UNIVERSITAT DE BARCELONA

WNT pathway regulation of lipid handling and inflammation in organ function: the role of LRP5

Aureli Luquero Gomez

WNT pathway regulation of lipid handling and inflammation in organ function: the role of LRP5

Aureli Luquero Gómez

Doctoral Thesis
2024

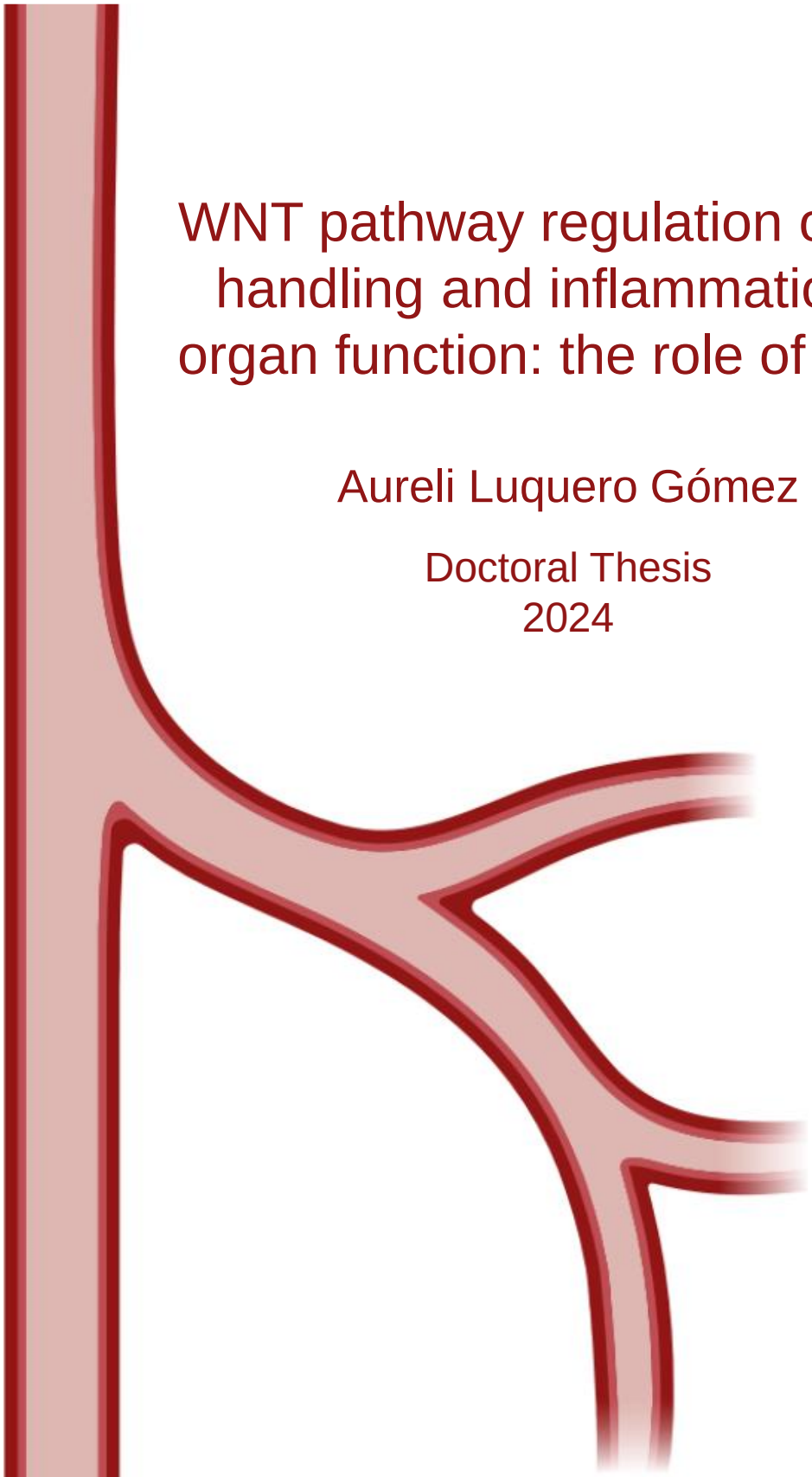

UNIVERSITAT DE BARCELONA

Programa de Doctorat en Biomedicina, Facultat de Biologia, Universitat de Barcelona

WNT pathway regulation of lipid handling and inflammation in organ function: the role of LRP5

Aureli Luquero Gómez

Directores: Dra. Maria Borrell Pagès i Prof. Lina Badimon Maestro

Tutora: Dra. Montserrat Corominas Guiu

Institut de Recerca de l'Hospital de la Santa Creu i Sant Pau

Memòria presentada per Aureli Luquero Gómez per optar al títol de doctor per la Universitat de Barcelona

Al meu germà,

la millor persona amb la que he pogut créixer i qui sé que en condicions normals hagués pogut fer un treball com aquest

Table of Contents

Acknowledgments

This section of the thesis will be written in Catalan language as the majority of the people I would like to express my gratitude preferentially speaks Catalan to me.

Aquesta tesis no hauria estat possible sense les contribucions i el suport de molta gent:

En primer lloc, m'agradaria poder donar les gràcies a la Professora Lina Badimon i a la Doctora Maria Borrell per acceptar-me el 2019 per a realitzar la tesis doctoral en el seu grup d'investigació de l'Institut de Recerca de l'Hospital de Sant Pau. Opino que hem fet un gran treball conjunt, fruit de l'esforç i dedicació que demostreu i que em vau inculcar des del primer moment, ha estat un llarg procés d'aprenentatge que m'ha ajudat a enriquir els meus coneixements científics. Per això, us estaré sempre agraït. També vull donar les gràcies a la Gemma Vilahur, la Gemma Arderiu, la Teresa Padró i l'Esther Peña, qui han estat referents per mí des del moment en que vaig arribar al centre.

M'agradaria mencionar especialment a la Sònia, la persona amb qui més properament he estat treballant i amb qui més relació he tingut en els darrers anys. Han estat molts moments de tensió, de ficar-nos l'un amb l'altre, de riure i de treballar durament, gràcies per ensenyar-me tant durant els primers anys i entendre'm en els últims, que mai ningú et digui que no ets la millor tècnic del món. També m'agradaria fer especial menció a la Nerea, que tot i marxar a meitat de la tesis, va ajudar-me a processar una infinitat de mostres i que, sense ella, tot hauria estat molt més difícil. També agrair a la resta de tècnics del centre, la Montse i la Mari, amb qui he passat moltes estones; l'Esther a qui li he demanat molts favors urgents; la Mònica, el Pablo i la Olaya.

No em vull oblidar dels meus companys de tesis, que en un trajecte llarg i gens fàcil sempre ens hem donat suport mutu i companyia, també

moments de riures en sopars i “anar a prendre algo”s, han estat molts moments que sempre tindré present. No em volia deixar ningú, doncs tots mereixeu estar en aquesta tesis perquè tots heu passat o haureu de passar per moments complicats que comporten el fet de realitzar una tesis doctoral: Soumaya, Elisa, Hue, Alex, Vicky, Pablo, Alba, Natalia, Leonie, Anna, Sebastià, Lisi i Sergi. En especial, m’agradaria mencionar la Noelia, qui va ser aire fresc pel nostre grup des del moment que va arribar i amb qui he tingut un vincle especial, gràcies de tot cor.

I will not pass on giving my most sincere thanks to Dr Melissa Reichelt and Dr Wally Thomas from the University of Queensland in Brisbane, Australia. I am so grateful for the opportunity that you gave me to come to your research group and visit your magnific country. I will always remember the knowledge I gained in your lab and the moments we shared. I will try to come back to visit you whenever I can, the experience in the *Down Under* land was terrific (as Wally would say).

Per altra banda, m’agradaria fer menció a la gent que ha estat fent-me costat des de sempre. Vull fer menció especial a cadascun dels meus grups d’amics:

- Al meu grup d’amics de l’escola, amb qui em sembla increïble que puguem seguir tanta gent tant unida des de fa temps i a qui he vist casar-se, tenir fills, anar-se’n a viure fora, etc. Però que sempre podem tornar a veure’ns per explicar-nos històries i recordar moments de tota la vida.
- Al meu grup d’amics de l’Institut. Dir-vos que sou els millors, no puc tenir gent amb qui riure més que amb vosaltres, esteu rematadament penjats i per això us estimo tant. Sé que no soc el que es queda fins els finals de les festes ni el que suma a més plans, potser perquè estava fent una tesis, espero que d’ara endavant ens puguem veure més sovint.

- Al grup de companys de la Universitat. No podria haver arribat fins aquí si no hagués estat pels moments que hem compartit mentre estudiàvem Bioquímica, em vau ensenyar que el més important no era aprendre ciència sinó formar amistats que perdurin. Cada vegada vivim més distanciats però això no treu que sempre podrem fer retrobaments i fer com si mai res ens hagués separat.
- En un grup a part tinc el Guillem, el Xavi i el Roger, amics però que pel temps i tants moments junts són també germans. Sé que sempre puc comptar amb vosaltres sigui allà on sigui i passi el que passi.

M'agradaria donar les més sinceres gràcies a la meva família, tiets i cosins, que m'han ajudat en tot moment des que era petit, ajudant-me a créixer com a persona. També, donar les gràcies als meus avis per fer de segons pares, cuidar-me en tot moment i donar-me uns valors extraordinaris. Als meus sogres, per sempre fer-me sentir benvingut a casa seva i adoptar-me com un nou membre de la seva família. Al meu pare, per sempre fer-me creure en mi mateix i fer-me suport en tot allò que sempre m'ha il·lusionat, gràcies papa. A la meva mare, per sempre ser-hi present, ser la persona més forta que conec i qui més m'ha estimat, gràcies mama. Al meu germà, per ser font d'inspiració i resiliència, la millor persona d'aquest món, saps que no hi ha ningú com tu, gràcies teti.

Per últim, donar les gràcies a l'Anna, qui fa 10 anys va entrar a la meva vida i que m'entusiasma dia a dia amb el seu somriure i la seva manera de ser. Hem compartit el viatge de fer una tesis doctoral i ara ens queda tota una vida per davant. Hem estat en els nostres millors moments i en els pitjors ajudant-me a tirar endavant, és per això que vull que sempre estiguis al meu costat. Gràcies per tot.

Sinopsi (in Catalan)

Introducció: les malalties cardiovascular són la primera causa de mort prematura a nivell mundial. L'aterosclerosis és la causa subjacent més comuna entre les malalties cardiovasculars, sent una patologia complexa que es desencadena després de l'acumulació de colesterol modificat en la paret del vas sanguini, induint processos inflamatoris i fibròtics. La via canònica WNT és una via de senyalització conservada evolutivament de la qual es coneix la seva importància durant el desenvolupament embrionari i en determinar el destí cel·lular. El "Low-density Lipoprotein Receptor – related protein 5" (LRP5) és un receptor que inicia la senyalització de la via canònica WNT i participa en la internalització de les lipoproteïnes de baixa densitat (LDL). És la nostra hipòtesi que el LRP5 i la via canònica WNT juguen un paper clau en la resposta cel·lular a l'exposició a colesterol en diferents teixits.

Objectiu: el focus de la tesis es centra en identificar el rol del LRP5 en diferents tipus cel·lulars i teixits que es veuen alterats per la hipercolesterolèmia incloent els macròfags circulats, així com línies cel·lulars del fetge o el teixit adipós. A més, en la tesis també s'ha estudiat el rol del LRP5 durant la resposta immunitària induïda per l'aterosclerosi i el seu rol en el cervell (un òrgan profundament afectat per la desregulació de l'homeòstasi del colesterol).

Mètodes: s'han fet servir tan models *in vitro* com *in vivo*. En estudis *in vitro* diferents línies cel·lulars i cultius primaris s'han sotmès a experiments de disminució d'expressió gènica selectiva contra certs gens diana (principalment LRP5, però també d'altres com el PCSK9, el SREBP2, el LDLR o el LRP1). Les cèl·lules eren posteriorment tractades amb diferents inductors d'estres, principalment LDL naturals o agregades però també peròxid d'hidrogen o estaurosporina, per després ser recol·lectades amb diferents tampons per a realitzar

experiments per avaluar el contingut transcriptòmic, proteòmic i lipidòmic.

Per experiments *in vivo*, es van fer servir ratolins C57Bl/6J amb deficiència sistèmica per LRP5 (*Lrp5*$^{-/-}$). Tan ratolins de genotip normal (*Wt*) com *Lrp5*$^{-/-}$ es van dividir en dos grups a les 8 setmanes d'edat que es van alimentar amb dieta normocolesterolémica (NC) o hipercolesterolèmica (HC) durant 10 setmanes, quan van ser sacrificats i es van obtenir mostres de sang i d'òrgan per fer anàlisis transcriptòmic, proteòmic i lipidòmic.

Resultats: l'expressió de LRP5 augmenta en macròfags després de l'estimulació amb lípids. Aquest augment d'expressió de LRP5 s'associa a una major captació de lípids. En els macròfags carregats de lípid, el LRP5 interacciona amb el PCSK9 i promou el seu alliberament a l'espai extracel·lular, desencadenant una resposta pro-inflamatòria. L'expressió d'ambdues proteïnes regula la internalització de colesterol en els macròfags.

El LRP5 i el PCSK9 demostren un comportament similar a l'anterior en cèl·lules hepàtiques estelades però no en els hepatòcits del fetge, revelant així que la interacció LRP5-PCSK9 és de tipus cèl·lula-específic. Tot i que el LRP5 indueix un perfil pro-inflamatori en macròfags carregats de lípids, també hem demostrat un rol anti-inflamatori pel LRP5 en les microvesícules derivades de macròfags (MVs). Els macròfags estimulats amb LRP5^{+}MVs mostren un perfil anti-inflamatori, mentre que el tractament de macròfags amb LRP5^{-}MVs indueix el canvi a un perfil pro-inflamatori similar a la inducció causada per MVs provinents de macròfags carregats de lípid.

La deficiència del LRP5 en ratolí bloqueja la proliferació del teixit adipós després de ser alimentats amb dieta HC. Aquest efecte és causat per una menor expressió de gens de resposta a insulina en ratolins HC

Lrp5$^{-/-}$ comparat amb ratolins HC *Wt*, però també per una reducció en l'infiltrat de cèl·lules del sistema immunitari en el teixit adipós.

En el cervell, el LRP5 no està involucrat en l'acumulació de colesterol en neurones; tot i això, el LRP5 participa en la senyalització de supervivència perquè les neurones silenciades per LRP5 mostren apoptosi promoguda. A més, en l'estudi de RNA-Seq de cervell de ratolí *Wt* i *Lrp5*$^{-/-}$ ha revelat alteracions significatives en processos metabòlics cerebrals com són el processament de l'àcid retinoic o l'àcid linoleic provocant una diferenciació neuronal i una formació de sinapsis defectuosa.

Conclusió: els resultats de la tesis mostren una important funció pel LRP5 en la resposta cel·lular i tissular al colesterol, però també en la preservació de l'homeòstasi de teixits. La reducció o la pèrdua d'expressió de LRP5 altera la fisiologia natural de cèl·lules i teixits fet que postula el LRP5 i la via canònica WNT com a reguladors clau en les malalties cardiovasculars.

Abstract

Introduction: cardiovascular diseases are the first cause of premature mortality worldwide. Atherosclerosis is the most common underlying cause of cardiovascular disease. This is a complex condition triggered by the accumulation of modified cholesterol in the vascular wall, which induces inflammatory and fibrotic processes. Hypercholesterolemia is the elevation of circulating cholesterol levels in blood, which affects cholesterol homeostasis in different tissues and organs. Canonical WNT pathway is an evolutionary conserved signalling pathway with a role in embryonic development and cell fate. Low-density Lipoprotein Receptor – related protein 5 (LRP5) is a receptor that triggers the canonical WNT signalling and uptakes circulating low-density lipoproteins (LDL). It is our hypothesis that LRP5 and the canonical WNT signalling play a key role in the cellular response to cholesterol exposure in different tissues.

Objectives: the aim of this thesis is to identify the role of LRP5 in different cell types and tissues modulated by hypercholesterolemia including circulating macrophages and cell lineages of the liver and the adipose tissue. Additionally, this thesis focuses on the study of LRP5 roles during the inflammatory response induced by atherosclerosis and its role in the brain (an organ with a heavily regulated cholesterol homeostasis).

Methods: both *in vitro* and *in vivo* models were used. In *in vitro* studies, different cell lineages and primary cultures were subjected to gene knockdown to silence the expression of selected genes (mainly LRP5, but also PCSK9, SREBP2, LDLR, or LRP1). Cells were then treated with different stressors, mainly native or aggregated LDLs but also H_2O_2 or staurosporine, and then harvested and collected with different buffers and further processed for transcriptomic, proteomic and lipidomic analyses.

C57Bl/6J mice with a systemic LRP5 deficiency (*Lrp5*$^{-/-}$) were used. Mice with wildtype (*Wt*) and *Lrp5*$^{-/-}$ genotypes were divided into two groups at 8 weeks old and fed a normocholesterolemic (NC) or hypercholesterolemic (HC) diet for further 10 weeks when they were sacrificed and blood and organ samples collected for transcriptomic, proteomic and lipidomic analyses.

Results: LRP5 expression increases in macrophages after lipid stimulation. This upregulation is associated to enhanced lipid accumulation in the cell. In lipid-loaded macrophages, LRP5 interacts with PCSK9 and promotes its release into the extracellular milieu, triggering a pro-inflammatory response. The expression of both proteins regulates macrophage cholesterol internalization.

LRP5 and PCSK9 display a similar behaviour in hepatic stellate cells but not in liver hepatocytes, revealing that LRP5-PCSK9 interaction is cell-type specific. Despite LRP5 pro-inflammatory roles in lipid-loaded macrophages, we have also observed an anti-inflammatory role for LRP5 in macrophage-derived microvesicles (MV). Macrophages stimulated with LRP5^{+}MVs show an anti-inflammatory profile; however, LRP5^{-}MVs treatment induce a pro-inflammatory switch in macrophages similar to the induction caused by MVs from lipid-loaded macrophages.

LRP5 deficiency in mice blocks adipose tissue proliferation after hypercholesterolemic feeding. This effect might be caused by a lower expression of insulin-responsive genes in HC *Lrp5*$^{-/-}$ mice compared to HC *Wt* mice but also by a reduced infiltration of immune inflammatory cells in the adipose tissue.

In the brain, LRP5 is not involved in neuronal cholesterol accumulation but participates in neuronal survival signalling as LRP5-silenced neurons display enhanced apoptosis. Additionally, RNA-seq analysis of brains of *Wt* and *Lrp5*$^{-/-}$ mice revealed significant alterations in different

metabolic processes such as retinoic acid or linoleic acid processing leading to defective neuronal differentiation and synapse formation.

Conclusion: the results of this thesis show an important function for LRP5 in cellular and tissular cholesterol response, but also in preserving tissue homeostasis. The reduction or deficiency of LRP5 expression alters the normal physiology of cells and tissues postulating LRP5 and the canonical WNT signalling key regulators of cardiovascular diseases.

Index for Figures

Index for Tables

Abbreviations

ABCA1 – ATP-Binding Cassette sub-family A member 1

ABCG1 – ATP-Binding Cassette sub-family G member 1

agLDL – aggregated Low-Density Lipoprotein

APC – Adenomatous Polyposis Coli

apoER2 – apolipoprotein E Receptor 2 / low-density lipoprotein receptor-related protein 8

apo(a) – apolipoprotein (a)

APP – Amyloid beta Precursor Protein

ARF1 – ADP-Ribosylation Factor 1

ARF6 – ADP-Ribosylation Factor 6

Aβ – Amyloid Beta

α-SMA – Alpha Smooth Muscle Actin

BACE1 – Beta-site Amyloid Precursor Protein Cleaving Enzyme 1

BAT – Brown Adipose Tissue

BBB – Blood-Brain Barrier

BMI – Body Mass Index

CAD – Coronary Artery Disease

CD(x) – Cluster of Differentiation (x)

CETP – Cholesteryl-Ester Transfer Protein

CHD – Coronary Heart Disease

CK1α – Casein Kinase I isoform Alpha

CM – Chylomicron

CMr – Chylomicron Remnant

CNS – Central Nervous System

CSF – Cerebrospinal Fluid

CSF-1 – Colony Stimulating Factor 1

CYP46A1 – Cytochrome P450 family 46 subfamily A member 1 / Cholesterol 24-hydroxylase

CVD – Cardiovascular Diseases

DAMP – Damage-Associated Molecular Pattern

Dkk1 – Dickkopf-related protein 1

EAT – Epicardial Adipose Tissue

EC – Endothelial Cell

ESCRT - Endosomal Complex Required for Transport

FATP – Fatty Acid Transport Protein

FFA – Free Fatty Acid

Fzd – Frizzled

GM-CSF – Granulocyte Macrophage - Colony Stimulating Factor

GSK3β – Glycogen Synthase Kinase-3 beta

GWAS – Genome-Wide Association Studies

HeFH – Heterozygous Familial Hypercholesterolemia

HF – Heart Failure

HIF1α – Hypoxia-Inducible Factor 1-alpha

HMGB1 – High Mobility Group Box 1

HMG-CoA – 3-hidroxi-3-metilglutaril-coenzim A

HLA-DR – Human Leukocyte Antigen - DR isotype

ICAM-1 – Intercellular Adhesion Molecule 1

IDL – Intermediate-Density Lipoprotein

IFNγ – Interferon γ

IL-(x) – interleukin - (x)

KLF2 – Krüppel-Like Factor 2

LCAT – Lecithin Cholesterol Acyl-Transferase

LDL – Low-Density Lipoprotein

LDLR – Low-Density Lipoprotein Receptor

LOX-1 – Lectin-type Oxidized LDL receptor 1

LPL – Lipoprotein Lipase

Lp(a) – Lipoprotein (a)

LRP(x) – Low-Density Lipoprotein Receptor-Related Protein (X)

LTP – Long-Term Potentiation

LXRα – Liver X Receptor alpha

MCP-1 – Monocyte Chemoattractant Protein 1 (also known as CCL2 – chemokine C-C motif ligand 2)

MDC – Macrophage-derived Chemokine (also known as CCL22 – chemokine C-C motif ligand 22)

MIP-1β – Macrophage Inflammatory Protein 1 beta

MI – Myocardial Infarction

miRNA – micro RNA

MMP(x) – Matrix Metalloproteinases (x)

MV – Microvesicle

MyD88 – Myeloid Differentiation Primary Response Protein 88

NET – Neutrophile Extracellular Traps

NeuroD1 – Neurogenic Differentiation 1

Nfe2r2 – Nuclear Factor Erythroid 2 Related Factor 2

NFκB – Nuclear Factor kappa-light-chain-enhancer of activated B cells

nLDL – Native Low-Density Lipoprotein

NO – Nitric Oxide

OXLAM – Oxidized Linoleic Acid Metabolites

PAD – Peripheral Artery Disease

PAR – Population Attributable Risk

PCSK9 – Proprotein Convertase Subtilisin/Kexin type 9

PECAM1 – Platelet Endothelial Cell Adhesion Molecule 1

PP2A – Protein Phosphatase 2a

PPARα – Peroxisome Proliferator-Activated Receptor alpha

PPARγ – Peroxisome Proliferator-Activated Receptor gamma

Prox1 – Prospero Homeobox Protein 1

Rab22a – Ras-related Protein Rab-22A

RAGE – Receptor for Advanced Glycation End Products

RAR – Retinoic Acid Receptor

RBP4 – Retinol Binding Protein 4

RoR – Receptor Tyrosine Kinase-like Orphan Receptor

ROS – Reactive Oxygen Species

RXR – Retinoic X Receptor

Ryk – Related to Receptor Tyrosine Kinase

SCAT – Subcutaneous Adipose Tissue

SCF – Skp-Cullin-F-box-Containing Complex

SNARE – Soluble NSF Attachment Protein

SREBP – Sterol Regulatory Element-Binding Protein

Src – Proto-oncogene Tyrosine-protein Kinase Src

SRSF1 – Serine/Arginine-rich splicing Factor 1

STRA6 – Stimulated by Retinoic Acid Gene 6

Tau – Tubulin Associated Unit

Tcf – T Cell Factor

TGF-β – Transforming Growth Factor beta

TIMP – Tissue Inhibitor of Matrix Metalloproteinases

TLR – Toll-like Receptors

TNFα – Tumour necrosis factor alpha

TREM-1 – Triggering Receptor Expressed on Myeloid Cells 1

UCP-1 – Uncoupling Protein 1

VAT – Visceral Adipose Tissue

VCAM-1 – Vascular Cell Adhesion Molecule 1

VEGF-A – Vascular Endothelial Growth Factor A

VSMC – Vascular Smooth Muscle Cell

VLDL – Very Low-Density Lipoprotein

VLDLR – Very Low-Density Lipoprotein Receptor

WAT – White Adipose Tissue

WASp1 – Wiskott-Aldrich Syndrome Protein 1

1. Introduction

“All we have to decide is what to do with the time that is given us.”

Gandalf to Frodo. *The Fellowship of the Ring. Chapter 2.* J.R.R. Tolkien

1.1 Introduction to Cardiovascular Biology

1.1.1 Epidemiology of CVD

According to the National Institutes of Health and the World Health Organization, cardiovascular diseases (CVD) encompass a group of disorders occurring in the heart and blood vessels. They are the leading cause of premature death and account for approximately 17.9 million deaths/year, being ischemic heart disease and stroke the world's leading death causes. CVD treatments are the costliest pathology-associated healthcare, with a calculated indirect cost of 237 billion dollars annually by 2015 and a projected increased cost of 368 billion dollars by 2035 (1).

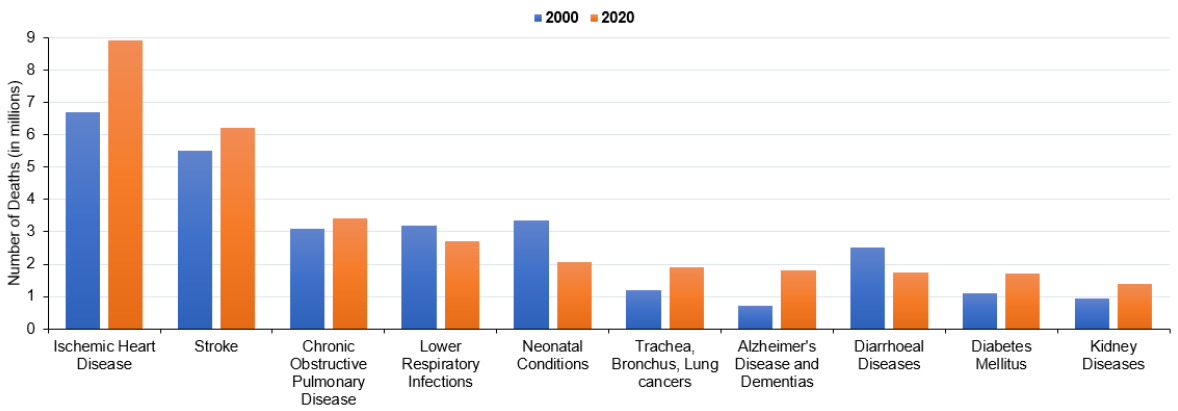

Figure 1. Ten most lethal diseases worldwide (number of total deaths caused in the years 2000 and 2020). Data obtained from the WHO website.

In the past, the incidence of CVD in the population was low. Back then, people worked on physically demanding jobs and the food intake was poor. However, the modern industrialized economy and consumerism produced a shift towards longer non-physically-demanding working periods, longer commutes, less leisure time, and higher food intake, which ultimately led to a progressive increase in CVD rates (2) (**Figure 1**). CVD exist in our society since the first civilizations, signs of atherosclerosis were found in pharaohs mummies from ancient Egypt

indicating that sedentary and high-caloric fed people always had enhanced CVD risk (3). In the mid-late 20th Century, there were few CVD cases/year in developing countries affecting ministers, political leaders, and other wealthy inhabitants with the “western” lifestyle (4).

There has been a rapid transition for CVD from a condition of developed countries to a global pandemic with a concerning continuous increase in the health system burden in lower-income countries (**Figure 2**). The main causes for the increased prevalence of CVD are the manifestation of risk factors and a relative lack of access to interventions against the disease (5).

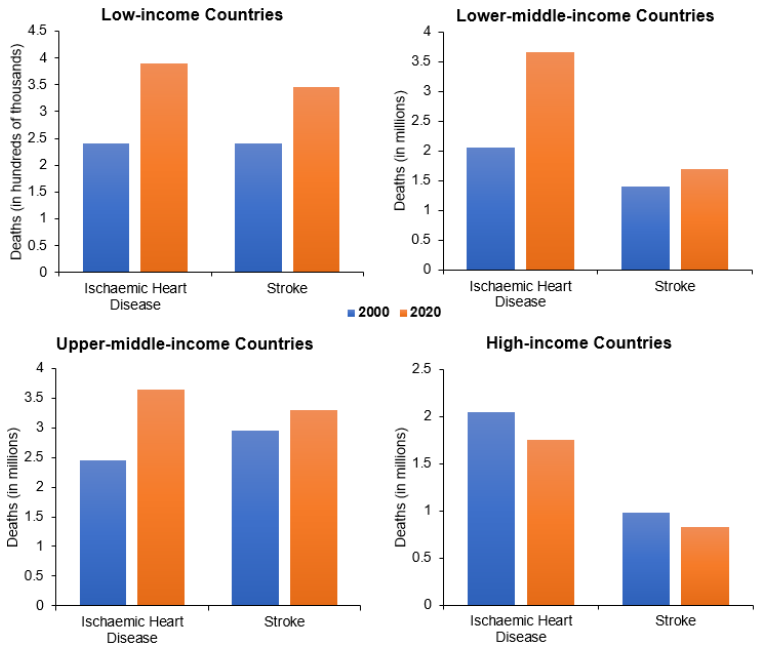

Figure 2. Evolution of Ischaemic Heart Disease and Stroke casualties in the years 2000 and 2020 classified by countries income. Country income classification was obtained by World Bank data from year 2020.

1.1.2 CVD risk factors

Two major case-control studies (INTERHEART and INTERSTROKE) resolved that nine modifiable risk factors explain more than 90% of the population attributable risk (PAR) of developing myocardial infarction

(MI) and stroke (6,7). The PAR value measures the incidence of a disease in the population caused by one risk factor by comparing the risk factor incidence in the exposed population fraction and in the non-exposed fraction (8). These risk factors include hypertension, tobacco smoking, waist-to-hip ratio, poor consumption of fruits and vegetables, limited physical activity, diabetes, alcohol intake, psychological stress and depression, cardiac causes, and the ratio between circulating apoB/apoA1. Collectively, these risk factors are consistent across different global regions, gender and age for both myocardial infarction and stroke.

Furthermore, non-modifiable risk factors include genetic background, previous cardiovascular events, ethnicity, gender, and age, which contribute to approximately 63-80% of CVD prognosis (9).

All these risk factors can induce the development of CVD by altering other parameters including the lipid profile, the inflammatory state, the oxidative stress or the development of thrombi either locally or systemically (10).

1.1.3 Clinical features of CVD

CVD comprehend different clinical features that share their origin in blood vessels and the heart. The American Heart Association classifies CVD in 4 groups depending on the location affected by the disease (11):

- Coronary Heart disease (CHD): encompassing coronary artery disease (CAD) and MI. Frequently, CHD initiates after the partial or complete reduction of blood supply to the heart. The appearance of these conditions usually triggers the development of heart failure (HF), characterized by a reduced cardiac output insufficient for the body needs. The causes for HF are diverse, from heart muscle hypertrophy to cardiomyocyte death after MI (12).

- Cerebrovascular disease (CBVD): includes ischemic stroke, transient ischemic attacks and carotid stenosis. CBVD initiates when the irrigation to the central nervous system is partially or completely blocked by vessel narrowing, clot formation, blockage or rupture of the blood vessel.
- Peripheral artery disease (PAD): occurs when blood flow to one or more limbs is restricted or blocked.
- Aortic diseases: include disorders or conditions affecting the integrity of the aorta. The pathological condition usually leads to the formation of aneurysms.

Therapeutical approaches targeting CVD can be differentiated into three major groups: primary, secondary and tertiary intervention, which focus into prevention, regression and slowing of CVD, respectively (13).

Primary intervention is the most effective approach to reduce CVD-related deaths. During 1980 to 2000 there were 70.000 fewer MI than predicted in the United Kingdom. The 41% of the decline was explained only by smoking cessation, as the percentage of smokers was reduced from 45% of the population to less than 28% because of consciousness-raising campaigns against tobacco consumption (14). However, CVD prevention is complicated as the clinical outcome is not obvious during the first stages of the disease. It is not until CVD is stablished and the patient is already in a life-threatening situation that the first symptomatology is reported, limiting in many cases the impact of primary interventions and requiring the application of secondary/tertiary interventions (15,16).

Secondary interventions also have a huge effect on reducing CVD-associated deaths. The effectiveness of statins in reducing circulating cholesterol levels lowers CVD-related deaths by 25% in hypercholesterolemic patients (17–19). Also, statin administration to

individuals between 75-94 years old in the United States would save 85.000 CHD cases, 269.000 disability-adjusted life years and a healthcare cost of 14.000.000.000 dollars (20). Statins act as competitive inhibitors of the enzyme 3-hidroxi-3-metilglutaril-coenzim A (HMG-CoA) reductase, the rate-limiting enzyme for cholesterol synthesis by the liver (21,22). This inhibition reduces very low-density lipoprotein (VLDL) production by hepatocytes and increases cholesterol uptake from blood mediated by the low-density lipoprotein receptor (LDLR) as a consequence of sterol receptor element-binding protein (SREBP) transcription factor activation (**Figure 3**).

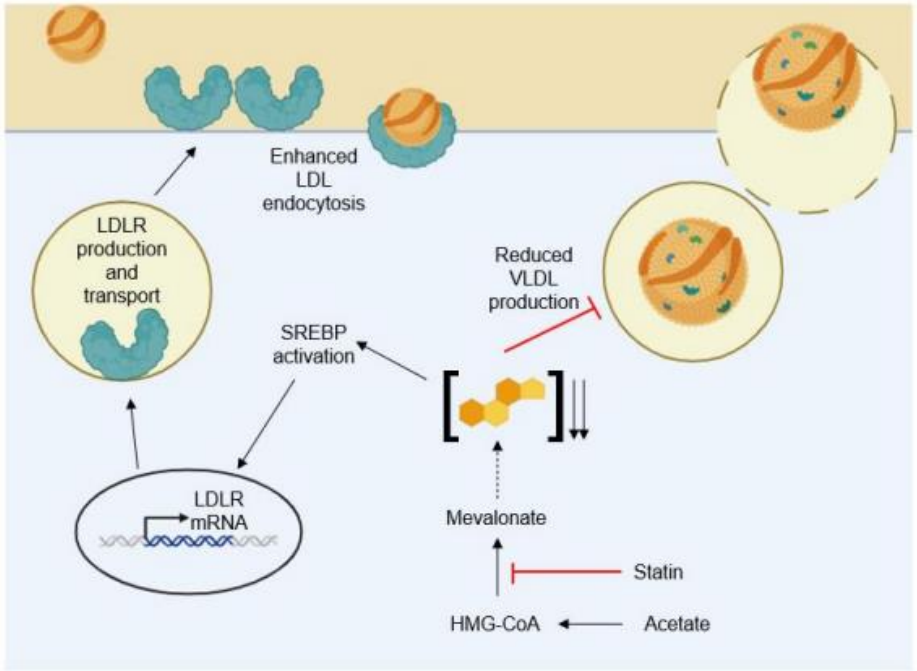

Figure 3. Statins effects on hepatocytes.

Tertiary interventions refer to the use of coronary interventions like the installation of pacemakers or left ventricular assistance devices. Surgical procedures such as coronary artery angioplasty or bypass are also included as tertiary procedures. However, these therapeutical approaches are expensive and the implementation of these techniques

on the global population at risk of CVD would suppose a huge cost for healthcare systems.

In order to reduce future CVD-related deaths, primary interventions should be made available to a broader spectrum of the population at risk. In addition, it is important to improve current therapies by finding new therapeutic targets discovered by high-quality translational research (13).

1.1.4 Obesity and adipose tissue in CVD

Obesity is a multi-factorial disease with a complex pathogenesis related to biological, psychosocial, socioeconomic and environmental components with multiple pathways activation leading to adipose tissue formation and proliferation due to hypercaloric ingestion (23). The World Health Organization criteria determines that obesity on humans is set above 30 kg/m^2 of body-mass index (BMI). Rather than the BMI indicator, clinicians prefer to use the waist circumference value or the waist-to-hip ratio as indicators of cardiovascular outcome due to obesity because they provide a better approach to the body fat distribution.

There are two types of adipose tissues in mammals: the white adipose tissue (WAT) and the brown adipose tissue (BAT), with opposite functions:

- WAT's most important function is as a fat reservoir. After food ingestion, WAT reacts to high insulin concentration generated by the pancreas and absorbs glucose and free fatty acids (FFA) from bloodstream preventing hyperglycaemia and hypercholesterolemia. Upon entrance into white adipocytes, glucose and FFA are used for the synthesis of triglycerides. In fasting periods, WAT hydrolyses the previously stored triglycerides and gradually release FFA to the circulation to be used as energy source for other tissues.

- BAT's most important function is to generate heat to maintain the body temperature. BAT absorbs glucose and FFA to be used in glycolysis and Krebs cycle, generating NADPH and $FADH_2$ metabolites, that finally donate their protons to the electron transport chain. BAT exclusively express the uncoupling protein 1 (UCP-1), which is located in the inner mitochondrial membrane of brown adipocytes and generate a secondary pathway for proton potential recovery, drastically impairing the oxidative phosphorylation process reducing ATP generation. Therefore, instead of producing ATP, brown adipocytes mitochondria dissipate the energy of the proton potential in the form of heat.

BAT is evolutionary conserved in individuals that are predisposed to temperature loss due to their small volume-to-surface ratio like small mammals and newborns. In large mammals, WAT frequently create an isolating layer to protect internal organs from cold temperatures. However, recent findings in adult humans reveal that an extra beige adipocyte phenotype exists. Beige adipocytes are derived from white adipocytes exposed to certain catecholamines and growth factors and have BAT characteristics. The presence of beige adipocyte islets in WAT is a beneficial indicator of health, as beige adipocytes burn lipids preventing fat accumulation in the tissue. The formation of beige adipocytes is being aimed as therapeutic target by many approaches to treat obesity (24).

The two major WAT depots in adulthood are subcutaneous adipose tissue (SCAT) and visceral adipose tissue (VAT). The importance of this classification is highlighted by studies revealing distinct transcriptomic and proteomic profiles between the different depots of adipose tissues, as well as studies that reveal a relationship between VAT and increased risk of CVD, while SCAT is considered to have a neutral or even cardioprotective profile (25). VAT is more innervated, irrigated and

vascularized than SCAT, which connects the fat depot closer to systemic regulation by nerves and hormones (26). In turn, the higher vascularization allows for a facilitated infiltration of inflammatory cells, which modulate adipocyte's activity (27).

SCAT acts as a metabolic sink for glucose and free-fatty acids in response to insulin and generates triglycerides that are stored in adipocytes, generating the energy reservoir (28). When the storage capacity of SCAT is exceeded, fat starts to accumulate in different regions of the abdominal cavity generating VAT (29). In normal conditions, SCAT is approximately 80% of the total WAT in human adults, while VAT accounts for 10-20% of total WAT in men and 5-8% in women (30). The distribution of adipose tissues in human and mouse is depicted in **Figure 4.**

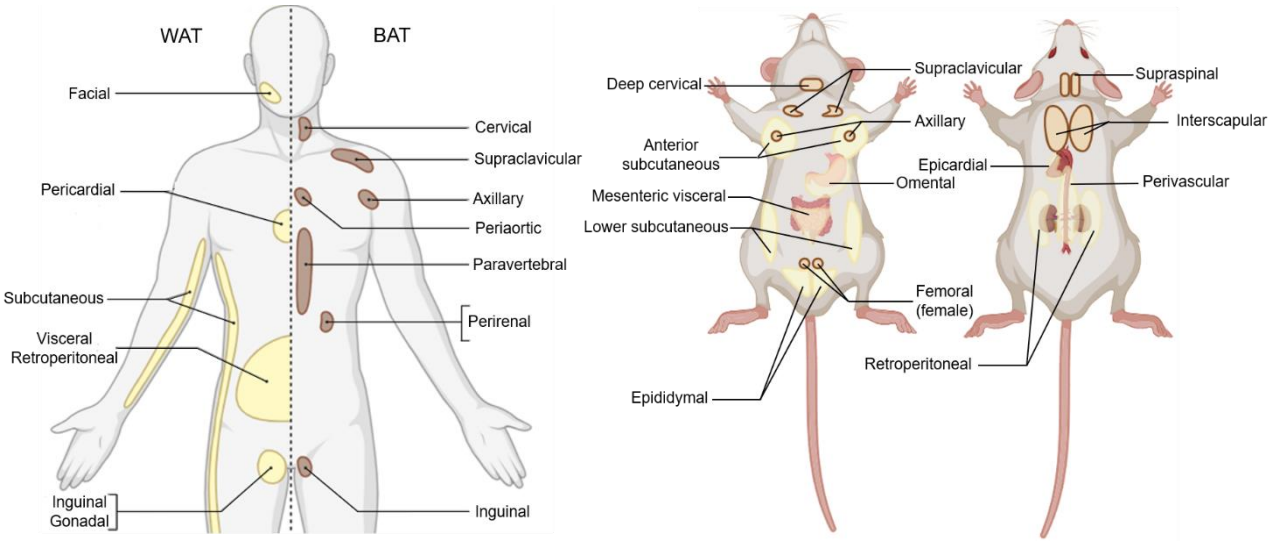

Figure 4. Fat depot location in the human and mouse organism. Yellow figures represent WAT and brown figures represent BAT. Adapted from Torres Irizarry, VC. et al. *Front Endocrinol*. 2022 Jun 9;13:898139.

Increased VAT, but not SCAT, enhances the risk of type I diabetes, elevates circulating cholesterol and triglycerides levels, hypertension, increases metabolic syndrome, increases the risk of stroke and peripheral artery disease, and reduces the thickness of the vascular wall

(31–34). Accordingly, the waist-to-hip ratio is a better indicator of cardiovascular outcome related to obesity than the BMI. The main differences between SCAT and VAT are found in **Table 1.**

	SCAT	**VAT**
Insulin sensitivity	High	Low
Lipogenesis capacity	High	Low
More sensitive to	Oestrogens	Catecholamines Glucocorticoids Androgens
Presence of beige adipocytes	Frequent	Almost inexistent
Immune response	Anti-atherogenic Anti-fibrotic	Pro-atherogenic Pro-fibrotic Neoangiogenic
Proportion in lean adults	80% men 95% women	20% men 5% women
Enhanced production	Leptin, adiponectin, resistin	TNFα, IL-6, IL-8, IL-13, MCP-1, eicosanoids, chemokines
Location	Beneath skin dermal layer	Associated with abdominal organs

Table 1. Differences between visceral and subcutaneous adipose tissue.

Metabolically, lean adipose tissue has more M2 macrophages with an anti-inflammatory phenotype while in obese adipose tissue the pro-inflammatory M1 macrophage phenotype prevails. The inflammatory state of the adipose tissue regulates the secretion of pro- and anti-inflammatory cytokines which affect the cardiovascular system. A pro-

inflammatory adipose tissue develops insulin resistance increasing cholesterol, triglyceride and FFA concentration in blood. Also, a proliferating adipose tissue switches its adipokine secreting profile as it releases less adiponectin, omentin-1, and nitric oxide (NO) while it increases the secretion of leptin, tumour necrosis factor alpha (TNFα), IL-6, interferon-γ (IFNγ), and reactive oxygen species (ROS).

The epicardial adipose tissue (EAT) is another WAT tissue located in the upper heart intimately related to the left auricula where it exerts protective functions in the myocardium. EAT protects the coronary arteries mechanically and metabolically, as it buffers the torsion generated by the arterial pulse and cardiac contraction and protects the myocardium from high concentrations of circulating inflammatory and pathogenic substances (35). Also, EAT serves as a source of fatty acids for the myocardium during high-demand moments as the heart is nurtured exclusively by fatty acids through β-oxidation (36). In obesity, EAT activity focuses on the release of pro-inflammatory adipokines and activates pro-fibrotic pathways. Subsequently, increased EAT thickness in patients is associated with increased insulin resistance, dyslipidaemia, hypertension, CAD, and enhanced risk of major cardiovascular events (37).

1.1.5 Lipoproteins

Lipoproteins are blood circulating large macromolecules that transport hydrophobic lipids across the organism (38). Lipoproteins have two main components: lipids and apolipoproteins. Different lipids can conform lipoproteins, which are distributed according to their hydrophobicity: the core is composed by hydrophobic lipids (cholesteryl esters and triglycerides) surrounded by a membrane of amphipathic lipids (phospholipids and free cholesterol) with their hydrophobic end facing towards the lipoprotein's core. Apolipoproteins are proteins embedded in the surface of the lipoproteins. Their functions include the

stabilisation of lipoproteins and conferring each lipoprotein type with unique biological properties (39). Lipoproteins, are classified according to their density (38) (**Table 2**):

- Chylomicrons (CMs): synthesized by the intestines, CMs transport dietary lipids from the intestines to the rest of the organism. Their lipid composition is high in triglycerides and low in cholesterol esters. The metabolization of CMs results in the formation of chylomicron remnants (CMr), which are smaller lipoproteins with higher cholesterol ester/triglyceride ratio than CMs.
- VLDLs: synthesized by the liver, VLDLs transport endogenously synthesized lipids from the liver to the rest of the organism. Their lipid content is enriched in triglycerides and poor in cholesterol, similar to CMs.
- Intermediate-density lipoproteins (IDLs): these lipoproteins are generated after triglycerides in VLDLs are metabolized in tissue capillaries.
- Low-density lipoproteins (LDLs): these lipoproteins are generated as a consequence of complete VLDL and IDL metabolization in the capillaries (which capture the majority of triglycerides), leaving a small cholesterol-enriched lipoprotein.
- Lipoprotein(a) (Lp(a)): this type of lipoprotein is generated as the consequence of an apolipoprotein (a) (apo(a)) protein binding to the canonical apoB-100 apolipoprotein of LDLs. Apo(a) confers extreme atherosclerotic properties to Lp(a) changing the lipoprotein density, its electrophoretic mobility, and molecular weight, which results in difficulties in Lp(a) removal from the vessel wall enhancing inflammatory, oxidative, and fibrotic processes (40).

- High-density lipoproteins (HDL): mainly generated in the liver and the intestines, HDL are responsible for the reverse cholesterol transport from the peripheral organs to the liver.

	CM 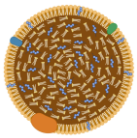	VLDL 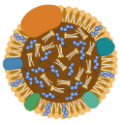	IDL 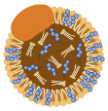	LDL 	Lp(a) 	HDL 
Size	> 100 µm	30-80 µm	25-35 µm	20-25 µM	20-25 µM	< 20 µM
Apolipoproteins	apoB48, ApoA-1, ApoA-II, apoC-I^{hi}, apoC-II^{hi}, apoE	apoB-100, ApoC-I^{hi}, apoC-II^{hi}	apoB-100, apoC-I^{low}, apoE^{low}	apoB-100	apoB-100, apo(a)	ApoA-I, ApoA-II, ApoC, ApoE
Source	Intestines	Liver	VLDL metabo-lization	VLDL and IDL metabo-lization	LDL modifi-cation	Intestines Liver
Cholesterol ester / triglyceride proportion	1:10	1:1	9:1	12:1	12:1	9:1
Lipid / protein proportion	99:1	9:1	4:1	4:1	4:1	3:2

Table 2. Main features of the most common circulating lipoproteins.

1.1.6 Cholesterol circulation and liver function

Cholesterol delivery is a well-regulated process where intestines, liver and cholesterol-demanding tissues communicate to keep balanced circulating cholesterol levels (41). Cholesterol has two main sources: *de novo* synthesis and diet. The liver is the main cholesterol-producing organ. Between 70-80% of the daily cholesterol need of an adult human (about 1 g/day) is synthesized by the liver, and is enough to completely sustain the organism (42,43). Cholesterol intake through diet is by

ingestion of animal-derived products as plants only produce cholesterol as a by-product to produce further metabolites like phytosterols (44).

After food intake, CM and VLDL are delivered to the systemic circulation where they reach their targeted tissues that are muscle and adipose tissue and, in minor proportion, other organs (45). In the capillaries surrounding the muscular and adipose tissues, CMs and VLDLs are recognised by the enzyme lipoprotein lipase (LPL). LPL recognizes ApoC-II of the surface of CMs and VLDL and promotes the hydrolyzation of triglycerides, resulting in the release of FFAs (46). Adjacent muscular and adipose cells absorb FFAs for energy production and storage, a process facilitated by membrane fatty-acid transport proteins: CD36 and fatty acid transport protein (FATP)-family members (47–49) . The metabolization of CMs and VLDLs-derived triglycerides empties the lipoprotein core and reduces the lipoprotein size which is followed by a change in apolipoprotein composition (45,50). ApoE incorporation in CMs and VLDLs, as well as loss of ApoC-II and ApoA-I in CMs leads to the formation of CMr and IDL/LDLs. Both CMr and IDL are rich in cholesterol esters and poor in triglycerides compared to their progenitors (51,52). The elimination of CMr from the systemic circulation by the liver is fast and mediated through specific recognition of ApoE by the LDLR present in the hepatocyte surface (53). However, LDLs are not cleared as efficiently as CMr, as ApoE is released from the lipoprotein surface during the IDL metabolization process. ApoB-100 is present in LDL surface and has a lower affinity for LDLR than for ApoE (39). The half-life of LDL in circulation is the longest amongst lipoproteins (approximately 3 days) as they lack active apolipoproteins and cholesteryl esters are very stable in LDL's core (54).

The main function of LDL is to transport cholesterol to extrahepatic tissues (55). Cholesterol is needed for many functions; thus, cells require limited but continuous supply of cholesterol to survive.

Approximately 70% of circulating LDL are cleared by liver's LDLR in normal conditions, and 30% is taken up by extrahepatic tissues (38). Hence, the liver, through the LDLR, is the main regulator of LDL circulating levels. LDLR is transcriptionally regulated by sterol regulatory element-binding protein (SREBPs) (56,57). This family of transcription factors sense the intracellular concentration of cholesterol and, upon activation, promote the transcription of cholesterol and fatty acid metabolism genes (58). Concretely, SREBPs induce the expression of LDLR and 3-hidroxi-3-metilglutaril-coenzim A (HMG-CoA) reductase, the rate-limiting enzyme in cholesterol *de novo* synthesis (59,60).

HDL particles are responsible for the reverse-cholesterol transport from extrahepatic tissues to the liver preventing cholesterol accumulation in cholesterol-overloaded cells and tissues (61). The generation of HDL starts with the liver production of Apo-AI that acquires cholesterol and phospholipids effluxed by cells, forming the mature HDL lipoprotein aided by the ATP-binding cassette sub-family A member 1 (ABCA1) transporter protein (61,62). In circulation, HDLs collect excess cholesterol from extrahepatic tissues but also FFA provided by LPL activity on circulating CM and VLDL. The lecithin cholesterol acyl-transferase (LCAT) enzyme mediates the transference of FFAs to unesterified cholesterol, forming cholesterol esters that move towards the HDL core (63). The ATP-binding cassette sub-family G member 1 (ABCG1) transporter is responsible for loading mature HDL with cholesteryl esters, regulating cholesterol efflux from cells to circulation (64). Another important enzyme in HDL metabolism is cholesteryl-ester transfer protein (CETP), a protein that promotes the exchange of cholesterol esters from HDL to apoB-containing lipoproteins and triglycerides from LDLs to HDLs (65,66). When fully loaded, HDL might

be cleared from the blood through the liver as scavenger receptor B-1 has a strong selective affinity for HDL (67) (**Figure 5**).

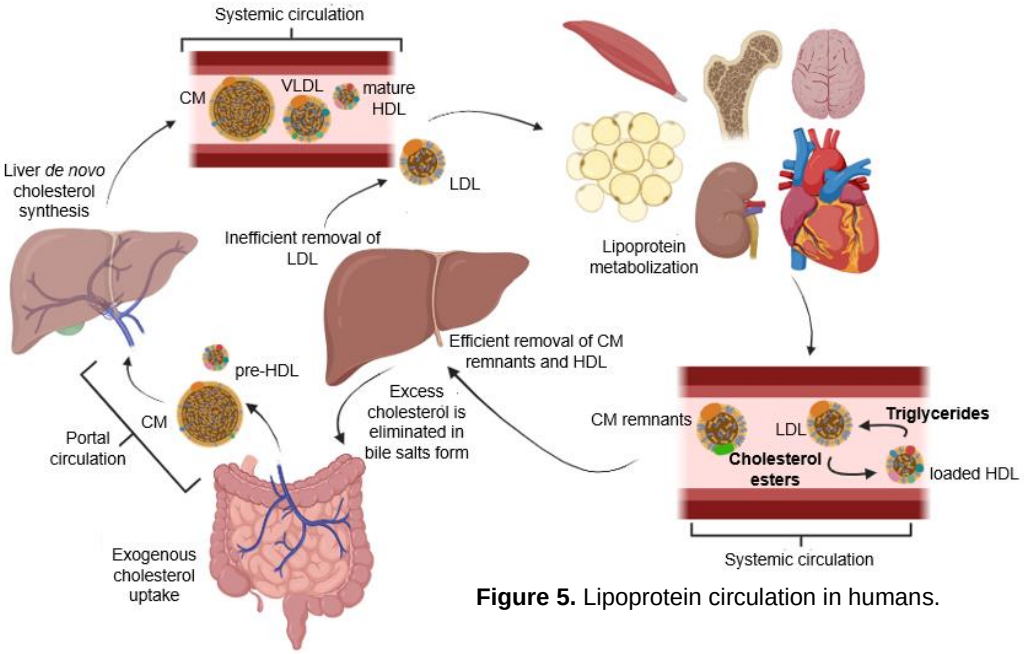

Figure 5. Lipoprotein circulation in humans.

1.1.7 Role of HSC in liver function

Besides its role as the main regulator of systemic blood cholesterol levels, the liver is a very complex organ which performs several functions that affect systemic circulation. It produces albumin, clears the blood from toxic substances, produces urea to eliminate the excess of nitrogen, supports digestion, and serves as energy and vitamin storage (68).

The liver receives a double blood supply from the portal vein and the hepatic artery, both located in the outer region of liver lobules which flow inwards fusing in the middle region and flowing into liver central veins (69). This creates concentration gradients for macromolecules and other blood components as they flow across the liver lobule. There are different resident cell subtypes in the liver and each has a unique role:

- Hepatocytes: they metabolize blood components and secrete most of the liver-derived proteins found in blood. Single-cell RNA-seq studies show that hepatocytes from the inner and outer liver lobule have distinct roles (70). Indeed, distal lobule hepatocytes are specialized in the production of blood proteins, gluconeogenesis, and urea synthesis while inner lobule hepatocytes are involved in cholesterol and lipid biosynthesis (71).
- Hepatic Stellate cells (HSCs): these cells are liver pericytes that surround liver sinusoids in the space of Disse, a liver-specific region between hepatocytes and sinusoids with a matrix resemblant function (72). HSC are quiescent cells that are the primary reservoir of fat and vitamin A in the liver (73). Their function during homeostasis remains unknown even though they constitute about 5% of the liver cell population (74).
- Kupffer cells: they are tissue-resident macrophages found in liver sinusoids. They contribute to the tissue homeostasis by providing innate immune surveillance (75).
- Liver sinusoidal ECs: these cells compose the endothelial layer of liver sinusoids. They form a highly specialised fenestrated endothelium, the most permeable in the organism. The liver endothelial layer is unique as it is the only endothelium without a base membrane. They contribute to the hepatic tone by maintaining a low portal vein pressure (76).

After liver damage, HSCs are activated, proliferate, and suffer a phenotype switch into fibber-producing myofibroblast-like cells (77). Collagen is the main extracellular protein produced by activated-HSC, contributing to liver fibrosis, a pathological state in which liver hepatocytes are replaced by extracellular matrix, reducing liver effective function and causing metabolic dysregulations (78) (**Figure 6**).

Advanced stages of fibrosis can lead to liver cirrhosis and hepatocarcinoma if the symptomatology is not reverted.

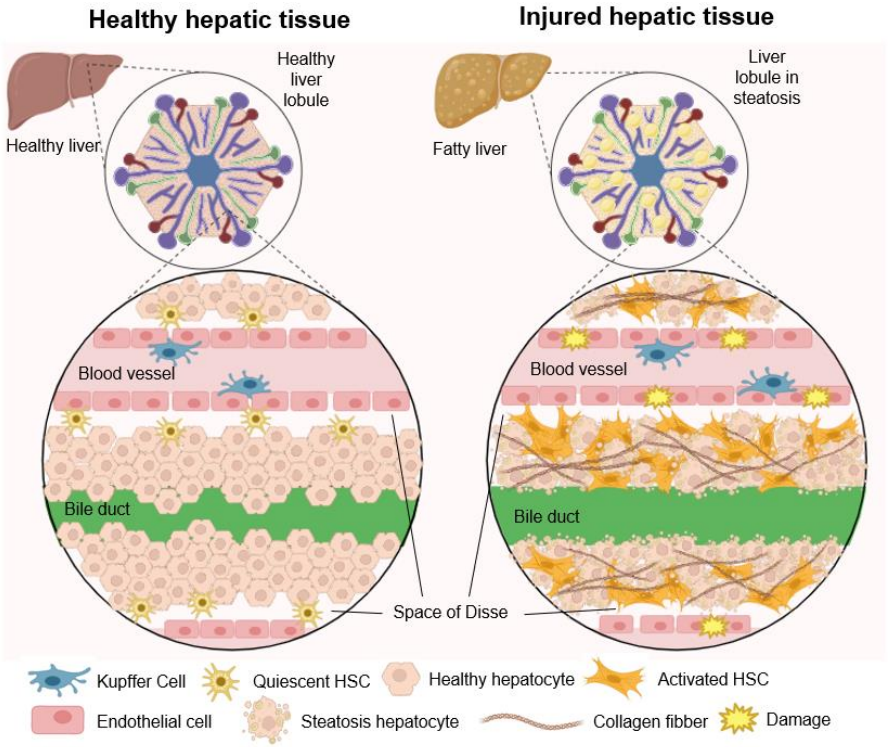

Figure 6. Schematic comparing the quiescent role of HSC in a healthy liver vs the HSC proliferative matrix-producing myofibroblast-like phenotype in injured liver.

Little is known about the mechanisms by which HSC accumulate lipids, nor the function that these lipids have. Retinoic acid (vitamin A) is accumulated in HSC's lipid droplets in the form of retinyl esters conjugated with either cholesterol or phospholipids. The HSC serve as a reservoir for retinoic acid that hepatocytes use as ligand for the activation of the transcription factors retinoic acid receptor (RAR) and retinoic X receptor (RXR) that control cellular differentiation, growth, and development (79). Retinoic acid is also used in the liver detoxification process, where it regulates the expression of detoxification enzymes, contributing to the organism's ability to eliminate toxins (80). HSC express peroxisome proliferator-activated receptor gamma (PPARγ)

and SREBP transcription factors which are involved in cholesterol and fatty acid storage metabolism. Constitutive activation of these regulators prevent HSC conversion into myofibroblasts (81), indicating that adipogenic-resemblant phenotypes for HSC might be beneficial to prevent liver diseases.

1.2 Atherosclerosis

The most common underlying cause for CVD is atherosclerosis (82), an almost asymptomatic condition. Atherosclerosis is the accumulation of lipids and fibrous elements inside the vessel walls of the arteries (83). Atherosclerosis develops as cholesterol, triglycerides, inflammatory cells and other substances slowly accumulate forming the atherosclerotic plaque. Progressive growth of the plaque produces a continuous narrowing of the vessel wall which leads to a reduced supply of oxygen and nutrients to the tissues downstream the blood vessel (84,85). Atherosclerosis pathophysiology is highly complex, with multiple biological processes modulating the progression of the disease (86).

1.2.1 Atherosclerosis initiation

The atherosclerotic process starts when the endothelial membrane from the inner part of the vascular wall is damaged (87). Blood vessels suffer different shear stress generated by circulating blood flow. Laminar unidirectional shear stress induces the expression of the transcription factor krüppel-like factor 2 (KLF2) in ECs, which activates genes to maintain the vascular barrier integrity and tissue-homeostasis by anti-inflammatory, anti-thrombotic and anti-atherogenic pathways (88,89). Regions with turbulent blood flow and low shear stress generate atherogenic haemodynamic signalling to ECs that activate the nuclear factor kappa-light-chain-enhancer of activated B cells (NFκB) transcription factor, which activates the transcription of hypoxia-inducible factor 1-alpha (HIF1α) (90). In turn, HIF1α activation induces the transcription of enzymes participating in glycolysis leading to local EC proliferation (91,92). These changes in the EC state lead to the release of inflammatory mediators, promoting a switch to a pro-inflammatory and pro-atherogenic phenotype (93–95).

The shear stress theory allows explaining why atherosclerosis develops in very specific regions of the cardiovascular system despite all ECs are subjected to the same biological conditions. Shear stress modulates the composition and thickness of the glycocalyx (96). The glycocalyx is the first regulator of the LDL trans endothelial passage. This extracellular layer consists of a thick negatively-charged matrix composed of glycoproteins, proteoglycans and hyaluronan (mainly membrane-bound components) which traps plasma- and endothelial-derived proteins (97). Inflammation increases the capacity of the glycocalyx to trap circulating LDLs which allows ECs to start the LDL-transcytosis process (98) (**Figure 7.1**).

Transcytosis is defined as the transport of LDL molecules from the lumen to the intima of the blood vessels (99). This process is performed mainly across the EC layer, but also between ECs (100). Transcytosis is performed by EC through several receptors that recognise circulating native LDL (nLDLs) and modified LDLs promoting their internalization via clathrin- and caveolin-endosomes (101–104). Exocytosis of LDL to the vessel intima occurs in a different process mediated by soluble NSF attachment protein (SNARE) receptors, which modulate the docking and fusion of vesicles with the cell membrane (99,105).

LDLs can also cross the endothelial barrier through junctions between the ECs (106). In normal conditions, tight-, adherent- and gap-junctions maintain the permeability of the endothelial layer blocking the crossing of macromolecules (107). However, in pathological conditions, junctions between ECs are weakened, generating structural changes in the endothelial layer and allowing LDLs to cross to the endothelial subintima (108–110).

Once in the arterial intima, LDL might suffer chemical enzymatic-driven modifications of its components including oxidation (111,112), acetylation (113,114), ethylation (115), methylation (115), glycation

(116) and others. These modifications modify lipids and aminoacids on the LDL surface, changing the affinity of LDLs for the cellular receptors that uptake nLDL in non-pathological conditions (117,118).

In the arterial intima, nLDL are modified by proteases, lipases and pro-oxidative agents, which are produced by ECs under stressful conditions (119,120). These modifications and the high concentration of modified LDL in the intima promote the formation of aggregated low-density lipoprotein (agLDL) (121,122), which can be a hundred times bigger than a circulating nLDLs (123).

1.2.2 Atherosclerosis progression

The inflammatory state of ECs leads to vascular wall dysfunction. ECs produce chemokines and inflammatory cytokines that activate and recruit inflammatory cells towards the injury site (124). Stressed ECs express adhesion molecules that allow leukocyte retention at the injury site and promote their transmigration across the EC layer (124–127). Macrophages play a major role during atherosclerosis while other leukocytes including dendritic cells, T lymphocytes and B lymphocytes also participate in enhancing atherosclerosis progression (128). When circulating monocytes are recruited to the vascular intima, a differentiation process is triggered to transform monocytes into tissue-resident macrophages (129).

At the same time, resident vascular smooth muscle cells (VSMCs) migrate from the outer arterial intima towards the lipid-accumulating zone (130). VSMC are not fully differentiated and can change their phenotype when stimulated with environmental factors such as growth factors, cell-cell or cell-matrix interactions, lipids, lipoproteins, and/or inflammatory mediators within the vessel wall intima (131). During the migratory process, VSMCs lose their low-proliferative contractile stable phenotype and dedifferentiate into high-rate proliferating cells, with

increased proteoglycan production and high lipid-engulfing capacity (132–134) (**Figure 7.2**).

Both macrophages and dedifferentiated VSMC express the receptors needed to endocytose both nLDL and modified LDL. These include the LDLR (135), the low-density lipoprotein receptor-related protein 1 (LRP1) (136), scavenger receptor A (SRA), CD36, and lectin-type oxidized LDL receptor 1 (LOX-1) (137–139). Hence, both cell types start to endocytose lipoproteins present in the arterial intima which activate the production of inflammatory cytokines/chemokines for continuous recruiting of VSMCs and macrophages. The persistent accumulation of lipids by macrophages and VSMC leads to the formation of foam cells, which are metabolically inactive as their function is to store lipids (140–142) (**Figure 7.3**).

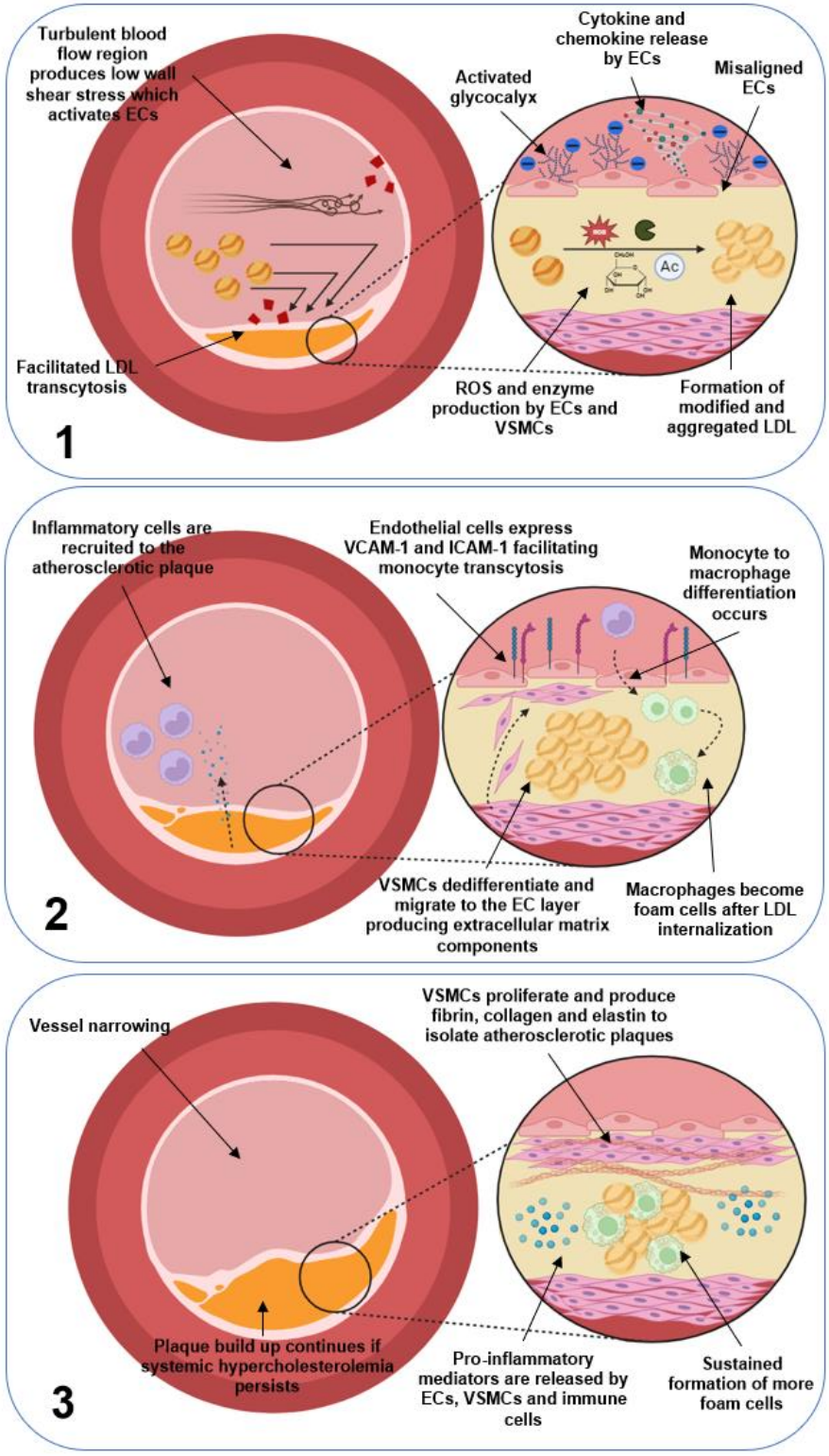
Turbulent blood flow region produces low wall shear stress which activates ECs
Cytokine and chemokine release by ECs
Misaligned ECs
Activated glycocalyx
Facilitated LDL transcytosis
ROS and enzyme production by ECs and VSMCs
Formation of modified and aggregated LDL
1
Inflammatory cells are recruited to the atherosclerotic plaque
Endothelial cells express VCAM-1 and ICAM-1 facilitating monocyte transcytosis
Monocyte to macrophage differentiation occurs
VSMCs dedifferentiate and migrate to the EC layer producing extracellular matrix components
Macrophages become foam cells after LDL internalization
2
Vessel narrowing
VSMCs proliferate and produce fibrin, collagen and elastin to isolate atherosclerotic plaques
Plaque build up continues if systemic hypercholesterolemia persists
Pro-inflammatory mediators are released by ECs, VSMCs and immune cells
Sustained formation of more foam cells
3

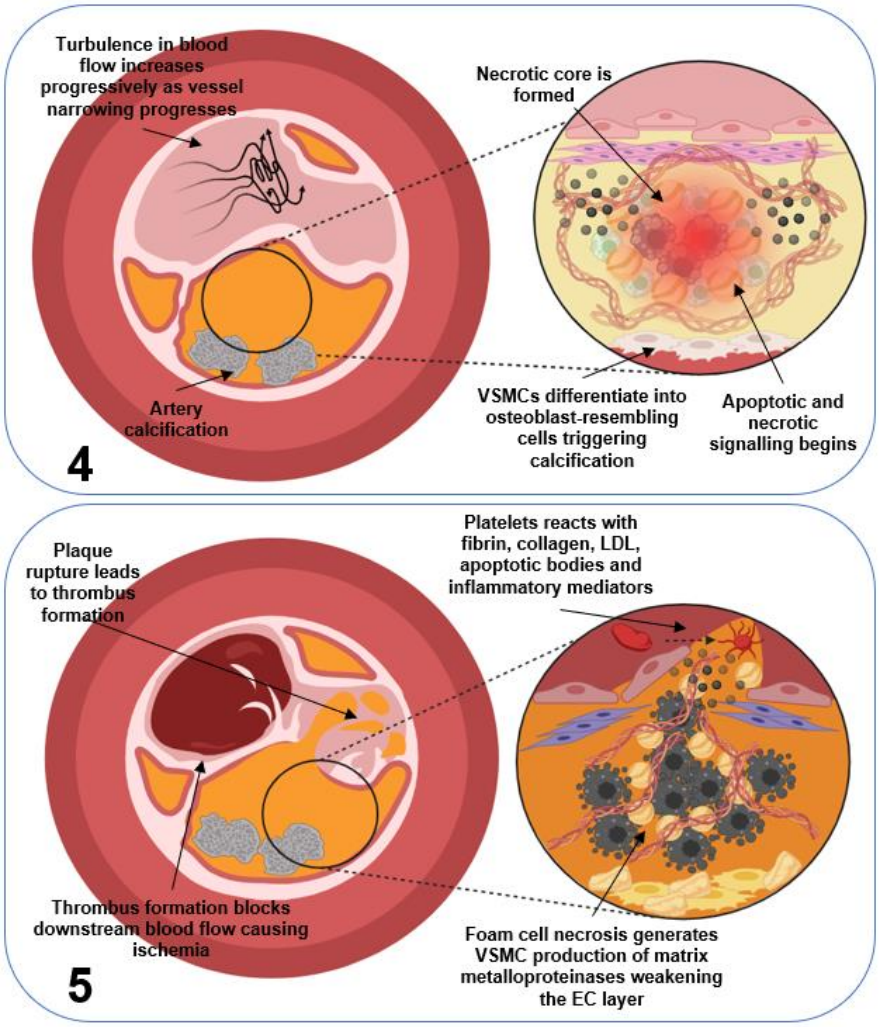

Figure 7. Cellular and tissue events during atherosclerosis progression.

1.2.3 Atherosclerosis final stage

As LDL accumulation persists in the arterial intima there is a sustained generation of foam cells, increasing the atherosclerotic lesion size, which progressively narrows the vessel reducing its nutrient-transporting capacity (84). Eventually, if the plaque core is big enough, nutrient supply does not reach cells in the lesion core and foam cells undergo a necrotic process (143). Necrosis occurs in plaques larger than 1 mm^2 and induces the initiation of the destabilization of the

atherosclerotic plaque (144). Almost 65% of plaque ruptures in humans have a necrotic area bigger than 25% of the atherosclerotic plaque (144). Cells undergoing necrosis lose cellular integrity and leak intracellular components into the media (145). Among these components, the release of damage-associated molecular patterns (DAMP) including high mobility group box 1 (HMGB1), receptor for advanced glycation end products (RAGE) or alarmins are recognised by toll-like receptors (TLR) or triggering receptor expressed on myeloid cells 1 (TREM-1) in macrophage's membrane triggering the production and release of pro-inflammatory cytokines and matrix metalloproteinases (MMPs) (146) (**Figure 7.4**). Vascular wall rupture due to necrosis causes the spilling of the plaque content into the blood, which generates thrombus that can trigger ischemic events (147,148) (**Figure 7.5**).

If LDL accumulation is blocked, foam cell formation is stopped and plaque is stabilized as VSMCs create a thick layer of collagen and elastin to protect vessel integrity and isolate the atherosclerotic plaque. In contrast, inflammatory cells produce collagen-degrading matrix metalloproteinases (MMPs) with plaque rupture potential. The balance between collagen production and degradation is key in plaque stabilisation/rupture fate (149). Slowly through time, HDL particles will remove the endocytosed cholesterol from foam cells (150,151). However, blood vessel narrowing prevails as tissue scar after atherosclerotic lesion stabilization. Tissue scar leads to reduced elasticity of the vasculature which can produce increased blood pressure (152). High blood pressure due to arterial stiffness is the most impactful risk factor to develop CVD, but can also damage other organs including kidney, brain or liver because high blood pressure leads to capillary breakdown (153,154).

1.2.4 Monocytes and macrophages involvement in atherosclerosis progression

Monocytes are continuously synthesized in the bone marrow from hematopoietic stem cells that enter the myeloid differentiation pathway (155). Myeloid precursors need further stimulus by growth factors and/or chemical signals to finally differentiate into neutrophiles, megakaryocytes, basophiles, eosinophiles, dendritic cells or monocytes (156).

Monocytes can be classified based on the expression levels of the surface markers CD14 and CD16. Human $CD14^{high}CD16^{low}$ monocytes are classical monocytes that migrate from blood to tissue and differentiate into macrophages. Upon differentiation, these macrophages can control infections by phagocytosis and trigger inflammatory and tissue-remodelling processes. The non-classical $CD14^{low}CD16^{high}$ monocytes, patrol the resting vasculature removing cellular debris and repairing the endothelium (157–159). In mice, this differentiation is based on the surface expression of Ly6C protein: $Ly6C^{high}$ monocytes are homologous to human $CD14^{high}CD16^{low}$ monocytes while $Ly6C^{low}$ monocytes are mirroring human $CD14^{low}CD16^{high}$. An important consideration is that human classical monocytes account for 85% of the monocyte population while only 15% are non-classical; instead, mice classical monocytes account for less than 40% of the total monocyte population while the remaining 60% are considered non-classical monocytes (160).

Macrophages are classified into M1 pro-inflammatory macrophages or M2 anti-inflammatory macrophages. There is ongoing controversy whether both populations are generated from the different monocyte populations or macrophages can shift from one phenotype to the other in response to microenvironmental signals (161–163). Several hypotheses attempt to explain this issue:

1. Macrophages derive from monocytes with a similar phenotype. According to this hypothesis, $CD14^{high}CD16^{low}$/$Ly6C^{+}$ monocytes would differentiate into M1 macrophages while $CD14^{low}CD16^{high}$/$Ly6C^{-}$ monocytes would differentiate into M2 macrophages. However, it has been reported that classical monocytes can differentiate into M2 macrophages, while non-classical monocytes can generate M1 macrophages (162).
2. Sequential waves of monocyte recruitment into the tissue lead to different macrophage phenotype fate. This hypothesis supports that the first waves of infiltrating monocytes are differentiated into M1 macrophages as a consequence of microenvironmental conditions triggered by pro-inflammatory cytokines like the granulocyte macrophage – colony stimulating factor (GM-CSF). In contrast, late waves of infiltrating monocytes find a different microenvironment enriched in other cytokines like colony stimulating factor 1 (CSF-1) that promote their differentiation into M2 macrophages specialised in tissue-repairing functions (162,164).
3. A third hypothesis stipulates that macrophages can switch from one phenotype to the other in response to the signals they receive independently of the original monocyte subtype. *In vitro* studies using human monocytes have proven that these acquire a M1 macrophage phenotype which further matures into M2 repairing macrophages if stimulated by different cytokines (165). Other studies have also proven a phenotype switch from M2 macrophages to M1 macrophages if cells are stimulated by TLR-ligands or IFN-γ (166,167).

Importantly, these results were obtained using only *in vitro* models, which do not fully resemble real case scenarios. Several features differentiate M1 from M2 macrophages, being the most relevant their

cytokine releasing profile. M1 macrophages release pro-inflammatory cytokines TNFα, IL-1β, IL-6, IL-8, type-1 interferons, and IFN-γ, while M2 macrophages release anti-inflammatory cytokines IL-10, TGF-β, and IL-1Ra (168). Also, M1 macrophages express high levels of iNOS which allows for NO production and ROS secretion with high potent killing activity against pathogens, while M2 macrophages fail to produce NO (169). Instead, M2 macrophages express the mannose receptor CD206, which allows them to bind and eliminate residual cellular debris and promote healing in the tissue (170) (**Table 3**).

	M1 macrophage	**M2 macrophage**
Cytokines inducing macrophage phenotype	GM-CSF, TNF, IFNα/β, IFNγ, TLR-ligands (LPS), IL-17a	CSF-1, IL-4, IL-10, IL-13, TGFβ, IL-21
Cytokines produced	TNFα, IL-1, IL-6, IL-12^{high}, Type 1 INF,CCL5, CXCL1-3, CXCL5, CXCL9-11	IL-10, IL-1Rα, TGFβ, CCL1, CCL17, CCL18, CCL22, CCL24, CXCL13, glucocorticoids
Activated transcription factors	STAT1, STAT5, NFκB, IRF3, IRF5	STAT6, STAT3, PPARγ, HIF-2α, KLF-4
Processes associated with the phenotype	Strong microbicidal and tumoricidal activity Promotion of Th1 response in T lymphocytes Tissue damage	Tissue remodelling Immune tolerance Tumor progression Parasite containment Promotion of Th2 response in T lymphocytes Secretion of growth factors (HGF, VEGF,etc) Angiogenesis
Main characteristics	High antigen presentation capacity High NO production High ROS production	High expression of scavenger receptors SR-A and SR-BI High ornithine and polyamine production High production of proteins that regulate matrix composition (MMPs/TIMP)
Surface markers	CD80, CD86, MHC-II, TLR2, TLR4	CD163, CD206, CD209, CD68, Ym1/2, Fizz1

Table 3. Main features differentiating M1 and M2 macrophage phenotypes.

During atherosclerosis progression, the inflammatory context in the vascular intima stimulates the production of GM-CSF, and the recruited monocytes proliferate and differentiate into M1 macrophages with enhanced capacity to accumulate cholesterol, become foam cells and further extent the inflammatory process (171). If the athero-inflammatory process is paused or reverted, macrophages can undergo a transdifferentiation process from M1 to M2 macrophages (172). M2

macrophages induce plaque stabilisation by expressing higher levels of ABCG1, promoting cholesterol-efflux towards HDL molecules, and producing anti-inflammatory proteins collagen, soluble IL-1R, and IL-10 (173,174).

Macrophages play a key role in the stabilisation of the fibrous cap and vascular wall thickness by modulating the degradation of collagen, fibrin, and elastin. M1 macrophages produce vast amounts of active MMP-1, -3, -10, -12, -14, and -25 in response to IL-1β, GM-CSF, and TNF-α, which cleave collagen and reduce the thickness of the vasculature, increasing plaque instability (175). However, M2 macrophages stimulated by IL-4 and IL-10 produce MMP-11 or MMP-12 while secreting tissue inhibitor of matrix metalloproteinase -1 and -3 (TIMP-1 and TIMP-3), inhibiting collagen degradation, and isolating the atherosclerotic lesion form general circulation (176,177). The balance between MMP and TIMP activity in the vascular wall is key to determine the fate of the atherosclerotic lesion (178). In conclusion, the M1/M2 macrophage ratio in the atherosclerotic lesion is an important factor that regulates atherosclerosis outcome. Hence, proteins regulating the phenotypic fate of macrophages are important to preserve lesion homeostasis and block atherosclerosis progression.

M(Hb) or Mox are other macrophage subtypes with anti-atherosclerotic properties in humans. M(Hb) macrophages engulf erythrocyte remnants and haemoglobin (179) activating the expression of the transcription factor liver X receptor alpha (LXRα), which promotes ABCA1 cholesterol-efflux regulating protein, reducing the possibilities for this macrophage subtype to become foam cells (180). Mox macrophages are induced by oxidized phospholipids and activate the nuclear factor erythroid 2 related factor 2 (Nfe2r2) transcription factor, which activates the secretion of antioxidant enzymes to the extracellular matrix including lipooxigenase-1, thioredoxin reductase-1, and sulfiredoxin-1 (181,182).

1.2.5 Microvesicles and their roles in atherosclerosis

Microvesicles (MVs) are extracellular vesicles composed of lipid bilayer-delimited particles released from cells. Extracellular vesicles include MVs, exosomes, apoptotic bodies, and exospheres (183). In the organism, MVs are found in the interstitial fluid between the cells and the systemic circulation. Their size oscillates between 30 to 100 nm in diameter. The role of MVs is to allow intercellular communication by transporting messenger RNA, microRNA (miRNA), proteins and/or lipids between cells in a selective process regulated by the expression of receptors at their membrane (184).

To generate MVs, an out-budding process in specific cell membrane locations enriched in lipids and proteins occurs. The cell, through different cellular pathways, selectively transports specific messenger RNAs, proteins, and other metabolites to the specialised cell-membrane regions. Tetraspanin proteins and the endosomal complex required for transport (ESCRT) complexes coordinate the formation of MV biogenesis, recruiting the MV-forming machinery to located regions of the cell membrane (185–187). The biogenesis of MVs is a highly complex process in which several proteins dictate which macromolecules need to be transported to the MV-generating cell membrane region (**Figure 8**).

Important mediators in this process are:

1. ADP-ribosylation factors 1 and 6 (ARF1 and ARF6): Ras GTPases that coordinate the selective recruitment of proteins into MVs, endosome trafficking, and membrane contractility, facilitating membrane fission and MV secretion (184,188). ARF6 activates phospholipase D, promoting the recruitment of extracellular signal-recruit kinase (ERK) to the out-budding membrane. ERK phosphorylates and activates the myosin light-

chain kinases that disrupts the union between actin chains from the MV and the cell, allowing the MV release (188).

2. Ras-related Protein Rab-22A (Rab22a): a GTPase which actively regulates the selection of MV cargo. The protein activity seems to be specially induced during hypoxic conditions (189).
3. Calcium signalling: an increase in cytoplasmic calcium concentration has been postulated as the initiating step in plasma membrane blebbing for MV generation (190,191).

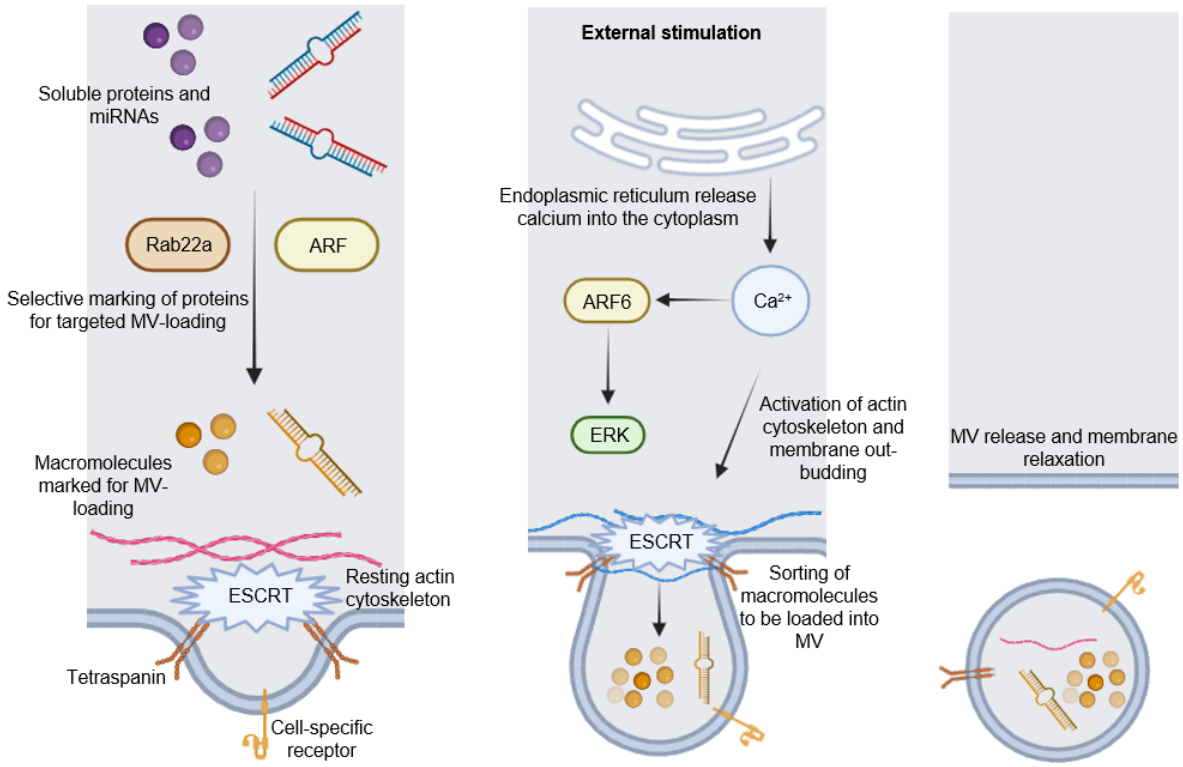

Figure 8. Microvesicles biosynthesis and the mediators involved in cargo sorting.

Many stimuli can trigger MV generation; however, it seems that each cell subtype reacts to a particular stimulus. Once released into the extracellular fluids, MVs interact with other cells by their surface receptors. The interaction and specific recognition between MVs and receptor cells produces the fusion of both membranes and the release

of MVs content (active metabolites and macromolecules) into the cytoplasm of the receptor cells (192).

The release of MVs is a paracrine and endocrine method of cell-cell communication (193). Protein receptors pattern expression at the MVs surface allows for the distinction of their cellular origin. Signalling through MVs is indispensable for the organism as it regulates multiple mechanisms including angiogenesis, immunity, cell-cell communication, transfer of proteins and miRNA, coagulation, inflammation, neuronal function, tissue-repair, and regeneration (194).

MVs play crucial roles in atherosclerosis and ischemic events (195). Human patients with increased circulating levels of platelet endothelial cell adhesion molecule 1 positive ($PECAM1^+$) and $AnnexinV^+$ MVs are more prone to die from major adverse cardiovascular events, revealing a potential role for MVs as CVD biomarker (196).

Macrophage-derived MVs trigger inflammation as their content includes cytokines, adhesion molecules, miRNAs, and receptor-specific ligands that modulate atherosclerosis progression (197–199). However, MVs produced by M2-macrophages contribute to maintaining the homeostasis in atherosclerosis and cardiac myocardium, stabilising the pathogenesis of the disease (200–202). In human atherosclerotic plaques, high Ca^{2+} concentration due to plaque calcification triggers macrophage release of MVs enriched in iNOS and IL-6 mRNAs, which enhance inflammation in receptor cells (203). Also, MVs produced by human plaque macrophages are enriched in CD40L and potentiate angiogenesis by stimulating EC proliferation both *in vitro* and in mice models (204).

Dysfunction of ECs caused by atherosclerosis increases leukocyte-derived extracellular vesicles in circulation (205). MVs produced by stressed ECs contain elevated levels of the proto-oncogene tyrosine-

protein kinase Src (Src) kinase; the recognition of Src-enriched MVs by receiving ECs reduced tight junctions and aggravates the EC barrier integrity (206). Also, EC-derived MVs display high concentrations of BMP-2 after incubation with TNFα. These BMP-2-enriched MVs act on VSMC triggering calcification, associated to atherosclerosis progression late-stages (207). Oxidized phospholipids also modify the cargo loaded into MVs by ECs increasing pro-inflammatory cytokine loading, and ICAM-1/VCAM-1 expression (208). Interestingly, KLF2-expressing ECs generated MVs enriched in miR-143 and miR-145, which reduce atherosclerotic lesions in *ApoE*$^{-/-}$ mice (209). However, incubation of ECs with oxLDL leads to MV enrichment in miR-155, which upon reception by macrophages induces its differentiation into M1 macrophages (210).

Finally, MVs secreted by activated platelets can also modulate macrophage pro-inflammatory phenotype. Thrombin-stimulated platelets, simulating thrombosis *in vitro*, produce MVs that trigger the oxLDL internalization by macrophages leading to foam cell formation and induce pro-inflammatory cytokine release by receptor macrophages (211).

The investigation on MVs ability to control key mechanisms regulating pathogenesis of diverse diseases is of high interest to create novel therapeutic approaches. In the recent years, the scientific community has postulated MVs as potential therapeutic vectors for their high biocompatibility, low immunogenic profile, and elevated malleability for delivery therapy. The objective is to modify MVs cytosol cargo in proteins and nucleic acids (but also synthetic components like nanoparticles) in order to transfer these bioactive molecules into receptor cells through highly-specific interactions modulated by MVs membrane receptors.

1.3 The WNT signalling pathway involvement in CVD

The WNT signalling pathways group three different pathways that are activated by WNT ligands: the canonical WNT pathway, the non-canonical WNT/Ca^{2+} pathway, and the non-canonical planar cell polarity (WNT/PCP) pathway (212). The determination of the signalling pathway being activated depends on the combination of WNT ligands that surround the cells and the expression of the receptors participating in the intracellular signal transduction (**Figure 9**).

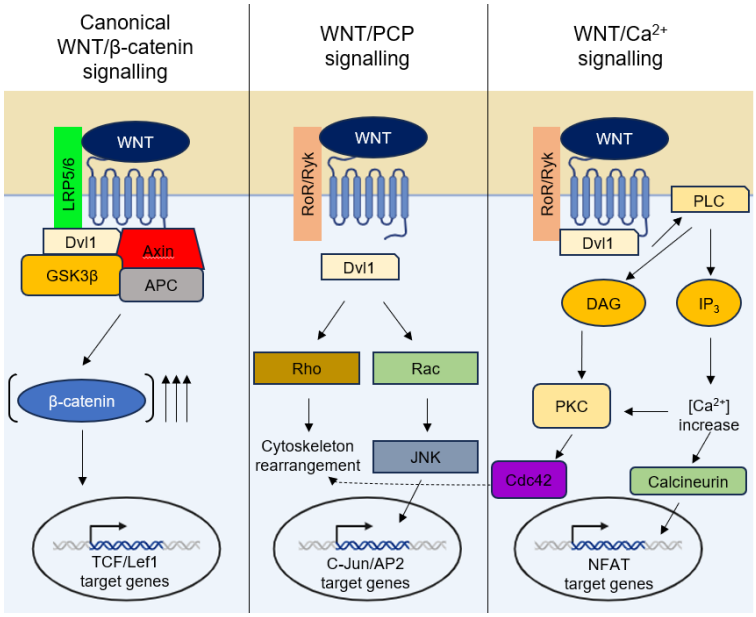

Figure 9. The three WNT ligand-dependent signalling pathways. Adapted from Ben-Ghedalia-Peled N. et al. *Cells*. 2022 Dec 5;11(23):3934.

The canonical WNT signalling pathway was first identified in *Drosophila*, where the signalling induced by *Wingless* (the WNT ligand *Drosophila* homologue) was found to be crucial for embryonic development as it controls body axis patterning, cell proliferation, migration and phenotypic fate (213,214). This thesis is focused on the regulation of the canonical WNT pathway.

The canonical WNT pathway triggers the expression of specific target genes regulated by β-catenin (215). In the absence of WNT ligand, frizzled (Fzd) and low-density lipoprotein receptor-related proteins 5 and 6 (LRP5 / LRP6) co-receptors remain inactive in the surface of the cell. In the cytoplasm, a multiproteic complex formed by Axin, adenomatous polyposis coli (APC), protein phosphatase 2a (PP2A), glycogen synthase kinase-3 beta (GSK3β), and casein kinase I isoform alpha (CK1α) continuously promotes the phosphorylation of β-catenin at specific aminoacids (216). These phosphorylations target β-catenin for ubiquitination and continuous proteasomal degradation. Upon WNT ligand's presence, Fzd and LRP5/6 create ternary complexes WNT ligand-Fzd-LRP5/6 (217). This activation leads to the phosphorylation of several serine and threonine residues in the LRP5/6 cytoplasmatic tail which recruit Axin towards the inner plasma membrane. This produces the disruption of the β-catenin destruction complex. As β-catenin is constitutively synthesized, the cytoplasmic levels rapidly increase allowing its translocation into the nucleus where it induces a cellular response via transcriptional activation of target genes by binding to T cell factor (TCF)/LEF1 transcription factors (218).

1.3.1 LRP5 and CVD

LRP5 is a member of the LDLR superfamily of receptors, which also include LDLR, very low-density lipoprotein receptor (VLDLR), LRP1, LRP2, LRP6, apolipoprotein E receptor 2 (apoER2) among others, most of them with cholesterol-regulating functions (219) (**Figure 10**). LRP5 was first discovered in *Drosophila,* as mutations in the fly homologous protein Arrow generated flies with similar phenotype as Wingless-null flies (220). LRP5 and LRP6 are both Arrow homologues in humans and mice (221).

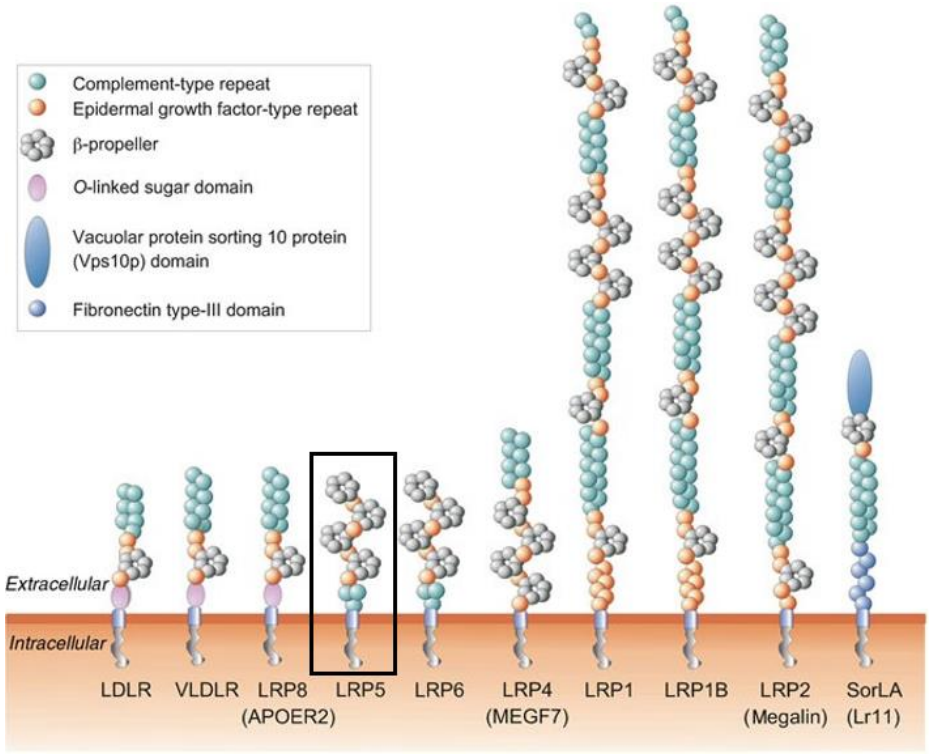

Figure 10. LDLR family of receptors showing the shared domains of the different members and their distribution. This figure is borrowed from the book section "Low-Density Lipoprotein Receptor Gene Family" by Thomas E. Willnow (222).

LRP5 is a single-pass transmembrane receptor ubiquitously expressed in cells and tissues of the organism. It is composed of 1615 aminoacids with a molecular weight of 179 kDa. The protein is divided in three regions: the extracellular domain (amino acids 32-1384), the transmembrane domain (amino acids 1385-1407), and the cytoplasmatic tail (amino acids 1408-1615). The extracellular domain is formed by 4 β-propeller domains 260 amino acids long separated by 4 EGF-A like domains about 40 amino acids long each (217,223). The intracellular domain contains five PPPSP motifs, that get phosphorylated upon ligand binding and trigger signal transduction (**Figure 11**).

Gain-of-function mutations in LRP5 produce increased bone density in humans and mice (224,225). Contrarily, LRP5 loss-of-function

mutations cause osteoporosis-pseudoglioma syndrome (226), a rare autosomal recessive disorder in which patients suffer impaired bone accrual (osteoporosis) and defective regression of the foetal ocular fibrovascular system (pseudoglioma) (227). Mutations in LRP5 can also cause familial exudative vitreoretinopathy or polycystic liver disease (226,228).

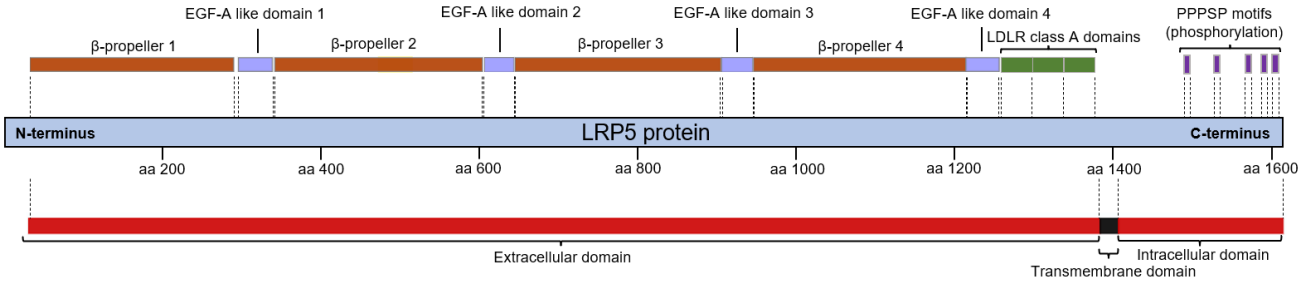

Figure 11. Linear representation of LRP5's amino acid sequence showing the distribution of the different domains.

In a cardiovascular context, LRP5-deficient mice (*Lrp5*$^{-/-}$ mice) show increased plasma cholesterol levels induced by reduced clearance of CMr by the liver after high-fat diet feeding generated by LRP5 ability to bind ApoE (229,230). In the same study, *Lrp5*$^{-/-}$ mice also showed reduced glucose sensitivity in pancreatic β-islets which, in turn, reduce insulin secretion (229). Furthermore, *Lrp5*$^{-/-}$ mice fed with a hypercholesterolemic diet develop larger atherosclerotic lesions revealing a protective role for LRP5 in atherosclerosis progression (231). *Lrp5*$^{-/-}$ mice with downregulated canonical WNT signalling have greater lipid infiltration in their aortas because of higher macrophage infiltrate in the aortic intima (232).

LRP5 also activates the canonical WNT pathway in isolated cardiomyocytes. Hypoxia and lipid-loading induce the expression of canonical WNT signalling proteins whereas this effect is blocked after LRP5 silencing in cardiomyocytes (233). An upregulation of LRP5 and proteins of the canonical WNT pathway was also observed in the

ischemic myocardium of hypercholesterolemic pigs and in human hearts of dyslipidemic patients with a previous episode of ischaemia (233). Finally, a protective role of LRP5 in the injured myocardium was also demonstrated as *Lrp5*$^{-/-}$ mice have larger infarcts than *Wt* mice (233).

The role of LRP5 in inflammation has also been studied. LRP5 is necessary for monocyte-to-macrophage differentiation, a process that involves the activation of the canonical WNT signalling pathway (234). Furthermore, upon macrophage lipid-loading, the canonical WNT signalling pathway is activated whereas the pathway remains inactive when macrophages' LRP5 expression is blocked (235). LRP5-expressing macrophages develop a protective anti-inflammatory phenotype *in vivo* with enhanced motility and phagocytic capacities (236).

In summary, LRP5 has protective roles in CVD development as it is expressed in M2 macrophages (with an anti-inflammatory and tissue-homeostatic function), it reduces the atherosclerosis progression, and it induces pro-survival signalling after myocardial infarction.

1.4 PCSK9 and CVD

The proprotein convertase subtilisin/kexin type 9 protein (PCSK9) was discovered in 2003 as a member of the mammalian proprotein convertases family, a group of proteins responsible for tissue-specific processing of secretory precursors (237). The hypothesis that another system to regulate cholesterol levels existed, besides that mediated by LDLR and apoB100, was raised after a study on two large French families. This study showed that heterozygous familial hypercholesterolemia (HeFH) patients had symptoms unrelated to mutations on LDLR and apoB100 genes, and pointed to variations in the p34.2-p32 region in human chromosome 1 (238). The exploration of the genetic region in detail determined the PCSK9 gene as a direct cause of HeFH (239–241).

PCSK9 modulates LDL clearance from the liver by downregulating LDLR on the hepatocyte's membrane. LDL particles are bound and internalized by LDLR via clathrin-mediated endocytosis. In cytoplasmic early-endosomes, the interaction between LDLR and LDL particles weakens; LDLR is sorted into recycling endosomes and recycled back to the cell surface while LDLs are guided towards late endosomes and degraded by lysosomes (242–245).

During hypercholesterolemia, PCSK9 is released into the circulation by the liver. Rapidly after, LDLR levels in the surface of hepatocytes drastically diminish, reducing the LDL clearing capacity from blood by the liver (246,247). PCSK9 has high affinity for LDLR binding by specific recognition of the receptor's EGF-A-like domains. When LDLRs bind LDLs, a ternary complex LDL-LDLR-PCSK9 is formed and internalized. After LDL-LDLR dissociation in early endosomes, PCSK9 prevents LDLR recycling to the cell membrane. This blocking guides LDLR towards the lysosome where it is degraded by the activity of acidic pH, proteases and lipases.

PCSK9 isoforms with gain-of-function mutations reduce the liver's ability to clear LDL-cholesterol from the blood, inducing hypercholesterolemia in patients (248). Patients carrying a PCSK9 loss-of-function mutation show a 40% decrease in LDL circulating levels (249). Statins are drugs used in clinical settings to treat hypercholesterolemia. Mechanistically, statins block the rate-limiting reaction for cholesterol biosynthesis, lowering the hepatocyte's intracellular cholesterol concentration and triggering the expression of SREBP-targeted genes, which include the LDLR (21,22,250). Surprisingly, statins induce PCSK9 expression because of the SREBP binding site in the promoter region of PCSK9 gene. However, as a consequence of statin treatment, SREBP activation also activates PCSK9 expression and release conferring statin-resistance specially to patients carrying PCSK9 gain-of-function mutations (251).

New therapies for statin-resistant hypercholesterolemic patients have been developed against PCSK9 with very positive outcomes in clinical trials. The most used approach to target PCSK9 activity is based on monoclonal antibodies (evolocumab and alirocumab) that target PCSK9 and neutralize its activity. Both antibodies produce ~60% reduction in circulating LDL cholesterol in patients under maximum tolerated statin dosage (252,253). Additionally, in long-term follow-up studies, alirocumab and evolocumab reduce major CVD events incidence by 15% (254,255). Other therapeutic approaches to target PCSK9 that have been launched to date are described in **Table 4**.

 Inclisiran	Inclisiran is a small-interfering RNA that selectively binds PCSK9 mRNA and suppresses the translation of the protein in the liver. Inclisiran therapy reduced non-HDL cholesterol and circulating apoB levels in patients with elevated LDL-cholesterol (256). Long-term studies proved that inclisiran reduces circulating LDL-cholesterol levels by 44%, with a reduction in PCSK9 levels ranging from 62-77% (257).
Adnectin-based recombinant protein  PCSK9-binding domain	Adnectins are proteins derived from human fibronectin with modifiable regions to selectively bind different targets. PCSK9-binding adnectin administration to mice led to a drastic reduction in circulating PCSK9 levels followed by a reduction in blood cholesterol levels (258). In a phase I clinical trial in humans, single-dose administration of PCSK9-binding adnectin reduced LDL-cholesterol by 48% between days 4 and 14 post-dose (259). However, this approach is no longer under investigation because better strategies have been developed.
Lerodalcibep 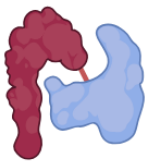	Lerodalcibep (LIB003) is a PCSK9-binding adnectin conjugated to human serum albumin. It has been tested in phase II and III clinical studies in patients with HeFH, reducing LDL-cholesterol levels by more than 50% with single monthly injections without producing considerable adverse events (260,261).

Antisense miRNA 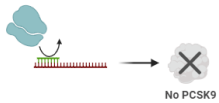	Orally administered antisense oligonucleotide against PCSK9 mRNA (AZD8233) have also shown promising results in early studies in mice, monkeys and humans. A single subcutaneous injection of the compound led to a 90% reduction of circulating PCSK9 in hypercholesterolemic patients for a month and to a 68% reduction in circulating LDL levels (262).
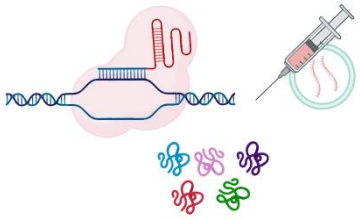	Other PCSK9-based therapy strategies are under investigation, including gene-editing using CRISPR (263), vaccines (264) and peptide-based small inhibitors (265).

Table 4. New generation therapies targeting PCSK9 activity.

Anti-PCSK9 based therapies induce a reduction in LDL-circulating levels by more than 50% in HeFH patients. More importantly, the use of anti-PCSK9 approaches diminishes the number of major cardiovascular events in 5 year of follow-up studies in HeFH patients and in hypercholesterolemic patients due to high-fat diets, sedentary life, and obesity (266,267). All these results indicate that PCSK9 is a major regulator in cholesterol levels regulation and atherosclerosis progression.

1.4.1 PCSK9 involvement in other processes

PCSK9 is an important player in other processes besides its LDL lowering capacity:

- Regulation of the lipid receptor expression:

During atherosclerosis progression, PCSK9 regulates cholesterol uptake of infiltrating macrophages by upregulating the expression of scavenger receptors and the LDLR-superfamily of receptors members (268).

- Pro-inflammatory mediator:

PCSK9 is produced in hypercholesterolemic rabbit aortas as a consequence of the activation of the TLR4-MyD88-NFκB pro-inflammatory pathway in ECs (269). Also, PCSK9-stimulated macrophages enhance the transcription of the pro-inflammatory cytokines tumour necrosis factor alpha (TNFα) and IL-1β while suppressing the expression of the anti-inflammatory markers IL-10 and arginase-1 (270).

PCSK9 inhibition leads to decreased expression of vascular adhesion molecules intercellular adhesion molecule-1 (ICAM-1) and vascular cell adhesion molecule 1 (VCAM-1) in the endothelium of atherosclerotic mice (271,272). Also, PCSK9 loss of expression produces a downregulation of inflammatory cell chemoattractant proteins monocyte chemoattractant protein-1 (MCP-1), macrophage inflammatory protein 1 beta (MIP-1β), macrophage-derived chemokine (MDC), skp-cullin-F-box-containing complex (SCF), and vascular endothelial growth factor A (VEGF-A) in the endothelium reducing the inflammatory infiltrate in the atherosclerotic lesions (272).

Antigen presentation is modulated by PCSK9 in cultured ox-LDL treated dendritic cells (273) inducing upregulation of pro-inflammatory CD80, CD83, CD86, human leukocyte antigen – DR isotype (HLA-DR), TNFα, IL-1β, and IL-6 in dendritic cells, which enhances T cell activation and differentiation towards Th1 or Th17 CD4+ T lymphocyte (273,274). Silencing of PCSK9 reverts ox-LDL effects on dendritic cells, limiting their maturation process, guiding T cells to differentiate into anti-inflammatory IL-10, and transforming growth factor beta (TGF-β) secreting T regulatory cells (273).

- Thrombus formation

Platelet aggregation and thrombus formation is also enhanced by PCSK9. Human platelets from healthy donors incubated with PCSK9 increase the platelet marker GPIIb/IIIa expression, which reduces the platelet's steady-state and facilitates their activation upon epinephrine or $FeCl_3$ stimulation (275). Also, PCSK9 facilitates NETosis as inferior vena cava ligation in *Pcsk9*$^{-/-}$ mice show reduced neutrophil extracellular trap (NET) formation than in *Wt* mice (276). Furthermore, PCSK9 increases the number of circulating platelets in patients with stable coronary artery disease (277) and promotes LDL oxidation by increasing platelet surface levels of LOX-1 and CD36 in hypercholesterolemic mice (278,279).

Detailed information on PCSK9 activities beyond the regulation of LDL cholesterol circulating levels is provided in our Review Manuscript published in *Frontiers in Cardiovascular Medicine* in 2021 (Annex 1).

1.5 Cholesterol homeostasis in the CNS

The central nervous system (CNS) is composed by the brain, the cerebellum, and the spinal cord. It is responsible for the processing, integration, and coordination of the information received from the organs; and the creation of physiological responses in the form of hormone secretion or muscle motor movement (280).

The CNS is composed of two different cell types:

- Neurons: cells that create electrical signals to transduce responses. Neuron stimulation consists in the creation of action potentials in their cell membranes, transmitted from their dendrites (receptor regions) towards their axons (emitting regions). Neurons can integrate the signals received from multiple sources and create a single output signal in the form of specific neurotransmitters released in synapses (the neuron-to-neuron communication regions), where the receptor neuron will be stimulated accordingly depending on the amount and type of neurotransmitter (281).
- Glial cells: their most important function is to preserve nervous tissue homeostasis and provide support, protection, and nutrients for neurons to maintain the CNS activity. Different cells are included in this group (282):
    - Astrocytes: produce extracellular matrix proteins that provide proper conditions for neuronal communication. Also, they provide nutrients for neurons, and can modulate neuronal stimulation by producing specific ligands.
    - Microglia: patrolling cells with phagocytic capacity that provide immune surveillance to the tissue.
    - Oligodendrocytes: cells that produce myelin, a fatty substance that forms sheaths around neuronal axons, providing insulation and facilitating the transport of the electrical signal along the neuronal body.

The CNS is isolated from the systemic circulation by the blood-brain barrier (BBB) (283). The BBB is a highly specialized endothelium in which tight-junctions are enriched in claudins and occludins that block any kind of paracellular transport (284). The limited transport through the intercellular space is counterbalanced by enhanced intracellular transcytosis. Transcytosis occurs in two directions, from blood to brain interstitial fluid and vice versa. ECs of the BBB express glucose, protein, and lipid transporters in their apical and basolateral membranes to transport substances across the BBB (285,286). The capillaries of the CNS are surrounded by pericytes that regulate the permeability and the receptor-mediated transport across the ECs (287). To avoid direct interaction of nutrients with neurons, astrocytes rapidly endocytose nutrients upon entrance into the CSF. They will then release nutrients in a highly-complex communication mechanism to cover the demand for specific metabolites needed for neuronal functions (288).

The brain accounts for only 2% of the total weight of the body, although it concentrates 20% of the organism's cholesterol (289) because oligodendrocyte's myelin sheaths are enriched in cholesterol, accounting for more than 80% of the brain's total cholesterol (290). However, neurons need cholesterol to maintain their cellular structure and to allow synapse. Although cholesterol can be synthesized by neurons, it is mainly synthesized and delivered by astrocytes in the adult brain (291). Of note, more than 95% of the cholesterol pool in the brain is synthesized *in situ* by astrocytes (292).

Neurons rely on cholesterol to generate structures to sustain neuron-to-neuron communication as cholesterol represents 40% of the lipids that constitute synaptic vesicles (293). Cholesterol facilitates vesicle fusion, formation of lipid rafts, and generation of ion currents, amongst other processes (294,295). Therefore, neurons need astrocytes to provide a constant supply of cholesterol in the adult brain.

In the cerebrospinal fluid (CSF), astrocytes release apoE-containing lipoproteins similar in size to HDL (296), which supply neuronal cholesterol demands. Cholesterol surplus is converted to 24S-hydroxycholesterol by the neuronal enzyme cholesterol 24-hydroxylase (CYP46A1), which can be eliminated from the CSF easily because of its increased solubility in water (297). 24S-hydroxycholesterol serves as a potent activator of astrocyte's LXR transcription factor, which regulates the expression of apoE, ABCA1, and ABCG1, responsible for the generation of brain-specific HDL-like lipoproteins, generating a feedback loop ensuring continuous cholesterol delivery by astrocytes to neurons (298). The recognition, binding, and endocytosis of HDL-like lipoproteins by neurons is performed by LDLR and LRP1; however, the involvement of other members of the LDLR superfamily is plausible as they are also expressed in neurons (299) (**Figure 12**).

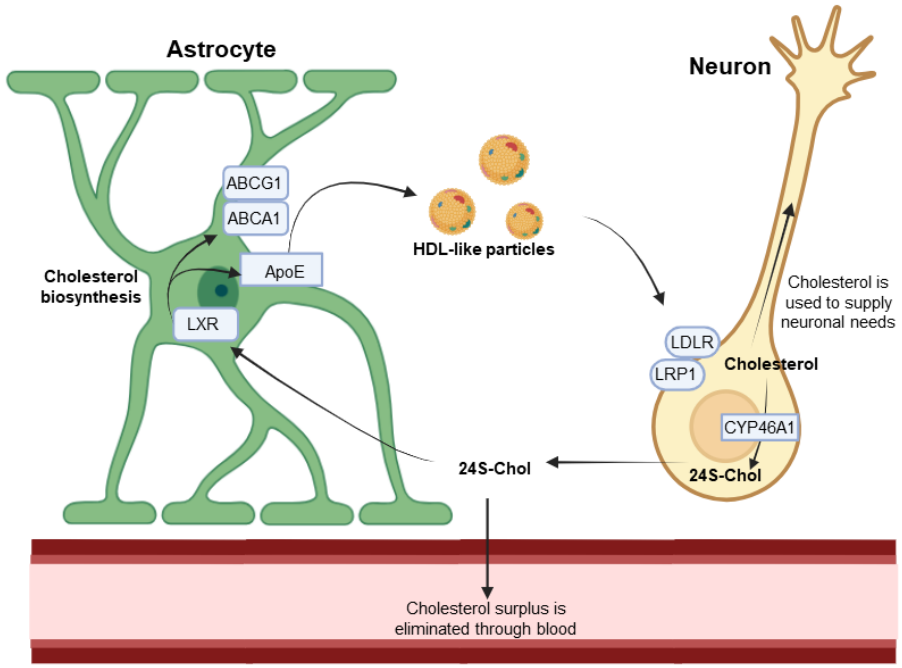

Figure 12. Cholesterol circulation in the CNS.

1.5.1 Cholesterol transport across the BBB

Although cholesterol *de novo* synthesis by astrocytes is the main source of cholesterol in the brain, there is an influx of cholesterol/oxysterols from systemic circulation to the CNS highly regulated by the BBB. Small soluble lipids can cross the BBB without much impediments, however lipoproteins and hydrophobic lipids need protein transporters to undergo transcytosis across BBB-ECs (300). Brain cholesterol metabolism in the CNS is strict and efficient. Because the half-life of a cholesterol pool in the adult brain is around 5 years, the BBB has an inefficient and not-specialised cholesterol transcytosis mechanism (301).

In normal conditions, lipoprotein transport in the BBB is inexistent. Systemic hypercholesterolemia damages brain ECs and disrupts BBB integrity, which induces a loss in CNS homeostasis affecting different brain functions. Several studies performed in mice have proven that alterations in the BBB permeability affect brain function (302,303).

1.5.2 Disrupted cholesterol homeostasis and brain diseases

In normal conditions, circulating LDL-cholesterol cannot interact with neurons. However, there is a significant correlation between systemic LDL-cholesterol levels, neurofibrillary tangles, β-amyloid protein and cerebral angiopathy (304,305). Also, systemic low LDL-cholesterol levels are associated with Parkinson's disease (306,307). Multiple *in vivo* studies have investigated the role of cholesterol in brain diseases.

- Rats fed a hypercholesterolemic diet significantly increased both systemic and cerebral cholesterol, triglyceride and LDL-cholesterol levels, which produced morphological changes in neurons, imbalanced neurotransmitter release and increased LDLR expression (308).
- High systemic LDL-cholesterol levels were associated with depression-like symptoms and psychomotor impairment, and

reduced dopamine and serotonin synthesis in the CNS of hypercholesterolemic mice (309).

- *Ldlr*$^{-/-}$ mice fed a high-fat diet exhibited memory loss in working, spatial and procedural domains (310).
- High fat diet induced the disruption of the BBB integrity by reducing the expression of the tight-junction proteins occluding-1 and claudin-5, increasing membrane permeability in wildtype and *Ldlr*$^{-/-}$ mice (302).
- High systemic LDL-cholesterol levels in *Ldlr*$^{-/-}$ mice have been associated with spatial memory defects, wider synaptic clefts, reduced synaptic markers in the hippocampus and neuron apoptosis and oedema (311).

In humans, patients with HeFH have a higher incidence of cognitive dysfunction, caused either by LDLR deficits or systemic high LDL levels (312). A study on healthy elderly population showed that those individuals with higher circulating levels of triglycerides and LDL are more susceptible to developing global cognitive decline in the future (313).

1.5.3 Canonical WNT signalling in the CNS

The canonical WNT signalling is involved in the differentiation and maturation process of progenitor cells during embryogenesis, guiding cell fate. In the brain, canonical WNT signalling regulates spatial patterning of the brain and neurogenesis (314). The signalling pathway is involved in the preservation of neurogenesis in the adult brain and in the maturation process of neuronal progenitors (315–317). Moreover, β-catenin activation in neuronal progenitor cells guides the transcription of the mitotic regulator survivin and neuron-specific neurogenic differentiation 1 (NeuroD1) and prospero homeobox protein 1 (Prox1) transcription factors, essential for the correct formation of hippocampal

neuronal cells (318,319). β-catenin is also involved in the formation of neuronal dendrites (320).

However, WNT signalling findings in the brain support a greater impact for β-catenin independent mechanisms. WNT ligands regulate synapse formation by controlling pre- and post-synaptic mechanisms in cellular regions that are distant from the nucleus, where β-catenin exerts its transcriptional function. Mice deficient for WNT7a or Dvl1 (a scaffold protein needed for WNT signal transduction) expression have defects in the pre-synaptic region of the cerebellar mossy-fibbers synapse (321). Likewise, WNT7a signalling through Fzd5 in the hippocampal region is necessary for the formation of pre-synaptic sites (322). WNT5a acts through receptor tyrosine kinase-like orphan receptor (RoR) receptors to increase pre-synaptic sites in the hippocampus (323), while WNT3a binds to Fzd1 to regulate protein clustering in pre-synaptic sites and neurotransmitter vesicle recycling (324). Also, the WNT7a-Dvl1 signalling promotes the formation of excitatory synapses and spine growth through calcium signalling, WNT7a-Dvl1 knockout mice display amplitude and frequency deficits in postsynaptic currents (325). In contrast to WNT7a, WNT5a promotes the formation of inhibitory synapses by increasing clustering of $GABA_R$ receptors and enhancing the inhibitory currents' amplitude (326).

Besides regulating pre- and post-synaptic formation, WNT ligands also modulate synaptic plasticity. Synaptic plasticity is defined as the dynamic changes in the structure of synapses in response to the environment and is considered the cellular basis of learning and memory, both processes associated with the hypothalamic region (327). Several studies have demonstrated that neuronal activity induces neuronal and astrocytic release of WNT ligands (328–330). Neuronal stimulation, both *in vitro* and *in vivo*, leads to WNT7a/b release and Fzd5 expression in dendrites (322). Synaptic plasticity is measured by the

long-term potentiation (LTP) parameter, which quantifies long-lasting increase in synapse strength (331). Blockade of WNT expression impairs the activity-mediated synapse formation (322). Moreover, inhibition of WNT7a/b by overexpression of soluble frizzled receptors severely impairs LTP while addition of WNT proteins significantly upregulates LTP, a mechanism in which the increase of AMPAR receptors localized in the post-synaptic dendrite is important (332). Similarly, WNT5a has also been involved in synaptic plasticity by promoting NMDA-receptor currents, adjusting the threshold of synaptic potentiation (333). Contrarily, mice with inducible expression of Dickkopf-related protein 1 (Dkk1), a WNT signalling inhibitor, show loss of excitatory synapses in the hippocampus, defects in LTP, and impaired long-term memory (334) (**Figure 13**).

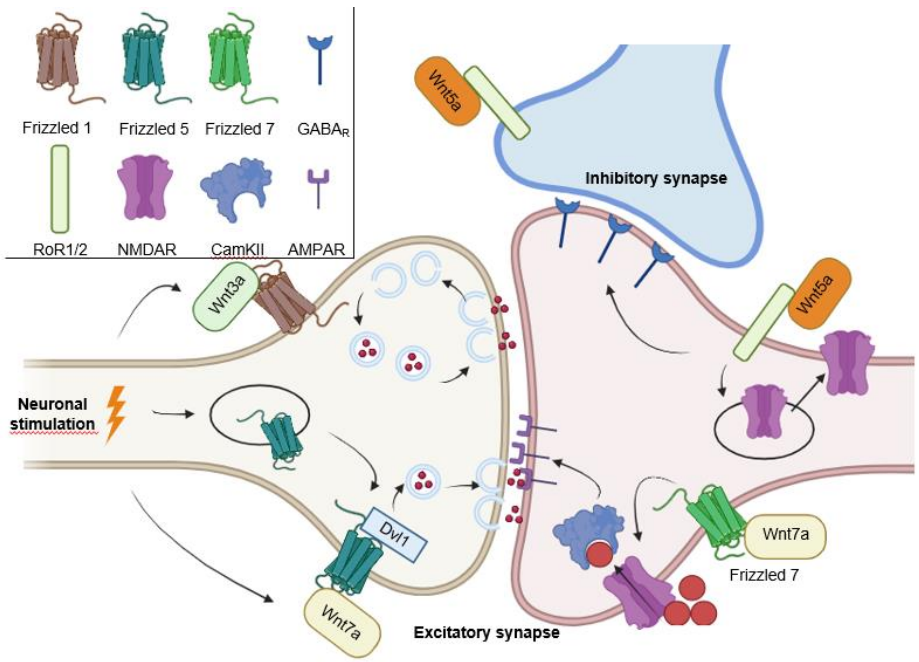

Figure 13. WNT ligands and Frizzled receptors regulate synapse formation and plasticity.

The role of LRP5 in the brain still remains to be elucidated. LRP5 expression pattern in the CNS is region- and cell-selective. There is high LRP5 expression in the cerebral cortex, the hippocampus, and the hypothalamus. Moreover, neurons constitutively express LRP5 (335). A hypothetical role for LRP5 in the brain can be inferred from the findings on Dkk1 protein. This protein selectively binds to LRP5 and LRP6 coreceptors preventing the binding of WNT ligands, inhibiting the canonical WNT signalling but enhancing other WNT-related pathways like the WNT/PCP or the WNT/Ca^{2+} (triggered by RoR and related to receptor tyrosine kinase (Ryk) coreceptors) (336). Loss of Dkk1 expression in mice shows impaired development of neural structures (337). Double knockout mice for LRP5 and LRP6 results in defective cerebellar foliation and lamination during postnatal development (338). Also, *in vivo* experiments show LRP5 expression to be protective in front of oxidative stress in a neuronal cell line (339). Additionally, variations in the LRP5 gene loci in human chromosome 11 have been associated with major depressive disorder, bipolar disorder, and schizophrenia in a meta-analysis including several genome-wide association studies (GWAS) (340). Also, allelic variants in LRP5 gene have been linked to attention-deficit/hyperactivity disorder only in females (341). Taken together, these results show that LRP5 contributes to brain maturation and development, and that defects on LRP5 signalling can be associated with brain dysfunction.

Dysregulation of the canonical WNT signalling has been involved in different CNS diseases. Nevertheless, its importance in Alzheimer's disease needs to be emphasized as β-catenin inactivity correlates directly with Alzheimer's progression. Canonical WNT signalling regulates the two main molecular alterations observed in Alzheimer's disease (**Figure 14**):

- The production of amyloid beta (Aβ) plaques. β-catenin activation leads to its binding with the transcription factor Tcf4, repressing the beta-site amyloid precursor protein cleaving enzyme 1 (BACE1) transcription, the protease responsible for Aβ-precursor protein (APP) cleavage and activation (342), leading to reduced Aβ deposition and aggregation (343). Defects in members of the canonical WNT signalling lead to accelerated Aβ formation and aggregation in different experimental models (344,345).
- The phosphorylation of tubulin associated unit (Tau). Besides inducing the phosphorylation of β-catenin for proteasomal degradation, GSK3β can also phosphorylate Tau in targeted residues associated with Alzheimer's disease (346). Tau phosphorylation leads to synaptic impairment and neuronal degeneration as it is responsible for the stabilization of microtubules in dendrites and axons (347). While canonical WNT pathway activators like Wiskott-Aldrich syndrome protein 1 (WASp1) reduce Tau phosphorylation (348), infusion of Dkk1 in rats leads to Tau phosphorylation and neuronal death in the hippocampus (349).

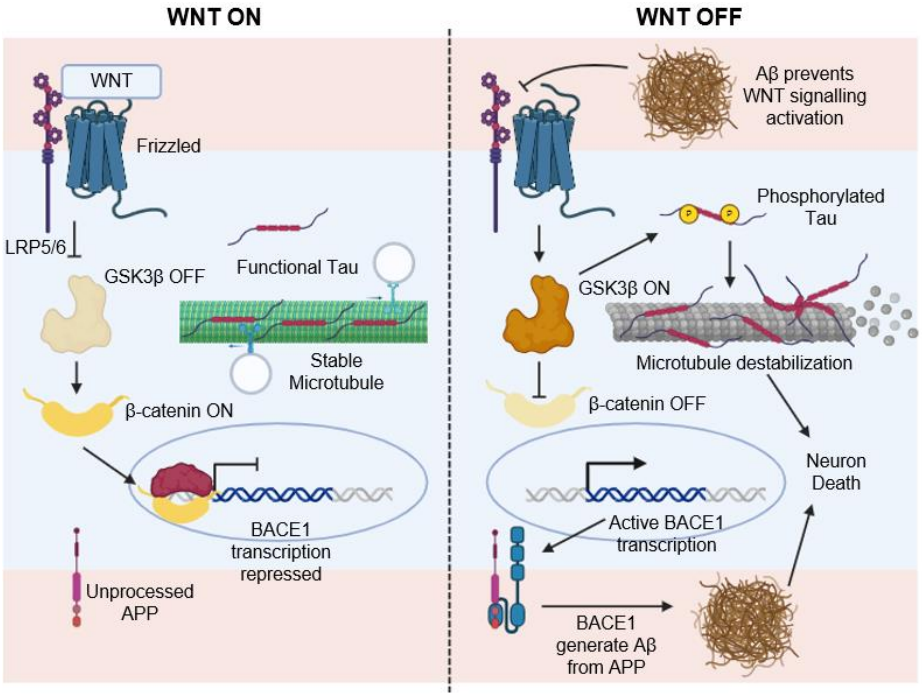

Figure 14. Canonical WNT signalling roles in the prevention of Alzheimer's Disease progression.

2. Hypothesis and Objectives

"I have found it is the small things, everyday deeds of ordinary folk, that keeps the darkness at bay. Simple acts of kindness and love."

Gandalf to Galadriel, from the film adaptation "The hobbit: an unexpected journey" from Peter Jackson. Based on *The Hobbit* by J.R.R. Tolkien.

LRP5 is a receptor of the canonical WNT signalling pathway, involved in many fundamental processes including organ and tissue development. LRP5 plays a key role in lipid metabolism and inflammation. Furthermore, LRP5 seems to play an important role in the brain.

It is our hypothesis that WNT, LRP5 and its cofactors have an important role in atherosclerosis progression, adipose tissue growth and brain cholesterol metabolism by mechanisms yet unknown.

The specific objectives designed to prove our hypothesis are:

Objective 1. To study if PCSK9 can interact with members of the LRP family of receptors to modulate cholesterol internalization.

Objective 2. To study the role of LRP5 in liver cholesterol metabolism.

Objective 3. To study the role of LRP5 in the expansion and distribution of the adipose tissue.

Objective 4. To study the role of LRP5 in inflammation, innate immunity cells and atherosclerotic plaques.

Objective 5 To study LRP5 in brain cholesterol homeostasis.

Objective 6. To study LRP5 transcriptomics in wildtype and Lrp5 knockout mice.

3. Results

“The world is not in your books and maps, it's out there.”

Gandalf to Bilbo, from the film adaptation “The Hobbit: An Unexpected Journey” by Peter Jackson. Based on the books by J.R.R. Tolkien.

3.1 Directors Report

SANT PAU
Campus Salut
Barcelona

Institut
de Recerca
Sant Pau

Directors Report

Dr Maria Borrell Pages and Prof. Lina Badimon Maestro, as directors of the doctoral thesis entitled "WNT pathway regulation of lipid handling and inflammation in organ function: the role of LRP5" of candidate Aureli Luquero Gomez, state the following:

The thesis entitled "WNT pathway regulation of lipid handling and inflammation in organ function: the role of LRP5" encompasses five original manuscripts, one review article, and one manuscript ready to be to submitted. The manuscripts have been accepted in scientific journals of the first quality quartile in their area of expertise, validating the quality of the data presented in the thesis.

Original Manuscripts:

Article 1: "PCSK9 and LRP5 in macrophage lipid internalization and inflammation" was published in *Cardiovascular Research*. Impact factor of the journal in 2021 was 14.239, ranking in Quartile 1, Decile 1 of Cardiac & Cardiovascular Systems journal category. Although the doctorate candidate is not the first author, he contributed significantly to the manuscript by performing the experiments shown in figures 5 and 6. Additionally, the candidate also assisted in manuscript reviewing.

Article 2: "Differential cholesterol uptake in liver cells: a role for PCSK9" was published in The FASEB Journal. Impact factor of the journal in 2022 was 4.8, ranking in Quartile 2, Decile 5 of Cell Biology journal category and Quartile 1, Decile 2 of Biology journal category. The doctorate candidate is first author of the publication and he participated in all steps in the preparation of the manuscript.

Article 3: "Canonical WNT pathway involvement in high fat diet-induced adipose tissue distribution" will be submitted in brief. The doctorate candidate will be first author of the publication and he participated in all steps in the preparation of the manuscript.

Article 4: "Microvesicles carrying LRP5 induce macrophage polarization to an anti-inflammatory phenotype" was published in *The Journal of Cellular and Molecular Medicine*. Impact factor of the journal in 2021 was 5.295, ranking in Quartile 2, Decile 5 of Cell Biology journal category. The doctorate candidate is first author of the publication and he participated in all steps in the preparation of the manuscript.

SANT PAU Campus Salut Barcelona

Institut de Recerca Sant Pau

Article 5: "Canonical WNT pathway and the LDL receptor superfamily in neuronal cholesterol homeostasis and function" was published in *Cardiovascular Research* in 2024. Impact factor of the journal in 2023 (the most recent update) was 10.2 which ranked in Quartile 1, Decile 1 of Cardiac & Cardiovascular Systems journal category. The doctorate candidate is first author of the publication and he participated in all steps in the preparation of the manuscript.

Article 6: "Unique splicing of LRP5 in the brain: a new player in neurodevelopment and brain maturation" was published in the *International Journal of Molecular Sciences*. Impact factor of the journal in 2023 (the most recent update) was 4.9 which ranked in Quartile 1, Decile 3 of Biochemistry & Molecular Biology journal category. The doctorate candidate is first author of the publication and he participated in all steps in the preparation of the manuscript.

Review Manuscript:

Article 7 (Annex): "PCSK9 functions in atherosclerosis are not limited to plasmatic LDL-cholesterol regulation" was published in *Frontiers of Cardiovascular Medicine*. Impact factor of the journal in 2021 was 5.848, which ranked in Quartile 2, Decile 4 of Cardiac & Cardiovascular System journal category. This Review was written during lockdown and the candidate is first author of the publication. He participated in all steps in the preparation of the manuscript.

We also certificate that none of the publications presented in the thesis have been used for any other Doctoral Thesis.

Barcelona, 18th of June 2024,

Dr. Maria Borrell Pages

Prof. Lina Badimon Maestro

3.2 Article 1

PCSK9 and LRP5 in macrophage lipid internalization and inflammation

By Lina Badimon, Aureli Luquero, Javier Crespo, Esther Peña and Maria Borrell-Pagès

Published in Cardiovascular Research. 2021 Jul 27;117(9):2054-2068.

doi: 10.1093/cvr/cvaa254.

Summary: Atherosclerosis is a condition driven by high cholesterol levels and chronic inflammation. During atherosclerosis progression, increased concentrations of modified LDLs downregulate LDLR expression. Whether PCSK9 binds to other members of the LDLR family of receptors and disrupts lipid uptake remains poorly studied. The aim of this study was to analyze whether PCSK9 interacts with LRP5 in human cultured macrophages challenged with lipids (agLDL). Results show that LRP5 binds and mediates the internalization of agLDL in human macrophages. More importantly, upon agLDL stimulation LRP5 translocalizes from the cytoplasm to the cell membrane and triggers the activation of the canonical WNT pathway. Both control monocytes and macrophages express PCSK9; however, upon agLDL-stimulation, intracellular PCSK9 levels are reduced because PCSK9 is released to the extracellular milieu. PCSK9 is regulated by SREBP2, which is downregulated upon lipid-loading in macrophages. PCSK9 and LRP5 colocalize in the perinuclear area of resting macrophages and coimmunoprecipitation analysis show an interaction between the two proteins that is stronger after lipid stimulation indicating a role for LRP5 in PCSK9 transport to the extracellular milieu. Both LRP5 and PCSK9 gene knockdown reduce macrophage's ability to internalize cholesterol, revealing a role for both proteins in lipid uptake. Additionally, LRP5-silencing in macrophages also reduce PCSK9 release after agLDL

stimulation. Finally, a role for PCSK9 in inflammation is also shown. The release of PCSK9 to the extracellular milieu induces the expression of the pro-inflammatory cytokines IL-1β and TNFα. Furthermore, its release also increases NFκB translocation into the nucleus revealing a pro-inflammatory role for PCSK9 in macrophages after lipid-loading.

ESC European Society of Cardiology
Cardiovascular Research (2021) **117**, 2054–2068
doi:10.1093/cvr/cvaa254

PCSK9 and LRP5 in macrophage lipid internalization and inflammation

Lina Badimon [1,2,3], Aureli Luquero [3], Javier Crespo [3], Esther Peña [3], and Maria Borrell-Pages [1,3]*

[1]CIBER-CV, Instituto de Salud Carlos III, Spain; [2]Cardiovascular Research Chair, UAB, Barcelona, Spain; and [3]Cardiovascular Research ICCC, IR-Hospital de la Santa Creu i Sant Pau, IIB-Sant Pau, Carrer Sant Antoni Maria Claret 165, 08025 Barcelona, Spain

Received 10 March 2020; revised 26 June 2020; editorial decision 18 August 2020; accepted 15 September 2020; online publish-ahead-of-print 29 September 2020

Time for primary review: 24 days

Aims Atherosclerosis, the leading cause of cardiovascular diseases, is driven by high blood cholesterol levels and chronic inflammation. Low-density lipoprotein receptors (LDLR) play a critical role in regulating blood cholesterol levels by binding to and clearing LDLs from the circulation. The disruption of the interaction between proprotein convertase subtilisin/kexin 9 (PCSK9) and LDLR reduces blood cholesterol levels. It is not well known whether other members of the LDLR superfamily may be targets of PCSK9. The aim of this work was to determine if LDLR-related protein 5 (LRP5) is a PCSK9 target and to study the role of PCSK9 and LRP5 in foam cell formation and lipid accumulation.

Methods and results Primary cultures of human inflammatory cells (monocytes and macrophages) were silenced for LRP5 or PCSK9 and challenged with LDLs. We first show that LRP5 is needed for macrophage lipid uptake since LRP5-silenced macrophages show less intracellular CE accumulation. In macrophages, internalization of LRP5-bound LDL is already highly evident after 5 h of LDL incubation and lasts up to 24 h; however, in the absence of both LRP5 and PCSK9, there is a strong reduction of CE accumulation indicating a role for both proteins in lipid uptake. Immunoprecipitation experiments show that LRP5 forms a complex with PCSK9 in lipid-loaded macrophages. Finally, PCSK9 participates in TLR4/NFkB signalling; a decreased TLR4 protein expression levels and a decreased nuclear translocation of NFκB were detected in PCSK9 silenced cells after lipid loading, indicating a downregulation of the TLR4/NFκB pathway.

Conclusion Our results show that both LRP5 and PCSK9 participate in lipid uptake in macrophages. In the absence of LRP5, there is a reduced release of PCSK9 indicating that LRP5 also participates in the mechanism of release of soluble PCSK9. Furthermore, PCSK9 up-regulates TLR4/NFκB favouring inflammation.

*Corresponding author. Tel: 34-935565621, E-mail: mborrellpa@santpau.cat

Graphical Abstract

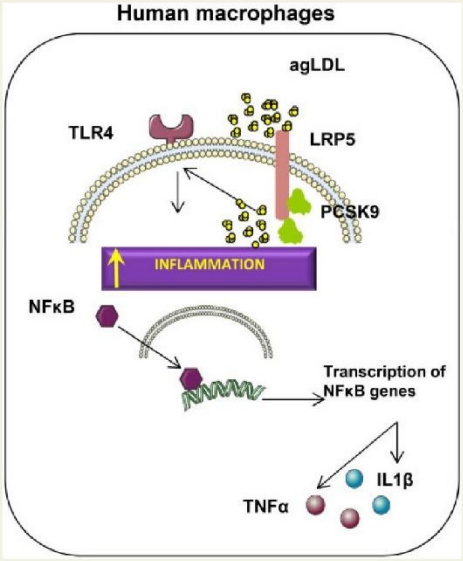

Keywords PCSK9 • Lipoproteins • Inflammation • Macrophages • lrp5

1. Introduction

Low-density lipoprotein receptors (LDLR) play a critical role in regulating blood cholesterol levels by binding to and clearing LDLs from the circulation. LDLR are particularly abundant in the liver and the number of LDLR determines how quickly LDLs are removed from the bloodstream.[1] Proprotein convertase subtilisin/kexin 9 (PCSK9) is a circulating protein that can reduce the amount of LDLR in hepatocytes. Indeed, circulating PCSK9 bind to the EGF domain of LDLRs causing the cointernalization of both PCSK9 and LDLR and directing the LDLR to degradation in the lysosomes, rather than its recycling to the plasma membrane.[2–4] Additionally, PCSK9 can also bind LDLR intracellularly.[5] Thus, by virtue of its role as a major inhibitor of the LDLR, PCSK9 has emerged as a new drug target to treat hypercholesterolaemia and reduce coronary heart disease.[6–8]

Cholesterol deposition is one of the prominent features of atherosclerotic lesion formation and aortic calcifications. Vascular disease is initiated by lipid retention, oxidation, and modification, which cause chronic inflammation, ultimately developing atheroma and thrombosis.[9] The initial step occurs when LDL particles infiltrate the arterial intima, where, if LDL concentration is exceedingly high they accumulate by binding to proteoglycans and forming aggregates.[10,11] LDL can then be modified by enzymes and oxidized into proinflammatory particles, which attract innate inflammatory cells to the intima. Both innate immunity cells and resident smooth muscle cells (SMC) internalize LDL by receptor-mediated processes, becoming foam cells and triggering further inflammation and progression of the atherosclerotic disease.[10–12] Upon entry, monocytes transform into macrophages, uptake lipids and become foam cells. This lipid accumulation is not facilitated by LDLR, because the LDLR downregulates by excess cholesterol. Instead internalization is facilitated by scavenger receptors[13] and the *LDL Receptor related Protein* family of receptors, including LRP5[14] and LRP1.[15] LDL accumulation in the intima induces changes in infiltrated and resident cell gene expression. Indeed, the expression of tissue factor, a procoagulant/angiogenic molecule is upregulated in human vascular smooth muscle cells and immune cells exerting changes in the plaque area that facilitates the transformation of chronic atherosclerosis into event-prone plaques.[16,17]

LRP5 is a single-pass transmembrane receptor member of the Wnt/β-catenin signalling pathway. LRP5-Wnt ligand binding results in the stabilization of β-catenin that then translocates to the nucleus, triggers TCF/LEF1 transcription factor activation and transcription of canonical Wnt target genes.[18,19] We have previously reported that LRP5 expression levels are increased in lipid-loaded macrophages.[14] PCSK9 expression has been shown in mice macrophages,[20] and PCSK9 secreted by human SMCs is functionally active and capable of reducing LDLR expression in macrophages.[21] Interestingly, suppression of LDLR and overexpression of PCSK9 has been linked to aortic calcification by a mechanism dependent on LRP5/canonical Wnt signalling.[22] In macrophages, PCSK9 reduces LDLR and LRP1 expression and increases atherosclerotic plaque inflammation in an LDLR-dependant and cholesterol-independent mechanism in mice.[23] However, the relation of PCSK9 and the LRP-receptor family is not fully understood. Indeed, members of the LDLR superfamily may be targets of PCSK9, and it is plausible that PCSK9 may have a direct role in foam cell formation, an LDLR-independent mechanism, and hence in lipid accumulation and atherosclerotic plaque progression.

In this study, we investigated the role of LRP5 and LRP5–PCSK9 interaction in lipid internalization and the inflammatory response in innate immunity cells.

2. Methods

2.1 Isolation of human monocytes and human macrophages primary cultures

Human monocytes were obtained by standard protocols from buffy coats of healthy blood donors. All procedures were approved by the Institutional Review and Ethics Committee and the investigation conformed to the principles outlined in the Declaration of Helsinki with informed consent given by donors. Cells were applied on 15 ml of Ficoll-Hypaque and centrifuged at 300 g for 1 h at 22 C, with no brake. Mononuclear cells were obtained from the central white band of the gradient, exhaustively washed in Dulbecco's phosphate buffer saline, and suspended in RPMI medium (Gibco) supplemented with 10% human serum AB (Sigma).[14] A set of cells (monocytes) was left overnight in culture, washed and treated with 100 μg/mL aggregated LDL (agLDL) for the described times. The second set of cells was left 7 days in culture and allowed to differentiate into macrophages by changing the cell culture media (RPMI supplemented with 10% human serum AB, 100 units/mL penicillin, and 100 μg/mL streptomycin) every 3 days. After several washings with PBS to completely remove serum, human macrophages were then incubated with 50 or 100 μg/mL nLDL (native LDL) or 100 μg/mL agLDL in serum-free medium. At the end of the experiments, human monocytes and macrophages were exhaustively washed and collected for both mRNA and protein detection or fixed with PFA4% for immunofluorescence as described below.

2.2. LDL isolation and modification

Human LDL (d1.019–d1.063 g/mL) was obtained as previously described.[12,24,25] Briefly, human LDLs were obtained from pooled sera of normocholesterolemic volunteers and isolated by sequential ultracentrifugation. LDLs were dialyzed three times against 200 volumes of 150 mmol/L NaCl, 1 mmol/L EDTA, and 20 mmol/L Tris-HCl, pH 7.4, overnight and once against 150 mmol/L NaCl. LDL protein concentration was determined by the bicinchoninic acid, and vortexing was monitored by measuring the turbidity (absorbance at 680 nm). The model system of agLDL was generated by vortexing LDL (1 mg/ml) for 4 min at room temperature at maximal speed. The percentage of LDL in aggregated form was calculated by measuring the fraction of protein recovered in the pellet obtained after centrifugation. The different fractions were analysed by agarose electrophoresis, and the precipitated fraction composed of 100% agLDL was added to cell cultures.

Lipoprotein purity analyses were performed enzymatically using commercial kits adapted to a COBAS c501 autoanalyzer (Roche Diagnostics). HDL cholesterol was measured through ApoA-I detection.

In order to label LDL particles, we incubated them with DiI. DiI stock solution was prepared dissolving 3 mg of DiI in 1 mL DMSO, obtaining a preparation of 3 mg/mL. This preparation was then diluted 1:60 in PBS/0.5% BSA with the desired concentration of LDL and left overnight at 37 C for proper lipoprotein staining. The DiI-labelled LDL was then isolated by ultracentrifugation, dialyzed and sterilized using a 0.45 μm filter. Finally, DiI-labelled LDL was stored at 4 C under sterile conditions. Labelled nLDL particles were used as DiI-nLDL or DiI-AgLDL.

2.3 LDL loading

After LDL (native or aggregated) incubation, cells were exhaustively washed (twice with PBS, twice with PBS/1% BSA, twice with PBS/1% BSA/heparin 100 U/mL, twice with PBS/1% BSA, and twice with PBS) and prepared for immunofluorescence analysis, and for the collection of mRNA and protein.

2.4 Immunofluorescence and DiI labelling

Human macrophages incubated or not with agLDL were fixed with 4% PFA and permeabilized (P) or not (NP) with 0.5% Tween in PBS at room temperature. After incubation in blocking buffer (3% bovine serum albumin in PBS), primary LRP5 or PCSK9 (Abcam) antibodies were added 1 h at room temperature in a moist chamber. Appropriate secondary antibodies Alexa Fluor anti-mouse 488 IgG (H + L), Alexa Fluor anti-rabbit 488 IgG (H + L), Alexa Fluor anti-rabbit 633 IgG (H + L) andHoechst 33342 or DiI staining (3,3-dimethyl-1-octadecylindol-1-ium-2-ylprop-2-enylidene-3,3-dimethyl-1-octadecylindole; 30 mg/mL in DMSO, Sigma were added for 1 h and stained cells were washed and covered with Prolong Gold antifade reagent (Molecular Probes). Images of 25–35 cells/condition/experiment were immunostained and recorded on a Leica inverted fluorescence confocal microscope (Leica TCS SP2-AOBS, Germany). Cells were viewed with HCX PL APO 63 /1.2 W Corr/0.17 CS objective. Fluorescent images were acquired in a scan format of 1024

1024 pixels in a spatial dataset (xyz) and were processed with the Leica Standard Software TCS-AOBS. Fluorescence was measured from individual stacks; number of pixels and the mean per field of view were measured blindly by two independent investigators. Controls without primary antibodies showed no fluorescence labelling.

2.5 Determination of free and esterified cholesterol content

Human macrophages were treated with 200 ng/mL Wnt3a (Sigma), 100 μg/mL agLDL, or 200 ng/mL Wnt3a + 100μg/ml agLDL for 8 h. In another set of experiments, macrophages were silenced for PCSK9, LRP5, both or LDLR as detailed below. 24h hours later, cells were treated with 100 μg/mL agLDL or nLDL (100 μg/mL) for further 24 h. Cells were exhaustively washed, twice with PBS, twice with PBS/1% BSA, and twice with PBS/1%BSA/heparin 100 U/mL before harvesting into 1 mL of 0.1 N NaOH. Lipid extraction and thin layer chromatography were performed as previously described.[26,27] Briefly, one aliquot of the cell suspension was extracted with methanol/dichloromethane (2:1, vol/vol). After solvent removal under an N_2 stream, the lipid extract was redissolved in dichloromethane and one aliquot was partitioned by TLC, which was performed on silica G-24 plates. Three different concentrations of standards (a mixture of cholesterol and cholesterol palmitate) were applied to each plate. The chromatographic developing solution was heptane/diethyl ether/acetic acid (74:21:4, vol/vol/vol). Plates were then stained with 26 mM/47.62 g/L molybdophosphoric acid solution of absolute ethanol/absolute sulfuric acid (95:5, vol/vol) for 1 min. After air drying, TLC plaques were heated at 100 C for 7 min. The spots corresponding to free cholesterol (Free C) and cholesteryl esters (CE) were quantified by densitometry against the standard curve of cholesterol and cholesterol palmitate, respectively, with the use of a computing densitometer (molecular dynamics).

2.6 LRP5 and PCSK9 silencing

Human macrophages were transfected with 100 nM of siRNA-Random (siR), siRNA-LRP5 (si5) siRNA-PCSK9 (siPCSK9), or siRNA-SREBP2

(siSREBP2) using HiPerfect® as recommended by the manufacturer. Small anti-LRP5, anti-PCSK9, or anti-SREBP2 interfering RNAs (si5, s8293; siPCSK9 s8569; siSREBP2 s8457) were synthesized by Applied Biotechnologies and Silencer Selective negative control #1 (siR, 4390843) by Ambion.

2.7 RNA isolation and real-time PCR

Total RNA was isolated from cultured human monocytes and macrophages using the Total RNA extraction kit (Qiagen). Total RNA concentration was determined on NanoDrop ND-1000 spectrophotometer (NanoDrop Technologies, Inc., Wilmington, DE, USA), and purity was checked by the A260/A280 ratio (ratios between 1.8 and 2.1 were considered acceptable), in addition, an agarose gel was run to assess quality. cDNA was synthesized from 1 μg RNA with cDNA Reverse transcription kit (Qiagen) The resulting cDNA samples were amplified by polymerase chain reaction (PCR) using a DNA thermal cycler (MJ Research, Watertown, MA, USA) and the following specific human probes from Applied Biotechnologies: LRP5, PCSK9, β-catenin, OPN, SREBP-2, TNF-α, and IL1β. Normalization was performed against r18S.

2.8 Western blot and antibodies

Sample extracts (cell lysates or supernatants, 20–50 μg protein) were resolved by SDS-PAGE and transferred to nitrocellulose membranes, blocked with 5% skim milk and probed for monoclonal (LRP5, TNF-α, IL1β, TGFβRII, osteopontin, β-catenin, and SREBP-2 from Abcam) or polyclonal (β-actin, TLR4, Histone H1, and PCSK9 from Millipore) primary antibodies. Membranes were then washed and blotted with appropriate anti-mouse or anti-rabbit secondary antibodies (Dako). Band densities were determined with the ChemiDoc XRS system (Bio-Rad) in chemiluminescence detection modus and Quantity-One software (Bio-Rad). Normalization was performed against β-actin.

2.9 Flow cytometry

LRP5 expression was assessed in primary cultures of human macrophages by FACS. Cell suspensions in FACS buffer (0.1% Sodium Azide/1%BSA/PBS) were stained for 15 min with a specific mouse monoclonal antibody against cell surface LRP5 (1:50; Abcam). Samples were then incubated for 15 min at 4 C with Alexa FluorTM 488-conjugated anti-mouse antibodies (1:100; Abcam) and washed with PBS prior to analysis. For each sample, at least 10 000 events were acquired on a FACS Cantoll (Beckton Dickinson). Data were analysed with a FACS Diva 6.0 Software. Samples incubated without primary antibodies were used as a negative control.

2.10 Immunoprecipitation and cellular subfractionation

Total protein content in cell lysates of human macrophages was estimated using the BCA protein assay (Pierce). IP was carried out on 500 μg of total protein. Total protein, cytoplasmic, and membrane fractions (obtained with the ProteoExtract Subcellular Proteome Extraction Kit following the manufacturer instructions) were incubated with 5 μL of unspecific IgG or ApoB, LRP5, or PCSK9 specific antibody at room temperature for 1 h enabling the antibody to bind to the protein in solution. The antibody/antigen complex was then pulled out of the sample using protein A/G-coupled agarose beads. The sample was then separated by SDS-PAGE for western blot analysis.

2.11 Statistical analysis

Results are expressed as mean ± SEM. A Stat View statistical package was used for all the analysis. When possible, comparisons among groups were performed by parametric (one factor ANOVA) analysis. Statistical significance was considered when $P < 0.05$. Non-parametric Mann–Whitney analyses were performed when described. All the experiments were performed at least three times.

3. Results

3.1 LRP5 mediates lipid uptake in human macrophages

To determine whether membrane expressed LRP5 is able to bind and internalize extracellular lipids, human macrophages were treated with aggregated LDL (agLDL, 100 μg/mL) and LRP5 and lipid colocalization was analysed by confocal microscopy (*Figure 1A*). In control conditions, when no agLDL was present in the media, a moderate DiI staining was observed in permeabilized macrophages. When agLDL was added, a strong DiI staining was observed as well as an increased expression of LRP5 (*Figure 1A*). Characterization of LRP5 and DiI staining by three-dimensional reconstruction (XYZ) identified agLDL-LRP5 merged staining inside the lipid-loaded macrophages (*Figure 1B*). To provide evidence that LDL preparations are not contaminated with HDL (high DL), we measured ApoA-I in three random LDL preparations showing that ApoA-I is not present in any of the LDL samples (Supplementary material online, *Figure S1A*).

Time-course confocal analyses in non-permeabilized (NP) human macrophages incubated with agLDL showed that while at baseline LRP5 staining was barely seen at the plasma membrane, there was an increase in LRP5 surface staining from 30 min up to 24 h (*Figure 1C* upper panels and *Figure 2A*). In permeabilized (P) cells, increased LRP5 in the cytoplasm was apparent at 5 h after agLDL loading suggesting that LRP5 is internalized with the lipids (*Figure 1C* lower panels and *Figure 2A*). Quantification analyses of DiI showed that at 30 min post-agLDL loading there was increased content of DiI in non-permeabilized macrophages (*Figure 2A*). Also, in permeabilized macrophages, the increased lipid staining was observed at 5 h and 24 h suggesting internalization of lipid (*Figure 2B*).

Flow cytometry analyses confirmed increased LRP5 expression after agLDL in human macrophages. Indeed, agLDL-treated human macrophages show a 48 + 1% increase in LRP5 intensity as compared to control macrophages (Supplementary material online, *Figure S1B*).

We then labelled agLDL with dil (dil-agLDL), treated human macrophages for 0.5 h, 5 h, and 24 h with 100 μg/mL dil-agLDL, fixed, and stained macrophages with LRP5 antibodies (Supplementary material online, *Figure S1C*). In control conditions only LRP5 staining is observed; however, in a similar way to unconjugated agLDL, dil-agLDL treatments show macrophage lipid internalization beginning at 30 min and up to 24 h (Supplementary material online, *Figure S1C*). For comparative purposes, we treated macrophages with native LDL (dil-nLDL) and stained them with LRP5 antibodies. Results show that the intracellular accumulation of nLDL is slower than that of agLDL (5 h vs. 30 min). As expected, no colocalization between nLDL and LRP5 is observed (Supplementary material online, *Figure S1D*).

3.2 LRP5 translocates to the membrane in the presence of extracellular lipids

Cellular subfractionation analyses in untreated and 24 h agLDL-loaded human macrophages followed by immunoprecipitation experiments with ApoB (present in agLDLs) and blotted against LRP5 or LDLR showed that in the absence of lipids, LRP5 is mainly in the cytoplasm. However, after agLDL treatment not only LRP5 levels are increased but there is also translocation to the membranes fraction (*Figure 2C*) supporting the immunofluorescence experiments (*Figure 1C*). As expected, LDLR expression decreased in the presence of lipids with respect to control cells and was found both in cytoplasm and membrane fractions of agLDL-treated human macrophages (*Figure 2C*). Quantification analyses of LRP5 and LDLR expression levels in the cytoplasmic and membrane fractions are also shown (*Figure 2C*). The cytoplasmic marker

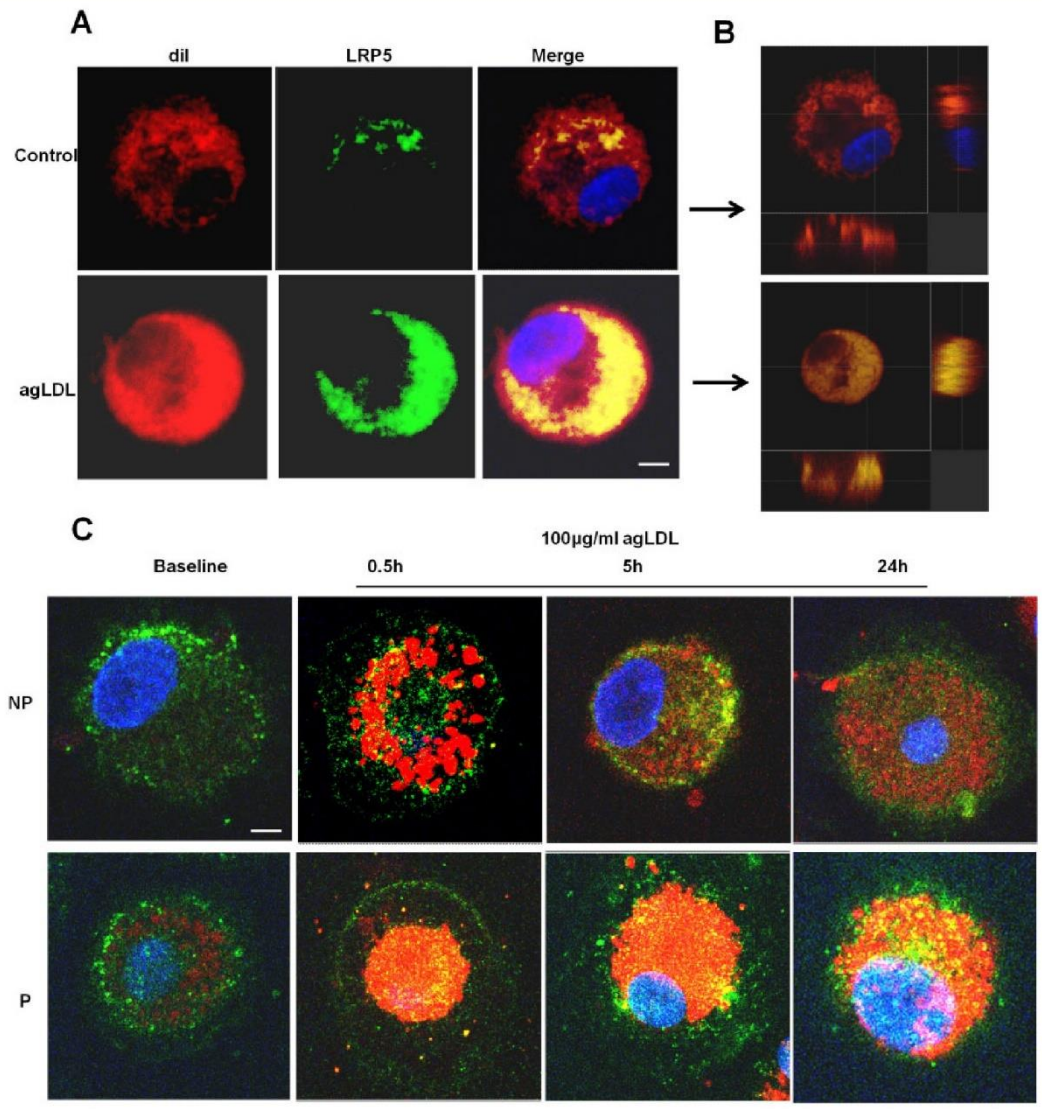

Figure 1 LRP5 participates in lipid internalization in human macrophages. (*A*) Human macrophages were treated with 100 µg/mL agLDL for 24 h and stained with mouse anti-LRP5 followed by Alexa Fluor anti-mouse 488, DiI, and Hoechst (permeabilized cells). (*B*) Fluorescence images were acquired in a spatial data set (xyz). *N* = 5 in duplicates (yellow, colocalization of LRP5 and DiI). (*C*) Human macrophages were treated for the indicated times with 100 µg/mL agLDL, permeabilized (P), or not (NP) and stained as in *A*. *N* = 5 in duplicates (LRP5-green; DiI-red; merge-yellow). Bar 5 µm.

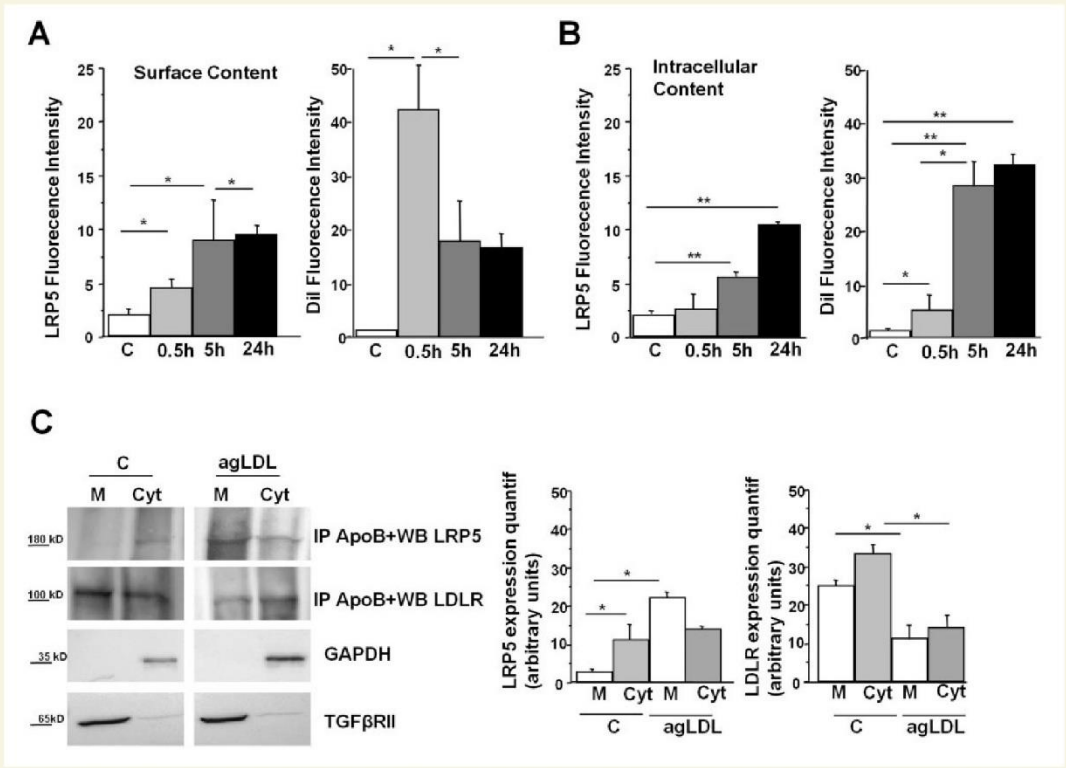

Figure 2 LRP5 and lipid internalization in human macrophages. Quantification of the fluorescence intensity for (*A*) LRP5 and (*B*) DiI staining of experiments depicted in *Figure 1C*, measured with the Leica Standard Software TCS-AOBS. (*C*) Human macrophages were treated with 100 μg/mL agLDL for 24 h, submitted to fractionation experiments and fractions were IP with ApoB antibodies; afterwards blots against LRP5, LDLR, GAPDH, and TGFβRII were performed. Bar graph showing the quantification of LRP5 and LDLR expression levels.*$P < 0.01$, **$P < 0.05$ for treated cells compared with controls (ANOVA); $n = 5$.

GAPDH and the nuclear marker TGFβRII were used as control of cellular fractionation.

3.3. Wnt3A increases canonical Wnt gene expression in human macrophages

To test if the activation of LRP5 by an extracellular ligand could lead to lipid uptake in human macrophages, we used Wnt3A an activator of the canonical Wnt pathway.[28] We first treated human macrophages with 200 ng/mL of Wnt3A and showed increased LRP5-mRNA expression levels, as well as increase in β-catenin and osteopontin mRNA levels (29 ± 2%, 47 ± 1%, and 66 ± 3%, respectively; *Figure 3A*) indicating that Wnt3A is able to induce canonical Wnt pathway activation in human macrophages. We then analysed the effect of agLDL in canonical Wnt gene expression and found that agLDL induced a 51 ± 2% increase in LRP5 expression level,[14] a 105 ± 7% increase in β-catenin expression levels, and a 87 ± 4% increase in OPN expression. This increase was also observed after combined treatments with Wnt3A and agLDL resulting in similar values to those observed with agLDL loading alone, indicating that there is little or no additive effect of both treatments but that both induce Wnt-pathway activation (*Figure 3A*). Protein analyses with LRP5, β-catenin and OPN antibodies showed similar results (*Figure 3A*).

3.4 LRP5 silencing inhibits agLDL-induced increased CE accumulation in human macrophages

The ability of activated LRP5 to induce lipid internalization was tested by intracellular cholesterol ester (CE) accumulation analyses in thin layer chromatography experiments. Wnt3A treatment in human macrophages was unable to induce CE accumulation in the absence of extracellular lipids (*Figure 3B*). When agLDL were added to the extracellular milieu, CE accumulation was increased by 1 μgCE/μgFC in human macrophages. Finally, when both treatments were combined, CE accumulation was increased, although similarly to agLDL-treated macrophages (*Figure 3B*).

To show that LRP5 participates in lipid internalization, human macrophages were silenced for LRP5 (siLRP5) and incubated with agLDL. Gene analyses showed a downregulation of LRP5 in silenced macrophages (Supplementary material online, *Figure S1E*). siLRP5-treated

macrophages had a significant, but nor complete, reduction of lipid internalization. CE accumulation was reduced to 0.55 μgCE/μgFC after agLDL loading (*Figure 3C*). Therefore, LRP5 contributes significantly to CE internalization in macrophages.[14] The role of LDLR in CE accumulation in human macrophages has already been studied in.[29] Indeed, after 24 h of lipid treatment, both nLDL and agLDL-induced CE accumulation in human macrophages (10.25 ± 0.54 μgCE/mg protein and 77.09 ± 1.2 μgCE/mg protein respectively).[29] Thin layer chromatography analyses of human macrophages silenced for LDLR and treated with nLDL showed a lower level of CE internalization from nLDL than from agLDL in macrophages, and that the silencing of LDLR reduces lipid internalization even further (Supplementary material online, *Figure S2A*).

Interestingly, increased LRP5 levels and Wnt activation are achieved both by Wnt3A and by agLDL (*Figure 3A*) but Wnt3A contribution to lipid uptake is smaller than agLDLs (*Figure 3B*). To test whether translocation of LRP5 occurs after Wnt activation, we performed cellular subfractionation analyses in untreated and 30 min Wnt3A-treated human macrophages (*Figure 3D*). In control conditions, LRP5 is mainly in the cytoplasm. However, after Wnt3A treatment LRP5 is translocated to the membrane fraction showing that Wnt3A activates the Wnt pathway and supporting the gene and protein analyses experiments (*Figure 3A*). The cytoplasmic marker GAPDH and the nuclear marker TGFβRII were used as control of cellular fractionation (*Figure 3D*).

3.5 SREBP-2 expression levels are decreased in inflammatory cells after agLDL treatments

SREBP-2 is a key modulator of lipoprotein receptor expression including LRP1and LDLR.[15,30] To determine if SREBP2 participates in the modulation of LRP5 expression, we analysed SREBP-2 (mRNA and protein levels) in human macrophages and monocytes in the presence of extracellular lipids. agLDL did not significantly alter SREBP-2 mRNA values in untreated or lipid-loaded human monocytes (Mo) or macrophages (Mac; *Figure 4A*). Interestingly, macrophages showed lower SREBP-2 mRNA expression than monocytes. Western blot analysis showed that although agLDL did not alter the precursor form of SREBP-2 in any of the inflammatory cells, the presence of extracellular lipids decreased the concentration of the active form of SREBP-2 in human macrophages but not in monocytes (*Figure 4B*). A quantification analysis of the active form of SREBP-2 in monocytes and macrophages is shown in *Figure 4B*.

LRP5 transcription and LRP5 protein were upregulated by agLDL loading in both monocytes and macrophages, further confirming previous results ([14]; *Figure 4C and D*). To test the possibility of SREBP-2 modulating LRP5, we silenced LRP5 in macrophages, before agLDL loading. Results show a decrease in the active form of SREBP-2 both in control and siLRP5 treated macrophages indicating that LRP5 is not regulated by SREBP-2 (*Figure 4E*). No variations were observed in the precursor form of SREBP-2 or in gene expression (*Figure 4E and F*). LRP5 mRNA transcript levels were reduced after silencing independently of lipid content (*Figure 4F*). We then analysed LRP5 expression levels in SREBP-2 silenced human macrophages and found increased LRP5 protein levels in the presence and absence of SREBP-2 further confirming that LRP5 is not under SREBP-2 regulation (Supplementary material online, *Figure 2B*).

3.6 PCSK9 in inflammatory cells

PCSK9 gene expression was analysed in monocytes (Mo), differentiating monocytes (MoMac), and fully differentiated macrophages (Mac). In monocytes, *Pcsk9* mRNA expression was almost undetectable, in MoMac was significantly upregulated and reached its highest expression in completely differentiated macrophages (*Figure 5A*). In macrophages, *Pcsk9* mRNA transcription was slightly and not significantly decreased by Wnt3A but was downregulated by LDL loading (40 ± 3% after 100 μg/mL agLDL treatment and 45 ± 1% after the combined treatment with 100 μg/mL agLDL and 200 ng/ml Wnt3A; *Figure 5B*).

Western blot of PCSK9 showed no differences between control and agLDL loaded human monocytes (*Figure 5C*). But similar to mRNA results (*Figure 5B*), PCSK9 protein expression was significantly reduced in agLDL-loaded human macrophages (*Figure 5C*). LDL-loaded macrophages secreted PCSK9 into the medium but not unloaded macrophages (*Figure 5D*).

3.7 PCSK9 binds to LRP5 at the perinuclear area of human macrophages

Human macrophages were incubated with 100 μg/mL agLDL for 24 h and stained with mouse anti-LRP5 followed by Alexa Fluor anti-mouse 488 IgG and with rabbit anti-PCSK9 followed by Alexa Fluor anti-rabbit 647 IgG, and Hoechst. Permeabilized cells showed a perinuclear staining for PCSK9 (red) and a membrane and perinuclear staining for LRP5 (green). A clear colocalization of both PCSK9 and LRP5 at the perinuclear area was observed suggesting a possible direct interaction between PCSK9 and LRP5 intracellularly (*Figure 5E*). IP experiments were performed in LDL-loaded macrophages showing that LRP5 and PCSK9 form a complex in the cytoplasm of macrophages and that the intensity of the interaction is higher after agLDL loading (*Figure 5F*). Reverse immunoprecipitation with PCSK9 antibodies and blotted against LRP5 confirmed these results (Supplementary material online, *Figure S2C*).

As PCSK9 and LRP5 interact directly intracellularly, we hypothesized that LRP5 was participating in the PCSK9 release pathway. We silenced human macrophages for LRP5 (*Figure 6A*) and analysed PCSK9 release to the extracellular milieu (*Figure 6B*). Results show decreased PCSK9 release in LRP5 silenced macrophages after agLDL treatments (*Figure 6B*).

For comparative purposes, we analysed the effect of PCSK9 on LDLR regulation in the macrophages. There is no variation in *Ldlr* expression levels in control and LRP5-silenced cells in the presence or absence of lipids suggesting that LRP5 and LDLR act through different mechanisms. As expected, in PCSK9-silenced macrophages, a significantly increased Ldlr expression was found after agLDL loading, both at gene and protein levels, supporting PCSK9 involvement in LDLR's downregulation (*Figure 6C*). Gene and protein analyses showed that silencing of LRP5 and PCSK9 was specific and selective (*Figure 6D and E*) and the absence of PCSK9 in human macrophages did not affect LRP5 expression levels and vice versa (*Figure 6D and E*).

To study the role of PCSK9 in macrophage intracellular cholesterol accumulation, human macrophages were silenced for PCSK9 (siPCSK9), LRP5 (siLRP5), or both (siLRP5+siPCSK9) and incubated with 100 μg agLDL. Both siPCSK9-macrophages and siLRP5-macrophages had a significantly reduced CE accumulation. When both proteins were silenced simultaneously, CE accumulation was reduced to 0.39 μgCE/μgFC (*Figure 6F*). Therefore, both LRP5 and PCSK9 contribute significantly to CE internalization in macrophages.

To further support that macrophage cholesterol content is decreasing in the absence of LRP5 and PCSK9, we analysed the protein levels of

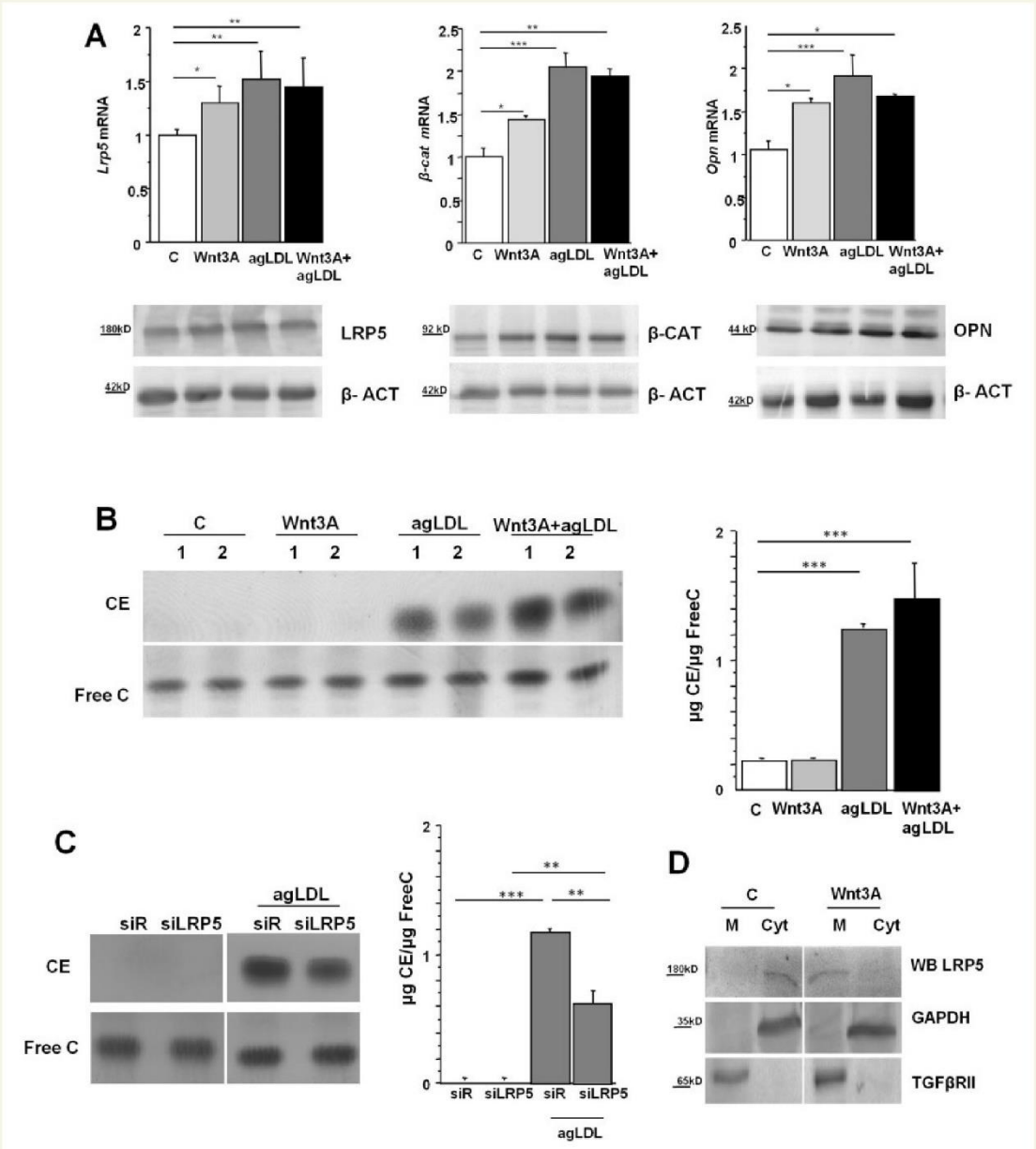

Figure 3 Wnt3A increases canonical Wnt gene expression in human macrophages. (*A*) Human macrophages were treated with agLDL, Wnt3A, or both for 24 h. *Lrp5*, *β-catenin*, and *Opn* levels from RNA extracts were quantified by RT-PCR and normalized to 18SrRNA, and lysis buffer samples were blotted against LRP5, *β*-CATENIN, OPN, and *β*-ACTIN. Experiments were performed four independent times in triplicates. (*B*) Human macrophages treated with Wnt3A, agLDL, or both were exhaustively washed and harvested to measure intracellular Free C and CE by TLC. Bar graph showing the quantification of cholesteryl esters respect to Free C. $N = 4$ in triplicates (*C*) Human macrophages containing siRNA-Random (siR) or siRNA-LRP5 (siLRP5) were agLDL-incubated (100 µg/mL). TLC and bar graphs were performed as in *B*. $N = 4$ in triplicates. (*D*) Human macrophages were treated with Wnt3A for 30 min, submitted to fractionation experiments and fractions were blotted against LRP5, GAPDH, and TGFβRII $^{*}P < 0.01$, $^{**}P < 0.05$, $^{***}P < 0.005$ for treated cells compared with controls (ANOVA).

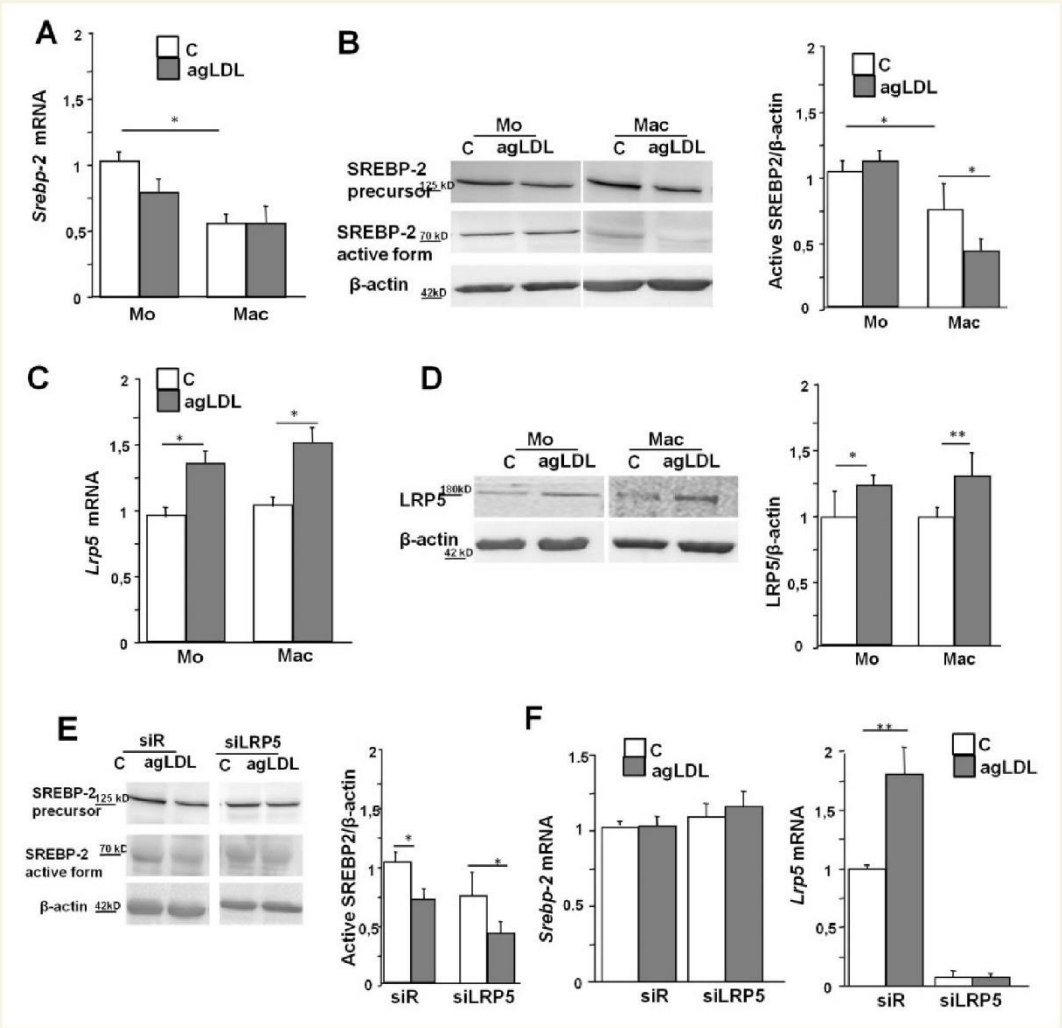

Figure 4 SREBP-2 expression levels are decreased in inflammatory cells after agLDL treatments. (*A*) Human monocytes or macrophages were incubated with 100 μg/mL agLDL for 24 h. *Srebp-2* levels from RNA extracts were quantified by RT-PCR and normalized to 18srRNA. $N = 4$ in triplicates. (*B*) Representative WB of the precursor and the active form of SREBP-2 and the analysis of active SREBP-2 expression in untreated and agLDL-treated human monocytes and macrophages. β-Actin was used as a loading control. (*C* and *D*) Same procedures as (*A* and *B*) for LRP5 gene and protein expression analyses. (*E*) Human macrophages were silenced for LRP5 and treated with agLDL for 24 h when the precursor and the active form of SREBP-2 were analysed by WB and quantified. (*F*) *Srebp-2* and *Lrp5* levels from RNA extracts were quantified by RT-PCR and normalized to 18srRNA $N = 4$ in duplicates $^{*}P < 0.01$, $^{**}P < 0.05$ for treated cells compared with controls (ANOVA).

another cholesterol-responsive gene, HMGCoA reductase. Results show increased HMGCoA reductase expression levels when there is a reduced accumulation of intracellular CE (*Figure 6G*).

3.8 PCSK9 and inflammatory mediators in macrophages

Because of the impact of macrophages/cytokines in atherosclerotic lesion development, we investigated whether *Tnf-α* and *Il1β* were changed by PCSK9-lipid internalization. We transduced human macrophages with a control siRNA (siR) or with siRNA-PCSK9 (siPCSK9) and incubated them with agLDL. Lipid loading reduced *Pcsk9* mRNA while *Tnf-α* and *Il1β* mRNA levels were moderately but significantly increased (*Figure 7A*). In the lipid-loaded siPCSK9 human macrophages *Tnf-α* and *Il1β* mRNA levels were reduced by 19 ± 2% and 21 ± 3%, respectively (both $P < 0.05$) (*Figure 7A*). Gene and protein analyses showed that silencing of PCSK9 was specific and selective (Supplementary material

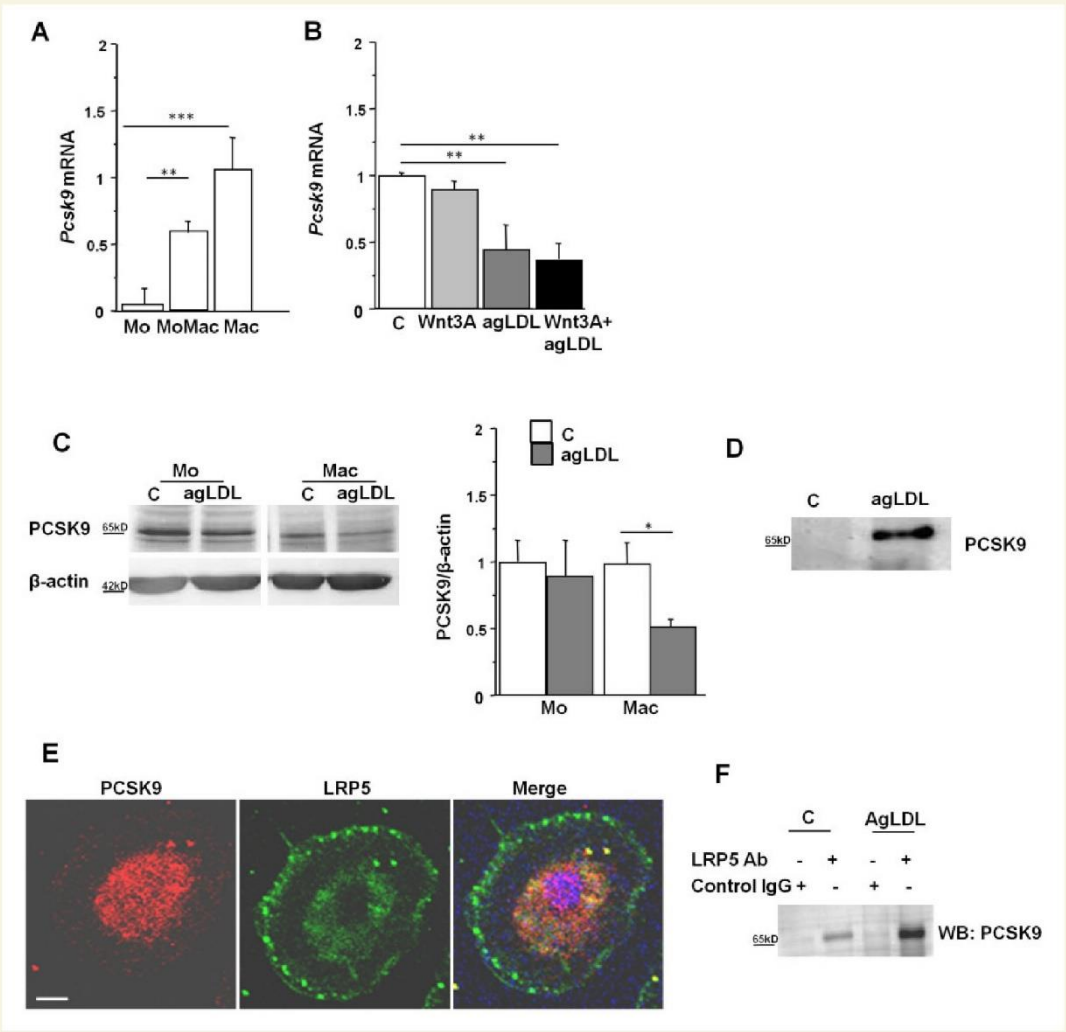

Figure 5 PCSK9 expression levels are decreased in human macrophages after agLDL treatments. (*A*) *Pcsk9* mRNA expression analyses were investigated in human monocytes (Mo), differentiating monocytes (MoMAc), and human macrophages (Mac). $N = 4$ in duplicates (*B*) Human macrophages were treated with Wnt3A, agLDL, or both for 24 h and *Pcsk9* gene levels were analysed by RT-PCR. $N = 4$. (*C*) Representative WB of macrophage PCSK9 expression levels. Bar graph to show the quantification of PCSK9 expression levels. $N = 3$. (*D*) Representative WB of soluble PCSK9 in the supernatants of agLDL-treated human macrophages. (*E*) Human macrophages were treated with 100 μg/mL agLDL for 24 h and stained with mouse anti-LRP5 followed by Alexa Fluor anti-mouse 488 IgG and rabbit anti-PCSK9 followed by Alexa Fluor anti-rabbit 647 IgG, and Hoechst. $N = 5$. Bar 5 μm. (*F*) Human macrophages were treated with 100 μg/mL agLDL, and IP with LRP5 antibody or unspecific IgG before WB against PCSK9 was performed. $N = 4$ $^{*}P < 0.01$, $^{**}P < 0.05$, $^{***}P < 0.005$ for treated cells compared with controls (ANOVA).

online, *Figure S2D*). Interestingly, agLDL loading induced the release of TNF-α and IL1β to the macrophage cell medium, and the silencing of PCSK9 reduced the release of TNF-α and IL1β to baseline control levels (*Figure 7B*). Additionally, AgLDL loading induced an increase in TLR4 expression levels that was partially but significantly abrogated by PCSK9 silencing to baseline control levels (*Figure 7C*). In these cells, LRP5 protein levels were increased after agLDL loading independently of the presence or absence of PCSK9 (*Figure 7C*). NFκB translocation to the nucleus was increased by LDL loading and reduced in siPCSK9/LDL-loaded macrophages (*Figure 7D*). Taken together, these data indicate that inhibition of PCSK9 reduces the proinflammatory state induced by agLDL in human macrophages (*Figure 7E*).

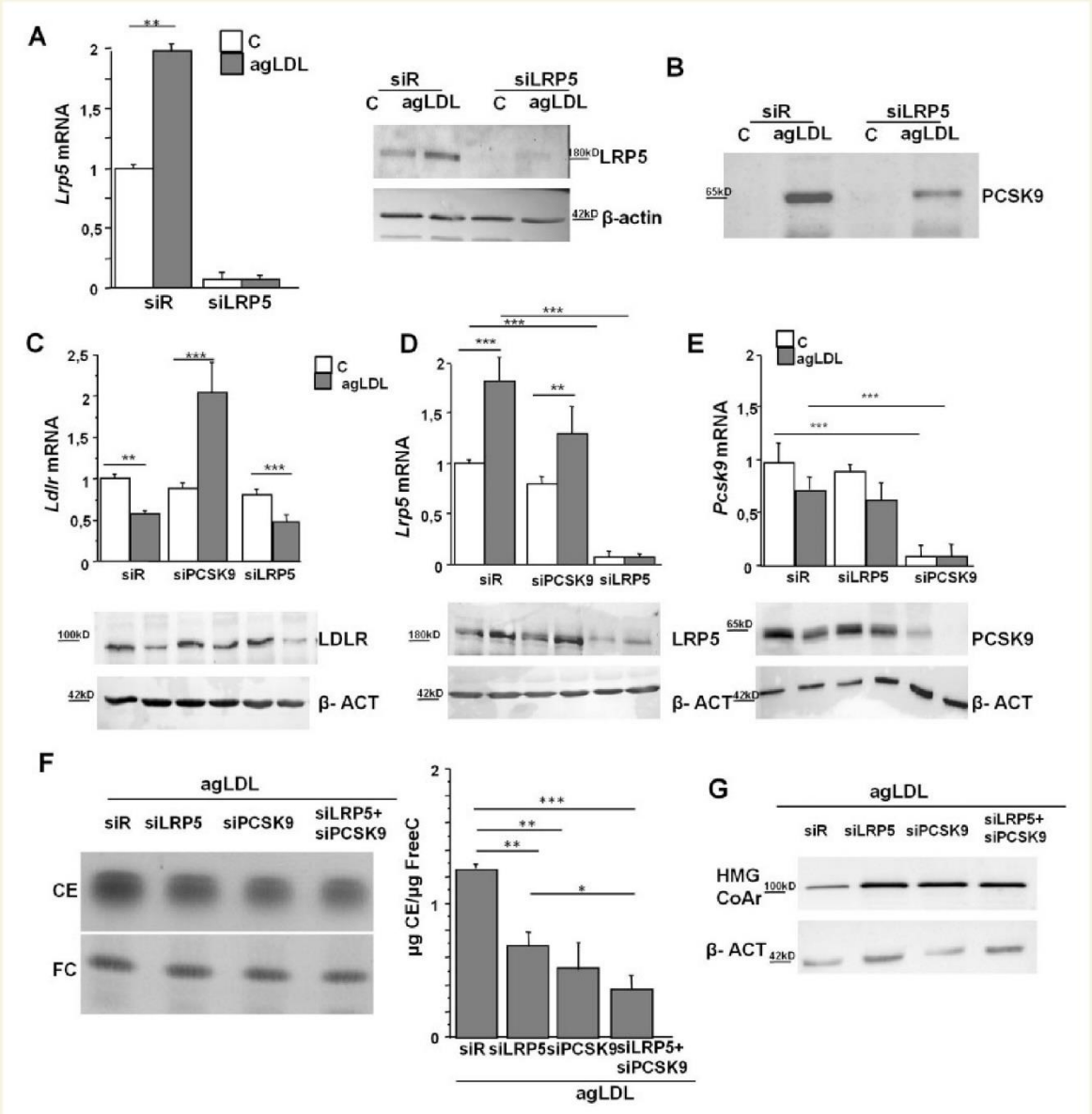

Figure 6 PCSK9 forms a complex with LRP5 in human macrophages. (*A*) LRP5 gene expression human macrophages containing siR or siLRP5 were agLDL-incubated (100 µg/mL) for 24 h and *Lrp5* levels from RNA extracts were quantified by RT-PCR and normalized to 18SrRNA and lysis buffer samples were blotted against LRP5 and *β*-ACTIN Experiments were performed four independent times in duplicates. (*B*) Representative WB of soluble PCSK9 in the supernatants of siR and siLRP5 agLDL-treated human macrophages. (*C*) Human macrophages were incubated with 100 µg/mL agLDL for 24 h. *Ldlr*, (*D*) *Lrp5* and (*E*) *Pcsk9* levels from RNA extracts were quantified by RT-PCR and normalized to 18srRNA. $N = 5$ in duplicates and lysis buffer samples were blotted against LDLR, LRP5, PCSK9, and *β*-ACTIN. (*F*) Human macrophages containing siR, siLRP5, siPCSK9, or both were agLDL-incubated (100 µg/mL) for 24 h and harvested to measure intracellular Free C and CE by TLC. Bar graph showing the quantification of cholesteryl esters respect to Free C. $N = 3$ in duplicates. (*G*) Samples were blotted against HMGCoAr and *β*-ACTIN $^{*}P < 0.01$, $^{**}P < 0.05$, $^{***}P < 0.005$ for treated cells compared with siR-C (ANOVA); (PCSK9-red; LRP5-green; merge-yellow).

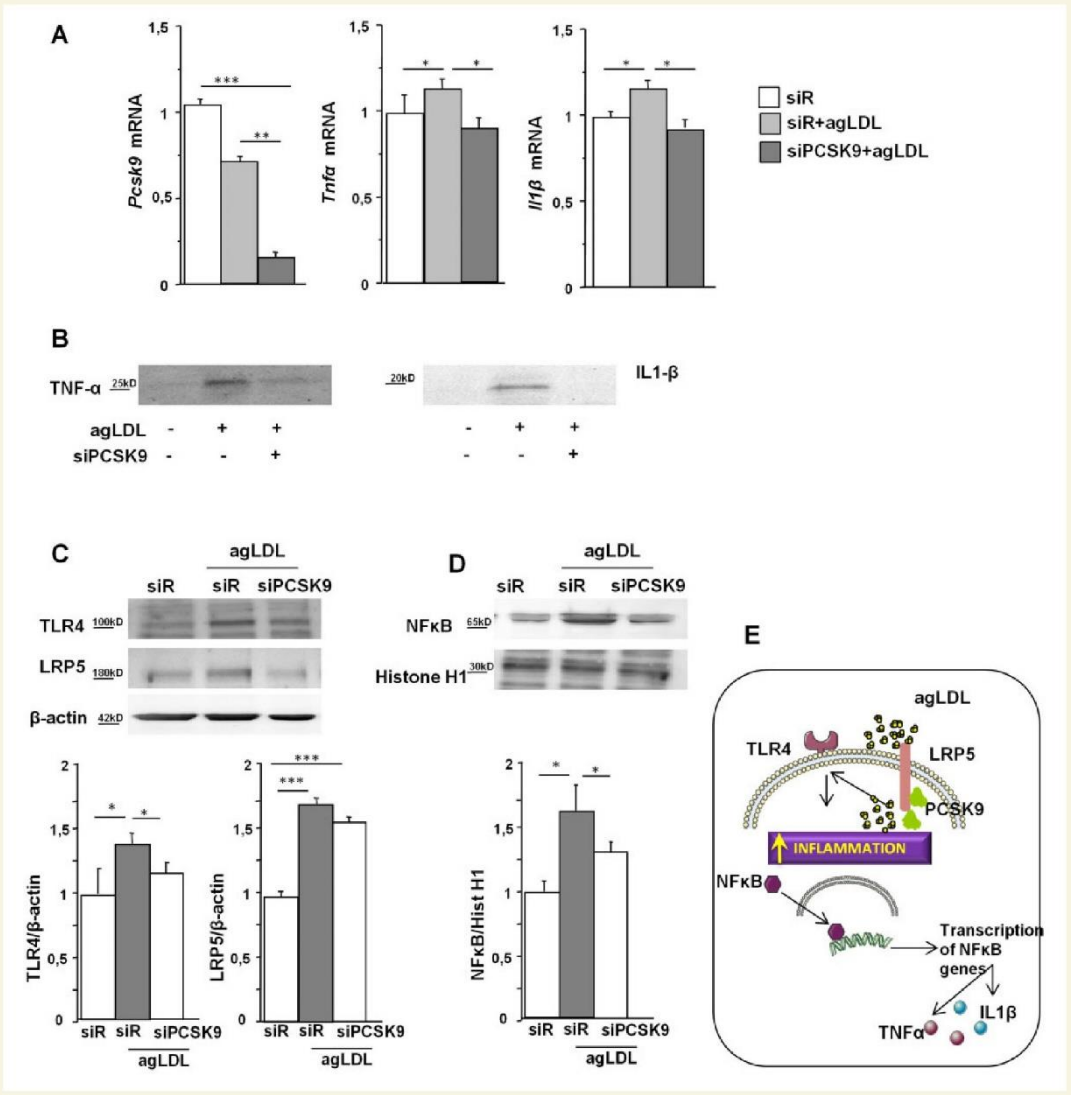

Figure 7 PCSK9 and TLR4 inflammatory pathway. (*A*) Human macrophages containing siRNA-random (siR) or siRNA-PCSK9 (siPCSK9) were agLDL-incubated (100 μg/mL) for 24 h. *Tnfα*, *Il1β*, and *Pcsk9* levels from RNA extracts were quantified by RT-PCR and normalized to 18SrRNA. Experiments were performed three independent times in triplicates. (*B*) Supernatants of human macrophages from (*A*) were blotted against TNF-α or IL1β. (*C*) Representative WB of TLR4 and LRP5 expression levels in total lysates of siR and siPCSK9 treated human macrophages after agLDL treatments. Bar graphs to show the quantification of TLR4 and LRP5 expression levels. (*D*) Level of nuclear NFκB p65 protein measured by WB analyses of human macrophages transfected with SiR or siPCSK9 in the presence or absence of agLDL for 24 h. $N = 4$. (*E*) Schematic showing TLR4/NFκB activation pathway with agLDL internalization by LRP5. $^{*}P < 0.01$, $^{***}P < 0.005$ for treated cells compared with controls (ANOVA).

4. Discussion

Hypercholesterolaemia induces LDL infiltration in the vascular wall. These LDL particles are retained by proteoglycans of the extracellular matrix inducing their modification. These modified lipoproteins are taken up by innate immunity cells and SMC initiating the cellular changes that contribute to the development of atherosclerosis.[9,10,14,26,31–33] In this study, we demonstrate that: (i) low-density lipoproteins strongly upregulate LRP5 in human monocytes and macrophages; (ii) LRP5 is found in the plasma membrane of macrophages, and (iii) after agLDL exposure,

LRP5 is localized in the cytoplasm of macrophages where it colocalizes with intracellular lipids suggesting that LRP5 and lipids are co-internalized. The co-internalization process is further supported by the translocation of LRP5 to the plasma membrane after lipid loading treatments and the induction of CE accumulation in lipid-loaded macrophages that express LRP5 and a decreased lipid uptake in the siLRP5 cells. Contrarily, Wnt3A (a Wnt signalling inducer) is not involved in lipid uptake. Wnt3A effects are limited to the activation of the canonical Wnt pathway as previously described.[28]

Inflammatory cells use SREBP-2 as a sensor for intracellular cholesterol levels. If there is a deficiency of intracellular cholesterol the cell starts producing cholesterol by an SREBP-2 dependent mechanism.[34] In this report, we show that intracellular levels of SREBP-2 decrease in lipid-loaded macrophages. However, in monocytes, SREBP-2 levels are similar in control and in lipid-loaded cells, indicating that SREBP-2 is only functional to intracellular cholesterol levels in macrophages. PCSK9 gene expression was increased in macrophages compared to monocytes indicating a role for PCSK9 in lipid-phagocyting cells as compared to inflammatory monocytes. PCSK9 gene and protein expression were also reduced in macrophages after lipid loading and were unchanged in monocytes, indicating that in macrophages PCSK9 is probably under the regulation of SREBP-2 as observed in mice models of hypercholesterolaemia.[35,36] Interestingly, PCSK9 is released from lipid-loaded macrophages possibly to regulate lipid internalization by a receptor-mediated process including LDLR, VLDLR and members of LRP family, including LRP5.

PCSK9 plasma levels have been described increased in various clinical settings, such as patients with acute myocardial infarction[37] and with coronary plaque inflammation.[38] Less is known about LRP5 but we have previously shown that LRP5 gene and protein expression levels are increased in lipid-loaded macrophages.[14] Here, we show that LRP5 is co-internalized with lipids. Although LRP5 expression is regulated by extracellular lipids,[39,40] our results do not support an involvement of SREBP-2 in LRP5 regulation since siLRP5-macrophages show a downregulation of SREBP-2 activity similar to control macrophages. In addition, macrophages silenced for SREBP-2 show similar LRP5 expression levels than control macrophages.

An interesting finding is that LRP5 and PCSK9 form a complex that immunoprecipitates together. Indeed, intracellular co-localization of LRP5 and PCSK9 was observed at the perinuclear area of human macrophages. Furthermore, LRP5 and PCSK9 can form a complex in the cytoplasm of macrophages and their interaction is stronger in lipid-loaded macrophages. In addition, macrophages silenced for LRP5 show a reduced release of PCSK9 demonstrating a role for LRP5 in PCSK9's transport to the plasma membrane. These results are also supported by the observed reduction in macrophage CE accumulation in the absence of PCSK9 and/or LRP5. Indeed, siRNA-PCSK9 THP-1-derived macrophages show less intracellular cholesterol accumulation after incubation with oxidized LDL for 24 h than control macrophages.[41] Also, severe aortic lesions and higher cholesterol accumulation are observed in overexpressing PCSK9 mice compared to wide-type controls. In contrast, PCKS9-knockout mice showed four-fold less aortic cholesterol than wild-type controls.[42] In this work, we take a step further and show that when both proteins are absent intracellular CE in the macrophage is drastically reduced, supporting an interaction of both proteins in the internalization of cholesterol from agLDL in innate immunity cells. A limitation of this study is that agLDL particle number was not measured; however, always the same procedure was followed to prepare agLDL and only the precipitated fraction composed of 100% agLDL was added to cell cultures.

Gain-of-function mutations in PCSK9 promote the progression of intima-media thickness[43] and plasma PCSK9 concentration is increased in atherosclerotic plaques.[44] Indeed, in patients with coronary artery disease, anti-PCSK9 antibodies in addition to statin therapy resulted in greater decreases in atheroma burden than statin therapy alone.[45] The FOURIER study showed that administration of PCSK9 inhibitors drastically reduced LDL cholesterol levels from the bloodstream leading to reduced myocardial infarction, stroke, and cardiovascular death.[7] The ODYSSEY OUTCOMES showed similar results in patients who had a more recent previous acute coronary syndrome.[8]

We studied the role of PCSK9 in macrophage inflammation through TLR4/NFkB signalling pathway. We show decreased TLR4 protein expression levels and decreased nuclear translocation of NFκB in PCSK9 silenced-inflammatory cells after lipid loading indicating a downregulation of the proinflammatory pathway TLR4/NFκB. Also, the increased *Tnfα* and *Il1β* expression observed after lipid loading is abolished in PCSK9-silenced macrophages. Furthermore, the release of the proinflammatory cytokines TNF-α and IL1β was decreased in PCSK9-silenced macrophages supporting the role of PCSK9 in increasing human inflammatory signalling. Interestingly, protein levels of both LRP5 and PCSK9 are increased in atherosclerotic plaques and their expression is very low in healthy aortas.[21,46,47]

In conclusion, our results show that both PCSK9 and LRP5 contribute to lipid uptake; that although PCSK9 does not regulate LRP5 levels, it does form an intracellular complex with LRP5; that LRP5 participates in PCSK9 transport to the plasma membrane and that PCSK9 inhibition protects against agLDL-induced inflammation associated with the TLR4/NFκB pathway.

Data availability statement

The data underlying this article are available in the article and in its online supplementary material.

Supplementary material

Supplementary material is available at *Cardiovascular Research* online.

Acknowledgements

We thank S. Huertas, M. A. Velasco and S. Florit for excellent technical assistance.

Conflict of interest: none declared.

Funding

This work was supported by the Spanish Ministry of Science and Innovation and FEDER funds (SAF2016-76819-R to L.B.); the Instituto de Salud Carlos III (CIBERCV CN16/11/00411 to LB, TERCEL RD16/0011/018 to L.B., and FIS2020-01282 to M.B-P.); the Generalitat of Catalunya-Secretaria d'Universitats i Recerca del Departament d'Economia i Coneixement de la Generalitat (2014SGR1303 to L.B.; PERIS SLT006 to L.B.) and the Spanish Society of Cardiology (FEC2019 to M.B-P.).

References

1. Jeon H, Blacklow SC. Structure and physiologic function of the low-density lipoprotein receptor. *Annu Rev Biochem* 2005;**74**:535–562.
2. Schmidt RJ, Beyer TP, Bensch WR, Qian Y-W, Lin A, Kowala M, Alborn WE, Konrad RJ, Cao G. Secreted proprotein convertase subtilisin/kexin type 9 reduces both hepatic and extrahepatic low-density lipoprotein receptors in vivo. *Biochem Biophys Res Commun* 2008;**370**:634–640.
3. Walley KR, Thain KR, Russell JA, Reilly MP, Meyer NJ, Ferguson JF, Christie JD, Nakada TA, Fjell CD, Thair SA, Cirstea MS, Boyd JH. PCSK9 is a critical regulator of the innate immune response and septic shock outcome. *Sci Transl Med* 2014;**6**:258.
4. Lambert G, Chariton F, Rye KA, Piper DE. Molecular basis of PCSK9 function. *Atherosclerosis* 2009;**203**:1–7.
5. Poirier S, Mayer G, Poupon V, McPherson PS, Desjardins R, Ly K, Asselin MC, Day R, Duclos FJ, Witmer M, Parker R, Prat A, Seidah NG. Dissection of the endogenous cellular pathways of PCSK9-induced LDL receptor degradation: evidence for an intracellular route. *J Biol Chem* 2009;**284**:28856–28864.
6. Li S, Guo YL, Xu RX, Zhang Y, Zhu CG, Sun J, Qing P, Wu NQ, Jiang LX, Li JJ. Association of plasma PCSK9 levels with white blood cell count and its subsets in patients with stable coronary artery disease. *Atherosclerosis* 2014;**234**:441–445.
7. Sabatine MS, Giugliano RP, Keech AC, Honarpour N, Wiviott SD, Murphy SA, Kuder JF, Wang H, Liu T, Wasserman SM, Sever PS, Pedersen TR; FOURIER Steering Committee and Investigators. Evolocumab and clinical outcomes in patients with cardiovascular disease. *N Engl J Med* 2017;**376**:1713–1722.
8. Schwartz GG, Steg PG, Szarek M, Bhatt DL, Bittner VA, Diaz R, Edelberg JM, Goodman SG, Hanotin C, Harrington RA, Jukema JW, Lecorps G, Mahaffey KW, Moryusef A, Pordy R, Quintero K, Roe MT, Sasiela WJ, Tamby JF, Tricoci P, White HD, Zeiher AM; ODYSSEY OUTCOMES Committees and Investigators. Alirocumab and cardiovascular outcomes after acute coronary syndrome. *N Engl J Med* 2018;**379**:2097–2107.
9. Badimon L, Vilahur G. Thrombosis formation on atherosclerotic lesions and plaque rupture. *J Intern Med* 2014;**276**:618–632.
10. Fuster V, Badimon L, Badimon JJ, Chesebro JH. The pathogenesis of coronary artery disease and the acute coronary syndromes (1). *N Engl J Med* 1992;**23**:242–250.
11. Hurt-Camejo E, Olsson U, Wiklund O, Bondjers G, Camejo G. Cellular consequences of the association of apoB lipoproteins with proteoglycans. Potential contribution to atherogenesis. *Arterioscler Thromb Vasc Biol* 1997;**17**:1011–1017.
12. Llorente-Cortés V, Otero-Viñas M, Camino-López S, Costales P, Badimon L. Cholesteryl esters of aggregated-LDL are internalized by selective uptake in HVSMC. *Arterioscler Thromb Vasc Biol* 2006;**26**:117–123.
13. Hiltunen TP, Luoma JS, Nikkari T, Ylä-Herttuala S. Expression of LDL-receptor, VLDL-receptor, LDL-receptor-related protein, and scavenger receptor in rabbit atherosclerotic lesions: marked induction of scavenger receptor and VLDL-receptor expression during lesion development. *Circulation* 1998;**97**:1079–1086.
14. Borrell-Pagès M, Romero JC, Juan-Babot O, Badimon L. Wnt pathway activation, cell migration, and lipid uptake is regulated by low-density lipoprotein receptor-related protein 5 in human macrophages. *Eur Heart J* 2011;**32**:2841–2850.
15. Llorente-Cortes V, Royo T, Otero-Vinas M, Berrozpe M, Badimon L. Sterol regulatory element binding proteins downregulate LRP1 expression and LRP1-mediated aggregated LDL uptake by human macrophages. *Cardiovasc Res* 2007;**74**:526–536.
16. Caminolopez S, Llorentecortes V, Sendra J, Badimon L. Tissue factor induction by aggregated LDL depends on LDL receptor-related protein expression (LRP1) and Rho A translocation in human vascular smooth muscle cells. *Cardiovasc Res* 2007;**73**:208–216.
17. Arderiu G, Espinosa S, Peña E, Crespo J, Aledo R, Bogdanov VY, Badimon L. Tissue factor variants induce monocyte transformation and transdifferentiation into endothelial cell-like cells. *J Thromb Haemost* 2017;**15**:1689–1703.
18. Li Y, Bu G. LRP5, a multifunctional cell surface receptor. *Curr Opin Lipidol* 2004;**3**:361–363.
19. Logan CY, Nusse R. The Wnt signalling pathway in development and disease. *Annu Rev Cell Dev Biol* 2004;**20**:781–810.
20. Ding Z, Liu S, Wang X, Theus S, Deng X, Fan Y, Zhou S, Mehta JL. PCSK9 regulates expression of scavenger receptors and ox-LDL uptake in macrophages. *Cardiovasc Res* 2018;**114**:1145–1153.
21. Ferri N, Tibolla G, Pirillo A, Cipollone F, Mezzetti A, Pacia S, Corsini A, Catapano AL. Proprotein convertase subtilisin kexin type 9 (PCSK9) secreted by cultured smooth muscle cells reduces macrophages LDLR levels. *Atherosclerosis* 2012;**220**:381–386.
22. Awan Z, Denis M, Bailey D, Giaid A, Prat A, Goltzman D, Seidah NG, Genest J. The LDLR deficient mouse as a model for aortic calcification and quantification by microcomputed tomography. *Atherosclerosis* 2011;**219**:455–462.
23. Giunzioni I, Tavori H, Covarrubias R, Major AS, Ding L, Zhang Y, DeVay RM, Hong L, Fan D, Predazzi IM, Rashid S, Linton MF, Fazio S. Local effects of human PCSK9 on the atherosclerotic lesion. *J Pathol* 2016;**238**:52–62.
24. Llorente-Cortés V, Martínez-González J, Badimon L. LDL receptor-related protein mediates uptake of aggregated LDL in human vascular smooth muscle cells. *Arterioscler Thromb Vasc Biol* 2000;**20**:1572–1579.
25. Llorente-Cortés V, Otero-Viñas M, Camino-López S, Llampayas O, Badimon L. Aggregated low-density lipoprotein uptake induces membrane tissue factor procoagulant activity and microparticle release in human vascular smooth muscle cells. *Circulation* 2004;**110**:452–459.
26. Llorente-Cortés V, Martínez-González J, Badimon L. Esterified cholesterol accumulation induced by aggregated LDL uptake in human vascular smooth muscle cells is reduced by HMG-CoA reductase inhibitors. *Arterioscler Thromb Vasc Biol* 1998;**18**:738–746.
27. Asmis R, Llorente VC, Gey KF. Prevention of cholesteryl ester accumulation in P388D1 macrophage-like cells by increased cellular vitamin E depends on species of extracellular cholesterol. Conventional heterologous non-human cell cultures are poor models of human atherosclerotic foam cell formation. *Eur J Biochem* 1995;**233**:171–178.
28. Schaale K, Neumann J, Schneider D, Ehlers S, Reiling N. Wnt signaling in macrophages: augmenting and inhibiting mycobacteria-induced inflammatory responses. *Eur J Cell Biol* 2011;**90**:553–559.
29. Llorente-Cortés V, Royo T, Juan-Babot O, Badimon L. Adipocyte differentiation-related protein is induced by LRP1-mediated aggregated LDL internalization in human vascular smooth muscle cells and macrophages. *J Lipid Res* 2007;**48**:2133–2140.
30. Sekar N, Veldhuis JD. Involvement of Sp1 and SREBP-1a in transcriptional activation of the LDL receptor gene by insulin and LH in cultured porcine granulosa-luteal cells. *Am J Physiol Endocrinol Metab* 2004;**287**:E128–135.
31. Tertov VV, Orekhov AN, Sobenin IA, Gabbasov ZA, Popov EG, Yaroslavov AA, Smirnov VN. Three types of naturally occurring modified lipoproteins induce intracellular lipid accumulation due to lipoprotein aggregation. *Circ Res* 1992;**71**:218–228.
32. Sakr SW, Eddy RJ, Barth H, Wang F, Greenberg S, Maxfield FR, Tabas I. The uptake and degradation of matrix-bound lipoproteins by macrophages require an intact actin Cytoskeleton, Rho family GTPases, and myosin ATPase activity. *J Biol Chem* 2001;**276**:37649–37658.
33. Morita SY, Kawabe M, Sakurai A, Okuhira K, Vertut-Doi A, Nakano M, Handa T. Ceramide in lipid particles enhances heparan-sulfate proteoglycan and low-density-lipoprotein-receptor-related protein-mediated uptake by macrophages. *J Biol Chem* 2004;**279**:24355–24361.
34. Brown MS, Goldstein JL. The SREBP pathway: regulation of cholesterol metabolism by proteolysis of a membrane-bound transcription factor. *Cell* 1997;**89**:331–340.
35. Sui GG, Xiao HB, Lu XY, Sun ZL. Naringin activates AMPK resulting in altered expression of SREBPs, PCSK9, and LDLR to reduce body weight in obese C57BL/6J mice. *J Agric Food Chem* 2018;**66**:8983–8990.
36. Chae HS, You BH, Kim DY, Lee H, Ko HW, Ko HJ, Choi YH, Choi SS, Chin YW. Sauchinone controls hepatic cholesterol homeostasis by the negative regulation of PCSK9 transcriptional network. *Sci Rep* 2018;**8**:6737.
37. Almontashiri NA, Vilmundarson RO, Ghasemzadeh N, Dandona S, Roberts R, Quyyumi AA, Chen HH, Stewart AF. Plasma PCSK9 levels are elevated with acute myocardial infarction in two independent retrospective angiographic studies. *PLoS One* 2014;**9**:e106294.
38. Cheng JM, Oemrawsingh RM, Garcia-Garcia HM, Boersma E, van Geuns RJ, Serruys PW, Kardys I, Akkerhuis KM. PCSK9 in relation to coronary plaque inflammation: results of the ATHEROREMO-IVUS study. *Atherosclerosis* 2016;**248**:117–122.
39. Borrell-Pages M, Carolina Romero J, Badimon L. LRP5 and plasma cholesterol levels modulate the canonical Wnt pathway in peripheral blood leukocytes. *Immunol Cell Biol* 2015;**93**:653–661.
40. Borrell-Pages M, Romero JC, Badimon L. Cholesterol modulates LRP5 expression in the vessel wall. *Atherosclerosis* 2014;**235**:363–370.
41. Tang Z, Jiang L, Peng J, Ren Z, Wei D, Wu C, Pan L, Jiang Z, Liu L. PCSK9 siRNA suppresses the inflammatory response induced by oxLDL through inhibition of NF-κB activation in THP-1-derived macrophages. *Int J Mol Med* 2012;**30**:931–938.
42. Denis M, Marcinkiewicz J, Zaid A, Gauthier D, Poirier S, Lazure C, Seidah NG, Prat A. Gene inactivation of proprotein convertase subtilisin/kexin type 9 reduces atherosclerosis in mice. *Circulation* 2012;**125**:894–901.
43. Norata GD, Garlaschelli K, Grigore L, Raselli S, Tramontana S, Meneghetti F, Artali R, Noto D, Cefalu AB, Buccianti G, Averna M, Catapano AL. Effects of PCSK9 variants on common carotid artery intima media thickness and relation to ApoE alleles. *Atherosclerosis* 2010;**208**:177–182.
44. Lee CJ, Lee YH, Park SW, Kim KJ, Park S, Youn JC, Lee SH, Kang SM, Jang Y. Association of serum proprotein convertase subtilisin/kexin type 9 with carotid intima media thickness in hypertensive subjects. *Metabolism* 2013;**62**:845–850.
45. Nicholls SJ, Puri R, Anderson T, Ballantyne CM, Cho L, Kastelein JJ, Koenig W, Somaratne R, Kassahun H, Yang J, Wasserman SM, Scott R, Ungi I, Podolec J, Ophuis AO, Cornel JH, Borgman M, Brennan DM, Nissen SE. Effect of evolocumab on progression of coronary disease in statin-treated patients: the GLAGOV randomized clinical trial. *JAMA* 2016;**316**:2373–2384.

46. Borrell-Pages M, Romero JC, Crespo J, Juan-Babot O, Badimon L. LRP5 associates with specific subsets of macrophages: molecular and functional effects. *J Mol Cell Cardiol* 2016;**90**:146–156.

47. Ding Z, Liu S, Wang X, Deng X, Fan Y, Shahanawaz J, Shmookler Reis RJ, Varughese KI, Sawamura T, Mehta JL. Cross-talk between LOX-1 and PCSK9 in vascular tissues. *Cardiovasc Res* 2015;**107**:556–567.

Translational perspective

We demonstrate that PCSK9 and LRP5 contribute to lipid uptake. We also show that LRP5 participates in PCSK9 transport to the plasma membrane and that PCSK9 inhibition protects against agLDL-induced inflammation associated with the TLR4/NFκB pathway. These results offer new targets to prevent the progression of inflammation and hypercholesterolaemia and their increased risk of cardiovascular events.

Supplemental Figure 1

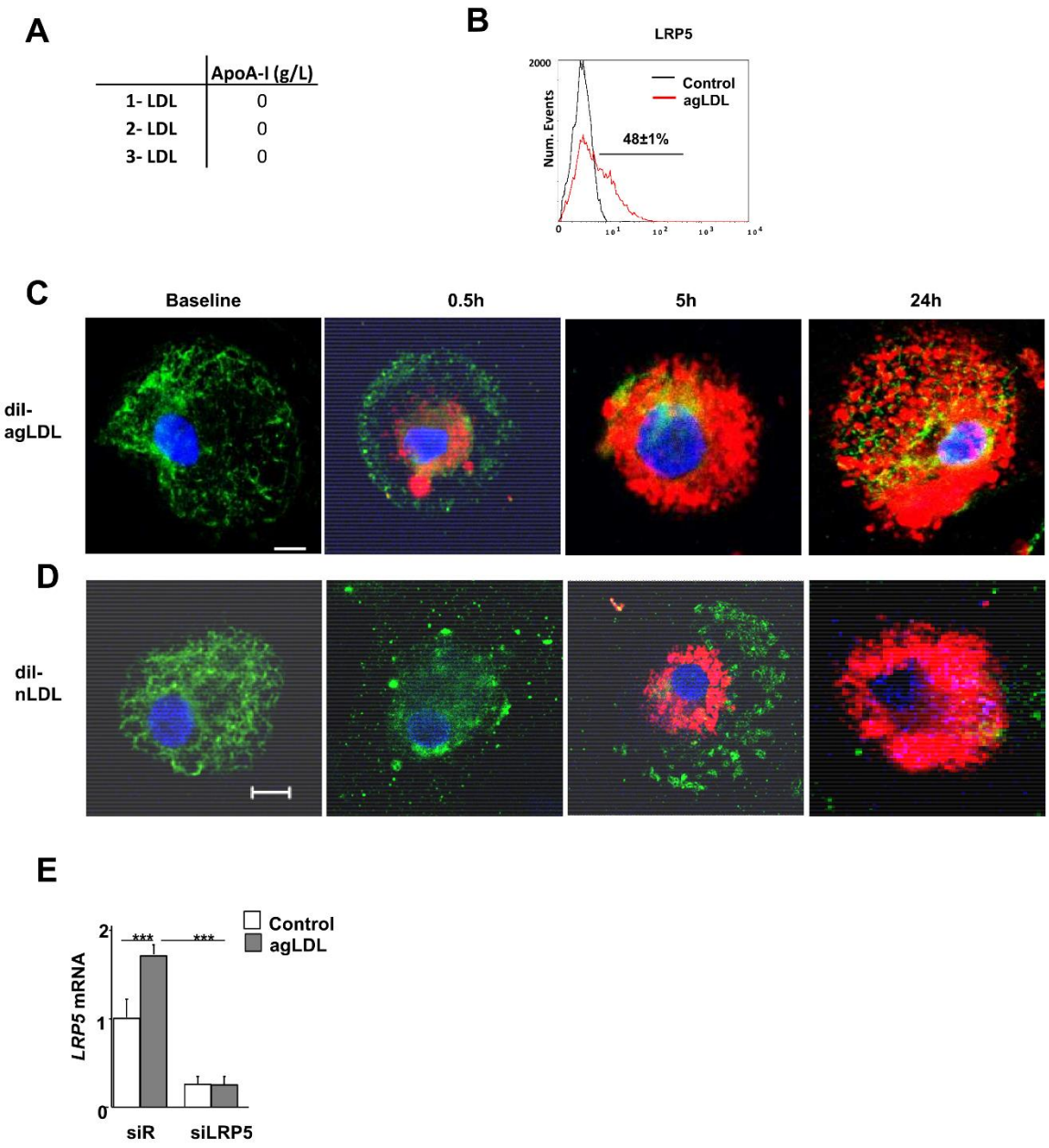

Supplemental Figure 1: LRP5 participates in lipid internalization in human macrophages. A) ApoA content measured by COBAS 501 in 3 independent LDL samples. **B)** Human macrophages were incubated or not with 100µg/ml agLDL for 5h when flow cytometry analysis of LRP5 expression was performed. **C)** dil was conjugated to agLDL or **D)** nLDL; human macrophages were treated for the indicated times and stained with LRP5 antibody. N=4 in duplicates. Bar 5µm. **E)** LRP5 gene expression human macrophages containing siRNA-Random (siR) or siRNA-LRP5 (siLRP5) were agLDL-incubated (100 µg/mL) for 24 h and *Lrp5* levels from RNA extracts were quantified by RT-PCR and normalized to 18SrRNA. ***P < 0.005 .

Supplemental Figure 2

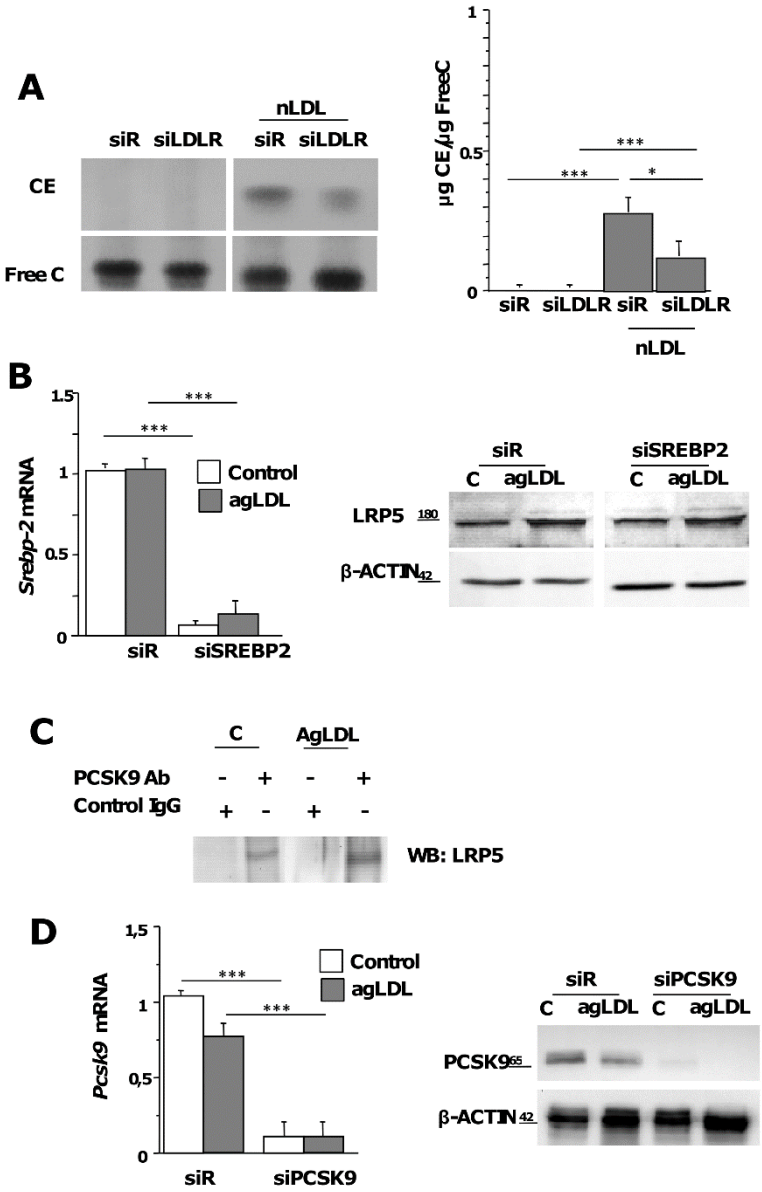

Supplemental Figure 2: LRP5 is not under SREBP-2 control. A) Human macrophages containing siRNA-Random (siR) or siRNA-LDLR (siLDLR) were incubated with native LDL (nLDL;100 µg/mL). TLC and Bar graphs are shown. N=5 in duplicates. **B)** *Srebp-2* gene expression in human macrophages containing siRNA-Random (siR) or siRNA-SREBP-2 (siSREBP2) were agLDL-incubated (100 µg/mL) for 24 h and *Srebp-2* levels from RNA extracts were quantified by RT-PCR and normalized to 18SrRNA. Experiments were performed three independent times in triplicates. Same samples were blotted against LRP5 or β actin. **C)** Human macrophages were treated with 100µg/mL agLDL, and IP with PCSK9 antibody or unspecific IgG before WB against LRP5 was performed. N=5 . *P < 0.01, ***P < 0.005

3.3 Article 2

Differential cholesterol uptake in liver cells: a role for PCSK9

By Aureli Luquero, Gemma Vilahur, Laura Casani, Lina Badimon and Maria Borrell-Pagès.

Published in The FASEB Journal. 2022 March 22;36:e22291.

DOI: 10.1096/fj.202101660RR

Summary: The liver regulates blood cholesterol levels by the clearance of LDL particles from the blood by hepatocyte's LDLR. PCSK9 regulates LDLR expression at the hepatocyte's plasma membrane and reduces lipid clearance from blood increasing systemic cholesterol levels. The interaction between LDLR and PCSK9 occurs by PCSK9's ability to bind the EGF-A like domain of LDLR. This domain is conserved in other receptors of the LDLR superfamily, raising the hypothesis that PCSK9 could be interacting with them too. *Wt* and *Lrp5*$^{-/-}$ mice were fed a normocholesterolemic (NC) or hypercholesterolemic (HC) diet to induce hypercholesterolemia. Results showed similar cholesteryl ester content in livers from HC *Wt* and HC *Lrp5*$^{-/-}$ mice. However, their lipid receptor profile was different. While HC *Wt* mice displayed high expression levels of VLDLR, LRP6 and LRP2, HC *Lrp5*$^{-/-}$ mice livers showed upregulation of the scavenger receptors SR-BI and CD36. Coimmunoprecipitation analysis indicated a lack of interaction between VLDLR, LRP2, LRP5, and LRP6 with PCSK9. Contrarily to the results observed in macrophages, lipid treatment in structural hepatocytes (HepG2 cells) did not induce PCSK9 release to the medium. Furthermore, PCSK9 and LRP5 did not interact in hepatocytes challenged with agLDL. We then analysed HSC (the liver's fat storing cells) response to lipid treatment and observed increased LRP5 expression and reduced PCSK9 expression levels. Coimmunoprecipitation studies in HSCs showed that LRP5 and PCSK9 bind intracellularly after lipid-loading. Additionally,

HSC lipid-loading triggered the release of PCSK9 into the extracellular medium. Gene silencing of LRP5 or PCSK9 led to reduced cholesteryl ester accumulation in HSCs, indicating that both proteins are needed for lipid uptake in HSC. This study shows that the interaction of LRP5 and PCSK9 is cell-specific and that both proteins contribute to HSC lipid uptake.

Received: 29 October 2021 | Revised: 11 March 2022 | Accepted: 20 March 2022

DOI: 10.1096/fj.202101660RR

THE FASEB JOURNAL

RESEARCH ARTICLE

Differential cholesterol uptake in liver cells: A role for PCSK9

Aureli Luquero[1] | **Gemma Vilahur**[1,2] | **Laura Casani**[1] | **Lina Badimon**[1,2,3] | **Maria Borrell-Pages**[1,2]

[1]Cardiovascular Program ICCC, Hospital de la Santa Creu i Sant Pau Research Institute, IIB-Sant Pau, Barcelona, Spain

[2]CIBER-CV, Instituto de Salud Carlos III, Spain

[3]Cardiovascular Research Chair, UAB, Barcelona, Spain

Correspondence
Maria Borrell-Pages, Cardiovascular Program ICCC, IR-Hospital de la Santa Creu i Sant Pau, C/Sant Antoni Maria Claret 167, Barcelona 08025, Spain.
Email: mborrellpa@santpau.cat

Funding information
Ministerio de Ciencia e Innovación (MICINN), Grant/Award Number: PID2019-107160RB-I00 and PGC 2018-094025-B-I00; MINECO | Instituto de Salud Carlos III (ISCIII), Grant/Award Number: CIBERCV CB16/11/00411, TERCEL RD16/0011/018 and FIS2020-01282; Generalitat de Catalunya (Government of Catalonia), Grant/Award Number: 2017SGR1480; Sociedad Española de Cardiología (Spanish Society of Cardiology), Grant/Award Number: FEC2019 and FEC2020; Government of Catalonia | Agència de Gestió d'Ajuts Universitaris i de Recerca (AGAUR), Grant/Award Number: 2016PROD00043

Abstract

The clearance of low-density lipoprotein (LDL) particles from the circulation is regulated by the LDL receptor (LDLR) and proprotein convertase subtilisin/kexin 9 (PCSK9) interaction. Its disruption reduces blood cholesterol levels and delays atherosclerosis progression. Whether other members of the LDLR superfamily are *in vivo* targets of PCSK9 has been poorly explored. The aim of this work was to study the interaction between PCSK9 and members of the LDLR superfamily in the regulation of liver cholesterol homeostasis in an in vivo low-density lipoprotein receptor related protein 5 (LRP5) deficient mice model challenged with high-fat diet. Our results show that *Wt* and *Lrp5*$^{-/-}$ mice fed a hypercholesterolemic diet (HC) have increased cholesterol ester accumulation and decreased liver LDLR and LRP5 gene and protein expression. Very low-density lipoprotein receptor (VLDLR), LRP6, LRP2, and LRP1 expression levels were analyzed in liver samples and show that they do not participate in *Lrp5*$^{-/-}$ liver cholesterol uptake. Immunoprecipitation experiments show that LRP5 forms a complex with PCSK9 in liver-specific fat-storing stellate cells but not in structural HepG2 cells. Hepatic stellate cells silenced for LRP5 and/or PCSK9 expression and challenged with lipids show reduced cholesterol ester accumulation, indicating that both proteins are involved in lipid processing in the liver. Our results indicate that cholesterol esters accumulate in livers of *Wt* mice in a LDLR-family-members dependent manner as VLDLR, LRP2, and LRP6 show increased expression in HC mice. However, this increase is lost in livers of *Lrp5*$^{-/-}$ mice, where scavenger receptors are involved in cholesterol uptake. PCSK9 expression is strongly downregulated in mice livers after HC feeding. However PCSK9 and LRP5 bind in the cytoplasm of fat storing liver cells, indicating that this PCSK9-LRP5 interaction is cell-type specific and that both proteins contribute to lipid uptake.

Abbreviations: agLDL, aggregated low-density lipoprotein; CE, cholesterol esters; FC, free cholesterol; HDL, high-density lipoprotein; HSCs, hepatic stellate cells; LDL, low-density lipoprotein; LDLR, low-density lipoprotein receptor; LRP5, low-density lipoprotein receptor related protein 5; PCSK9, proprotein convertase subtilisin/kexin 9; SRBI, scavenger receptor class B, type 1; SREBP-2, sterol regulatory element-binding protein 2; TLC, thin layer chromatography; VLDL, very low-density lipoprotein; VLDLR, very low-density lipoprotein receptor; VSMCs, vascular smooth muscle cells.

KEYWORDS
cholesterol uptake, hepatic stellate cells, liver, LRP5, PCSK9

1 | INTRODUCTION

One of the main causal factors of atherosclerosis is hypercholesterolemia. Because cholesterol is a highly insoluble molecule, it has to be transported in the circulation in the form of lipoproteins that include low-density lipoprotein (LDL), very low-density lipoprotein (VLDL), and high-density lipoprotein (HDL).[1] Cholesterol balance variations that lead to low plasma HDL and high plasma LDL increase the risk for CVD. Therefore, efficient strategies to protect against CVDs are interventions that focus on down-regulating plasma LDL levels. Cholesterol homeostasis is regulated by the liver.[2] LDL receptor (LDLR) expressed in the liver mediates LDL uptake from the circulation by endocytosis.[3] Hence, to maintain a correct cholesterol balance, it is crucial to maintain optimal LDLR levels.[4] LDLR levels are controlled, at transcriptional levels by sterol regulatory element-binding protein 2 (SREBP-2) and post-transcriptionally by proprotein convertase subtilisin/kexin 9 (PCSK9), a circulating protein that can reduce the amount of LDLR in hepatocytes by promoting LDLR to degradation in the lysosomes, rather than its recycling to the plasma membrane.[5–7] LDLR degradation is prevented by PCSK9 inhibition that causes more expression of LDLR in hepatocytes cell membranes to facilitate LDL clearance. Thus, by virtue of its role as a major inhibitor of the LDLR, PCSK9 inhibitors have been developed as novel drugs for CVDs.[8,9] Indeed, in patients with coronary artery disease, anti-PCSK9 antibodies in addition to statin therapy resulted in greater decreases in atheroma burden, compared with statins alone.[10–12]

Correct lipoprotein transport and plasma cholesterol clearance can also involve other members of the LDLR superfamily besides LDLR.[13,14] Lipid accumulation in aortas is not facilitated by LDLR because excess cholesterol downregulates its expression in the vessel wall; instead, other receptors including scavenger receptors[15] and low-density lipoprotein receptor-related proteins including LRP1[16] and low-density lipoprotein receptor related protein 5 (LRP5)[17] are involved in vessel wall lipid accumulation. We have recently demonstrated that LRP5 regulates cell mobility and human macrophage binding to extracellular lipids activating canonical Wnt signaling.[17] Indeed, extracellular Wnt glycoproteins or circulating lipids bind to the LRP5-frizzled complex stabilizing cytoplasmic β-catenin and leading to the translocation of β-catenin into the nucleus, where it activates the TCF/LEF1 family of transcriptional factors to promote target gene transcription.[18,19] LRP5 is also involved in the induction of macrophage apoptosis and in the differentiation of monocytes into macrophages by the induction of the canonical Wnt pathway.[20] Additionally, arterial LRP5 can be modulated by plasma lipid levels in mice fed a high-fat diet and a reduction in LRP5 arterial protein levels reduces cholesterol ester content in atherosclerotic plaques.[21–23]

Interestingly, the overexpression of PCSK9 in *Ldlr*$^{-/-}$ mice showed increased aortic calcification by a mechanism dependent on LRP5/canonical Wnt signaling suggesting a participation of LRP5 in PCSK9 activity.[24] Other members of the LDLR superfamily are known targets of PCSK9. Indeed, PCSK9 degrades very low-density lipoprotein receptor (VLDLR) and LRP1 in a fashion similar to the manner in which it degrades LDLR,[25–27] and in mice neurons, PCSK9 interacts with the apolipoprotein E Receptor 2 (LRP8) to regulate apoptosis.[28] These results show that there is a relationship between PCSK9 and the LRP-family of receptors that is still poorly understood, and that the role of LRPs during PCSK9 inhibition therapy is largely unknown. It seems that members of the LDLR super-family may be targets of PCSK9, and it is plausible that PCSK9 has a direct role in foam cell formation and hence in the mechanism of lipid accumulation and atherosclerotic plaque progression. Indeed, we have recently shown that in the absence of LRP5, there is a reduced release of PCSK9, indicating that LRP5 participates in PCSK9 release to the plasma membrane in the primary cultures of human macrophages.[29] However, the in vivo consequences of the interaction between LRP5 and PCSK9 have still not been addressed.

We hypothesized that members of the LDLR family that participate in liver cholesterol homeostasis are targets of PCSK9. Here, we have investigated the role of PCSK9 and members of the LDLR superfamily in liver regulation of plasma cholesterol in an in vivo *Lrp5* deficient mice model challenged with high-fat diet.

2 | MATERIALS AND METHODS

2.1 | Animal models and experimental design

The study protocols for mice were approved by the institutional Animal Care and Use Committee (ICCC051/5422) and authorized by the local government commission. All animal procedures conform the

guidelines from Directive 2010/63/EU of the European Parliament and the "Position of the American Heart Association on Research Animals use" (November 11, 1984). At the IR, we are committed to the "3Rs" principle, and hence, we used the minimum of animals required to achieve statistical significance.

Lrp5$^{-/-}$ mice, a kind gift from Dr. Bart William[30,31] were maintained in a C57BL/6 background. Mice were housed in cages under controlled temperature (21 ± 2°C) on a 12h light/dark cycle with food and water ad libitum. Homozygous wild-type C57BL/6 mice (*Wt*; $n = 24$) and LRP5 knockout C57BL/6 mice (*Lrp5*$^{-/-}$; $n = 24$) were used for the protocols. The presence of LRP5 alleles was assessed by PCR amplification from DNA extracted from tail biopsies in *Wt*, *Lrp5*$^{-/+}$ and *Lrp5*$^{-/-}$ littermates. *Wt* and *Lrp5*$^{-/-}$ mice were fed a normal chow diet (NC; Tekland diet, Harlan Labs, Berkeley, CA, USA) for 10 weeks. Animals were then divided into 2 groups to be fed with NC or western-type cafeteria diet with high cholesterol (HC, TD.88137, Harlan Labs) for further 8 weeks ($n = 8$–12/group). Cardiac puncture was performed in mice under terminal anesthesia (1 mg/kg Medetomidine and 75 mg/kg Ketamine, ip).

In accordance with the guidelines from the "International Committee on Standardized Genetic Nomenclature for Mice and the Rat Genome", 2010, genes are written in italics and capital letter (*Lrp5*) and proteins in straight block letters (LRP5).

2.2 | Determination of free and esterified cholesterol content

Liver tissues (5 mg) were homogenized in NaOH 0.1 N. Lipid extraction and thin layer chromatography were performed as previously described.[32,33] Briefly, one aliquot of the cell suspension was extracted with methanol/dichloromethane (2:1, vol/vol). After solvent removal under an N_2 steam, the lipid extract was dissolved in dichloromethane, and one aliquot was partitioned by thin layer chromatography (TLC), which was performed on silica G-24 plates. Three different concentrations of standards (a mixture of cholesterol and cholesterol palmitate) were applied to each plate. The chromatographic developing solution was heptane/diethyl ether/acetic acid (74:21:4, vol/vol/vol). Plates were then stained with 26 mM/47.62 g/L molybdophosphoric acid solution of absolute ethanol/absolute sulfuric acid (95:5, vol/vol) for 1 min. After air drying, TLC plaques were heated at 100°C for 7 min. The spots corresponding to cholesteryl ester and free cholesterol (FC) were quantified by densitometry against the standard curve of cholesterol and cholesterol palmitate respectively, with the use of a computing densitometer (Molecular Dynamics).

Human hepatic stellate cells (HSCs) were provided by Innoprot and isolated by ScienCell Research Laboratories (Carlsbad, CA) from human liver. Human HSCs were guaranteed to further expand for 15 population doublings in the conditions provided by ScienCell Research Laboratories. Cells were used between passages 2 and 8. Human HSCs were grown in DMEM supplemented with fetal bovine serum (FBS) (10%), penicillin/streptomycin (1%) and L-glutamine (1%). HSC or HepG2 cells were silenced for PCSK9, LRP5 or both and treated with 100 μg/ml aggregated low-density lipoprotein (agLDL) as detailed below. Cells were exhaustively washed, twice with PBS, twice with PBS/1% BSA and twice with PBS/1%BSA/heparin 100 U/ml before being harvested with 1ml of 0.1 N NaOH.

2.3 | Mice serum lipid determinations

Mice blood samples were collected and the serum was obtained by centrifugation at 3000 rpm for 20 min at room temperature. Cholesterol and HDL levels were measured enzymatically by using commercially available kits (GERNON reagents; RAL, Barcelona, Catalonia, Spain) and read with a spectrophotometer (MC-15 SOFT; RAL). Non-HDL levels were obtained by calculating "Total Cholesterol"-"HDL Cholesterol".

2.4 | RNA isolation and real time PCR

Liver tissues were frozen in liquid nitrogen and RNA was isolated with the Trizol® Reagent (Invitrogen, Carlsbad, CA, USA) ($n = 5$–7 mice/group). Alternatively, total RNA was isolated from cultured HSC or HepG2 cells using the total RNA extraction kit (Qiagen). Total RNA concentration from cells or livers was determined on NanoDrop ND-1000 spectrophotometer (NanoDrop Technologies, Inc., Wilmington, DE, USA) and purity was checked by the A260/A280 ratio (ratios between 1.8 and 2.1 were considered acceptable); in addition, an agarose gel was run to assess its quality. cDNA was synthesized from 1 μg RNA with cDNA reverse transcription kit (QIAGEN Inc.), and the resulting cDNA samples were amplified by real-time polymerase chain reaction (RT-PCR) with the following specific probes from Applied Biosystems (Carlsbad, CA, USA): Lrp5 (Mm_01227476_m1), Vldlr (Mm00443298_m1), CD36 (Mm00489652_m1), SRBI (Mm00567812_m1) and PCSK9 (Mm_01340178_m1) and from Integrated DNATechnologies, Inc. (Coralville, IA, USA): Ldlr (Mm.

PT.49a.9930556), Lrp1 (Mm.PT.49a.7750137), Lrp2 (Mm.PT.49a.11916154), LRP6 (Mm.PT.56a.6383636), and SREBP-2 (Mm.PT.58a.5689751). Normalization was performed against r18S (Applied Biosystems).

2.5 | Western blot and antibodies

Sample extracts (20–40 μg protein) were resolved by SDS-PAGE and transferred to nitrocellulose membranes, blocked with 5% skim milk and probed for monoclonal (LRP5, LRP6, CD36, SRBI and β-actin from Abcam, Cambridge, UK; VLDLR, SREBP-2 and LDLR from Santa Cruz Biotechnology Inc, Santa Cruz, CA, USA; and LRP1 from Research Diagnostics Inc., Flanders, NJ, USA) or polyclonal (LRP2 and PCSK9 from Millipore) primary antibodies. Membranes were then washed and blotted with anti-mouse, anti-rabbit or anti-chicken secondary antibodies (Dako, Glostrup, Denmark). Band densities were determined with the ChemiDoc XRS system (Bio-Rad Laboratories Inc., Hercules, CA, USA) in chemiluminescence detection modus and Quantity-One software (Bio-Rad Laboratories Inc). Normalization was performed against β-actin.

2.6 | Immunoprecipitation analyses

Total protein content in livers of *Wt* and *Lrp5*$^{-/-}$ mice was estimated using the BCA protein assay (Pierce). IP was carried out on 500 μg of total protein that was incubated with 5 μl of unspecific IgG or PCSK9 specific antibody at room temperature for 1h enabling the antibody to bind to the protein in solution. The antibody/antigen complex was then pulled out of the sample using protein A/G-coupled agarose beads. The sample was then separated by SDS-PAGE for western blot analysis.

HepG2 or HSC were treated with 100 μg/ml agLDL as explained below for 24h when samples were PBS washed and collected for IP experiments.

2.7 | LDL isolation and modification

Human LDL (d1.019–d1.063 g/ml) were obtained as previously described.[29,34,35] Briefly, human LDLs were obtained from pooled sera of normocholesterolemic volunteers and isolated by sequential ultracentrifugation. LDLs were dialyzed three times against 200 volumes of 150 mmol/L NaCl, 1 mmol/L EDTA and 20 mmol/L Tris-HCl, pH 7.4, overnight and once against with 150 mmol/L NaCl. LDL protein concentration was determined by the bicinchoninic acid, vortexing was monitored by measuring the turbidity (absorbance at 680 nm). The model system of agLDL was generated by vortexing LDL (1 mg/ml) for 4 min at room temperature at maximal speed. The percentage of LDL in aggregated form was calculated by measuring the fraction of protein recovered in the pellet obtained after centrifugation at 10 000 *g* for 10 min. The different fractions were analyzed by agarose electrophoresis and the precipitated fraction composed of 100% agLDL was added to cell cultures.

2.8 | LRP5 and PCSK9 silencing

HSC were transfected with 25 nM of siRNA-Random (siR), siRNA-LRP5 (si5) or siRNA-PCSK9 (siP9) using HiPerfect® as recommended by the manufacturer. Small anti-LRP5 or anti-PCSK9 interfering RNAs (si5, s8293; siP9 s8569) were synthesized by Applied Biotechnologies and Silencer Selective negative control #1 (siR, 4390843) by Ambion.

2.9 | Statistical analysis

Results are expressed as mean ± SEM. A Stat View statistical package was used for all the analysis. Comparisons among groups were performed by two-way ANOVA analysis. Regression analyses were performed by applying $Y = a + b * X$ lineal pattern besides using Stat View for Windows program, selecting just highly adjusted equations. Statistical significance was considered when $p < .05$.

3 | RESULTS

3.1 | Hypercholesterolemic diet effect in liver cholesterol and LRP5 expression

Wt and *Lrp5*$^{-/-}$ mice were fed a NC for 10 weeks when they were divided into 2 groups to be fed with NC or HC diet for further 8 weeks (n = 8–12/group) when we analyzed the intracellular cholesterol esters (CE) and neutral acylglyceride lipid content in livers by semi-quantitave thin layer chromatography (TLC). CE content/mg liver tissue in *Wt* and *Lrp5*$^{-/-}$ mice increased significantly after HC feeding, while FC levels remained constant (Figure 1A). *Wt* and *Lrp5*$^{-/-}$ mice showed similar neutral acylglycerides levels independent of diet (Figure 1B).

We then analyzed *Lrp5* and *Ldlr* gene expression levels in livers of *Wt* and *Lrp5*$^{-/-}$ mice. Results showed a 29 ± 4% decrease in *Lrp5* gene expression in livers of *Wt* mice after HC diet while *Lrp5* expression was undetectable

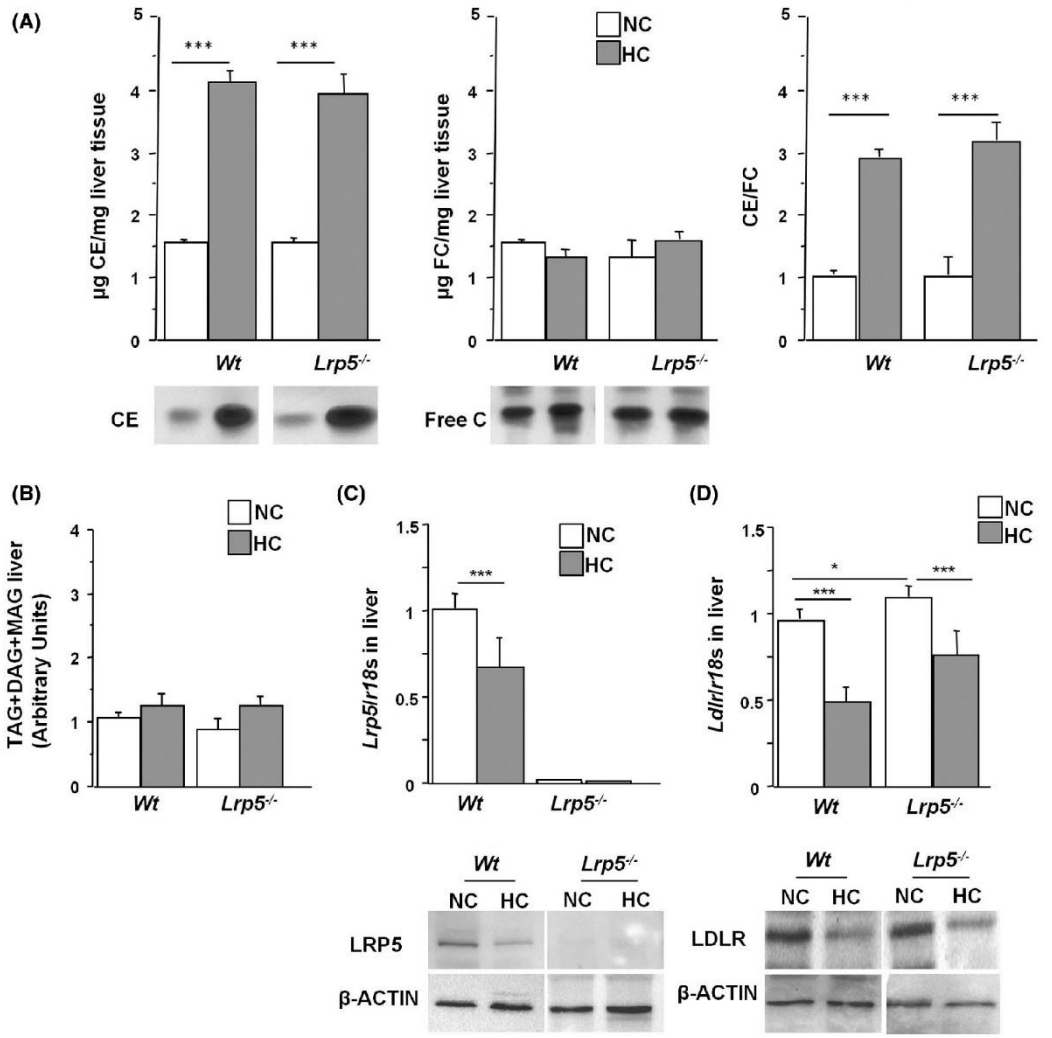

FIGURE 1 Lipid composition and gene and protein expression in mice livers. (A) Micrograms of cholesteryl esters (CE)/mg liver tissue; micrograms of free cholesterol (FC)/mg liver tissue; ratio between CE/FC and (B) acylglycerol content in livers of *Wt* and *Lrp5*$^{-/-}$ mice fed a normocholesterolemic (NC) or a hypercholesterolemic (HC) diet. (C) LRP5 and (D) LDLR gene and protein expression levels in livers of *Wt* and *Lrp5*$^{-/-}$ mice fed a NC or a HC diet. *$p < .05$; ***$p < .005$

in *Lrp5*$^{-/-}$ mice (Figure 1C). LRP5 protein expression analyzed by western blot showed similar results. β-actin was used for normalization purposes (Figure 1C). *Ldlr* gene expression was reduced in both *Wt* and *Lrp5*$^{-/-}$ by HC diet (56 ± 3% and 28 ± 2% respectively). LDLR protein expression was also reduced in livers of HC *Wt* and *Lrp5*$^{-/-}$ mice (Figure 1D).

The analyses of *Wt* and *Lrp5*$^{-/-}$ mice serum cholesterol profiles showed that HC diet increased total cholesterol levels both in *Wt* and in *Lrp5*$^{-/-}$ mice (Figure S1A). Interestingly, NC *Lrp5*$^{-/-}$ mice had lower cholesterol serum levels than NC *Wt* mice, and the overall increase in HC diets with respect to NC diets was double in *Lrp5*$^{-/-}$ mice than in *Wt* mice (125.69 mg/dl versus 62.25 mg/dl, Figure S1B, $p < .05$). Serum levels of non-HDL cholesterol were significantly increased in HC *Wt* (25 ± 3mg/dl) and HC *Lrp5*$^{-/-}$ (101 ± 17 mg/dl) with respect to their NC littermates ($p < .005$, Figure S1C). In a similar way, serum

levels of HDL cholesterol were increased after HC diets in both genotypes (Figure S1D).

3.2 | LDL-receptor family expression in the liver

To understand the mechanisms of hepatic CE accumulation when both LDLR and LRP5 are downregulated, we analyzed gene and protein expression levels of other receptors of the LDLR superfamily. VLDLR is widely known for its participation in hepatic lipoprotein clearance. Consequently its gene and protein expression levels were increased in *Wt* mice after HC feeding (Figure 2A). Interestingly, *Vldlr* gene and protein levels remained constantly low in *Lrp5*$^{-/-}$ mice liver, independently of diet, suggesting that in *Lrp5*$^{-/-}$ mice, VLDLR does not participate in CE liver accumulation. Similarly, *Lrp6* gene expression was induced by HC diets only in *Wt* mice (Figure 2B) and *Lrp2* gene expression levels were increased by 28 ± 2% only in HC *Wt* mice with respect to NC *Wt* mice (Figure 2C). Protein analyses confirm gene expression results strongly suggesting that neither VLDR, LRP2 nor LRP6 participate in hepatic CE accumulation in *Lrp5*$^{-/-}$ mice. *Lrp1* gene and protein levels remained constant among dietary treatment groups; interestingly *Lrp1* gene expression levels were significantly lower in NC *Lrp5*$^{-/-}$ mice than in NC *Wt* mice (Figure 2D).

Scavenger receptors can internalize modified forms of LDL through mechanisms not inhibited by cellular cholesterol content; therefore, we analyzed the expression of CD36 and SRBI, two scavenger receptors that belong to the BI subfamily. Increased liver CD36 expression was observed in *Lrp5*$^{-/-}$ mice as compared to *Wt* mice; however, CD36 expression levels did not increase after HC feeding (Figure 2E). In contrast, SRBI expression increased by 32 ± 3% in HC *Lrp5*$^{-/-}$ mice as compared to NC *Lrp5*$^{-/-}$ mice, indicating a role for this receptor in the uptake of lipids after HC feeding *Lrp5*$^{-/-}$ mice (Figure 2F).

3.3 | PCSK9 is downregulated in livers of HC Wt and HC Lrp5$^{-/-}$ mice

Pcsk9 gene and protein expression were downregulated in livers of mice after HC feeding independently of genotype (Figure 3A). Similarly, the analyses of the expression of SREBP-2 in liver showed that *Srebp-2* gene and protein levels were reduced when mice were fed a HC diet in both genotypes (31 ± 2% in HC *Wt* and 56 ± 5% in HC *Lrp5*$^{-/-}$ mice with respect to their NC littermates; Figure 3B).

Furthermore, after NC treatments, there is high expression of both *Pcsk9* and *Ldlr* independent of mice genotype while after HC feeding there is a decrease in *Ldlr* and *Pcsk9* expression levels both in *Wt* and *Lrp5*$^{-/-}$ mice. Interestingly, significantly higher *Pcsk9* expression levels were observed with higher *Ldlr* expression, both in *Wt* and *Lrp5*$^{-/-}$ mice but the slope for the correlation was significantly steeper in *Wt* mice, indicating that *Lrp5*$^{-/-}$ mice have less *Pcsk9* gene expression per unit of *Ldlr* gene expression than *Wt* mice (Figure 3C,D).

3.4 | PCSK9 forms a complex with LRP5 in hepatic stellate cells

To further understand the role of PCSK9 and the LRP family in lipid homeostasis, we performed IP analyses with different lipoprotein receptors. Liver samples of NC and HC *Wt* mice were IP with PCSK9 antibody and blotted with antibodies against LRP2 or LRP6 showing no interaction between these proteins (Figure 4A). Similar results were obtained in livers from *Lrp5*$^{-/-}$ mice (Figure 4B). When liver samples from *Wt* mice were IP with PCSK9 and blotted against LRP5, no band could be observed indicating that, contrarily to human macrophages, PCSK9 does not interact with LRP5 in liver samples (Figure 4A).[29] Liver samples from *Wt* and *Lrp5*$^{-/-}$ mice that were immunoprecipitated with PCSK9 antibody and blotted with antibody against LDLR show a clear band, indicating an interaction for LDLR and PCSK9 in mice livers (Figure 4A,B). We then studied the human liver cell line HepG2. Protein expression analyses showed that, similar to liver samples, there was a decrease in LRP5 and PCSK9 expression after lipid loading (Figure 4C). Immunoprecipitation experiments in HepG2 cells revealed no interaction between LRP5 and PCSK9 similar to the results in liver samples (Figure 4D).

HSC, also known as the liver fat storing cells, show increased LRP5 protein levels and decreased PCSK9 protein levels after lipid loading (Figure 4E). When lipid-loaded HSC were immunoprecipitated with PCSK9 antibodies and blotted against LRP5, a clear band was observed in both control and lipid loaded cells indicating that LRP5 and PCSK9 bind intracellularly in HSC (Figure 4F).

3.5 | LRP5 and PCSK9 silencing inhibit agLDL-induced increased CE accumulation in HSC cells

To characterize further the direct interaction between PCSK9 and LRP5, HSC were silenced for LRP5 (si5) and incubated with agLDL. In contrast to mice liver samples and HepG2 cells, LRP5 gene and protein

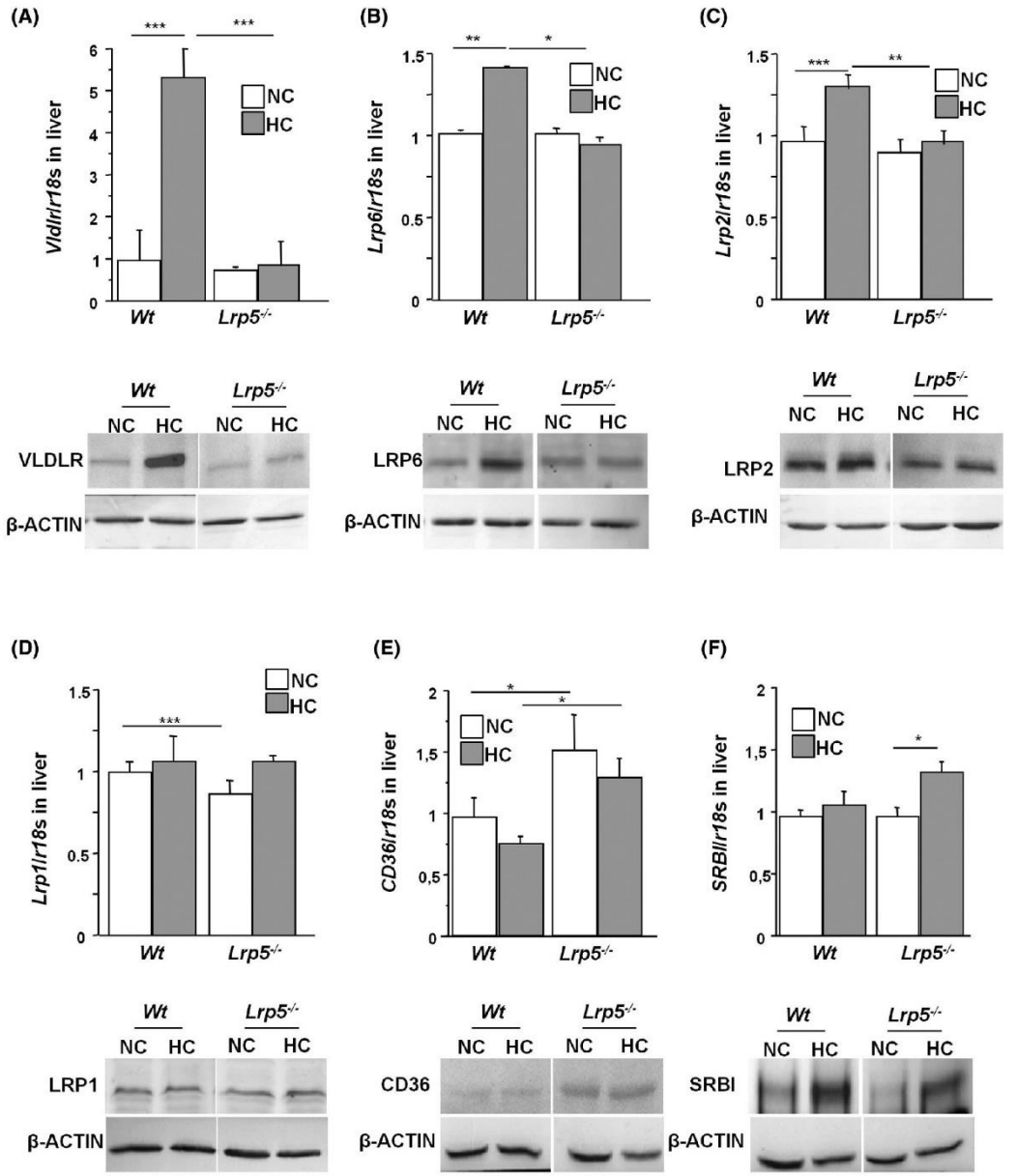

FIGURE 2 Receptor expression in mice livers. Gene and protein expression levels of (A) VLDLR (B) LRP6, (C) LRP2, (D) LRP1, (E) CD36 and (F) SRBI in livers of NC and HC *wt* and *Lrp5*$^{-/-}$ mice. *$p < .05$; **$p < .01$ ***$p < .005$

expression were upregulated after agLDL treatments in HSC (Figure 5A,B). A downregulation of LRP5 in silenced HSC was observed indicating the correct silencing of the gene (Figure 5A,B). We then analyzed the release of PCSK9 to the extracellular milieu in control and si5 HSC to show an increased release of PCSK9 in lipid-loaded control cells (Figure 5C). However, this increased release was lost in si5 lipid-loaded HSC suggesting the

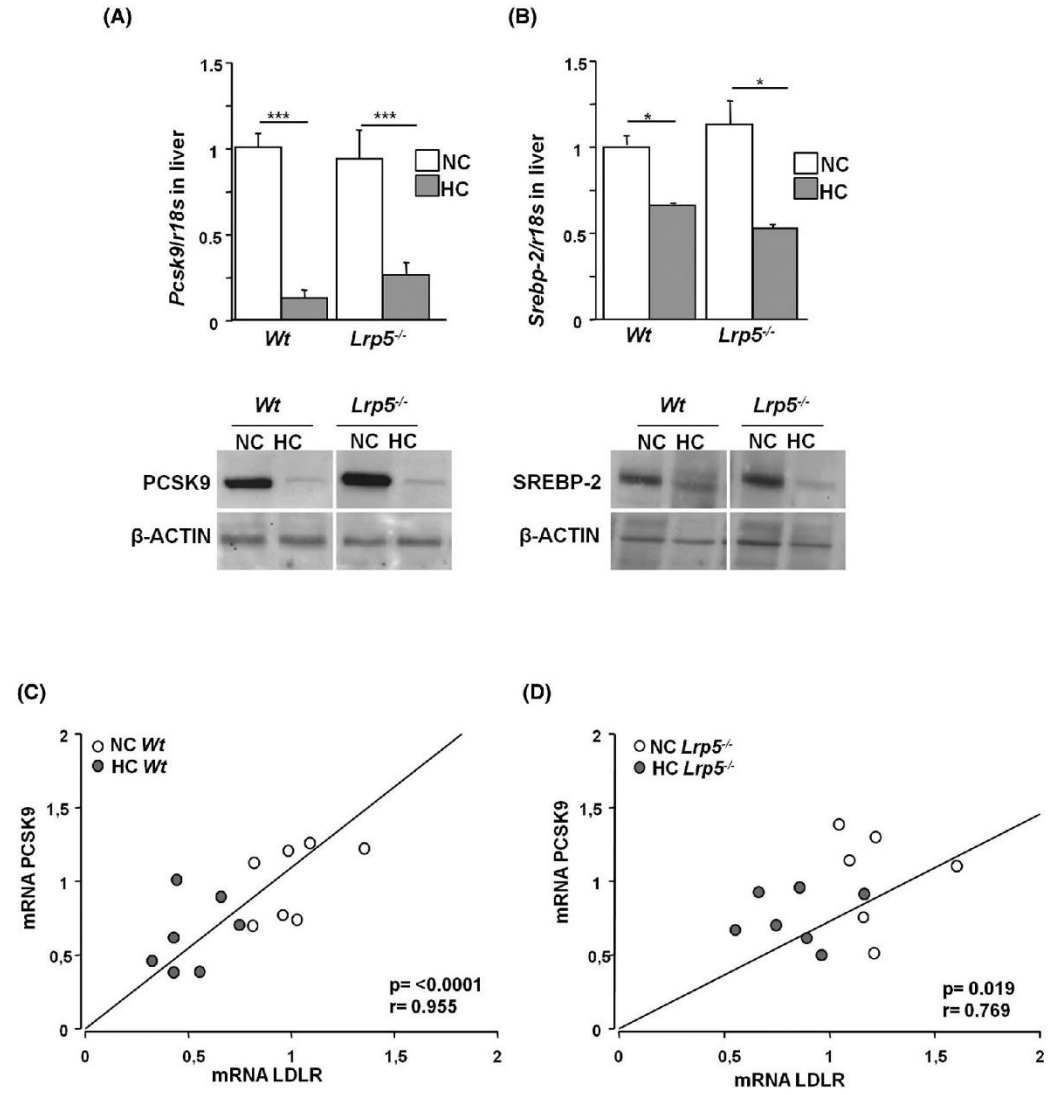

FIGURE 3 PCSK9 expression in mice livers. Gene and protein expression levels of (A) PCSK9 and (B) SREBP-2 in livers of *Wt* and *Lrp5*$^{-/-}$ mice fed a NC or a HC diet. (C) Regression analyses between *Pcsk9* and *Ldlr* gene expression in *Wt* or (D) *Lrp5*$^{-/-}$ mice fed a NC or a HC diet with their statistical significances (p) and correlation coefficients (r). $^{*}p < .05$; $^{***}p < .005$

involvement of LRP5 in the PCSK9 release pathway in high lipid atmospheres (Figure 5C).

To study the role of LRP5 and PCSK9 in HSC intracellular cholesterol accumulation, HSC were silenced for LRP5 (si5), PCSK9 (siP9) or both (si5+siP9), incubated with 100 μg/ml agLDL for 24 h when cells were collected and TLC was performed. A control siRNA random was used (siR). Without the addition of extracellular lipids, no CE accumulation was observed under any condition; however, after lipid treatment, CE accumulation was significantly increased in control HSC (Figure 5D). Both si5-HSC and siP9-HSC reduced their CE content after lipid loading indicating that they both participate in lipid uptake. Similarly, when both proteins were silenced simultaneously, CE accumulation was also significantly reduced (Figure 5D), suggesting that both

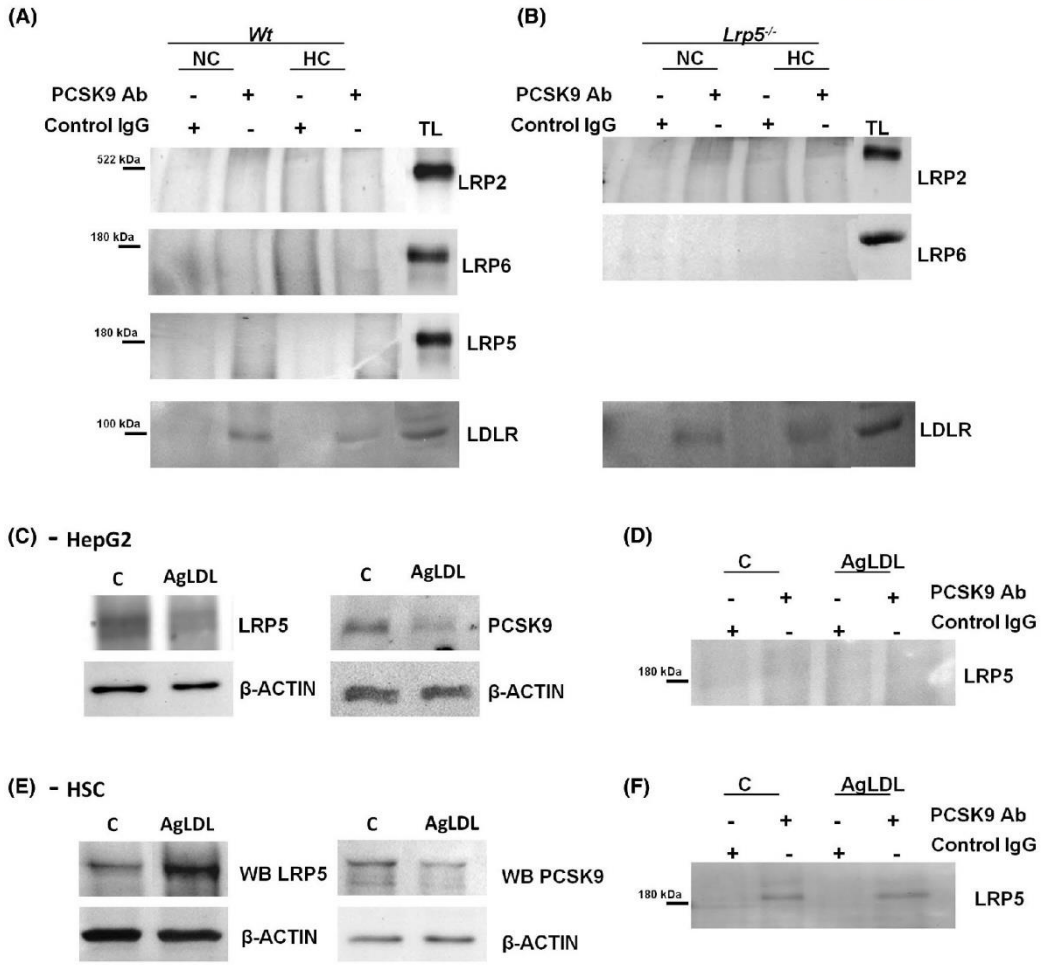

FIGURE 4 Immunoprecipitation analyses in mice liver. (A) Liver samples of NC or HC *Wt* mice were immunoprecipitated with PCSK9 antibody or unspecific IgG before WB against LRP2, LRP6, LRP5 or LDLR was performed ($n = 6$/WB). (B) Same procedure as in A for *Lrp5*$^{-/-}$ mice liver samples; TL: Total lysate. (C) HepG2 cells were lipid-loaded (agLDL) or not (C) and protein expression was analyzed by WB for LRP5 and PCSK9; and (D) another set of HepG2 cells was IP with PCSK9 antibody or unspecific IgG before WB against LRP5 was performed. (E) HSC were treated or not with agLDL and LRP5 and PCSK9 protein expression was analyzed by WB. (F) HSC were IP with PCSK9 antibody or unspecific IgG before WB against LRP5 was performed

LRP5 and PCSK9 participate in CE-internalization in HSC. Gene analyses showed that silencing of LRP5 and PCSK9 was specific and selective, and the absence of PCSK9 in HSC did not affect LRP5 expression levels and vice versa (Figure 5E).

When similar experiments were performed on HepG2 cells, there was a decrease in CE accumulation after siRNA-LRP5 treatments indicating that, although its expression is downregulated after lipid treatments (Figure S2B), LRP5 plays a role in CE uptake (Figure S2A). However, when HepG2 cells were silenced for PCSK9, no decrease in CE accumulation was observed indicating that in this cell type, PCSK9 is not needed for CE uptake. LRP5 gene and protein levels were decreased after lipid treatments, (Figure S2B) probably contributing to the lower CE accumulation observed in HepG2 control cells (siR-HepG2 cells) as compared to HSC control cells (siR-HSC, Figure 5D) after lipid loading. PCSK9 gene and expression levels analyses showed that HepG2 cells were silenced after silencing treatments (Figure S2C).

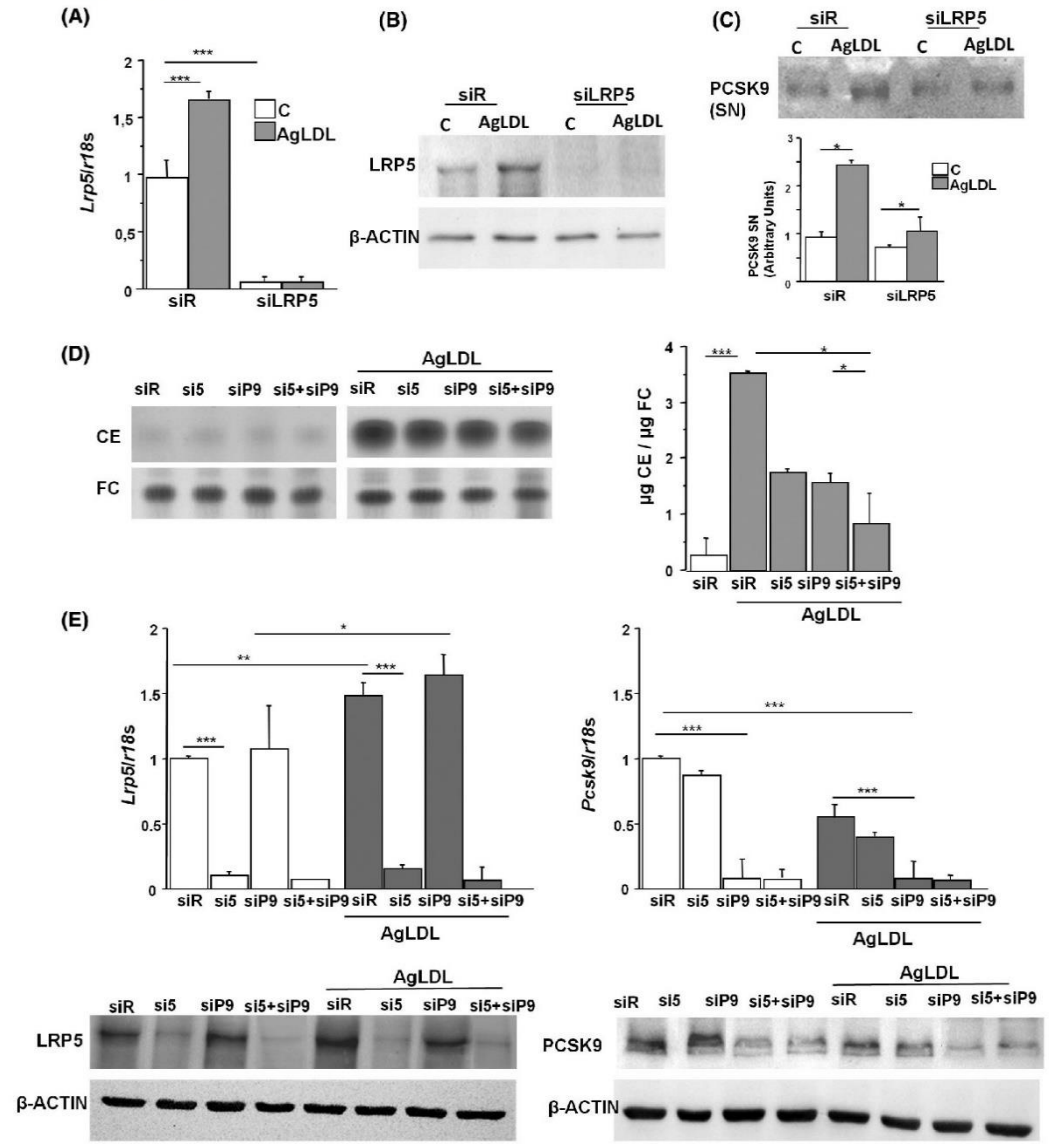

FIGURE 5 PCSK9 forms a complex with LRP5 in HSC. (A) *Lrp5* gene levels were determined in HSC lipid-loaded cells containing siRNA-Random (siR) or siRNA-LRP5 (si5). (B) Representative WB of LRP5 expression in agLDL treated HSC. β-ACTIN was used as a loading control. (C) Representative WB and bar graph quantification of soluble PCSK9 in the supernatants of siR and si5 agLDL treated HSC cells. (D) HSC cells containing siR, siRNA-LRP5 (si5), siRNA-PCSK9 (siP9) or both were agLDL-incubated (100 µg/ml) for 24h, exhaustively washed and harvested to measure intracellular free cholesterol (FC) and cholesteryl esters (CE) by TLC. Bar graph showing µg CE/µg FC content. $n = 3$ in duplicates. (E) Gene and protein levels of LRP5 and PCSK9 in HSC containing siR, si5, siP9 or both, agLDL-incubated (100 µg/ml) for 24h. $^{*}p < .05$; $^{***}p < .005$

4 | DISCUSSION

Several lines of evidence indicate that the LRP family of receptors is involved in promoting hypercholesterolemia. HC *Lrp5*$^{-/-}$ mice show increased protein expression of LRP6 in aortas that directly correlate with the injured area.[23] Furthermore, LDLR internalization is severely diminished in LRP6 knock-out cells suggesting that LRP6 can also modulate LDLR-mediated lipid uptake.[36] Overexpression of LRP6[37] and LRP1[38] has been found in human atherosclerotic lesions. Indeed, LRP1 upregulation is induced by extracellular lipids in human macrophages and vascular smooth muscle cells (VSMCs) present in human advanced atherosclerotic lesions.[38] A proatherogenic role for LRP1 has been suggested as aortas of swine and rabbits after HC diets show increased expression of LRP1.[39] Consistently, enhanced LRP1 expression after HC diets in *Wt* and *Lrp5*$^{-/-}$ mice aortas has been shown.[23] Taken together, these results indicate that LRP1 and LRP6 could participate in the proatherogenic effect of hypercholesterolemia. However, there is little understanding on the role of LRPs in liver cholesterol processing.

The liver is the main regulator of circulating lipoproteins. Lipids accumulate in the liver in the form of phospholipids, cholesterol including CE and neutral lipids including acylglycerides.[40,41] Neutral lipids carry a high unsaturated pool of fatty acyl groups that release fatty acids.[42] We performed TLC in the livers of *Wt* and *Lrp5*$^{-/-}$ mice to study the effect of hypercholesterolemia in the accumulation of CE and neutral lipids and found increased CE content while neutral acylglycerides lipids accumulation was similar in *Wt* and in *Lrp5*$^{-/-}$ mice after hypercholesterolemic diets. Interestingly, LRP5 gene and protein expression levels in the liver were decreased during hypercholesterolemia. This was an unexpected result as different primary cultures including human monocytes, human macrophages, human VSMCs, and an endothelial cell line all show increased LRP5 gene and protein levels after lipid loading.[17] Furthermore, LRP5 gene and protein levels are also upregulated in the hearts of hypercholesterolemic mice and in hypercholesterolemic ischemic human hearts.[43,44]

Liver LDLR expression levels were also downregulated after HC feeding in *Wt* and *Lrp5*$^{-/-}$ mice. This result raises the question of how does liver cholesterol uptake take place in *Lrp5*$^{-/-}$ mice. Indeed, LRP5 and LDLR protein levels are downregulated in HC *Lrp5*$^{-/-}$ mice. Similarly, other lipoprotein receptors including LRP1, LRP2 and LRP6 show similar expression levels in HC *Lrp5*$^{-/-}$ mice than in NC *Lrp5*$^{-/-}$ mice. However, the fact that all these receptors are not upregulated does not mean that they are not expressed in the livers of HC *Lrp5*$^{-/-}$ mice. They are indeed expressed, opening the possibility that they could all be uptaking plasma cholesterol although at slower rates. To test if other receptors such as scavenger receptors, could also be uptaking plasma cholesterol we analyzed CD36 and SRBI expression levels in mice livers.[45,46] CD36 expression levels did not increase in HC with respect to NC in either genotype; however, SRBI expression increased after HC feeding in livers of *Lrp5*$^{-/-}$ mice as compared to NC *Lrp5*$^{-/-}$ mice, indicating a role for this receptor in liver cholesterol uptake in HC *Lrp5*$^{-/-}$ mice. These results are supported by the analyses of plasma cholesterol levels in mice. Indeed, SRBI's main role is the uptake of HDL-C; therefore, plasmatic non-HDL-C content is significantly higher in HC *Lrp5*$^{-/-}$ mice as compared to HC *Wt* mice.

The observed higher plasma cholesterol levels in HC *Lrp5*$^{-/-}$ mice as compared to HC *Wt* mice could also be due to impaired lipoprotein clearance. Indeed, hepatic expression of receptors from the LDLR superfamily that have been described to participate in lipoprotein clearance were analyzed and the upregulation of VLDLR after HC diets was found only in *Wt* mice. *Lrp5*$^{-/-}$ mice showed similar liver VLDLR expression levels in both NC and HC conditions probably due to a decreased clearance of lipoprotein particles by their livers. Indeed, ectopic expression by adenoviral virus of the VLDLR in mouse liver resulted in enhanced internalization of lipoproteins.[47] Therefore, liver VLDLR seems to act as a clearance receptor for circulating lipoprotein particles. HC *Lrp5*$^{-/-}$ mice have increased plasmatic VLDL particles[48] and the injection of fluorescently labeled chylomicron particles into HC *Lrp5*$^{-/-}$ mice showed that only 20% of labeled chylomicrons disappeared from the plasma of *Lrp5*$^{-/-}$ mice 30 min after injection, suggesting that LRP5 is needed for correct hepatic clearance.[48] Supporting these results, we find that VLDLR expression levels do not increase after HC feeding in *Lrp5*$^{-/-}$ mice. This could explain the increased serum levels of non-HDL cholesterol (which includes LDL and VLDL) in *Lrp5*$^{-/-}$ mice after HC feeding by a decreased clearance of lipoprotein particles from the liver. LRP6 and LRP2 also contribute to lipoprotein clearance. Indeed, LRP2 contributes to HDL metabolism by internalizing structural components of HDLs, namely, ApoA-I and ApoA-II[48]; and *Lrp6*$^{-/-}$ hepatic cells show decreased LDL uptake because LDLR internalization is severely downregulated.[36] Both receptors have a reduced expression in the livers of HC *Lrp5*$^{-/-}$ mice strongly supporting their participation in the clearance of lipoprotein particles in *Wt* mice. We also analyzed LRP1 as it has been shown to participate in hepatic remnant clearance.[49,50] Nonetheless, LDLR can fully compensate for LRP1 deficiency,[49,50] consequently *Wt* and *Lrp5*$^{-/-}$ mice showed similar hepatic LRP1 expression levels independent of diet.

PCSK9 is involved in the control of LDL-cholesterol plasma concentration by regulating hepatic expression of LDLR.[9] Also, PCSK9 and LDLR are coordinately regulated by a transcription factor that activates different genes involved in cholesterol metabolism, SREBP-2.[51,52] The dual regulation of PCSK9 and LDLR by SREBP-2 allows the exploitation of this pathway for cholesterol-lowering therapies. Indeed, statin administration downregulates plasma LDL by inducing SREBP-2 expression levels that in turn increase LDLR expression.[53,54] PCSK9 gene and protein expression is also increased in response to statins attenuating the cholesterol-lowering effect of statins.[55,56] Furthermore, mice without PCSK9 show increased statin-induced LDLR expression and accelerated LDL-cholesterol clearance.[55]

We have previously shown an interaction between LRP5 and PCSK9 in human macrophages.[29] However, when liver samples from *Wt* mice were immunoprecipitated with antibodies against PCSK9 and blotted against LRP5 no interaction could be observed. Similarly, in liver samples of *Wt* or *Lrp5*$^{-/-}$ mice PCSK9 did not interact with LRP2 nor LRP6. Hepatocytes are the main resident cell type in the liver. Hence, we studied the hepatocyte cell line HepG2 and observed a similar behavior than that of liver samples: low LRP5 and PCSK9 protein expression levels after lipid loading without interaction between these proteins. Thin layer chromatography analyses in HepG2 cells showed that PCSK9 is not involved in CE accumulation after lipid loading. We then analyzed hepatic stellate cells, which are fat storing cells that constitute about 8% of cells present in liver. They contain big lipid droplets to store the liver's Vitamin A as well as other non-retinoid lipids including free fatty acids, cholesterol, CE, and triglycerides.[57,58] PCSK9 activity is tightly controlled at a post-translational level by proteins that regulate its secretion, its extracellular inhibition and its clearance from the circulation. Our results show increased LRP5 protein expression and decreased PCSK9 protein expression after lipid loading. Immunoprecipitation experiments show that PCSK9 and LRP5 form a complex in the cytoplasm of stellate cells and that the interaction is stronger in lipid-loaded cells. Furthermore, reduced release of PCSK9 is observed in si5 stellate cells demonstrating a role for LRP5 in PCSK9's transport to the plasma membrane in a similar way to that observed in lipid-loaded human macrophages. Therefore, the results shown here indicate that the PCSK9-LRP5 interaction is a cell specific interaction as it does not take place in HepG2 cells, suggesting that upon lipid challenge, only lipid-primed tissue-specific cells (macrophages in atherosclerotic lesions in vascular walls or stellate cells in fat livers) release PCSK9 in a LRP5- dependent manner.

The relevance of PCSK9-LRP5 union is supported by the reduction in CE accumulation in the absence of PCSK9 and/or LRP5 in HSC. Indeed, when both PCSK9 and LRP5 proteins are absent, there is a strong reduction in the intracellular CE content in stellate cells supporting a role of both proteins in the internalization of cholesterol in hepatic stellate cells and therefore in the liver.

This study has three main limitations. First, gene knockdown analyses in HSC and HepG2 cells are performed with silencing RNAs. This technique allows for a 70–90% gene inhibition but not for a complete gene knockdown. Second, we have only analyzed PSK9-LRP5 interaction in mice livers, structural HepG2 liver cells and fat storing stellate liver cells. Still, there are other liver resident cells including Kupffer cells that are liver macrophages with altered functions in several pathologies; however, their main function is the phagocytosis and defense of the liver against infections rather than lipid uptake. Third, broader analyses in mice livers including RNAseq or LC-MS/MS could provide wide-range information about compensative mechanisms in mice liver in *Wt* and *Lrp5*$^{-/-}$ mice at baseline and after HC feeding.

In conclusion our results show that CE accumulate in livers of *Wt* and *Lrp5*$^{-/-}$ mice; that LRP5, LDLR, PCSK9 and SREBP-2 are downregulated in livers of HC mice; that PCSK9 and LRP5 bind intracellularly in fat storing liver cells and that both proteins are involved in CE accumulation in mice livers.

ACKNOWLEDGEMENTS

We thank S. Huertas for excellent technical assistance. This work was supported by the Spanish Ministry of Science and Innovation and FEDER funds [PID2019-107160RB-I00 to LB and PGC 2018-094025-B-I00 to GV]; the Instituto de Salud Carlos III [CIBERCV CB16/11/00411 to LB, TERCEL RD16/0011/018 to LB and FIS2020-01282 to MBP]; the Generalitat of Catalunya-Secretaria d'Universitats i Recerca del Departament d'Economia i Coneixement de la Generalitat [2017SGR1480 to LB] and Agencia Gestió Ajudes Universitàries Recerca: AGAUR [2016PROD00043 to LB]; the Spanish Society of Cardiology [FEC 2019 to MBP and FEC 2020 to GV] and the Fundación Investigación Cardiovascular-Fundación Jesus Serra for their continuous support.

DISCLOSURES

The authors have stated explicitly that there are no conflicts of interest in connection with this article.

AUTHOR CONTRIBUTIONS

Design research was carried out by Aureli Luquero and Maria Borrell-Pages. Aureli Luquero, Gemma Vilahur and Laura Casani performed the research. Aureli Luquero,

Gemma Vilahur, Laura Casani, Maria Borrell-Pages and Lina Badimon contributed new reagents and analytic tools. Aureli Luquero, Maria Borrell-Pages, Gemma Vilahur and Lina Badimon analyzed the data. Aureli Luquero, Lina Badimon and Maria Borrell-Pages wrote the article.

DATA AVAILABILITY STATEMENT

The data that support the findings of this study are available in the methods and Supporting Information of this article.

ORCID

Maria Borrell-Pages https://orcid.org/0000-0002-1759-9756

REFERENCES

1. Libby P, Buring JE, Badimon L, et al. Atherosclerosis. *Nat Rev Dis Primers*. 2019;5:56.
2. Accad M, Farese RV. Cholesterol homeostasis: a role for oxysterols. *Curr Biol*. 1998;8:R601-R604.
3. Brown MS, Goldstein JL. A receptor-mediated pathway for cholesterol homeostasis. *Science*. 1986;232:34-47.
4. Ishibashi S, Brown MS, Goldstein JL, Gerard RD, Hammer RE, Herz J. Hypercholesterolemia in low density lipoprotein receptor knockout mice and its reversal by adenovirus-mediated gene delivery. *J Clin Invest*. 1993;92:883-893.
5. Schmidt RJ, Beyer TP, Bensch WR, et al. Secreted proprotein convertase subtilisin/kexin type 9 reduces both hepatic and extrahepatic low-density lipoprotein receptors in vivo. *Biochem Biophys Res Commun*. 2008;370:634-640.
6. Walley KR, Thain KR, Russell JA, et al. PCSK9 is a critical regulator of the innate immune response and septic shock outcome. *Sci Transl Med*. 2014;6:258ra143.
7. Lambert G, Charlton F, Rye KA, Piper DE. Molecular basis of PCSK9 function. *Atherosclerosis*. 2009;203:1-7.
8. Abifadel M, Varret M, Rabés JP, et al. Mutations in PCSK9 cause autosomal dominant hypercholesterolemia. *Nat Genet*. 2003;34:154-156.
9. Seidah NG. PCSK9 as a therapeutic target of dyslipidemia. *Expert Opin Ther Targets*. 2009;13:19-28.
10. Nicholls SJ, Puri R, Anderson T, et al. Effect of evolocumab on progression of coronary disease in statin-treated patients: the GLAGOV randomized clinical trial. *JAMA*. 2016;316:2373-2384.
11. Sabatine MS, Giugliano RP, Keech AC, et al.; FOURIER Steering Committee and Investigators. Evolocumab and clinical outcomes in patients with cardiovascular disease. *N Engl J Med*. 2017;376:1713-1722.
12. Schwartz GG, Steg PG, Szarek M, et al. Alirocumab and cardiovascular outcomes after acute coronary syndrome. *N Engl J Med*. 2018;379:2097-2107.
13. Jeon H, Blacklow SC. Structure and physiologic function of the low-density lipoprotein receptor. *Annu Rev Biochem*. 2005;74:535-562.
14. Go GW, Mani A. Low-density lipoprotein receptor (LDLR) family orchestrates cholesterol homeostasis. *Yale J Biol Med*. 2012;85:19-28.
15. Hiltunen TP, Luoma JS, Nikkari T, Ylä-Herttuala S. Expression of LDL receptor, VLDL receptor, LDL receptor-related protein, and scavenger receptor in rabbit atherosclerotic lesions: marked induction of scavenger receptor and VLDL receptor expression during lesion development. *Circulation*. 1998;97:1079-1086.
16. Llorente-Cortés V, Royo T, Otero-Viñas M, Berrozpe M, Badimon L. Sterol regulatory element binding proteins downregulate LDL receptor-related protein (LRP1) expression and LRP1-mediated aggregated LDL uptake by human macrophages. *Cardiovasc Res*. 2007;74:526-536.
17. Borrell-Pagès M, Romero JC, Juan-Babot O, Badimon L. Wnt pathway activation, cell migration and lipid uptake is regulated by LRP5 in human macrophages. *Eur Heart J*. 2011;32:2841-2850.
18. Miller JR, Hocking AM, Brown JD, Moon RT. Mechanism and function of signal transduction by the Wnt/beta-catenin and Wnt/Ca2+ pathways. *Oncogene*. 1999;18:7860-7872.
19. Barker N, Morin PJ, Clevers H. The Yin-Yang of TCF/beta-catenin signaling. *Adv Cancer Res*. 2000;77:1-24.
20. Borrell-Pagès M, Romero JC, Badimon L. LRP5 negatively regulates differentiation of monocytes through abrogation of Wnt signalling. *J Cell Mol Med*. 2014;18:314-325.
21. Borrell-Pages M, Romero JC, Badimon L. Cholesterol modulates LRP5 expression in the vessel wall. *Atherosclerosis*. 2014;235:363-370.
22. Borrell-Pagès M, Carolina Romero J, Badimon L. LRP5 and plasma cholesterol levels modulate the canonical Wnt signalling in peripheral blood leukocytes. *Immunol Cell Biol*. 2015;93:653-661.
23. Borrell-Pagès M, Romero JC, Badimon L. LRP5 deficiency downregulates Wnt pathway and promotes aortic lipid accumulation in hypercholesterolemic mice. *J Cell Mol Med*. 2015;19:770-777.
24. Awan Z, Denis M, Bailey D, et al. The LDLR deficient mouse as a model for aortic calcification and quantification by microcomputed tomography. *Atherosclerosis*. 2011;219:455-462.
25. Canuel M, Sun X, Asselin MC, Paramithiotis E, Prat A, Seidah NG. Proprotein convertase subtilisin/kexin type 9 (PCSK9) can mediate degradation of the low-density lipoprotein receptor-related protein 1 (LRP-1). *PLoS One*. 2013;8:e64145.
26. Liu M, Wu G, Baysarowich J, et al. PCSK9 is not involved in the degradation of LDL receptors and BACE1 in the adult mouse brain. *J Lipid Res*. 2010;51:2611-2618.
27. Poirier S, Mayer G, Benjannet S, et al. The proprotein convertase PCSK9 induces the degradation of low density lipoprotein receptor (LDLR) and its closest family members VLDLR and ApoER2. *J Biol Chem*. 2008;283:2363-2372.
28. Kysenius K, Muggalla P, Matlik K, Arumae U, Huttunen HJ. PCSK9 regulates neuronal apoptosis by adjusting ApoER2 levels and signaling. *Cell Mol Life Sci*. 2012;69:1903-1916.
29. Badimon L, Luquero A, Crespo J, Peña E, Borrell-Pages M. PCSK9 and LRP5 in macrophage lipid internalization and inflammation. *Cardiovasc Res*. 2021;117(9):2054-2068.
30. Holmen SL, Giambernardi TA, Zylstra CR, et al. Decreased BMD and limb deformities in mice carrying mutations in both Lrp5 and Lrp6. *J Bone Miner Res*. 2004;19:2033-2040.
31. Cui Y, Niziolek PJ, MacDonald BT, et al. Lrp5 functions in bone to regulate bone mass. *Nat Med*. 2011;17:684-691.

32. Llorente-Cortés V, Martínez-González J, Badimon L. Esterified cholesterol accumulation induced by aggregated LDL uptake in human vascular smooth muscle cells is reduced by HMG-CoA reductase inhibitors. *Arterioscler Thromb Vasc Biol*. 1998;18:738-746.
33. Asmis R, Llorente-Cortes V, Gey KF. Prevention of cholesteryl ester accumulation in P388D1 macrophage-like cells by increased cellular vitamin E depends on species of extracellular cholesterol. Conventional heterologous non-human cell cultures are poor models of human atherosclerotic foam cell formation. *Eur J Biochem*. 1995;233:171-178.
34. Llorente-Cortes V, Otero-Viñas M, Camino-Lopez S, Costales P, Badimon L. Cholesteryl esters of aggregated-LDL are internalized by selective uptake in HVSMC. *Arterioscler Thromb Vasc Biol*. 2006;26:117-123.
35. Llorente-Cortés V, Martínez-González J, Badimon L. LDL receptor-related protein mediates uptake of aggregated LDL in human vascular smooth muscle cells. *Arterioscler Thromb Vasc Biol*. 2000;20:1572-1579.
36. Ye ZJ, Go GW, Singh R, Liu W, Keramati AR, Mani A. LRP6 protein regulates low density lipoprotein (LDL) receptor-mediated LDL uptake. *J Biol Chem*. 2012;287:1335-1344.
37. Keramati AR, Singh R, Lin A, et al. Wild-type LRP6 inhibits, whereas atherosclerosis-linked LRP6R611C increases PDGF-dependent vascular smooth muscle cell proliferation. *Proc Natl Acad Sci U S A*. 2011;108:1914.
38. Llorente-Cortés V, Otero-Viñas M, Sánchez S, Rodríguez C, Badimon L. Low-density lipoprotein upregulates low-density lipoprotein receptor-related protein expression in vascular smooth muscle cells: possible involvement of sterol regulatory element binding protein-2-dependent mechanism. *Circulation*. 2002;106:3104-3110.
39. Llorente-Cortés V, Badimon L. LDL receptor-related protein and the vascular wall: implications for atherothrombosis. *Arterioscler Thromb Vasc Biol*. 2005;25:497-504.
40. Puri P, Baillie RA, Wiest MM, et al. A lipidomic analysis of nonalcoholic fatty liver disease. *Hepatology*. 2007;46:1081-1090.
41. Laurell S, Lundquist A. Lipid composition of human liver biopsy specimens. *Acta Med Scand*. 1971;189:65-68.
42. Kruth HS. Localization of unesterified cholesterol in human atherosclerotic lesions. Demonstration of filipin-positive, oil-red-O-negative particles. *Am J Pathol*. 1984;114:201-208.
43. Borrell-Pages M, Vilahur G, Romero JC, Casaní L, Bejar MT, Badimon L. LRP5/canonical Wnt signaling in healing of ischemic myocardium. *Basic Res Cardiol*. 2016;111:67.
44. Badimon L, Casaní L, Camino-Lopez S, Juan-Babot O, Borrell-Pages M. GSK3β inhibition and canonical Wnt signaling in mice hearts after myocardial ischemic damage. *PLoS One*. 2019;14:e0218098.
45. Brundert M, Heeren J, Merkel M, et al. Scavenger receptor CD36 mediates uptake of high density lipoproteins in mice and by cultured cells. *J Lipid Res*. 2011;52:745-758.
46. Krieger M. Scavenger receptor class B type I is a multiligand HDL receptor that influences diverse physiologic systems. *J Clin Invest*. 2001;108:793-797.
47. Kobayashi K, Oka K, Forte T, et al. Reversal of hypercholesterolemia in low density lipoprotein receptor knockout mice by adenovirus mediated gene transfer of the very low density lipoprotein receptor. *J Biol Chem*. 1996;271:6852-6860.
48. Fujino T, Asaba H, Kang MJ, et al. Low-density lipoprotein receptor-related protein 5 (LRP5) is essential for normal cholesterol metabolism and glucose-induced insulin secretion. *Proc Natl Acad Sci U S A*. 2003;100:229-234.
49. Willnow TE, Sheng Z, Ishibashi S, Herz J. Inhibition of hepatic chylomicron remnant uptake by gene transfer of a receptor antagonist. *Science*. 1994;264:1471-1474.
50. Rohlmann A, Gotthardt M, Hammer RE, Herz J. Inducible inactivation of hepatic LRP gene by cre-mediated recombination confirms role of LRP in clearance of chylomicron remnants. *J Clin Invest*. 1998;101:689-695.
51. Maxwell KN, Soccio RE, Duncan EM, Sehayek E, Breslow JL. Novel putative SREBP and LXR target genes identified by microarray analysis in liver of cholesterol-fed mice. *J Lipid Res*. 2003;44:2109-2119.
52. Horton JD, Shah NA, Warrington JA, et al. Combined analysis of oligonucleotide microarray data from transgenic and knockout mice identifies direct SREBP target genes. *Proc Natl Acad Sci U S A*. 2003;100:12027-12032.
53. Hua X, Yokoyama C, Wu J, et al. SREBP-2, a second basic–helix–loop–helix–leucine zipper protein that stimulates transcription by binding to a sterol regulatory element. *Proc Natl Acad Sci U S A*. 1993;90:11603-11607.
54. Sheng Z, Otani H, Brown MS, Goldstein JL. Independent regulation of sterol regulatory element-binding proteins 1 and 2 in hamster liver. *Proc Natl Acad Sci U S A*. 1995;92:935-938.
55. Rashid S, Curtis DE, Garuti R, et al. Decreased plasma cholesterol and hypersensitivity to statins in mice lacking Pcsk9. *Proc Natl Acad Sci U S A*. 2005;102:5374-5379.
56. Dubuc G, Chamberland A, Wassef H, et al. Statins upregulate PCSK9, the gene encoding the proprotein convertase neural apoptosis-regulated convertase-1 implicated in familial hypercholesterolemia. *Arterioscler Thromb Vasc Biol*. 2004;24:1454-1459.
57. Blaner WS, O'Byrne SM, Wongsiriroj N, et al. Hepatic stellate cell lipid droplets: a specialized lipid droplet for retinoid storage. *Biochim Biophys Acta*. 2009;1791:467-473.
58. Moriwaki H, Blaner WS, Piantedosi R, Goodman DS. Effects of dietary retinoid and triglyceride on the lipid composition of rat liver stellate cells and stellate cell lipid droplets. *J Lipid Res*. 1988;29:1523-1534.

SUPPORTING INFORMATION

Additional supporting information may be found in the online version of the article at the publisher's website.

How to cite this article: Luquero A, Vilahur G, Casani L, Badimon L, Borrell-Pages M. Differential cholesterol uptake in liver cells: A role for PCSK9. *FASEB J*. 2022;36:e22291. doi:10.1096/fj.202101660RR

3.4 Article 3

Canonical WNT pathway involvement in high fat diet-induced adipose tissue distribution

By Aureli Luquero, Noelia Pimentel, Lina Badimon and Maria Borrell-Pages

Submitted in June 2024.

Summary: Obesity is a real-threat epidemic in the world and a major comorbidity in many diseases including metabolic syndrome or cardiovascular diseases. Understanding the mechanisms that promote the generation of fat tissue is of interest for human health. In this study we investigated the mechanisms by which the canonical WNT receptor LRP5 participates in adipose tissue differentiation induced by hypercholesterolemia in mice.

We performed extensive gene expression analysis on adiposity and inflammation markers in WAT and BAT tissues of Wt and Lrp5-/- mice fed a chow or hypercholesterolemic diet and found that LRP5 expression is promoted by hypercholesterolemia in visceral and subcutaneous adipose tissue. LRP5 expression is also increased in human adipose tissues of obese patients. Moreover, the absence of LRP5 expression resulted in impaired adipose tissue growth, reduced adipocyte differentiation and altered inflammatory profile; particularly a decrease in pro-inflammatory macrophage markers.

This study sheds light on the significance of LRP5 in regulating adipose tissue dynamics, offering valuable insights into the molecular mechanisms governing obesity development. Although deeper investigation is required to clarify the modulation of the molecular pathways triggered after LRP5 activation, potential therapies can arise

from the investigation of canonical WNT signalling pathway in adipose tissue to prevent obesity-related diseases.

"Canonical WNT pathway involvement in high fat diet-induced adipose tissue distribution"

by Aureli Luquero [(1), (2)], Noelia Pimentel [(1), (2)], Lina Badimon [(1), (3), *] and Maria Borrell-Pages [(1), (3)]

[1]: Institut de Recerca Sant Pau, Barcelona, Spain

[2]: Biomedicine Doctorate Program, Universitat de Barcelona, Barcelona, Spain

[3]: CIBER-CV, Instituto de Salud Carlos III, Madrid, Spain

[*]Address for correspondence: Dr. Lina Badimon

Sant Pau Institute for Biomedical Research (IIB-Sant Pau)

C/ Sant Antoni Maria Claret 167

08025 Barcelona, Spain

Tel: 34-935565621

E-mail: lbadimon@santpau.cat

Figures: 6 Figures

Manuscript Category: Research article

Word Count: 4500 words+ References

Keywords: LRP5, adipose tissue, VAT, SCAT, inflammation

Abstract

Obesity is a world epidemic threat and a major cause of chronic diseases morbimortality. Understanding the mechanisms that promote the generation of adipose tissues will allow the development of effective treatments for patients at risk. Cardiovascular disease is associated to high fat diet intake, however how adiposity is distributed in relation to common fat intake is not fully known.

The lipoprotein receptor LRP5 is involved in lipid handling in several cells and tissues. Whether LRP5 and its downstream signalling pathway, the canonical WNT pathway are involved in high fat diet-induced adipose tissues distribution is not known. We fed *Wt* and *Lrp5*$^{-/-}$ mice with a high cholesterol diet and analysed adipose and inflammatory markers in their brown and white adipose tissues. We show more fat deposition in *Wt* mice than in *Lrp5*$^{-/-}$ mice upon high fat diets intake. LRP5 and LRP1 expression are increased in mice visceral and subcutaneous adipose tissues of hypercholesterolemic mice. Markers of adiposity and inflammation show that absence of LRP5 induces reduced adipocyte growth and differentiation and decreased expression of macrophage markers indicating a role for LRP5 in lipid metabolism homeostasis. LRP5 expression is also increased in human adipose tissues of obese patients. We show that LRP5 is involved in adipose tissue growth by inducing tissue proliferation and insulin sensitivity and, simultaneously, by enhancing macrophage's infiltrating capacity into the adipose tissue triggering the inflammatory process associated to proliferating adipose tissue. This study shows that therapies can arise from the investigation of the canonical WNT signalling pathway in adipose tissues to prevent obesity-related diseases.

Introduction

The relationship between obesity and cardiovascular diseases is undeniable. Weight-gain in obese humans is characterized by adipose tissue hypertrophy, that eventually leads to cardiovascular diseases (1,2). Before the year 2000, to evaluate obesity, researchers focused mainly on the amount of adipose tissue. However, it is now known that adipose tissue distribution is more important for cardiovascular diseases' incidence (1,2). Adipose tissues have unique properties and can be classified in white adipose tissue (WAT) and brown adipose tissue (BAT). While WAT function is to serve as a fat deposit, BAT is metabolically more active as its main function is to regulate body temperature (3,4). WAT is enough to isolate internal organs from extreme cold temperatures from outside in adulthood and in big mammals (5). BAT is evolutionary conserved in individuals that suffer from temperature loss due to a small volume/surface ratio like small mammals and newborns (6,7). Hence, WAT accumulates fat and BAT uses fat to generate heat.

The two major reservoirs of WAT in adulthood are subcutaneous and abdominal fat. Subcutaneous white adipose tissue (SCAT) is the physiologic buffer for excess of energy intake (hypercaloric diets), absorbing circulating sugars and fats in response to insulin and generating triglycerides that are stored in adipocytes (8). When the storage capacity of SCAT is exceeded, fat starts to accumulate in different regions of the abdominal cavity in visceral adipose tissue (VAT) (9). In normal conditions, SCAT is approximately 80% of the total WAT in human adults, while VAT accounts for 10-20% of total WAT in men and 5-8% in women (10,11). The amount of VAT increases with age in both genders (10).

Increased VAT but not SCAT induces increased risk of type I diabetes, elevated circulating cholesterol and triglycerides, hypertension, metabolic syndrome, stroke, peripheral artery disease and/or reduced thickness in vascular walls (12–15). This is because there is higher innervation, irrigation and vascularization in VAT compared to SCAT, connecting the fat depot to systemic regulation by nerves and hormones (12). As VAT becomes more vascularized, inflammatory cells infiltrate VAT and are found in high levels (16). VAT is more sensible than SCAT in response to glucocorticoid- and androgen-stimulus while SCAT reacts preferentially to catecholamine- and oestrogen stimulus (17–20).

Epicardial adipose tissue (EAT) is the WAT tissue that covers the heart surface, being more abundant in the atrioventricular node, the interventricular groves and the right ventricle where it exerts protective functions in the myocardium (21). EAT protects the coronary arteries mechanically and metabolically, as it buffers the torsion generated by the arterial pulse and cardiac contraction and protects the myocardium from high concentrations of circulating inflammatory and pathogenic substances (22). Also, EAT serves as a source of fatty acids for the myocardium during periods of high-demand as the heart is nurtured by fatty acids through β-oxidation (23,24).

BAT is present in the cervical, supraclavicular, axillary and paravertebral regions of adult mammals and is specialised for energy expenditure. BAT adipocytes are characterized by multiple small lipid droplets and many mitochondria needed to release energy as heat in a non-shivering thermogenesis process (25). BAT exclusively express the mitochondrial protein Uncoupling Protein 1 (UCP-1), that blocks ATP synthesis and dissipates energy as heat (26). This thermogenic capacity makes BAT an interesting tissue to fight the complications of human obesity (27–29).

Canonical WNT signalling is an evolutionary conserved pathway needed in cellular proliferation and morphogenesis, the maintenance of tissue homeostasis and the regulation of developmental processes (30). The pathway activates by binding of canonical WNT ligands to membrane-bound low-density lipoprotein-related proteins 5 and 6 (LRP5 / LRP6) and to Frizzled coreceptors inducing the stabilisation and accumulation of β-catenin in the cytoplasm that will translocate into the nucleus to activate the transcription factors TCF/Lef1, which regulate the expression of canonical WNT target genes (31).

Activation of canonical WNT signalling in preadipocytes by overexpression of Wnt1 or Wnt10a (two WNT ligands), gain-of-function mutations in β-catenin or pharmacological inhibition of glycogen synthase kinase 3 beta (GSK3β, a WNT inhibitor), block adipogenesis by suppressing the expression of the adipogenic transcription factors peroxisome proliferator-activated receptor gamma (PPARγ) and CCAAT/enhancer-binding protein alpha (C/EBPα) (32). Also, inhibition of WNT signalling in preadipocytes using secreted Frizzled-Related protein 1 and 2 (sFRP1 and sFRP2) soluble inhibitors or enhanced expression of the negative regulator Axin results in spontaneous adipogenic differentiation, indicating that canonical WNT signalling and β-catenin activity are important repressors for adipocyte differentiation (33,34). Furthermore, during mesenchymal stem cell differentiation, canonical WNT signalling stimulates the differentiation of multipotent cells into pre-osteoblastic cells blocking differentiation into pre-adipocytic cells (35). Taken together, these results indicate that in early-stages of mesenchymal stem cell differentiation the canonical WNT pathway is a repressor of adipose tissue generation.

Mice and human patients with gain-of-function mutations in LRP5 exhibit high-bone mass (HBM) phenotype (36,37) while loss-of-function mutations lead to osteoporosis (38), which in a small study with 12 subjects of two different families was also coupled with increased prevalence of Type-2 Diabetes (39). Also, patients carrying LRP5 gain-of-function mutations show increased amount of lower-body fat, enhanced insulin sensitivity and lower inflammatory profile in subcutaneous adipocytes compared to non-related-to-LRP5 HBM patients indicating a role for canonical WNT signalling in modulating human fat distribution (40). Furthermore, the expression of the rs559083 allele, associated with reduced LRP5 function, correlates with an increased upper-body fat accumulation (40). In mice, loss of LRP5 expression in osteoblasts induces loss of insulin

sensitivity and ectopic lipid accumulation during high-fat diet treatments (41). *Lrp5*$^{-/-}$ mice pre-adipocytes show impaired DNA repair, that results in increased inflammation in gluteal cells and in a reduced ability of SCAT to proliferate (42).

Because weight gain induces increased adipose tissue, we hypothesized that high-fat fed mice have different adipose tissue distribution than normocholesterolemic mice. We also hypothesized that LRP5 is involved in adipose tissue distribution because of its different functions in lipid metabolism. We analysed the role of LRP5 in WAT and BAT mice adipose tissue depots and found that LRP5-dependent canonical WNT signalling is involved in changes in insulin sensitivity and adipose tissue proliferation and differentiation. Furthermore, LRP5 expression is needed for the infiltration of immune cells into the adipose tissue and the triggering of inflammatory processes.

Methods

Animal protocols

Experimental procedures were reviewed and approved by the Institutional Animal Care and Use Committee of the Sant Pau Research Institute and authorized by the Animal Experimental Committee of the local government authority (Generalitat de Catalunya, authorization No. ICCC051/5422) in accordance to the Spanish Law (RD 53/2013) and the European Directive 2010/63/EU. Procedures were performed at the Animal Experimentation Service,ISO 9001:2015 certified. In addition, the investigation conforms to the Guide for the Care and Use of Laboratory Animals published by the US National Institutes of Health (NIH Publication No. 85–23, revised 1985), follows the ARRIVE guidelines (Animal Research: Reporting of In Vivo Experiments), and is committed to the 3Rs of laboratory animal research and consequently used the minimal number of animals to reach statistical significance.

Lrp5 alleles were amplified by using PCR of DNA extracted from tail biopsies. Primers sequence for PCR amplification were as follows S17 (GGC TCG GAG GAC AGA CCT GAG), S23 (CTG TCA GTG CCT GTA TCT GTC C) and IRES31 (AGG GGC GGA ATT CGA TAG CT). *Wt* and *Lrp5*$^{-/-}$ mice were fed a normal chow diet for the first 10 weeks (NC, Tekland Diet, Harland Labs Berkeley, CA, USA). Animals of both genotypes were the divided into two groups to be fed a NC or a HC diet (42% fat; TD.88137, Harland Labs) for the following 8 weeks (8-12 mice per group). Mice were weighed weekly from 10 to 18 weeks.

At 18 weeks old, mice were terminally anesthetised by intraperitoneal injection of 1 mg/kg medetomidine and 75 mg/kg ketamine. Cardiac puncture was performed to obtain the maximum blood volume. Immediately after, fat depots were collected and frozen by immersion in liquid nitrogen for further processing. SCAT contained the fat depots in the inguinal and axillar areas; VAT contained the fat depots in the omental and mesenchymal areas; EAT contained the fat depot covering the upper region of the heart and BAT contained the fat depots in the interscapular dorsal region of the mice. Before freezing, each adipose tissue mass was weighed.

Human adipose tissue collection

SCAT and VAT were obtained via surgical resection from young individuals with morbid obesity (BMI > 40 kg/m^2) who underwent bypass gastric surgery. In these obese patients, AT was obtained simultaneously from subcutaneous and visceral depots during surgery. Additionally, adipose tissue was collected from young individuals with normal weight (BMI < 25 kg/m^2) who underwent abdominal lipectomy. Informed consent was obtained from all donors and the study protocol was approved by the Centro Medico Teknon Ethical Committee that is in accordance with the principles of the Declaration of Helsinki.

Tissue processing

Frozen tissue samples were smashed in liquid nitrogen and 1 gram of each sample was processed using a RNeasy Extraction Kit (Qiagen) to obtain pure RNA. RNA concentration and purity was determined using a NanoDrop ND-1000 spectrophotometer (Nanodrop Technologies) and only samples with ratios 260/280 and 260/230 between 1.8-2.2 were considered acceptable. cDNA was synthesised using a cDNA Reverse Transcription kit (Qiagen). The resulting cDNA samples were amplified in a RT-qPCR thermal cycler (Applied Biosystems) using the following probes LRP5 (Mm00493187_m1 / Hs00182031_m1), LRP1 (Mm00464608_m1 / Hs00233856_m1), Fabp4 (Mm00445878_m1), LPL (Mm00434764_m1), CD36 (Mm00432403_m1), CD68 (Mm03047343_m1), CD11b (Mm00434455_m1), F4/80 (Mm00802529_m1), Nos2 (Mm00440502_m1), CD80 (Mm00711660_m1), CCR7 (Mm00432608_m1), Pcsk9 (Mm01263610_m1), Arg1 (Mm00475988_m1), CD163 (Mm00474091_m1) and CD206 (Mm01329359_m1).

Statistical analysis

Results are found expressed as mean ± standard error of the mean. A StatView statistical software was used for all the analysis. Comparisons among groups was performed using One-way Anova analysis. Differences between groups were performed using Fisher's test. Statistical significance was considered when $p<0.05$.

Results

Reduced adipose tissue growth in *Lrp5*$^{-/-}$ mice

Wt and *Lrp5*$^{-/-}$ mice were fed a normocholesterolemic (NC) or a hypercholesterolemic (HC) diet for 8 weeks when mice were sacrificed and adipose tissue samples including VAT, SCAT, EAT and BAT were obtained. *Wt* and *Lrp5*$^{-/-}$ mice fed NC diets showed similar weight at sacrifice (Fig 1A). Adipose tissue weights (VAT, SCAT, EAT and BAT) and the ratio between adipose tissue weight and total body weight were also similar in both genotypes (Figures B-F). The role of HC on mice total body weight and adipose tissue weight was then analyzed. After hypercholesterolemic feeding, HC *Wt* mice show a 10 g gain in total body weight compared to their NC littermates while HC *Lrp5*$^{-/-}$ mice weight increased only by 2,5 g compared to NC *Lrp5*$^{-/-}$ mice (Fig 1A, 1G and 1M). Although adipose tissue weights were also increased after HC feeding in both *Wt* and *Lrp5*$^{-/-}$ mice, *Wt* mice show more fat deposits (Fig H-K, M). The ratio between adipose tissue weight and total body weight shows increased fat accumulation in HC *Wt* mice compared to HC *Lrp5*$^{-/-}$ mice indicating that mice without LRP5 accumulate less fat after high fat diets (Fig 1L).

Increased LRP1 and LRP5's expression in hypercholesterolemic mice

VAT and SCAT from HC *Wt* mice show increased LRP5 gene expression levels compared to NC *Wt* mice (Fig 2A). Interestingly, LRP5 expression levels are downregulated in EAT after HC diets while they remain constant in BAT. LRP5 expression is undetectable in adipose tissues from *Lrp5*$^{-/-}$ mice (Fig 2A). Gene expression of LRP1, known to contribute to lipoprotein internalization, is also increased in VAT and SCAT from HC *Wt* and HC *Lrp5*$^{-/-}$ mice compared to NC *Wt* and NC *Lrp5*$^{-/-}$ mice respectively revealing that diets induce similar LRP1 upregulation in mice of both genotypes (Fig 2B). LRP1 gene expression levels in VAT and SCAT of *Lrp5*$^{-/-}$ mice are lower than in *Wt* mice independent of diets indicating that LRP1 expression is downregulated in the absence of LRP5 expression in these tissues. LRP1 expression levels in EAT and BAT is lower than that of VAT and SCAT and are not modified by diets nor genotype (Fig 2B). The increase in LRP1 gene expression levels in VAT and SCAT of *Wt* mice is bigger than that of *Lrp5*$^{-/-}$ mice (Fig 2C).

Increased LRP1 and LRP5's expression in obese patients

We also analysed lipoprotein receptor's expression in adipose tissues of obese and lean individuals. VAT and SCAT from obese patients show increased LRP5 gene expression levels compared to SCAT from lean patients (Fig 2D). LRP1 expression is increased in SCAT from obese patients compared to SCAT obtained from lean patients (Fig 2E). Interestingly, LRP1 expression levels in VAT from obese patients is lower than in SCAT from lean and obese patients, suggesting a minor role for LRP1 in lipid uptake in VAT from obese patients (Fig 2E).

Adipocyte markers are increased in hypercholesterolemic mice

The ability of *Wt* and *Lrp5*$^{-/-}$ mice to generate new adipose tissue was then evaluated. VAT and SCAT from HC *Wt* and HC *Lrp5*$^{-/-}$ show increased expression of the adipocyte marker FABP4 suggesting increased presence of mature adipocytes (Fig 3A). FABP4 gene expression is very low in EAT but shows a similar pattern in VAT and SCAT (Fig 3A). FABP4 expression in BAT remains constant independently of dietary treatments or genotype (Fig 3A). VAT and SCAT from both genotypes show similar increase in FABP4 gene levels suggesting that both adipose tissues have the ability to generate new adipose tissue after HC diets (Figure 3B). LPL gene expression levels are increased in VAT and SCAT from HC *Wt* mice compared to NC *Wt* mice while *Lrp5*$^{-/-}$ mice show similar LPL gene expression levels independently of dietary treatments (Fig 3C). Also, VAT and SCAT of HC *Lrp5*$^{-/-}$ mice show lower LPL gene expression compared to HC *Wt* mice indicating reduced lipoprotein degradation in *Lrp5*$^{-/-}$ mice adipose tissue (Figure 3D). CD36 gene expression levels are upregulated by HC diets in *Wt* and *Lrp5*$^{-/-}$ mice suggesting increased fatty acid absorption in HC mice adipocytes (Figure 3E). Interestingly, CD36 expression levels in HC *Lrp5*$^{-/-}$ mice is significantly lower than in HC *Wt* mice indicating reduced fatty acid absorption in *Lrp5*$^{-/-}$ mice (Figure 3F). EAT expression levels for LPL and CD36 are very low compared to the other adipose tissues. Similar to FABP4, LPL and CD36 gene expression levels in BAT are moderately high and are not modified by diets or genotype.

Macrophage markers are reduced in *Lrp5*$^{-/-}$ mice adipose tissues

To analyse the inflammatory profile of the different adipose tissues, we characterised gene expression levels of well-defined macrophage markers. Gene expression levels of CD68, CD11b and F4/80 are upregulated in VAT and SCAT of HC animals compared to NC mice independently of genotype (Fig 4A, 4C and 4E). However, this upregulation is significantly lower in HC *Lrp5*$^{-/-}$ mice compared to HC *Wt* mice indicating reduced presence of macrophages in *Lrp5*$^{-/-}$ mice adipose tissues (Fig 4B, 4D and 4F). NC *Lrp5*$^{-/-}$ mice show less CD68, CD11b and F4/80 gene expression levels in VAT, SCAT and EAT compared to NC *Wt* mice suggesting that *Lrp5*$^{-/-}$ mice have fewer resident macrophages. In contrast to VAT and SCAT, gene expression of macrophage markers in BAT is extremely low, revealing a very small resident macrophage population in the tissue.

Pro-inflammatory profile in mice adipose tissues

To better define the role of the inflammatory cells in the different adipose tissues, we further studied their inflammatory profile. NC *Wt* and NC *Lrp5*$^{-/-}$ mice show similar expression levels of the pro-inflammatory marker CD80 in VAT and SCAT (Fig 5A). HC treatments upregulate CD80 gene expression in VAT and SCAT of *Wt* mice, and to a lesser extent of *Lrp5*$^{-/-}$ mice (Fig 5B). EAT shows the highest CD80 expression, while CD80 expression in BAT is almost undetectable.

Adipose tissues pro-inflammatory profile was further assessed by the analyses of Nos2 and PCSK9 gene expression levels. After HC diets Nos2 gene expression is increased in VAT of both HC *Wt* and HC *Lrp5*$^{-/-}$ mice indicating increased inflammation in HC fed mice compared to NC mice (Fig 5B). HC *Lrp5*$^{-/-}$ mice show less increase in Nos2 gene expression than HC *Wt* mice, both in VAT and SCAT, indicating less inflammation in these adipose tissues in *Lrp5*$^{-/-}$ mice (Fig 5C). Nos2 gene expression in EAT and BAT remained unchanged after HC treatments; however, as observed in CD80, EAT of *Lrp5*$^{-/-}$ mice show less expression of Nos2 than *Wt* mice.

VAT and EAT have relatively high PCSK9 gene expression levels independently of genotype or dietary treatments while SCAT and BAT have relatively low PCSK9 gene expression levels (Fig 5D). Interestingly, HC diets do not modify PCSK9 gene expression levels in the tissues suggesting that PCSK9 in the adipose tissues is not regulated by lipids. Also, PCSK9 gene expression remains constant in *Wt* and *Lrp5*$^{-/-}$ mice suggesting that LRP5 is not involved in PCSK9's adipose tissue gene expression regulation.

We also analysed gene expression of CCR7, a lymphocyte and dendritic cell marker. Very low CCR7 gene expression is observed in VAT and BAT of *Wt* and *Lrp5*$^{-/-}$ mice. SCAT and EAT express CCR7 independent of genotype (Fig 5E). HC feeding induced upregulation of CCR7 gene expression levels only in SCAT of HC *Wt* mice suggesting lower lymphocyte accumulation in adipose tissues of HC *Lrp5*$^{-/-}$ mice (Fig 5F).

Anti-inflammatory profile is preserved in *Lrp5*$^{-/-}$ mice adipose tissues

To better understand the inflammatory process in adipose tissues, the anti-inflammatory macrophage markers CD163, CD206 and Arginase 1 (Arg1) were analysed. VAT and SCAT of *Wt* mice show higher CD163 expression than *Lrp5*$^{-/-}$ mice (Fig 6A). Interestingly, while mice from both genotypes increase their CD163 gene levels after HC feeding, the increase in adipose tissues of *Lrp5*$^{-/-}$ mice is steeper (Fig 6B). CD206 gene expression levels are also increased in VAT and SCAT of *Wt* mice compared to *Lrp5*$^{-/-}$ mice (Fig 6C). However, HC treatments increase CD206 gene expression levels in both *Wt* and *Lrp5*$^{-/-}$ mice in a similar manner (Fig 6D). CD163 and CD206 gene expression levels in EAT and BAT are very low and do not increase after HC treatments (Fig 6A, 6C). Finally, Arg1 gene expression analyses show a consistently low expression of this macrophage marker in all adipose tissues (Fig 6E-F).

Discussion

The role of canonical WNT signalling in adipocyte's is still under debate. LRP5 is involved in cell fate determination as canonical WNT signalling promotes osteoblastic rather than adipocytic differentiation in human mesenchymal stem cells (43). Nonetheless, nuclear β-catenin-TCF/Lef1 complex can interact with the transcription factor p300 initiating adipocyte differentiation (44). Therefore, it seems that not only extracellular WNT ligands induce mesenchymal cells proliferation or differentiation programmes but also downstream intranuclear interactions. Also, the signals that lead to the promotion/inhibition of adipogenesis by the canonical WNT pathway are still not known. For example, Wnt5a, a canonical ligand inhibitor is a negative regulator of adipogenesis, while vascular endothelial growth factor (VEGF), a target of the canonical WNT signalling is closely involved in the growth and proliferation of adipocytes (45). Our results support a role for LRP5 in the regulation of proliferation in mice adipose tissues. Indeed, *Lrp5*$^{-/-}$ mice show less weight gain than *Wt* mice after HC diets. Furthermore, VAT, SCAT, EAT and BAT weights at sacrifice are also higher in HC *Wt* mice than in HC *Lrp5*$^{-/-}$ mice indicating that mice without LRP5 accumulate less fat after high fat diets.

LRP1 mediates the internalization of chylomicron remnants and LDL-bound LPL in the liver (46). When adipocytes are stimulated by insulin, LRP1-mediated uptake of triglycerides and cholesteryl esters increases together with LPL expression (47). Interestingly, LRP1 and LPL showed similar gene expression levels in *Wt* mice and their expression increased after HC diets, when blood insulin concentration is higher. Loss of LRP5 expression in the adipose tissue significantly reduced LRP1 and LPL gene expression, indicating that tissue sensitivity to insulin is reduced, which probably resulted in reduced fat internalization and lower weight-gain in HC *Lrp5*$^{-/-}$ mice. Furthermore, CD36 gene expression levels are also low in HC *Lrp5*$^{-/-}$ mice compared to HC *Wt* mice. CD36 is a well-stablished marker for adipocyte differentiation and a high-affinity receptor for circulating long-chain fatty acids that contributes to lipid accumulation in adipose tissue (48,49). Lack of CD36 expression has also been associated with insulin resistance (50,51). Human volunteers with low insulin sensitivity show decreased gene expression of LRP5, Wnt10b, Frizzled-1, Frizzled-8 and β-catenin indicating that an active canonical WNT pathway is needed for correct insulin sensitivity in white adipose tissue (52). Also, a crosstalk between WNT signalling and insulin signalling where LRP5 is a coreceptor of both pathways leading to the phosphorylation of Akt, ERK1/2 and GSK3β in undifferentiated adipocytes has also been demonstrated (53). These findings not only support our hypothesis of impaired insulin sensitivity in *Lrp5*$^{-/-}$ mice white adipose tissues but also suggest a link between LRP5-dependent canonical WNT signalling, insulin sensitivity and adipose tissue proliferation.

FABP4 is a protein of the "fatty acid binding protein" family that regulates lipid trafficking (54,55). It accounts for 1% of all soluble proteins in WAT and indicates presence of mature adipocytes (56,57). High fat diets increase adipocytes FABP4 gene expression in mice and humans as WAT specialises in energy storing and proliferation (58). Our results show increased FABP4 gene expression levels in HC mice compared to NC mice, with no differences between animals of different genotypes. This indicates that the adipose tissue is able to generate fully-differentiated adipocytes after HC diets in both *Wt* and *Lrp5*$^{-/-}$ mice. Hence, differences in total body weight and adipose tissue weight cannot be explained by the inability of *Lrp5*$^{-/-}$ mice's adipose tissue to mature correctly.

Inflammatory cells play key roles in the differentiation process of the adipose tissues (59). Increased monocyte/macrophage recruitment in HC *Wt* mice compared to NC *Wt* mice was observed by increased gene expression levels of CD68, CD11b and F4/80. Interestingly, VAT and SCAT of HC *Lrp5*$^{-/-}$ mice show reduced expression of these markers compared to HC *Wt* mice, revealing a reduced population of inflammatory macrophages in HC *Lrp5*$^{-/-}$ mice. LRP5 is expressed in macrophages infiltrated into the vessel intima of human atherosclerotic plaques with a migratory function (60). It is then plausible that *Lrp5*$^{-/-}$ mice macrophages show reduced migratory function and their infiltration into the adipose tissue is reduced.

While in normal-weight patients macrophages show anti-inflammatory properties, adipose tissue macrophages (ATMs) in obese patients shift to a pro-inflammatory phenotype (61). Numerous studies have demonstrated a role for ATMs and inflammatory mediators in the impairment of insulin signalling pathways (62–64). We observe a significant increase in the pro-inflammatory macrophage marker CD80 in VAT of HC *Wt* compared to HC *Lrp5*$^{-/-}$ mice indicating higher infiltration of inflammatory macrophages. Soluble PCSK9 participates in LDL- and VLDL-derived triglyceride accumulation in mice adipose tissues (65,66). PCSK9 expression in adipocytes is also regulated by insulin and may contribute to the impaired insulin sensitivity of *Lrp5*$^{-/-}$ mice. Our results show that PCSK9 is mainly expressed in VAT and EAT. In humans, PCSK9 gene expression in VAT is associated with an elevated body mass index and a pro-inflammatory profile, which is consistent with the elevated PCSK9 gene levels observed in mice (67). Interestingly, the interaction observed between LRP5 and PCSK9 in human macrophages does not seem to be taking place in mice adipose tissue (68). PCSK9 intracellular levels of lipid-loaded macrophages are low because it is transported to the plasma membrane and released to the extracellular milieu in a process that involves LRP5 (68). However, because PCSK9 levels do not decrease after HC diets in adipose tissue mice we believe this mechanism takes place in macrophages but not in adipocytes.

The anti-inflammatory macrophage markers CD163 and CD206 increase their gene expression in VAT and SCAT of HC *Wt* and HC *Lrp5*$^{-/-}$ mice compared to their NC littermates. Interestingly, *Lrp5*$^{-/-}$ mice consistently show lower expression of macrophage anti-inflammatory markers than *Wt* mice suggesting an anti-inflammatory role for LRP5 in VAT and SCAT and in line with previous results where LRP5 expression is associated to the anti-inflammatory macrophage phenotype (69).

While low-bone-mineral-density LRP5 alleles correlate with increased abdominal adiposity, LRP5 high-bone-density phenotypes are associated with a healthier lower-body fat accumulation suggesting a role for LRP5 and the canonical WNT pathway in the distribution of body fat (40). Also, LRP5 expression in humans is higher in abdominal fat than in gluteal fat (40). LRP5 knockdown in human VAT or SCAT adipocytes reduced their proliferation; however while SCAT adipocytes also showed a limited differentiation, the differentiation process in LRP5 deficient VAT adipocytes remained unaltered (40). Mutations in other canonical WNT signalling regulators including the leucine-rich repeat containing G protein-coupled receptor-4 (LGR4), the zinc and ring finger 3 (ZNRF3) or R-spondin 3 (Rspo3) have been associated to adiposity as well. ZNRF3 is a transmembrane protein that regulates Frizzled receptors levels by ubiquitination, promoting its degradation and reducing canonical WNT signalling (70). LGR proteins, on the other hand, promote canonical WNT signalling by stabilising the signal transducing LRP5/6-Frizzled complex on the surface (71). R-spondin proteins are soluble ligands that bind to both receptors inhibiting ZNRF3 and activating LGR (72). A gain-of-function mutation in LGR4 is associated with increased central obesity, as human carriers are characterized by abdominal visceral fat accumulation (73). In a meta-analysis of GWAS for waist-to-hip ratio, the Rspo3 and the ZNRF3 locis were disclosed as regulators of waist-to-hip ratio, a rare SNP in Rspo3 correlated with an increased waist-to-hip ratio while a SNP in ZNRF3 correlated with reduced waist-to-hip ratio (74). In mice, β-catenin was shown to have distinct activity in mature adipocytes and in adipocyte progenitors. Mature adipocyte β-catenin expression contributed to adipocyte lipid metabolism preservation but adipocyte progenitor β-catenin expression induced a loss in adiposity as cells were differentiated into a fibroblastic-like subtype (75). These results indicate that canonical WNT signalling has distinct roles over the adipocyte differentiation process inhibiting adipocyte differentiation in mesenchymal stem cells but preserving adipocyte's lipid metabolism in mature adipose tissues. Our results show that not only weight gain due to HC diets was reduced in HC *Lrp5*$^{-/-}$ mice compared to HC *Wt* mice, but the amount of adipose tissues compared to total body weight was significantly reduced in HC *Lrp5*$^{-/-}$ mice indicating that LRP5 in the adipose tissue has a role on the regulation of obesity. In line with our results, loss of Wntless expression, a downstream effector of canonical WNT pathway, protects mice from diet-induced obesity and metabolic dysfunction (76). It also has been reported that *β-catenin*$^{-/-}$ mice are resistant to obesity

induced by diet compared to control mice, while improving insulin sensitivity at the same time (77). A recent study also demonstrated that exclusive lack of β-catenin expression in mice adipocytes fed a high-fat diet exhibit decreased adiposity in mature adipose tissue, indicating that the pathway is a key regulator of mature adipocyte *de novo* lipogenesis and fatty acid desaturation (78). Also, a potential role for stromovascular cells (mesenchymal stem cell progenitors located in the adipose tissue) to replace the loss of function in β-catenin-deficient differentiated adipocytes has been suggested indicating an homeostatic role for canonical WNT signalling in WAT lipid metabolism (78). Interestingly, results observed in *β-catenin*$^{-/-}$ mice challenged with high-fat diets support the results observed in *Lrp5*$^{-/-}$ mice as HC *β-catenin*$^{-/-}$ mice are also leaner than their *Wt* littermates indicating reduced obesity when the canonical WNT signalling pathway is downregulated.

Of note, gene expression in EAT and BAT are not modified by HC treatments nor by the presence/absence of LRP5 expression. EAT has a very specific function in maintaining the heart protected and nourished. Obesity enhances cardiovascular risk factors, such as hypertension, which correlates directly with cardiac hypertrophy (79). Also, as mice size increases due to high-fat diets, so does the heart (80). Hence, we show that EAT needs to proliferate and increase its mass and volume to maintain cardiac function and heart integrity. Differences in BAT mass between HC *Wt* and HC *Lrp5*$^{-/-}$ mice can also be explained by total body weight increase.

Our study has limitations. The study provides transcriptomic data without protein expression analysis. However, we believe that these RNA-based findings are enough to sustain our conclusions. Also, the research provides data from a *Lrp5*-deficient mice model; similar analysis conducted in other research models with lack of expression of canonical WNT signalling members would be of great interest.

In conclusion, our results show that high-fat fed mice have different adipose tissue distribution than normocholesterolemic mice. Furthermore, we unravel a mechanism where LRP5 is involved in adipose tissue growth by inducing tissue proliferation and insulin sensitivity and, simultaneously, by enhancing macrophage's infiltrating capacity into the adipose tissue triggering the inflammatory process associated to proliferating adipose tissue.

References

1. Longo M, Zatterale F, Naderi J, Parrillo L, Formisano P, Raciti GA, Beguinot F, Miele C. Adipose Tissue Dysfunction as Determinant of Obesity-Associated Metabolic Complications. Int J Mol Sci. 2019 May 13;20(9):2358.

2. Bays HE, González-Campoy JM, Bray GA, Kitabchi AE, Bergman DA, Schorr AB, Rodbard HW, Henry RR. Pathogenic potential of adipose tissue and metabolic consequences of adipocyte hypertrophy and increased visceral adiposity. Expert Rev Cardiovasc Ther. 2008 Mar;6(3):343-68.

3. Smorlesi A, Frontini A, Giordano A, Cinti S. The adipose organ: White-brown adipocyte plasticity and metabolic inflammation. Obesity Reviews. 2012;13(Suppl 2):83–96.

4. Rosenwald M, Wolfrum C. The origin and definition of brite versus white and classical brown adipocytes. Adipocyte. 2014;3(1):4–9.

5. Finlin BS, Memetimin H, Confides AL, Kasza I, Zhu B, Vekaria HJ, Harfmann B, Jones KA, Johnson ZR, Westgate PM, Alexander CM, Sullivan PG, Dupont-Versteegden EE, Kern PA. Human adipose beiging in response to cold and mirabegron. JCI Insight. 2018 Aug 9;3(15):e121510.

6. Saely CH, Geiger K, Drexel H. Brown versus white adipose tissue: A mini-review. Gerontology. 2011;58(1):15–23.

7. Lidell ME. Brown adipose tissue in human infants. In: Handbook of Experimental Pharmacology. 2019. p. 107–23.

8. Wajchenberg BL. Subcutaneous and visceral adipose tissue: Their relation to the metabolic syndrome. Endocrine Reviews. 2000;21(6):697–738.

9. Chait A, den Hartigh LJ. Adipose Tissue Distribution, Inflammation and Its Metabolic Consequences, Including Diabetes and Cardiovascular Disease. Frontiers in Cardiovascular Medicine. 2020;7:22.

10. González Jiménez E. Body composition: Assessment and clinical value. Endocrinología y Nutrición (English Edition). 2013;60(2):69–75.

11. Moschonis G, Chrousos GP, Lionis C, Mougios V, Manios Y. Association of total body and visceral fat mass with iron deficiency in preadolescents: The Healthy Growth Study. British Journal of Nutrition. 2012;108(4):710–9.

12. Ibrahim MM. Subcutaneous and visceral adipose tissue: Structural and functional differences. Obesity Reviews. 2010;11(1):11–8.

13. Medina-Inojosa JR, Batsis JA, Supervia M, Somers VK, Thomas RJ, Jenkins S, Grimes C, Lopez-Jimenez F. Relation of Waist-Hip Ratio to Long-Term Cardiovascular Events in Patients With Coronary Artery Disease. Am J Cardiol. 2018 Apr 15;121(8):903-909.

14. Jung UJ, Choi MS. Obesity and its metabolic complications: the role of adipokines and the relationship between obesity, inflammation, insulin resistance, dyslipidemia and nonalcoholic fatty liver disease. Int J Mol Sci. 2014 Apr 11;15(4):6184-223.

15. Guo X, Xu Y, He H, Cai H, Zhang J, Li Y, Yan X, Zhang M, Zhang N, Maddela RL, Ma G. Visceral fat reduction is positively associated with blood pressure reduction in overweight or obese males but not females: an observational study. Nutr Metab (Lond). 2019 Jul 10;16:44.

16. Li X, Ren Y, Chang K, Wu W, Griffiths HR, Lu S, Gao D. Adipose tissue macrophages as potential targets for obesity and metabolic diseases. Front Immunol. 2023 Apr 19;14:1153915.

17. Freedland ES. Role of a critical visceral adipose tissue threshold (CVATT) in metabolic syndrome: Implications for controlling dietary carbohydrates: A review. Nutrition and Metabolism. 2004;1(1):12.

18. Lee RA, Harris CA, Wang JC. Glucocorticoid Receptor and Adipocyte Biology. Nucl Receptor Res. 2018;5:101373.

19. Araiz C, Yan A, Bettedi L, Samuelson I, Virtue S, McGavigan AK, Dani C, Vidal-Puig A, Foukas LC. Publisher Correction: Enhanced β-adrenergic signalling underlies an age-dependent beneficial metabolic effect of PI3K p110α inactivation in adipose tissue. Nat Commun. 2020 Feb 21;11(1):1078. Erratum for: Nat Commun. 2019 Apr 4;10(1):1546.

20. Bracht JR, Vieira-Potter VJ, De Souza Santos R, Öz OK, Palmer BF, Clegg DJ. The role of estrogens in the adipose tissue milieu. Ann N Y Acad Sci. 2020 Feb;1461(1):127-143.

21. Cherian S, Lopaschuk GD, Carvalho E. Cellular cross-talk between epicardial adipose tissue and myocardium in relation to the pathogenesis of cardiovascular disease. American Journal of Physiology - Endocrinology and Metabolism. 2012;303(8):E937–49.

22. Antonopoulos AS, Antoniades C. The role of epicardial adipose tissue in cardiac biology: classic concepts and emerging roles. Journal of Physiology. 2017;595(12):3907–17.

23. Nelson RH, Prasad A, Lerman A, Miles JM. Myocardial uptake of circulating triglycerides in nondiabetic patients with heart disease. Diabetes. 2007;56(2):527–30.

24. Iacobellis G. Epicardial adipose tissue in contemporary cardiology. Nat Rev Cardiol. 2022 Sep;19(9):593-606.

25. Sacks H, Symonds ME. Anatomical locations of human brown adipose tissue: Functional relevance and implications in obesity and type 2 diabetes. Diabetes. 2013;62(6):1783–90.

26. Nøhr MK, Bobba N, Richelsen B, Lund S, Pedersen SB. Inflammation Downregulates UCP1 Expression in Brown Adipocytes Potentially via SIRT1 and DBC1 Interaction. Int J Mol Sci. 2017 May 8;18(5):1006.

27. Singh R, Barrios A, Dirakvand G, Pervin S. Human Brown Adipose Tissue and Metabolic Health: Potential for Therapeutic Avenues. Cells. 2021 Nov 5;10(11):3030.

28. Park A. Distinction of white, beige and brown adipocytes derived from mesenchymal stem cells. World Journal of Stem Cells. 2014;6(1):33–42.

29. Gómez-Hernández A, Beneit N, Díaz-Castroverde S, Escribano Ó. Differential Role of Adipose Tissues in Obesity and Related Metabolic and Vascular Complications. International Journal of Endocrinology. 2016;2016:1216783.

30. Nusse R, Clevers H. Wnt/β-Catenin Signaling, Disease, and Emerging Therapeutic Modalities. Cell. 2017;169(6):985–99.

31. Liu J, Xiao Q, Xiao J, Niu C, Li Y, Zhang X, et al. Wnt/β-catenin signalling: function, biological mechanisms, and therapeutic opportunities. Signal Transduction and Targeted Therapy. 2022 Jan 3;7(1):3.

32. Kang S, Bennett CN, Gerin I, Rapp LA, Hankenson KD, MacDougald OA. Wnt signaling stimulates osteoblastogenesis of mesenchymal precursors by suppressing CCAAT/enhancer-binding protein α and peroxisome proliferator-activated receptor γ. Journal of Biological Chemistry. 2007;282(19):14515–24.

33. Cristancho AG, Schupp M, Lefterova MI, Cao S, Cohen DM, Chen CS, et al. Repressor transcription factor 7-like 1 promotes adipogenic competency in precursor cells. Proceedings of the National Academy of Sciences of the United States of America. 2011;108(39):16271–6.

34. Kennell JA, O'Leary EE, Gummow BM, Hammer GD, MacDougald OA. T-Cell Factor 4N (TCF-4N), a Novel Isoform of Mouse TCF-4, Synergizes with β-Catenin To Coactivate C/EBPα and Steroidogenic Factor 1 Transcription Factors. Molecular and Cellular Biology. 2003;23(15):5366–75.

35. Liu G, Vijayakumar S, Grumolato L, Arroyave R, Qiao H, Akiri G, et al. Canonical Wnts function as potent regulators of osteogenesis by human mesenchymal stem cells. Journal of Cell Biology. 2009;185(1):67–75.

36. Little RD, Carulli JP, Del Mastro RG, Dupuis J, Osborne M, Folz C, et al. A mutation in the LDL receptor-related protein 5 gene results in the autosomal dominant high-bone-mass trait. American Journal of Human Genetics. 2002;70(1).

37. Boyden LM, Mao J, Belsky J, Mitzner L, Farhi A, Mitnick MA, et al. High Bone Density Due to a Mutation in LDL-Receptor–Related Protein 5. New England Journal of Medicine. 2002;346(20).

38. Gong Y, Slee RB, Fukai N, Rawadi G, Roman-Roman S, Reginato AM, Wang H, Cundy T, Glorieux FH, Lev D, Zacharin M, Oexle K, Marcelino J, Suwairi W, Heeger S, Sabatakos G, Apte S, Adkins WN, Allgrove J, Arslan-Kirchner M, Batch JA, Beighton P, Black GC, Boles RG, Boon LM, Borrone C, Brunner HG, Carle GF, Dallapiccola B, De Paepe A, Floege B, Halfhide ML, Hall B, Hennekam RC, Hirose T, Jans A, Jüppner H, Kim CA, Keppler-Noreuil K, Kohlschuetter A, LaCombe D, Lambert M, Lemyre E, Letteboer T, Peltonen L, Ramesar RS, Romanengo M, Somer H, Steichen-Gersdorf E, Steinmann B, Sullivan B, Superti-Furga A, Swoboda W, van den Boogaard MJ, Van Hul W, Vikkula M, Votruba M, Zabel B, Garcia T, Baron R, Olsen BR, Warman ML; Osteoporosis-Pseudoglioma Syndrome Collaborative Group. LDL receptor-related protein 5 (LRP5) affects bone accrual and eye development. Cell. 2001 Nov 16;107(4):513-23

39. Mäkitie O, Saarinen A, Saukkonen T, Kivelä T, Lahtinen U, Laine C, et al. Low density lipoprotein receptor-related protein 5 (LRP5) mutations and osteoporosis, impaired glucose metabolism and hypercholesterolaemia. Clinical Endocrinology. 2010;72(4):481–8.

40. Loh NY, Neville MJ, Marinou K, Hardcastle SA, Fielding BA, Duncan EL, et al. LRP5 regulates human body fat distribution by modulating adipose progenitor biology in a dose- and depot-specific fashion. Cell Metabolism. 2015;21(2):262–73.

41. Kim SP, Frey JL, Li Z, Goh BC, Riddle RC. Lack of Lrp5 signaling in osteoblasts sensitizes male mice to diet-induced disturbances in glucose metabolism. Endocrinology. 2017;158(11):3805–16.

42. Nellie Y. Loh, Senthil K. Vasan, Manu Verma, Agata Wesolowska-Andersen, Matt J. Neville, Clive Osmond, et al. LRP5 promotes adipose progenitor cell fitness and adipocyte insulin sensitivity. bioRxiv 2020.03.04.976647

43. Qiu W, Andersen TE, Bollerslev J, Mandrup S, Abdallah BM, Kassem M. Patients with high bone mass phenotype exhibit enhanced osteoblast differentiation and inhibition of adipogenesis of human mesenchymal stem cells. Journal of Bone and Mineral Research. 2007;22(11):1720–31.

44. Chen N, Wang J. Wnt/β-Catenin signaling and obesity. Frontiers in Physiology. 2018;9:792.

45. Hutchings G, Janowicz K, Moncrieff L, Dompe C, Strauss E, Kocherova I, et al. The proliferation and differentiation of adipose-derived stem cells in neovascularization and angiogenesis. International Journal of Molecular Sciences. 2020;21(11):3790.

46. Au DT, Strickland DK, Muratoglu SC. The LDL Receptor-Related Protein 1: At the Crossroads of Lipoprotein Metabolism and Insulin Signaling. J Diabetes Res. 2017;2017:8356537.

47. Masson O, Chavey C, Dray C, Meulle A, Daviaud D, Quilliot D, Muller C, Valet P, Liaudet-Coopman E. LRP1 receptor controls adipogenesis and is up-regulated in human and mouse obese adipose tissue. PLoS One. 2009 Oct 12;4(10):e7422.

48. Pepino MY, Kuda O, Samovski D, Abumrad NA. Structure-function of CD36 and importance of fatty acid signal transduction in fat metabolism. Annual Review of Nutrition. 2014;34:281–303.

49. Durandt C, van Vollenstee FA, Dessels C, Kallmeyer K, de Villiers D, Murdoch C, et al. Novel flow cytometric approach for the detection of adipocyte subpopulations during adipogenesis. Journal of Lipid Research. 2016 Apr;57(4):729–42.

50. Yamashita S, Hirano KI, Kuwasako T, Janabi M, Toyama Y, Ishigami M, et al. Physiological and pathological roles of a multi-ligand receptor CD36 in atherogenesis; insights from CD36-deficient patients. Molecular and Cellular Biochemistry. 2007;299(1–2):19–22.

51. Vroegrijk IOCM, Van Klinken JB, Van Diepen JA, Van Den Berg SAA, Febbraio M, Steinbusch LKM, et al. CD36 is important for adipocyte recruitment and affects lipolysis. Obesity. 2013;21(10):2037–45.

52. Karczewska-Kupczewska M, Stefanowicz M, Matulewicz N, Nikołajuk A, Straczkowski M. Wnt signaling genes in adipose tissue and skeletal muscle of humans with different degrees of insulin sensitivity. Journal of Clinical Endocrinology and Metabolism. 2016;101(8):3079–87.

53. Palsgaard J, Emanuelli B, Winnay JN, Sumara G, Karsenty G, Kahn CR. Cross-talk between insulin and Wnt signaling in preadipocytes: Role of Wnt co-receptor low density lipoprotein receptor-related protein-5 (LRP5). Journal of Biological Chemistry. 2012;287(15):12016–26.

54. Furuhashi M, Hotamisligil GS. Fatty acid-binding proteins: Role in metabolic diseases and potential as drug targets. Nature Reviews Drug Discovery. 2008;7(6):489–503.

55. Furuhashi M, Ishimura S, Ota H, Miura T. Lipid Chaperones and Metabolic Inflammation. International Journal of Inflammation. 2011;2011:642612.

56. Ron I, Mdah R, Zemet R, Ulman RY, Rathaus M, Brandt B, Mazaki-Tovi S, Hemi R, Barhod E, Tirosh A. Adipose tissue-derived FABP4 mediates glucagon-stimulated hepatic glucose production in gestational diabetes. Diabetes Obes Metab. 2023 Nov;25(11):3192-3201.

57. Shan T, Liu W, Kuang S. Fatty acid binding protein 4 expression marks a population of adipocyte progenitors in white and brown adipose tissues. FASEB Journal. 2013;27(1):277–87.

58. Furuhashi M, Saitoh S, Shimamoto K, Miura T. Fatty acid-binding protein 4 (FABP4): Pathophysiological insights and potent clinical biomarker of metabolic and cardiovascular diseases. Clinical Medicine Insights: Cardiology. 2015;8(Suppl 3):23–33.

59. Weisberg SP, McCann D, Desai M, Rosenbaum M, Leibel RL, Ferrante AW. Obesity is associated with macrophage accumulation in adipose tissue. Journal of Clinical Investigation. 2003 Dec 15;112(12):1796–808.

60. Borrell-Pages M, Romero JC, Crespo J, Juan-Babot O, Badimon L. LRP5 associates with specific subsets of macrophages: Molecular and functional effects. Journal of Molecular and Cellular Cardiology. 2016;90:146–56.

61. Russo L, Lumeng CN. Properties and functions of adipose tissue macrophages in obesity. Immunology. 2018;155(4):407–17.

62. Arkan MC, Hevener AL, Greten FR, Maeda S, Li ZW, Long JM, et al. IKK-β links inflammation to obesity-induced insulin resistance. Nature Medicine. 2005;11(2):191–8.

63. Baker RG, Hayden MS, Ghosh S. NF-κB, inflammation, and metabolic disease. Cell Metabolism. 2011;13(1):11–22.

64. Zick Y. Ser/Thr phosphorylation of IRS proteins: a molecular basis for insulin resistance. Science's STKE : signal transduction knowledge environment. 2005;2005(268):pe4.

65. Roubtsova A, Munkonda MN, Awan Z, Marcinkiewicz J, Chamberland A, Lazure C, et al. Circulating proprotein convertase subtilisin/kexin 9 (PCSK9) regulates VLDLR protein and triglyceride accumulation in visceral adipose tissue. Arteriosclerosis, Thrombosis, and Vascular Biology. 2011;31(4):785–91.

66. Roubtsova A, Chamberland A, Marcinkiewicz J, Essalmani R, Fazel A, Bergeron JJ, et al. PCSK9 deficiency unmasks a sex- And tissue-specific subcellular distribution of the LDL and VLDL receptors in mice. Journal of Lipid Research. 2015;56(11):2133–42.

67. Bordicchia M, Spannella F, Ferretti G, Bacchetti T, Vignini A, Di Pentima C, et al. PCSK9 is expressed in human visceral adipose tissue and regulated by insulin and cardiac natriuretic peptides. International Journal of Molecular Sciences. 2019;20(2):245.

68. Badimon L, Luquero A, Crespo J, Peña E, Borrell-Pages M. PCSK9 and LRP5 in macrophage lipid internalization and inflammation. Cardiovascular Research. 2021;117(9):2054–68.

69. Luquero A, Vilahur G, Crespo J, Badimon L, Borrell-Pages M. Microvesicles carrying LRP5 induce macrophage polarization to an anti-inflammatory phenotype. Journal of Cellular and Molecular Medicine. 2021;25(16):7935–47.

70. Hao HX, Xie Y, Zhang Y, Zhang O, Oster E, Avello M, et al. ZNRF3 promotes Wnt receptor turnover in an R-spondin-sensitive manner. Nature. 2012;485(7397):195–200.

71. Carmon KS, Gong X, Lin Q, Thomas A, Liu Q. R-spondins function as ligands of the orphan receptors LGR4 and LGR5 to regulate Wnt/β-catenin signaling. Proceedings of the National Academy of Sciences of the United States of America. 2011;108(28):11452–7.

72. Xie Y, Zamponi R, Charlat O, Ramones M, Swalley S, Jiang X, et al. Interaction with both ZNRF3 and LGR4 is required for the signalling activity of R-spondin. EMBO Reports. 2013;14(12):1120–6.

73. Zou Y, Ning T, Shi J, Chen M, Ding L, Huang Y, et al. Association of a gain-of-function variant in LGR4 with central obesity. Obesity. 2017;25(1):252–60.

74. Heid IM, Jackson AU, Randall JC, Winkler TW, Qi L, Ssteinthorsdottir V, et al. Meta-analysis identifies 13 new loci associated with waist-hip ratio and reveals sexual dimorphism in the genetic basis of fat distribution. Nature Genetics. 2010;42(11):949–60.

75. Zeve D, Seo J, Suh JM, Stenesen D, Tang W, Berglund ED, et al. Wnt signaling activation in adipose progenitors promotes insulin-independent muscle glucose uptake. Cell Metabolism. 2012;15(4):492–504.

76. Bagchi DP, Li Z, Corsa CA, Hardij J, Mori H, Learman BS, et al. Wntless regulates lipogenic gene expression in adipocytes and protects against diet-induced metabolic dysfunction. Molecular Metabolism. 2020;39:100992.

77. Chen M, Lu P, Ma Q, Cao Y, Chen N, Li W, et al. CTNNB1/β-catenin dysfunction contributes to adiposity by regulating the cross-talk of mature adipocytes and preadipocytes. Science Advances. 2020;6(2):eaax9605.

78. Bagchi DP, Nishii A, Li Z, DelProposto JB, Corsa CA, Mori H, et al. Wnt/β-catenin signaling regulates adipose tissue lipogenesis and adipocyte-specific loss is rigorously defended by neighboring stromal-vascular cells. Molecular Metabolism. 2020;42:101078.

79. Woodiwiss AJ, Libhaber CD, Majane OHI, Libhaber E, Maseko M, Norton GR. Obesity promotes left ventricular concentric rather than eccentric geometric remodeling and hypertrophy independent of blood pressure. American Journal of Hypertension. 2008;21(10):1144–51.

80. Calligaris SD, Lecanda M, Solis F, Ezquer M, Gutiérrez J, Brandan E, et al. Mice Long-Term High-Fat Diet Feeding Recapitulates Human Cardiovascular Alterations: An Animal Model to Study the Early Phases of Diabetic Cardiomyopathy. PLoS ONE. 2013;8(4):e60931.

FIGURE 1

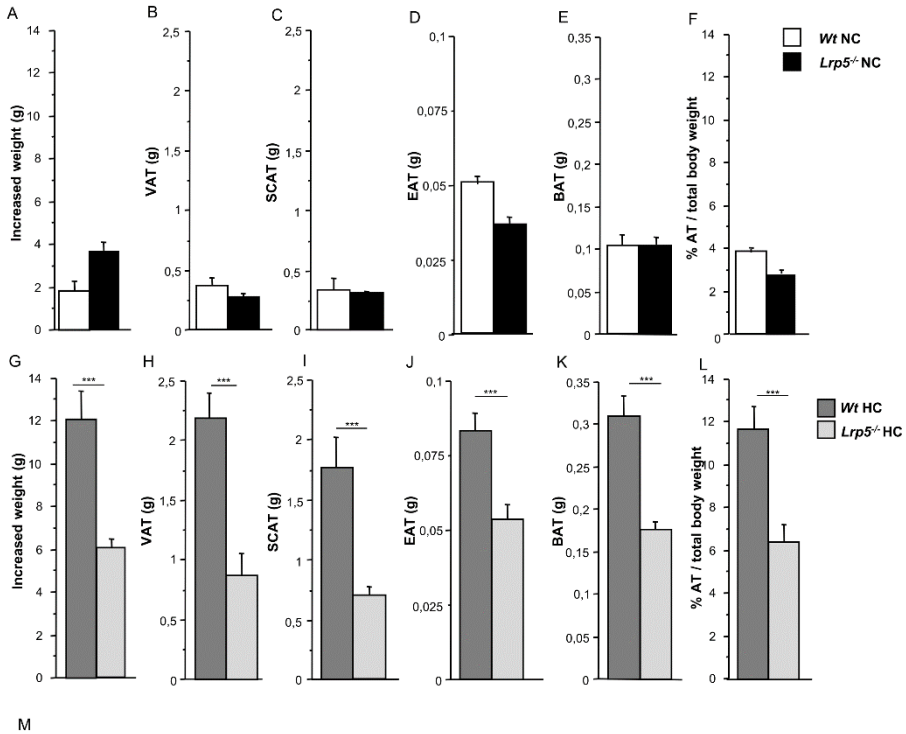

M

	Increased Weight	VAT	SCAT	EAT	BAT	%AT/total body weight
Wt NC vs HC	***	***	***	***	***	***
Lrp5$^{-/-}$ NC vs HC	*	*	*	*	*	***

Figure 1. Mice total body weight and adipose tissue weight. *Wt* and *Lrp5*$^{-/-}$ mice (A) weight-gain after 8 weeks of NC feeding. (B) VAT, (C) SCAT, (D) EAT and (E) BAT weight at sacrifice. (F) *Wt* and *Lrp5*$^{-/-}$ mice total adipose tissues weights against mice total body weight in NC mice. *Wt* and *Lrp5*$^{-/-}$ mice (G) weight-gain after 8 weeks of HC feeding and (H) VAT, (I) SCAT, (J) EAT and (K) BAT weight at sacrifice. (L) *Wt* and *Lrp5*$^{-/-}$ mice total adipose tissues weights against mice total body weight in HC mice. (M) Table of significances between *Wt* NC vs HC mice and *Lrp5*$^{-/-}$ NC vs HC mice. *p<0,05, ***p<0,001.

FIGURE 2

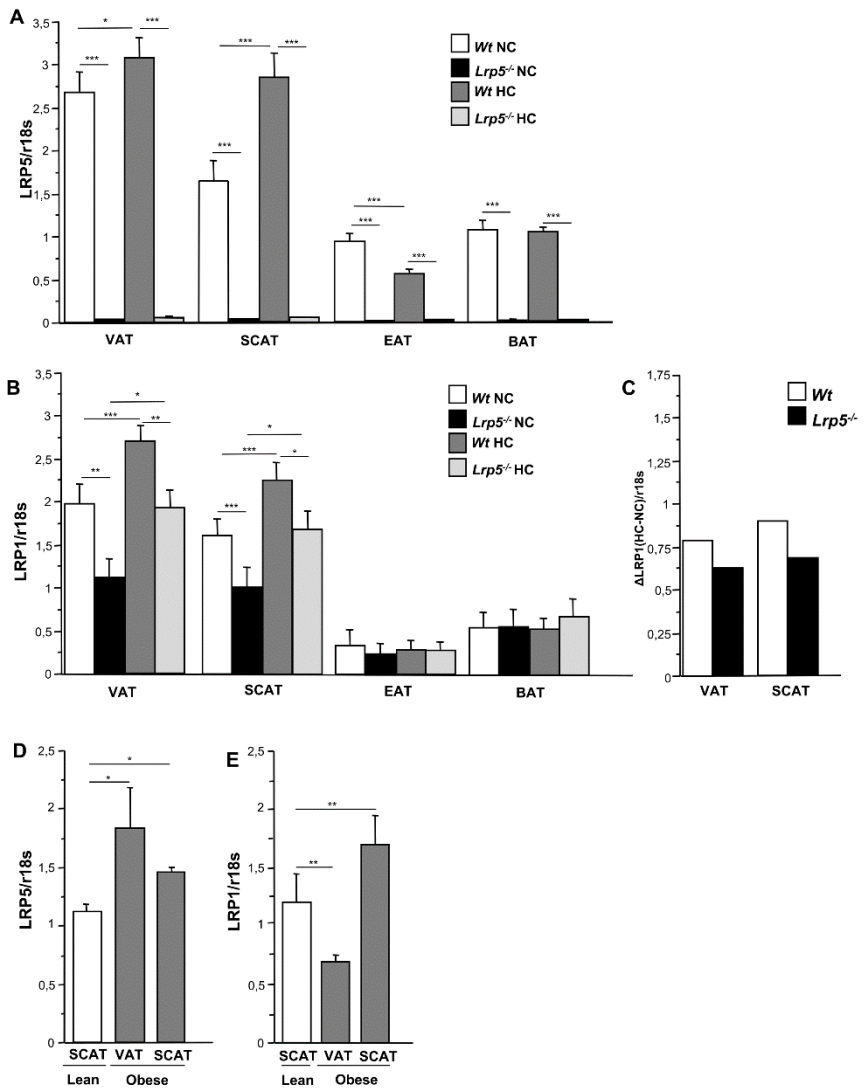

Figure 2. **Low-density lipoprotein receptors gene expression in mice and humans.** (A) LRP5 and (B) LRP1 gene expression in adipose tissue of *Wt* and *Lrp5*$^{-/-}$ mice fed a NC or HC diet. (C) Increased LRP1 gene expression in VAT and SCAT of *Wt* and *Lrp5*$^{-/-}$ mice after HC diets lean and obese patients. (D) LRP5 and (E) LRP1 gene expression in adipose tissue of lean and obese patients. *p<0,05, **p<0,01, ***p<0,001.

FIGURE 3

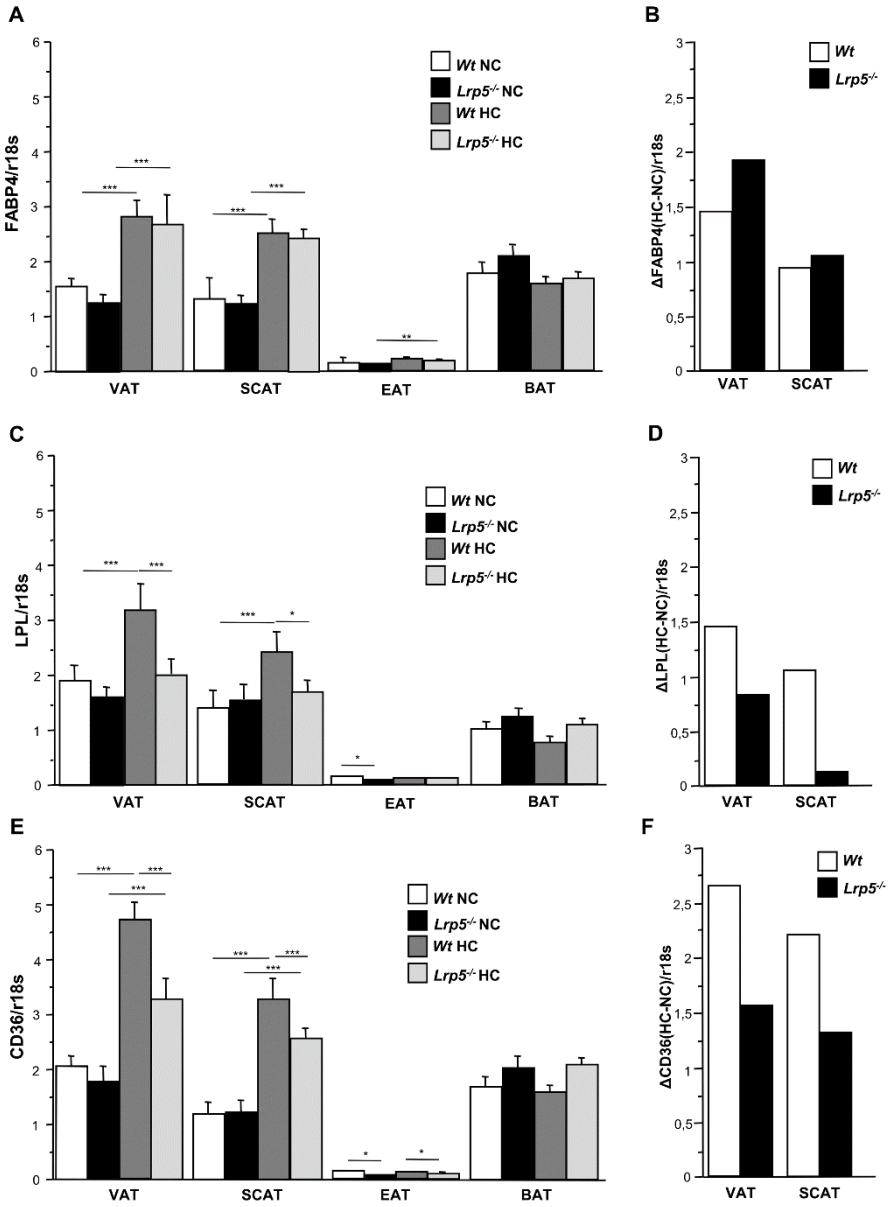

Figure 3. **Adipogenic markers' gene expression in mice.** (A) FABP4, (C) LPL and (E) CD36 gene expression in adipose tissues of *Wt* and *Lrp5*$^{-/-}$ mice fed a NC or a HC diet. Increased (B) FABP4, (D) LPL or (F) CD36 gene expression in VAT and SCAT from *Wt* and *Lrp5*$^{-/-}$ mice after HC diets. *p<0,05,***p<0,001.

FIGURE 4

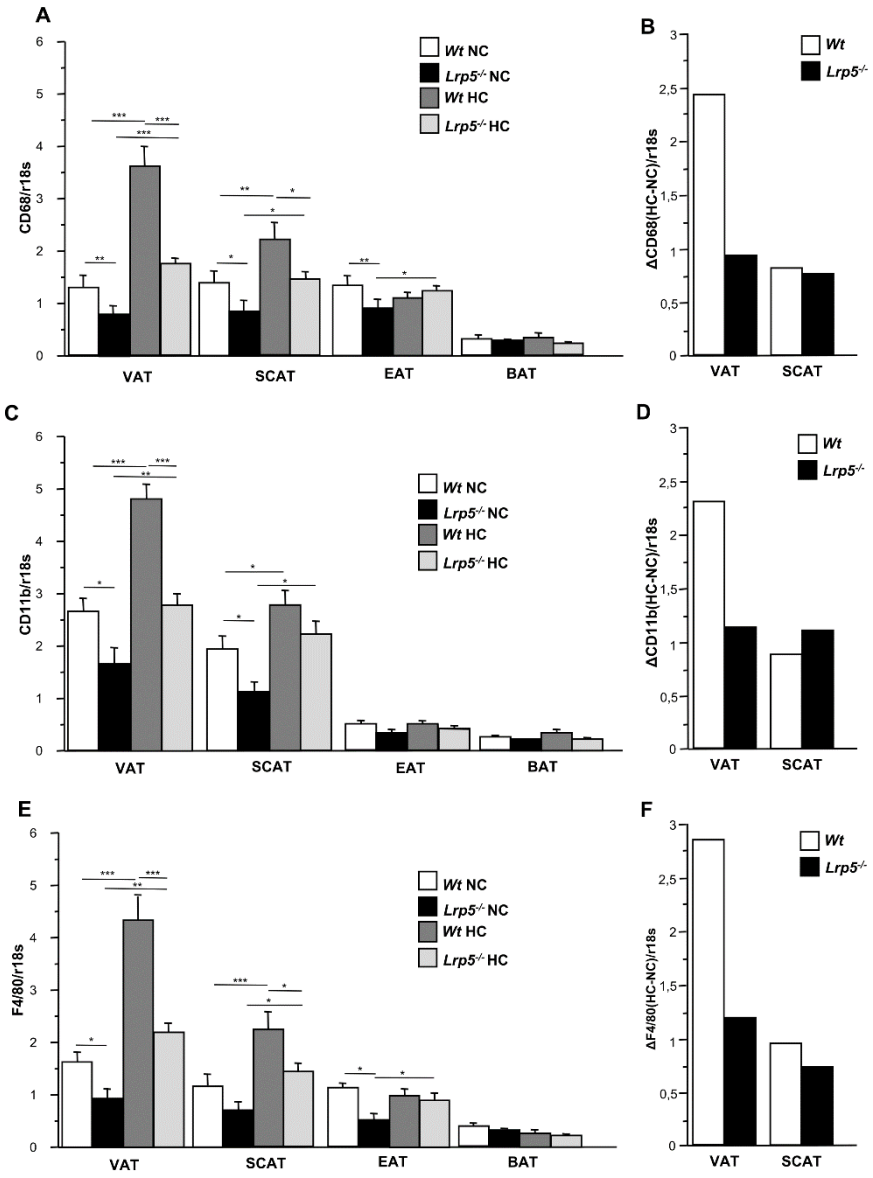

Figure 4. **Macrophage markers in mice.** (A) CD68, (C) CD11b and (E) F4/80 gene expression in adipose tissues of *Wt* and *Lrp5*$^{-/-}$ mice fed NC or HC diets. Increase in (B) CD68, (D) CD11b or (F) F4/80 gene expression levels in VAT and SCAT after HC diets. *p<0,05, **p<0,01, ***p<0,001.

FIGURE 5

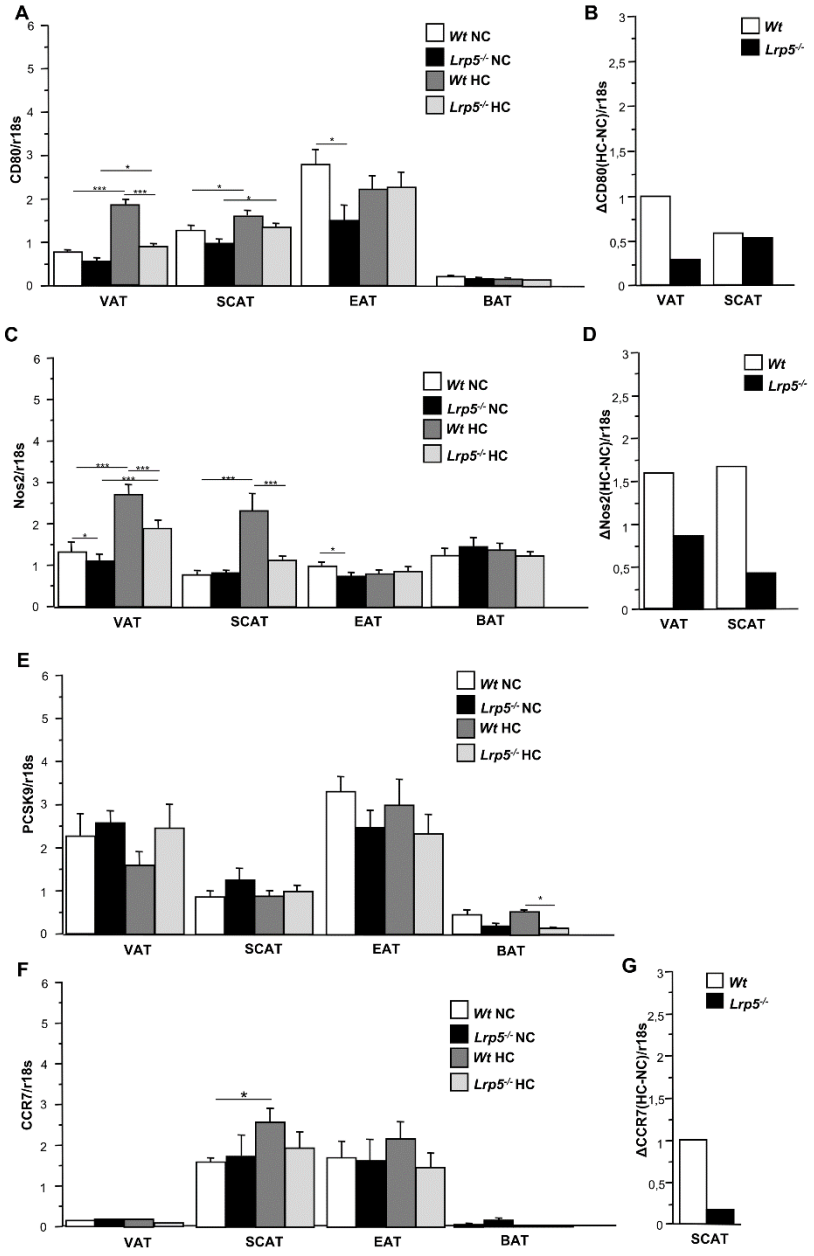

Figure 5. **Pro-inflammatory markers in mice adipose tissues.** (A) CD80, (C) Nos2, (E) PCSK9 and (G) CCR7 gene expression in adipose tissues of *Wt* and *Lrp5*$^{-/-}$ mice fed NC and HC diets. Increase in (B) CD80, (D) Nos2 or (F) CCR7 gene expression levels in VAT and SCAT of *Wt* and *Lrp5*$^{-/-}$ mice after HC diets. *p<0,05, **p<0,01, ***p<0,001.

FIGURE 6

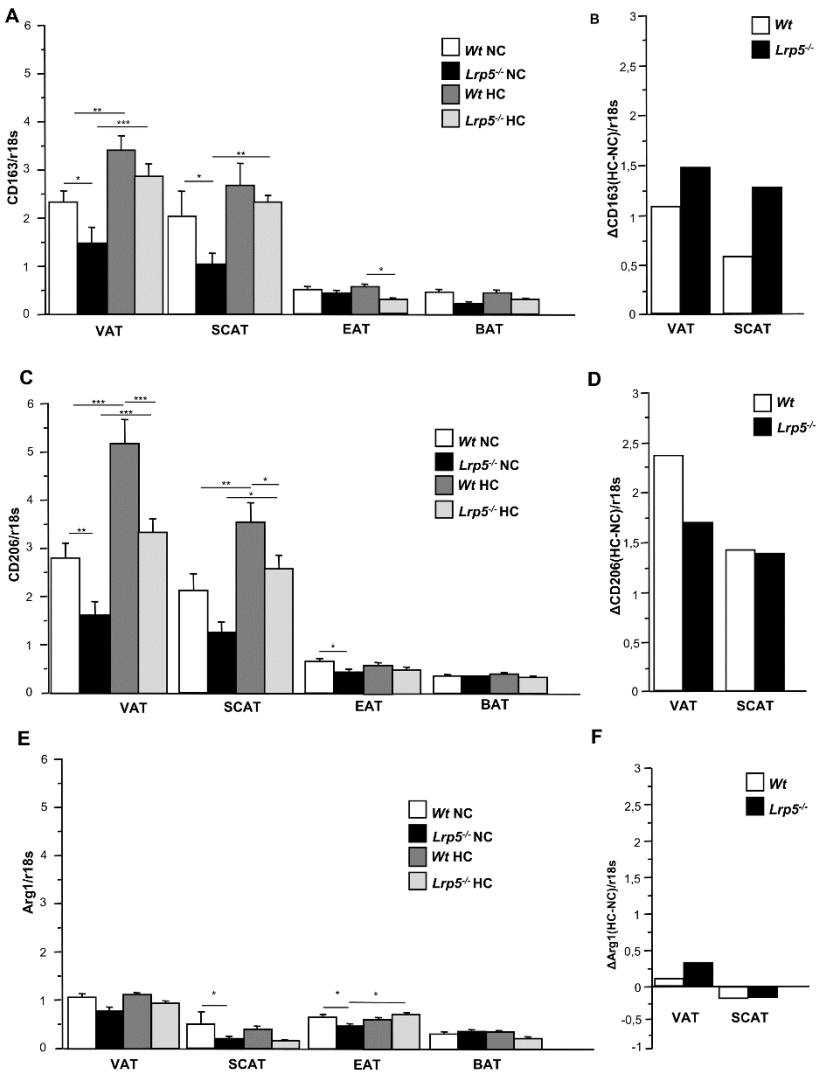

Figure 6. **Anti-inflammatory markers in mice adipose tissues.** (A) CD163, (C) CD206 and (E) Arg1 gene expression in adipose tissues of *Wt* and *Lrp5*$^{-/-}$ mice fed a NC or a HC diet. Increase in (B) CD163, (D) CD206 and (F) Arg1 gene expression in VAT and SCAT of *Wt* and *Lrp5*$^{-/-}$ mice after HC diets. *p<0,05, **p<0,01, ***p<0,001.

3.5 Article 4

Microvesicles carrying LRP5 induce macrophage polarization to an anti-inflammatory phenotype

By Aureli Luquero, Gemma Vilahur, Javier Crespo, Lina Badimon and Maria Borrell-Pages

Published in Journal of Cell and Molecular Medicine. 2021 May 29;25:7935-7947.

doi: 10.1093/cvr/cvaa254.

Summary: Microvesicles (MVs) have been associated with atherosclerosis initiation and progression and participate in the inflammatory process. Macrophages have a role in atherosclerosis progression and are responsible for the release of cytokines, chemokines and MVs that mediate the communication of macrophages with other cells. MVs contain miRNAs, long-non-coding RNAs, soluble proteins, and receptors expressed in the surface. We aimed to investigate whether LRP5 is expressed in macrophage-derived MVs and whether it plays a role in cell communication. Monocytes and macrophages were isolated from human buffy coats and results show that they both constitutively release $LRP5^{+}$MVs. Lipid treatments increased MV release on monocytes and macrophages; however, $LRP5^{+}$MVs release was only increased in macrophages. Treatment with agLDL induced a pro-inflammatory phenotype in macrophages with increased expression of CD80, CD83 and decreased expression of the anti-inflammatory markers CD163, CD206 and CD16. MVs from lipid treated macrophages also displayed increased expression of CD80 and CD86, but not of CD163, CD206, or CD16. LRP5 gene expression levels were increased in both pro-inflammatory and anti-inflammatory macrophages after lipid-loading, but the percentage of $LRP5^{+}$

macrophage was bigger in anti-inflammatory macrophages. LRP5-silenced macrophages produced LRP5-depleted MVs. The incubation of control macrophages with LRP5-depleted MVs triggered the expression of the pro-inflammatory markers iNOS and CD83 in naïve macrophages while $LRP5^{+}$MVs did not induce them, revealing a role for LRP5 in maintaining macrophage's anti-inflammatory state. Loss of LRP5 expression in macrophages induce the generation of pro-inflammatory proteins in their MVs that will induce the generation of further pro-inflammatory macrophages indicating an anti-inflammatory role for LRP5 in macrophage-derived MVs.

Received: 26 December 2020 | Revised: 19 May 2021 | Accepted: 29 May 2021

DOI: 10.1111/jcmm.16723

ORIGINAL ARTICLE

WILEY

Microvesicles carrying LRP5 induce macrophage polarization to an anti-inflammatory phenotype

Aureli Luquero[1] | Gemma Vilahur[1,2] | Javier Crespo[1] | Lina Badimon[1,2,3] | Maria Borrell-Pages[1,2]

[1]Cardiovascular Program ICCC, IR-Hospital de la Santa Creu i Sant Pau, IIB-Sant Pau, Barcelona, Spain

[2]CIBER-CV, Instituto de Salud Carlos III, Madrid, Spain

[3]Cardiovascular Research Chair, UAB, Barcelona, Spain

Correspondence
Maria Borrell-Pages, Cardiovascular Research Program, IR-Hospital de la Santa Creu i Sant Pau, C/Sant Antoni Maria Claret 167, 08025 Barcelona, Spain.
Email: mborrellpa@santpau.cat

Funding information
Instituto de Salud Carlos III, Grant/Award Number: CIBERCV CN16/11/00411, FIS2019-01282, TERCEL RD16/0011/018, CIBERCV CB16/11/00411 and FIS2020-01282; Generalitat of Catalunya-Secretaria d'Universitats i Recerca del Departament d'Economia i Coneixement de la Generalitat, Grant/Award Number: 2014SGR1303, PERIS SLT006 and 2017SGR1480; Spanish Ministry of Science and Innovation, Grant/Award Number: SAF2016-76819-R and PID2019-107160RB-I00; Spanish Society of Cardiology, Grant/Award Number: FEC2019

Abstract

Microvesicles (MV) contribute to cell-to-cell communication through their transported proteins and nucleic acids. MV, released into the extracellular space, exert paracrine regulation by modulating cellular responses after interaction with near and far target cells. MV are released at high concentrations by activated inflammatory cells. Different subtypes of human macrophages have been characterized based on surface epitopes being $CD16^+$ macrophages associated with anti-inflammatory phenotypes. We have previously shown that low-density lipoprotein receptor-related protein 5 (LRP5), a member of the LDLR family that participates in lipid homeostasis, is expressed in macrophage $CD16^+$ with repair and survival functions. The goal of our study was to characterize the cargo and tentative function of macrophage-derived MV, whether LRP5 is delivered into MV and whether these MV are able to induce inflammatory cell differentiation to a specific $CD16^-$ or $CD16^+$ phenotype. We show, for the first time, that lipid-loaded macrophages release MV containing LRP5. LDL loading induces increased expression of macrophage pro-inflammatory markers and increased release of MV containing pro-inflammatory markers. Conditioning of fresh macrophages with MV released by *Lrp5*-silenced macrophages induced the transcription of inflammatory genes and reduced the transcription of anti-inflammatory genes. Thus, MV containing LRP5 induce anti-inflammatory phenotypes in macrophages.

KEYWORDS

inflammation, lipids, LRP5, macrophages, MV

1 | INTRODUCTION

Extracellular microvesicles (MV) are cell shed particles (diameter ranging from 0.1 to 1 μm) released when cells are stimulated, damaged or undergoing apoptosis.[1-9] They can also be released by healthy cells.[10] MV are formed by direct budding of small cytoplasmatic protrusions that are detached from the cell surface into the extracellular space. They are characterized by the externalization of the procoagulant anionic phosphatidylserine making MV Annexin V positive.[11,12] Their cargo defines their shape, size and function. Because MV reflect the condition of their parental cells, they represent a potential diagnostic tool to identify diverse diseases, including cancer, metabolic and cardiovascular diseases. When MV are shed from their cells of origin, they circulate in blood carrying messengers for recipient cells that will receive the signal and regulate their cellular growth, differentiation and transformation.[4-10,13-16] Indeed, the

interaction of MV with target cells and the release of their content modulate cell responses.[17] MV have been described in inflammatory processes and associated with several cardiovascular risk factors[18] contributing to the initiation and progression of cardiovascular diseases, including atherosclerosis.

Atherosclerosis is characterized by chronic inflammation induced by increasing accumulation of low-density lipoproteins (LDL) and apoptotic cells in the intima layer of the arteries.[19] The low-density lipoprotein receptor-related protein 5 (LRP5) is a multifunctional receptor involved in both endocytosis of lipids and the canonical Wnt signalling pathway.[20] LRP5 is a single-pass transmembrane receptor that participates in the Wnt/β-catenin signalling pathway. LRP5 activation causes the stabilization of β-catenin that translocates into the nucleus, binds to the transcription factor TCF/LEF1 and starts the transcription of Wnt target genes that regulate fundamental aspects of embryonic cell development[21] and adult cell function.[20,22,23]

LDL loading induces high LRP5 expression in human macrophages.[20] Macrophages can be classified into classical activated $CD14^+CD16^-$, pro-inflammatory macrophages and alternatively activated $CD14^-CD16^+$, anti-inflammatory macrophages.[24,25] LRP5 participates in inflammation and macrophage polarization by association with the anti-inflammatory macrophage subtype $CD16^+$ derived from $CD14^+CD16^+$ patrolling circulating monocytes.[26] LRP5 confers the motile function to $CD16^+$ macrophages by triggering the canonical Wnt signalling. Furthermore, $CD16^+LRP5^+$ macrophages, found in advanced atherosclerotic human plaques, trigger an anti-inflammatory, defensive and repair response.[26]

The in-depth understanding of the formation, cargo and function of MV is an ongoing task in the field. The objectives of this study were (a) to characterize the cargo and function of macrophage-derived MV and their ability to induce inflammatory cell differentiation to a $CD16^-$ or a $CD16^+$ phenotype, and (b) to investigate whether LRP5 is delivered into MV and whether it can exert paracrine functions.

We show that LDL-loaded macrophages release MV carrying LRP5 and exert paracrine and/or autocrine regulation. LDL loading induces increased expression of macrophage cellular pro-inflammatory markers and increased release of MV. Interestingly, LRP5 is released in MV that contain both pro- and anti-inflammatory markers. Conditioning of recipient macrophages with MV released by *Lrp5*-silenced macrophages induced pro-inflammatory gene transcription and a reduced expression of anti-inflammatory genes indicating that LRP5 induces macrophage differentiation into the anti-inflammatory phenotype.

2 | METHODS

2.1 | Isolation of human monocytes and human macrophages primary cultures and LDL loading

Human monocytes were obtained by standard protocols from buffy coats of healthy blood donors.[20,26-28] All procedures were approved by the Institutional Review and Ethics Committee, and the investigation conformed to the principles outlined in the Declaration of Helsinki with informed consent given by donors. Briefly, blood was applied on 15 mL of Ficoll-Hypaque and centrifuged at 300 g for 1 hour at 22°C, with no brake. Mononuclear cells were obtained from the central white band of the gradient, exhaustively washed in Dulbecco's phosphate buffer saline, and suspended in RPMI medium (Gibco) supplemented with 10% human serum AB (Sigma). Isolated monocytes (Mo) were left overnight in culture, washed and treated with 100 μg/mL nLDL (native LDL) or agLDL (aggregated LDL) for the described times. A second set of isolated Mo were left 7 days in culture and allowed to differentiate into macrophages (Mac) by changing the cell culture media (RPMI supplemented with 10% human serum AB, 100 units/mL penicillin and 100 μg/mL streptomycin) every 3 days. After several washings with PBS to completely remove serum, human macrophages were incubated with 100 μg/mL nLDL or 100 μg/mL agLDL in serum-free medium.[20,26-28] At the end of the experiments, human Mo and Mac were exhaustively washed (twice with PBS, twice with PBS/1% BSA, once with PBS/1%BSA/heparin 100 U/mL, twice with PBS/1% BSA and twice with PBS) and prepared for the collection of mRNA and protein detection as described below.

2.2 | LDL isolation and modification

Human LDL (d1.019-d1.063 g/mL) were obtained as previously described.[28] Briefly, human LDLs were obtained from pooled sera of normocholesterolemic volunteers and isolated by sequential ultracentrifugation. LDLs were dialyzed three times against 200 volumes of 150 mmol/L NaCl, 1 mmol/L EDTA, and 20 mmol/L Tris-HCl, pH 7.4, overnight and once against 150 mmol/L NaCl. LDL protein concentration was determined by the bicinchoninic acid, and vortexing was monitored by measuring the turbidity (absorbance at 680 nm). The model system of agLDL was generated by vortexing LDL (1 mg/mL) for 4 minutes at room temperature at maximal speed. The percentage of LDL in aggregated form was calculated by measuring the fraction of protein recovered in the pellet obtained after centrifugation at 10 000 *g* for 10 minutes. The different fractions were analysed by agarose electrophoresis, and the precipitated fraction composed of 100% agLDL was added to cell cultures.

2.3 | MV isolation and quantification

LDL-loaded or non-loaded human Mo and Mac were cultured for 24 or 48 hours and the MV released into the supernatants collected. MV were isolated by five-step high-speed centrifugations. Briefly, 2 mL of fresh supernatant aliquots were centrifuged at 3200 *g* for 20 minutes to guarantee complete cell and debris removal. The recovered supernatants were centrifuged at room temperature at 300 *g*, (10 minutes); at 1200 *g*, (20 minutes); and at 12 500 *g* (5 minutes) in two repeated processes to ensure the elimination of nLDL or agLDL. The cleared supernatants were transferred to another vial and centrifuged at 20 500 *g* for 150 minutes at RT to pellet the MV.

Supernatants were removed and the MV-enriched pellets (MVp) were suspended in 100 μL citrate-PBS.

MVp (5 μL) in combination with 2-3 specific monoclonal antibodies (1-5 μL each) labelled with phycoerythrin, 488 or the isotype-matched control antibodies were added in a final volume of 50 μL annexin binding buffer with 5 μL of Annexin V (AV) to label and characterize AV^+MV with bioactive and biomarker molecules from their parental cells. Table S1 shows the different antibodies and the concentrations used for microvesicle identification and characterization. Samples were incubated 20 minutes at room temperature in the dark and diluted with annexin binding buffer before being immediately analysed and counted on a FACSCanto II flow cytometer. The number of monocytes or macrophage per well were counted using Neubauer chambers, and the number of MV/cell type was obtained.

AV binding level was corrected for autofluorescence using fluorescence signals obtained with MV in a calcium-free buffer PBS. MV were identified and quantified based on their forward scatter/side scatter characteristics according to their size, binding or not to AV and reactivity to specific monoclonal antibodies. Figure S1 shows representative plots for MV identification and characterization by flow cytometry analysis.

Acquisition was performed at 1 minute per sample and flow rate was measured before each experiment. Forward scatter, side scatter and fluorescence data were obtained with the settings in the logarithmic scale. The lower detection limit was placed as a threshold above the electronic noise of the flow cytometer. To identify positive marked events, thresholds were also set based on samples incubated with the same final concentration of isotype-matched control antibodies after titration experiments. Data were analysed with the FACSDivaTM software (version 6.1.3; Becton Dickinson). To reduce background noise, buffers were prepared on the same day and filtered through 0.2 μm pore size filters under vacuum.

2.4 | Macrophages isolation by flow cytometry

Cellular protein expression was assessed in primary cultures of human macrophages by flow cytometry. Cell suspensions in flow cytometry buffer (0.1% sodium azide/1%BSA/PBS) were gently centrifuged at 200 *g*, 10 minutes, RT. Pellet samples were then suspended in flow cytometry buffer and stained for 20 minutes with specific antibodies as described in Table S2. Figure S2 shows the gating strategy for live macrophages by flow cytometry analysis. Samples were diluted with 400 μL flow cytometry buffer prior to being immediately analysed. For each sample, at least 10 000 events were acquired on a FACSCantoII (Beckton Dickinson). Data was analysed with the FACSDiva 6.1.3 software.

2.5 | Macrophages isolation by cell sorter

Lipid loaded macrophages were gently detached from culture dishes and stained with CD11b, CD14 and CD206 or CD80 antibodies (Table S2) for 30 minutes in 100 μL 0.5%BSA/PBS. The reaction was stopped by adding 4 volumes of 0.5%BSA/PBS to the mix. Cells were sorted using a FACSAria-I (BD Biosciences) operated using a 100 μm nozzle with the 488 nm and 633 nm laser lines. After positive selection of $CD11b^+CD14^+$ cells, two populations were sorted: $CD11b^+CD14^+CD206^+$/$CD11b^+CD14^+CD206^-$ or $CD11b^+CD14^+CD80^+$/$CD11b^+CD14^+CD80^-$. After sorting, macrophage populations were centrifuged separately for 10 minutes at 200 *g*. Then, cells were suspended in RPMI GlutaMax medium supplemented with 10% AB human serum with 1% penicillin/streptomycin and seeded into 6-well plates for 24 hours. Flow cytometry data acquisition, analysis and image preparation were performed using the FACSDiva software (BD Bioscience).

2.6 | Supernatant collection

Cell sorted macrophages were cultured in serum-free RPMI GlutaMax medium for 2 days when supernatants were collected and centrifuged at 15 000 *g*, 15 minutes, 4°C. Pellets were discharged and supernatants were precipitated using a methanol/chloroform protocol. Briefly, one volume of supernatant was mixed with three volumes of cold methanol and one volume of chloroform, vortexed vigorously for 30 seconds, and then, three volumes of H_2O were added to the sample to induce phase separation. The mix was centrifuged at 10 000 *g* for 5 minutes, and the upper phase was eliminated without disturbing the interphase. Three volumes of methanol were added to the mix, and samples were centrifuged at 10 000 *g* for 5 minutes. Supernatants were discharged and the precipitated proteins (pellet) were let to air-dry. Finally, samples were suspended in 100 μL of lysis protein buffer solution and frozen at −20°C until western blots were performed.

2.7 | Western blot

Protein extracts (50 μL) were resolved by SDS-PAGE and transferred to nitrocellulose membranes, blocked with 5% bovine serum albumin and probed for monoclonal primary antibodies against IL-1β, TNFα and TGF-β from Cell Signalling. Membranes were then washed and blotted with antimouse secondary antibodies (Dako). Band densities were determined with the ChemiDoc XRS system (Bio-Rad) in chemiluminescence detection modus and Quantity-One software (Bio-Rad).

2.8 | LRP5 silencing

Human macrophages were transfected with 100 nmol/L of siRNA-Random (siR) or siRNA-LRP5 (si5) using HiPerfect® as recommended by the manufacturer. Small anti-LRP5 interfering RNAs (si5, s8293) were synthesized by Applied Biotechnologies and Silencer Selective Negative Control #1 (siR, 4390843) by Ambion.

2.9 | RNA isolation and Real time PCR

Total RNA was isolated from cultured human monocytes and macrophages using the total RNA extraction kit (Qiagen). Total RNA concentration was determined by NanoDrop ND-1000 spectrophotometer (NanoDrop Technologies, Inc), and purity was checked by the A260/A280 ratio (ratios between 1.8 and 2.1 were considered acceptable), in addition, an agarose gel was run to assess quality. cDNA was synthesized from 1 μg RNA with cDNA reverse transcription kit (Qiagen) The resulting cDNA samples were amplified by polymerase chain reaction (PCR) using a DNA thermal cycler (MJ Research) and the following specific human probes from Applied Biotechnologies: LRP5, iNOS, CD80, CD163 and IL1Ra. Normalization was performed against r18S.

2.10 | Statistical analysis

A StatView statistical package was used for all the analysis. Results are expressed as mean ± SD or n (%) when indicated. When possible, comparisons among groups were performed by parametric (one factor ANOVA) analysis. Statistical significance was considered when $P < .05$. All the experiments were performed at least three times.

3 | RESULTS

3.1 | Monocytes and macrophages induce LRP5+MV secretion

To characterize the released MV, supernatants of primary cultures of monocytes and macrophages were collected after 24 hours and 48 hours (Figure 1A). Mo release around 200 000 MV/mL after 24 hours and around 250 000 MV/mL after 48 hours in culture (Figure 1A). Mac release around 52 000 MV/mL after 24 hours and almost 100 000 MV/mL after 48 hours in culture (Figure 1A). These time differences in MV release did not reach statistical significance. However, there was a statistically significant difference in MV release between Mo and Mac both at 24 hours and at 48 hours (Figure 1A).

We then analysed released Annexin V-positive MV (AV^+MV) and no significant differences were found between MV release at 24 hours and 48 hours neither in Mo nor in Mac. Mo released higher number of AV^+MV than Mac both at 24 hours and at 48 hours (Figure 1B). AV^+MV released by monocytes and by macrophages at 24 hours and 48 hours contained LRP5 (Figure 1C).

3.2 | Lipid loading increases $LRP5^+MV$ secretion

We have previously shown that lipid loading with modified lipoproteins (agLDL) increases LRP5 expression in macrophages.[20,26] We hypothesized that the LDL loading would increase the generation of MV carrying LRP5. Primary cultures of human monocytes and macrophages were treated with 100 μg/mL nLDL or agLDL for 24 hours or 48 hours and, indeed, agLDL loading induced a massive generation of AV^+MV from monocytes while a modest amount of AV^+MV were released by macrophages (Figure 1D). LDL loading induced the release of AV^+LRP5^+MV in larger quantities in monocytes than in macrophages (Figure 1E). However, the relative release of AV^+LRP5^+MV (normalized by total AV^+MV) was significantly induced by LDL loading in macrophages both after 24 hours and 48 hours incubation (Figure 1F).

We then estimated the amount of MV produced by each monocyte or macrophage (MV/Mo and MV/Mac). Lipid-loaded Mo release more AV^+ MV than Mac after 24 hours (175 ± 21 AV^+MV/Mo vs 6 ± 0.8 AV^+MV/Mac, Figure S3A) and 48 hours agLDL incubation (108 ± 15 AV^+MV/Mo vs 6 ± 0.4 AV^+MV/Mac, Figure S3A). AgLDL treatments induced more $LRP5^+MV$ release in individual monocytes than in macrophages both after 24 hours and 48 hours incubation (Figure S3B). Finally, the relative amount of AV^+LRP5^+MV/cell type (normalized by AV^+MV/cell type) released by macrophages was higher than that released by monocytes after 24 hours and 48 hours agLDL incubation (Figure S3C).

3.3 | agLDL loading induces macrophage polarization

We previously observed that LRP5 is mainly expressed in $CD16^+$ macrophages and lipid loading induces LRP5 expression in these cells[20,26]; therefore we investigated whether macrophage polarization could be induced by agLDL. Lipid-loaded macrophages were gently detached from the culture dish and these live macrophages were counted by flow cytometry showing that the agLDL loading did not affect cell survival (Figure 2A). Macrophage population was defined by size, with specific pro- and anti-inflammatory antibodies and with the well-known macrophage markers CD11b and CD14. Figure S2 shows the gating strategy for live macrophages by flow cytometry analysis. Results show that lipid loading induces the expression of $CD80^+$ and $CD83^+$ and reduces the expression of cell surface CD16 ($CD80^+$: 2.16% expression in control conditions to 15.81% expression after agLDL loading; $CD83^+$: 2.06% expression in control conditions to 8.65% expression after lipid loading and $CD16^-$: 77.3% expression in control conditions and 86.3% expression in lipid loaded cells). The expression levels of the anti-inflammatory marker $CD16^+$ was reduced in lipid loaded macrophages while the expression levels of the anti-inflammatory proteins, $CD206^+$ and $CD163^+$ did not vary with respect to control conditions. Therefore, lipid loading induces a pro-inflammatory polarization in macrophages with increased $CD80^+$, $CD83^+$ and $CD16^-$ expression in cells (Figure 2B,C).

Macrophage pro-inflammatory phenotype after lipid loading was confirmed by pro and anti-inflammatory protein secretion analyses. Cell sorting was performed on lipid loaded macrophages to obtain $CD11b^+CD14^+CD206^-$ and $CD11b^+CD14^+CD206^+$ or $CD11b^+CD14^+CD80^-$ and $CD11b^+CD14^+CD80^+$ macrophage

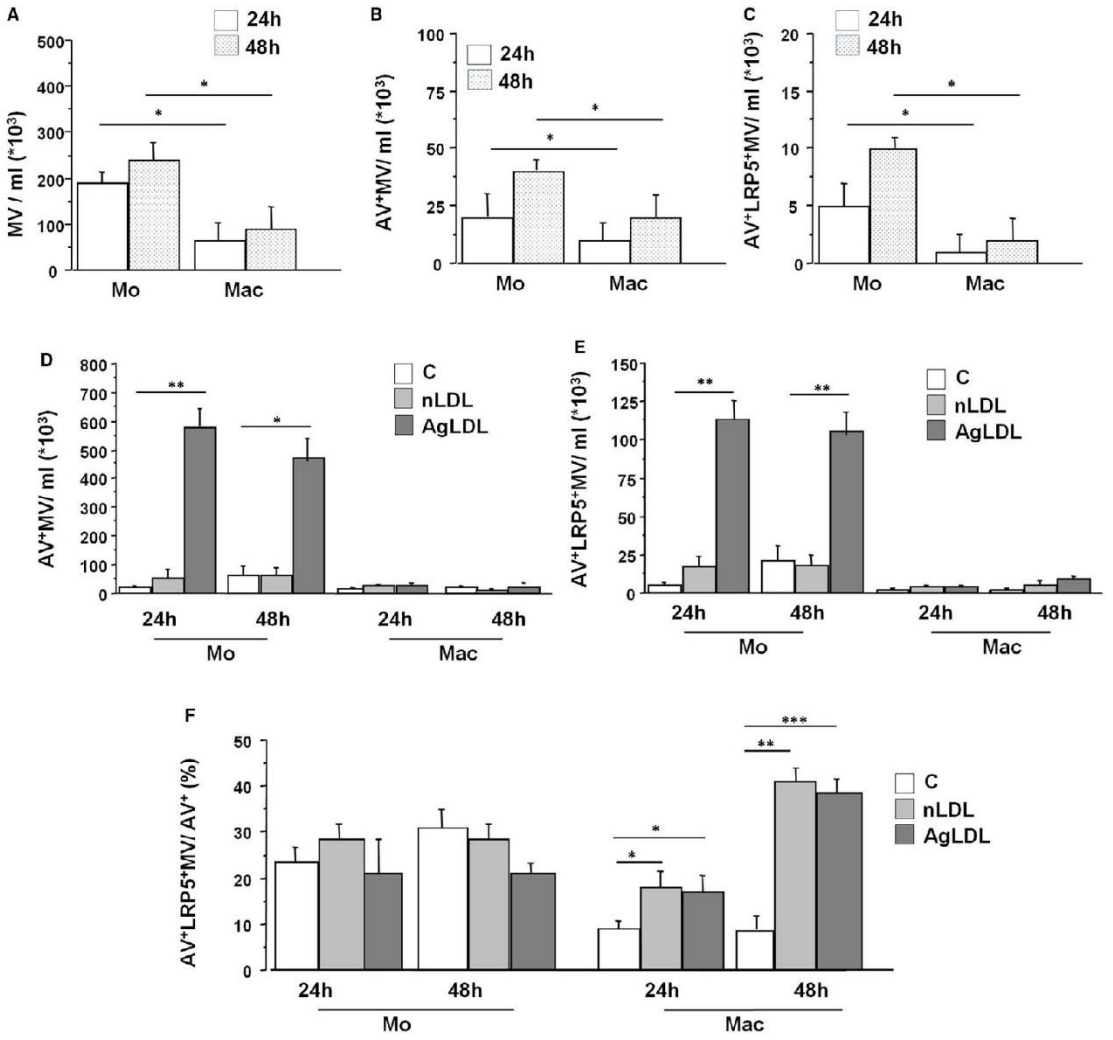

FIGURE 1 AgLDL treatments in macrophages induce LRP5$^+$MV secretion. 24 hours or 48 hours supernatants from undifferentiated monocytes (Mo) or from 7 to 10 days fully differentiated macrophages (Mac) were collected and the amount of (A) microvesicles/mL; (B) Annexin V$^+$ microvesicles/mL and (C) Annexin V$^+$ LRP5$^+$ microvesicles/mL were analysed. (D) Monocytes (Mo) or macrophages (Mac) were treated with 100 μg/mL nLDL or 100 μg/mL agLDL for 24 hours or 48 hours and the amount of AV$^+$ MV/mL and of (E) AV$^+$ LRP5$^+$ MV/mL was analysed. (F) The ratio between MV that are AV$^+$LRP5$^+$/AV$^+$ in control and lipid-loaded monocytes (Mo) and macrophages (Mac). All experiments were performed at least four times in duplicates or triplicates. *$P < .05$, **$P < .01$, ***$P < .005$

subpopulations. The different macrophage subpopulations were seeded in culture dishes and supernatants were collected after 48 hours. Increased release of the pro-inflammatory proteins TNFα and IL1β was observed in the pro-inflammatory CD80$^+$ subpopulation while the levels remained low in the anti-inflammatory CD206$^+$ subpopulation (Figure 2D). Conversely, the release of the anti-inflammatory protein TGFβ was higher in the CD206$^+$ macrophage subpopulation than in the CD80$^+$ macrophage subpopulation (Figure 2D). Therefore, inflammatory protein release confirms the pro-inflammatory polarized phenotype in macrophages observed by cell surface markers expression after lipid loading.

3.4 | Lipid loading induces LRP5 expression in macrophages

We next examined the expression levels of LRP5 in the different macrophage subpopulations by staining macrophages with a

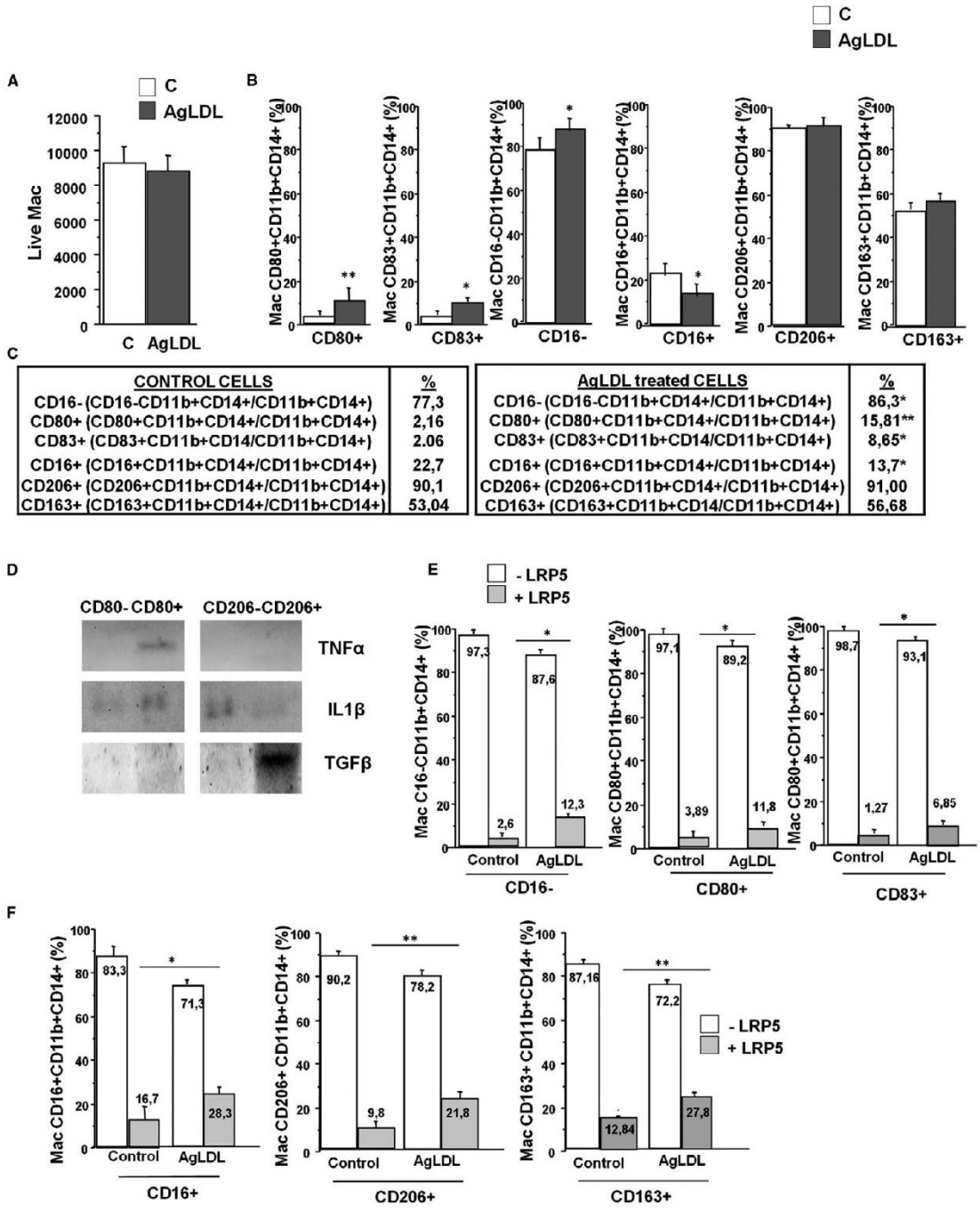

FIGURE 2 AgLDL treatments induce LRP5 expression in pro- and anti-inflammatory macrophages. (A) Flow cytometry was used to quantify live macrophages after treatment or not with 100 μg/mL agLDL. (B) Cellular expression of CD80, CD83, CD16, CD206 and CD163 in control and agLDL-treated macrophages. (C) Quantification of the graphs depicted in (B). (D) TNFα, IL1β and TGFβ expression in supernatants of agLDL-treated and cell sorted macrophage subpopulations. (E) LRP5 expression levels by flow cytometry in $CD16^{-}$, $CD80^{+}$ and $CD83^{+}$ pro-inflammatory macrophages in control and after agLDL treatment. (F) Same in anti-inflammatory $CD16^{+}$, $CD2016^{+}$ and $CD163^{+}$ expressing macrophages. All experiments were performed at least four times in duplicates or triplicates. $^{*}P < .05$, $^{**}P < .01$

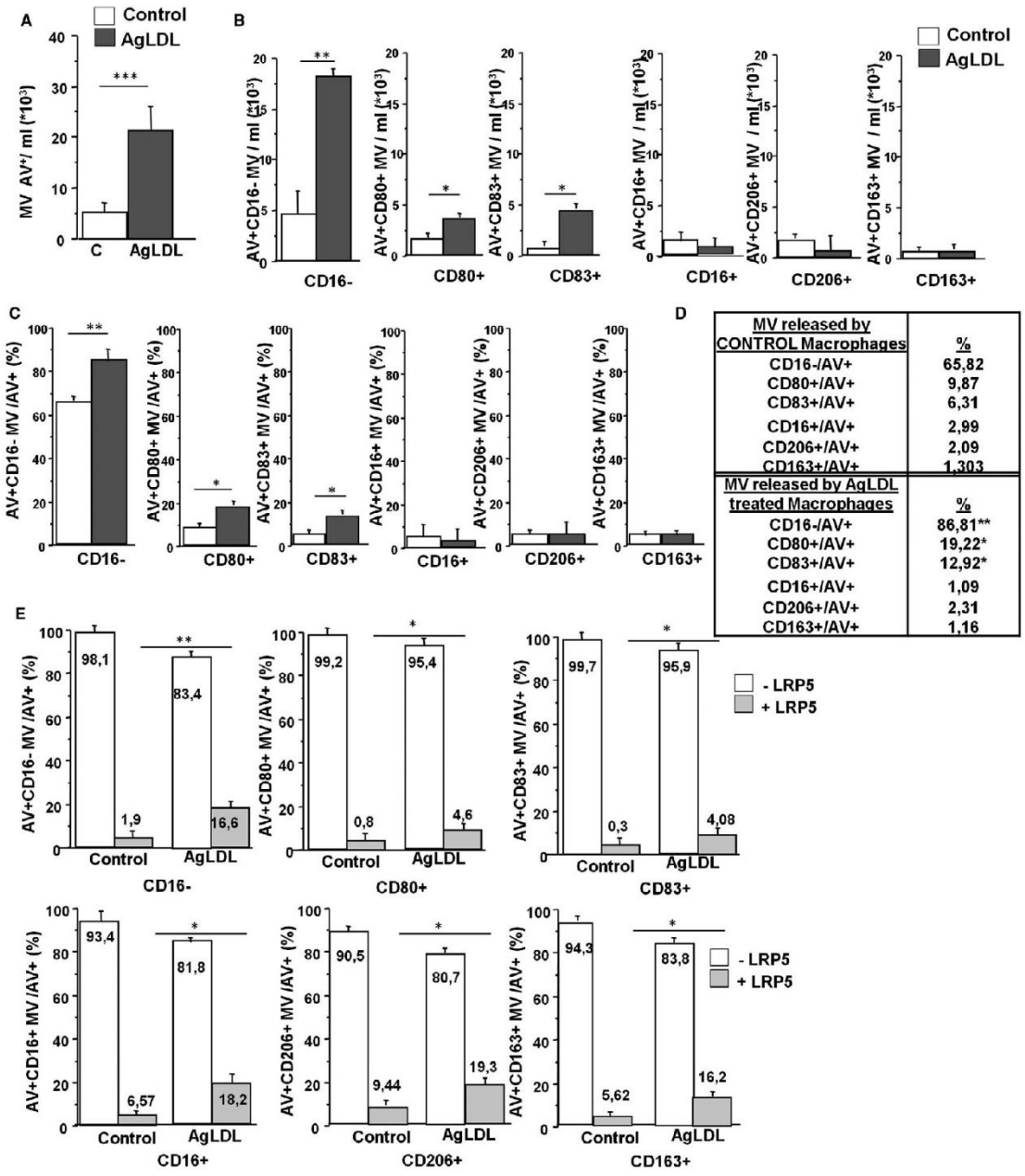

MV released by CONTROL Macrophages	%
CD16-/AV+	65,82
CD80+/AV+	9,87
CD83+/AV+	6,31
CD16+/AV+	2,99
CD206+/AV+	2,09
CD163+/AV+	1,303

MV released by AgLDL treated Macrophages	%
CD16-/AV+	86,81**
CD80+/AV+	19,22*
CD83+/AV+	12,92*
CD16+/AV+	1,09
CD206+/AV+	2,31
CD163+/AV+	1,16

FIGURE 3 Macrophages treated with agLDL release LRP5⁺MV. (A) Flow cytometry was used to quantify AV⁺ MV secreted by control and 100 μg/mL AgLDL-treated macrophages. (B) CD16⁻ MV/mL, CD80⁺ MV/mL, CD16⁺ MV/mL and CD206⁺ MV/mL released by control and agLDL-treated macrophages (C) Same as in (B) but performing the ratio against AV⁺MV. (D) Quantification of the graphs shown in (C). (E) Flow cytometry detection of LRP5 expression in CD16⁻MV, CD80⁺MV, CD16⁺MV and CD206⁺MV released by control and agLDL-treated macrophages. All experiments were performed at least four times in duplicates or triplicates. *$P < .05$, **$P < .01$, ***$P < .005$

specific antibody for LRP5. Pro-inflammatory CD16⁻ macrophages show increased LRP5 cellular expression after agLDL loading compared to controls (12.3% and 2.6% respectively; Figure 2E). Similarly, CD80⁺ and CD83⁺ macrophages showed increased levels of cellular LRP5 after lipid loading compared to controls (CD80⁺: 3.89% expression in control conditions to 11.8% expression after

lipid loading; $CD83^+$: 1.27% expression in control conditions to 6.85% expression after agLDL loading; Figure 2E). Interestingly, macrophages that express the anti-inflammatory markers $CD16^+$, $CD206^+$ or $CD163^+$ also showed significantly increased LRP5 expression after agLDL loading ($CD16^+$: 16.7% in control conditions to 28.3% in lipid-loaded macrophages, $CD206^+$: 9.8% in controls to 21.8% in lipid-loaded macrophages and $CD163^+$: 12.84% in controls to 27.8% in agLDL-treated macrophages) indicating that lipid loading induce LRP5 expression in both pro- and anti-inflammatory macrophages but with a higher expression in anti-inflammatory macrophages (Figure 2F).

3.5 | Inflammatory profile of MV after lipid loading

MV release was investigated in supernatants from LDL-loaded macrophage (100 μg/mL agLDL). Lipid loading induced significantly higher release of AV^+MV (Figure 3A). LDL loading induced a significant increase in the release of $CD16^-$, $CD80^+$ and $CD83^+$ MV but not $CD16^+$, $CD206^+$ and $CD163^+$ MV (Figure 3B). Normalization by total AV^+ MV showed that only $CD16^-$, $CD80^+$ and $CD83^+$ MV levels were increased after agLDL loading ($CD16^-$: 65.82% in control conditions to 86.81% after lipid loading, $CD80^+$: 9.87% in control conditions to 19.22% after lipid loading and $CD83^+$: 6.31% in control conditions to 12.92% after lipid loading, Figure 3C,D). Macrophage-derived MV containing $CD16^+$, $CD206^+$ and $CD163^+$ anti-inflammatory markers remained constant before and after macrophage lipid loading ($CD16^+$: 2.99% in control conditions vs 1.09% in lipid-loaded macrophages, $CD206^+$: 2.09% in control conditions vs 2.31% after agLDL loading and $CD163^+$: 1.30% in control conditions to 1.16% after lipid loading Figure 3C,D) indicating that lipid loading induces the release of MV containing pro-inflammatory markers.

3.6 | $LRP5^+MV$ contain pro-inflammatory and anti-inflammatory proteins

MV released from lipid-loaded and non-loaded macrophages were isolated and stained for pro-inflammatory and anti-inflammatory markers and for LRP5. Interestingly, LRP5 was delivered into MV containing both pro-inflammatory and anti-inflammatory proteins, indicating that the delivery of LRP5 into MV is independent of the inflammatory proteins delivered into the MV (Figure 3E).

3.7 | Characterization of donor macrophages and their released MV

Macrophage specific inhibition of LRP5 expression (with siRNA) was used to identify whether LRP5 was playing a role in macrophage differentiation towards a $CD16^-$ or a $CD16^+$ phenotype. Macrophages were silenced or not for LRP5 and agLDL-loaded or not (Figure 4A). Analysis of donor macrophages mRNA expression by RT-PCR showed a 92 ± 3% LRP5 reduction in siRNA-LRP5 control cells and a 90 ± 2% LRP5 reduction in siRNA-LRP5 lipid-loaded macrophages. LRP5 mRNA expression was increased in lipid-loaded macrophages (Figure 4B). LRP5 silencing did not modify the number of AV^+MV/mL released by macrophages neither in control nor in lipid-loaded conditions (Figure 4C). However, a consistent reduction in $LRP5^+AV^+MV$ release by siRNA-LRP5-treated macrophages was observed both in untreated and agLDL-loaded macrophages (Figure 4D).

3.8 | Gene expression levels in conditioned macrophages

MV released by the different sets of donor macrophages were isolated and used to condition naive macrophages and monocytes. Treatment of naive macrophages with macrophage-derived MV released by control macrophages or with MV released by siRNA-LRP5-treated macrophages did not modify their LRP5 cellular mRNA expression (Figure 5A). Similarly, treatment with MV released by control or lipid-loaded macrophages did not modify LRP5 gene expression levels in recipient macrophages indicating that LRP5 contained in MV does not affect LRP5 gene transcription (Figure 5A).

However, macrophage gene transcription of the pro-inflammatory molecules iNOS and CD80 was increased by MV devoid of LRP5 indicating that LRP5 blocks the expression of pro-inflammatory genes in recipient macrophages (Figure 5B,C). Treatment with MV released by lipid-loaded macrophages induced iNOS and CD80 gene transcription in recipient macrophages independent of LRP5 expression (Figure 5B,C). The anti-inflammatory genes CD163 and IL1Ra showed decreased expression levels in macrophages conditioned with MV released by siRNA-LRP5 macrophages, indicating that $LRP5^+MV$ induce higher levels of anti-inflammatory genes expression in recipient macrophages (Figure 5D,E). Anti-inflammatory gene transcription in macrophages conditioned with MV released by lipid-loaded macrophages remained constant independently of LRP5 expression in donor macrophages (Figure 5D,E).

3.9 | Gene transcription in conditioned monocytes

LRP5 gene expression levels remained constant in monocytes treated with MV released by both LRP5-expressing and LRP5-silenced macrophages. Interestingly LRP5 gene levels were increased in monocytes conditioned with MV released by lipid-loaded macrophages (Figure 5F). However, iNOS and CD80 expression levels in monocytes conditioned with MV released by untreated and lipid-loaded macrophages in the presence or absence of LRP5 were not significantly modified (Figure 5G,H) as did the expression levels of the anti-inflammatory genes CD163 and IL1Ra (Figure 5I,J) indicating that monocyte gene expression is unaffected by $LRP5^+MVs$.

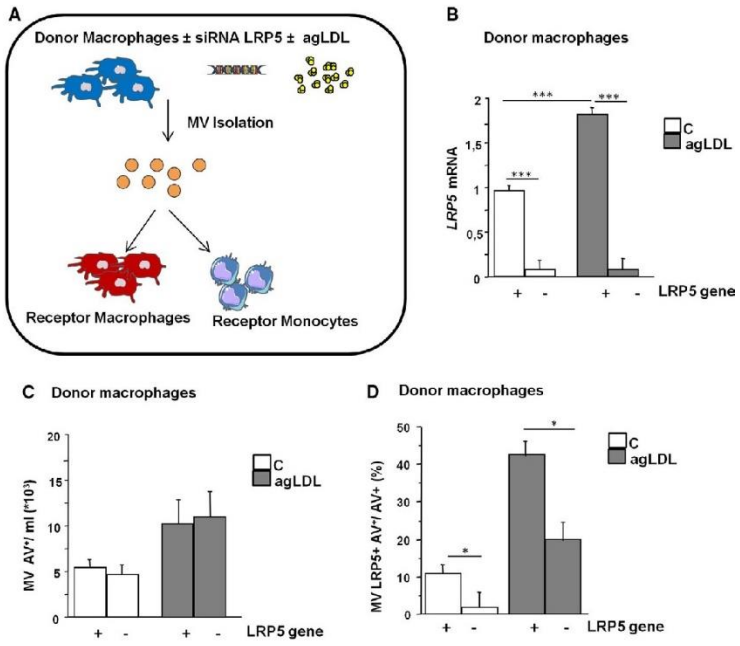

FIGURE 4 Characterization of donor macrophages and their secreted MV. (A) Schematic of experiment. Donor macrophages were silenced or not for LRP5 (siLRP5) and treated or not with agLDL. After 48 hours, macrophage secreted MV were isolated and suspended to treat receptor macrophages or receptor monocytes. (B) LRP5 gene expression in donor macrophages after LRP5 silencing and agLDL treatments. (C) Macrophage-derived AV^+MV/mL secreted by donor macrophages. (D) Macrophage-derived $LRP5^+$MV released by donor macrophages. Experiments were performed four times in triplicates. $^*P < .05$, $^{**}P < .01$, $^{***}P < .005$

4 | DISCUSSION

Microvesicles can stimulate targets cells by direct interaction with target receptors and the transfer of the bioactive molecules they contain.[2,3,7,8,10,13,15] Here, we show, for the first time, that LRP5 is delivered into MV released by macrophages and monocytes. However, the release of $LRP5^+$MV is only significantly increased in fully differentiated lipid-loaded macrophages.

In general, macrophages are classified into two main phenotypes, classical M1 $CD16^-$ activated macrophages and alternative M2 $CD16^+$ activated macrophages, which regulate pro-inflammatory and anti-inflammatory responses, respectively.[29] Regulation of lipid-induced macrophage polarization is a very new field of investigation. A recent study showed that saturated fatty acid treatment induced M1-predominant macrophages, while polyunsaturated fatty acid induced M2-predominant macrophages.[30] Treatment of hepatocytes with conditioned media from M1-polarized macrophages promoted lipid synthesis and accumulation indicating that lipid-induced macrophage M1 polarization stimulates hepatic lipid metabolism.[30] In this study, we show that lipid-loaded macrophages show high cell surface expression of pro-inflammatory proteins while cell surface expression of anti-inflammatory proteins ($CD16^+$, $CD163^+$ and $CD206^+$) remains constantly low indicating that lipid loading induces M1 polarization. This results are supported by cell sorting experiments where isolated specific pro-inflammatory subpopulations of macrophages release pro-inflammatory proteins. LRP5 expression levels are higher in $CD16^+$ expressing macrophages as compared to $CD16^-$ macrophages. Indeed, in control conditions there is a 2.6% expression of cell surface LRP5 in $CD16^-$ macrophages as compared to 16.7% in $CD16^+$ macrophages. These results are in line with our previous findings where LRP5 immunofluorescent staining was increased in $CD16^+$ macrophages as compared to $CD16^-$ macrophages.[26] Here, we show that LRP5 expression levels in control macrophages expressing anti-inflammatory proteins are higher than in macrophages expressing pro-inflammatory markers ($CD16^-$, $CD80^+$ and $CD83^+$) indicating that in control conditions, there is more LRP5 expressed in macrophages with anti-inflammatory phenotype. Interestingly, LRP5 cell surface expression is increased in all lipid-loaded macrophages. Indeed, macrophages expression of pro-inflammatory or anti-inflammatory markers on their cell surface is independent of LRP5 expression levels, indicating that LRP5 expression is upregulated in lipid-loaded macrophages irrespective of the macrophage inflammatory phenotype.

In the presence of extracellular lipids, there is increased release of MV. This is in line with previous studies where statin treatment (a lipid lowering agent) reduced MV shedding from platelets, endothelial cells and leukocytes carrying markers of cell activation.[31] Similarly, decreased MV release and decreased cargo of cell activation markers after statin treatment in different cell lineages have also been described.[32-36] We have explored whether MV show different inflammatory phenotypes if they are released by untreated or lipid-loaded macrophages. Because MV are released from the cell surface of their cells of origin, we used the same pro-inflammatory and anti-inflammatory markers used to characterize $CD16^-$ and $CD16^+$ macrophages to map their released MV. Lipid-loaded macrophages show increased release of $CD16^-$MV, $CD80^+$MV and $CD83^+$MV,

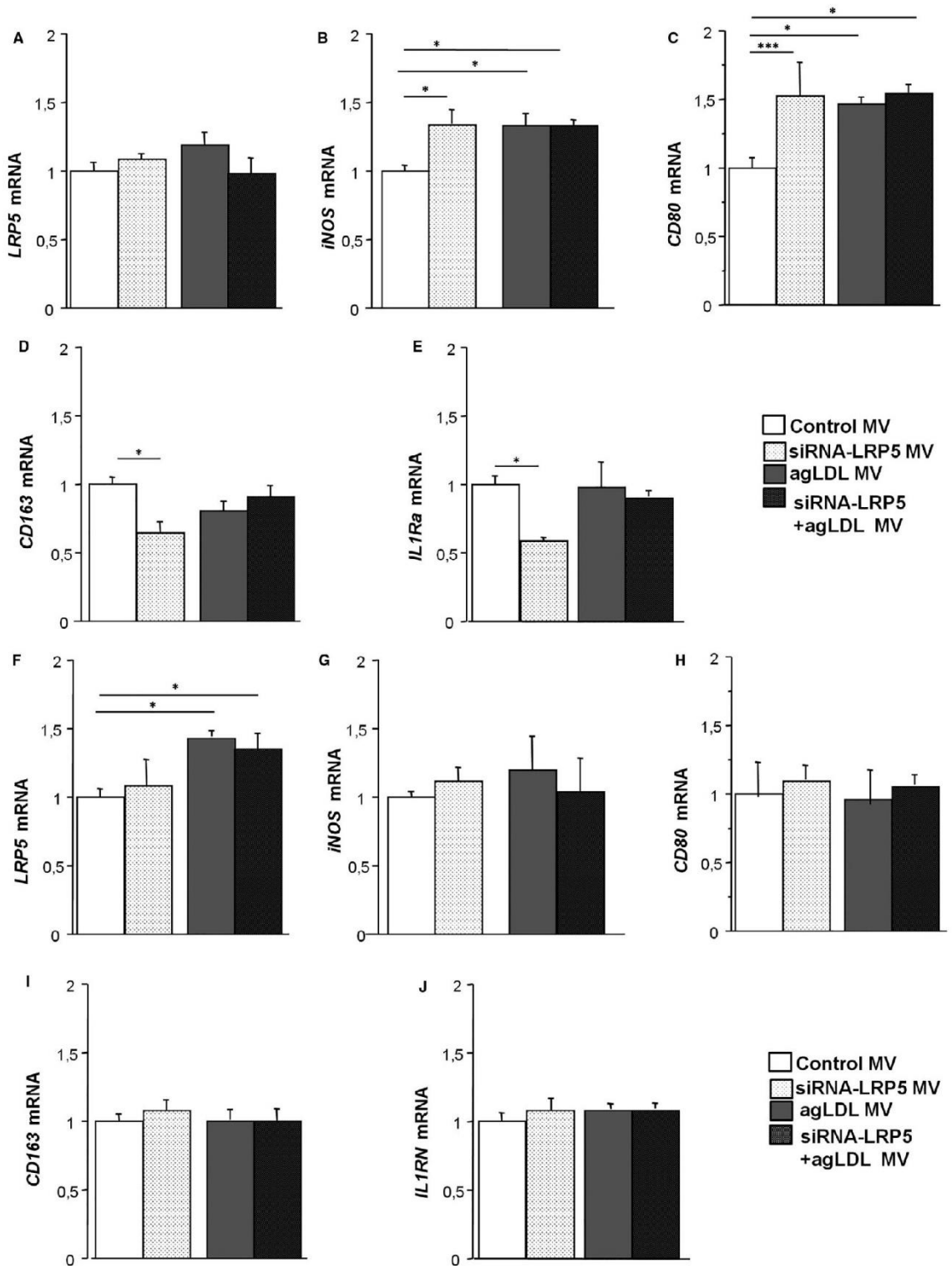
A
LRP5 mRNA
B
iNOS mRNA
C
CD80 mRNA
D
CD163 mRNA
E
IL1Ra mRNA
Control MV
siRNA-LRP5 MV
agLDL MV
siRNA-LRP5 +agLDL MV
F
LRP5 mRNA
G
iNOS mRNA
H
CD80 mRNA
I
CD163 mRNA
J
IL1RN mRNA
Control MV
siRNA-LRP5 MV
agLDL MV
siRNA-LRP5 +agLDL MV

FIGURE 5 Gene expression levels in receptor macrophages and monocytes. Receptor macrophages were treated with macrophage-derived MV released by Control macrophages, siRNA-LRP5-treated macrophages, 100 μg/mL agLDL-treated macrophages or siRNA-LRP5+AgLDL-treated macrophages and mRNA expression levels of (A) *LRP5*, (B) *iNOS*, (C) *CD80*, (D) *CD163* and (E) *IL1Ra* were analysed. Receptor monocytes were treated with macrophage-derived MV released by Control macrophages, siRNA-LRP5-treated macrophages, 100 μg/mL agLDL-treated macrophages or siRNA-LRP5+AgLDL-treated macrophages and mRNA expression levels of (F) *LRP5*, (G) *iNOS*, (H) *CD80*, (I) *CD163* and (J) *IL1Ra* were analysed. Experiments were performed four times in triplicates. $^{*}P < .05$, $^{***}P < .005$

while the release of MV containing anti-inflammatory markers ($CD16^+$, $CD163^+$ and $CD206^+$) remained similar to untreated macrophages indicating that lipid-loaded macrophages release MV with a pro-inflammatory phenotype. The molecular mechanisms behind the preferential incorporation of different proteins into budding MV remain to be elucidated, but it has been suggested that it could be mediated by the cytoplasmic domains of the protein to be included into the MV.[37]

Similar to the increased cellular expression of LRP5 in lipid-loaded $CD16^-$ and $CD16^+$ macrophages, lipid loading induced increased release of $LRP5^+$MV in both $CD16^-$MV and $CD16^+$MV indicating that the expression of inflammatory markers in MV is independent of the delivery of LRP5 into MV. However, after lipid loading, only pro-inflammatory MV were released. Therefore, only $LRP5^+CD16^-$MV, $LRP5^+CD80^+$MV and $LRP5^+CD83^+$MV were released. This raises the very interesting question of how is LRP5 delivered and released with MV containing pro-inflammatory markers. Notably, MV production and release are stimuli and signal dependent.[38,39] For example, cytokine IL1β induces MV shedding from circulating monocytes.[40] Accordingly, here we show that lipid stimuli induce pro-inflammatory MV release. As lipid loaded macrophages show increased expression of LRP5 at the cell surface, it is plausible that this LRP5 will be delivered to their MV and released as $LRP5^+$MV. Human macrophages expressing LRP5 have been shown to provide survival and repair to damaged tissues.[26] It is our hypothesis that this is the function of $LRP5^+$MV but further work needs to be performed to prove it.

We also explored the function of macrophage-derived $LRP5^+$MV in the polarization fate of macrophages. Lipid-loaded macrophages that did not express LRP5 showed similar MV release than lipid-loaded $LRP5^+$ macrophages indicating that LRP5 does not participate in the MV release pathway. A reduction in $LRP5^+$MV release from macrophages without LRP5 was observed.

Classically activated $CD16^-$ macrophages are characterized by the expression of several pro-inflammatory markers, including iNOS and CD80[41,42] while alternatively activated anti-inflammatory $CD16^+$ macrophages express CD163 and IL1Ra.[42,43] Treatment with MV released by macrophages devoid of LRP5 induced iNOS and CD80 expression and reduced CD163 and IL1Ra expression in naive macrophages indicating that $LRP5^+$MV induce macrophages to differentiate towards an anti-inflammatory phenotype. A limitation of this study is that the size of $LRP5^+$MV was not assessed; therefore, we could not determine if $LRP5^+$MV have a different size than MV devoid of LRP5. However, always the same procedure was followed to prepare MV and only MV released by control macrophages were unable to induce high expression of pro-inflammatory genes. Also, MV released by lipid-loaded macrophages induced increased expression of pro-inflammatory genes independent of LRP5 expression further supporting that different stimulus in the cells of origin generates MV with different cargoes that will have different functions in the target cells.

In conclusion, here we demonstrate for the first time that a lipoprotein receptor, LRP5, is delivered into MV. MV released by lipid-loaded macrophages contain mainly pro-inflammatory proteins and LRP5. $LRP5^+$MV induce an anti-inflammatory genotype in naive macrophages. Therefore, a systematic blockade of monocyte/macrophage infiltration in the prevention of atherosclerosis may be less effective than originally expected if the levels of macrophage-derived $LRP5^+$MV are affected and reduced.

ACKNOWLEDGEMENTS

We thank S. Huertas for excellent technical assistance. This work was supported by the Spanish Ministry of Science and Innovation and FEDER funds [PID2019-107160RB-I00 to LB]; the Instituto de Salud Carlos III [CIBERCV CB16/11/00411 to LB, TERCEL RD16/0011/018 to LB and FIS2020-01282 to MBP]; the Generalitat of Catalunya-Secretaria d'Universitats i Recerca del Departament d'Economia i Coneixement de la Generalitat [2017SGR1480 to LB; PERIS SLT006 to LB]; the Spanish Society of Cardiology [FEC2019 to MBP] and the Fundación Investigación Cardiovascular-Fundación Jesus Serra for their continuous support.

CONFLICT OF INTEREST

The authors confirm that there are no conflicts of interest.

AUTHOR CONTRIBUTION

Aureli Luquero: Data curation (lead); Formal analysis (equal); Investigation (equal); Methodology (lead); Software (equal); Visualization (equal); Writing-review & editing (equal). **Gemma Vilahur:** Conceptualization (equal); Formal analysis (equal); Methodology (equal); Writing-review & editing (equal). **Javier Crespo:** Formal analysis (supporting); Methodology (supporting); Software (equal); Writing-review & editing (equal). **Lina Badimon:** Conceptualization (lead); Funding acquisition (lead); Methodology (equal); Resources (equal); Supervision (equal); Writing-review & editing (equal). **Maria Borrell-Pages:** Conceptualization (supporting); Data curation (equal); Formal analysis (equal); Funding acquisition (supporting); Investigation (lead); Methodology (equal); Supervision (lead); Writing-original draft (lead); Writing-review & editing (lead).

DATA AVAILABILITY STATEMENT

The data underlying this article are available in the article and in its online supplementary material.

ORCID

Maria Borrell-Pages https://orcid.org/0000-0002-1759-9756

REFERENCES

1. Ridger VC, Boulanger CM, Angelillo-Scherrer A, et al. Microvesicles in vascular homeostasis and diseases position paper of the European society of cardiology (ESC) working group on atherosclerosis and vascular biology. *Thromb Haemost*. 2017;117:1296-1316.
2. Mathivanan S, Ji H, Simpson RJ. Exosomes: extracellular organelles important in intercellular communication. *J Proteomics*. 2010;73:1907-1920.
3. Camussi G, Deregibus MC, Bruno S, Cantaluppi V, Biancone L. Exosomes/microvesicles as a mechanism of cell-to-cell communication. *Kidney Int*. 2010;78:838-848.
4. Taylor DD, Gercel-Taylor C. Exosomes/microvesicles: mediators of cancer-associated immunosuppressive microenvironments. *Semin Immunopathol*. 2011;33:441-454.
5. Cocucci E, Racchetti G, Meldolesi J. Shedding microvesicles: artefacts no more. *Trends Cell Biol*. 2009;19:43-51.
6. Février B, Raposo G. Exosomes: endosomal-derived vesicles shipping extracellular messages. *Curr Opin Cell Biol*. 2004;16:415-421.
7. Hunter MP, Ismail N, Zhang X, et al. Detection of microRNA expression in human peripheral blood microvesicles. *PLoS One*. 2008;3:e3694.
8. Ratajczak J, Wysoczynski M, Hayek F, Janowska-Wieczorek A, Ratajczak MZ. Membrane-derived microvesicles: important and underappreciated mediators of cell-to-cell communication. *Leukemia*. 2006;20:1487-1495.
9. Valadi H, Ekström K, Bossios A, Sjöstrand M, Lee JJ, Lötvall JO. Exosome-mediated transfer of mRNAs and microRNAs is a novel mechanism of genetic exchange between cells. *Nat Cell Biol*. 2007;9:654-659.
10. Baj-Krzyworzeka M, Szatanek R, Węglarczyk K, et al. Tumour-derived microvesicles carry several surface determinants and mRNA of tumour cells and transfer some of these determinants to monocytes. *Cancer Immunol Immunother*. 2006;55:808-818.
11. MacKenzie A, Wilson HL, Kiss-Toth E, Dower SK, North RA, Surprenant A. Rapid secretion of interleukin-1β by microvesicle shedding. *Immunity*. 2001;15:825-835.
12. Frey B, Munoz LE, Pausch F, et al. The immune reaction against allogeneic necrotic cells is reduced in Annexin A5 knock out mice whose macrophages display an anti-inflammatory phenotype. *J Cell Mol Med*. 2009;13:1391-1399.
13. Martínez MC, Larbret F, Zobairi F, et al. Transfer of differentiation signal by membrane microvesicles harboring hedgehog morphogens. *Blood*. 2006;108:3012-3020.
14. Ratajczak J, Miekus K, Kucia M, et al. Embryonic stem cell-derived microvesicles reprogram hematopoietic progenitors: evidence for horizontal transfer of mRNA and protein delivery. *Leukemia*. 2006;20:847-856.
15. Collino F, Deregibus MC, Bruno S, et al. Microvesicles derived from adult human bone marrow and tissue specific mesenchymal stem cells shuttle selected pattern of miRNAs. *PLoS One*. 2010;5:e11803.
16. Montecalvo A, Larregina AT, Shufesky WJ, et al. Mechanism of transfer of functional microRNAs between mouse dendritic cells via exosomes. *Blood*. 2012;119:756-766.
17. Arderiu G, Peña E, Badimon L. Angiogenic microvascular endothelial cells release microparticles rich in tissue factor that promotes postischemic collateral vessel formation. *Arterioscler Thromb Vasc Biol*. 2015;35:348-357.
18. Boulanger CM, Loyer X, Rautou PE, Amabile N. Extracellular vesicles in coronary artery disease. *Nat Rev Cardiol*. 2017;14:259-272.
19. Badimon L, Vilahur G. Thrombosis formation on atherosclerotic lesions and plaque rupture. *J Intern Med*. 2014;276:618-632.
20. Borrell-Pages M, Romero JC, Juan-Babot O, Badimon L. Wnt pathway activation, cell migration, and lipid uptake is regulated by low-density lipoprotein receptor-related protein 5 in human macrophages. *Eur Heart J*. 2011;32:2841-2850.
21. Clevers H, Nusse R. Wnt/β-catenin signaling and disease. *Cell*. 2012;149:1192-1205.
22. Borrell-Pages M, Vilahur G, Romero JC, Casaní L, Bejar MT, Badimon L. LRP5/canonical Wnt signalling and healing of ischemic myocardium. *Basic Res Cardiol*. 2016;111:67.
23. Badimon L, Casaní L, Camino-Lopez S, Juan-Babot O, Borrell-Pages M. GSK3β inhibition and canonical Wnt signaling in mice hearts after myocardial ischemic damage. *PLoS One*. 2019;14:e0218098.
24. Mosser DM, Edwards JP. Exploring the full spectrum of macrophage activation. *Nat Rev Immunol*. 2008;8:958-969.
25. Murray PJ, Wynn TA. Protective and pathogenic functions of macrophage subsets. *Nat Rev Immunol*. 2011;11:723-737.
26. Borrell-Pages M, Romero JC, Crespo J, Juan-Babot O, Badimon L. LRP5 associates with specific subsets of macrophages: molecular and functional effects. *J Mol Cell Cardiol*. 2016;90:146-156.
27. Borrell-Pagès M, Romero JC, Badimon L. LRP5 negatively regulates differentiation of monocytes through abrogation of Wnt signalling. *J Cell Mol Med*. 2014;18:314-325.
28. Badimon L, Luquero A, Crespo J, Peña E, Borrell-Pages M. PCSK9 and LRP5 in macrophage lipid internalization and inflammation. *Cardiovasc Res*. 2020;cvaa254. https://doi.org/10.1093/cvr/cvaa254
29. Tacke F, Zimmermann HW. Macrophage heterogeneity in liver injury and fibrosis. *J Hepatol*. 2014;60:1090-1096.
30. Wu HM, Ni XX, Xu QY, Wang Q, Li XY, Hua J. Regulation of lipid-induced macrophage polarization through modulating peroxisome proliferator-activated receptor-gamma activity affects hepatic lipid metabolism via a Toll-like receptor 4/NF-κB signaling pathway. *J Gastroenterol Hepatol*. 2020;35:1998-2008.
31. Suades R, Padró T, Alonso R, Mata P, Badimon L. Lipid-lowering therapy with statins reduces microparticle shedding from endothelium, platelets and inflammatory cells. *Thromb Haemost*. 2013;110:366-377.
32. Nomura S, Shouzu A, Omoto S, et al. Effects of eicosapentaenoic acid on endothelial cell-derived microparticles, angiopoietins and adiponectin in patients with type 2 diabetes. *J Atheroscler Thromb*. 2009;16:83-90.
33. Nomura S, Inami N, Shouzu A, Rase F, Maeda Y. The effects of pitavastatin, eicosapentaenoic acid and combined therapy on platelet-derived microparticles and adiponectin in hyperlipidemic, diabetic patients. *Platelets*. 2009;20:406-414.
34. Tramontano AF, O'Leary J, Black AD, Muniyappa R, Cutaia MV, El-Sherif N. Statin decreases endothelial microparticle release from human coronary artery endothelial cells: implication for the Rho-kinase pathway. *Biochem Biophys Res Commun*. 2004;320:34-38.
35. Sommeijer DW, Joop K, Leyte A, Reitsma PH, Ten Cate H. Pravastatin reduces fibrinogen receptor gpIIIa on platelet-derived microparticles in patients with type 2 diabetes. *J Thromb Haemost*. 2005;3:1168-1171.
36. Mobarrez F, He S, Bröijersen A, et al. Atorvastatin reduces thrombin generation and expression of tissue factor, p-selectin and GPIIIa on platelet-derived microparticles in patients with peripheral arterial occlusive disease. *Thromb Haemost*. 2011;106:344-352.
37. Barclay AN, Brown M, Law SKA, McKnight A, Tomlinson M, Van der Merwe P. *The Leucocyte Antigen Factsbook*. Oxford, UK: Elsevier, Academic Press; 1997:231.

38. Williams C, Palviainen M, Reichardt NC, Siljander PRM, Falcón-Pérez JM. Metabolomics applied to the study of extracellular vesicles. *Metabolites*. 2019;9:276.
39. Turchinovich A, Drapkina O, Tonevitsky A. Transcriptome of extracellular vesicles: state-of-the-art. *Front Immunol*. 2019;10:202.
40. Ward JR, West PW, Ariaans MP, et al. Temporal interleukin-1β secretion from primary human peripheral blood monocytes by P2X7-independent and P2X7-dependent mechanisms. *J Biol Chem*. 2010;285:23147-23158.
41. Xue Q, Yan Y, Zhang R, Xiong H. Regulation of iNOS on immune cells and its role in diseases. *Int J Mol Sci*. 2018;19:3805.
42. Bertani FR, Mozetic P, Fioramonti M, et al. Classification of M1/M2-polarized human macrophages by label-free hyperspectral reflectance confocal microscopy and multivariate analysis. *Sci Rep*. 2017;7:8965.
43. Alvarado-Vazquez PA, Bernal L, Paige CA, et al. Macrophage-specific nanotechnology-driven CD163 overexpression in human macrophages results in an M2 phenotype under inflammatory conditions. *Immunobiology*. 2017;222:900-912.

SUPPORTING INFORMATION

Additional supporting information may be found online in the Supporting Information section.

How to cite this article: Luquero A, Vilahur G, Crespo J, Badimon L, Borrell-Pages M. Microvesicles carrying LRP5 induce macrophage polarization to an anti-inflammatory phenotype. *J Cell Mol Med*. 2021;25:7935–7947. https://doi.org/10.1111/jcmm.16723

Supplemental Figure 1

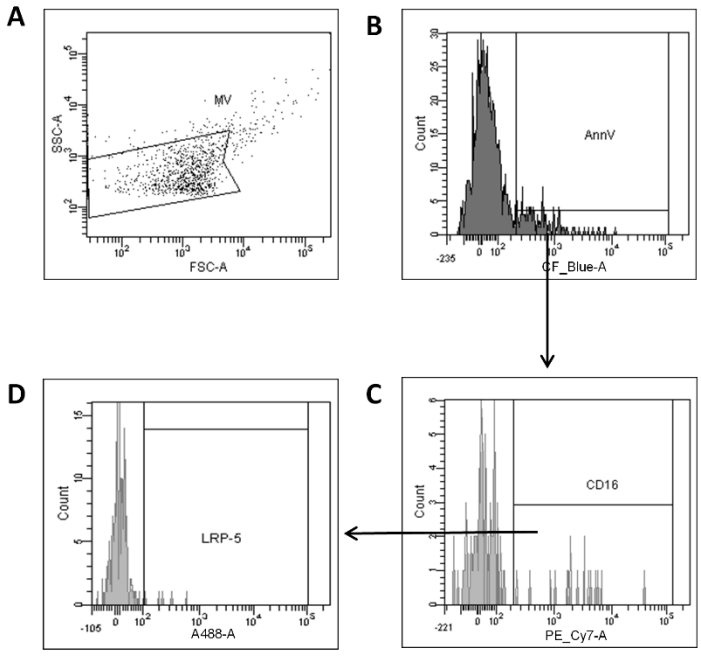

Supplemental Figure 1: Representative plots for macrophage-derived-microvesicles identification and characterization. **A)** MV gate was set according to MV size. **B)** Annexin V CFBlue$^+$ MV were selected from the MV gate. **C)** PECy7 and **D)** 488 labelled antibodies were quantified. FSC means forward scatter; SSC, side scatter; PE, phycoerithrin.

Supplemental Figure 2

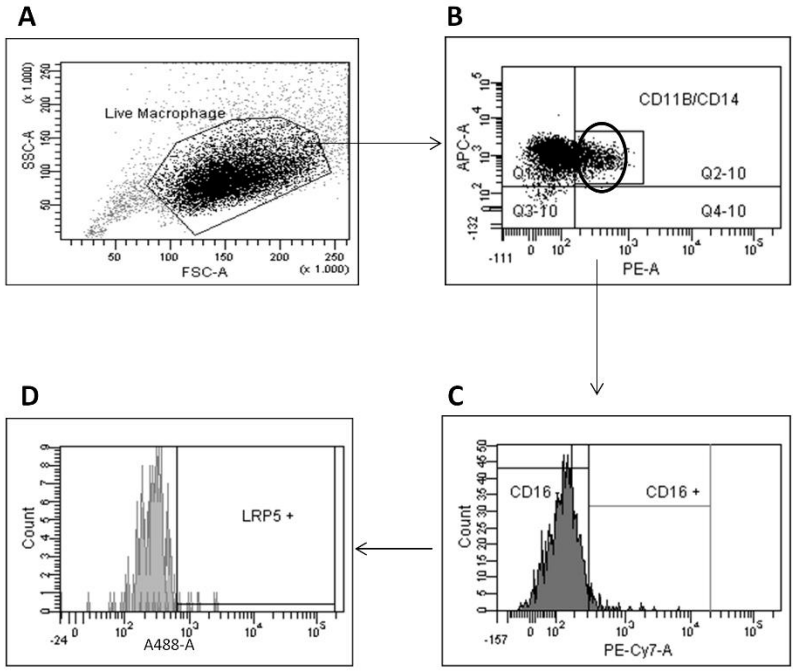

Supplemental Figure 2: Gating Strategy for $CD11b^{+}CD14^{+}CD16^{-}LRP5^{+}$ macrophages and $CD11b^{+}CD14^{+}CD16^{+}LRP5^{+}$ macrophages by flow cytometry analysis. A) Live macrophage gate was set according to macrophages size and complexity (FSC/SSC). **B)** Live macrophages were gated on positive co-expression of $CD11b^{+}$ and $CD14^{+}$ for macrophage determination. **C)** Events were then gated for CD16 positive or negative expression. **D)** Finally LRP5 expression levels was analyzed in these cells. FSC means forward scatter; SSC, side scatter; PE, phycoerityhrin.

Supplemental Figure 3

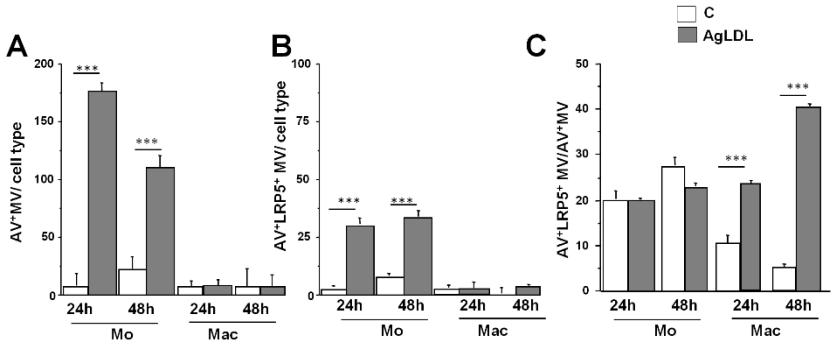

Supplemental Figure 3: AgLDL treatment induce MV secretion. Monocytes (Mo) or macrophages (Mac) were treated with 100µg/ml agLDL for 24h or 48h and the amount of **A)** Annexin V^{+} microvesicles per cell and **B)** Annexin V^{+} $LRP5^{+}$ microvesicles per cell was analyzed. **C)** The ratio between MV per cell that are $AV^{-}LRP5^{+}/AV^{-}$ in control and lipid-loaded Mo and Mac is shown. All experiments were performed at least 4 times in duplicates or triplicates. **$P<0.05$, ***$P<0.005$.

Supplemental Tables

Supplemental Table I. Cell molecules for circulating microvesicle identification and characterization.

mAb	Alternative name	Conjugation	Clone	µL/test	Company	Reference
CD16	Fc gamma RIII	PE-Cyanine7	eBioCB16	2,5	Invitrogen	25-0168-42
CD206	Macrophage mannose receptor	PE-Cyanine7	19.2	2,5	Invitrogen	25-2069-42
CD163	Haemoglobin-Heptaglobin complex Receptor	PE-Cyanine7	eBioGHI/61 (GHI/61)	5	Invitrogen	25-1639-42
CD80	B7-1 Membrane Protein	Super Bright 436	2D10.4	5	Invitrogen	62-0809-42
CD83	B-cell activation protein	PerCP-eFluo 710	HB15e	5	Invitrogen	46-0839-42
LRP5	LRP5	488	Polyclonal	1	Bioss	bs-411R
AV	PS- Binding protein	CF Blue	---	5	Immunostep	ANVCFB-200

mAb indicates monoclonal antibody; PE, phycoerithrin; AV Annexin V; PS, phosphatidylserine.

Supplemental Table II. Cell molecules for macrophage identification and characterization.

mAb	Alternative name	Conjugation	Clone	µL/test	Company	Reference
CD16	Fc gamma RIII	PE-Cyanine7	eBioCB16	5	Invitrogen	25-0168-42
CD206	Macrophage mannose receptor	PE-Cyanine7	19.2	5	Invitrogen	25-2069-42
CD163	Haemoglobin-Heptaglobin complex Receptor	PE-Cyanine7	eBioGHI/61 (GHI/61)	5	Invitrogen	25-1639-42
CD11b	Macrophage-1 Antigen (Mac-1)	PE	M1/70	5	Invitrogen	12-0112-82
CD14	LPS Receptor	PerCPCyanine5.5	Sa2-8	5	Invitrogen	45-0141-82
CD14	LPS Receptor	PE	61D3	5	Invitrogen	12-0149-42
CD80	B7-1 Membrane Protein	Super Bright 436	2D10.4	5	Invitrogen	62-0809-42
CD83	B-cell activation protein	PerCP-eFluor710	HB15e	5	Invitrogen	46-0839-42
LRP5	LRP 5	488	Polyclonal	1	Bioss	bs-411R

mAb indicates monoclonal antibody; PE, phycoerithrin; APC, allophycocyanin; LPS, lipopolysaccharide.

3.6 Article 5

Canonical Wnt pathway and the LDL receptor superfamily in neuronal cholesterol homeostasis and function

By Aureli Luquero, Maria Borrell-Pages, Gemma Vilahur, Teresa Padró and Lina Badimon.

Published in Cardiovascular Research. 2024;120:140-151.
doi.org/10.1093/cvr/cvad159

*An erratum is pendent of being published regarding this manuscript. The erratum corrects author affiliation data for Aureli Luquero, adding the affiliation: Biomedicine Doctorate Program, Universitat de Barcelona, 08007 Barcelona, Spain.

Summary: The canonical WNT signalling pathway is associated with multiple brain processes and enhanced or repressed activity of the pathway can induce brain diseases. Cholesterol is necessary for neuronal homeostasis as it contributes to synaptic vesicle trafficking and formation of lipid rafts. LDL do not typically interact with neurons directly but pathological conditions like hypercholesterolemia can disrupt the blood-brain barrier integrity and allow for LDL leaks into the cerebrospinal fluid which breaks neuronal homeostasis. To analyze the role of LRP5 and the canonical WNT signalling pathway in brain cholesterol homeostasis we first studied the expression of LRP5 and other canonical WNT proteins in brains of *Wt* and *Lrp5*$^{-/-}$ mice. Results show that in *Lrp5*$^{-/-}$ mice, Lrp5 expression is absent from all extracranial tissues but is conserved in the brain. Transcriptional activity of canonical WNT signalling pathway target genes including VEGF-A or OPN is also present in *Lrp5*$^{-/-}$ mice brains, indicating the viability of the signalling pathway. The neuronal cell line SH-SY5y was exposed to lipids and

LRP5 expression levels were increased. Lipid exposure also increased cholesteryl ester accumulation in the cells. However, LRP5-silencing did not reduce cholesterol accumulation, suggesting that LRP5 does not participate in lipid uptake in SH-SY5y cells. Further analyses show that LDLR, but not LRP5, LRP1, or CD36, induce cholesterol internalization in differentiated neurons. LDL stimulation triggered the expression of canonical WNT signalling members' and targets. We hypothesized that LRP5 and the canonical WNT signalling might exert a pro-survival protective function in neuronal cells because we have previously shown a protective role for LRP5 in atherosclerosis progression and MI. We incubated LRP5-silenced differentiated neurons with H_2O_2 (oxidative-stress inducer) or staurosporine (kinase inhibitor) to induce apoptosis. After exposure to H_2O_2, high Bax/Bcl2 ratio was observed in LRP5-silenced cells, indicating enhanced apoptosis, a result further confirmed by flow cytometry experiments with staining of AnnexinV and propidium iodide. The apoptotic protein profile of SH-SY5y cells after H_2O_2 treatments show higher active caspase 3 expression in LRP5-silenced cells than in control cells. In staurosporine treated cells, we observed enhanced apoptosis in LRP5-silenced cells which was further confirmed by higher active caspase 3 expression. Finally, we also evaluated the involvement of LRP5 in autophagy of neuronal cells, a physiological process that is involved in cell survival. Neurons stimulated with H_2O_2 or staurosporine had reduced autophagy as demonstrated by the reduced expression of autophagy markers LC3b and p62. However, no differences were observed between control and LRP5-silenced cells indicating that LRP5 does not participate in the neuronal autophagic process. In conclusion, we demonstrate that LRP5 and the canonical WNT pathway are important regulators of neuron survival.

ESC European Society of Cardiology
Cardiovascular Research (2024) **120**, 140–151
https://doi.org/10.1093/cvr/cvad159

Canonical Wnt pathway and the LDL receptor superfamily in neuronal cholesterol homeostasis and function

Maria Borrell-Pages [1,2*†], Aureli Luquero [1,2†], Gemma Vilahur[1,2], Teresa Padró[1,2], and Lina Badimon [1,2,3]

[1]Cardiovascular Program ICCC, Sant Pau Institute for Biomedical Research (IIB-Sant Pau), C/Sant Antoni Maria Claret 167, Barcelona 08025, Spain; [2]CIBER-CV, Av. Monforte de Lemos, 3-5, 28029 Madrid, Spain; and [3]Cardiovascular Research Chair, Universitat Autònoma de Barcelona, Plaça Cívica, 08193 Bellaterra, Barcelona, Spain

Received 9 May 2023; revised 13 July 2023; accepted 4 September 2023; online publish-ahead-of-print 26 October 2023

Time of primary review: 48 days

Aims There is little information on the regulation of cholesterol homeostasis in the brain. Whether cholesterol crosses the blood–brain barrier is under investigation, but the present understanding is that cholesterol metabolism in the brain is independent from that in peripheral tissues. Lipoprotein receptors from the LDL receptor family (LRPs) have key roles in lipid particle accumulation in cells involved in vascular and cardiac pathophysiology; however, their function on neural cells is unknown.

Methods and results The expression of LRP5 and the components and targets of its downstream signalling pathway, the canonical Wnt pathway, including β-catenin, LEF1, VEGF, OPN, MMP7, and ADAM10, is analysed in the brains of *Wt* and *Lrp5*$^{-/-}$ mice and in a neuroblastoma cell line. LRP5 expression is increased in a time- and dose-dependent manner after lipid loading in neuronal cells; however, it does not participate in cholesterol homeostasis as shown by intracellular lipid accumulation analyses. Neurons challenged with staurosporin and H_2O_2 display an anti-apoptotic protective role for LRP5.

Conclusions For the first time, it has been shown that neurons can accumulate intracellular lipids and lipid uptake is performed mainly by the LDLR, while CD36, LRP1, and LRP5 do not play a major role. In addition, it has been shown that LRP5 triggers the canonical Wnt pathway in neuronal cells to generate pro-survival signals. Finally, *Lrp5*$^{-/-}$ mice have maintained expression of LRP5 only in the brain supporting the biological plausible concept of the need of brain LRP5 to elicit pro-survival processes and embryonic viability.

* Corresponding author. Tel: +34 935565621; fax: +34 93 5565600, E-mail: mborrellpa@santpau.cat
† The first two authors share the equal first authorship.

Graphical Abstract

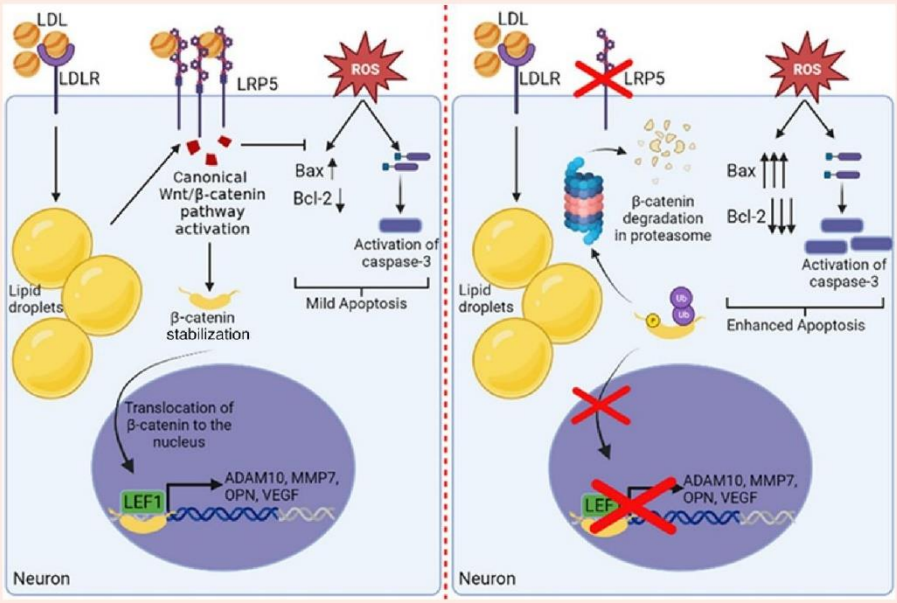

Keywords LRP • Lipids • Cholesterol homeostasis • Neurons

1. Introduction

The canonical Wnt signalling pathway is mainly involved in cell proliferation and survival in vital biological processes, including organogenesis and embryogenesis.[1,2] It is activated by LDL receptor–related protein 5 (LRP5), a receptor of the LDL receptor superfamily. In the adult, LRPs are involved for their role in the clearance of cholesterol and cholesteryl ester–containing LDL particles from the blood.[3] Together with its co-receptor Frizzled, LRP5 binds specific Wnt ligands or extracellular lipids and induces an intracellular signalling cascade by the phosphorylation of different proteins allowing cytoplasmic β-catenin to translocate to the nucleus and bind the LEF family of transcription factors. This binding induces the transcription of canonical Wnt direct and indirect target genes, including c-jun,[4] cyclin D1,[5] VEGF,[6] MMP7,[7] ADAM 10,[8] and Opn.[9] A role for both LRP5 and LRP6 has been described in the cerebellum where the deletion of both LRP5 and LRP6 together, but not individually, resulted in defective foliation and lamination of the cerebellum during post-natal development.[10] However, whether LRP5 is involved in cholesterol metabolism in the brain is unknown.

The canonical Wnt signalling pathway participates in the formation of the antero-posterior axis patterning in axonal pathfinding and in synaptogenesis.[11–13] In the mammalian central nervous system, dysregulation of the Wnt pathway inhibits timely myelination and remyelination of neurons,[14] and Dkk-1, a canonical Wnt inhibitor, is released into the circulation after the occurrence of cerebral ischaemia events.[15] Inhibition of canonical Wnt signalling is also observed in a variety of central nervous system diseases. During the progression of Alzheimer's disease, the β-amyloid protein can bind to the Frizzled receptor inhibiting downstream phosphorylation and preventing canonical Wnt signalling induction.[16] β-Amyloid can also increase the activity of the Wnt pathway inhibitor GSK3β, inducing neuronal apoptosis and increasing the neurotoxicity associated with β-amyloid.[17] Taken together, these results show that the canonical Wnt pathway has to be finely regulated to avoid brain diseases.

Early studies addressing the topic of cholesterol content in human brain arteries show that atherosclerosis is 6- to 19-fold greater in extracranial arteries than in intracranial arteries, mostly due to the anti-oxidant enzymes present in brain arteries that provide resistance to atherosclerosis lesion development.[18] Furthermore, a comparison of intracranial vs. extracranial fatty streak formation of human foetuses from normocholesterolaemic and hypercholesterolaemic mothers shows that, in the absence of other atherogenic risk factors, hypercholesterolaemia during foetal development induces an extensive formation of fatty streaks in extracranial arteries but not in intracranial arteries.[19] Cholesterol in the central nervous system is mainly synthesized by astrocytes.[20] Transcytosis across the blood–brain barrier (BBB) occurs as an efflux mechanism to eliminate cholesterol excess.[21] Blood-circulating LDL molecules can also cross the BBB in a process mediated by the LDLR expressed in caveolin- or clathrin-coated vesicles in specialized BBB-endothelial cells.[22] In addition, disruption of BBB integrity can lead to an increased permeability of the endothelium for cholesterol-carrying lipoproteins and facilitate the exposure of blood-circulating components to neurons.[23–25]

Here, we investigated the role of brain cells in cholesterol regulation. We have previously shown that LRP5 is an alternative to the LDLR for cholesterol internalization, and the role of LRP5 in lipid homeostasis has been proven previously in a variety of organs and tissues. Increased LRP5 expression is induced by extracellular lipids in the primary cultures of human monocytes and macrophages and human vascular smooth muscle cells[3] and *in vivo* in $ApoE^{-/-}$ mice.[26] Also, macrophages that do not express LRP5 show less intracellular cholesterol ester accumulation than *Wt* macrophages.[3] Furthermore, aortas from $Lrp5^{-/-}$ mice show less lipid

content than those from *Wt* mice[27,28] and LRP5 gene and protein levels are also upregulated in the hearts of hypercholesterolaemic mice and in hypercholesterolaemic ischaemic human hearts.[29,30] Here, we investigated whether LRP5 and the canonical Wnt pathway participate in brain cholesterol metabolism.

2. Methods

2.1 Organ distribution in *Wt* and *Lrp5*$^{-/-}$ mice

The study protocols for mice were approved by the institutional Animal Care and Use Committee (ICCC051/5422) and authorized by the local government commission. All animal procedures conform to the guidelines from Directive 2010/63/EU of the European Parliament and the 'Position of the American Heart Association on Research Animals use' (11 November 1984). We are committed to the '3Rs' principle and hence used the minimum number of animals required to achieve statistical significance.

Lrp5$^{-/-}$ mice, a kind gift from Dr Bart Williams,[31,32] were maintained in a C57BL/6 background. The mice were housed in cages under controlled temperature (21 ± 2°C) on a 12 h light/dark cycle with food and water *ad libitum*. Homozygous wild-type C57BL/6 mice (*Wt*) and *Lrp5*$^{-/-}$ C57BL/6 mice (*Lrp5*$^{-/-}$) were used for organ extraction. The presence of LRP5 alleles was assessed by polymerase chain reaction (PCR) amplification from DNA extracted from tail biopsies in wild-type, heterozygous, and homozygous littermates. The primers used were S17 (GGC TCG GAG GAC AGA CCT GAG), S23 (CTG TCA GTG CCT GTA TCT GTC C), and IRES31 (AGG GGC GGA ATT CGA TAG CT). *Lrp5*$^{-/-}$ and *Wt* mice were fed a normal chow diet (Tekland diet, Harlan Labs, Shardlow, UK) for 18 weeks. Cardiac puncture was performed in mice under terminal anaesthesia (1 mg/kg Medetomidine and 75 mg/kg Ketamine, ip).

2.2 Human neuronal cell line

Human SHSY5Y were purchased from the European Collection of Authenticated Cell Cultures (Salisbury, UK). Human SHSY5Y were grown in Dulbecco's modified Eagle's medium:F12 (1:1), FBS (Fetal Bovine Serum; 10%), penicillin (1%), and streptomycin (1%). Previous to any experiment, SHSY5Y cells were induced to differentiate by the addition of 10 μM retinoic acid (RA) to the growth medium for 7 days. Differentiated SHSY5Y cells were silenced for LRP5, LRP1, CD36, or LDLR and treated with different nLDL concentrations as detailed below.

2.3 Real-time reverse transcriptase-PCR

Organs were frozen in liquid nitrogen and RNA was isolated with Trizol® Reagent (Invitrogen, Paisley, UK). Alternatively, total RNA was isolated from cultured SHSY5Y using the Total RNA extraction kit (Qiagen, Germantown, MD, USA). The concentration was determined by using a NanoDrop ND-1000 spectrophotometer (NanoDrop Technologies, Inc., Wilmington, DE, USA), and purity was checked by using the A260/A280 ratio (ratios between 1.8 and 2.1 were considered acceptable). cDNA was synthesized from 1 μg RNA by using a cDNA reverse transcription kit (Qiagen). The resulting cDNA samples were amplified with a reverse transcriptase-PCR (RT–PCR) thermal cycler (Applied Biosystems 7900HT) and the following specific probes from Applied Biosystems: Lrp5, Lrp1, Ldlr, β-catenin, Lef1, Vegf, Mmp7, Adam10, and Opn. The results were normalized with 18S probe from Applied Biosystems (San Francisco, CA, USA).

2.4 Determination of free and esterified cholesterol content by thin-layer chromatography

After the treatments, SHSY5Y cells were homogenized in NaOH 0.1 N. Lipid extraction and thin-layer chromatography (TLC) were performed as previously described.[33,34] Briefly, one aliquot of the cell suspension was extracted with methanol/dichloromethane (2:1, vol/vol). After solvent removal under an N_2 steam, the lipid extract was dissolved in dichloromethane, and one aliquot was partitioned by TLC, which was performed on silica G-24 plates. Three different concentrations of standards (a mixture of cholesterol and cholesterol palmitate) were applied to each plate. The chromatographic developing solution was heptane/diethyl ether/acetic acid (74:21:4, vol/vol/vol). The plates were then stained with 26 mM/47.62 g/L molybdophosphoric acid solution of absolute ethanol/absolute sulphuric acid (95:5, vol/vol) for 1 min. After air drying, TLC plaques were heated at 100°C for 7 min. The spots corresponding to cholesteryl ester and free cholesterol were quantified by densitometry against the standard curve of cholesterol and cholesterol palmitate, respectively, with the use of a computing densitometer (Molecular Dynamics, Chatsworth, CA, USA).

2.5 LDL isolation and modification

Human LDLs (d1.019–d1.063 g/mL) were obtained as previously described.[34] Briefly human LDLs were obtained from the pooled sera of normocholesterolemic volunteers and isolated by sequential ultracentrifugation. LDLs were dialyzed three times against 200 volumes of 150 mmol/L NaCl, 1 mmol/L ethylenediaminetetraacetic acid, and 20 mmol/L Tris-HCl, pH 7.4, overnight, and once against 150 mmol/L NaCl. LDL protein concentration was determined by using the bicinchoninic acid, and vortexing was monitored by measuring the turbidity (absorbance at 680 nm).

In order to label LDL particles, they were incubated with DiI. DiI stock solution was prepared dissolving 3 mg of DiI in 1 mL DMSO (Dimethylsulfoxide) (3 mg/mL). This preparation was then diluted 1:60 in phosphate-buffered saline (PBS)/0.5% bovine serum albumin (BSA) with the desired concentration of LDL and left overnight at 37°C for proper lipoprotein staining. DiI-labelled LDL was stored at 4°C under sterile conditions.

2.6 Immunofluorescence analyses

SHSY5Y cells incubated or not with nLDL and silenced or not for LRP5 were fixed with 4% PFA and permeabilized with 0.5% Tween in PBS at room temperature. After incubation in a blocking buffer (3% BSA in PBS), primary LRP5 (Abcam, Cambridge, UK) antibodies were added 1 h at room temperature in a moist chamber. Appropriate secondary antibodies [Alexa Fluor anti-mouse 488 IgG (H + L)] and Hoechst 33342 were added for 1 h, and stained cells were washed and covered with Prolong Gold antifade reagent (Molecular Probes, Eugene, OR, USA). Images of 25–35 cells/condition/experiment were immunostained and recorded on a Leica inverted fluorescence confocal microscope (Leica TCS SP2-AOBS, Berlin, Germany). Cells were viewed with HCX PL APO 63×/1.2 W Corr/0.17 CS objective. Fluorescent images were acquired in a scan format of 1024 × 1024 pixels in a spatial data set (*xyz*) and were processed with the Leica Standard Software TCS-AOBS. Fluorescence was measured from individual stacks; the number of pixels and the mean per field of view were measured blindly by two independent investigators. Controls without primary antibodies showed no fluorescence labelling.

2.7 Western blot and antibodies

Cell lysates 20–50 μg protein were resolved by sodium dodecyl sulphate-polyacrylamide gel electrophoresis and transferred to nitrocellulose membranes, blocked with 5% skim milk, and probed for monoclonal (LRP5, p62, Caspase 3, β-catenin, and β-tubulin from Abcam) or polyclonal (β-actin, MMP7, CD36, and LDLR from Millipore, Temecula, CA, USA; LC3B from Fisher Scientific, Waltham, MA, USA; and ADAM10 and LDLR from Santa Cruz Antibodies, Dallas, TX, USA) primary antibodies. Membranes were then washed and blotted with appropriate anti-mouse or anti-rabbit secondary antibodies (Dako). Band densities were determined by using the ChemiDoc XRS system (Bio-Rad, Hercules, CA, USA) in chemiluminescence detection modus and Quantity-One software (Bio-Rad). Normalization was performed against β-actin.

2.8 LRP5 silencing

About 4×10^6 RA-differentiated SH-SY5Y cells in 100 µL of Cell Line Nucleofector® Solution V and 800 nM of siRNA-random (siR) or siLRP5 were transfected with G-004 program in a Nucleofector® II Device (Lonza, Basel, Switzerland). siR was used as a control and did not exert any effect on LRP5 expression. Twenty-four hours after transfection, complete cell medium was removed and serum-deprived medium containing the desired treatment was added to the cells for a further 24 h. Transfection efficiency was analysed by LRP5 RNA expression by real-time RT–PCR and normalized to r18S RNA expression. Small anti-LRP5-interfering RNAs (si5, s8293, si1 s5681, and siLDLR s9357) were synthesized by Applied Biotechnologies (Sutton, UK) and Silencer Selective negative control #1 (siR, 4390843) by Ambion (Austin, TX, USA).

2.9 SHSY5Y cell cytotoxicity assays

Twenty-four hours after RNA silencing by electroporation, SHSY5Y cells were incubated with 250 µM H_2O_2 (Sigma, Macquarie Park, NSW, Australia, #H1009) or 1 µM staurosporin (STP; Sigma #62996) for a further 24 h when apoptotic/necrotic induction was evaluated by flow cytometry. SHSY5Y cells were counted, separated in pools of 2×10^6 cells, and centrifuged at 300 *g* 10 min. The cells were suspended in 100 µL Annexin V Binding Buffer (BD Pharmingen, #51-66121E, San Diego, CA, USA) and incubated with 5 µL of Annexin V CF-Blue (Immunostep, #ANXVCFB-200T) for 25 min at dark at room temperature. Then, 2.5 µL of propidium iodide (BD Pharmingen, #51-66211E) was added for 5 more minutes. The reaction was stopped by adding four volumes of Annexin V Binding Buffer. For each sample, at least 10 000 events were acquired on a MACSQuant Analyzer 10 (Miltenyi Biotec, Bergisch Gladbach, Germany). Data were analysed using MACSQuantify software.

2.10 Statistical analysis

Results are expressed as mean ± SEM. A Stat View statistical package was used for all the analyses. Comparisons among groups were performed by two-way analysis of variance analysis. For comparisons between groups, Bonferroni's multiple-comparison test was used. Regression analyses were performed by applying $Y = a + b \times X$ lineal pattern besides using Stat View for the Windows program, selecting only highly adjusted equations. Statistical significance was considered when $P < 0.05$.

3. Results

3.1 LRP5 expression in *Wt* and *Lrp5*$^{-/-}$ mice organs

Lrp5$^{-/-}$ mice showed the absence of LRP5 gene transcription in all organs except for the brain. LRP5 gene transcription levels were assessed in the aorta, heart, liver, spleen, jejunum, and brain samples of *Wt* mice and in *Lrp5*$^{-/-}$ mice. Interestingly, LRP5 was highly transcribed in the aorta, heart, and liver of *Wt* mice. LRP5 gene expression in *Lrp5*$^{-/-}$ mice brains showed a 48 ± 2% reduction in that observed in *Wt* mice brains (*Figure 1A*). In a similar way, LRP5 protein expression is readily detected in the aorta, heart, liver, spleen, jejunum, and brain of *Wt* mice. Again, LRP5 protein expression in *Lrp5*$^{-/-}$ mice is undetectable in all the organs except for the brain, where a faint band of a similar molecular weight than that observed in *Wt* mice was detected (*Figure 1B*).

The expression of canonical Wnt pathway members (β-catenin and LEF1) and targets (VEGF, Opn, MMP7, and ADAM10) was observed in the brain samples of both *Wt* and *Lrp5*$^{-/-}$ mice, indicating the pathway viability in the brains of *Lrp5*$^{-/-}$ mice (*Figure 1C*).

3.2 LRP5 and neuronal LDL handling

Human neuronal cells were obtained by making a differentiation of neuroblastoma cells SHSY5Y treated with 10 µM of all-trans-RA for 7 days. *Figure 2A* shows representative images of SHSY5Y cells without RA treatment (left panels) or after 7 days of RA treatment (right panels) when we assessed the uptake of extracellular LDL (native LDL, nLDL). The cells were treated for different time periods with 200 µg/mL of DiI-stained nLDL particles. The results show intracellular DiI-nLDL depositions immediately upon 2 h of treatment and these lasted for 48 h. The highest staining intensity was observed at 24 h (*Figure 2B*). TLC analyses showed DiI-nLDL intracellular accumulation in a concentration-dependent manner (*Figure 2C* and *D*). LRP5 expression analyses showed a mild 23.2 ± 2% increase in LRP5 expression at 24 h of DiI-nLDL incubation (*Figure 2E*), which was not concentration dependent (*Figure 2F*). Protein analyses supported the gene transcription results (*Figure 2E* and *F*).

A strong LRP5 staining was observed after 24 h DiI-nLDL (200 µg/mL nLDL) treatment confirming RNA and Western Blot (WB) analyses. However, no colocalization between LRP5 and nLDL was observed, suggesting that LRP5 is not involved in neuronal SHSY5Y lipid uptake (*Figure 3A*). To confirm this result, neuronal cells were transfected with a siR or siRNA-LRP5 (si5), lipid loaded with 200 µg/mL of nLDL, and intracellular cholesteryl esters were quantified by TLC. Lipid uptake down-regulation is not observed in LRP5-silenced cells, confirming that LRP5 is not involved in lipid uptake in neurons (*Figure 3C*). For transfection efficiency analyses, LRP5 gene and protein expression were determined (*Figure 3D*). Finally, siR and si-LRP5-transfected neuronal cells were lipid-loaded with DiI-stained nLDL particles. The results do not show a reduction in intracellular DiI staining in LRP5-silenced neuronal cells compared with control cells (*Figure 3E* and *F*), further supporting our previous results.

3.3 LDLR but not LRP1 or CD36 induces lipid uptake in neuronal SHSY5Y cells

Because LRP5 is not involved in lipid uptake in neuronal cells, we sought to determine whether another member of the LRP family was involved in this process. We transfected the cells with siRNA-LRP1, treated them with lipids, and analysed the cholesteryl ester intracellular accumulation and did not find any variations between control and LRP1-silenced cells, indicating that LRP1 is not responsible for lipid uptake in these cells either (*Figure 4A* and *B*). We then silenced the scavenger receptor CD36 (siCD36) and, similar to LRP1 results, we did not find any differences in cholesterol uptake between the silenced and the control cells (*Figure 4C* and *D*). Finally, we performed the same experiment in LDLR-silenced neuronal cells (siLDLR), and the results show that LDLR-silenced cells contain less intracellular lipids than their controls, suggesting that the classic LDLR is in charge of lipid uptake in neuronal cells (*Figure 4E* and *F*).

3.4 Effect of nLDL on Wnt signalling pathway

To determine whether nLDL could induce the canonical Wnt signalling pathway, we analysed the gene and protein levels of several Wnt proteins in the control and nLDL-treated neuronal cells in the presence and absence of LRP5. Twenty-four hours after nLDL treatment, both mRNA and protein levels of the structural canonical Wnt proteins β-catenin and LEF1 increased. In a similar way, the mRNA and protein levels of MMP7, ADAM10, Opn, and VEGF, four Wnt targets also increased (*Figure 5A–D*).

To test whether LRP5 was needed for canonical Wnt signalling activation, we silenced LRP5 prior to nLDL treatments. Interestingly, LDL-induced expression of β-catenin and LEF1 was abrogated in si-LRP5 cells. Similar results are observed for MMP7 and ADAM10. In contrast, Opn and VEGF were not affected by LRP5 silencing. These results indicate that in neurons, LDL triggers the activation of the canonical Wnt pathway with different activations of target gene expression depending on LRP5 (*Figure 5A–D*).

3.5 Anti-apoptotic role of LRP5 in neurons

We have previously shown a pro-survival role for LRP5 in peripheral blood leucocytes[35] and in cardiomyocytes.[29,30] We now tested whether LRP5 could also exert pro-survival functions in neurons. We treated siR or si5 neuronal cells with 250 µM H_2O_2 to induce apoptosis and analysed apoptosis-related proteins. The results show a 52 ± 9% increase in the

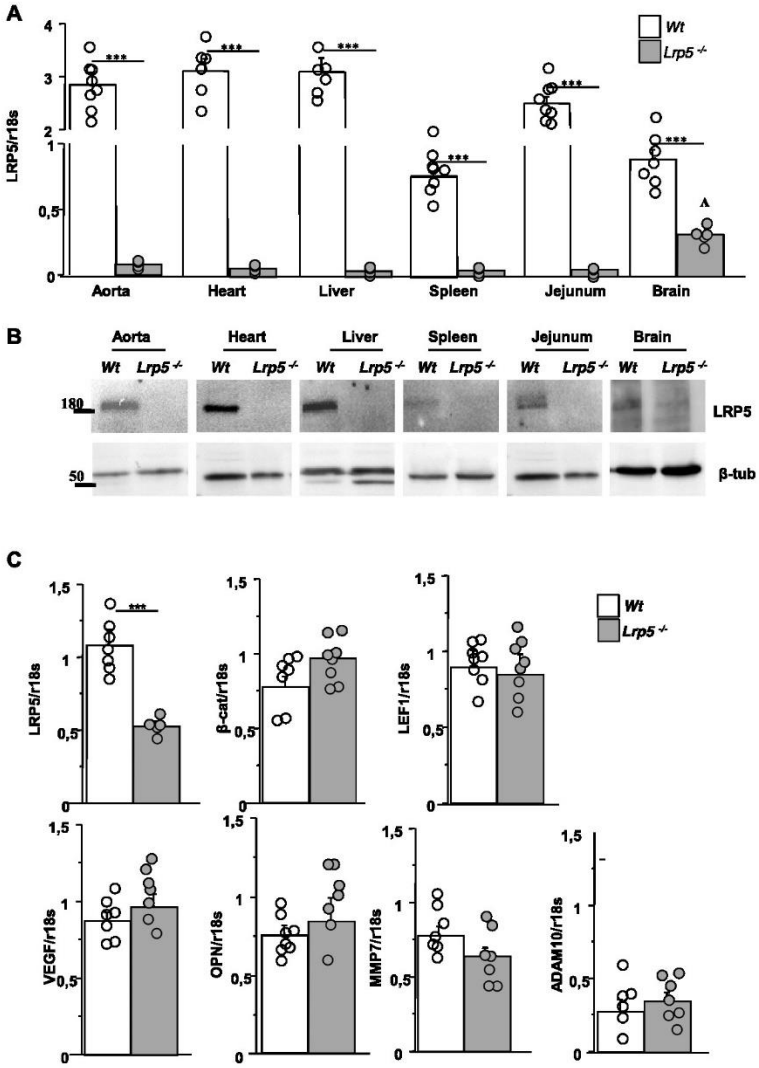

Figure 1 LRP5 expression in mice organs. (*A*) Gene and (*B*) protein expression levels of LRP5 in different organs of *Wt* and *Lrp5*$^{-/-}$ mice $n = 6$–8 organs/mice and genotype. (*C*) Gene expression levels of different proteins and targets of the canonical Wnt pathway in the brains of *Wt* and *Lrp5*$^{-/-}$ mice $n = 6$–8 brains/genotype (***$P < 0.005$, *Wt* vs. *Lrp5*$^{-/-}$ mice; ∧ = $P < 0.005$ mice brain *Lrp5*$^{-/-}$ vs. all other organs).

expression levels of the pro-apoptotic protein Bax after H_2O_2 treatments in control cells (*Figure 6A*). In cells without LRP5, this increase was of 98 ± 11%. We also determined the levels of expression of the anti-apoptotic gene Bcl2 and found a 49 ± 3% reduced expression after H_2O_2 treatments in control cells, while in cells without LRP5, this decrease was of 27 ± 1%. Therefore, there was a significant increase in the Bax/Bcl2 ratio of LRP5-silenced and H_2O_2-treated cells compared with control cells, indicating increased cell death in cells without LRP5 (*Figure 6A*).

To characterize this increased neuronal apoptotic cell death, LRP5-dependent apoptotic features were measured using the Annexin V fluorescein isothiocyanate/propidium iodide (FITC/PI) assay kit. Twenty-four hours after H_2O_2 treatments, there was a 52 ± 3% increase in early apoptosis ($AnnV^+$ cells) and a 36 ± 6% increase in late apoptosis in the control cells ($AnnV^+/PI^+$ cells; *Figure 6B*). siRNA-LRP5 H_2O_2-treated cells showed a 91 ± 4% increase in early apoptosis and a 654 ± 8% increase in late apoptosis when compared with control cells (untreated siR SHSY5Y cells), indicating an anti-apoptotic role for LRP5 (*Figure 6B*). Supporting these results, the cells that were silenced for LRP5 showed increased early and late apoptosis even in the absence of H_2O_2 treatments (*Figure 6B*). Necrotic cells (PI^+ cells) were increased after H_2O_2 treatments

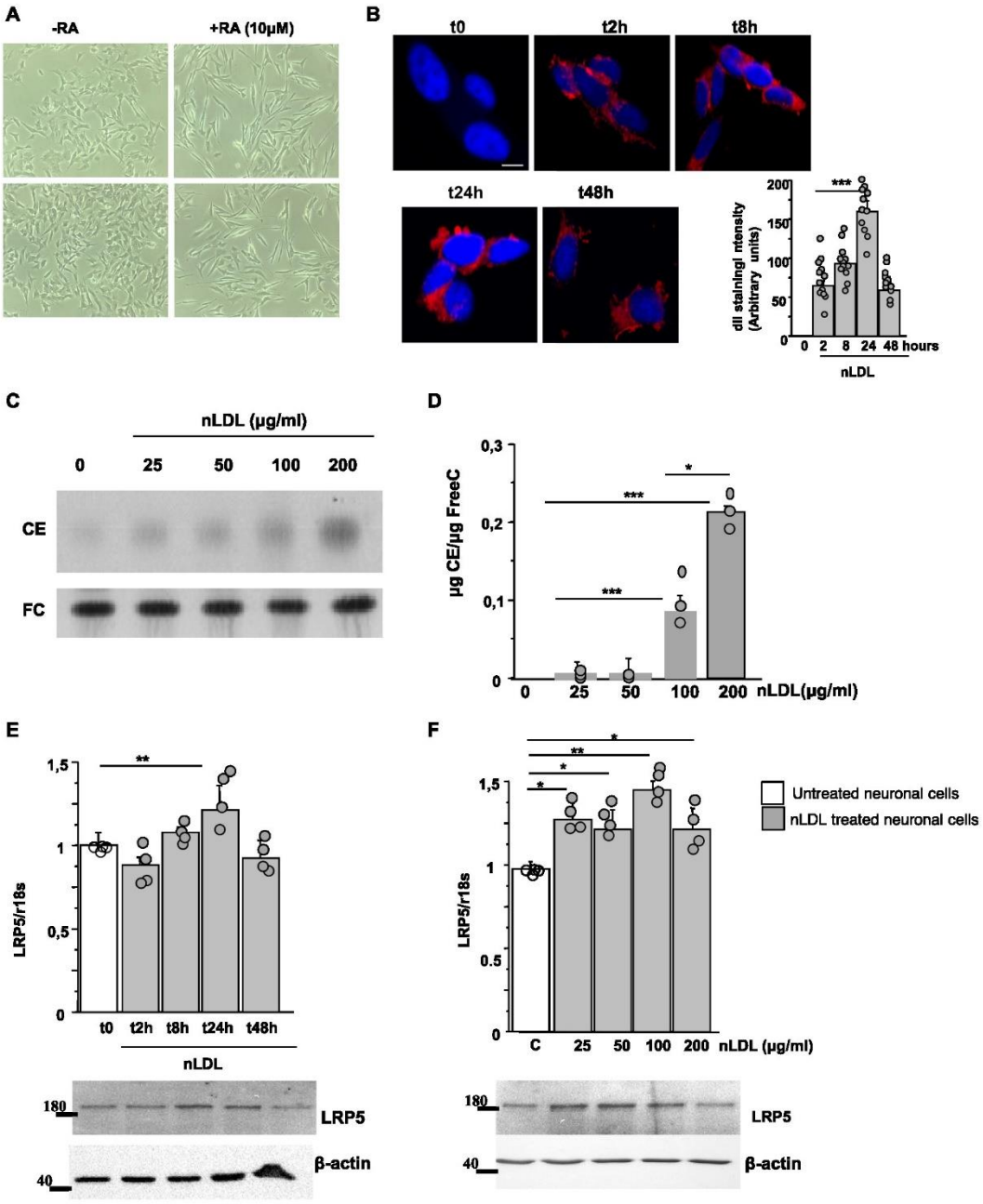

Figure 2 LRP5 is expressed in differentiated neurons. (*A*) Representative images of undifferentiated and differentiated neuronal cells. (*B*) Confocal microscopy images of neuronal cells treated with 200 μg/mL DiI-nLDL for 2, 8, 24, and 48 h. A bar graph shows the quantification of DiI staining. Bar 10 μM ($n = 4$). (*C*) Neurons were incubated with increasing amounts of nLDL for 24 h and exhaustively washed and harvested to measure intracellular free cholesterol (FC) and cholesteryl esters (CE) by TLC. (*D*) A bar graph showing μg CE/μg FC content. $n = 3$ in duplicates. Gene and protein expression levels of LRP5 (*E*) after a time-course of treatment with 200 μg/mL nLDL and (*F*) after treatment with increasing concentrations of nLDL. $n = 4$. *$P < 0.05$; **$P < 0.01$; ***$P < 0.005$.

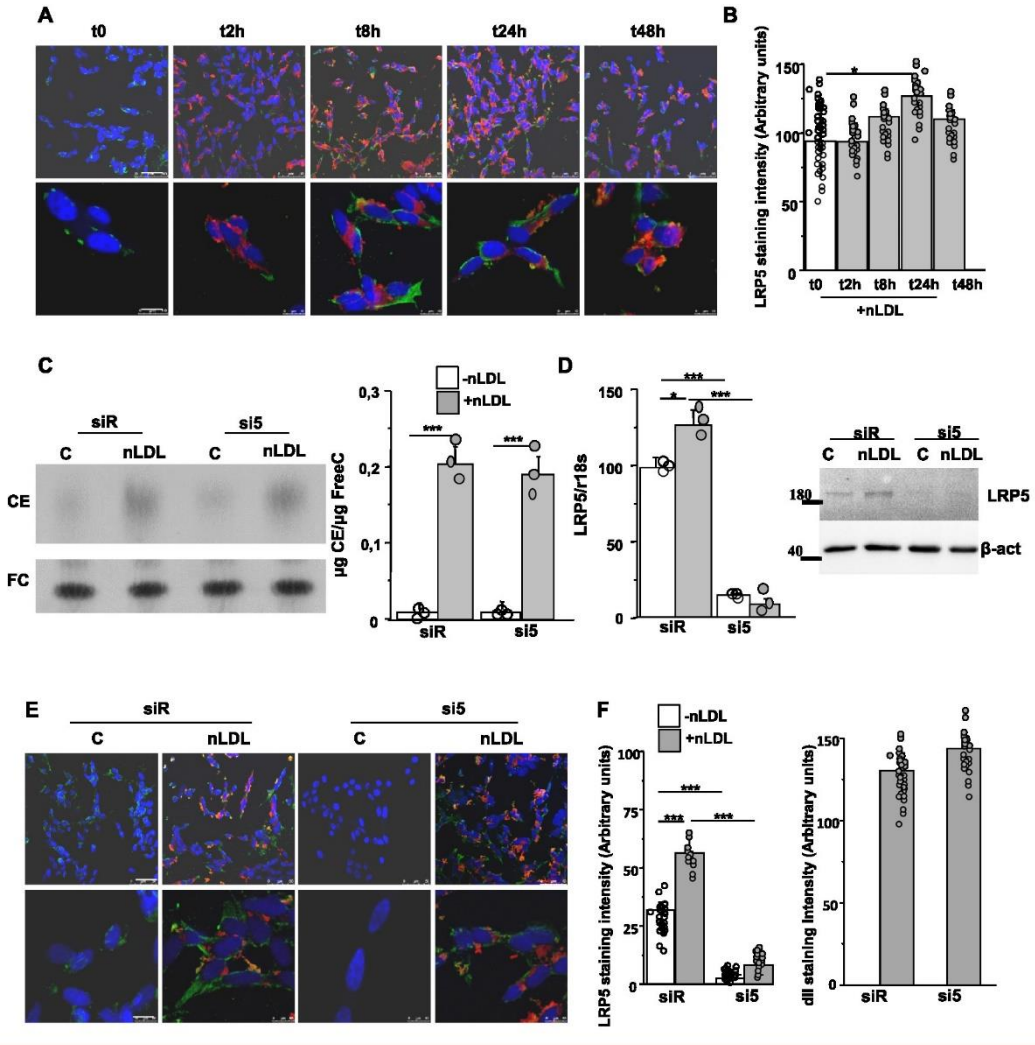

Figure 3 LRP5 does not colocalize with nLDL in differentiated neurons. (*A*) Representative confocal images of neuronal cells treated with 200 µg/mL Dil-nLDL and stained with LRP5-FITC. An upper panel bar 50 µM and lower panel bar 10 µM. (*B*) A bar graph showing LRP5 staining quantification. $n = 3$ in duplicates. (*C*) TLC was performed in cells transfected with siR or siRNA-LRP5 (si5) and incubated with 200 µg/mL nLDL for 24 h. A bar graph showing µg CE/µg FC content. $n = 3$ in duplicates. (*D*) Gene and protein expression levels of LRP5 in cells from *C*. (*E*) Confocal images of cells silenced or not for LRP5 and treated with 200 µg/mL nLDL. An upper bar 50 µM and lower bar 10 µM. (*F*) A bar graph showing LRP5 and Dil staining intensity. $n = 4$. $^{*}P < 0.05$; $^{***}P < 0.005$.

by 96 ± 7% in the control situation. However, siRNA-LRP5 SHSY5Y cells after H_2O_2 treatments showed similar PI staining than control cells, suggesting that LRP5 does not participate in the necrotic process (*Figure 6C*). The analyses of the intracellular pro-apoptotic protein Caspase 3 showed that cells without LRP5 express more active Caspase 3 than control cells, supporting the anti-apoptotic role of LRP5 (*Figure 6D*).

STP induces apoptotic cell death by different protein kinases inhibition. We treated cells with 1 µM STP after being silenced or not for LRP5. Similar to the results of H_2O_2 treatments, the results of STP treatments show increased early and late apoptosis in cells without LRP5 (*Figure 6E*), while no differences in LRP5-silenced cells in respect to control cells were observed after cellular necrosis staining (*Figure 6F*). An anti-apoptotic role for LRP5 was further supported by Caspase 3 western blotting, where cells without LRP5 expressed more active Caspase 3 than control cells (*Figure 6G*).

Finally, we aimed to investigate the function of LRP5 in the regulation of autophagy, a cellular pro-survival mechanism. We analysed the autophagic proteins p62 and LC3B. Both of them accumulate when autophagy is inhibited; therefore, decreased levels are observed when

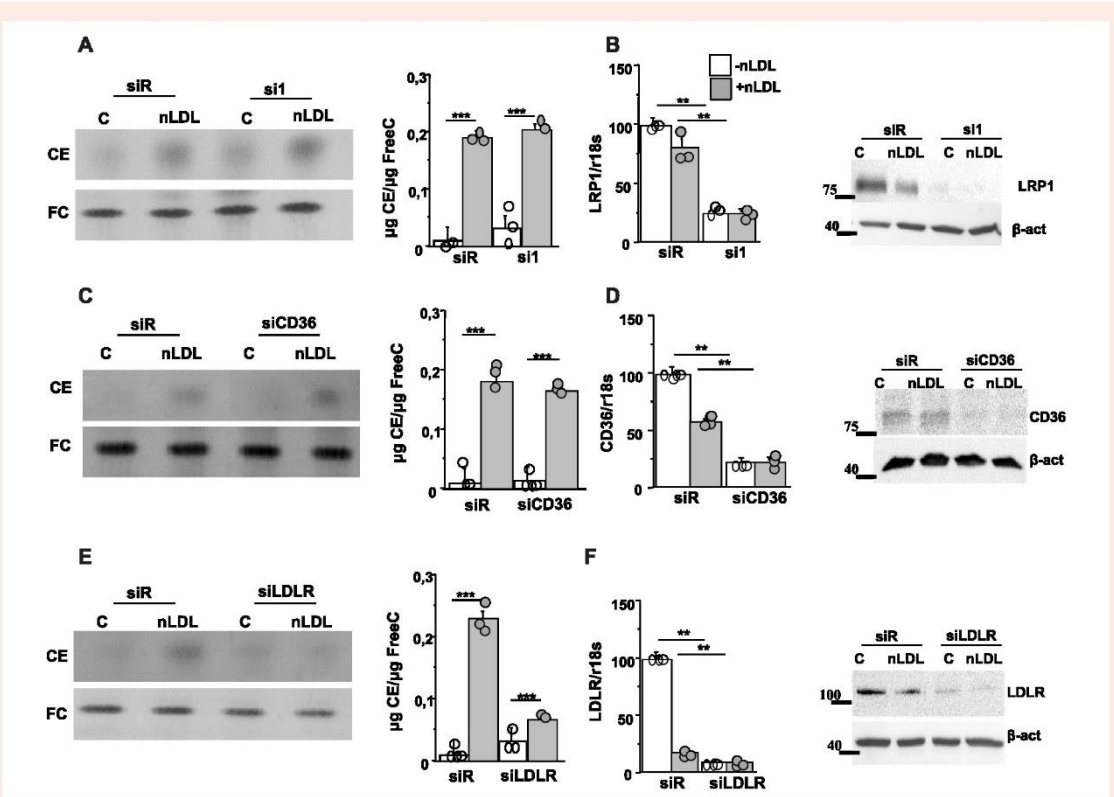

Figure 4 Neuronal cell uptake lipids by LDLR. (*A*) TLC was performed in cells transfected with siR or siRNA-LRP1 (si1) and incubated with 200 µg/mL nLDL for 24 h. A bar graph showing µg CE/µg FC content. $n = 3$ in duplicates. (*B*) Gene and protein expression levels of LRP1 in cells from *A*. (*C* and *D*) Same as *A* and *B*, but cells were silenced for CD36. (*E* and *F*) Same as *A* and *B*, but cells were silenced for LDLR. $n = 3$ in duplicates ***$P < 0.005$, **$P < 0.01$.

autophagy is induced. The results show that both p62 and LC3B are down-regulated in control conditions when autophagy is promoted by H_2O_2 treatments (*Figure 6H*) or by STP treatments (*Figure 6I*). However, there were no significant differences between LRP5-silenced and control cells after H_2O_2 or STP treatments, suggesting that LRP5 does not play a major role in cellular autophagic processes in neuronal cells (*Figure 6H* and *I*).

4. Discussion

LRP5 is a transmembrane receptor that belongs to the LDL receptor family. It has traditionally been associated with the regulation of lipid metabolism in peripheral cells involved in the cardiovascular system. Here, we show a completely different role for this receptor in neuronal cells. Indeed, we first show there is a low, but significant expression of LRP5 in the brain of *Lrp5*$^{-/-}$ mice. This is an unexpected finding as *Lrp5*$^{-/-}$ mice do not show LRP5 expression in any other organ. It is important to highlight that all *Lrp5*$^{-/-}$ mice showed LRP5 expression in brain, suggesting that a complete absence of LRP5 in the brain is incompatible with life. To further understand the role of LRP5 and the canonical Wnt pathway in the brain, we analysed the expression of different proteins and target genes of the pathway and found that they were all expressed, indicating that the pathway is functional and can be activated in both wild-type and *Lrp5*$^{-/-}$ mice.

Cholesterol does not cross the BBB in normal physiological conditions; therefore, cholesterol metabolism in the brain is independent from that in peripheral tissues. Cholesterol *de novo* synthesis is higher in astrocytes than in neuronal cells in post-natal rats.[20] Cholesterol is needed for brain survival during development, and in the adult life, and for a correct brain function, the amount of cholesterol in the brain has to be accurately maintained.[36–38] Several brain disorders including Alzheimer's disease, Huntington's disease, and Parkinson's disease run with defects in brain cholesterol metabolism.[39–41] Cholesterol is essential for neurons, because a lack of cholesterol leads to synapse degeneration, impaired synaptic vesicle exocytosis and neurotransmission, and overall decreased neuronal activity.[42–44] In this study, we have used a human neuroblastoma SHSY5Y cell line that is widely used as an *in vitro* model for neurotoxicity experiments. The addition of all-trans-RA promotes and maintains the neuronal phenotype. Treatment of neurons with lipids showed a time- and dose-dependent lipid uptake, indicating that neurons can accumulate small amounts of intracellular lipids.

A role for LRP5 has been described in the formation of the cerebellum.[10] However, the role of LRP5 in the brain has not yet been defined. Here, we show that although there is an increased expression of neuronal LRP5 after lipid exposure, LRP5 does not play a major role in lipid uptake in neurons. The absence of LRP5 does not reduce neuronal intracellular cholesteryl esters nor intracellular lipids. LRP1 belongs to the same family as LRP5 and is known to regulate crucial processes that help maintain synaptic integrity

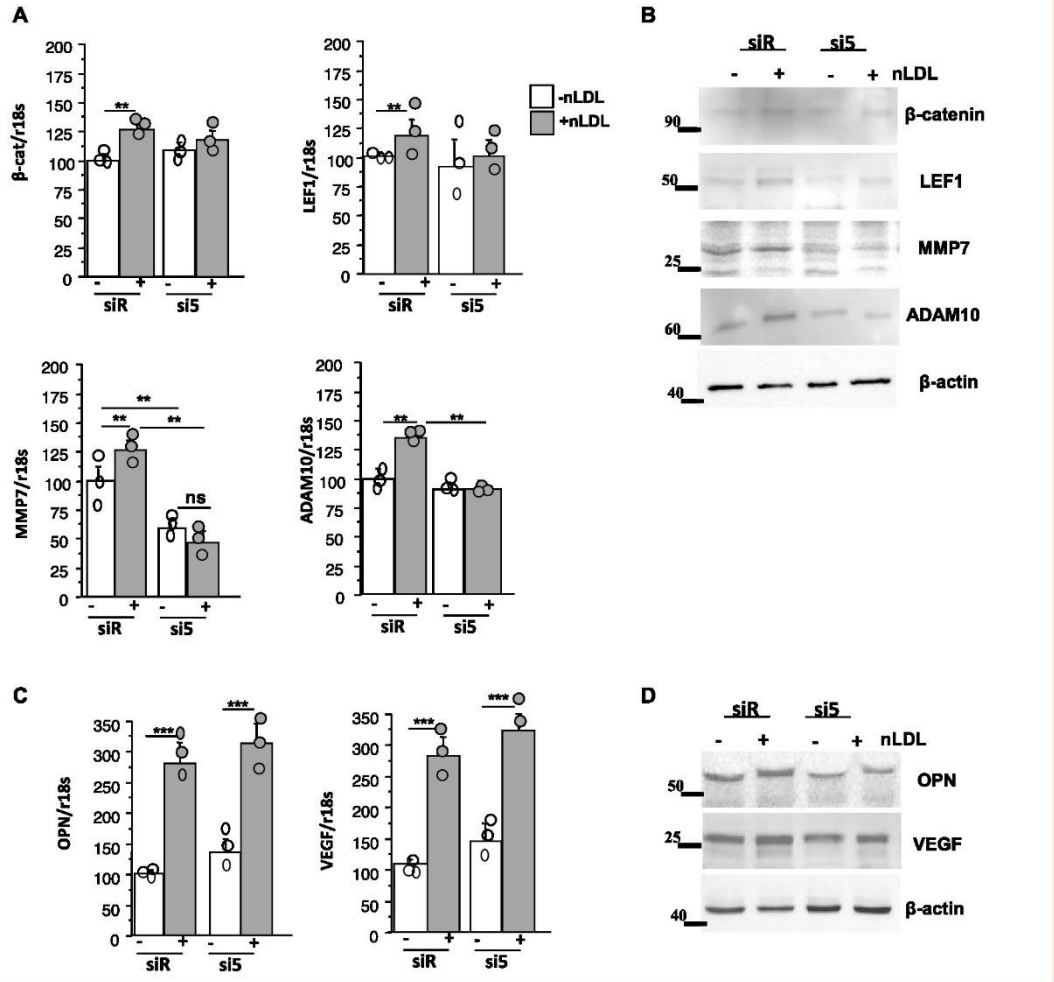

Figure 5 Effect of nLDL on Wnt activation in neuronal cells. (*A*) Gene and (*B*) protein expression levels of β-catenin, LEF1, MMP7, and ADAM10 in SHSY5Y cells transfected with siR or si5 and incubated with 200 μg/mL nLDL for 24 h. (*C* and *D*) Same as *A* and *B*, but the expression levels of OPN and VEGF were analysed. $n = 3$. ***$P < 0.005$, **$P < 0.01$.

and cholesterol homeostasis in the brain.[44–46] Therefore, we tested whether LRP1 was responsible for the lipid internalization of neuronal cells. Again, no intracellular lipid accumulation reduction was observed in neurons without LRP1, indicating that LRP1 is not accountable for neuronal lipid uptake. The same was true for CD36. Finally, we analysed the role of the LDLR, a receptor that plays a major role in the regulation of liver lipid homeostasis,[47] and found a reduced lipid uptake in siLDLR-neuronal cells, indicating that the LDLR is the receptor involved in lipid uptake in neuronal cells.

After nLDL incubation, the neuronal cells showed increased gene and protein levels of Wnt pathway proteins and targets, including LRP5, β-catenin, LEF1, Opn, VEGF, MMP7, and ADAM10, indicating that Wnt pathway activation is induced after lipid loading. Importantly, the increased expression of these Wnt proteins and targets was greatly reduced in the absence of LRP5 only in Wnt structural proteins (β-catenin and LEF1) and in some Wnt targets (MMP7 and ADAM10), while other indirect Wnt targets (OPN and VEGF) are induced, suggesting that OPN and VEGF are regulated by pathways independent of the LRP5/Wnt signalling pathway. Indeed, OPN expression is increased after NFκB pathway activation[48] and is known to influence PI3K/AKT/mTOR signalling[49] to regulate migration, phagocytosis, and the expression of inflammatory factors in microglia.[50] Also, following an acute ischaemic stroke, the PKC pathway in endothelial cells is activated and the expression of VEGF and HIF1α is enhanced.[51]

ADAM10 and MMP7 seem to be under canonical Wnt pathway regulation. ADAM10 has key roles in neural development,[52] is involved in axonal growth and myelination,[52] and has a major role in the shedding of β-amyloid protein, therefore possessing the ability to prevent the

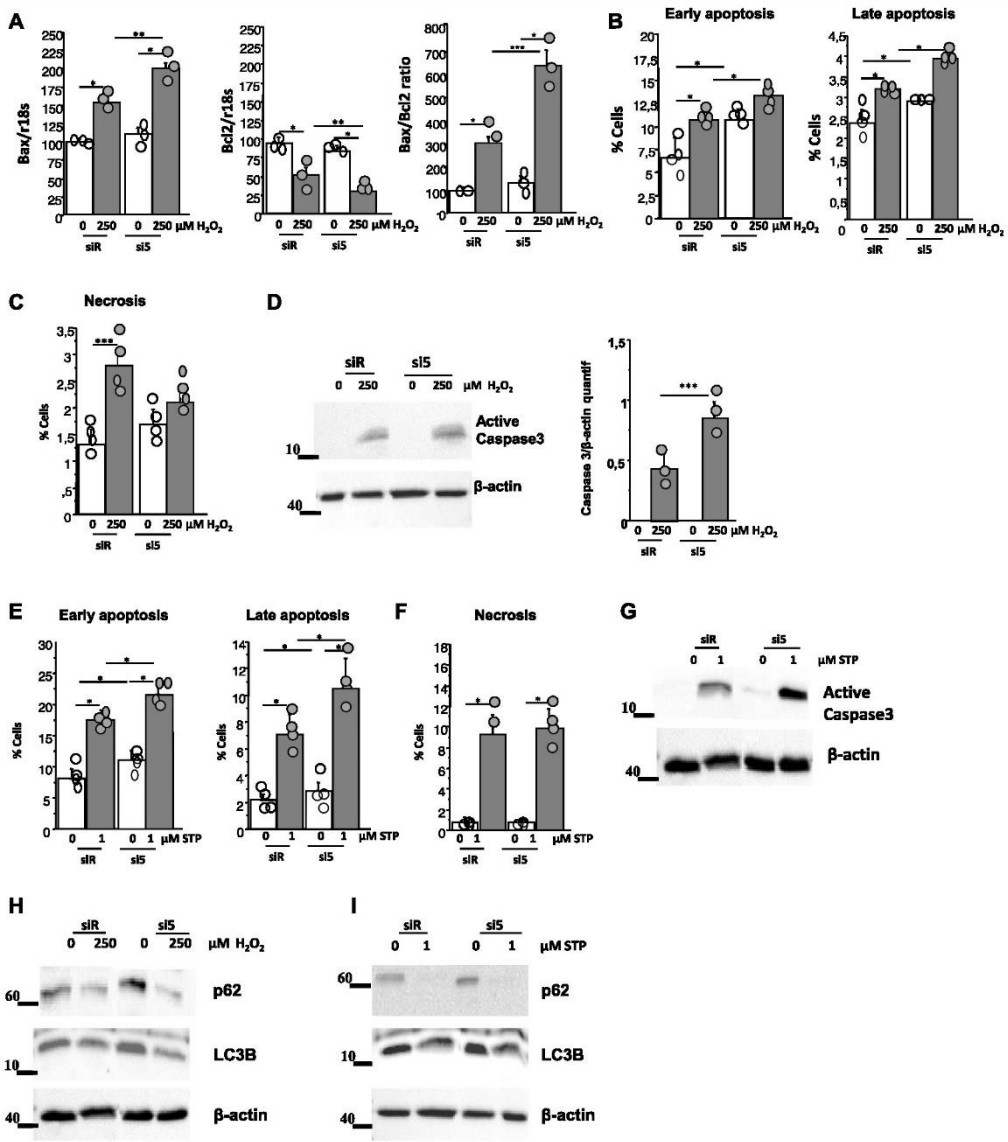

Figure 6 LRP5 expression reduces apoptosis. (*A*) Neuronal cells were transfected for 24 h to silence siLRP5 and were treated with 250 µM of H_2O_2 to induce apoptosis when the expression levels of Bax and Bcl2 were measured and Bax/Bcl2 ratio was analysed. $n = 3$ in duplicates. (*B*) Cells were collected, washed, and stained with Annexin V, PI, or both following the manufacturer's instructions and analysed by flow cytometry: Early apoptotic cells were stained for $AnnV^{+}/PI^{-}$, late apoptotic cells $AnnV^{+}/PI^{+}$ and (*C*) necrotic cells $AnnV^{-/}PI^{+}$. $n = 4$. (*D*) Active Caspase 3 protein levels were measured in cells, silenced for LRP5, and treated with H_2O_2. A bar graph showing Caspase 3 quantification. $n = 3$. (*E–G*) Same as *B–D* in STP-treated neuronal cells. $n = 3$. p62 and LC3B protein levels were determined by WB (*H*) in H_2O_2-treated cells and (*I*) in STP-treated cells. $^{***}P < 0.005$, $^{**}P < 0.01$, $^{*}P < 0.05$.

generation of the pathogenic Aβ peptide in Alzheimer's disease.[53,54] MMP7 promotes survival and regeneration in renal tubes, inducing protection against acute kidney injury.[55] In the brain, MMP7 participates in the regeneration of injured peripheral nerves[56] and in the removal of neuronal myelinization, protecting against fibronectin aggregates in multiple sclerosis lesions.[57] Furthermore, its expression is greatly increased after injury in rat sciatic nerves.[58] Taken together, these results point to ADAM10 and MMP7 as regulators of protective functions in the brain. Therefore, these

results suggest that in neurons, nLDL triggers the Wnt pathway only in the presence of LRP5 to induce the transcription of proteins that will develop pro-survival mechanisms.

We have previously shown a protective role for LRP5 in the vascular wall. Indeed, *Lrp5*$^{-/-}$ mice fed a high fat diet have increased serum cholesterol, increased cholesterol ester accumulation in aortas, and larger aortic lipid infiltrations than hypercholesterolaemic *Wt* mice.[28] LRP5 and the canonical Wnt pathway also exert pro-survival roles in peripheral blood leucocytes[35] and induce a pro-survival healing response of cardiomyocytes upon injury.[29,30] Here, we show the involvement of LRP5 in survival processes in neurons. Two cytoplasmic proteins, B-cell lymphoma protein 2 (Bcl2)-associated X (Bax) and Bcl2, act as a promoter and an inhibitor of apoptosis, respectively. We explored the relationship of Bax and Bcl-2 gene expression and their ratio in cells treated with H_2O_2 to trigger apoptosis in the presence or absence of LRP5. Cells without LRP5 expressed higher levels of Bax and lower levels of Bcl2 than control cells, suggesting that LRP5 is involved in the H_2O_2-induced apoptotic pathway with an anti-apoptotic function. These results were supported by flow cytometry experiments, where early and late apoptosis was increased in both H_2O_2 and STP-treated cells devoid of LRP5. Furthermore, the analyses of intracellular levels of Caspase 3 in neuronal cells also showed high levels of the activated form in cells without LRP5, further supporting an anti-apoptotic role of LRP5 in neurons. Autophagy also plays a major role in determining cellular fate. We analysed two autophagic proteins, p62 and LC3B, in neurons. p62 is an autophagic adaptor that mediates the selective recognition and degradation of specific autophagy substrates including protein aggregates[59,60] and intracellular bacteria.[61] p62 binds LC3B to deliver the substrate to the lysosome for degradation.[62] Interestingly, LRP5 does not seem to play a major role in the autophagic processes of neuronal cells.

A limitation of this study is that high cholesterol–induced functions have been studied in cultured neurons. Further analysis performed in mice brains will help determine the role of cholesterol and LRPs in complex biological contexts. The translation of the putative novel therapies, identified by the understanding of the pathophysiologic basis of the disease, into effective treatment for human patients will be the next challenge.

In summary, here we show for the first time that neurons can accumulate intracellular lipids and lipid uptake is performed mainly by the LDLR, while CD36, LRP1, and LRP5 do not play a major role. We also show that LRP5 triggers the canonical Wnt pathway in neuronal cells to generate pro-survival signals. Interestingly, we show that mice knock-out for LRP5 has maintained the expression of LRP5 only in the brain, supporting the biologically plausible concept of the need for brain LRP5 to elicit pro-survival processes and embryonic viability.

Acknowledgements

The authors thank S. Huertas and N. Garcia for providing excellent technical assistance.

Conflict of interest: The authors have stated explicitly that there are no conflicts of interest in connection with this article. L.B. declares to have acted as a SAB member of Sanofi, Novo Nordisk, Ionis, and IAF. L.B., G.V., and T.P. declare to be cofounders of the Spin-offs Glycardial Diagnostics SL and Ivastatin Therapeutics SL (all unrelated to this work). The remaining authors have nothing to disclose. This manuscript was handled by Consultant Editor Henning Morawietz.

Funding

This work was supported by funds from the Spanish Ministerio de Ciencia e Innovación (PID2019-107160RB-I00 to L.B. and PGC 2018-094025-B-I00 to G.V.); funds from the Instituto de Salud Carlos III (CIBERCV CB16/11/00411 and ERA-CVD JTC 202-023/AC 209-00054 to L.B. and PI23-00589 to M.B.-P.); funds from the Sociedad Española de Cardiologia (FEC 2022 to M.B.-P. and FEC 2020 to G.V.); and funds from the Fundación Investigación Cardiovascular-Fundación Jesus Serra. A.L. is a predoctoral fellow (PRE2020-096422) associated with L.B.'s grant PID2019-107160RB-I00.

Data availability

The data underlying this article are available in the article.

References

1. Mao J, Wang J, Liu B, Pan W, Farr GH III, Flynn C, Yuan H, Takada S, Kimelman D, Li L, Wu D. Low-density lipoprotein receptor-related protein-5 binds to axin and regulates the canonical Wnt signaling pathway. *Mol Cell* 2001;**7**:801–809.
2. Johnson ML. The high bone mass family—the role of Wnt/Lrp5 signaling in the regulation of bone mass. *J Musculoskel Neuron Interact* 2004;**4**:135–138.
3. Borrell-Pagès M, Romero JC, Juan-Babot O, Badimon L. Wnt pathway activation, cell migration, and lipid uptake is regulated by low-density lipoprotein receptor-related protein 5 in human macrophages. *Eur Heart J* 2011;**32**:2841–2850.
4. Mann B, Gelos M, Siedow A, Hanski ML, Gratchev A, Ilyas M, Bodmer WF, Moyer MP, Riecken EO, Buhr HJ, Hanski C. Target genes of beta-catenin-T cell-factor/lymphoid-enhancer-factor signaling in human colorectal carcinomas. *Proc Natl Acad Sci U S A* 1999;**96**:1603–1608.
5. Shtutman M, Zhurinsky J, Simcha I, Albanese C, D'Amico M, Pestell R, Ben-Ze'ev A. The cyclin D1 gene is a target of the beta-catenin/LEF-1 pathway. *Proc Natl Acad Sci U S A* 1999;**96**:5522–5527.
6. Qu B, Liu BR, Du YJ, Chen J, Cheng YQ, Xu W, Wang XH. Wnt/β-catenin signaling pathway may regulate the expression of angiogenic growth factors in hepatocellular carcinoma. *Oncol Lett* 2014;**7**:1175–1178.
7. Crawford HC, Fingleton BM, Rudolph-Owen LA, Goss KJ, Rubinfeld B, Polakis P, Matrisian LM. The metalloproteinase matrilysin is a target of beta-catenin transactivation in intestinal tumors. *Oncogene* 1999;**18**:2883–2891.
8. Reiss K, Maretzky T, Ludwig A, Tousseyn T, de Strooper B, Hartmann D, Saftig P. ADAM10 cleavage of N-cadherin and regulation of cell-cell adhesion and beta-catenin nuclear signalling. *EMBO J* 2005;**24**:742–752.
9. Müller T, Bain G, Wang X, Papkoff J. Regulation of epithelial cell migration and tumor formation by beta-catenin signaling. *Exp Cell Res* 2002;**280**:119–133.
10. Huang Y, Zhang Q, Song NN, Zhang L, Sun YL, Hu L, Chen JY, Zhu W, Li J, Ding YQ. Lrp5/6 are required for cerebellar development and for suppressing TH expression in Purkinje cells via β-catenin. *Mol Brain* 2016;**9**:7.
11. Yamaguchi TP. Heads or tails: Wnts and anterior–posterior patterning. *Curr Biol* 2001;**11**:R713–R724.
12. Ciani L, Salinas PC. WNTs in the vertebrate nervous system: from patterning to neuronal connectivity. *Nat Rev Neurosci* 2005;**6**:351–362.
13. Salinas PC, Zou Y. Wnt signaling in neural circuit assembly. *Annu Rev Neurosci* 2008;**31**:339–358.
14. Fancy SP, Baranzini SE, Zhao C, Yuk DI, Irvine KA, Kaing S, Sanai N, Franklin RJ, Rowitch DH. Dysregulation of the Wnt pathway inhibits timely myelination and remyelination in the mammalian CNS. *Genes Dev* 2009;**23**:1571–1585.
15. Seifert-Held T, Pekar T, Gattringer T, Simmet NE, Scharnagl H, Stojakovic T, Fazekas F, Storch MK. Circulating Dickkopf-1 in acute ischemic stroke and clinically stable cerebrovascular disease. *Atherosclerosis* 2011;**218**:233–237.
16. Magdesian MH, Carvalho MM, Mendes FA, Saraiva LM, Juliano MA, Juliano L, Garcia-Abreu J, Ferreira ST. Amyloid-beta binds to the extracellular cysteine-rich domain of Frizzled and inhibits Wnt/beta-catenin signaling. *J Biol Chem* 2008;**283**:9359–9368.
17. Farías GG, Godoy JA, Hernández F, Avila J, Fisher A, Inestrosa NC. M1 muscarinic receptor activation protects neurons from beta-amyloid toxicity. A role for Wnt signaling pathway. *Neurobiol Dis* 2004;**17**:337–348.
18. D'Armiento FP, Bianchi A, de Nigris F, Capuzzi DM, D'Armiento MR, Crimi G, Abete P, Palinski W, Condorelli M, Napoli C. Age-related effects on atherogenesis and scavenger enzymes of intracranial and extracranial arteries in men without classic risk factors for atherosclerosis. *Stroke* 2001;**32**:2472–2489.
19. Napoli C, Witztum JL, de Nigris F, Palumbo G, D'Armiento FP, Palinski W. Intracranial arteries of human fetuses are more resistant to hypercholesterolemia-induced fatty streak formation than extracranial arteries. *Circulation* 1999;**99**:2003–2010.
20. Nieweg K, Schaller H, Pfrieger FW. Marked differences in cholesterol synthesis between neurons and glial cells from postnatal rats. *J Neurochem* 2009;**109**:125–134.
21. Pifferi F, Laurent B, Plourde M. Lipid transport and metabolism at the blood-brain interface: implications in health and disease. *Front Physiol* 2021;**12**:645646.
22. Dehouck B, Fenart L, Dehouck MP, Pierce A, Torpier G, Cecchelli R. A new function for the LDL receptor: transcytosis of LDL across the blood-brain barrier. *J Cell Biol* 1997;**138**:877–889.
23. Finch CE, Laping NJ, Morgan TE, Nichols NR, Pasinetti GM. TGF-beta 1 is an organizer of responses to neurodegeneration. *J Cell Biochem* 1993;**53**:314–322.
24. Lin YL, Chang HC, Chen TL, Chang JH, Chiu WT, Lin JW, Chen RM. Resveratrol protects against oxidized LDL-induced breakage of the blood-brain barrier by lessening disruption of tight junctions and apoptotic insults to mouse cerebrovascular endothelial cells. *J Nutr* 2010;**140**:2187–2192.
25. Acharya NK, Levin EC, Clifford PM, Han M, Tourtellotte R, Chamberlain D, Pollaro M, Coretti NJ, Kosciuk MC, Nagele EP, Demarshall C, Freeman T, Shi Y, Guan C, Macphee CH, Wilensky RL, Nagele RG. Diabetes and hypercholesterolemia increase blood-brain barrier permeability and brain amyloid deposition: beneficial effects of the LpPLA2 inhibitor darapladib. *J Alzheimers Dis* 2013;**35**:179–198.

26. Fujino T, Asaba H, Kang MJ, Ikeda Y, Sone H, Takada S, Kim DH, Ioka RX, Ono M, Tomoyori H, Okubo M, Murase T, Kamataki A, Yamamoto J, Magoori K, Takahashi S, Miyamoto Y, Oishi H, Nose M, Okazaki M, Usui S, Imaizumi K, Yanagisawa M, Sakai J, Yamamoto TT. Low-density lipoprotein receptor-related protein 5 (LRP5) is essential for normal cholesterol metabolism and glucose-induced insulin secretion. *Proc Natl Acad Sci U S A* 2003; **100**:229–234.
27. Borrell-Pages M, Romero JC, Badimon L. Cholesterol modulates LRP5 expression in the vessel wall. *Atherosclerosis* 2014;**235**:363–370..
28. Borrell-Pagès M, Romero JC, Badimon L. LRP5 deficiency down-regulates Wnt signalling and promotes aortic lipid infiltration in hypercholesterolaemic mice. *J Cell Mol Med* 2015;**19**: 770–777.
29. Borrell-Pages M, Vilahur G, Romero JC, Casaní L, Bejar MT, Badimon L. LRP5/canonical Wnt signalling and healing of ischemic myocardium. *Basic Res Cardiol* 2016;**111**:67.
30. Badimon L, Casaní L, Camino-Lopez S, Juan-Babot O, Borrell-Pages M. GSK3β inhibition and canonical Wnt signaling in mice hearts after myocardial ischemic damage. *PLoS One* 2019;**14**: e0218098.
31. Holmen SL, Giambernardi TA, Zylstra CR, Buckner-Berghuis BD, Resau JH, Hess JF, Glatt V, Bouxsein ML, Ai M, Warman ML, Williams BO. Decreased BMD and limb deformities in mice carrying mutations in both Lrp5 and Lrp6. *J Bone Miner Res* 2004;**19**:2033–2040.
32. Cui Y, Niziolek PJ, MacDonald BT, Zylstra CR, Alenina N, Robinson DR, Zhong Z, Matthes S, Jacobsen CM, Conlon RA, Brommage R, Liu Q, Mseeh F, Powell DR, Yang QM, Zambrowicz B, Gerrits H, Gossen JA, He X, Bader M, Williams BO, Warman ML, Robling AG. Lrp5 functions in bone to regulate bone mass. *Nat Med* 2011;**17**:684–691.
33. Badimon L, Luquero A, Crespo J, Peña E, Borrell-Pages M. PCSK9 and LRP5 in macrophage lipid internalization and inflammation. *Cardiovasc Res* 2021;**117**:2054–2068.
34. Luquero A, Vilahur G, Casani L, Badimon L, Borrell-Pages M. Differential cholesterol uptake in liver cells: a role for PCSK9. *FASEB J* 2022;**36**:e22291.
35. Borrell-Pages M, Carolina Romero J, Badimon L. LRP5 and plasma cholesterol levels modulate the canonical Wnt pathway in peripheral blood leukocytes. *Immunol Cell Biol* 2015;**93**: 653–661.
36. Goritz C, Mauch DH, Pfrieger FW. Multiple mechanisms mediate cholesterol-induced synaptogenesis in a CNS neuron. *Mol Cell Neurosci* 2005;**29**:190–201.
37. Takamori S, Holt M, Stenius K, Lemke EA, Grønborg M, Riedel D, Urlaub H, Schenck S, Brügger B, Ringler P, Müller SA, Rammner B, Gräter F, Hub JS, De Groot BL, Mieskes G, Moriyama Y, Klingauf J, Grubmüller H, Heuser J, Wieland F, Jahn R. Molecular anatomy of a trafficking organelle. *Cell* 2006;**127**:831–846.
38. Pfenninger KH. Plasma membrane expansion: a neuron's Herculean task. *Nat Rev Neurosci* 2009;**10**:251–261.
39. Block RC, Dorsey ER, Beck CA, Brenna JT, Shoulson I. Altered cholesterol and fatty acid metabolism in Huntington disease. *J Clin Lipidol* 2010;**4**:17–23.
40. Di Paolo G, Kim TW. Linking lipids to Alzheimer's disease: cholesterol and beyond. *Nat Rev Neurosci* 2011;**12**:284–296.
41. Wang Q, Yan J, Chen X, Li J, Yang Y, Weng J, Deng C, Yenari MA. Statins: multiple neuroprotective mechanisms in neurodegenerative diseases. *Exp Neurol* 2011;**230**:27–34.
42. Björkhem I, Meaney S. Brain cholesterol: long secret life behind a barrier. *Arterioscler Thromb Vasc Biol* 2004;**24**:806–815.
43. Linetti A, Fratangeli A, Taverna E, Valnegri P, Francolini M, Cappello V, Matteoli M, Passafaro M, Rosa P. Cholesterol reduction impairs exocytosis of synaptic vesicles. *J Cell Sci* 2010;**123**: 595–605.
44. Liu Q, Trotter J, Zhang J, Peters MM, Cheng H, Bao J, Han X, Weeber EJ, Bu G. Neuronal LRP1 knockout in adult mice leads to impaired brain lipid metabolism and progressive, age-dependent synapse loss and neurodegeneration. *J Neurosci* 2010;**30**:17068–17078.
45. Herz J, Strickland DK. LRP: a multifunctional scavenger and signaling receptor. *J Clin Invest* 2001;**108**:779–784.
46. Lillis AP, Van Duyn LB, Murphy-Ullrich JE, Strickland DK. LDL receptor-related protein 1: unique tissue-specific functions revealed by selective gene knockout studies. *Physiol Rev* 2008;**88**:887–918.
47. Go GW, Mani A. Low-density lipoprotein receptor (LdLr) family orchestrates cholesterol homeostasis. *Yale J Biol Med* 2012;**85**:19–28.
48. Kariya Y, Kariya Y. Osteopontin in cancer: mechanisms and therapeutic targets. *Int J Transl Med* 2022;**2**:419–447.
49. Ahmed M, Kundu GC. Osteopontin selectively regulates p70S6K/mTOR phosphorylation leading to NF-κB dependent AP-1-mediated ICAM-1 expression in breast cancer cells. *Mol Cancer* 2010;**9**:101.
50. Yu H, Liu X, Zhong Y. The effect of osteopontin on microglia. *Biomed Res Int* 2017:**2017**: 1879437.
51. Moon S, Chang MS, Koh SH, Choi YK. Repair mechanisms of the neurovascular unit after ischemic stroke with a focus on VEGF. *Int J Mol Sci* 2021;**22**:8543.
52. Yang P, Baker KA, Hagg T. The ADAMs family: coordinators of nervous system development, plasticity and repair. *Prog Neurobiol* 2006;**79**:73–94.
53. Lammich S, Kojro E, Postina R, Gilbert S, Pfeiffer R, Jasionowski M, Haass C, Fahrenholz F. Constitutive and regulated α-secretase cleavage of Alzheimer's amyloid precursor protein by a disintegrin metalloprotease. *Proc Natl Acad Sci U S A* 1999;**96**:3922–3927.
54. Kuhn P-H, Wang H, Dislich B, Colombo A, Zeitschel U, Ellwart JW, Kremmer E, Rossner S, Lichtenthaler SF. ADAM10 is the physiologically relevant, constitutive α-secretase of the amyloid precursor protein in primary neurons. *EMBO J* 2010;**29**:3020–3032.
55. Fu H, Zhou D, Zhu H, Liao J, Lin L, Hong X, Hou FF, Liu Y. Matrix metalloproteinase-7 protects against acute kidney injury by priming renal tubules for survival and regeneration. *Kidney Int* 2019;**95**:1167–1180.
56. Wang H, Zhang P, Yu J, Zhang F, Dai W, Yi S. Matrix metalloproteinase 7 promoted Schwann cell migration and myelination after rat sciatic nerve injury. *Mol Brain* 2019;**12**:101.
57. Wang P, Gorter RP, de Jonge JC, Nazmuddin M, Zhao C, Amor S, Hoekstra D, Baron W. MMP7 cleaves remyelination-impairing fibronectin aggregates and its expression is reduced in chronic multiple sclerosis lesions. *Glia* 2018;**66**:1625–1643.
58. Qin J, Zha GB, Yu J, Zhang HH, Yi S. Differential temporal expression of matrix metalloproteinases following sciatic nerve crush. *Neural Regen Res* 2016;**11**:1165–1171.
59. Pankiv S, Clausen TH, Lamark T, Brech A, Bruun JA, Outzen H, Overvatn A, Bjorkoy G, Johansen T. P62/SQSTM1 binds directly to Atg8/LC3 to facilitate degradation of ubiquitinated protein aggregates by autophagy. *J Biol Chem* 2007;**282**:24131–24145.
60. Clausen TH, Lamark T, Isakson P, Finley K, Larsen KB, Brech A, Overvatn A, Stenmark H, Bjorkoy G, Simonsen A, Johansen T. P62/SQSTM1 and ALFY interact to facilitate the formation of p62 bodies/ALIS and their degradation by autophagy. *Autophagy* 2010;**6**:330–344.
61. Zheng YT, Shahnazari S, Brech A, Lamark T, Johansen T, Brumell JH. The adaptor protein p62/SQSTM1 targets invading bacteria to the autophagy pathway. *J Immunol* 2009;**183**: 5909–5916.
62. Bjorkoy G, Lamark T, Brech A, Outzen H, Perander M, Overvatn A, Stenmark H, Johansen T. P62/SQSTM1 forms protein aggregates degraded by autophagy and has a protective effect on huntingtin-induced cell death. *J Cell Biol* 2005;**171**:603–614.

Translational perspective

This investigation describes a new role for LRP5 in brain homeostasis. Promoting LRP5 function and boosting canonical Wnt signalling might ameliorate neuronal related diseases. The translation of the putative novel therapies, identified by the understanding of the pathophysiologic basis of the disease, into effective treatment for human patients will be the next challenge.

3.7 Article 6

Unique splicing of Lrp5 in the brain: A new player in neurodevelopment and brain maturation.

By Aureli Luquero, Noelia Pimentel, Gemma Vilahur, Lina Badimon and Maria Borrell-Pagès.

Accepted for publication in *International Journal of Molecular Sciences* in June 2024.

Summary: The expression of LRP5 is undetectable in extracranial tissues of *Lrp5*$^{-/-}$ mice; however, *Lrp5*$^{-/-}$ mice brains show reduced but detectable LRP5 expression. We analysed the breeding of the *Lrp5*$^{-/-}$ mice colony and observed that mice with a *Lrp5*$^{-/-}$ genotype are born less frequently than expected. We hypothesized that LRP5 might be needed for mice embryonic development and performed a RNA-Seq based analysis where we studied the transcriptomic expression of brains and livers of *Wt* and *Lrp5*$^{-/-}$ mice brains and livers. Two different LRP5 transcripts are generated by alternative splicing: *Lrp5-201* and *Lrp5-202*. The *Lrp5-201* transcript contains all LRP5 exons and codes for the full-length LRP5 protein while the *Lrp5-202* transcript only contains exons 1 to 8 and codes for a truncated LRP5 protein. *Wt* mice expressed the *Lrp5-201* transcript in both livers and brains and did not express *Lrp5-202* transcript. Contrarily, *Lrp5*$^{-/-}$ mice only express the *Lrp5-202* transcript in the liver. In *Lrp5*$^{-/-}$ mice brains, there is high expression of the *Lrp5-202* transcript but there is also expression of the *Lrp5-201* transcript. Functional analysis on RNA-seq data showed that *Lrp5*$^{-/-}$ mice brains have impaired synapse formation and neuronal differentiation compared to *Wt* mice. Additionally, gene-set enrichment analysis showed a downregulation of genes associated with specific metabolic pathways including retinoic acid and linoleic acid pathways,

known to participate in brain development. In conclusion, we show that LRP5 expression in mice brains is necessary for proper organ development. *Lrp5*$^{-/-}$ mice show a low LRP5 expression that is enough to ensure mice embryonic development but not sufficient to maintain retinoic and linoleic acid signalling pathways which affect neuronal differentiation and synapse formation. Of note, we have not observed a downregulated expression of canonical WNT signalling pathway transcripts in *Lrp5*$^{-/-}$ mice brains indicating that LRP5 function in the brain might act through other metabolic pathways.

International Journal of
Molecular Sciences

MDPI

Artide

Unique Splicing of Lrp5 in the Brain: A New Player in Neurodevelopment and Brain Maturation

Aureli Luquero [1,2], Noelia Pimentel [1,2], Gemma Vilahur [1,3], Lina Badimon [1,3,4] and Maria Borrell-Pages [1,3,*]

1 Cardiovascular Program, Institut de Recerca de Sant Pau, 08025 Barcelona, Spain; aluquero@santpau.cat (A.L.); npimentel@santpau.cat (N.P.); gvilahur@santpau.cat (G.V.); lbadimon@santpau.cat (L.B.)
2 Biomedicine Doctorate Program, Universitat de Barcelona, 08007 Barcelona, Spain
3 Centro Investigación Biomédica en Red-Cardiovascular (CIBER-CV), Instituto de Salud Carlos III, 28029 Madrid, Spain
4 Universitat Autònoma de Barcelona, 08193 Barcelona, Spain
* Correspondence: mborrellpa@santpau.cat; Tel.: +34-935565621

Abstract: Low-density lipoprotein receptor-related protein 5 (LRP5) is a constitutively expressed receptor with observed roles in bone homeostasis, retinal development, and cardiac metabolism. However, the function of LRP5 in the brain remains unexplored. This study investigates LRP5's role in the central nervous system by conducting an extensive analysis using RNA-seq tools and in silico assessments. Two protein-coding Lrp5 transcripts are expressed in mice: full-length Lrp5-201 and a truncated form encoded by Lrp5-202. Wt mice express Lrp5-201 in the liver and brain and do not express the truncated form. $Lrp5^{-/-}$ mice express Lrp5-202 in the liver and brain and do not express Lrp5-201 in the liver. Interestingly, $Lrp5^{-/-}$ mouse brains show full-length Lrp5-201 expression, suggesting that LRP5 has a role in preserving brain function during development. Functional gene enrichment analysis on RNA-seq unveils dysregulated expression of genes associated with neuronal differentiation and synapse formation in the brains of $Lrp5^{-/-}$ mice compared to Wt mice. Furthermore, Gene Set Enrichment Analysis highlights downregulated expression of genes involved in retinol and linoleic acid metabolism in $Lrp5^{-/-}$ mouse brains. Tissue-specific alternative splicing of Lrp5 in $Lrp5^{-/-}$ mice supports that the expression of LRP5 in the brain is needed for the correct synthesis of vitamins and fatty acids, and it is indispensable for correct brain development.

Keywords: LRP5; brain; RNA-seq; liver; transcriptome; synapse; retinoic acid

Citation: Luquero, A.; Pimentel, N.; Vilahur, G.; Badimon, L.; Borrell-Pages, M. Unique Splicing of Lrp5 in the Brain: A New Player in Neurodevelopment and Brain Maturation. Int. J. Mol. Sci. **2024**, 25, 6763. https://doi.org/10.3390/ijms25126763

Academic Editor: Mario Costa

Received: 16 May 2024
Revised: 11 June 2024
Accepted: 13 June 2024
Published: 20 June 2024

1. Introduction

Low-density lipoprotein receptor (LDLR)-related protein 5 (LRP5) induces the canonical WNT/β-catenin signalling pathway after the extracellular binding of WNT ligands or extracellular lipids [1–3]. LRP5 was identified when a loss-of-function mutation in Arrow (the Drosophila melanogaster homologue LRP5 gene) generated flies without functional wings due to impaired development [4]. In normal conditions, the canonical WNT pathway is inactive, and there is constant phosphorylation, ubiquitination and degradation of β-catenin monomers [5,6]. Canonical WNT signalling activation through LRP5 leads to β-catenin stabilisation in the cytoplasm and translocation into the nucleus where it triggers the activation of the T cell factor/Lymphoid enhancer-binding factor 1 (TCF/LEF1) transcription factors [7,8]. TCF/LEF1 recruits other transcriptional co-activators to the promoter region of targeted genes such as cydin D1, Bmp2, and Opn, inducing their expression [9,10].

Canonical WNT signalling is crucial in the central nervous system, as it regulates, amongst other processes, brain development, synapse formation, and neurogenesis [11–16]. Defects in canonical WNT signalling have been associated with central nervous system malfunction, including neural tube closure defects, medulloblastoma, bipolar disorder,

schizophrenia, and Alzheimer's disease [17–19]. In the brain, there is constitutive expression of LRP5 [20]. However, there is little knowledge on the role of LRP5 in brain development. In a human meta-analysis, two different single nucleotide polymorphisms (SNPs) in *LRP5* causing Ala1330Val amino acid changes have been associated with attention-deficit/hyperactivity disorder in females with altered brain maturation [21]. LRP5 is also necessary in zebrafish, where WNT3 binding to Frizzled1 activates the canonical WNT pathway that regulates brain development [22].

We have previously shown a role for LRP5 in extracranial tissues and organs. Indeed, LRP5 is involved in the healing process of the heart after myocardial infarctions in mice, pigs, and humans [23]. Furthermore, LRP5 expression is protective in the vascular wall, as LRP5 deficiency leads to increased aortic lipid accumulation, macrophage infiltration into the vessel wall, and increased pro-inflammatory cytokines in the blood of hypercholesterolemic mice [24,25]. Additionally, LRP5 is also involved in cholesterol ester accumulation in inflammatory cells [3], a process in which proprotein convertase subtilisin kexin 9 (PCSK9) is also involved [26]. Finally, LRP5 generates pro-survival signalling by stimulating the WNT/β-catenin pathway in neurons [27]. Taken together, these results indicate a protective and pro-survival role for LRP5 in tissue homeostasis.

Lrp5$^{-/-}$ mice are generated by the insertion of an IRES-*LacZ-neomycin* cassette to interrupt the sixth exon of the mouse *Lrp5* gene at amino acid 373, generating a premature stop codon and blocking the synthesis of a full-length LRP5 protein [28]. This modification should affect all cells in mice. However, full-length LRP5 expression is observed in the brains of *Lrp5*$^{-/-}$ mice. To understand these data, we analysed different organs of *Wt* and *Lrp5*$^{-/-}$ mice.

2. Results

2.1. Non-Mendelian Pattern in *Lrp5*$^{-/-}$ Mouse Births

The analyses of the breeding of heterozygous (*Hz*; −/+ × −/+) mice from our *Lrp5*$^{-/-}$ mouse colony showed that the offspring did not follow a Mendelian pattern. The observed births of *Lrp5*$^{-/-}$ mice were less than expected (16.97% instead of the expected 25%), and there were increased *Hz* mouse births (60.57% instead of the expected 50%; Figure 1A,C). Similarly, the breeding of *Hz* mice to *Lrp5*$^{-/-}$ mice (−/+ × −/−) also showed decreased births of *Lrp5*$^{-/-}$ mice (93 births observed versus 107 expected; Figure 1B,D).

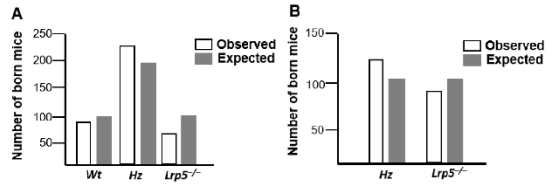

C

Hz (−/+) *Hz* (−/+)	*Wt* (+/+)	*Hz* (−/+)	*Lrp5*$^{-/-}$ (−/−)	Total
Observed births (number)	86	232	65	383
Expected births (number)	95.75	191.5	95.75	
Observed frequency (%)	22.45	60.57	16.97	
Expected frecuency (%)	25	50	25	

D

Hz (−/+)x *Lrp5*$^{-/-}$ (−/−)	*Hz* (−/+)	*Lrp5*$^{-/-}$ (−/−)	Total
Observed births (number)	121	93	214
Expected births (number)	107	107	
Observed frequency (%)	56.54	43.46	
Expected frecuency (%)	50	50	

Figure 1. Analysis of *Lrp5*$^{-/-}$ mouse offspring. Observed and expected births of wildtype (*Wt*; +/+), heterozygous (*Hz*; −/+), and knockout (*Lrp5*$^{-/-}$; −/−) mice from (**A**,**C**) *Hz* crossbreeding (−/+ × −/+; $p < 0.001$) or (**B**,**D**) *Hz* and *Lrp5*$^{-/-}$ crossbreeding (−/+ × −/−; $p = 0.05$) for over 10 years.

2.2. LRP5 Is Expressed in Brains of $Lrp5^{-/-}$ Mice

Two *Lrp5* protein-coding transcripts were generated from the *Lrp5 Mus musculus* gene by alternative splicing according to the Ensembl database [29]. The *Lrp5-201* transcript codes for the full-length *LRP5* protein, containing exons 1 to 23. The *Lrp5-202* transcript codes for a truncated protein containing exons 1 to 8; therefore, it codes for a short portion of the extracellular domain (Figure 2A).

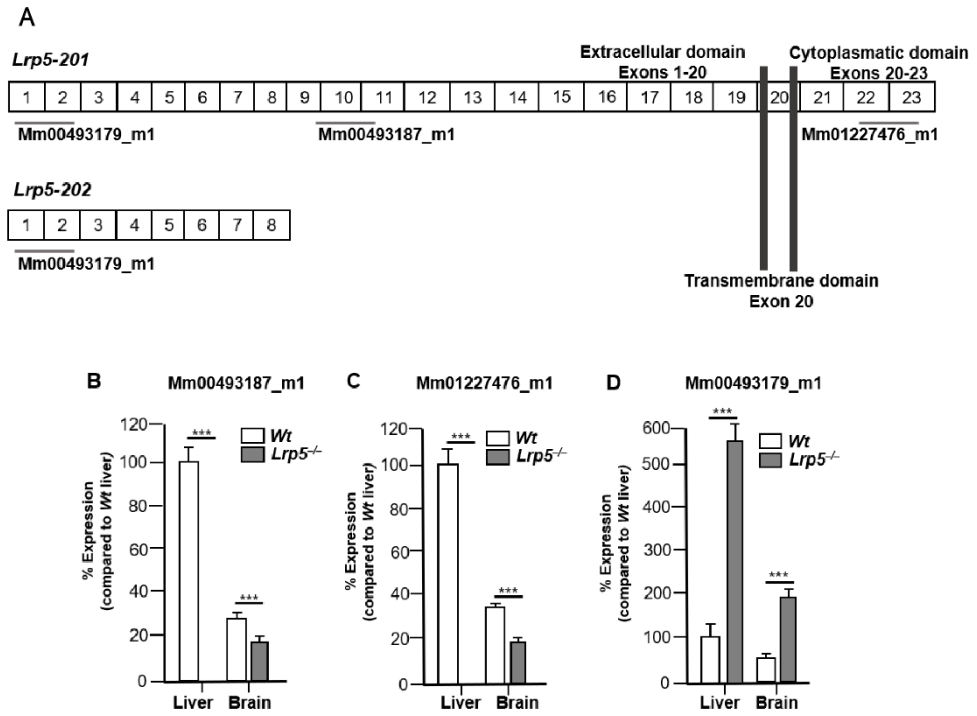

Figure 2. *LRP5* gene expression in the brains and livers of Wt and $Lrp5^{-/-}$ mice. (**A**) The *Lrp5-201* transcript was detected by LP5 probes against exons 1–2, exons 9–10–11, and exons 22–23, whereas the *Lrp5-202* transcript was only detected by the *LRP5* probe against exons 1-2. *LRP5* gene expression in the liver and brain tissues of *Wt* and $Lrp5^{-/-}$ mice using (**B**) *LRP5* probe Mm00493187_m1; (**C**) *LRP5* probe Mm_01227476; and (**D**) *LRP5* probe Mm_00493179. *** $p < 0.001$.

We first studied *Lrp5* gene expression in the brains and livers of *Wt* and $Lrp5^{-/-}$ mice. Organs were analysed with the *LRP5* probe Mm_00493187, which detected exons 9–10–11. *LRP5* gene expression was expected in the livers and brains of *Wt* mice, and no *LRP5* gene expression was expected in the organs of $Lrp5^{-/-}$ mice. Surprisingly, low but consistent expression of *LRP5* in the brains of $Lrp5^{-/-}$ mice was detected (Figure 2B). To further confirm this unexpected result, we used a second probe, Mm_01227476, which detected exons 22–23. Again, *LRP5* expression was detected in the livers and brains of *Wt* mice and in the brains but not the livers of $Lrp5^{-/-}$ mice (Figure 2C). We then tested a third probe, Mm_00493179, which detected exons 1–2–3 and therefore detected both the full-length *Lrp5-201* and the truncated *Lrp5-202* transcript. The expression of *LRP5* in the livers and brains of $Lrp5^{-/-}$ mice was greater than the expression in *Wt* mice, indicating that the *Lrp5-202* transcript was expressed predominantly in the livers and brains of $Lrp5^{-/-}$ mice (Figure 2D). These results indicate that *Lrp5* transcript expression is variable in different mouse tissues.

2.3. Lrp5 Transcriptome Is Different in Livers and Brains of Lrp5$^{-/-}$ Mice

To further understand differential *Lrp5* gene expression in *Lrp5*$^{-/-}$ mouse organs, samples of livers and brains were analysed by whole-tissue RNA-seq analyses. *Wt* mice livers showed 15-fold increased *Lrp5-201* expression compared to *Wt* mouse brain samples (Figure 3A), supporting the results from Figure 2B,C. Comparisons between *Wt* and *Lrp5*$^{-/-}$ mouse liver samples revealed that *Wt* mice had an approximated 100-fold increase in *Lrp5-201* expression levels (Figure 3A,B). Contrarily, brain samples from *Wt* and *Lrp5*$^{-/-}$ animals did not show statistically significant differences in *Lrp5-201* expression (Figure 3A,B).

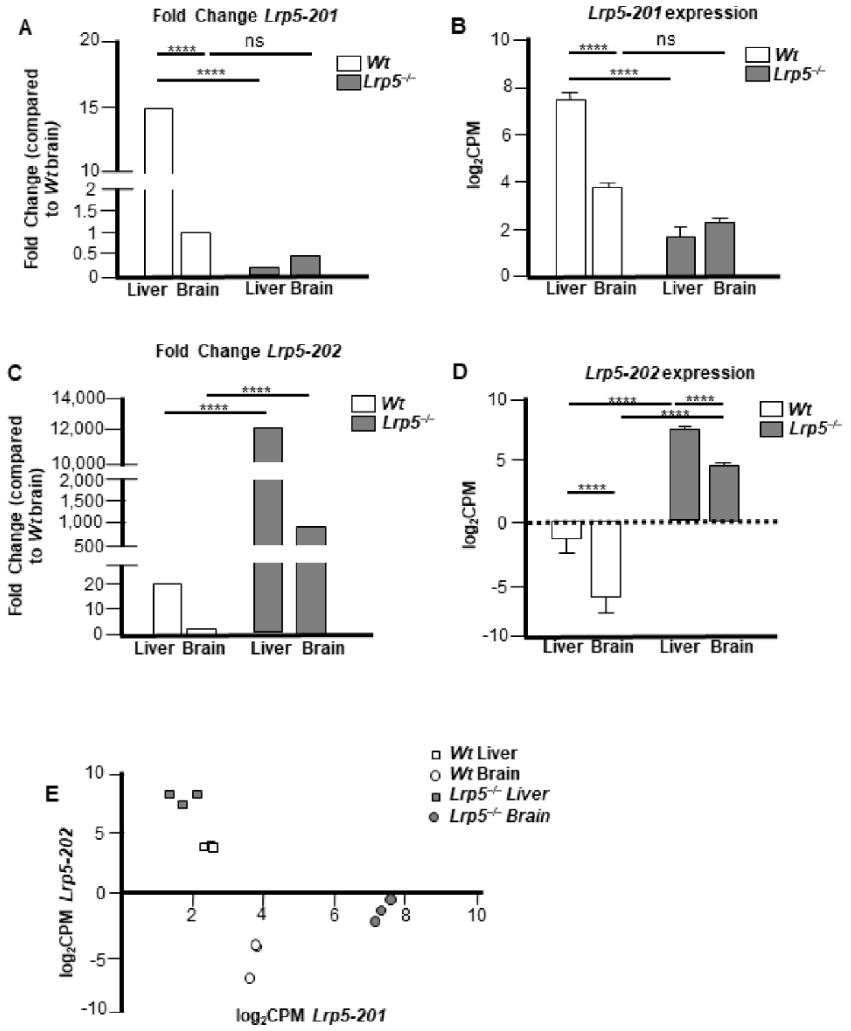

Figure 3. *Lrp5-201* and *Lrp5-202* transcript expression in the livers and brains of *Wt* and *Lrp5*$^{-/-}$ mice. (**A**) Fold change in *Lrp5-201* transcript expression. (**B**) *Lrp5-201* transcript expression in the brains and livers of *Wt* and *Lrp5*$^{-/-}$ mice expressed in $\log_2$CPM. (**C**) Same as (**A**) for *Lrp5-202*. (**D**) Same as (**B**) for *Lrp5-202*. (**E**) *Lrp5-201* transcript expression on the *X* axis and *Lrp5*-202 transcript expression on the *Y* axis for each tissue sample. Data are expressed as mean ± S.E.M. **** $p < 0.0001$; ns: non-statistically significant.

Lrp5-202 expression was increased in the livers (450-fold) and brains (850-fold) of *Lrp5*$^{-/-}$ mice compared to *Wt* mice (Figure 3C,D). Similar to *Lrp5-201*, *Lrp5-202* transcript expression was higher in the livers than that in the brains of *Lrp5*$^{-/-}$ mice (Figure 3D). These RNA-seq results confirm that the *Lrp5-201* transcript is expressed in the brains of *Lrp5*$^{-/-}$ mice. More importantly, the RNA-seq analyses did not show statistical differences in *Lrp5-201* expression in *Wt* or *Lrp5*$^{-/-}$ brain samples. The tissue expression of *Lrp5-201* and *Lrp5-202* using the $\log_2$CPM value in an *XY* axis indicated a similar *Lrp5* transcript pattern expression for each sample of the same group (Figure 3E).

2.4. LRP5 Deficiency Leads to Alterations in the Transcriptome of Livers and Brains

To assess if *LRP5* deficiency can modulate the expression of other genes, we compared gene expression in the livers of *Wt* and *Lrp5*$^{-/-}$ mice. The transcription factor encoded in transcript *Mdfic-206*, with other transcripts including non-protein coding *Tcf2l7-213* or *Gm12191-201* and the *LRP5* truncated isoform *Lrp5-202*, were significantly reduced in the livers of *Wt* mice compared to the livers of *Lrp5*$^{-/-}$ mice, indicating that *Lrp5-201* deficiency modifies the liver transcriptomic pattern (Figure 4A). Table 1 shows a list of the transcripts that were significantly modified in the livers of *Lrp5*$^{-/-}$ mice compared to *Wt* mice. When the brain samples of *Wt* and *Lrp5*$^{-/-}$ mice were analysed, the results showed increased expression of *Lrp5-202* transcripts in the brains of *Lrp5*$^{-/-}$ animals. Other transcripts with modified expression in *Lrp5*$^{-/-}$ mouse brains compared to *Wt* mouse brains included protein-coding transcripts *Rab11fip3-201*, *FGFbp3-201*, or *Rbfox1-202* (Figure 4B). Table 2 shows a list of the transcripts that were significantly modified in the brains of *Lrp5*$^{-/-}$ mice compared to *Wt* mice.

Table 1. List of transcripts with significantly altered expression in livers of *Lrp5*$^{-/-}$ mice compared to *Wt* mice. p value < 0.05.

Gene Transcripts with Altered Expression in Livers of *Lrp5*$^{-/-}$ Mice								
Mdfic-206	*Myo5a-204*	*Lpin2-204*	*Wnk2-211*	*Rida-201*	*Fbxo16-204*	*Otud1-201*	*Ranbp10-201*	*1500011B03Rik-204*
Lrp5-201	*Dpys-201*	*Gabrb3-201*	*Tlcd4-207*	*Xlr3a-201*	*Irf6-201*	*Aplp2-203*	*Atp5pb-203*	*0610030E20Rik-201*
Fam222b-203	*Slc13a3-201*	*Nat8f2-201*	*Wdr77-201*	*Eml1-202*	*Kif26b-202*	*Tbp-211*	*Med13l-201*	*1110032F04Rik-201*
Tcf7l2-213	*Ppm1k-201*	*Papola-202*	*Serpinc1-207*	*Dph7-201*	*Zhx3-202*	*Ifnar2-201*	*Fech-201*	*D5Ertd579e-201*
Camsap3-209	*Bend6-201*	*Sptan1-202*	*Fus-204*	*Fzd8-201*	*Zfp703-202*	*Gmppb-202*	*Tmem25-204*	*AW209491-202*
Dctn1-203	*Fgd6-201*	*Hnrnpa1-202*	*Gsap-201*	*Lipa-201*	*Yy1-201*	*Mat1a-201*	*Btg1-202*	*Cdc42bpb-201*
Ankrd33b-202	*Clk3-201*	*Zmynd8-203*	*Xpo4-209*	*Ppm1b-201*	*Eif5-201*	*Lrrc73-204*	*Bptf-203*	*2810021J22Rik-201*
Lrp5-202	*Hddc3-208*	*Dpys-202*	*mt-Atp6-201*	*St6gal1-205*	*Aacs-201*	*Ide-201*	*Ankrd11-202*	*A630089N07Rik-202*
Ociad2-205	*Stom-201*	*Pxmp2-201*	*Tab2-204*	*Crebrf-201*	*Relch-205*	*Tmpo-201*	*Mcfd2-204*	*2410002F23Rik-202*
Meis3-205	*Tspyl5-201*	*Slc8b1-202*	*Cyp39a1-203*	*Cog8-201*	*Map2k3-201*	*N4bp2l2-201*	*Pwwp2a-203*	*Nr1i2-201*
Cps1-201	*Zfand5-205*	*Irgm1-202*	*Bet1l-201*	*Rhod-201*	*Hes6-202*	*Nr1h2-201*	*Dcaf12l1-202*	*Wbp1l-201*
Slc15a2-205	*Inpp5f-208*	*Myef2-201*	*Rab9-202*	*Zfp120-201*	*Wnk2-201*	*Dst-201*	*Elf1-201*	*Srp54a-202*
Rapgef1-207	*Jmy-201*	*Rsph1-201*	*Pxmp4-201*	*Znfx1-201*	*Tfdp1-204*	*Gpbp1-202*	*Mphosph8-201*	*Slc4a2-201*
Pnrc1-201	*Traf4-201*	*Dclk2-206*	*Rnf186-201*	*Csnk1d-202*	*Scaf11-204*	*Rabep1-207*	*Chd4-203*	*Dtymk-201*
Gamt-202	*Brap-201*	*Srsf7-201*	*Kdm2a-202*	*Etv6-202*	*Pik3r1-202*	*Bhlhe41-201*	*Pi4ka-201*	*Ip6k2-206*
Prxl2c-207	*Gria4-203*	*Pdcd11-201*	*Esyt2-201*	*Stxbp3-201*	*Ahctf1-201*	*Slc38a2-201*	*Pkp4-211*	*Gemin5-205*
Aktip-204	*Gabarapl1-201*	*Slc39a14-202*	*Qdpr-201*	*Sgsh-201*	*Atp6ap2-201*	*Gpbp1l1-201*	*Per2-201*	*Azin1-203*
Zfyve1-201	*Irs2-201*	*Elfn2-201*	*Dnajc13-203*	*Rsph4a-201*	*Rai1-202*	*Cmtm4-201*	*Slc43a1-201*	*Zrsr2-201*
Slc25a33-201	*Spns2-201*	*Papss2-201*	*Mxd4-201*	*Fah-201*	*Epm2aip1-201*	*Cyp2c70-201*	*Grb10-203*	*Ttc14-211*
Tpm1-215	*Dtx3l-201*	*Uox-201*	*Hdac5-202*	*Csad-211*	*Irf2bp2-201*	*Pfkfb2-204*	*Dusp3-201*	*Snrnp48-201*
Klf11-201	*Maoa-201*	*Inf2-201*	*Pspc1-201*	*Prpsap1-201*	*Tbc1d20-201*	*Flcn-203*	*Cebpb-201*	*Gpcpd1-202*
Dctn1-202	*Tor1aip2-205*	*Epc2-201*	*Rabggtb-201*	*Abat-201*	*Bdp1-204*	*Hbp1-202*	*Atrip-201*	*Iigp1-202*
Evi5l-207	*Pparg-202*	*Dennd11-202*	*Fn3krp-201*	*Serpinf2-202*	*Jmjd1c-206*	*C9orf72-203*	*Riok2-201*	*Sstr4-201*
Klhl24-201	*Cnppd1-201*	*Foxp4-208*	*Cdc42bpg-201*	*Hnrnpa3-203*	*Fnip1-201*	*Smc5-202*	*Bzw1-201*	*Unc13b-201*

Table 1. *Cont.*

Gene Transcripts with Altered Expression in Livers of *Lrp5*$^{-/-}$ Mice								
Cyria-205	*Dach1-202*	*Stk24-201*	*Aldh3a2-202*	*Tro-204*	*Tmf1-202*	*Atxn2-201*	*Slc25a47-201*	*Ciart-201*
Il13ra1-201	*Erbb3-201*	*Serpinb9-201*	*Agxt2-204*	*Ubiad1-201*	*Clic5-203*	*Chn2-202*	*Zfp955a-201*	*Elac1-201*
Trim46-201	*Spryd4-201*	*Ilrun-203*	*Pcdh1-204*	*Gorasp1-201*	*Upp2-202*	*Atpsckmt-201*	*Ap4m1-201*	*Nfyc-204*
Gclc-201	*Sesn2-201*	*Mmab-201*	*Zfand6-208*	*Dyrk3-201*	*Csnk1g1-202*	*Stat5b-201*	*Hsd17b7-201*	*Ipmk-203*
Dgkb-203	*Dlg4-205*	*Thrsp-201*	*Fbxl19-201*	*Blvrb-201*	*Slc25a22-225*	*Lats2-201*	*Fbxl3-201*	*Mef2d-204*
Gla-201	*Nr2c2-201*	*Klhl42-201*	*Ppp1r3b-201*	*Pcsk9-201*	*Paqr5-201*	*Sf3a1-201*	*Nars-205*	*Rnf125-202*
Muc3a-202	*Stard4-201*	*Tstd3-201*	*Inf2-203*	*Cpeb2-202*	*Tmc6-201*	*Map3k11-201*	*Stau2-212*	*Dcaf11-202*
Aldh1l1-201	*Slc38a3-209*	*Bcan-201*	*Mtdh-202*	*Gnpnat1-201*	*Rnd1-201*	*Tfe3-201*	*Ss18l2-201*	*Dhtkd1-202*
Smurf1-203	*Ccng2-201*	*Atad3a-201*	*Mink1-201*	*Zfp266-202*	*Arhgef3-202*	*Elp1-201*	*Hmgb1-201*	*Ttbk2-202*
Wnt7b-201	*Elovl6-201*	*Chic1-201*	*Pck1-201*	*Zswim4-201*	*Aqp11-205*	*Mthfr-201*	*Gpr146-201*	*Mapk3-202*
Lnx2-201	*Psmc3-210*	*Slc38a3-201*	*Gtf2ird1-229*	*Ccdc39-201*	*Slc38a3-202*	*Oser1-201*	*P2ry1-203*	*Heatr1-206*
Zfp386-204	*Gprc5b-204*	*Serpind1-202*	*Fam47e-202*	*Arg1-201*	*Ankrd13c-202*	*Zfp592-201*	*Tmem98-201*	*Tmub2-202*
Creg1-202	*Calcoco1-201*	*Nme5-204*	*Map1lc3a-201*	*Mid1ip1-201*	*Ints6-201*	*Net1-201*	*Zfp322a-201*	*Rb1cc1-214*
Rbm33-204	*Pou2af2-202*	*Laptm4b-201*	*Dnajb11-203*	*Tbcel-203*	*Smad4-201*	*Ewsr1-205*	*Zkscan8-201*	*Kdm3a-201*
Fam135a-206	*Rpl30-201*	*Fads6-201*	*Ppp1r3g-201*	*Srsf1-205*	*Slc20a2-201*	*Slc9a3-203*	*Gpx6-201*	*Map4k4-209*
Rnf38-202	*Pde4b-207*	*Lrfn3-201*	*Dyrk1b-201*	*Ddx42-201*	*Map3k5-202*	*Hnrnpf-202*	*Cstf2t-201*	
Ephx1-201	*Sec24c-201*	*Gpam-202*	*Tacc2-205*	*Mbd5-203*	*Suds3-202*	*Crebbp-205*	*Tbc1d14-201*	
Rtl5-201	*Stard13-208*	*Raf1-201*	*Ttc38-203*	*Meiob-201*	*Plekhm1-201*	*Proca1-201*	*Acbd5-213*	
Uqcc1-204	*Mok-202*	*Aox1-201*	*Atat1-203*	*Fem1a-201*	*Net1-202*	*Rims2-201*	*Mtmr3-203*	
Abcb4-201	*Mrtfb-204*	*Ube2h-202*	*Wac-201*	*Cpeb2-204*	*Serpina3n-201*	*Shroom1-201*	*Cyth2-203*	
Cpq-201	*Ttll11-202*	*Zfp446-203*	*Fus-201*	*Csad-205*	*Lrp6-201*	*Ano1-203*	*Chrm3-202*	
Heca-201	*Septin9-204*	*Anks4b-201*	*Tomm40-202*	*Mul1-201*	*Fnbp1-210*	*Leng8-203*	*Opn3-201*	
Nlgn3-201	*Ctdsp2-202*	*Kctd7-201*	*Tesk1-201*	*Efr3a-212*	*Taok3-201*	*Pnn-201*	*H2az1-201*	
Map3k13-203	*Nfil3-201*	*Gbp7-201*	*Hlcs-201*	*Evi5-201*	*Mpv17l-201*	*Pon2-201*	*Ppp2r2d-201*	
Btg1-201	*Arl4a-201*	*Ypel2-201*	*Casp7-201*	*Ptpn21-203*	*Mettl1-201*	*Hmgcr-201*	*Nup50-201*	
Tcp11l2-201	*Zfp740-201*	*Plec-218*	*Rrp9-201*	*Khnyn-203*	*Wdr45-204*	*Mtss1-201*	*Magi1-203*	
Tmem64-201	*Pcdh1-203*	*Atosa-201*	*Hnrnpd-211*	*Cyp39a1-204*	*Kcna2-202*	*Ephb6-201*	*Mterf2-201*	
Zfp13-201	*Hsdl2-201*	*Txndc11-202*	*Ankrd46-203*	*Zdhhc2-201*	*Dtx4-201*	*Itgb1-201*	*Abhd8-201*	
Azin1-201	*Aldh1l1-203*	*Nhlrc1-201*	*Echdc3-201*	*Lrrfip2-205*	*Rbbp6-202*	*Tmx2-201*	*Akap8-206*	
Emc2-201	*Gpr17-201*	*Znrf3-201*	*Dnmbp-206*	*Lcorl-212*	*Rabl3-201*	*Acaca-201*	*Csad-201*	
Tgoln1-201	*Sppl3-201*	*Pomk-201*	*Triobp-203*	*Rnf11-201*	*Phf13-201*	*Otud3-201*	*Rdx-204*	
Pde4dip-201	*Tlcd4-203*	*Zfp715-203*	*Stat1-206*	*Axin1-201*	*Tmem44-204*	*Ranbp10-203*	*Snap25-201*	

Table 2. List of transcripts with significantly altered expression in brains of *Lrp5*$^{-/-}$ mice compared to *Wt* mice. p value < 0.05.

Gene Transcripts with Altered Expression in Brains of *Lrp5*$^{-/-}$ Mice				
Fgfbp3-201	*Pde4d-202*	*Cramp1-201*	*Ttyh1-201*	*Brap-205*
Eps8l2-206	*Ankrd33b-202*	*H2-Q7-201*	*Erich5-201*	*Ighg2c-202*
Rab11fip3-201	*Cask-210*	*Gm17167-201*	*Ube2d2a-210*	*Abi1-205*
Lrp5-202	*Zfp386-204*	*Gm8116-201*	*Bcat2-205*	*Atp6v1c1-202*
Gm12191-201	*Rpl30-201*	*Aldh1l1-204*	*Baalc-202*	*Ywhaz-203*
Rbfox1-202	*Ciz1-202*	*Atp6v1c1-201*	*Slc29a1-222*	*Lzts3-202*
Ndn-201	*Atg16l2-211*	*Fn1-204*	*Rpl30-ps9-201*	*Rspo2-201*
Hax1-207	*Gm8276-201*	*Cobl-210*	*Ankrd46-204*	*Pak3-210*
Ptpn6-203	*Marveld2-201*	*Btaf1-201*	*Gm54215-201*	*Meg3-201*
Ankrd33b-203	*Ywhaz-207*	*Eif3s6-ps2-201*	*Ywhaz-201*	

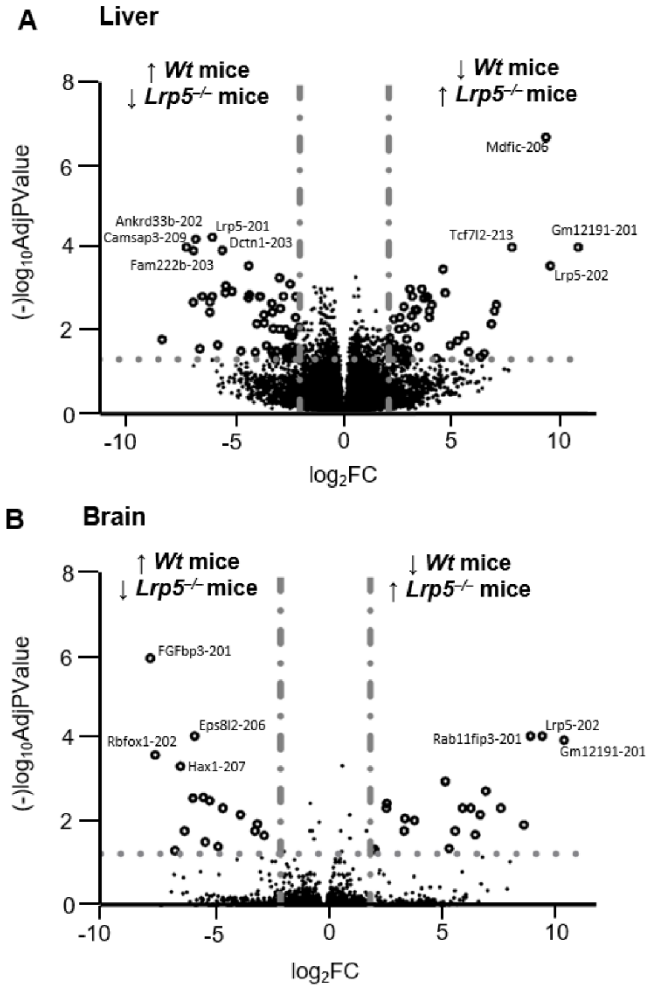

Figure 4. Volcano plots for liver and brain samples. Volcano plot comparing transcript expression in (**A**) livers of *Lrp5*$^{-/-}$ mice vs. livers of Wt mice and in (**B**) brains of *Lrp5*$^{-/-}$ mice vs. brains of *Wt* mice. Data are expressed as $\log_2$FC on the *X* axis and as $(-)\log_{10}$AdjPvalue on the *Y* axis. Transcripts above the horizontal grey dotted line (···) show significantly modified expression in *Lrp5*$^{-/-}$ mice compared to *Wt* mice. Vertical grey bar-dot lines (— · — ·) indicate thresholds where transcripts reduced expression by ½-fold or increased by 2-fold in mouse *Lrp5*$^{-/-}$ tissue compared to *Wt* mice tissue. Empty dots (○) indicate transcripts with highly modified expression in *Lrp5*$^{-/-}$ tissues. ↑ indicates that the transcript expression is significantly higher in animals of the genotype and ↓ indicates that transcript expression is significantly lower in animals of the genotype.

2.5. Lrp5 Quantity Is Different in Livers and Brains of Lrp5$^{-/-}$ *Mice*

The balance of the different *Lrp5* transcripts in each tissue was then evaluated. Differential transcript usage (DTU) analysis showed that the livers and brains of *Wt* mice expressed only the *Lrp5-201* transcript (Figure 5A,B). In *Lrp5*$^{-/-}$ mice, the liver's *Lrp5-201* transcript accounted for less than 2% of *Lrp5* transcripts, whereas *Lrp5-202* accounted for more than 98% (Figure 5C). However, in the brains of *Lrp5*$^{-/-}$ mice, *Lrp5-201* accounted for 27% of *Lrp5*-encoding transcripts, whereas 73% were *Lrp5-202* transcripts (Figure 5D).

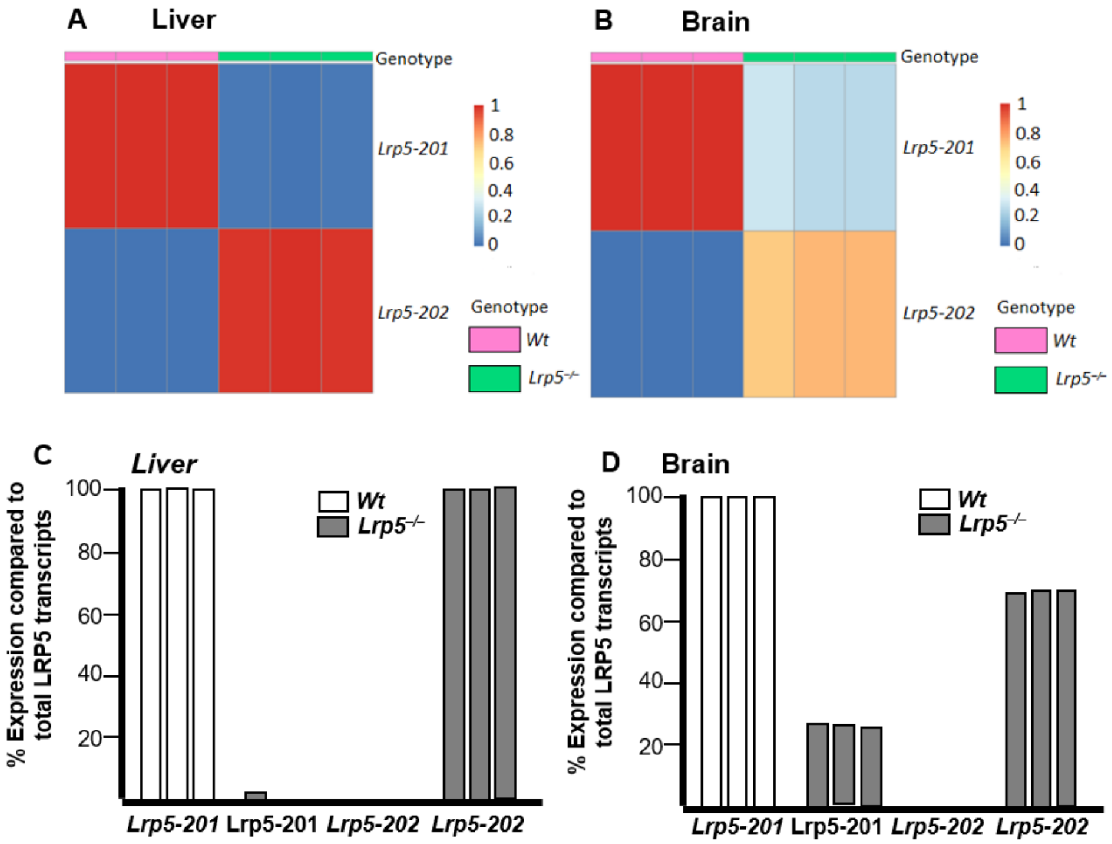

Figure 5. *Lrp5* transcript variability depending on tissue and mouse genotype. Heat map with the number of *Lrp5-201* and *Lrp5-202* transcripts in the (**A**) livers and (**B**) brains of *Wt* and *Lrp5*$^{-/-}$ mice. *Lrp5-201* and *Lrp5-202* expression compared to total *Lrp5* transcripts in *Wt* and *Lrp5*$^{-/-}$ mouse (**C**) livers and (**D**) brains.

2.6. Functional Studies Show Modified Functions in Brains of Lrp5$^{-/-}$ *Mice*

To study the effects of *LRP5* deficiency on brain functionality, functional gene enrichment analysis was performed on RNA-seq data from the brains of *Wt* and *Lrp5*$^{-/-}$ mice, showing that *LRP5* transcripts are associated with specific functions of the brain, including "Cell morphogenesis involved in neuron differentiation" and "Synapsis formation" (Table 3). Gene Set Enrichment Analysis (GSEA) showed that genes involved in retinol and linoleic acid metabolism are downregulated in the brains of *Lrp5*$^{-/-}$ mice compared to *Wt* mice (Figure 6A–C). Other pathways with downregulated gene expression in *Lrp5*$^{-/-}$ mouse brains are steroid hormone biosynthesis, porphyrin and chlorophyll metabolism, chemical carcinogenesis, and ascorbate and aldarate metabolism (Figure 6D–G).

Network analysis using Cytoscape software based on the STRING database showed that several genes with modified expression in *Lrp5*$^{-/-}$ mice not only participate in the WNT/β-catenin signalling pathway but are also involved in abnormal neuron morphology and abnormal central nervous system physiology (Figure 7A,B). All these findings suggest that dysregulation in the WNT/β-catenin pathway can be the cause for a deficient retinol acid and linoleic acid metabolism, which, in turn, can produce deficits in neuron differentiation and neuron synapsis formation.

Table 3. Altered functions in the brains of *Lrp5*$^{-/-}$ mice according to functional gene enrichment analysis. The 1st column indicates the altered function; the 2nd column shows the *p* value associated with each function; the 3rd column shows the Gene Ontology subhierarchy associated with the altered function; the 4th column lists the transcripts with altered expression in the brains of *Lrp5*$^{-/-}$ mice that are associated with the altered function (GO:BP stands for Gene Ontology:Biological Process; GO:CC stands for Gene Ontology:Cellular Component; GO:MF stands for Gene Ontology:Molecular Function).

Altered Function	*p*-Value	Source	Significantly Altered Transcripts
Cell morphogenesis involved in differentiation	0.00713631	GO:BP	*Necdin-201; Ptpn6-203; Cask-210; Fn1-204; Cobl-210; Abi-205; Ltzs3-202; Pak3-210*
Cell morphogenesis involved in neuron differentiation	0.03526747	GO:BP	*Necdin-201; Cask-210; Fn1-204; Cobl-210; Abi-205; Ltzs3-202; Pak3-210*
Postsynaptic density	0.00032878	GO:CC	*Cask-210; Rpl30-201; Ywhaz-207; Baalc-202; Abi1-205; Ltzs3-202; Pak3-210*
Postsynapse	0.00037269	GO:CC	*Rab11fip3-201; Slc29a1-222; Cask-210; Rpl30-201; Ywhaz-207; Baalc-202; Abi1-205; Ltzs3-202; Pak3-210*
Asymmetric synapse	0.00043165	GO:CC	*Cask-210; Rpl30-201; Ywhaz-207; Baalc-202; Abi1-205; Ltzs3-202; Pak3-210*
Postsynaptic specialization	0.00060115	GO:CC	*Cask-210; Rpl30-201; Ywhaz-207; Baalc-202; Abi1-205; Ltzs3-202; Pak3-210*
Neuron to neuron synapse	0.00072925	GO:CC	*Cask-210; Rpl30-201; Ywhaz-207; Baalc-202; Abi1-205; Ltzs3-202; Pak3-210*
Cell junction	0.00111901	GO:CC	*Rab11fip3-201; Ptpn6-203; Cask-210; Rpl30-201; Ywhaz-207; Baalc-202; Slc29a1-222; Marveld2-201; Atp6v1c1-201; Ttyh1-201; Abi1-205; Ltzs3-202; Pak3-210*
Synapse	0.00187814	GO:CC	*Rab11fip3-201; Slc29a1-222; Cask-210; Rpl30-201; Ywhaz-207; Baalc-202; Atp6v1c1-201; Abi1-205; Ltzs3-202; Pak3-210*
Apical part of cell	0.01692298	GO:CC	*Hax1-207; Pde4d-202; Marveld2-201; Atp6v1c1-201; Fn1-204; Cobl-210*
Plasma membrane region	0.01918133	GO:CC	*Rab11fip3-201; Eps8l2-206; Hax1-207; Pde4d-202; Cask-210; Marveld2-201; Fn1-204; Ttyh1-201; Slc29a1-222*
Protein domain specific binding	0.00720761	GO:MF	*Hax1-207; Ptpn6-203; Cask-210; Ywhaz-207; Fn1-204; Abi1-205; Lzts3-202; Pak3-210*
Protein binding	0.04096533	GO:MF	*Fgfbp3-201; Eps8l2-206; Rab11fip3-201; Ndn-201; Hax1-207; Ptpn6-203; Pde4d-204; Cask-210; Marveld2-201; Ywhaz-207; Fn1-204; Cobl-210; Ankrd46-204; Abi1-205; Lzts3-202; Pak3-210; Lrp5-202; Ankrd33b-206; Ciz1-202; Atg16l2-211; H2-Q7-201; Aldh1l1-204; Btaf1-201; Ube2d2a-210; Brap-205; Ighg2c-202; Rspo2-201*

Int. J. Mol. Sci. **2024**, *25*, 6763

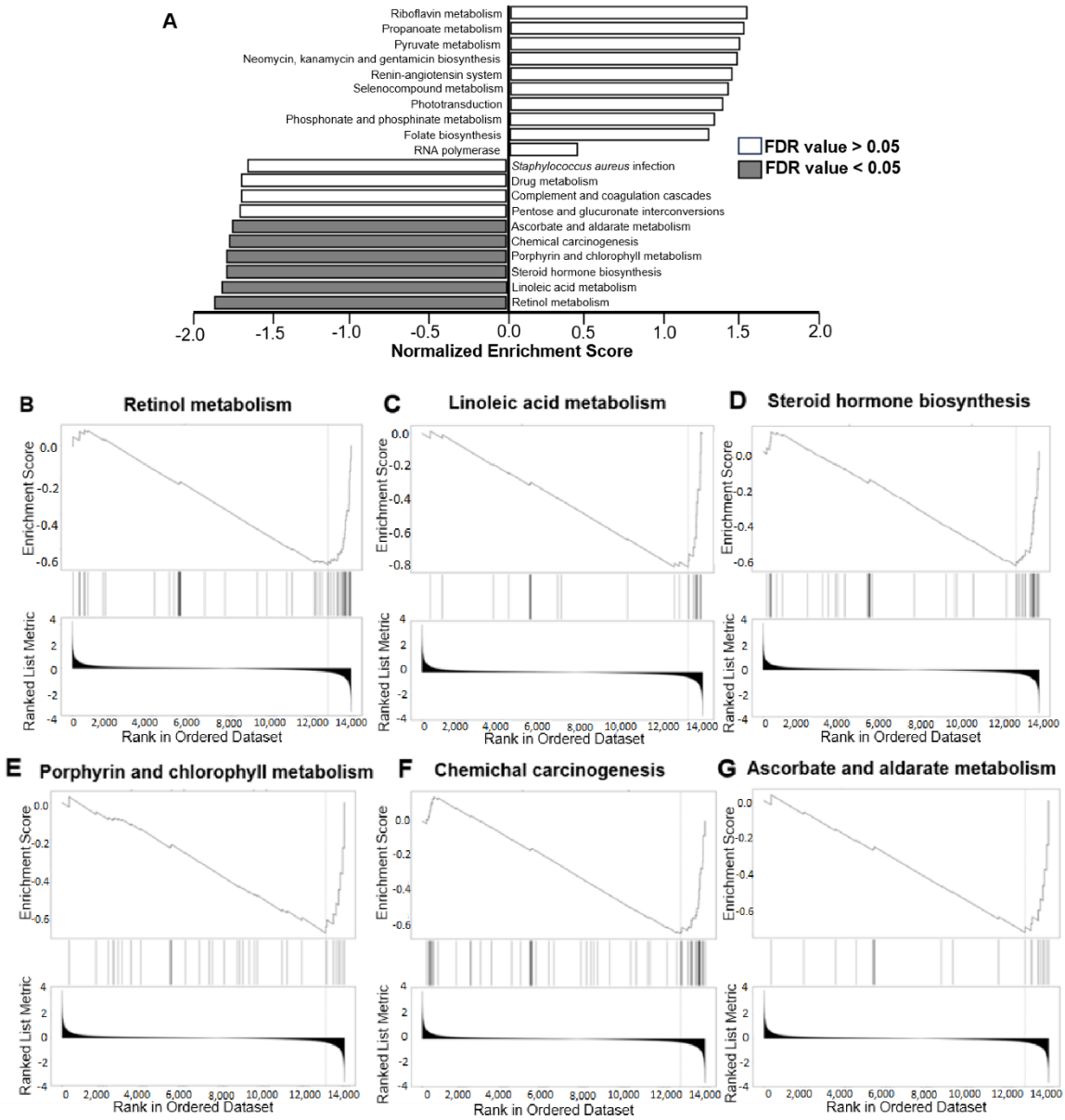

Figure 6. Gene Set Enrichment Analyses (GSEA) on the brains of Wt and Lrp5$^{-/-}$ mice. (**A**) List of the top 10 most dysregulated pathways in the brains of *Lrp5*$^{-/-}$ mice. Positive values on the *X* axis indicate upregulation, and negative values on the *X* axis indicate downregulation compared to the brains of *Wt* mice. (**B**–**G**) GSEA plots for pathways with FDR < 0.05, (**B**) retinol metabolism, (**C**) linoelic acid metabolism, (**D**) steroid hormone biosynthesis, (**E**) porphyrin and chlorophyll metabolism, (**F**) chemichal carcinogenesis, and (**G**) ascorbate and aldarate metabolism. All gene sets available in the Gene Ontology database were considered. Figures (**B**–**G**): *X*-axis is the Rank in Ordered Dataset ranging from 0 to 14,000; superior *Y*-axis is the Enrichment Score ranging from 0.0 to −0.8; inferior *Y*-axis is the Ranked List Metric ranging from 4 to −4.

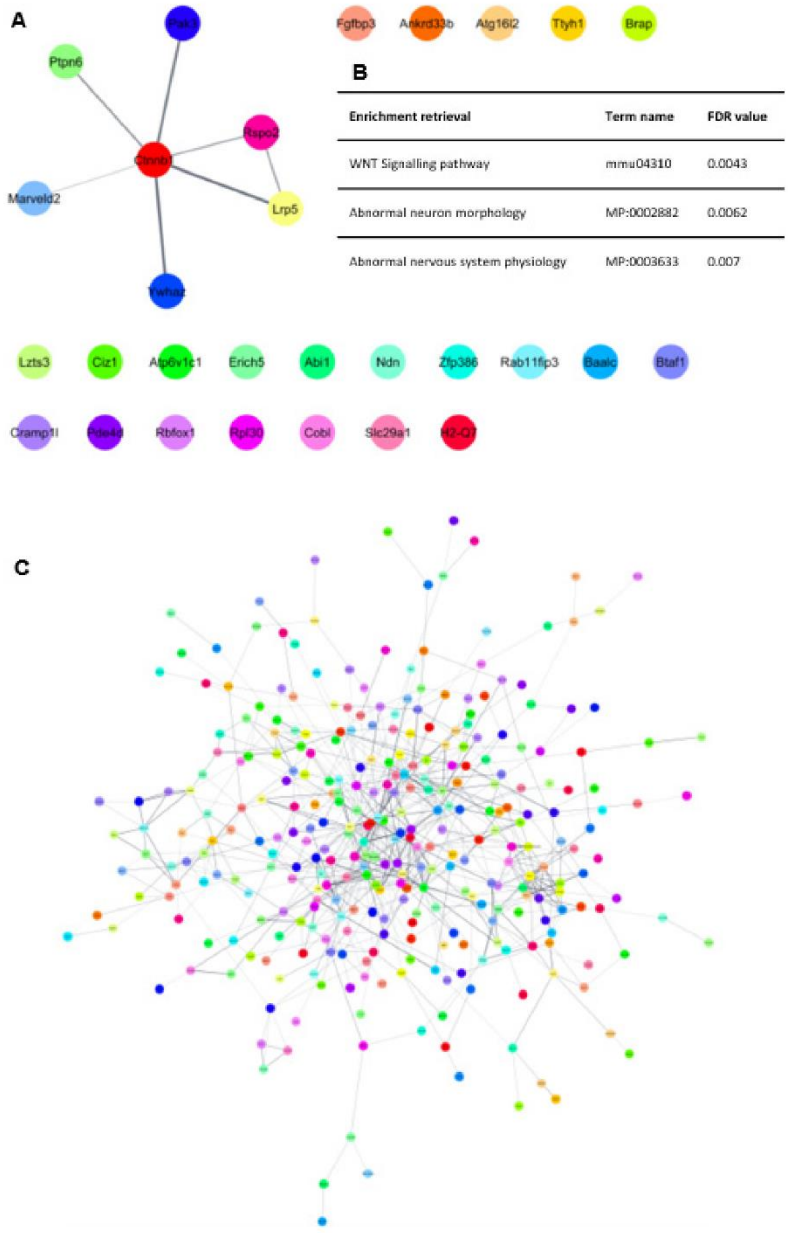

Figure 7. Network analysis of RNA-seq data. (**A**) Protein–protein interaction network of transcripts with modified expression in Lrp5$^{-/-}$ mice brains. Only interactions with a confidence score higher than 0.4 are shown. A β-catenin node was added to generate a cluster of interacting proteins. Singletons were included in the figure to show that the majority of proteins with altered expression did not interact with each other. (**B**) Table showing functional gene enrichment retrieved from proteins forming the cluster in A. Singletons were not included for the enrichment. Term names and FDR data are included in the table. (**C**) Protein–protein interaction network of transcripts with modified expression in *Lrp5*$^{-/-}$ mice livers. Only interactions with a confidence score higher than 0.4 are shown.

2.7. Functional Studies Show Impaired Functions in Livers of $Lrp5^{-/-}$ Mice

Functional gene enrichment analysis on RNA-seq data from the livers of *Wt* and $Lrp5^{-/-}$ mice showed that over 300 liver functions were significantly modified in $Lrp5^{-/-}$ mice compared to *Wt* mice, including processes involving cellular and metabolic pathways (Table 4). Liver RNA-seq data were also subjected to network analysis, resulting in 319 proteins that had their expression modified in the livers of $Lrp5^{-/-}$ mice (Figure 7C). Furthermore, clustering of the network followed by functional gene enrichment analysis revealed that each group of closely interacting proteins are associated with specific modified functions (Supplementary Figure S1, Supplementary Table S1). Network analyses support that the livers of $Lrp5^{-/-}$ mice were more severely affected than their brains by the loss of *Lrp5-201* expression as more functions were altered in their gene expression profiles.

Table 4. Altered functions in livers of $Lrp5^{-/-}$ mice according to functional gene enrichment analysis. The 1st column indicates the altered process; the 2nd column shows the *p* value associated with each function; the 3rd column shows the Gene Ontology subhierarchy associated with the altered function; the 4th column shows the number of altered transcripts associated with the function. Only the 28 functions with the smallest *p* values are listed, as more than 300 functions were altered in the livers of $Lrp5^{-/-}$ mice (based on the Gene Ontology database) (GO:BP stands for Gene Ontology:Biological Process; GO:CC stands for Gene Ontology:Cellular Component; GO:MF stands for Gene Ontology:Molecular Function).

Altered Function	*p*-Value	Source	Number of Significantly Altered Transcripts
Regulation of cellular metabolic process	1.54×10^{-19}	GO:BP	193
Regulation of cellular process	2.68×10^{-18}	GO:BP	325
Regulation of primary metabolic process	4.22×10^{-18}	GO:BP	199
Biological regulation	1.31×10^{-16}	GO:BP	347
Reguation of metabolic process	2.41×10^{-16}	GO:BP	223
Regulation of nitrogen compound metabolic process	7.82×10^{-16}	GO:BP	189
Regulation of biological process	1.66×10^{-15}	GO:BP	337
Organic substance biosynthetic process	3.49×10^{-15}	GO:BP	190
Biosynthetic process	3.75×10^{-15}	GO:BP	192
Cellular process	6.86×10^{-15}	GO:BP	446
Positive regulation of biological process	1.45×10^{-14}	GO:BP	207
Positive regulation of cellular process	4.05×10^{-14}	GO:BP	190
Regulation of macromolecule metabolic process	2.91×10^{-13}	GO:BP	204
Cellular metabolic process	2.50×10^{-12}	GO:BP	299
Cellular biosynthetic process	3.84×10^{-12}	GO:BP	173
Regulation of biosynthetic process	1.43×10^{-11}	GO:BP	143
Organonitrogen compund metabolic process	3.46×10^{-11}	GO:BP	192
Anatomical structural development	4.95×10^{-11}	GO:BP	186
Developmental process	6.58×10^{-11}	GO:BP	199
Metabolic process	1.18×10^{-10}	GO:BP	344
Primary metabolic process	1.37×10^{-10}	GO:BP	318
Negative regulation of cellular process	1.92×10^{-10}	GO:BP	157
Regulation of macromolecule biosynthetic process	3.05×10^{-10}	GO:BP	133
Regulation of cellular biosynthetic process	3.16×10^{-10}	GO:BP	136
Multicellular organism development	3.37×10^{-10}	GO:BP	154
Positive regulation of cellular metabolic process	6.09×10^{-10}	GO:BP	111
System development	6.42×10^{-10}	GO:BP	136
Localization	1.11×10^{-9}	GO:BP	166
.			
.			
.			

3. Discussion

We analysed the breeding of our *Lrp5*$^{-/-}$ mice colony in the last 10 years and observed that, after mating heterozygous mice, *Lrp5*$^{-/-}$ mice were born less frequently than expected. Furthermore, the mating of heterozygous with knockout mice also showed reduced births of *Lrp5*$^{-/-}$ mice. This finding suggests that *LRP5* expression might be essential for mouse embryonic development.

Lrp5-201 is not expressed in the peripheral tissues of *Lrp5*$^{-/-}$ mice, including the liver, aorta, heart, spleen, and jejunum [27], but it is expressed in their brains, showing a mosaic expression of the *Lrp5-201* transcript in *Lrp5*$^{-/-}$ mice. Indeed, the protein expression pattern of full-length *LRP5* resembles that of gene *Lrp5-201*. Interestingly, all *Lrp5*$^{-/-}$ mice showed similar *Lrp5-201* expression in their brains, supporting a role for *Lrp5-201* in survival. *Lrp5*$^{-/-}$ mice expressed significantly fewer *Lrp5-201* transcripts than *Wt* mice in the brain. The insertion of the IRES-*LacZ-Neomycin* cassette at the end of exon 6 abrogated full-length *LRP5* transcript formation; however, the brain splicing machinery could avoid the inserted sequence producing the *Lrp5-201* transcript. The inserted cassette probably hampered the efficiency of the splicing process, as the immature *Lrp5* transcript was mostly converted into an *Lrp5-202* transcript.

Because *LRP5* was not expressed in extracranial tissues in *Lrp5*$^{-/-}$ mice, *LRP5* must not be required in the organogenesis of extracranial organs. However, *LRP5* is active after hypercholesterolemia or ischemia [3,26,30,31], indicating that particular RNA splicing in the *Lrp5* transcript must occur exclusively in the brains of *Lrp5*$^{-/-}$ mice to generate an *Lrp5* transcript similar to full-length *Lrp5-201* that can generate a functional protein.

Lrp5-202 expression in the livers of *Lrp5*$^{-/-}$ mice was higher than that of *Lrp5-201* in the livers of *Wt* mice. This indicates that a lack of *Lrp5-201* induces the synthesis of high levels of *Lrp5-202* truncated transcripts in an attempt, probably, to counterbalance the loss of *LRP5* function.

Similarly, reduced expression of *Lrp5-201* transcripts in the brains of *Lrp5*$^{-/-}$ mice led to the overexpression of *Lrp5-202*. This could be explained because of an insufficient quantity of full-length *LRP5* proteins being produced by the *Lrp5-201* transcript or that the full-length *LRP5* protein encoded by the *Lrp5-201* transcript could not reproduce *LRP5*'s normal functions. We hypothesise that only those embryos that showed brain *Lrp5-201* transcript expression were viable. We showed that *Lrp5*$^{-/-}$ mice had similar brain expression of *Lrp5-201* transcripts (Figure 5B), further supporting that mouse embryos that do not express more than 25% of *Lrp5-201* transcripts are not viable and probably die during the early gestation stages.

RNA-seq analysis revealed differential expression of *Lrp5-201* and *Lrp5-202* transcripts in the livers and brains of *Wt* mice compared to their *Lrp5*$^{-/-}$ littermates. *Lrp5*$^{-/-}$ mouse brains showed modified expression of 48 mature RNAs, 35 of which were protein coding mRNAs. In contrast, *Lrp5*$^{-/-}$ mouse livers showed modified expression of 546 transcripts, 488 of them being protein-coding mRNAs. This finding suggests that, by the preservation of full-length *LRP5* expression, the brain transcriptome is less modified than the liver transcriptome, which shows a complete loss of *LRP5* expression and function. This finding is further confirmed by the network in silico analysis, in which brain altered transcripts needed at least the β-catenin node addition to generate a minimum network of interacting proteins. Hence, this finding supports our hypothesis that, in *Lrp5*$^{-/-}$ mice, there is expression of fully active *LRP5* and that the *LRP5* brain's expression must be preserved to ensure survival. Of note, we believe that the generation of *Lrp5-201* transcripts in *Lrp5*$^{-/-}$ mouse brains is not an efficient process, as most of the *LRP5* transcripts synthesised were *Lrp5-202* transcripts. Hence, in order to have enough functional *LRP5* in the brains of *Lrp5*$^{-/-}$ mice, vast quantities of *Lrp5-202* transcripts were synthesised as a by-product.

Liver altered transcripts generated a huge network with hundreds of interacting proteins. Further clustering of liver genes followed by functional gene enrichment analysis showed that multiple functions were dysregulated in the livers of *Lrp5*$^{-/-}$. These functions

comprise essential cellular metabolic pathways, including regulation of transcription, control of mRNA splicing, catabolism, autophagy, and others.

Functional gene enrichment analysis in *Wt* and *Lrp5*$^{-/-}$ mouse brains revealed that different genes are involved in the same cellular functions. Also, the proteins can be grouped and associated with different pathways, including neuronal differentiation and synapsis formation. Therefore, downregulation of these pathways could explain the low number of *Lrp5*$^{-/-}$ mouse births. Furthermore, if full-length *Lrp5-201* expression was completely abolished from *Lrp5*$^{-/-}$ mouse brains, increased modified gene transcripts (similar to the liver samples) would be expected.

GSEA revealed significant downregulation of genes associated with retinol, linoleic acid, and other biosynthetic pathways in the brains of *Lrp5*$^{-/-}$ mice. A deficit in retinol acid metabolism is associated with impaired neuronal plasticity and defects in the development of the central nervous system, as retinoic acid has very specific effects on neuronal differentiation [32–35]. Linoleic acid and derivates have also been involved in mouse reflex maturation and memory improvement [36], and elevated linoleic acid concentrations in the blood can lead to mouse brain malfunction and inflammation [37]. Our findings show downregulation of the retinol and linoleic acid pathways in the brains of *Lrp5*$^{-/-}$ mice, suggesting that a reduction in the expression of full-length *LRP5* causes deficits in neuronal differentiation and synapsis formation.

Full-length *LRP5* is transported to the cell membrane in endosomal bodies from the endoplasmic reticulum [38]. *LRP5*'s transmembrane domain allows the receptor's insertion into the plasma membrane. An artificial dominant-negative soluble form of *LRP5* lacking the transmembrane and cytoplasmatic domains has been used as a WNT/β-catenin pathway inhibitor. Soluble *LRP5* contains the full extracellular protein sequence (exons 1–19) and shows *LRP5* antagonist properties preventing WNT ligands from binding full-length *LRP5*, suppressing the expression of tumorigenic and metastatic proteins and inducing an epithelial to mesenchymal transition in Saos-2 cells [39]. Soluble *LRP5* also reduces 143B cell tumour growth in nude mice [40]. The *Lrp5-202* transcript encodes for a protein containing only a fraction of the extracellular domain (exons 1–6), opening the possibility that it can also act as a WNT pathway repressor; however, functional studies are needed to determine the possible roles for this isoform. To the best of our knowledge, no protein similar to that encoded by the *Lrp5-202* transcript has been described.

This study highlights the importance of *LRP5* expression in the brain. We observed fewer births of mice with a *Lrp5*$^{-/-}$ genotype as opposed to a *Wt* genotype and were able to demonstrate that mice unable to express full-length *LRP5* in the brain die during embryonic stages. Furthermore, we showed a protective mechanism that involves the alternative splicing of *Lrp5* transcripts to avoid a premature stop codon and generate a full-length *Lrp5* transcript in mouse brains, suggesting a role for *LRP5* in the preservation of brain function during development. Finally, Gene Set Enrichment Analysis highlighted the downregulated expression of genes involved in retinol and linoleic acid metabolism in *Lrp5*$^{-/-}$ mouse brains, supporting that the expression of *LRP5* in the brain is needed for the correct synthesis of vitamins and fatty acids, and it indispensable for correct brain development.

4. Materials and Methods

4.1. Animal Models and Experimental Design

Genes and proteins from mouse and human samples are written in accordance with the guidelines from the "International Committee on Standardized Genetic Nomenclature for Mice and the Rat Genome", 2010. Briefly, mouse genes and transcripts are written in italics (*Lrp5*), human genes are written in italics and capital block letters (*LRP5*) and proteins from the two species are written in straight capital block letters (*LRP5*) [41].

The study protocols for mice were approved by the institutional Animal Care and Use Committee (ICCC051/5422) and authorised by the local government commission. Animal procedures conformed to guidelines published in directive 2010/63/EU of the European Parliament and the "Position of the American Heart Association on Research Animal use"

(11 November 1984). At the research institute, we are committed to the "3R"s principle, using the minimum number of animals required to accomplish statistical significance.

Lrp5$^{-/-}$ mice were a kind gift from Dr. Bart Williams [42]. Mouse strains were maintained in a C57bl/6J genetic background. Animals were housed in cages under controlled monitoring of temperature (21 ± 2 °C) on a 12 h light/dark cycle with food and water ad libitum. Genotyping was performed on mice 4 weeks after birth using PCR amplification from DNA extracted from tail biopsies, resulting in the identification of *Wt*, *Lrp5*$^{-/+}$, or *Lrp5*$^{-/-}$ mouse genotypes. Heterozygous *Lrp5*$^{-/+}$ mice were discarded for this work. Adult animals were sacrificed at 16–18 weeks old after terminal anaesthesia (ketamine/medetomidine, 75 mg/kg and 1 mg/kg, respectively, i.p.). Mouse organs were collected, washed extensively in sterile saline, and frozen immediately in liquid nitrogen.

4.2. RNA Isolation and Real-Time PCR

Frozen mouse tissue samples from livers and brains were smashed to dust using mortar and liquid nitrogen. Pulverised tissues were processed for RNA extraction using RNEasy Kit from Qiagen (Qiagen, Hilden, Germany). Total RNA concentration and purity were determined using a Nanodrop ND-1000 Spectrophotometer (Nanodrop Technologies, Inc., Wilmington, DE, USA). For purity standards, only samples in which A260/A280 ratios were between 1.8 and 2.1 were considered acceptable. cDNA synthesis was performed using 1 µg RNA and cDNA reverse-transcription kit (Applied Biosystems, Foster City, CA, USA). The generated cDNA was amplified by real-time polymerase chain reaction in a 7900HT Fast Real-Time PCR System (Applied Biosystems, Foster City, CA, USA) using probes from Applied Biosystems. Different *LRP5* probes were used to detect different regions of the transcript: for exons 1–2, probe Mm00493179_m1 was used; for exons 9–10–11, probe Mm00493187_m1 was used; and for exons 22–23, probe Mm01227476_m1 was used (ThermoFisher, Waltham, MA, USA). Results were normalised against r18s mRNA expression, which was measured using a specific r18s probe from Applied Biosystems.

4.3. RNA-Seq Analysis

RNA was isolated from *Wt* or *Lrp5*$^{-/-}$ mouse brain and liver samples using the RNAEasy extraction kit from Qiagen. RNA samples were sent to "Centro Nacional de Análisis Genómico" (CNAG) for RNA sequencing and analysis. RNA purity was checked by A260/A280 and A260/A230 ratios, and only RNA with ratios between 1.8 and 2.1 was used for this analysis. RNA integrity was further analysed by Bioanalyzer 2100 (Agilent Tech, Santa Clara, CA, USA) using an Agilent RNA nano 6000 kit (Agilent Tech, Santa Clara, CA, USA), and only RNAs with an RNA Integrity Number >8 were accepted. RNA-seq reads were trimmed with TrimGalore (version 0.6.10, 2 Feb 2023) [43] and mapped against the *Mus musculus* reference genome (GRCm39) with STAR/2.7.8a [44] using ENCODE parameters. Genes and isoforms were quantified with RSEM/1.3.0 [45] with default parameters using the gencode.M32 annotation. Differential expression was performed with the R Package limma-voom (https://bioconductor.org/packages/release/bioc/html/limma.html (accessed on 15 May 2024)) [46], and differential transcript usage was determined with the DTUrtle R Package (https://tobitekath.github.io/DTUrtle/ (accessed on 15 May 2024)) [47].

4.4. In Silico Systems Biology Analysis

Data from the RNA-seq analysis of differentially expressed genes were imported into Cytoscape 3.10.0 to build a protein–protein interaction (PPI) network based on STRING database interaction data. The confidence cut-off value was set to 0.4. An additional node was added to the brain network to generate a minimal network of interacting proteins. To generate the networks, only protein-coding transcripts that showed altered expression between tissues from animals of different genotypes in the RNA-seq analysis were included for this study. In order to identify protein–protein interaction clusters, the community

cluster strategy GLay algorithm was used. Functional enrichment was performed with g:profiler [48] using as input a list of differentially expressed genes.

Gene Set Enrichment Analysis (GSEA) was performed using WebGestalt: update 2013 (Web-based Gene Set Analysis Toolkit) [49], and the "Geneontology" functional database was selected for the analysis. The top 10 most significant categories are shown in the results. Significance was considered for FDR values < 0.05. For GSEA, we used $\log_2$FC values, comparing the transcript expression of *Lrp5*$^{-/-}$ brain samples against *Wt* brain samples to rank genes.

4.5. Statistical Analysis

Experimental data were expressed as mean ± S.E.M. To assess alterations in the frequency of the genotypes of the different born mice, the chi-squared goodness-of-fit test was used. To establish significance, data were subjected to a one-way ANOVA followed by Bonferroni's multiple-comparisons test using GraphPad Prism software statistical package 10 (GraphPad Software, San Diego, CA, USA). The criterion for significance was set as a p value ≤ 0.05.

5. Conclusions

We describe for the first time that *LRP5* pre-mRNA undergoes differential splicing during mRNA maturation and that this splicing is tissue-dependent. *Lrp5*$^{-/-}$ mice that are unable to generate brain full-length *LRP5* cannot develop during the embryonic stages, explaining the unbalanced Mendelian pattern observed at birth. Our results support that *LRP5*'s brain expression is needed for the correct synthesis of vitamins and fatty acids, and subsequently, it is indispensable for normal brain development.

Supplementary Materials: The supporting information can be downloaded at https://www.mdpi.com/article/10.3390/ijms25126763/s1.

Author Contributions: Conceptualisation, A.L. and M.B.-P.; methodology, A.L.; software, A.L. and N.P.; validation, G.V., L.B. and M.B.-P.; formal analysis, A.L. and M.B.-P.; investigation, A.L., N.P. and M.B.-P.; resources, G.V., L.B. and M.B.-P.; data curation, A.L., N.P. and M.B.-P.; writing—original draft preparation, A.L. and M.B.-P.; writing—review and editing, G.V. and M.B.-P.; visualisation, L.B. and M.B.-P.; supervision, M.B.-P.; project administration, L.B. and M.B.-P.; funding acquisition, G.V., L.B. and M.B.-P. All authors have read and agreed to the published version of the manuscript.

Funding: This work was supported by the Spanish Ministry of Economy and Competitiveness of Science "Agencia Estatal de Investigación (AEI)" Proj. Ref. AEI/10.13039/501100011033-[PID2019-107160RB-I00]; Project PMP22/00108 to LB cofounded by FEDER "Una Manera de Hacer Europa"; the Institute of Health Carlos III (ISCIII) CIBERCV-CB16/11/00411 and ERA-CVD JTC 202-023/AC 209-00054 to LB and PI23-00589 to MBP; Red RICORS TERAV-RD21/0017/0013 to LB; FEC 2022 to MBP and Marato de TV3 202304-10 to MBP. AL is a predoctoral fellow (PRE2020-096422) associated to LB's grant PID2019-107160RB-I00. NP is part of the INVESTIGO-Program of the Spanish Ministery of Science.

Institutional Review Board Statement: The study protocol was conducted in conformity with the Public Health Service (PHS) Policy on Humane Care and Use of Laboratory Animals and was approved by the local institutional animal research committee (ICCC051/5422 date 11 March 2021).

Informed Consent Statement: Not applicable.

Data Availability Statement: The data that support the findings of this study are available from the corresponding author (MBP) upon reasonable request.

Acknowledgments: We thank S. Huertas for excellent technical assistance. We also thank A. Esteve and the CNAG team for assistance with the RNA-seq analysis.

Conflicts of Interest: Badimon L. declares to have acted as an SAB member of Sanofi, Novo Nordisk, Ionis, and IAF. Badimon L. and Vilahur G. are co-founders of the spin-off Ivestatin Therapeutics SL (unrelated to this work). The remaining authors have nothing to disclose.

References

1. Bhanot, P.; Brink, M.; Samos, C.H.; Hsieh, J.C.; Wang, Y.; Macke, J.P.; Andrew, D.; Nathans, J.N.R. A new member of the frizzled family from Drosophila functions as a Wingless receptor. *Nature* **1996**, *382*, 225–230. [CrossRef] [PubMed]
2. Yang-Snyder, J.; Miller, J.R.; Brown, J.D.; Lai, C.J.; Moon, R.T. A frizzled homolog functions in a vertebrate Wnt signaling pathway. *Curr. Biol.* **1996**, *6*, 1302–1306. [CrossRef] [PubMed]
3. Borrell-Pags, M.; Romero, J.C.; Juan-Babot, O.; Badimon, L. Wnt pathway activation, cell migration, and lipid uptake is regulated by low-density lipoprotein receptor-related protein 5 in human macrophages. *Eur. Heart J.* **2011**, *32*, 2841–2850. [CrossRef] [PubMed]
4. Wehrli, M.; Dougan, S.T.; Caldwell, K.; O'Keefe, L.; Schwartz, S.; Valzel-Ohayon, D.; Schejter, E.; Tomlinson, A.; DiNardo, S. Arrow encodes an LDL-receptor-related protein essential for Wingless signalling. *Nature* **2000**, *407*, 527–530. [CrossRef] [PubMed]
5. Siegfried, E.; Chou, T.B.; Perrimon, N. wingless signaling acts through zeste-white 3, the drosophila homolog of glycogen synthase kinase-3, to regulate engrailed and establish cell fate. *Cell* **1992**, *71*, 1167–1179. [CrossRef] [PubMed]
6. Behrens, J.; Jerchow, B.A.; Würtele, M.; Grimm, J.; Asbrand, C.; Wirtz, R.; Kühl, M.; Wedlich, D.; Birchmeier, W. Functional interaction of an axin homolog, conductin, with β-catenin, APC, and GSK3β. *Science* **1998**, *280*, 596–599. [CrossRef]
7. Behrens, J.; Von Kries, J.P.; Kühl, M.; Bruhn, L.; Wedlich, D.; Grosschedl, R.; Birchmeier, W. Functional interaction of β-catenin with the transcription factor LEF- 1. *Nature* **1996**, *382*, 638–642. [CrossRef] [PubMed]
8. Billin, A.N.; Thirlwell, H.; Ayer, D.E. β-Catenin–Histone Deacetylase Interactions Regulate the Transition of LEF1 from a Transcriptional Repressor to an Activator. *Mol. Cell. Biol.* **2000**, *20*, 6882–6890. [CrossRef]
9. He, T.C.; Sparks, A.B.; Rago, C.; Hermeking, H.; Zawel, L.; Da Costa, L.T.; Morin, P.J.; Vogelstein, B.; Kinzler, K.W. Identification of c-MYC as a target of the APC pathway. *Science* **1998**, *281*, 1509–1512. [CrossRef]
10. Shtutman, M.; Zhurinsky, J.; Simcha, I.; Albanese, C.; D'Amico, M.; Pestell, R.; Ben-Ze'ev, A. The cyclin D1 gene is a target of the β-catenin/LEF-1 pathway. *Proc. Natl. Acad. Sci. USA* **1999**, *96*, 5522–5527. [CrossRef]
11. Carter, M.; Chen, X.; Slowinska, B.; Minnerath, S.; Glickstein, S.; Shi, L.; Campagne, F.; Weinstein, H.; Ross, M.E. Crooked tail (Cd) model of human folate-responsive neural tube defects is mutated in Wnt coreceptor lipoprotein receptor-related protein 6. *Proc. Natl. Acad. Sci. USA* **2005**, *102*, 12843–12848. [CrossRef] [PubMed]
12. Ciani, L.; Salinas, P.C. WNTs in the vertebrate nervous system: From patterning to neuronal connectivity. *Nat. Rev. Neurosci.* **2005**, *6*, 351–362. [CrossRef] [PubMed]
13. Ahmad-Annuar, A.; Ciani, L.; Simeonidis, I.; Herreros, J.; Fredj, N.B.; Rosso, S.B.; Hall, A.; Brickley, S.; Salinas, P.C. Signaling across the synapse: A role for Wnt and Dishevelled in presynaptic assembly and neurotransmitter release. *J. Cell Biol.* **2006**, *174*, 127–139. [CrossRef] [PubMed]
14. Zechner, D.; Müller, T.; Wende, H.; Walther, I.; Taketo, M.M.; Crenshaw, E.B.; Treier, M.; Birchmeier, W.; Birchmeier, C. Bmp and Wnt/β-catenin signals control expression of the transcription factor Olig3 and the specification of spinal cord neurons. *Dev. Biol.* **2007**, *303*, 181–190. [CrossRef] [PubMed]
15. Varela-Nallar, L.; Alfaro, I.E.; Serrano, F.G.; Parodi, J.; Inestrosa, N.C. Wingless-type family member 5A (Wnt-5a) stimulates synaptic differentiation and function of glutamatergic synapses. *Proc. Natl. Acad. Sci. USA* **2010**, *107*, 21164–21169. [CrossRef] [PubMed]
16. Clark, C.E.J.; Nourse, C.C.; Cooper, H.M. The tangled web of non-canonical wnt signalling in neural migration. *NeuroSignals* **2012**, *20*, 202–220. [CrossRef] [PubMed]
17. Okerlund, N.D.; Cheyette, B.N.R. Synaptic Wnt signaling-a contributor to major psychiatric disorders? *J. Neurodev. Disord.* **2011**, *3*, 162–174. [CrossRef] [PubMed]
18. Valvezan, A.J.; Klein, P.S. GSK-3 and Wnt signaling in neurogenesis and bipolar disorder. *Front. Mol. Neurosci.* **2012**, *5*, 1. [CrossRef] [PubMed]
19. Jia, L.; Piña-Crespo, J.; Li, Y. Restoring Wnt/β-catenin signaling is a promising therapeutic strategy for Alzheimer's disease. *Mol. Brain* **2019**, *12*, 104. [CrossRef]
20. Ren, Q.; Chen, J.; Liu, Y. LRP5 and LRP6 in Wnt Signaling: Similarity and Divergence. *Front. Cell Dev. Biol.* **2021**, *9*, 670960. [CrossRef]
21. Grünblatt, E.; Nemoda, Z.; Werling, A.M.; Roth, A.; Angyal, N.; Tarnok, Z.; Thomsen, H.; Peters, T.; Hinney, A.; Hebebrand, J.; et al. The involvement of the canonical Wnt-signaling receptor LRP5 and LRP6 gene variants with ADHD and sexual dimorphism: Association study and meta-analysis. *Am. J. Med. Genet. Part B Neuropsychiatr. Genet.* **2019**, *180*, 365–376. [CrossRef]
22. Veerapathiran, S.; Teh, C.; Zhu, S.; Kartigayen, I.; Korzh, V.; Matsudaira, P.T.; Wohland, T. Wnt3 distribution in the zebrafish brain is determined by expression, diffusion and multiple molecular interactions. *eLife* **2020**, *9*, e59489. [CrossRef]
23. Borrell-Pages, M.; Vilahur, G.; Romero, J.C.; Casaní, L.; Bejar, M.T.; Badimon, L. LRP5/canonical Wnt signalling and healing of ischemic myocardium. *Basic. Res. Cardiol.* **2016**, *111*, 67. [CrossRef]
24. Borrell-Pagès, M.; Romero, J.C.; Badimon, L. LRP5 deficiency down-regulates Wnt signalling and promotes aortic lipid infiltration in hypercholesterolaemic mice. *J. Cell. Mol. Med.* **2015**, *19*, 770–777. [CrossRef]
25. Borrell-Pages, M.; Carolina Romero, J.; Badimon, L. LRP5 and plasma cholesterol levels modulate the canonical Wnt pathway in peripheral blood leukocytes. *Immunol. Cell Biol.* **2015**, *93*, 653–661. [CrossRef]
26. Badimon, L.; Luquero, A.; Crespo, J.; Peña, E.; Borrell-Pages, M. PCSK9 and LRP5 in macrophage lipid internalization and inflammation. *Cardiovasc. Res.* **2021**, *117*, 2054–2068. [CrossRef]

27. Borrell-Pages, M.; Luquero, A.; Vilahur, G.; Padró, T.; Badimon, L. Canonical Wnt pathway and the LDL receptor superfamily in neuronal cholesterol homeostasis and function. *Cardiovasc. Res.* **2023**, *120*, 140–151. [CrossRef]
28. Kato, M.; Patel, M.S.; Levasseur, R.; Lobov, I.; Chang, B.H.J.; Glass, D.A.; Hartmann, C.; Li, L.; Hwang, T.H.; Brayton, C.F.; et al. Cbfa1-independent decrease in osteoblast proliferation, osteopenia, and persistent embryonic eye vascularization in mice deficient in Lrp5, a Wnt coreceptor. *J. Cell Biol.* **2002**, *157*, 303–314. [CrossRef]
29. Ensembl. Mouse LRP5 Gene [Internet]. Available online: https://www.ensembl.org/Mus_musculus/Gene/Summary?db=core;g=ENSMUSG00000024913;r=19:3634828-3736564 (accessed on 1 May 2023).
30. Badimon, L.; Casaní, L.; Camino-Lopez, S.; Juan-Babot, O.; Borrell-Pages, M. GSK3β inhibition and canonical Wnt signaling in mice hearts after myocardial ischemic damage. *PLoS ONE* **2019**, *14*, e0218098. [CrossRef]
31. Luquero, A.; Vilahur, G.; Casani, L.; Badimon, L.; Borrell-Pages, M. Differential cholesterol uptake in liver cells: A role for PCSK9. *FASEB J.* **2022**, *36*, e22291. [CrossRef]
32. McCaffery, P.; Dräger, U.C. Regulation of retinoic acid signaling in the embryonic nervous system: A master differentiation factor. *Cytokine Growth Factor. Rev.* **2000**, *11*, 233–249. [CrossRef] [PubMed]
33. Maden, M. Retinoid signalling in the development of the central nervous system. *Nat. Rev. Neurosci.* **2002**, *3*, 843–853. [CrossRef] [PubMed]
34. Glaser, T.; Brüstle, O. Retinoic acid induction of ES-cell-derived neurons: The radial glia connection. *Trends Neurosci.* **2005**, *28*, 397–400. [CrossRef] [PubMed]
35. Olson, C.R.; Mello, C.V. Significance of vitamin A to brain function, behavior and learning. *Mol. Nutr. Food Res.* **2010**, *54*, 489–495. [CrossRef] [PubMed]
36. Queiroz, M.P.; Da Silva Lima, M.; Barbosa, M.Q.; De Melo, M.F.F.T.; De Menezes Santos Bertozzo, C.C.; De Oliveira, M.E.G.; Branquinho Bessa, R.J.; Almeida Alves, S.P.; Souza, M.I.A.; de Cassia Ramos do Egypto Queiroga, R.; et al. Effect of conjugated linoleic acid on memory and reflex maturation in rats treated during early life. *Front. Neurosci.* **2019**, *13*, 370. [CrossRef] [PubMed]
37. Taha, A.Y. Linoleic acid–good or bad for the brain? *NPJ Sci. Food* **2020**, *4*, 1. [CrossRef] [PubMed]
38. Wolffe, A.P.; Cooper, G.M. The Cell: A Molecular Approach. *Q. Rev. Biol.* **1998**, *73*, 69–70. [CrossRef]
39. Guo, Y.; Zi, X.; Koontz, Z.; Kim, A.; Xie, J.; Gorlick, R.; Holcombe, R.F.; Hoang, B.H. Blocking Wnt/LRP5 signaling by a soluble receptor modulates the epithelial to mesenchymal transition and suppresses met and metalloproteinases in osteosarcoma Saos-2 cells. *J. Orthop. Res.* **2007**, *25*, 964–971. [CrossRef]
40. Guo, Y.; Rubin, E.M.; Xie, J.; Zi, X.H.B. Dominant Negative LRP5 Decreases Tumorigenicity and Metastasis of Osteosarcoma in an Animal Model. *Clin. Orthop. Relat. Res.* **2008**, *466*, 2039–2045. [CrossRef]
41. Davisson, M.T. Rules and guidelines for nomenclature of mouse genes. *Gene* **1994**, *147*, 157–160. [CrossRef]
42. Holmen, S.L.; Giambernardi, T.A.; Zylstra, C.R.; Buckner-Berghuis, B.D.; Resau, J.H.; Hess, J.F.; Glatt, V.; Bouxsein, M.L.; Ai, M.; Warman, M.L.; et al. Decreased BMD and limb deformities in mice carrying mutations in both Lrp5 and Lrp6. *J. Bone Miner. Res.* **2004**, *19*, 2033–2040. [CrossRef] [PubMed]
43. Krueger, F. TrimGalore [Internet]. Available online: https://github.com/FelixKrueger/TrimGalore (accessed on 1 May 2023).
44. Dobin, A.; Davis, C.A.; Schlesinger, F.; Drenkow, J.; Zaleski, C.; Jha, S.; Batut, P.; Chaisson, M.; Gingeras, T.R. STAR: Ultrafast universal RNA-seq aligner. *Bioinformatics* **2013**, *29*, 15–21. [CrossRef] [PubMed]
45. Li, B.; Dewey, C.N. RSEM: Accurate transcript quantification from RNA-Seq data with or without a reference genome. *BMC Bioinform.* **2011**, *12*, 323. [CrossRef] [PubMed]
46. Ritchie, M.E.; Phipson, B.; Wu, D.; Hu, Y.; Law, C.W.; Shi, W.; Smyth, G.K. Limma powers differential expression analyses for RNA-sequencing and microarray studies. *Nucleic Acids Res.* **2015**, *43*, e47. [CrossRef] [PubMed]
47. Tekath, T.; Dugas, M. Differential transcript usage analysis of bulk and single-cell RNA-seq data with DTUrtle. *Bioinformatics* **2021**, *37*, 3781–3787. [CrossRef] [PubMed]
48. Raudvere, U.; Kolberg, L.; Kuzmin, I.; Arak, T.; Adler, P.; Peterson, H.; Vilo, J. G:Profiler: A web server for functional enrichment analysis and conversions of gene lists (2019 update). *Nucleic Acids Res.* **2019**, *47*, W191–W198. [CrossRef]
49. Wang, J.; Duncan, D.; Shi, Z.; Zhang, B. WEB-based GEne SeT AnaLysis Toolkit (WebGestalt): Update 2013. *Nucleic Acids Res.* **2013**, *41*, W77–W83. [CrossRef]

Supplementary Figure S1

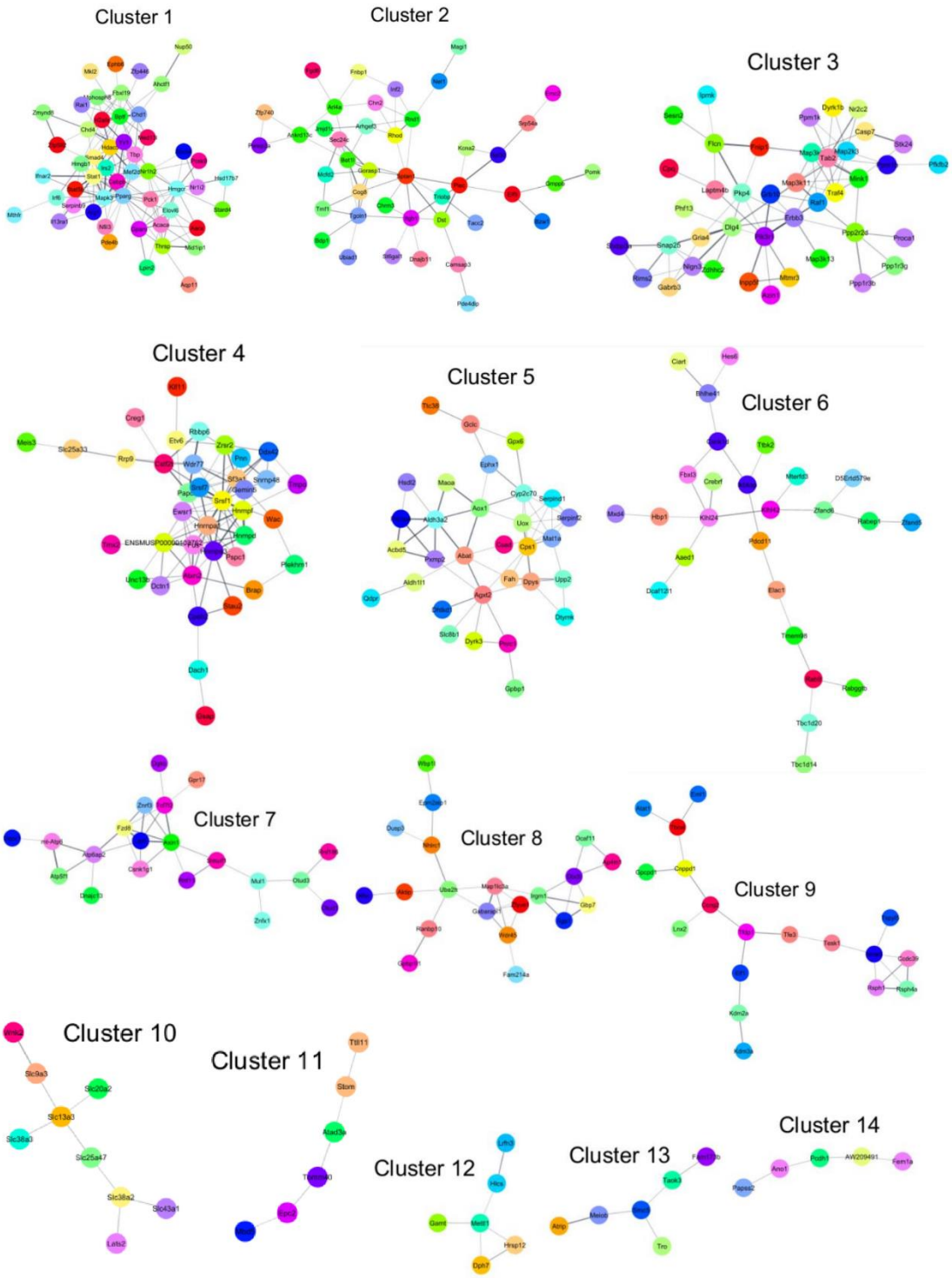

Supplementary Table S1

Cluster #	Enrichment retrieval	Term name	FDR value
Cluster 1	Regulation of cellular biosynthetic process	GO:0031326	4.33×10^{-9}
	Regulation of transcription	GO:0006355	3.82×10^{-8}
Cluster 2	Transport to the Golgi and subsequent modification	MMU-948021	8.48×10^{-5}
	Organelle	GO:0043226	0.005
Cluster 3	Positive regulation of signalling	GO:0023056	6.11×10^{-10}
	Regulation of phosphate metabolic processes	GO:0019220	3.56×10^{-9}
Cluster 4	Nucleic acid binding	GO:0003676	8.53×10^{-14}
	mRNA splicing	MMU-72172	6.48×10^{-13}
Cluster 5	Small molecule metabolic process	GO:0044281	6.75×10^{-10}
	Cellular catabolic process	GO:0044248	3.12×10^{-8}
Cluster 6	Circadian rhythm	CL:4564	2.5×10^{-4}
Cluster 7	WNT Signalling Pathway	KW-0879	7.88×10^{-6}
Cluster 8	Autophagy	GO:0006914	4.1×10^{-4}
Cluster 9	Mixed, incl. axoneme assembly, and Trichohyalin-plectin-homology domain	CL:11382	0.0017
Cluster 10	Transport of inorganic cations/anions and amino acids/oligopeptides	MMU-425393	2.83×10^{-7}
Cluster 11	Ganglion	BTO:0000497	0.0372
Cluster 13	DNA repair	GO:0006281	0.029

Supplementary Figure S1. Clustering of liver protein-protein interaction network. Clustering was performed using Glay clustering algorithm in Cytoscape software. Clustering resulted in the formation of 14 isolated clusters. Data available upon demand to authors.

Supplementary Table S1. Functional gene enrichment analysis was performed separately for each of the clusters generated using Glay clustering algorithm. Table shows cellular functions altered in Lrp5-/- mice livers, with the corresponding term name and a FDR value calculated by STRING enrichment algorithm in Cytoscape software.

4. Discussion

“Even the smallest person can change the course of the future”

Galadriel to Frodo, from the film adaptation “The Lord of the Rings: The Fellowship of the Ring” by Peter Jackson. Based on the books by J.R.R.Tolkien.

The canonical WNT signalling is an ancient evolutionary pathway conserved in multicellular organisms (350). The role of the different members of the canonical WNT pathway is under constant investigation as new roles for the molecular pathway are continuously described.

Both LRP5 and LRP6 trigger the canonical WNT signalling pathway and share 71% sequence homology. Deficit of LRP5 might be partially covered by LRP6 and vice versa (351). However, the expression of both receptors is needed for canonical WNT signalling activation in osteoblasts for normal skeletal homeostasis in mice (352). Moreover, in mammary epithelial cells both receptors need to form an heterodimer to transduce WNT ligand signalling (353). Nonetheless, our results in cell models lacking LRP5 expression and in the *Lrp5*$^{-/-}$ mice model show that LRP5 has unique roles in anti-inflammatory, anti-apoptotic and pro-survival processes.

Atherosclerosis remains a life-threatening disease with a complicated diagnosis and a complicated therapeutical approach. The total annual costs of treating people with atherosclerosis-derived CVD only in the US is of 431.8 billion dollars with a projected cost of 1.1 trillion dollars by 2035 (11). Subsequently, the investment on CVD research is also gigantic. The Global Cardiovascular Research Funders Forum (GCRFF), which includes the American Heart Association and its homologues in Britain, Canada, Australia and others support more than 600 million dollars in CVD annually. The investment from public funds and pharmaceutical companies surpasses that quantity by far. This allows the development of precise biologically-based therapies including Sanofi's alirocumab or Amgen's evolocumab, both PCSK9 inhibitors (254,255).

4.1 LRP5 has different roles in macrophages during atherosclerosis progression

One of the PCSK9's main functions is the regulation of circulating LDL cholesterol through LDLR processing in liver cells; however, it has additional CVD-related roles. PCSK9 induces foam cell formation as loss of PCSK9 in human macrophages reduces modified lipid internalization and atherosclerosis progression (354). Hence, besides lowering LDL cholesterol levels, it is likely that PCSK9 inhibitors are preventing atherosclerotic plaque build-up. LRP5 and PCSK9 are needed for lipid uptake in macrophages. When the expression of either of the two proteins is blocked, there is less intracellular cholesterol accumulation. Furthermore, LRP5 participates in the secretion of PCSK9 pathway. However, silencing LRP5 expression does not completely abolish PCSK9 release to the extracellular milieu indicating that other pathways are involved in PCSK9's endosome trafficking to the cell membrane.

We have described a dual role for LRP5 in macrophages. After lipid exposure, LRP5 participates in PCSK9 release which then facilitates lipid accumulation triggering a pro-inflammatory signal that induces IL-1β and TNFα release. As well, LRP5 promotes an anti-inflammatory phenotype in macrophages treated with LRP5-containing MVs, while LRP5-depleted MVs promote a pro-inflammatory phenotype. However, these two mechanisms do not necessarily exclude each other. Furthermore, LRP5 expression increases in human macrophages after lipid-loading (Article 1 and Article 4). LRP5 participates in PCSK9 release as an early-response to lipid exposure. After lipid-loading, LRP5 exerts a secondary anti-inflammatory role by regulating cell-cell communication through MVs. Our findings reveal that in control conditions, LRP5 is located in the vesicular bodies of the cytoplasm of the macrophage and after lipid exposure LRP5 is transported to the

plasma membrane together with PCSK9. PCSK9 is then released to the extracellular media while LRP5 remains in the macrophage cell membrane. This process occurs in pro-inflammatory macrophages, generating an early response to lipid rich milieu that leads to lipid uptake.

LRP5 expression increases in macrophages and macrophage derived-MVs of both M1 and M2 macrophage subtypes, revealing a role for the receptor in both pro- and anti-inflammatory responses. M2 macrophages can differentiate to M1 macrophages after exposure to pro-inflammatory stimuli (355), for example high lipid concentrations. Therefore, a phenotype switch can occur between resting macrophages with cytoplasm-located-LRP5 and activated membrane-located-LRP5 macrophages. Reasonably, LRP5 has to be located at the cell membrane in order to be included in macrophage-derived MVs; which, once released, will regulate the anti-inflammatory response in receiving macrophages. Lack of LRP5 in MV-derived from donor macrophages triggers an inflammatory response in the receiving cells indicating an anti-inflammatory role for LRP5 in lipid loaded macrophages. Although we do not know the mechanism, it is plausible that MVs from LRP5-depleted macrophage when fusing with the membranes of naïve macrophage reduce the concentration of LRP5 that could lead to a reduction in canonical WNT signalling in the host macrophage and hence reduced pro-survival signalling. This would guide naïve macrophage to a higher pro-inflammatory state. Our group has previously shown that M2 macrophages express LRP5 in advanced human atherosclerotic plaques indicating that LRP5 participates in the remodelling process of the vascular wall (236). This indicates that LRP5 is playing a role in the early-inflammatory response by promoting macrophage lipid internalization together with PCSK9, while, during the tissue-remodelling phase MVs released by macrophages containing

LRP5 can display a homeostatic function regulating the motility and phagocytic process of macrophages (**Figure 15**).

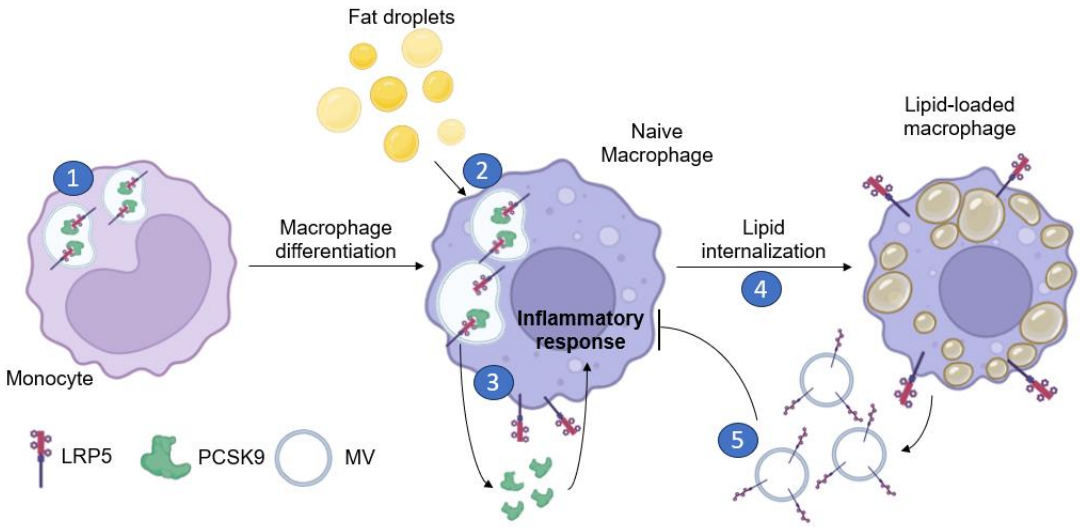

Figure 15. LRP5-related mechanisms in macrophages during atherosclerosis.

(1) Monocyte express LRP5 and PCSK9 in internal vesicles.
(2) Lipid exposure induces a rapid release of PCSK9 aided by LRP5.
(3) PCSK9 release triggers an inflammatory response and induces LRP5 translocation to the cell membrane leading to lipid internalization.
(4) Lipid-loading reduces PCSK9 gene expression and LRP5 is highly expressed in the cell membrane.
(5) LRP5^{+}MVs released by lipid-loaded macrophages prevent inflammatory responses in macrophages.

A similar anti-inflammatory role is described for LRP5 in adipose tissue. Indeed, the anti-inflammatory macrophage markers CD163 and CD206 increase their gene expression in VAT and SCAT of HC Wt and HC Lrp5-/- mice compared to their NC littermates. Interestingly, Lrp5-/- mice consistently show lower expression of macrophage anti-inflammatory markers than Wt mice suggesting an anti-inflammatory role for LRP5 in VAT and SCAT and in line with our previous results where LRP5 expression is associated to the anti-inflammatory macrophage phenotype (Article 4).

SREBP2 transcription factor, the main regulator of PCSK9 gene transcription, has a different role in monocytes and macrophages (251). Monocytes are non-adherent cells that do not express cholesterol ester internalization receptors; therefore, intracellular cholesterol levels in monocytes are low, SREBP2 transcription factor is active and PCSK9 levels are high (356,357). However, when monocytes differentiate into tissue-resident macrophages and are treated with lipids they release PCSK9. In lipid-loaded macrophages, SREBP2 is inactive, preventing PCSK9 protein expression (358). Therefore, monocyte-derived macrophages release PCSK9 after lipid exposure and intracellular concentrations of PCSK9 remain low.

Macrophages infiltrating capacity into the adipose tissue is induced by LRP5. We show that LRP5 activation by hypercholesterolemia can trigger adipose tissue growth by inducing tissue proliferation and insulin sensitivity and it can simultaneously enhance the infiltration of macrophages into adipose tissues that will start the inflammatory process associated to a proliferating adipose tissue (Article 3).

4.2 LRP5 roles in liver cholesterol metabolism

PCSK9 expression and release pattern by HSC is very similar to that observed in human macrophages. Cultured HSC have a phenotype that resembles the myofibroblast pathogenic phenotype associated to liver fibrosis, with high expression of desmin and alpha-smooth muscle actin (α-SMA) and without retinyl ester lipid droplets (359). However, agLDL exposure to HSCs induces intracellular cholesterol accumulation that is reduced by LRP5 and/or PCSK9 downregulated expression. Hence, high cholesterol levels can repress HSC proliferation and induce their dedifferentiation into cholesterol accumulating cells, with a lower fibrotic phenotype. Previous results showed reduced cholesteryl ester internalization by PCSK9 in hepatocytes (246,247). However, PCSK9-silencing in HepG2 cells did not affect cholesterol ester accumulation

(Article 2). This might happen because HepG2 cells are fully loaded with lipids and their capacity to keep uptaking lipids is blocked. Therefore, whether PCSK9 is or not released does not affect hepatocyte's lipid internalization. The *in vitro* model does not fully resemble the *in vivo* situation where excessive hepatocyte's cholesterol can be secreted through bile salts. Cholesterol secretion through bile salts allows a continuous lipid uptake and PCSK9 actually exerts its blocking function. Hence, PCSK9 function is cell specific; while it blocks lipid accumulation in hepatocytes, it triggers the accumulation of cholesteryl esters in HSCs or macrophages, cell subtypes that typically accumulate fat. In structural hepatocytes (HepG2), cholesterol accumulates by LDLR, which without PCSK9 regulation, would induce exacerbated lipid-loading and a liver-steatosis phenotype as a result of increased oxidative stress and endoplasmic reticulum stress (360–362). Therefore, we show that cells that accumulate lipids share a common pathway to uptake cholesterol.

Interestingly, the interaction observed between LRP5 and PCSK9 in human macrophages does not seem to be taking place in mice adipose tissue. PCSK9 intracellular levels of lipid-loaded macrophages are low because it is transported to the plasma membrane and released to the extracellular milieu in a process that involves LRP5. However, because PCSK9 levels do not decrease after HC diets in mice adipose tissue we believe this mechanism takes place in macrophages but not in adipocytes. Indeed, our results show that PCSK9 is highly expressed in mice VAT and EAT. In a similar way, human PCSK9 gene expression in VAT is associated with an elevated body mass index and a pro-inflammatory profile, which is consistent with the elevated PCSK9 gene levels observed in mice (363).

Hepatocytes and HSC are not exposed to agLDL *in vivo*, as this form of LDL is only generated in the intima vasculature. Nevertheless, both cellular types uptake cholesterol from agLDLs revealing that both cell

types express the receptors needed for agLDL internalization. Scavenger receptors SR-BI/SR-BII and CD36 are known to participate in this process (364,365). Additionally, we show that PCSK9 and LRP5 also participate in HSC cholesterol uptake.

High VLDLR, LRP2, and LRP6 expression are found in livers of hypercholesterolemic *Wt* mice but not in livers of hypercholesterolemic *Lrp5*$^{-/-}$ mice. VLDLR and LRP2 expression are regulated in the liver by peroxisome proliferator-activated receptor alpha (PPARα), a transcription factor that responds to polyunsaturated free-fatty acids (366,367). Upon liver pathogenic stimuli, *β-catenin*$^{-/-}$ mice show disrupted PPARα signalling leading to fatty acid accumulation, steatosis, and redox imbalance, ultimately leading to steatohepatitis development (368,369). Hence, it is likely that *Lrp5*$^{-/-}$ mice have similar liver complications, which would result in the downregulation of VLDLR and LRP2 expression levels. Reduction of LRP6 expression levels in hypercholesterolemic *Lrp5*$^{-/-}$ mice might be caused by the negative feedback loop that the triggering of the canonical WNT signalling induces in the expression of its own members (370). In fact, RNA-seq analysis show that the logFC value for VLDLR, LRP2 and LRP6 protein-coding transcripts between *Lrp5*$^{-/-}$ mice liver samples and *Wt* mice liver samples were -1.95, -1.14, and -0.44, respectively, indicating that the average gene expression for these receptors is downregulated in *Lrp5*$^{-/-}$ mice. Additionally, functional gene enrichment analysis on RNA-seq data of *Lrp5*$^{-/-}$ mice liver samples unmasked dysregulations in several signalling pathways that can affect liver integrity.

4.3 LRP5 role in the brain

The canonical WNT signalling pathway regulates synapse formation and neuronal function (315–317). However, the specific role of LRP5 in the brain has been poorly studied. We first analysed the role of LRP5 in neuronal cholesterol homeostasis in the SH-SY5y neuroblastoma cell

line that has been extensively used as an *in vitro* model to assess neurotoxicity, ischemia and other processes (371,372). SH-SY5y cells were differentiated to mature neurons by retinoic acid (373–375).

Hypercholesterolemic diets increase the BBB permeability to blood metabolites allowing for the leaking of nLDL into the brain interstitial fluid (302). Furthermore, the BBB leakage of cholesterol has been associated with morphological changes in mice brain, reduced synaptic formation, and cell death in *Ldlr*$^{-/-}$ mice (311). Cholesterol overload in neurons increases endoplasmic reticulum stress and induces neuronal apoptosis, resulting in brain atrophy and reduced cognitive function in mice (376). Rats fed a hypercholesterolemic diet display brain reduced LDLR expression levels to compensate for cholesterol overload in neurons (308). Our results support these reports as only LDLR-silenced SH-SY5y showed reduced cholesterol internalization after LDL incubation. LRP1, LRP5, or CD36 are not involved in neuronal cholesterol accumulation (Article 5).

The canonical WNT signalling is involved in pro-survival mechanisms in neurons (377–379). Activation of the canonical WNT signalling in SH-SY5y cells results in doxorubicin resistance inducing cell survival (380,381). Doxorubicin is a potent chemotherapeutic drug that induces DNA cross-linking, oxidative stress, and cell death (382). Also, LRP5 gene expression is upregulated in neuroblastoma patients samples with high *Myc* (a canonical WNT target gene) expression, suggesting that LRP5 is involved in neuronal cell proliferation and survival (383). Our results support a role for LRP5 in neuronal survival too. LRP5-silenced differentiated SH-SY5y exposed to H_2O_2 or staurosporine showed increased levels of active caspase-3 levels and more Annexin V in the outer plasma membrane.

Incubation of SH-SY5y with nLDL led to enhanced expression of canonical WNT signalling proteins. Lipid-loading induces lipotoxicity as neurons start to use fatty acids as their energy source; however, neurons lack the appropriate antioxidative mechanisms to compensate for ROS generation associated to lipid β-oxidation and require of glial cells to counteract ROS generation (384). It is our hypothesis that differentiated SH-SY5y cells overexpress canonical WNT signalling to compensate for the toxic effects of lipid loading by the triggering of pro-survival signals.

Retinoic acid is essential for a correct brain development both in embryonic and postnatal stages as it regulates brain development, neurogenesis, neuronal plasticity and synapses formation (385–387). Retinoic acid signals through RAR and RXR, transcription factors with a wide expression in rodent and human brains (388,389). Retinol/ Vitamin A, the retinoic acid precursor, is transported through the bloodstream bound to retinol binding protein 4 (RBP4) (390). Once inside the cell, retinol is oxidized to retinaldehyde by retinol dehydrogenases or alcohol dehydrogenases in the rate-limiting reaction of the retinoic acid metabolic pathway (391). Gene expression levels of both dehydrogenases are downregulated in brains of *Lrp5*$^{-/-}$ mice. As a consequence, retinoic acid levels in brains of *Lrp5*$^{-/-}$ mice are much lower than in *Wt* mice, limiting the activation of RAR and RXR transcription factors and reducing the transcription of retinoic acid target genes including members of the P450 cytochrome or the UDP glucuronosyltransferases. These proteins are involved in retinoic acid release by increasing the conversion rate of retinoic acid into polar metabolites with increased capacity to cross the cell plasma membrane (392,393). It is conceivable that the lower intracellular concentration of retinoic acid downregulates the expression of the enzymes required for its cellular release to prevent excessive retinoic acid loss.

A significant downregulation of genes associated with linoleic acid metabolism was observed in *Lrp5*$^{-/-}$ mice brains compared to *Wt* mice brains. When linoleic acid enters the brain, it is rapidly oxidized into acetyl-CoA and derivatives, which are used for *de novo* cholesterol synthesis (394). However, linoleic acid also participates in the synthesis of oxidized linoleic acid metabolites (OXLAMs), which are lipid mediators regulating inflammatory and pain responses in the central nervous system (395). The cytochrome P450 is involved in the generation of a particular type of OXLAM, the epoxy-polyunsaturated fatty acids (epoxy-PUFAs), known to have neuroprotective and analgesic effects in the brain (396,397). Phospholipase A2 expression is also downregulated in *Lrp5*$^{-/-}$ mice brains. This enzyme catalyses the hydrolyzation of glycerophospholipids into FFAs and glycerol (398), suggesting a reduced FFA availability in brains of *Lrp5*$^{-/-}$.

The combined signalling by retinoic and linoleic acid seems to be crucial to preserve the functional integrity of mice brains. Functional Gene Enrichment analysis showed reduced synapses formation and plasticity and less neuronal differentiation in brains of *Lrp5*$^{-/-}$ mice. However, the link between LRP5 deficiency and the alterations observed in their brains is difficult to establish. In hepatocytes, β-catenin induces the expression of cytochrome P450 isoform 1a1 (399). In mice mammary cells, the stimulated by retinoic acid gene 6 (STRA6) retinol transporter expression is induced by Wnt3a and Wnt1 synergistically with retinoic acid (400,401). Also, β-catenin has been shown to interact directly with RARs in a retinoic acid-dependent manner inducing RAR activity in cancerous cells (402,403). We did not observe reduced expression of transcripts coding for protein members of the canonical WNT pathway in *Lrp5*$^{-/-}$ mice brains, suggesting that the pathway is open and may be active. To explore this possibility, proteomic analysis to assess which

proteins are activated by canonical WNT ligand incubation in neurons with or without LRP5 expression could be performed.

The persistent expression of a full-length LRP5 transcript in *Lrp5*$^{-/-}$ mice brains was an unexpected result. The *Lrp5*$^{-/-}$ mice colony was generated by an insertion of an IRES-βGal-PGKNeo cassette in exon 6, impairing the natural splicing of the transcript and generating an aberrant LRP5 isoform (404). This should have led to the complete abolishment of LRP5 expression in *Lrp5*$^{-/-}$ mice. Indeed, the expression of the full-length LRP5 transcript is absent from all mice tissues and organs except for the brain. Hence, we hypothesize that LRP5 brain expression is required to ensure mice survival. The reduced expression of the full-length LRP5 transcript in *Lrp5*$^{-/-}$ mice brains reduce synapse formation and neuronal differentiation involving a downregulation of retinoic and linoleic acid signalling.

During development and neuronal cell differentiation splicing regulators determine transcripts formation (405). For example, serine/arginine-rich splicing factor 1 (SRSF1) blocks the insertion of exon 19 in the apoER2 final transcript in neurons in a mice transgenic model for Alzheimer's disease. Inhibition of SRSF1 binding to apoER2 mRNA with antisense oligonucleotides generates a functional apoER2 transcript (406). Although the expression of a full-length LRP5 protein is observed in brains of *Lrp5*$^{-/-}$ mice (Article 5), non-functional proteins can be generated in *Lrp5*$^{-/-}$ mice brains according to the following possibilities:

- The insertion of an IRES-βGal-PGKNeo cassette generates a premature STOP codon in exon 6. When the full-length LRP5 transcript is produced, it should only contain the first 6 exons of LRP5. This protein would contain aminoacids that form the extracellular domain of LRP5; therefore, when synthesized, it would be transported through the Golgi apparatus and, upon reaching the

cell membrane, would be released into the extracellular medium as it would lack any transmembrane domain. In this scenario, soluble LRP5-like protein would act as a repressor of canonical WNT signalling (as soluble Frizzled receptors) by competing with canonical receptors for the binding of WNT ligands, reducing signal transduction (407). Soluble LRP5 can also participate in modulating the activity of other signalling pathways.

- The alternative splicing of the LRP5 transcript undergoes alternative splicing in *Lrp5*$^{-/-}$ mice brains that manage to skip exon 6 during the transcript maturation process. Although unlikely, the generation of this alternative transcript would generate a shorter protein. Exon 6 contains aminoacids 338 to 470 of mice LRP5 which are part of the second β-propeller and the LDL-receptor class B domains 6 and 7, necessary for the correct folding of the receptor and WNT ligand recognition (218).

We observed a faint, yet non-negligible, ~180 kDa protein in brains of *Lrp5*$^{-/-}$ mice (Article 5). The existence of this protein could be explained by the alternative splicing of Lrp5 transcript that manages to skip exon 6 during transcript maturation. Future studies will attempt to determine if this isoform is functional by studying its interactome and its ability to transduce canonical WNT signalling.

Our results support that LRP5-dependent signalling is crucial to ensure proper brain development and mice survival. To further analyze LRP5 transcript composition in *Lrp5*$^{-/-}$ mice exon sequencing would need to be performed. Behavioural and memory tests in *Wt* and *Lrp5*$^{-/-}$ mice would help define the functional consequences of LRP5 deficiency in mice brains.

4.4 Summary of LRP5 function

In summary, the novel findings of this thesis include the definition of properties and functions of the canonical WNT signalling receptor LRP5 in multiple tissues: (1) we have identified LRP5 as a major regulator of the immune response to cholesterol accumulation in the vessel wall during early and late stages of atherosclerosis; (2) we have identified a function for LRP5 in liver hepatic stellate cells during hypercholesterolemia; (3) we have described a role for LRP5 in neuronal survival and brain development; and, (4) we have shown that LRP5 is involved in adipose tissue growth in mice fed a hypercholesterolemic diet by regulating adipose tissue insulin-sensitivity and inflammatory cell infiltration (**Figure 16**).

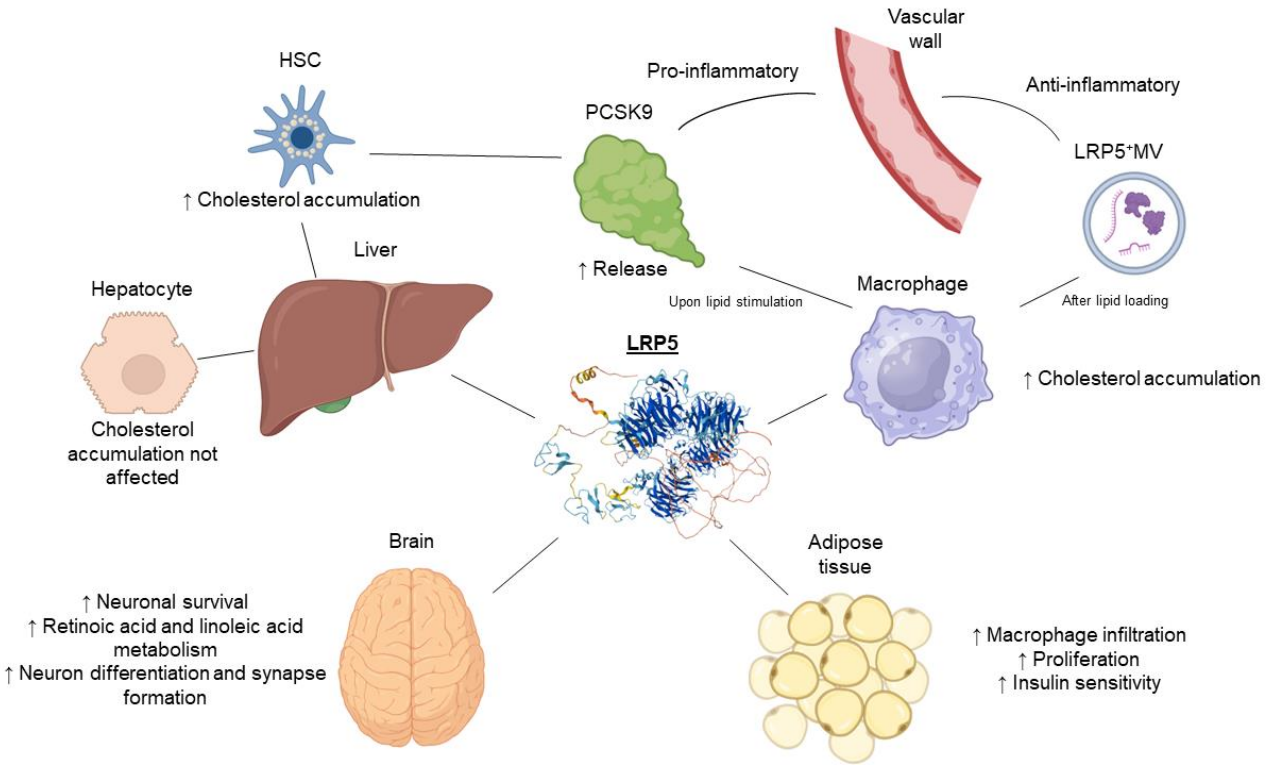

Figure 16. Summary of functions related to LRP5 in the different organs studied in this thesis.

The findings on adipose tissue and brain revealed interactions of LRP5 and canonical WNT signalling with other important cellular pathways including retinoic acid metabolism and insulin response. Hence, it is conceivable that to understand the complete dysregulation triggered by LRP5 deficiency, the focus needs not only be centred on modulations of canonical WNT signalling but also on other important regulators of cellular response.

Long-term studies might lead to the generation of therapies targeting LRP5 function in disease progression. These therapies will need to be cell-specific because systemic therapies targeting LRP5 activity may yield unwanted effects since they could affect several molecular and cellular mechanisms affecting the homeostasis of multiple tissues. In 2018, a LRP5/6 antagonist product developed by Boehringer Ingelheim, BI 905677, was tested in patients with advanced, unresectable, and/or metastatic tumours but the results of the study have yet to be published. BI 905677 is a humanized biparatopic nanobody that blocks WNT ligand binding to LRP5/6 and reduces canonical WNT signalling activation in cancerous cells, which stops cell proliferation and survival signalling (408).

5. Conclusions

“Faithless is he that says farewell when the road darkens.”

Gimli to the Fellowship of the Ring members*. The Fellowship of the Ring, Chapter 3*. J.R.R. Tolkien

LRP5 regulates biological processes that take place in different tissues and organs. Specifically, the novel main findings of this thesis are as follows:

1. LRP5 and PCSK9 participate in lipid uptake in fat-storing cells including macrophages and HSC.
2. LRP5 expressed in human macrophages binds PCSK9 in the early cellular endosomes and regulates PCSK9 release into the extracellular media.
3. PCSK9 blocks lipid internalization in HepG2, while it triggers the accumulation of cholesteryl esters in HSC indicating that structural hepatocytes and HSCs uptake lipids in a different manner.
4. LRP5 is involved in adipose tissue growth by inducing tissue proliferation and insulin sensitivity and, simultaneously, by enhancing macrophages infiltrating capacity into the adipose tissue triggering the inflammatory response.
5. In resting macrophages, LRP5 overexpression triggers a pro-inflammatory response by inducing PCSK9 release. However, in lipid-loaded macrophages, LRP5 exerts an anti-inflammatory response mediated by MVs as $LRP5^{+}$MVs induce macrophage differentiation to an anti-inflammatory phenotype.
6. LRP5 and the canonical WNT signalling do not participate in cholesterol uptake in neurons. LRP5 expression induces survival in stress-exposed neurons by preserving cell viability and reducing apoptosis.
7. LRP5-deficiency in mice brains induces a downregulation in the expression of genes associated with synapse formation and neuronal differentiation. The alteration in these functions is a consequence of reduced signalling of the retinoic and linoleic acid pathways.

6. References

“The burned hand teaches best. After that, advice about fire goes to the heart”.

Gandalf to Aragorn, Legolas and Gimli. *The Two Towers, Chapter 5*. J.R.R. Tolkien

1. Dunbar SB, Khavjou OA, Bakas T, Hunt G, Kirch RA, Leib AR, et al. Projected Costs of Informal Caregiving for Cardiovascular Disease: 2015 to 2035: A Policy Statement From the American Heart Association. Circulation. 2018;137(19):e558–77.

2. Olvera Lopez E, Ballard BD JA. Cardiovascular Disease [Internet]. StatPearls [Internet]. 2023 [cited 2023 Aug 22]. Available from: https://www.ncbi.nlm.nih.gov/books/NBK535419/

3. Allam AH, Thompson RC, Wann LS, Miyamoto MI, Thomas GS. Computed tomographic assessment of atherosclerosis in ancient Egyptian mummies. JAMA. 2009;302(19):2091–4.

4. Teo KK, Rafiq T. Cardiovascular Risk Factors and Prevention: A Perspective From Developing Countries. Canadian Journal of Cardiology. 2021;37(5):733–43.

5. Gaziano TA, Bitton A, Anand S, Abrahams-Gessel S, Murphy A. Growing Epidemic of Coronary Heart Disease in Low- and Middle-Income Countries. Current Problems in Cardiology. 2010;35(2):72–115.

6. Yusuf PS, Hawken S, Ôunpuu S, Dans T, Avezum A, Lanas F, et al. Effect of potentially modifiable risk factors associated with myocardial infarction in 52 countries (the INTERHEART study): Case-control study. Lancet. 2004;364(9438):937–52.

7. O'Donnell MJ, Chin SL, Rangarajan S, Xavier D, Liu L, Zhang H, et al. Global and regional effects of potentially modifiable risk factors associated with acute stroke in 32 countries (INTERSTROKE): a case-control study. The Lancet. 2016;388(10046):761–75.

8. Hoffman JIE. Odds Ratio, Relative Risk, Attributable Risk, and Number Needed to Treat. In: Basic Biostatistics for Medical and Biomedical Practitioners. 2019. p. 295–310.

9. Pencina MJ, Navar AM, Wojdyla D, Sanchez RJ, Khan I, Elassal J, et al. Quantifying Importance of Major Risk Factors for Coronary Heart Disease. Circulation. 2019;139(13):1603–11.

10. Bays HE, Kulkarni A, German C, Satish P, Iluyomade A, Dudum R, et al. Ten things to know about ten cardiovascular disease risk factors – 2022. American Journal of Preventive Cardiology. 2022;10:100342.

11. Benjamin EJ, Virani SS, Callaway CW, Chamberlain AM, Chang AR, Cheng S, et al. American Heart Association Council on Epidemiology and Prevention Statistics Committee and Stroke Statistics Subcommittee Heart Disease and Stroke Statistics-2018 Update: A Report From the American Heart Association. Circulation. 2018;137:e67–492.

12. Jenča D, Melenovský V, Stehlik J, Staněk V, Kettner J, Kautzner J, et al. Heart failure after myocardial infarction: incidence and predictors. ESC Heart Failure. 2021;8(1):222–37.

13. Prasad K. Current Status of Primary, Secondary, and Tertiary Prevention of Coronary Artery Disease. International Journal of Angiology. 2021;30(3):177–86.

14. Unal B, Critchley JA, Capewell S. Explaining the Decline in Coronary Heart Disease Mortality in England and Wales between 1981 and 2000. Circulation. 2004;109(9):1101–7.

15. Christopher Jones R, Pothier CE, Blackstone EH, Lauer MS.

Prognostic importance of presenting symptoms in patients undergoing exercise testing for evaluation of known or suspected coronary disease. American Journal of Medicine. 2004;117(6):380–9.

16. Master AM, Geller AJ. The extent of completely asymptomatic coronary artery disease. The American Journal of Cardiology. 1969;23(2):173–9.

17. Vallejo-Vaz AJ, Robertson M, Catapano AL, Watts GF, Kastelein JJ, Packard CJ, et al. Low-density lipoprotein cholesterol lowering for the primary prevention of cardiovascular disease among men with primary elevations of low-density lipoprotein cholesterol levels of 190 mg/dL or above: Analyses from the WOSCOPS (West of Scotland coronary prevention study) 5-year randomized trial and 20-year observational follow-up. Circulation. 2017;136(20):1878–91.

18. Collins R, Armitage J, Parish S, Sleight P, Peto R. MRC/BHF Heart Protection Study of cholesterol lowering with simvastatin in 20 536 high-risk individuals: A randomised placebo-controlled trial. Lancet. 2002;360(9326):7–22.

19. Simes RJ, Hunt D, Kirby A, Tonkin A, Keech A, Aylward P, et al. Long-term effectiveness and safety of pravastatin in 9014 patients with coronary heart disease and average cholesterol concentrations: The LIPID trial follow-up. Lancet. 2002;359(9315):1379–87.

20. Odden MC, Pletcher MJ, Coxson PG, Thekkethala D, Guzman D, Heller D, et al. Cost-effectiveness and population impact of statins for primary prevention in adults aged 75 years or older in the United States. Annals of internal medicine. 2015 Apr

21;162(8):533–41.

21. Istvan ES, Deisenhofer J. Structural mechanism for statin inhibition of HMG-CoA reductase. Science. 2001;292(5519):1160–4.

22. Corsini A, Maggi FM, Catapano AL. Pharmacology of competitive inhibitors of HMg-CoA reductase. Pharmacological Research. 1995;31(1):9–27.

23. Gordon-Larsen P, Heymsfield SB. Obesity as a Disease, Not a Behavior. Circulation. 2018;137(15):1543–5.

24. Lizcano F. The beige adipocyte as a therapy for metabolic diseases. International Journal of Molecular Sciences. 2019;20(20):5058.

25. Britton KA, Massaro JM, Murabito JM, Kreger BE, Hoffmann U, Fox CS. Body fat distribution, incident cardiovascular disease, cancer, and all-cause mortality. Journal of the American College of Cardiology. 2013;62(10):921–5.

26. Ibrahim MM. Subcutaneous and visceral adipose tissue: structural and functional differences. Obesity reviews : an official journal of the International Association for the Study of Obesity. 2010 Jan;11(1):11–8.

27. Weisberg SP, McCann D, Desai M, Rosenbaum M, Leibel RL, Ferrante AW. Obesity is associated with macrophage accumulation in adipose tissue. The Journal of clinical investigation. 2003 Dec;112(12):1796–808.

28. Freedland ES. Role of a critical visceral adipose tissue threshold (CVATT) in metabolic syndrome: implications for controlling

dietary carbohydrates: a review. Nutrition & metabolism. 2004 Nov 5;1(1):12.

29. Chait A, den Hartigh LJ. Adipose Tissue Distribution, Inflammation and Its Metabolic Consequences, Including Diabetes and Cardiovascular Disease. Frontiers in cardiovascular medicine. 2020;7:22.

30. González Jiménez E. [Body composition: assessment and clinical value]. Endocrinologia y nutricion : organo de la Sociedad Espanola de Endocrinologia y Nutricion. 2013 Feb;60(2):69–75.

31. Sironi AM, Gastaldelli A, Mari A, Ciociaro D, Positano V, Buzzigoli E, et al. Visceral fat in hypertension: influence on insulin resistance and beta-cell function. Hypertension (Dallas, Tex : 1979). 2004 Aug;44(2):127–33.

32. Lemieux S, Després JP. Metabolic complications of visceral obesity: contribution to the aetiology of type 2 diabetes and implications for prevention and treatment. Diabete & metabolisme. 1994;20(4):375–93.

33. Neeland IJ, Ross R, Després J-P, Matsuzawa Y, Yamashita S, Shai I, et al. Visceral and ectopic fat, atherosclerosis, and cardiometabolic disease: a position statement. The lancet Diabetes & endocrinology. 2019 Sep;7(9):715–25.

34. Snijder MB, Flyvbjerg A, Stehouwer CDA, Frystyk J, Henry RMA, Seidell JC, et al. Relationship of adiposity with arterial stiffness as mediated by adiponectin in older men and women: the Hoorn Study. European journal of endocrinology. 2009 Mar;160(3):387–95.

35. Antonopoulos AS, Antoniades C. The role of epicardial adipose tissue in cardiac biology: classic concepts and emerging roles. The Journal of physiology. 2017 Jun 15;595(12):3907–17.

36. Wisneski JA, Gertz EW, Neese RA, Mayr M. Myocardial metabolism of free fatty acids. Studies with 14C-labeled substrates in humans. The Journal of clinical investigation. 1987 Feb;79(2):359–66.

37. Iacobellis G, Willens HJ. Echocardiographic epicardial fat: a review of research and clinical applications. Journal of the American Society of Echocardiography : official publication of the American Society of Echocardiography. 2009 Dec;22(12):1311–9; quiz 1417–8.

38. Feingold KR. Introduction to Lipids and Lipoproteins [Internet]. Endotext. 2024 [cited 2024 Jan 14]. Available from: https://www.ncbi.nlm.nih.gov/books/NBK305896/

39. Smith LC, Pownall HJ, Gotto AM. The plasma lipoproteins: structure and metabolism. Annual review of biochemistry. 1978;47:751–7.

40. Lampsas S, Xenou M, Oikonomou E, Pantelidis P, Lysandrou A, Sarantos S, et al. Lipoprotein(a) in Atherosclerotic Diseases: From Pathophysiology to Diagnosis and Treatment. Molecules. 2023;28(3):969.

41. Groen AK, Bloks VW, Verkade H, Kuipers F. Cross-talk between liver and intestine in control of cholesterol and energy homeostasis. Molecular Aspects of Medicine. 2014;37:77–88.

42. Püschel GP, Henkel J. Dietary cholesterol does not break your

heart but kills your liver. Porto Biomedical Journal. 2018;3(1):e12.

43. Goldstein JL, Brown MS. Regulation of the mevalonate pathway. Nature. 1990;343(6257):425–30.

44. Xu Z, McClure ST, Appel LJ. Dietary cholesterol intake and sources among U.S adults: Results from national health and nutrition examination surveys (NHANES), 2001–2014. Nutrients. 2018;10(6):771.

45. Brunzell JD, Hazzard WR, Porte D, Bierman EL. Evidence for a common, saturable, triglyceride removal mechanism for chylomicrons and very low density lipoproteins in man. Journal of Clinical Investigation. 1973;52(7):1578–85.

46. Olivecrona G, Beisiegel U. Lipid binding of apolipoprotein CII is required for stimulation of lipoprotein lipase activity against apolipoprotein CII-deficient chylomicrons. Arteriosclerosis, Thrombosis, and Vascular Biology. 1997;17(8):1545–9.

47. Abumrad NA, El-Maghrabi MR, Amri EZ, Lopez E, Grimaldi PA. Cloning of a rat adipocyte membrane protein implicated in binding or transport of long-chain fatty acids that is induced during preadipocyte differentiation: Homology with human CD36. Journal of Biological Chemistry. 1993;268(24):17665–8.

48. Ibrahimi A, Bonen A, Blinn WD, Hajri T, Li X, Zhong K, et al. Muscle-specific overexpression of FAT/CD36 enhances fatty acid oxidation by contracting muscle, reduces plasma triglycerides and fatty acids, and increases plasma glucose and insulin. Journal of Biological Chemistry. 1999;274(38):26761–6.

49. Kazantzis M, Stahl A. Fatty acid transport proteins, implications

in physiology and disease. Biochimica et Biophysica Acta. 2012;1821(5):852–7.

50. Björkegren J, Packard CJ, Hamsten A, Bedford D, Caslake M, Foster L, et al. Accumulation of large very low density lipoprotein in plasma during intravenous infusion of a chylomicron-like triglyceride emulsion reflects competition for a common lipolytic pathway. Journal of Lipid Research. 1996;37(1):76–86.

51. Mjos OD, Faergeman O, Hamilton RL, Havel RJ. Characterization of remnants produced during the metabolism of triglyceride rich lipoproteins of blood plasma and intestinal lymph in the rat. Journal of Clinical Investigation. 1975;56(3):603–15.

52. Pagnan A, Havel RJ, Kane JP, Kotite L. Characterization of human very low density lipoproteins containing two electrophoretic populations: double pre-beta lipoproteinemia and primary dysbetalipoproteinemia. Journal of Lipid Research. 1977;18(5):613–22.

53. Mahley RW, Hui DY, Innerarity TL, Beisiegel U. Chylomicron remnant metabolism. Role of hepatic lipoprotein receptors in mediating uptake. Arteriosclerosis. 1989;9(1 SUPPL.):I14–8.

54. Langer T, Strober W, Levy RI. The metabolism of low density lipoprotein in familial type II hyperlipoproteinemia. The Journal of clinical investigation. 1972;51(6):1528–36.

55. Osono Y, Woollett LA, Herz J, Dietschy JM. Role of the low density lipoprotein receptor in the flux of cholesterol through the plasma and across the tissues of the mouse. Journal of Clinical Investigation. 1995;95(3):1124–32.

56. Horton JD, Goldstein JL, Brown MS. SREBPs: Activators of the complete program of cholesterol and fatty acid synthesis in the liver. Journal of Clinical Investigation. 2002;109(9):1125–31.

57. Streicher R, Kotzka J, Müller-Wieland D, Siemeister G, Munck M, Avci H, et al. SREBP-1 mediates activation of the low density lipoprotein receptor promoter by insulin and insulin-like growth factor-I. Journal of Biological Chemistry. 1996;271(12):7128–33.

58. Daemen S, Kutmon M, Evelo CT. A pathway approach to investigate the function and regulation of SREBPs. Genes and Nutrition. 2013;8(3):289–300.

59. Yokoyama C, Wang X, Briggs MR, Admon A, Wu J, Hua X, et al. SREBP-1, a basic-helix-loop-helix-leucine zipper protein that controls transcription of the low density lipoprotein receptor gene. Cell. 1993;75(1):187–97.

60. Wu N, Sarna LK, Hwang SY, Zhu Q, Wang P, Siow YL, et al. Activation of 3-hydroxy-3-methylglutaryl coenzyme A (HMG-CoA) reductase during high fat diet feeding. Biochimica et Biophysica Acta - Molecular Basis of Disease. 2013;1832(10):1560–8.

61. Ouimet M, Barrett TJ, Fisher EA. HDL and Reverse Cholesterol Transport. Circulation Research. 2019;124(10):1505–18.

62. Assmann G, Gotto AM. HDL cholesterol and protective factors in atherosclerosis. Circulation. 2004;109(23 SUPPL 1):III8–14.

63. Glomset JA. The plasma lecithins:cholesterol acyltransferase reaction. Journal of Lipid Research. 1968;9(2):155–67.

64. Kennedy MA, Barrera GC, Nakamura K, Baldán Á, Tarr P, Fishbein MC, et al. ABCG1 has a critical role in mediating

cholesterol efflux to HDL and preventing cellular lipid accumulation. Cell Metabolism. 2005;1(2):121–31.

65. Tall AR. Plasma cholesteryl ester transfer protein. Journal of Lipid Research. 1993;34(8):663–72.

66. Barter PJ, Brewer HB, Chapman MJ, Hennekens CH, Rader DJ, Tall AR. Cholesteryl ester transfer protein: A novel target for raising HDL and inhibiting atherosclerosis. Vol. 23, Arteriosclerosis, Thrombosis, and Vascular Biology. 2003. p. 160–7.

67. Krieger M. Charting the fate of the “good cholesterol”: Identification and characterization of the high-density lipoprotein receptor SR-BI. Annual Review of Biochemistry. 1999;68:523–58.

68. Kalra A, Yetiskul E, Wehrle CJ, Tuma F. Physiology, Liver. 2024.

69. Ben-Moshe S, Itzkovitz S. Spatial heterogeneity in the mammalian liver. Nature Reviews Gastroenterology and Hepatology. 2019;16(7):395–410.

70. Halpern KB, Shenhav R, Matcovitch-Natan O, Tóth B, Lemze D, Golan M, et al. Single-cell spatial reconstruction reveals global division of labour in the mammalian liver. Nature. 2017;542(7641):352–6.

71. Cunningham RP, Porat-Shliom N. Liver Zonation – Revisiting Old Questions With New Technologies. Frontiers in Physiology. 2021;12:732929.

72. Hendriks HFJ, Verhoofstad WAMM, Brouwer A, De Leeuw AM, Knook DL. Perisinusoidal fat-storing cells are the main vitamin A

storage sites in rat liver. Experimental Cell Research. 1985;160(1):138–49.

73. Yamada M, Blaner WS, Soprano DR, Dixon JL, Kjeldbye HM, Goodman DS. Biochemical characteristics of isolated rat liver stellate cells. Hepatology. 1987;7(6):1224–9.

74. Giampieri MP, Jezequel AM, Orlandi F. The lipocytes in normal human liver. A quantitative study. Digestion. 1981;22(4):165–9.

75. Dixon LJ, Barnes M, Tang H, Pritchard MT, Nagy LE. Kupffer cells in the liver. Comprehensive Physiology. 2013;3(2):785–97.

76. Poisson J, Lemoinne S, Boulanger C, Durand F, Moreau R, Valla D, et al. Liver sinusoidal endothelial cells: Physiology and role in liver diseases. Journal of Hepatology. 2017;66(1):212–27.

77. Mederacke I, Hsu CC, Troeger JS, Huebener P, Mu X, Dapito DH, et al. Fate tracing reveals hepatic stellate cells as dominant contributors to liver fibrosis independent of its aetiology. Nature Communications. 2013;4:2823.

78. Friedman SL, Roll FJ, Boyles J, Bissell DM. Hepatic lipocytes: The principal collagen-producing cells of normal rat liver. Proceedings of the National Academy of Sciences of the United States of America. 1985;82(24):8681–5.

79. Gudas LJ. Retinoid metabolism: new insights. Journal of Molecular Endocrinology. 2022;69(4):T37–49.

80. Qian L, Zolfaghari R, Ross AC. Liver-specific cytochrome P450 CYP2C22 is a direct target of retinoic acid and a retinoic acid-metabolizing enzyme in rat liver. Journal of Lipid Research. 2010;51(7):1781–92.

81. Miyahara T, Schrum L, Rippe R, Xiong S, Yee J, Motomura K, et al. Peroxisome proliferator-activated receptors and hepatic stellate cell activation. Journal of Biological Chemistry. 2000;275(46):35715–22.

82. Frostegård J. Immunity, atherosclerosis and cardiovascular disease. BMC Medicine. 2013;11:117.

83. Lusis AJ. Atherosclerosis. Nature [Internet]. 2000 Sep 14 [cited 2022 Apr 26];407(6801):233–41. Available from: https://pubmed.ncbi.nlm.nih.gov/11001066/

84. Holzapfel GA, Sommer G, Regitnig P. Anisotropic mechanical properties of tissue components in human atherosclerotic plaques. Journal of Biomechanical Engineering. 2004;126(5):657–65.

85. Kobielarz M, Kozuń M, Gąsior-Głogowska M, Chwiłkowska A. Mechanical and structural properties of different types of human aortic atherosclerotic plaques. Journal of the Mechanical Behavior of Biomedical Materials. 2020;109:103837.

86. Singh RB, Mengi SA, Xu YJ, Arneja AS, Dhalla NS. Pathogenesis of atherosclerosis: A multifactorial process. Experimental and Clinical Cardiology. 2002;7(1):40–53.

87. Vanhoutte PM. Endothelial dysfunction - The first step toward coronary arteriosclerosis. Circulation Journal. 2009;73(4):595–601.

88. Lin Z, Natesan V, Shi H, Dong F, Kawanami D, Mahabeleshwar GH, et al. Kruppel-like factor 2 regulates endothelial barrier function. Arteriosclerosis, Thrombosis, and Vascular Biology.

2010;30(10):1952–9.

89. Dekker RJ, Van Thienen J V., Rohlena J, De Jager SC, Elderkamp YW, Seppen J, et al. Endothelial KLF2 links local arterial shear stress levels to the expression of vascular tone-regulating genes. American Journal of Pathology. 2005;167(2):609–18.

90. Huang H, Ren P, Zhao Y, Weng H, Jia C, Yu F, et al. Low shear stress induces inflammatory response via CX3CR1/NF-κB signal pathway in human umbilical vein endothelial cells. Tissue and Cell. 2023;82:102043.

91. Wu D, Huang RT, Hamanaka RB, Krause M, Oh MJ, Kuo CH, et al. HIF-1α is required for disturbed flow-induced metabolic reprogramming in human and porcine vascular endothelium. eLife. 2017;6:e25217.

92. Feng S, Bowden N, Fragiadaki M, Souilhol C, Hsiao S, Mahmoud M, et al. Mechanical Activation of Hypoxia-Inducible Factor 1α Drives Endothelial Dysfunction at Atheroprone Sites. Arteriosclerosis, Thrombosis, and Vascular Biology. 2017 Nov;37(11):2087–101.

93. Cramer T, Yamanishi Y, Clausen BE, Förster I, Pawlinski R, Mackman N, et al. HIF-1α Is Essential for Myeloid Cell-Mediated Inflammation. Cell. 2003 Mar 7;112(5):645–57.

94. Rius J, Guma M, Schachtrup C, Akassoglou K, Zinkernagel AS, Nizet V, et al. NF-κB links innate immunity to the hypoxic response through transcriptional regulation of HIF-1α. Nature. 2008;453(7196):807–11.

95. Urschel K, Cicha I, Daniel WG, Garlichs CD. Shear stress patterns affect the secreted chemokine profile in endothelial cells. Clinical Hemorheology and Microcirculation. 2012;50(1–2):143–52.

96. Yao Y, Rabodzey A, Dewey CF. Glycocalyx modulates the motility and proliferative response of vascular endothelium to fluid shear stress. American Journal of Physiology - Heart and Circulatory Physiology. 2007;293(2):H1023–30.

97. Weinbaum S, Tarbell JM, Damiano ER. The structure and function of the endothelial glycocalyx layer. Annual Review of Biomedical Engineering. 2007;9:121–67.

98. Liu X, Fan Y, Deng X. Effect of the endothelial glycocalyx layer on arterial LDL transport under normal and high pressure. Journal of Theoretical Biology. 2011;283(1):71–81.

99. Predescu SA, Predescu DN, Malik AB. Molecular determinants of endothelial transcytosis and their role in endothelial permeability. American Journal of Physiology - Lung Cellular and Molecular Physiology. 2007;293(4):L823–42.

100. Komarova YA, Kruse K, Mehta D, Malik AB. Protein Interactions at Endothelial Junctions and Signaling Mechanisms Regulating Endothelial Permeability. Circulation Research. 2017;120(1):179–206.

101. Sun SW, Zu XY, Tuo QH, Chen LX, Lei XY, Li K, et al. Caveolae and caveolin-1 mediate endocytosis and transcytosis of oxidized low density lipoprotein in endothelial cells. Acta Pharmacologica Sinica. 2010;31(10):1336–42.

102. Ramirez CM, Zhang X, Bandyopadhyay C, Rotllan N, Sugiyama MG, Aryal B, et al. Caveolin-1 regulates atherogenesis by attenuating low-density lipoprotein transcytosis and vascular inflammation independently of endothelial nitric oxide synthase activation. Circulation. 2019;140(3):225–39.

103. Huang L, Chambliss KL, Gao X, Yuhanna IS, Behling-Kelly E, Bergaya S, et al. SR-B1 drives endothelial cell LDL transcytosis via DOCK4 to promote atherosclerosis. Nature. 2019;569(7757):565–9.

104. Kraehling JR, Chidlow JH, Rajagopal C, Sugiyama MG, Fowler JW, Lee MY, et al. Genome-wide RNAi screen reveals ALK1 mediates LDL uptake and transcytosis in endothelial cells. Nature Communications. 2016;7:13516.

105. Clary DO, Rothman JE. Purification of three related peripheral membrane proteins needed for vesicular transport. Journal of Biological Chemistry. 1990;265(17):10109–17.

106. Nordestgaard BG, Nielsen LB. Atherosclerosis and arterial influx of lipoproteins. Current Opinion in Lipidology. 1994;5(4):252–7.

107. Jang E, Robert J, Rohrer L, von Eckardstein A, Lee WL. Transendothelial transport of lipoproteins. Atherosclerosis. 2020;315:111–25.

108. Schwenke DC, Carew TE. Initiation of atherosclerotic lesions in cholesterol-fed rabbits. II. Selective retention of LDL vs. selective increases in LDL permeability in susceptible sites of arteries. Arteriosclerosis. 1989;9(6):908–18.

109. Ross R, Glomset J, Harker L. Response to injury and

atherogenesis. American Journal of Pathology. 1977;86(3):675–84.

110. Zhang X, Sessa WC, Fernández-Hernando C. Endothelial Transcytosis of Lipoproteins in Atherosclerosis. Frontiers in Cardiovascular Medicine. 2018;5:130.

111. Steinbrecher UP, Parthasarathy S, Leake DS, Witztum JL, Steinberg D. Modification of low density lipoprotein by endothelial cells involves lipid peroxidation and degradation of low density lipoprotein phospholipids. Proceedings of the National Academy of Sciences of the United States of America. 1984;81(12):3883–7.

112. Schuh J, Fairclough GF, Haschemeyer RH. Oxygen-mediated heterogeneity of apo-low-density lipoprotein. Proceedings of the National Academy of Sciences of the United States of America. 1978;75(7):3173–7.

113. Goldstein JL, Ho YK, Basu SK, Brown MS. Binding site on macrophages that mediates uptake and degradation of acetylated low density lipoprotein, producing massive cholesterol deposition. Proceedings of the National Academy of Sciences of the United States of America. 1979;76(1):333–7.

114. Henriksen T, Mahoney EM, Steinberg D. Enhanced macrophage degradation of low density lipoprotein previously incubated with cultured endothelial cells: Recognition by receptors for acetylated low density lipoproteins. Proceedings of the National Academy of Sciences of the United States of America. 1981;78(10):6499–503.

115. Steinbrecher UP, Fisher M, Witztum JL, Curtiss LK.

Immunogenicity of homologous low density lipoprotein after methylation, ethylation, acetylation, or carbamylation: Generation of antibodies specific for derivatized lysine. Journal of Lipid Research. 1984;25(10):1109–16.

116. Bucala R, Makita Z, Koschinsky T, Cerami A, Vlassara H. Lipid advanced glycosylation: Pathway for lipid oxidation in vivo. Proceedings of the National Academy of Sciences of the United States of America. 1993;90(14):6434–8.

117. Avogaro P, Cazzolato G, Bittolo-Bon G. Some questions concerning a small, more electronegative LDL circulating in human plasma. Atherosclerosis. 1991;91(1–2):163–71.

118. Orekhov AN, Bobryshev Y V., Sobenin IA, Melnichenko AA, Chistiakov DA. Modified low density lipoprotein and lipoprotein-containing circulating immune complexes as diagnostic and prognostic biomarkers of atherosclerosis and type 1 diabetes macrovascular disease. International Journal of Molecular Sciences. 2014;15(7):12807–41.

119. Williams KJ, Tabas I. The response-to-retention hypothesis of early atherogenesis. Arteriosclerosis, Thrombosis, and Vascular Biology. 1995;15(5):551–61.

120. Borén J, John Chapman M, Krauss RM, Packard CJ, Bentzon JF, Binder CJ, et al. Low-density lipoproteins cause atherosclerotic cardiovascular disease: Pathophysiological, genetic, and therapeutic insights: A consensus statement from the European Atherosclerosis Society Consensus Panel. European Heart Journal. 2020;41(24):2313–30.

121. Lu M, Gursky O. Aggregation and fusion of low-density

lipoproteins in vivo and in vitro. Biomolecular Concepts. 2013;4(5):501–18.

122. Oorni K, Pentikainen MO, Ala-Korpela M, Kovanen PT. Aggregation, fusion, and vesicle formation of modified low density lipoprotein particles: Molecular mechanisms and effects on matrix interactions. Journal of Lipid Research. 2000;41(11):1703–14.

123. Öörni K, Kovanen PT. Aggregation susceptibility of low-density lipoproteins—a novel modifiable biomarker of cardiovascular risk. Journal of Clinical Medicine. 2021;10(8):1769.

124. Szmitko PE, Wang CH, Weisel RD, De Almeida JR, Anderson TJ, Verma S. New Markers of Inflammation and Endothelial Cell Activation Part I. Circulation. 2003;108(16):1917–23.

125. Ohta H, Wada H, Niwa T, Kirii H, Iwamoto N, Fujii H, et al. Disruption of tumor necrosis factor-α gene diminishes the development of atherosclerosis in ApoE-deficient mice. Atherosclerosis. 2005;180(1):11–7.

126. Johnson-Tidey RR, McGregor JL, Taylor PR, Poston RN. Increase in the adhesion molecule P-selectin in endothelium overlying atherosclerotic plaques: Coexpression with intercellular adhesion molecule-1. American Journal of Pathology. 1994;144(5):952–61.

127. Nakashima Y, Raines EW, Plump AS, Breslow JL, Ross R. Upregulation of VCAM-1 and ICAM-1 at atherosclerosis-prone sites on the endothelium in the apoE-deficient mouse. Arteriosclerosis, Thrombosis, and Vascular Biology. 1998;18(5):842–51.

128. Razeghian-Jahromi I, Karimi Akhormeh A, Razmkhah M, Zibaeenezhad MJ. Immune system and atherosclerosis: Hostile or friendly relationship. International Journal of Immunopathology and Pharmacology. 2022;36:3946320221092188.

129. Ley K, Miller YI, Hedrick CC. Monocyte and macrophage dynamics during atherogenesis. Arteriosclerosis, Thrombosis, and Vascular Biology. 2011;31(7):1506–16.

130. Alexander MR, Owens GK. Epigenetic control of smooth muscle cell differentiation and phenotypic switching in vascular development and disease. Annual Review of Physiology. 2012;74:13–40.

131. Owens GK, Kumar MS, Wamhoff BR. Molecular regulation of vascular smooth muscle cell differentiation in development and disease. Physiological Reviews. 2004;84(3):767–801.

132. Orekhov AN, R. Andreeva E, Mikhailova IA, Gordon D. Cell proliferation in normal and atherosclerotic human aorta: Proliferative splash in lipid-rich lesions. Atherosclerosis. 1998;139(1):41–8.

133. Mulvihill ER, Jaeger J, Sengupta R, Ruzzo WL, Reimer C, Lukito S, et al. Atherosclerotic plaque smooth muscle cells have a distinct phenotype. Arteriosclerosis, Thrombosis, and Vascular Biology. 2004;24(7):1283–9.

134. Allahverdian S, Chaabane C, Boukais K, Francis GA, Bochaton-Piallat ML. Smooth muscle cell fate and plasticity in atherosclerosis. Cardiovascular Research. 2018;114(4):540–50.

135. Herijgers N, Van Eck M, Groot PHE, Hoogerbrugge PM, Van

Berkel TJC. Low Density Lipoprotein Receptor of Macrophages Facilitates Atherosclerotic Lesion Formation in C57Bl/6 Mice. Arteriosclerosis, Thrombosis, and Vascular Biology. 2000 Aug;20(8):1961–7.

136. Yancey PG, Blakemore J, Ding L, Fan D, Overton CD, Zhang Y, et al. Macrophage LRP-1 controls plaque cellularity by regulating efferocytosis and Akt activation. Arteriosclerosis, Thrombosis, and Vascular Biology. 2010;30(4):787–95.

137. Manning-Tobin JJ, Moore KJ, Seimon TA, Bell SA, Sharuk M, Alvarez-Leite JI, et al. Loss of SR-A and CD36 activity reduces atherosclerotic lesion complexity without abrogating foam cell formation in hyperlipidemic mice. Arteriosclerosis, Thrombosis, and Vascular Biology. 2009;29(1):19–26.

138. Kunjathoor V V., Febbraio M, Podrez EA, Moore KJ, Andersson L, Koehn S, et al. Scavenger receptors class A-I/II and CD36 are the principal receptors responsible for the uptake of modified low density lipoprotein leading to lipid loading in macrophages. Journal of Biological Chemistry. 2002;277(51):49982–8.

139. Yoshida H, Kondratenko N, Green S, Steinberg D, Quehenberger O. Identification of the lectin-like receptor for oxidized low-density lipoprotein in human macrophages and its potential role as a scavenger receptor. Biochemical Journal. 1998;334(1):9–13.

140. Moore KJ, Tabas I. Macrophages in the pathogenesis of atherosclerosis. Cell. 2011;145(3):341–55.

141. Pan H, Xue C, Auerbach BJ, Fan J, Bashore AC, Cui J, et al. Single-Cell Genomics Reveals a Novel Cell State During Smooth Muscle Cell Phenotypic Switching and Potential Therapeutic

Targets for Atherosclerosis in Mouse and Human. Circulation. 2020;142(21):2060–75.

142. Maguire EM, Pearce SWA, Xiao Q. Foam cell formation: A new target for fighting atherosclerosis and cardiovascular disease. Vascular Pharmacology. 2019;112:54–71.

143. Tabas I. Consequences and therapeutic implications of macrophage apoptosis in atherosclerosis: The importance of lesion stage and phagocytic efficiency. Arteriosclerosis, Thrombosis, and Vascular Biology. 2005;25(11):2255–64.

144. Virmani R, Burke AP, Kolodgie FD, Farb A. Vulnerable plaque: The pathology of unstable coronary lesions. Journal of Interventional Cardiology. 2002;15(6):439–46.

145. Rock KL, Kono H. The Inflammatory Response to Cell Death. Annual Review of Pathology: Mechanisms of Disease. 2008 Feb 1;3(1):99–126.

146. Rai V, Agrawal DK. The role of damage- and pathogen-associated molecular patterns in inflammation-mediated vulnerability of atherosclerotic plaques. Canadian Journal of Physiology and Pharmacology. 2017 Oct;95(10):1245–53.

147. Falk E. Unstable angina with fatal outcome: dynamic coronary thrombosis leading to infarction and/or sudden death. Autopsy evidence of recurrent mural thrombosis with peripheral embolization culminating in total vascular occlusion. Circulation. 1985;71(4):699–708.

148. Falk E, Shah PK, Fuster V. Coronary plaque disruption. Circulation. 1995;92(3):657–71.

149. Braganza DM, Bennett MR. New insights into atherosclerotic plaque rupture. Postgraduate Medical Journal. 2001;77(904):94–8.

150. Hara H, Yokoyama S. Interaction of free apolipoproteins with macrophages: Formation of high density lipoprotein-like lipoproteins and reduction of cellular cholesterol. Journal of Biological Chemistry. 1991;266(5):3080–6.

151. Oram JF, Albers JJ, Cheung MC, Bierman EL. The effect of subfractions of high density lipoprotein on cholesterol efflux from cultured fibroblasts. Regulation of low density lipoprotein receptor activity. Journal of Biological Chemistry. 1981;256(16):8348–56.

152. Palombo C, Kozakova M. Arterial stiffness, atherosclerosis and cardiovascular risk: Pathophysiologic mechanisms and emerging clinical indications. Vascular Pharmacology. 2016;77:1–7.

153. Martinez-Quinones P, McCarthy CG, Watts SW, Klee NS, Komic A, Calmasini FB, et al. Hypertension Induced Morphological and Physiological Changes in Cells of the Arterial Wall. American Journal of Hypertension. 2018 Sep 11;31(10):1067–78.

154. Fuchs FD, Whelton PK. High Blood Pressure and Cardiovascular Disease. Hypertension. 2020 Feb;75(2):285–92.

155. Akashi K, Traver D, Miyamoto T, Weissman IL. A clonogenic common myeloid progenitor that gives rise to all myeloid lineages. Nature. 2000;404(6774):193–7.

156. Mueller UG, Malloch D, Rehner S a, Schultz TR, Currie CR, Adams RMM, et al. A clonogenic Bone Marrow Progenitor Specific for Macrophages and Dendritic cells. Science.

2006;311(5757):83–7.

157. Auffray C, Fogg D, Garfa M, Elain G, Join-Lambert O, Kayal S, et al. Monitoring of blood vessels and tissues by a population of monocytes with patrolling behavior. Science. 2007;317(5838):666–70.

158. Carlin LM, Stamatiades EG, Auffray C, Hanna RN, Glover L, Vizcay-Barrena G, et al. Nr4a1-dependent Ly6Clow monocytes monitor endothelial cells and orchestrate their disposal. Cell. 2013;153(2):362–75.

159. Wolf AA, Yáñez A, Barman PK, Goodridge HS. The ontogeny of monocyte subsets. Frontiers in Immunology. 2019;10:1642.

160. Italiani P, Boraschi D. From Monocytes to M1/M2 Macrophages: Phenotypical vs. Functional Differentiation. Frontiers in Immunology. 2014;5:514.

161. Nahrendorf M, Swirski FK, Aikawa E, Stangenberg L, Wurdinger T, Figueiredo J-L, et al. The healing myocardium sequentially mobilizes two monocyte subsets with divergent and complementary functions. The Journal of Experimental Medicine. 2007 Nov 26;204(12):3037–47.

162. Arnold L, Henry A, Poron F, Baba-Amer Y, van Rooijen N, Plonquet A, et al. Inflammatory monocytes recruited after skeletal muscle injury switch into antiinflammatory macrophages to support myogenesis. The Journal of Experimental Medicine. 2007 May 14;204(5):1057–69.

163. Crane MJ, Daley JM, van Houtte O, Brancato SK, Henry WL, Albina JE. The Monocyte to Macrophage Transition in the Murine

Sterile Wound. PLoS ONE. 2014 Jan 22;9(1):e86660.

164. Fleetwood AJ, Lawrence T, Hamilton JA, Cook AD. Granulocyte-Macrophage Colony-Stimulating Factor (CSF) and Macrophage CSF-Dependent Macrophage Phenotypes Display Differences in Cytokine Profiles and Transcription Factor Activities: Implications for CSF Blockade in Inflammation. The Journal of Immunology. 2007 Apr 15;178(8):5245–52.

165. Italiani P, Mazza EMC, Lucchesi D, Cifola I, Gemelli C, Grande A, et al. Transcriptomic Profiling of the Development of the Inflammatory Response in Human Monocytes In Vitro. PLoS ONE. 2014 Feb 3;9(2):e87680.

166. Mylonas KJ, Nair MG, Prieto-Lafuente L, Paape D, Allen JE. Alternatively Activated Macrophages Elicited by Helminth Infection Can Be Reprogrammed to Enable Microbial Killing. The Journal of Immunology. 2009 Mar 1;182(5):3084–94.

167. Stout RD, Jiang C, Matta B, Tietzel I, Watkins SK, Suttles J. Macrophages Sequentially Change Their Functional Phenotype in Response to Changes in Microenvironmental Influences. The Journal of Immunology. 2005 Jul 1;175(1):342–9.

168. Strizova Z, Benesova I, Bartolini R, Novysedlak R, Cecrdlova E, Foley LK, et al. M1/M2 macrophages and their overlaps - myth or reality? Clinical science (London, England : 1979). 2023 Aug 14;137(15):1067–93.

169. Kovacevic Z, Sahni S, Lok H, Davies MJ, Wink DA, Richardson DR. Regulation and control of nitric oxide (NO) in macrophages: Protecting the “professional killer cell” from its own cytotoxic arsenal via MRP1 and GSTP1. Biochimica et Biophysica Acta

(BBA) - General Subjects. 2017 May;1861(5):995–9.

170. Azad AK, Rajaram MVS, Schlesinger LS. Exploitation of the Macrophage Mannose Receptor (CD206) in Infectious Disease Diagnostics and Therapeutics. Journal of cytology & molecular biology. 2014 Jan 10;1(1):1000003.

171. Anzinger JJ, Chang J, Xu Q, Barthwal MK, Bohnacker T, Wymann MP, et al. Murine bone marrow-derived macrophages differentiated with GM-CSF become foam cells by PI3Kγ-dependent fluid-phase pinocytosis of native LDL. Journal of Lipid Research. 2012;53(1):34–42.

172. Cardilo-Reis L, Gruber S, Schreier SM, Drechsler M, Papac-Milicevic N, Weber C, et al. Interleukin-13 protects from atherosclerosis and modulates plaque composition by skewing the macrophage phenotype. EMBO Molecular Medicine. 2012 Oct 2;4(10):1072–86.

173. Bi Y, Chen J, Hu F, Liu J, Li M, Zhao L. M2 Macrophages as a Potential Target for Antiatherosclerosis Treatment. Neural Plasticity. 2019;2019:6724903.

174. Wei H, Tarling EJ, McMillen TS, Tang C, LeBoeuf RC. ABCG1 regulates mouse adipose tissue macrophage cholesterol levels and ratio of M1 to M2 cells in obesity and caloric restriction. Journal of Lipid Research. 2015;56(12):2337–47.

175. Zhang Y, McCluskey K, Fujii K, Wahl LM. Differential Regulation of Monocyte Matrix Metalloproteinase and TIMP-1 Production by TNF-α, Granulocyte-Macrophage CSF, and IL-1β Through Prostaglandin-Dependent and -Independent Mechanisms. The Journal of Immunology. 1998;161(6):3071–6.

176. Huang W-C, Sala-Newby GB, Susana A, Johnson JL, Newby AC. Classical Macrophage Activation Up-Regulates Several Matrix Metalloproteinases through Mitogen Activated Protein Kinases and Nuclear Factor-κB. PLoS ONE. 2012 Aug 3;7(8):e42507.

177. Newby AC. Metalloproteinase production from macrophages – a perfect storm leading to atherosclerotic plaque rupture and myocardial infarction. Experimental Physiology. 2016 Nov 5;101(11):1327–37.

178. Johnson JL, Jenkins NP, Huang W-C, Di Gregoli K, Sala-Newby GB, Scholtes VPW, et al. Relationship of MMP-14 and TIMP-3 expression with macrophage activation and human atherosclerotic plaque vulnerability. Mediators of inflammation. 2014;2014:276457.

179. Nielsen MJ, Møller HJ, Moestrup SK. Hemoglobin and heme scavenger receptors. Antioxidants and Redox Signaling. 2010;12(2):261–73.

180. Finn A V., Nakano M, Polavarapu R, Karmali V, Saeed O, Zhao XQ, et al. Hemoglobin directs macrophage differentiation and prevents foam cell formation in human atherosclerotic plaques. Journal of the American College of Cardiology. 2012;59(2):166–77.

181. Kadl A, Meher AK, Sharma PR, Lee MY, Doran AC, Johnstone SR, et al. Identification of a novel macrophage phenotype that develops in response to atherogenic phospholipids via Nrf2. Circulation Research. 2010;107(6):737–46.

182. Russo L, Lumeng CN. Properties and functions of adipose tissue macrophages in obesity. Immunology. 2018;155(4):407–17.

183. Raposo G, Stoorvogel W. Extracellular vesicles: Exosomes, microvesicles, and friends. Journal of Cell Biology. 2013;200(4):373–83.

184. Tricarico C, Clancy J, D'Souza-Schorey C. Biology and biogenesis of shed microvesicles. Small GTPases. 2017;8(4):220–32.

185. Jankovičová J, Sečová P, Michalková K, Antalíková J. Tetraspanins, more than markers of extracellular vesicles in reproduction. International Journal of Molecular Sciences. 2020;21(20):7568.

186. Nabhan JF, Hu R, Oh RS, Cohen SN, Lu Q. Formation and release of arrestin domain-containing protein 1-mediated microvesicles (ARMMs) at plasma membrane by recruitment of TSG101 protein. Proceedings of the National Academy of Sciences of the United States of America. 2012;109(11):4146–51.

187. Wehman AM, Poggioli C, Schweinsberg P, Grant BD, Nance J. The P4-ATPase TAT-5 inhibits the budding of extracellular vesicles in C. elegans embryos. Current Biology. 2011;21(23):1951–9.

188. Muralidharan-Chari V, Clancy J, Plou C, Romao M, Chavrier P, Raposo G, et al. ARF6-Regulated Shedding of Tumor Cell-Derived Plasma Membrane Microvesicles. Current Biology. 2009;19(22):1875–85.

189. Wang T, Gilkes DM, Takano N, Xiang L, Luo W, Bishop CJ, et al. Hypoxia-inducible factors and RAB22A mediate formation of microvesicles that stimulate breast cancer invasion and

metastasis. Proceedings of the National Academy of Sciences of the United States of America. 2014;111(31):E3234–42.

190. Morrell AE, Brown GN, Robinson ST, Sattler RL, Baik AD, Zhen G, et al. Mechanically induced Ca2+ oscillations in osteocytes release extracellular vesicles and enhance bone formation. Bone Research. 2018;6(1):11.

191. Taylor J, Azimi I, Monteith G, Bebawy M. Ca2+ mediates extracellular vesicle biogenesis through alternate pathways in malignancy. Journal of extracellular vesicles. 2020;9(1):1734326.

192. Cocucci E, Racchetti G, Meldolesi J. Shedding microvesicles: artefacts no more. Trends in Cell Biology. 2009;19(2):43–51.

193. Deatheragea BL, Cooksona BT. Membrane vesicle release in bacteria, eukaryotes, and archaea: A conserved yet underappreciated aspect of microbial life. Infection and Immunity. 2012;80(6):1948–57.

194. Liu YJ, Wang C. A review of the regulatory mechanisms of extracellular vesicles-mediated intercellular communication. Cell Communication and Signaling. 2023;21(1):77.

195. Sarlon-Bartoli G, Bennis Y, Lacroix R, Piercecchi-Marti MD, Bartoli MA, Arnaud L, et al. Plasmatic level of leukocyte-derived microparticles is associated with unstable plaque in asymptomatic patients with high-grade carotid stenosis. Journal of the American College of Cardiology. 2013;62(16):1436–41.

196. Sinning J-M, Losch J, Walenta K, Bohm M, Nickenig G, Werner N. Circulating CD31+/Annexin V+ microparticles correlate with cardiovascular outcomes. European Heart Journal. 2011 Aug

2;32(16):2034–41.

197. Niu C, Wang X, Zhao M, Cai T, Liu P, Li J, et al. Macrophage foam cell-derived extracellular vesicles promote vascular smooth muscle cell migration and adhesion. Journal of the American Heart Association. 2016;5(10):e004099.

198. Biemmi V, Milano G, Ciullo A, Cervio E, Burrello J, Cas MD, et al. Inflammatory extracellular vesicles prompt heart dysfunction via TRL4-dependent NF-κB activation. Theranostics. 2020;10(6):2773–90.

199. New SEP, Goettsch C, Aikawa M, Marchini JF, Shibasaki M, Yabusaki K, et al. Macrophage-derived matrix vesicles : An alternative novel mechanism for microcalcification in atherosclerotic plaques. Circulation Research. 2013;113(1):72–7.

200. Liu H, Gao W, Yuan J, Wu C, Yao K, Zhang L, et al. Exosomes derived from dendritic cells improve cardiac function via activation of CD4+ T lymphocytes after myocardial infarction. Journal of Molecular and Cellular Cardiology. 2016;91:123–33.

201. Xia N, Lu Y, Gu M, Li N, Liu M, Jiao J, et al. A Unique Population of Regulatory T Cells in Heart Potentiates Cardiac Protection From Myocardial Infarction. Circulation. 2020;142(20):1956–73.

202. Yan W, Li T, Yin T, Hou Z, Qu K, Wang N, et al. M2 macrophage-derived exosomes promote the c-KIT phenotype of vascular smooth muscle cells during vascular tissue repair after intravascular stent implantation. Theranostics. 2020;10(23):10712–28.

203. New SEP, Goettsch C, Aikawa M, Marchini JF, Shibasaki M, Yabusaki K, et al. Macrophage-derived matrix vesicles: an alternative novel mechanism for microcalcification in atherosclerotic plaques. Circulation research. 2013 Jun 21;113(1):72–7.

204. Leroyer AS, Rautou P-E, Silvestre J-S, Castier Y, Lesèche G, Devue C, et al. CD40 Ligand+ Microparticles From Human Atherosclerotic Plaques Stimulate Endothelial Proliferation and Angiogenesis. Journal of the American College of Cardiology. 2008 Oct;52(16):1302–11.

205. Chironi G, Simon A, Hugel B, Pino M Del, Gariepy J, Freyssinet JM, et al. Circulating leukocyte-derived microparticles predict subclinical atherosclerosis burden in asymptomatic subjects. Arteriosclerosis, Thrombosis, and Vascular Biology. 2006;26(12):2775–80.

206. Chatterjee V, Yang X, Ma Y, Cha B, Meegan JE, Wu M, et al. Endothelial microvesicles carrying Src-rich cargo impair adherens junction integrity and cytoskeleton homeostasis. Cardiovascular Research. 2020;116(8):1525–38.

207. Buendía P, Oca AM, Madueño JA, Merino A, Martín-Malo A, Aljama P, et al. Endothelial microparticles mediate inflammation-induced vascular calcification. The FASEB Journal. 2015 Jan 23;29(1):173–81.

208. Huber J, Vales A, Mitulovic G, Blumer M, Schmid R, Witztum JL, et al. Oxidized membrane vesicles and blebs from apoptotic cells contain biologically active oxidized phospholipids that induce monocyte-endothelial interactions. Arteriosclerosis, Thrombosis, and Vascular Biology. 2002;22(1):101–7.

209. Hergenreider E, Heydt S, Tréguer K, Boettger T, Horrevoets AJG, Zeiher AM, et al. Atheroprotective communication between endothelial cells and smooth muscle cells through miRNAs. Nature Cell Biology. 2012;14(3):249–56.

210. He S, Wu C, Xiao J, Li D, Sun Z, Li M. Endothelial extracellular vesicles modulate the macrophage phenotype: Potential implications in atherosclerosis. Scandinavian Journal of Immunology. 2018;87(4):e12648.

211. Feng C, Chen Q, Fan M, Guo J, Liu Y, Ji T, et al. Platelet-derived microparticles promote phagocytosis of oxidized low-density lipoprotein by macrophages, potentially enhancing foam cell formation. Annals of Translational Medicine. 2019;7(18):477.

212. Komiya Y, Habas R. Wnt signal transduction pathways. Organogenesis. 2008;4(2):68–75.

213. Sharma RP, Chopra VL. Effect of the wingless (wg1) mutation on wing and haltere development in Drosophila melanogaster. Developmental Biology. 1976;48(2):461–5.

214. Babu P. Early developmental subdivisions of the wing disk in Drosophila. MGG Molecular & General Genetics. 1977;151(3):289–94.

215. Cruciat CM, Niehrs C. Secreted and transmembrane Wnt inhibitors and activators. Cold Spring Harbor Perspectives in Biology. 2013;5(3):a015081.

216. Liu J, Xiao Q, Xiao J, Niu C, Li Y, Zhang X, et al. Wnt/β-catenin signalling: function, biological mechanisms, and therapeutic opportunities. Signal Transduction and Targeted Therapy.

2022;7(1):3.

217. He X, Semenov M, Tamai K, Zeng X. LDL receptor-related proteins 5 and 6 in Wnt/β-catenin signaling: Arrows point the way. Development. 2004;131(8):1663–77.

218. MacDonald BT, He X. Frizzled and LRp5/6 receptors for wnt/β-catenin signaling. Cold Spring Harbor Perspectives in Biology. 2012;4(12):a007880.

219. Go GW, Mani A. Low-density lipoprotein receptor (LDLR) family orchestrates cholesterol homeostasis. Yale Journal of Biology and Medicine. 2012;85(1):19–28.

220. Nüsslein-Volhard C, Wieschaus E, Kluding H. Mutations affecting the pattern of the larval cuticle in Drosophila melanogaster - I. Zygotic loci on the second chromosome. Wilhelm Roux's Archives of Developmental Biology. 1984;193(5):267–82.

221. Wehrli M, Dougan ST, Caldwell K, O'Keefe L, Schwartz S, Valzel-Ohayon D, et al. Arrow encodes an LDL-receptor-related protein essential for Wingless signalling. Nature. 2000;407(6803):527–30.

222. Willnow TE. Low-density Lipoprotein Receptor Gene Family. In: Encyclopedia of Molecular Pharmacology. Berlin, Heidelberg: Springer Berlin Heidelberg; 2008. p. 705–8.

223. Ahn VE, Chu MLH, Choi HJ, Tran D, Abo A, Weis WI. Structural basis of Wnt signaling inhibition by Dickkopf binding to LRP5/6. Developmental Cell. 2011;21(5):862–73.

224. Boyden LM, Mao J, Belsky J, Mitzner L, Farhi A, Mitnick MA, et al. High Bone Density Due to a Mutation in LDL-Receptor–

Related Protein 5. New England Journal of Medicine. 2002;346(20):1513–21.

225. Little RD, Carulli JP, Del Mastro RG, Dupuis J, Osborne M, Folz C, et al. A mutation in the LDL receptor-related protein 5 gene results in the autosomal dominant high-bone-mass trait. American Journal of Human Genetics. 2002;70(1):11–9.

226. Gong Y, Slee RB, Fukai N, Rawadi G, Roman-Roman S, Reginato AM, et al. LDL receptor-related protein 5 (LRP5) affects bone accrual and eye development. Cell. 2001 Nov 16;107(4):513–23.

227. Ai M, Heeger S, Bartels CF, Schelling DK, Warman ML. Clinical and molecular findings in osteoporosis-pseudoglioma syndrome. American Journal of Human Genetics. 2005;77(5):741–53.

228. Cnossen WR, Te Morsche RHM, Hoischen A, Gilissen C, Chrispijn M, Venselaar H, et al. Whole-exome sequencing reveals LRP5 mutations and canonical Wnt signaling associated with hepatic cystogenesis. Proceedings of the National Academy of Sciences of the United States of America. 2014;111(14):5343–8.

229. Fujino T, Asaba H, Kang MJ, Ikeda Y, Sone H, Takada S, et al. Low-density lipoprotein receptor-related protein 5 (LRP5) is essential for normal cholesterol metabolism and glucose-induced insulin secretion. Proceedings of the National Academy of Sciences of the United States of America. 2003 Jan 7;100(1):229–34.

230. Kim DH, Inagaki Y, Suzuki T, Ioka RX, Yoshioka SZ, Magoori K, et al. A new low density lipoprotein receptor related protein,

LRP5, is expressed in hepatocytes and adrenal cortex, and recognizes apolipoprotein E. Journal of Biochemistry. 1998;124(6):1072–6.

231. Borrell-Pages M, Romero JC, Badimon L. Cholesterol modulates LRP5 expression in the vessel wall. Atherosclerosis. 2014 Aug 1;235(2):363–70.

232. Borrell-Pagès M, Romero JC, Badimon L. LRP5 deficiency down-regulates Wnt signalling and promotes aortic lipid infiltration in hypercholesterolaemic mice. Journal of Cellular and Molecular Medicine. 2015;19(4):770–7.

233. Borrell-Pages M, Vilahur G, Romero JC, Casaní L, Bejar MT, Badimon L. LRP5/canonical Wnt signalling and healing of ischemic myocardium. Basic Research in Cardiology. 2016;111(6):67.

234. Borrell-Pagès M, Romero JC, Badimon L. LRP5 negatively regulates differentiation of monocytes through abrogation of Wnt signalling. Journal of cellular and molecular medicine. 2014 Feb;18(2):314–25.

235. Borrell-Pages M, Carolina Romero J, Badimon L. LRP5 and plasma cholesterol levels modulate the canonical Wnt pathway in peripheral blood leukocytes. Immunology and Cell Biology. 2015;93(7):653–61.

236. Borrell-Pages M, Romero JC, Crespo J, Juan-Babot O, Badimon L. LRP5 associates with specific subsets of macrophages: Molecular and functional effects. Journal of Molecular and Cellular Cardiology. 2016;90:146–56.

237. Seidah NG, Benjannet S, Wickham L, Marcinkiewicz J, Bélanger Jasmin S, Stifani S, et al. The secretory proprotein convertase neural apoptosis-regulated convertase 1 (NARC-1): Liver regeneration and neuronal differentiation. Proceedings of the National Academy of Sciences of the United States of America. 2003;100(3):928–33.

238. Varret M, Rabès JP, Saint-Jore B, Cenarro A, Marinoni JC, Civeira F, et al. A third major locus for autosomal dominant hypercholesterolemia maps to 1p34.1-p32. American Journal of Human Genetics. 1999;64(5):1378–87.

239. Abifadel M, Varret M, Rabès JP, Allard D, Ouguerram K, Devillers M, et al. Mutations in PCSK9 cause autosomal dominant hypercholesterolemia. Nature Genetics. 2003;34(2):154–6.

240. Timms KM, Wagner S, Samuels ME, Forbey K, Goldfine H, Jammalapati S, et al. A mutation in PCSK9 causing autosomal-dominant hypercholesterolemia in a Utah pedigree. Human Genetics. 2004;114(4):349–53.

241. Leren TP. Mutations in the PCSK9 gene in Norwegian subjects with autosomal dominant hypercholesterolemia. Clinical Genetics. 2004;65(5):419–22.

242. Davis CG, Goldstein JL, Südhof TC, Anderson RGW, Russell DW, Brown MS. Acid-dependent ligand dissociation and recycling of LDL receptor mediated by growth factor homology region. Nature. 1987;326(6115):760–5.

243. Miyake Y, Tajima S, Funahashi T, Yamamoto A. Analysis of a recycling-impaired mutant of low density lipoprotein receptor in familial hypercholesterolemia. Journal of Biological Chemistry.

1989;264(28):16584–90.

244. van der Westhuyzen DR, Stein ML, Henderson HE, Marais AD, Fourie AM, Coetzee GA. Deletion of two growth-factor repeats from the low-density-lipoprotein receptor accelerates its degradation. Biochemical Journal. 1991;277(3):677–82.

245. Van Hoof D, Rodenburg KW, Van der Horst DJ. Intracellular fate of LDL receptor family members depends on the cooperation between their ligand-binding and EGF domains. Journal of Cell Science. 2005;118(6):1309–20.

246. Maxwell KN, Fisher EA, Breslow JL. Overexpression of PCSK9 accelerates the degradation of the LDLR in a post-endoplasmic reticulum compartment. Proceedings of the National Academy of Sciences of the United States of America. 2005;102(6):2069–74.

247. Maxwell KN, Breslow JL. Adenoviral-mediated expression of Pcsk9 in mice results in a low-density lipoprotein receptor knockout phenotype. Proceedings of the National Academy of Sciences of the United States of America. 2004;101(18):7100–5.

248. Pandit S, Wisniewski D, Santoro JC, Ha S, Ramakrishnan V, Cubbon RM, et al. Functional analysis of sites within PCSK9 responsible for hypercholesterolemia. Journal of Lipid Research. 2008;49(6):1333–43.

249. Cohen J, Pertsemlidis A, Kotowski IK, Graham R, Garcia CK, Hobbs HH. Low LDL cholesterol in individuals of African descent resulting from frequent nonsense mutations in PCSK9. Nature Genetics. 2005;37(2):161–5.

250. Tam SP, Brissette L, Ramharack R, Deeley RG. Differences

between the regulation of 3-hydroxy-3-methylglutarylcoenzyme a reductase and low density lipoprotein receptor in human hepatoma cells and fibroblasts reside primarily at the translational and post-translational levels. Journal of Biological Chemistry. 1991;266(25):16764–73.

251. Dong B, Wu M, Li H, Kraemer FB, Adeli K, Seidah NG, et al. Strong induction of PCSK9 gene expression through HNF1α and SREBP2: Mechanism for the resistance to LDL-cholesterol lowering effect of statins in dyslipidemic hamsters. Journal of Lipid Research. 2010;51(6):1486–95.

252. Sabatine MS, Giugliano RP, Wiviott SD, Raal FJ, Blom DJ, Robinson J, et al. Efficacy and safety of evolocumab in reducing lipids and cardiovascular events. New England Journal of Medicine. 2015;372:1500–9.

253. Robinson JG, Farnier M, Krempf M, Bergeron J, Luc G, Averna M, et al. Efficacy and safety of alirocumab in reducing lipids and cardiovascular events. New England Journal of Medicine. 2015;372:1489–99.

254. Schwartz GG, Steg PG, Szarek M, Bhatt DL, Bittner VA, Diaz R, et al. Alirocumab and cardiovascular outcomes after acute coronary syndrome. New England Journal of Medicine. 2018;379:2097–107.

255. Sabatine MS, Giugliano RP, Keech AC, Honarpour N, Wiviott SD, Murphy SA, et al. Evolocumab and Clinical Outcomes in Patients with Cardiovascular Disease. The New England journal of medicine. 2017 May 4;376(18):1713–22.

256. Ray KK, Kallend D, Leiter LA, Raal FJ, Koenig W, Jaros MJ, et

al. Effect of inclisiran on lipids in primary prevention: the ORION-11 trial. European Heart Journal. 2022;43(48):5047–57.

257. Ray KK, Troquay RPT, Visseren FLJ, Leiter LA, Scott Wright R, Vikarunnessa S, et al. Long-term efficacy and safety of inclisiran in patients with high cardiovascular risk and elevated LDL cholesterol (ORION-3): results from the 4-year open-label extension of the ORION-1 trial. The Lancet Diabetes and Endocrinology. 2023;11(2):109–19.

258. Mitchell T, Chao G, Sitkoff D, Lo F, Monshizadegan H, Meyers D, et al. Pharmacologic profile of the adnectin BMS-962476, a small protein biologic alternative to PCSK9 antibodies for low-density lipoprotein lowering. Journal of Pharmacology and Experimental Therapeutics. 2014;350(2):412–24.

259. Stein EA, Kasichayanula S, Turner T, Kranz T, Arumugam U, Biernat L, et al. Ldl cholesterol reduction with BMS-962476, an adnectin inhibitor of PCSK9: results of a single ascending dose study. Journal of the American College of Cardiology. 2014;63(12):A1372.

260. Stein E, Toth P, Butcher MB, Kereiakes D, Magnu P, Bays H, et al. Safety, Tolerability And Ldl-C Reduction With A Novel Anti-Pcsk9 Recombinant Fusion Protein (Lib003): Results Of A Randomized, Double-Blind, Placebo-Controlled, Phase 2 Study. Atherosclerosis. 2019;287(E7):e1–27.

261. Raal F, Fourie N, Scott R, Blom D, De Vries Basson M, Kayikcioglu M, et al. Long-term efficacy and safety of lerodalcibep in heterozygous familial hypercholesterolaemia: the LIBerate-HeFH trial. European Heart Journal. 2023;44(40):4272–80.

262. Gennemark P, Walter K, Clemmensen N, Rekić D, Nilsson CAM, Knöchel J, et al. An oral antisense oligonucleotide for PCSK9 inhibition. Science Translational Medicine. 2021;13(593):eabe9117.

263. Musunuru K, Chadwick AC, Mizoguchi T, Garcia SP, DeNizio JE, Reiss CW, et al. In vivo CRISPR base editing of PCSK9 durably lowers cholesterol in primates. Nature. 2021;593(7859):429–34.

264. Momtazi-Borojeni AA, Jaafari MR, Banach M, Gorabi AM, Sahraei H, Sahebkar A. Pre-clinical evaluation of the nanoliposomal antipcsk9 vaccine in healthy non-human primates. Vaccines. 2021;9(7):749.

265. Ahamad S, Mathew S, Khan WA, Mohanan K. Development of small-molecule PCSK9 inhibitors for the treatment of hypercholesterolemia. Drug Discovery Today. 2022;27(5):1332–49.

266. O'Donoghue ML, Giugliano RP, Wiviott SD, Atar D, Keech A, Kuder JF, et al. Long-Term Evolocumab in Patients with Established Atherosclerotic Cardiovascular Disease. Circulation. 2022;146(15):1109–19.

267. Goodman SG, Steg PG, Poulouin Y, Bhatt DL, Bittner VA, Diaz R, et al. Long-Term Efficacy, Safety, and Tolerability of Alirocumab in 8242 Patients Eligible for 3 to 5 Years of Placebo-Controlled Observation in the ODYSSEY OUTCOMES Trial. Journal of the American Heart Association. 2023;12(18):e029216.

268. Ding Z, Liu S, Wang X, Theus S, Deng X, Fan Y, et al. PCSK9 regulates expression of scavenger receptors and ox-LDL uptake

in macrophages. Cardiovascular Research. 2018;114(8):1145–53.

269. Liu S, Deng X, Zhang P, Wang X, Fan Y, Zhou S, et al. Blood flow patterns regulate PCSK9 secretion via MyD88-mediated pro-inflammatory cytokines. Cardiovascular Research. 2019;116(10):1721–32.

270. Giunzioni I, Tavori H, Covarrubias R, Major AS, Ding L, Zhang Y, et al. Local effects of human PCSK9 on the atherosclerotic lesion. Journal of Pathology. 2016;238(1):52–62.

271. Ding Z, Liu S, Wang X, Deng X, Fan Y, Shahanawaz J, et al. Cross-Talk between LOX-1 and PCSK9 in vascular tissues. Cardiovascular Research. 2015;107(4):556–67.

272. Landlinger C, Pouwer MG, Juno C, Van Der Hoorn JWA, Pieterman EJ, Jukema JW, et al. The AT04A vaccine against proprotein convertase subtilisin/kexin type 9 reduces total cholesterol, vascular inflammation, and atherosclerosis in APOE∗3Leiden.CETP mice. European Heart Journal. 2017;38(32):2499–507.

273. Liu A, Frostegård J. PCSK9 plays a novel immunological role in oxidized LDL-induced dendritic cell maturation and activation of T cells from human blood and atherosclerotic plaque. Journal of Internal Medicine. 2018;284(2):193–210.

274. Kim YU, Kee P, Danila D, Teng BB. A critical role of PCSK9 in mediating il-17-producing T cell responses in hyperlipidemia. Immune Network. 2019;19(6):e41.

275. Camera M, Rossetti L, Barbieri SS, Zanotti I, Canciani B,

Trabattoni D, et al. PCSK9 as a Positive Modulator of Platelet Activation. Journal of the American College of Cardiology. 2018;71(8):952–4.

276. Wang H, Wang Q, Wang J, Guo C, Kleiman K, Meng H, et al. Proprotein convertase subtilisin/kexin type 9 (PCSK9) Deficiency is Protective Against Venous Thrombosis in Mice. Scientific Reports. 2017;30(1):14360.

277. Li S, Zhu CG, Guo YL, Xu RX, Zhang Y, Sun J, et al. The Relationship between the Plasma PCSK9 Levels and Platelet Indices in Patients With Stable Coronary Artery Disease. Journal of Atherosclerosis and Thrombosis. 2015;22(1):76–84.

278. Chen K, Febbraio M, Li W, Silverstein RL. A specific cd36-dependent signaling pathway is required for platelet activation by oxidized low-density lipoprotein. Circulation Research. 2008;102(12):1512–9.

279. Shen MY, Chen FY, Hsu JF, Fu RH, Chang CM, Chang CT, et al. Plasma L5 levels are elevated in ischemic stroke patients and enhance platelet aggregation. Blood. 2016;127(10):1336–45.

280. Ludwig PE, Reddy V, Varacallo M. Neuroanatomy, Central Nervous System (CNS). 2024.

281. Ludwig PE, Reddy V, Varacallo M. Neuroanatomy, Neurons. 2024.

282. Allen NJ, Lyons DA. Glia as architects of central nervous system formation and function. Science. 2018;362(6411):181–5.

283. Dotiwala AK, McCausland C, Samra NS. Anatomy, Head and Neck: Blood Brain Barrier. 2024.

284. Jiao H, Wang Z, Liu Y, Wang P, Xue Y. Specific role of tight junction proteins claudin-5, occludin, and ZO-1 of the blood-brain barrier in a focal cerebral ischemic insult. Journal of Molecular Neuroscience. 2011;44(2):130–9.

285. Stewart PA. Endothelial vesicles in the blood-brain barrier: Are they related to permeability? Cellular and Molecular Neurobiology. 2000;20(2):149–63.

286. Pardridge WM. The blood-brain barrier: Bottleneck in brain drug development. NeuroRx. 2005;2(1):3–14.

287. Brown LS, Foster CG, Courtney JM, King NE, Howells DW, Sutherland BA. Pericytes and neurovascular function in the healthy and diseased brain. Frontiers in Cellular Neuroscience. 2019;13:282.

288. Beard E, Lengacher S, Dias S, Magistretti PJ, Finsterwald C. Astrocytes as Key Regulators of Brain Energy Metabolism: New Therapeutic Perspectives. Frontiers in Physiology. 2022;12:825816.

289. Björkhem I, Meaney S, Fogelman AM. Brain Cholesterol: Long Secret Life behind a Barrier. Arteriosclerosis, Thrombosis, and Vascular Biology. 2004;24(5):806–15.

290. Dietschy JM, Turley SD. Thematic review series: brain Lipids. Cholesterol metabolism in the central nervous system during early development and in the mature animal. Journal of Lipid Research. 2004;45(8):1375–97.

291. Pfrieger FW. Outsourcing in the brain: Do neurons depend on cholesterol delivery by astrocytes? BioEssays. 2003;25(1):72–8.

292. Dietschy JM. Central nervous system: Cholesterol turnover, brain development and neurodegeneration. Biological Chemistry. 2009;390(4):287–93.

293. Tong J, Borbat PP, Freed JH, Shin YK. A scissors mechanism for stimulation of SNARE-mediated lipid mixing by cholesterol. Proceedings of the National Academy of Sciences of the United States of America. 2009;106(13):5141–6.

294. Zamir O, Charlton MP. Cholesterol and synaptic transmitter release at crayfish neuromuscular junctions. Journal of Physiology. 2006;571(1):83–99.

295. Jia JY, Lamer S, Schümann M, Schmidt MR, Krause E, Haucke V. Quantitative proteomics analysis of detergent-resistant membranes from chemical synapses: Evidence for cholesterol as spatial organizer of synaptic vesicle cycling. Molecular and Cellular Proteomics. 2006;5(11):2060–71.

296. Shanmugaratnam J, Berg E, Kimerer L, Johnson RJ, Amaratunga A, Schreiber BM, et al. Retinal Muller glia secrete apolipoproteins E and J which are efficiently assembled into lipoprotein particles. Molecular Brain Research. 1997;50(1–2):113–20.

297. Lund EG, Xie C, Kotti T, Turley SD, Dietschy JM, Russell DW. Knockout of the cholesterol 24-hydroxylase gene in mice reveals a brain-specific mechanism of cholesterol turnover. Journal of Biological Chemistry. 2003;278(25):22980–8.

298. Olkkonen VM, Béaslas O, Nissilä E. Oxysterols and their cellular effectors. Biomolecules. 2012;2(1):76–103.

299. Hussain G, Wang J, Rasul A, Anwar H, Imran A, Qasim M, et al.

Role of cholesterol and sphingolipids in brain development and neurological diseases. Lipids in Health and Disease. 2019;18(1):26.

300. Rhea EM, Banks WA. Interactions of Lipids, Lipoproteins, and Apolipoproteins with the Blood-Brain Barrier. Pharmaceutical Research. 2021;38(9):1469–75.

301. Wang H, Eckel RH. What are lipoproteins doing in the brain? Trends in Endocrinology and Metabolism. 2014;25(1):8–14.

302. De Oliveira J, Engel DF, De Paula GC, Dos Santos DB, Lopes JB, Farina M, et al. High Cholesterol Diet Exacerbates Blood-Brain Barrier Disruption in LDLr-/- Mice: Impact on Cognitive Function. Journal of Alzheimer's Disease. 2020;78(1):97–115.

303. Saeed AA, Genové G, Li T, Lütjohann D, Olin M, Mast N, et al. Effects of a disrupted blood-brain barrier on cholesterol homeostasis in the brain. Journal of Biological Chemistry. 2014;289(34):23712–22.

304. Sparks DL, Scheff SW, Hunsaker JC, Liu H, Landers T, Gross DR. Induction of Alzheimer-like β-amyloid immunoreactivity in the brains of rabbits with dietary cholesterol. Experimental Neurology. 1994;126(1):88–94.

305. Wingo AP, Vattathil SM, Liu J, Fan W, Cutler DJ, Levey AI, et al. LDL cholesterol is associated with higher AD neuropathology burden independent of APOE. Journal of Neurology, Neurosurgery and Psychiatry. 2022;93(9):930–8.

306. Rozani V, Gurevich T, Giladi N, El-Ad B, Tsamir J, Hemo B, et al. Higher serum cholesterol and decreased Parkinson's disease

risk: A statin-free cohort study. Movement Disorders. 2018;33(8):1298–305.

307. Fu X, Wang Y, He X, Li H, Liu H, Zhang X. A systematic review and meta-analysis of serum cholesterol and triglyceride levels in patients with Parkinson's disease. Lipids in Health and Disease. 2020;19(1):97.

308. Yang W, Shen Z, Wen S, Wang W, Hu M. Mechanisms of multiple neurotransmitters in the effects of Lycopene on brain injury induced by Hyperlipidemia. Lipids in Health and Disease. 2018;17(1):13.

309. Paul R, Choudhury A, Chandra Boruah D, Devi R, Bhattacharya P, Choudhury MD, et al. Hypercholesterolemia causes psychomotor abnormalities in mice and alterations in cortico-striatal biogenic amine neurotransmitters: Relevance to Parkinson's disease. Neurochemistry International. 2017;108:15–26.

310. Moreira ELG, De Oliveira J, Nunes JC, Santos DB, Nunes FC, Vieira DSC, et al. Age-Related cognitive decline in hypercholesterolemic LDL receptor knockout mice (LDLr-/-): Evidence of antioxidant imbalance and increased acetylcholinesterase activity in the prefrontal cortex. Journal of Alzheimer's Disease. 2012;32(2):495–511.

311. Wang SH, Huang Y, Yuan Y, Xia WQ, Wang P, Huang R. LDL receptor knock-out mice show impaired spatial cognition with hippocampal vulnerability to apoptosis and deficits in synapses. Lipids in Health and Disease. 2014;13(1):175.

312. Zambón D, Quintana M, Mata P, Alonso R, Benavent J, Cruz-

Sánchez F, et al. Higher incidence of mild cognitive impairment in familial hypercholesterolemia. American Journal of Medicine. 2010;123(3):267–74.

313. Ma C, Yin Z, Zhu P, Luo J, Shi X, Gao X. Blood cholesterol in late-life and cognitive decline: A longitudinal study of the Chinese elderly. Molecular Neurodegeneration. 2017;12(1):24.

314. Rosso SB, Inestrosa NC. WNT signalling in neuronal maturation and synaptogenesis. Frontiers in Cellular Neuroscience. 2013;7:103.

315. Lie DC, Colamarino SA, Song HJ, Désiré L, Mira H, Consiglio A, et al. Wnt signalling regulates adult hippocampal neurogenesis. Nature. 2005;437(7063):1370–5.

316. Mardones MD, Andaur GA, Varas-Godoy M, Henriquez JF, Salech F, Behrens MI, et al. Frizzled-1 receptor regulates adult hippocampal neurogenesis. Molecular Brain. 2016;9(1):29.

317. Qu Q, Sun G, Murai K, Ye P, Li W, Asuelime G, et al. Wnt7a Regulates Multiple Steps of Neurogenesis. Molecular and Cellular Biology. 2013;33(13):2551–9.

318. Karalay Ö, Doberauer K, Vadodaria KC, Knobloch M, Berti L, Miquelajauregui A, et al. Prospero-related homeobox 1 gene (Prox1) is regulated by canonical Wnt signaling and has a stage-specific role in adult hippocampal neurogenesis. Proceedings of the National Academy of Sciences of the United States of America. 2011;108(14):5807–12.

319. Kuwabara T, Hsieh J, Muotri A, Yeo G, Warashina M, Lie DC, et al. Wnt-mediated activation of NeuroD1 and retro-elements

during adult neurogenesis. Nature Neuroscience. 2009;12(9):1097–105.

320. Yu X, Malenka RC. β-catenin is critical for dendritic morphogenesis. Nature Neuroscience. 2003;6(11):1169–77.

321. Ahmad-Annuar A, Ciani L, Simeonidis I, Herreros J, Fredj N Ben, Rosso SB, et al. Signaling across the synapse: A role for Wnt and Dishevelled in presynaptic assembly and neurotransmitter release. Journal of Cell Biology. 2006;174(1):127–39.

322. Sahores M, Gibb A, Salinas PC. Frizzled-5, a receptor for the synaptic organizer Wnt7a, regulates activity-mediated synaptogenesis. Development. 2010;137(13):2215–25.

323. Paganoni S, Bernstein J, Ferreira A. Ror1-Ror2 complexes modulate synapse formation in hippocampal neurons. Neuroscience. 2010;165(4):1261–74.

324. Varela-Nallar L, Grabowski CP, Alfaro IE, Alvarez AR, Inestrosa NC. Role of the Wnt receptor Frizzled-1 in presynaptic differentiation and function. Neural Development. 2009;4(1):41.

325. Ciani L, Boyle KA, Dickins E, Sahores M, Anane D, Lopes DM, et al. Wnt7a signaling promotes dendritic spine growth and synaptic strength through Ca 2+/Calmodulin-dependent protein kinase II. Proceedings of the National Academy of Sciences of the United States of America. 2011;108(26):10732–7.

326. Cuitino L, Godoy JA, Farías GG, Couve A, Bonansco C, Fuenzalida M, et al. Wnt-5a modulates recycling of functional GABAA receptors on hippocampal neurons. Journal of Neuroscience. 2010;30(25):8411–20.

327. McLeod F, Salinas PC. Wnt proteins as modulators of synaptic plasticity. Current Opinion in Neurobiology. 2018;53:90–5.

328. Okamoto M, Inoue K, Iwamura H, Terashima K, Soya H, Asashima M, et al. Reduction in paracrine Wnt3 factors during aging causes impaired adult neurogenesis. The FASEB Journal. 2011;25(10):3570–82.

329. Ataman B, Ashley J, Gorczyca M, Ramachandran P, Fouquet W, Sigrist SJ, et al. Rapid Activity-Dependent Modifications in Synaptic Structure and Function Require Bidirectional Wnt Signaling. Neuron. 2008;57(5):705–18.

330. Chen J, Chang SP, Tang SJ. Activity-dependent synaptic Wnt release regulates hippocampal long term potentiation. Journal of Biological Chemistry. 2006;281(17):11910–6.

331. Takeuchi T, Duszkiewicz AJ, Morris RGM. The synaptic plasticity and memory hypothesis: Encoding, storage and persistence. Philosophical Transactions of the Royal Society B: Biological Sciences. 2014;369(1633):20130288.

332. McLeod F, Bossio A, Marzo A, Ciani L, Sibilla S, Hannan S, et al. Wnt Signaling Mediates LTP-Dependent Spine Plasticity and AMPAR Localization through Frizzled-7 Receptors. Cell Reports. 2018;23(4):1060–71.

333. Cerpa W, Gambrill A, Inestrosa NC, Barria A. Regulation of NMDA-receptor synaptic transmission by Wnt signaling. Journal of Neuroscience. 2011;31(26):9466–71.

334. Marzo A, Galli S, Lopes D, McLeod F, Podpolny M, Segovia-Roldan M, et al. Reversal of Synapse Degeneration by Restoring

Wnt Signaling in the Adult Hippocampus. Current Biology. 2016;26(19):2551–61.

335. Figueroa DJ, Hess JF, Ky B, Brown SD, Sandig V, Hermanowski-Vosatka A, et al. Expression of the type I diabetes-associated gene LRP5 in macrophages, vitamin A system cells, and the islets of Langerhans suggests multiple potential roles in diabetes. Journal of Histochemistry and Cytochemistry. 2000;48(10):1357–68.

336. Bafico A, Liu G, Yaniv A, Gazit A, Aaronson SA. Novel mechanism of Wnt signalling inhibition mediated by Dickkopf-1 interaction with LRP6/Arrow. Nature Cell Biology. 2001;3(7):683–6.

337. Mukhopadhyay M, Shtrom S, Rodriguez-Esteban C, Chen L, Tsukui T, Gomer L, et al. Dickkopf1 Is Required for Embryonic Head Induction and Limb Morphogenesis in the Mouse. Developmental Cell. 2001;1(3):423–34.

338. Huang Y, Zhang Q, Song NN, Zhang L, Sun YL, Hu L, et al. Lrp5/6 are required for cerebellar development and for suppressing TH expression in Purkinje cells via β-catenin. Molecular Brain. 2016;9:7.

339. Zhang L, Bahety P, Ee PLR. Wnt co-receptor LRP5/6 overexpression confers protection against hydrogen peroxide-induced neurotoxicity and reduces tau phosphorylation in SH-SY5Y cells. Neurochemistry International. 2015;87:13–21.

340. Zhao H, Nyholt DR. Gene-based analyses reveal novel genetic overlap and allelic heterogeneity across five major psychiatric disorders. Human Genetics. 2017;136(2):263–74.

341. Grünblatt E, Nemoda Z, Werling AM, Roth A, Angyal N, Tarnok Z, et al. The involvement of the canonical Wnt-signaling receptor LRP5 and LRP6 gene variants with ADHD and sexual dimorphism: Association study and meta-analysis. American Journal of Medical Genetics, Part B: Neuropsychiatric Genetics. 2019;180(6):365–76.

342. Zhang S, Wang Z, Cai F, Zhang M, Wu Y, Zhang J, et al. BACE1 cleavage site selection critical for amyloidogenesis and Alzheimer's pathogenesis. Journal of Neuroscience. 2017;37(29):6915–25.

343. Parr C, Mirzaei N, Christian M, Sastre M. Activation of the Wnt/β-catenin pathway represses the transcription of the β-amyloid precursor protein cleaving enzyme (BACE1) via binding of T-cell factor-4 to BACE1 promoter. FASEB Journal. 2015;29(2):623–35.

344. Liu CC, Tsai CW, Deak F, Rogers J, Penuliar M, Sung YM, et al. Deficiency in LRP6-Mediated Wnt Signaling Contributes to Synaptic Abnormalities and Amyloid Pathology in Alzheimer's Disease. Neuron. 2014;84(1):63–77.

345. Tapia-Rojas C, Burgos P V., Inestrosa NC. Inhibition of Wnt signaling induces amyloidogenic processing of amyloid precursor protein and the production and aggregation of Amyloid-β (Aβ)42 peptides. Journal of Neurochemistry. 2016;139(6):1175–91.

346. Sayas CL, Ávila J. GSK-3 and tau: A key duet in alzheimer's disease. Cells. 2021;10(4):721.

347. Barbier P, Zejneli O, Martinho M, Lasorsa A, Belle V, Smet-Nocca C, et al. Role of tau as a microtubule-associated protein:

Structural and functional aspects. Frontiers in Aging Neuroscience. 2019;10:204.

348. Vargas JY, Ahumada J, Arrázola MS, Fuenzalida M, Inestrosa NC. WASP-1, a canonical Wnt signaling potentiator, rescues hippocampal synaptic impairments induced by Aβ oligomers. Experimental Neurology. 2015;264:14–25.

349. Scali C, Caraci F, Gianfriddo M, Diodato E, Roncarati R, Pollio G, et al. Inhibition of Wnt signaling, modulation of Tau phosphorylation and induction of neuronal cell death by DKK1. Neurobiology of Disease. 2006;24(2):254–65.

350. Coates JC. Armadillo repeat proteins: Beyond the animal kingdom. Trends in Cell Biology. 2003;13(9):463–71.

351. Kelly OG, Pinson KI, Skarnes WC. The Wnt co-receptors Lrp5 and Lrp6 are essential for gastrulation in mice. Development. 2004;131(12):2803–15.

352. Riddle RC, Diegel CR, Leslie JM, van Koevering KK, Faugere MC, Clemens TL, et al. Lrp5 and Lrp6 Exert Overlapping Functions in Osteoblasts during Postnatal Bone Acquisition. PLoS ONE. 2013;8(5):e63323.

353. Goel S, Chin EN, Fakhraldeen SA, Berry SM, Beebe DJ, Alexander CM. Both LRP5 and LRP6 receptors are required to respond to physiological Wnt ligands in mammary epithelial cells and fibroblasts. Journal of Biological Chemistry. 2012;287(20):16454–66.

354. Kim JA, Montagnani M, Chandrasekran S, Quon MJ. Role of Lipotoxicity in Endothelial Dysfunction. Heart Failure Clinics.

2012;8(4):589–607.

355. Porcheray F, Viaud S, Rimaniol AC, Léone C, Samah B, Dereuddre-Bosquet N, et al. Macrophage activation switching: An asset for the resolution of inflammation. Clinical and Experimental Immunology. 2005;142(3):481–9.

356. Kusnadi A, Park SH, Yuan R, Pannellini T, Giannopoulou E, Oliver D, et al. The Cytokine TNF Promotes Transcription Factor SREBP Activity and Binding to Inflammatory Genes to Activate Macrophages and Limit Tissue Repair. Immunity. 2019;51(2):241–57.

357. Ecker J, Liebisch G, Englmaier M, Grandl M, Robenek H, Schmitz G. Induction of fatty acid synthesis is a key requirement for phagocytic differentiation of human monocytes. Proceedings of the National Academy of Sciences of the United States of America. 2010;107(17):7817–22.

358. Jaén RI, Povo-Retana A, Rosales-Mendoza C, Capillas-Herrero P, Sánchez-García S, Martín-Sanz P, et al. Functional Crosstalk between PCSK9 Internalization and Pro-Inflammatory Activation in Human Macrophages: Role of Reactive Oxygen Species Release. International Journal of Molecular Sciences. 2022;23(16):9114.

359. Chang W, Yang M, Song L, Shen K, Wang H, Gao X, et al. Isolation and culture of hepatic stellate cells from mouse liver. Acta Biochimica et Biophysica Sinica. 2014;46(4):291–8.

360. Rennert C, Heil T, Schicht G, Stilkerich A, Seidemann L, Kegel-Hübner V, et al. Prolonged lipid accumulation in cultured primary human hepatocytes rather leads to er stress than oxidative

stress. International Journal of Molecular Sciences. 2020;21(19):7097.

361. Seki S, Kitada T, Yamada T, Sakaguchi H, Nakatani K, Wakasa K. In situ detection of lipid peroxidation and oxidative DNA damage in non-alcoholic fatty liver diseases. Journal of Hepatology. 2002;37(1):56–62.

362. Lake AD, Novak P, Hardwick RN, Flores-Keown B, Zhao F, Klimecki WT, et al. The Adaptive endoplasmic reticulum stress response to lipotoxicity in progressive human nonalcoholic fatty liver disease. Toxicological Sciences. 2014;137(1):26–35.

363. Bordicchia M, Spannella F, Ferretti G, Bacchetti T, Vignini A, Di Pentima C, et al. PCSK9 is Expressed in Human Visceral Adipose Tissue and Regulated by Insulin and Cardiac Natriuretic Peptides. International journal of molecular sciences. 2019 Jan 9;20(2):245.

364. Terpstra V, Van Amersfoort ES, Van Velzen AG, Kuiper J, Van Berkel TJC. Hepatic and extrahepatic scavenger receptors function in relation to disease. Arteriosclerosis, Thrombosis, and Vascular Biology. 2000;20(8):1860–72.

365. Patten DA, Wilkinson AL, O'Keeffe A, Shetty S. Scavenger Receptors: Novel Roles in the Pathogenesis of Liver Inflammation and Cancer. Seminars in Liver Disease. 2022;42(1):61–76.

366. Gao Y, Shen W, Lu B, Zhang Q, Hu Y, Chen Y. Upregulation of hepatic VLDLR via PPARα is required for the triglyceride-lowering effect of fenofibrate. Journal of Lipid Research. 2014;55(8):1622–33.

367. Cabezas F, Lagos J, Céspedes C, Vio CP, Bronfman M, Marzolo MP. Megalin/LRP2 expression is induced by peroxisome proliferator-activated receptor -alpha and -gamma: Implications for PPARs' roles in renal function. PLoS ONE. 2011;6(2):e16794.

368. Behari J, Yeh TH, Krauland L, Otruba W, Cieply B, Hauth B, et al. Liver-specific β-catenin knockout mice exhibit defective bile acid and cholesterol homeostasis and increased susceptibility to diet-induced steatohepatitis. American Journal of Pathology. 2010;176(2):744–53.

369. Lehwald N, Tao G, Jang KY, Papandreou I, Liu B, Lia B, et al. β-catenin regulates hepatic mitochondrial function and energy balance in mice. Gastroenterology. 2012;143(3):754–64.

370. MacDonald BT, Tamai K, He X. Wnt/β-Catenin Signaling: Components, Mechanisms, and Diseases. Developmental Cell. 2009;17(1):9–26.

371. Lopez-Suarez L, Awabdh S Al, Coumoul X, Chauvet C. The SH-SY5Y human neuroblastoma cell line, a relevant in vitro cell model for investigating neurotoxicology in human: Focus on organic pollutants. NeuroToxicology. 2022;92:131–55.

372. Liu Y, Eaton ED, Wills TE, McCann SK, Antonic A, Howells DW. Human ischaemic cascade studies using SH-SY5Y cells: A systematic review and meta-analysis. Translational Stroke Research. 2018;9(6):564–74.

373. Adem A, Mattsson MEK, Nordberg A, Påhlman S. Muscarinic receptors in human SH-SY5Y neuroblastoma cell line: regulation by phorbol ester and retinoic acid-induced differentiation. Developmental Brain Research. 1987;33(2):235–42.

374. Tosetti P, Taglietti V, Toselli M. Functional changes in potassium conductances of the human neuroblastoma cell line SH-SY5Y during in vitro differentiation. Journal of Neurophysiology. 1998;79(2):648–58.

375. Lopes FM, Schröder R, Júnior MLC da F, Zanotto-Filho A, Müller CB, Pires AS, et al. Comparison between proliferative and neuron-like SH-SY5Y cells as an in vitro model for Parkinson disease studies. Brain Research. 2010;1337:85–94.

376. Djelti F, Braudeau J, Hudry E, Dhenain M, Varin J, Bièche I, et al. CYP46A1 inhibition, brain cholesterol accumulation and neurodegeneration pave the way for Alzheimer's disease. Brain. 2015 Aug;138(8):2383–98.

377. Vieira GC, Chockalingam S, Melegh Z, Greenhough A, Malik S, Szemes M, et al. LGR5 regulates pro-survival MEK/ERK and proliferative Wnt/β-catenin signalling in neuroblastoma. Oncotarget. 2015;6(37):40053–67.

378. Zhang L, Li K, Lv Z, Xiao X, Zheng J. The effect on cell growth by Wnt1 RNAi in human neuroblastoma SH-SY5Y cell line. Pediatric Surgery International. 2009;25(12):1065–71.

379. Zins K, Schäfer R, Paulus P, Dobler S, Fakhari N, Sioud M, et al. Frizzled2 signaling regulates growth of high-risk neuroblastomas by interfering with β-catenin-dependent and β-cateninindependent signaling pathways. Oncotarget. 2016;7(29):46187–202.

380. Flahaut M, Meier R, Coulon A, Nardou KA, Niggli FK, Martinet D, et al. The Wnt receptor FZD1 mediates chemoresistance in neuroblastoma through activation of the WntB-catenin pathway.

Oncogene. 2009;28(23):2245–56.

381. Suebsoonthron J, Jaroonwitchawan T, Yamabhai M, Noisa P. Inhibition of WNT signaling reduces differentiation and induces sensitivity to doxorubicin in human malignant neuroblastoma SH-SY5Y cells. Anti-Cancer Drugs. 2017;28(5):469–79.

382. Thorn CF, Oshiro C, Marsh S, Hernandez-Boussard T, McLeod H, Klein TE, et al. Doxorubicin pathways: Pharmacodynamics and adverse effects. Pharmacogenetics and Genomics. 2011;21(7):440–6.

383. Liu X, Mazanek P, Dam V, Wang Q, Zhao H, Guo R, et al. Deregulated Wnt/β-catenin program in high-risk neuroblastomas without MYCN amplification. Oncogene. 2008 Feb 28;27(10):1478–88.

384. Ioannou MS, Jackson J, Sheu SH, Chang CL, Weigel A V., Liu H, et al. Neuron-Astrocyte Metabolic Coupling Protects against Activity-Induced Fatty Acid Toxicity. Cell. 2019;177(6):1522–35.

385. McCaffery PJ, Adams J, Maden M, Rosa-Molinar E. Too much of a good thing: Retinoic acid as an endogenous regulator of neural differentiation and exogenous teratogen. European Journal of Neuroscience. 2003;18(3):457–72.

386. McCaffery P, Zhang J, Crandall JE. Retinoic acid signaling and function in the adult hippocampus. Journal of Neurobiology. 2006;66(7):780–91.

387. Jacobs S, Lie DC, DeCicco KL, Shi Y, DeLuca LM, Gage FH, et al. Retinoic acid is required early during adult neurogenesis in the dentate gyrus. Proceedings of the National Academy of Sciences

of the United States of America. 2006;103(10):3902–7.

388. Zetterstrom RH, Simon A, Giacobini MMJ, Eriksson U, Olson L. Localization of cellular retinoid-binding proteins suggests specific roles for retinoids in the adult central nervous system. Neuroscience. 1994;62(3):899–918.

389. Rioux L, Arnold SE. The expression of retinoic acid receptor alpha is increased in the granule cells of the dentate gyrus in schizophrenia. Psychiatry Research. 2005;133(1):13–21.

390. Kawaguchi R, Yu J, Honda J, Hu J, Whitelegge J, Ping P, et al. A membrane receptor for retinol binding protein mediates cellular uptake of vitamin A. Science. 2007;315(5813):820–5.

391. Napoli JL. Retinol metabolism in LLC-PK1 Cells. Characterization of retinoic acid synthesis by an established mammalian cell line. The Journal of biological chemistry. 1986 Oct 15;261(29):13592–7.

392. Ross AC, Zolfaghari R. Cytochrome P450s in the regulation of cellular retinoic acid metabolism. Annual Review of Nutrition. 2011;31:65–87.

393. Samokyszyn VM, Gall WE, Zawada G, Freyaldenhoven MA, Chen G, Mackenzie PI, et al. 4-Hydroxyretinoic acid, a novel substrate for human liver microsomal UDP-glucuronosyltransferase(s) and recombinant UGT2B7. Journal of Biological Chemistry. 2000;275(10):6908–14.

394. DeMar JC, Lee HJ, Ma K, Chang L, Bell JM, Rapoport SI, et al. Brain elongation of linoleic acid is a negligible source of the arachidonate in brain phospholipids of adult rats. Biochimica et

Biophysica Acta - Molecular and Cell Biology of Lipids. 2006;1761(9):1050–9.

395. Schuster S, Johnson CD, Hennebelle M, Holtmann T, Taha AY, Kirpich IA, et al. Oxidized linoleic acid metabolites induce liver mitochondrial dysfunction, apoptosis, and NLRP3 activation in mice. Journal of Lipid Research. 2018;59(9):1597–609.

396. Bazinet RP, Layé S. Polyunsaturated fatty acids and their metabolites in brain function and disease. Nature Reviews Neuroscience. 2014;15(12):771–85.

397. Inceoglu B, Zolkowska D, Yoo HJ, Wagner KM, Yang J, Hackett E, et al. Epoxy fatty acids and inhibition of the soluble epoxide hydrolase selectively modulate GABA mediated neurotransmission to delay onset of seizures. PLoS ONE. 2013;8(12):e80922.

398. Farooqui AA, Yang HC, Rosenberger TA, Horrocks LA. Phospholipase A2 and its role in brain tissue. Journal of Neurochemistry. 1997;69(3):889–901.

399. Braeuning A, Köhle C, Buchmann A, Schwarz M. Coordinate regulation of cytochrome P450 1a1 expression in mouse liver by the aryl hydrocarbon receptor and the β-catenin pathway. Toxicological Sciences. 2011;122(1):16–25.

400. Szeto W, Jiang W, Tice DA, Rubinfeld B, Hollingshead PG, Fong SE, et al. Overexpression of the retinoic acid-responsive gene Stra6 in human cancers and its synergistic induction by Wnt-1 and retinoic acid. Cancer Research. 2001;61(10):4197–205.

401. Tice DA, Szeto W, Soloviev I, Rubinfeld B, Fong SE, Dugger DL,

et al. Synergistic induction of tumor antigens by Wnt-1 signaling and retinoic acid revealed by gene expression profiling. Journal of Biological Chemistry. 2002;277(16):14329–35.

402. Easwaran V, Pishvaian M, Salimuddin, Byers S. Cross-regulation of β-catenin-LEF/TCF and retinoid signaling pathways. Current Biology. 1999;9(23):1415–9.

403. Dhokia V, Macip S. A master of all trades – linking retinoids to different signalling pathways through the multi-purpose receptor STRA6. Cell Death Discovery. 2021;7(1):358.

404. Kato M, Patel MS, Levasseur R, Lobov I, Chang BHJ, Glass DA, et al. Cbfa1-independent decrease in osteoblast proliferation, osteopenia, and persistent embryonic eye vascularization in mice deficient in Lrp5, a Wnt coreceptor. Journal of Cell Biology. 2002;157(2):303–14.

405. Su CH, Dhananjaya D, Tarn WY. Alternative splicing in neurogenesis and brain development. Frontiers in Molecular Biosciences. 2018;5:12.

406. Hinrich AJ, Jodelka FM, Chang JL, Brutman D, Bruno AM, Briggs CA, et al. Therapeutic correction of ApoER2 splicing in Alzheimer's disease mice using antisense oligonucleotides. EMBO Molecular Medicine. 2016;8(4):328–45.

407. Kawano Y, Kypta R. Secreted antagonists of the Wnt signalling pathway. Journal of Cell Science. 2003;116(13):2627–34.

408. Zinzalla V, Drobits-Handl B, Savchenko A, Rinnenthal J, Bauer MJ, Sanderson M, et al. Abstract DDT01-01: BI 905677: A first-in-class LRP5/6 antagonist targeting Wnt-driven proliferation and

immune escape. Cancer Research. 2019;79(13_Supplement).

7. Annex

"It's the job that's never started that takes the longest to finish."

Gandalf to Frodo. *The Fellowship of the Ring, Chapter 3*. J.R.R. Tolkien

7.1 Article 7. Review: PCSK9 roles beyond lipid-lowering

Title: PCSK9 functions in atherosclerosis are not limited to plasmatic LDL-cholesterol Regulation

By Aureli Luquero, Lina Badimon and Maria Borrell-Pagès.

Published in Frontiers in Cardiovascular Medicine. 2021 March 23;8:639727.

doi: 10.3389/fcvm.2021.639727

frontiers in Cardiovascular Medicine

REVIEW
published: 23 March 2021
doi: 10.3389/fcvm.2021.639727

PCSK9 Functions in Atherosclerosis Are Not Limited to Plasmatic LDL-Cholesterol Regulation

Aureli Luquero[1], *Lina Badimon*[1,2,3] *and Maria Borrell-Pages*[1,2]

[1]*Cardiovascular Program ICCC, IR-Hospital de la Santa Creu i Sant Pau, IIB-Sant Pau, Barcelona, Spain,* [2]*Centro de Investigación en Red- Área Cardiovascular, Instituto de Salud Carlos III, Madrid, Spain,* [3]*Cardiovascular Research Chair, Universitat Autònoma de Barcelona, Barcelona, Spain*

The relevance of PCSK9 in atherosclerosis progression is demonstrated by the benefits observed in patients that have followed PCSK9-targeted therapies. The impact of these therapies is attributed to the plasma lipid-lowering effect induced when LDLR hepatic expression levels are recovered after the suppression of soluble PCSK9. Different studies show that PCSK9 is involved in other mechanisms that take place at different stages during atherosclerosis development. Indeed, PCSK9 regulates the expression of key receptors expressed in macrophages that contribute to lipid-loading, foam cell formation and atherosclerotic plaque formation. PCSK9 is also a regulator of vascular inflammation and its expression correlates with pro-inflammatory cytokines release, inflammatory cell recruitment and plaque destabilization. Furthermore, anti-PCSK9 approaches have demonstrated that by inhibiting PCSK9 activity, the progression of atherosclerotic disease is diminished. PCSK9 also modulates thrombosis by modifying platelets steady-state, leukocyte recruitment and clot formation. In this review we evaluate recent findings on PCSK9 functions in cardiovascular diseases beyond LDL-cholesterol plasma levels regulation.

Keywords: atherosclerosis, PCSK9 (proprotein convertase subtilisin kexin type 9), lipoprotein receptors, inflammation, lipid loading, LDL—cholesterol

OPEN ACCESS

Edited by:
Gabrielle Fredman,
Albany Medical College, United States

Reviewed by:
Marit Westerterp,
University of Groningen, Netherlands
Jürgen Bernhagen,
Ludwig Maximilian University of Munich, Germany

****Correspondence:***
Maria Borrell-Pages
mborrellpa@santpau.cat

Specialty section:
This article was submitted to Atherosclerosis and Vascular Medicine, a section of the journal Frontiers in Cardiovascular Medicine

Received: *10 December 2020*
Accepted: *01 March 2021*
Published: *23 March 2021*

Citation:
Luquero A, Badimon L and Borrell-Pages M (2021) PCSK9 Functions in Atherosclerosis Are Not Limited to Plasmatic LDL-Cholesterol Regulation. Front. Cardiovasc. Med. 8:639727. doi: 10.3389/fcvm.2021.639727

INTRODUCTION

Proprotein Convertase Subtilisin/Kexin Type 9 (PCSK9) is a soluble protein synthesized as a zymogen that undergoes autocatalytic cleavage in the endoplasmic reticulum (1). In 2007, PCSK9 was found to be a ligand for Low Density Lipoprotein Receptor (LDLR) a key cell membrane receptor in cholesterol homeostasis regulation (2). LDLRs bind and internalize low density lipoproteins (LDL) from the bloodstream, clearing the blood from highly-enriched cholesterol lipoproteins. The LDL-LDLR complex is guided to the lysosome where LDLs are digested and LDLRs are recycled to the cell surface to keep clearing LDL particles from the circulation. PCSK9 inhibits LDLR recirculation by promoting its degradation in the lysosomes along with LDLs (3). This effect highly reduces the presence of LDLR at the hepatocyte's cell surface and consequently, there is an increase in LDL particles in the bloodstream.

Although PCSK9 is known since 2003 (4) and was almost immediately associated with hypercholesterolemia (5), the knowledge of its potential role on LDL metabolism regulation and its associated diseases is increasing over the years (6, 7). It was first described that mutations on PCSK9 that lead to gain-of-function variants of the protein were responsible for different cases of human familial hypercholesterolemia [FH; (8, 9)]. FH is an inherited disease where patients have LDL plasma levels above 190 mg/dL, contributing to an elevated risk of atherosclerotic plaque formation and coronary adverse events. Contrarily, PCSK9 loss-of-function mutations are associated with very low levels of LDL in blood reducing the cardiovascular associated risk (10, 11). These data encouraged studies to test if PCSK9 was a good target for clinical trials to treat hypercholesterolemia. Hypercholesterolemia is commonly treated with statins, which are drugs that inhibit HMG-CoA reductase, a key enzyme for cholesterol biosynthesis that reduces cholesterol production and lowers LDL concentration in plasma. However, some patients present statin intolerance which hampers the treatment (12). Both PCSK9 and LDLR gene expression are regulated by SREBP2 [Sterol Regulatory Element-Binding Protein 2; (13–15)]. When intracellular levels of cholesterol are low (as after statin treatments), there is activation of SREBP2 that promotes PCSK9 and LDLR transcription. Therefore, both LDLR and LDLR's inhibitor protein levels increase resulting in an intrinsic loop that limits statin therapy efficacy (16–18). SREBP2 transcriptional activity is regulated upstream by AMPK (AMP-activated protein Kinase). Activation of AMPK leads to SREBP2 phosphorylation and its inability to promote transcription of target genes (19, 20).

Anti-PCSK9 drugs started to be developed as a secondary approach to reduce LDL cholesterol levels in hypercholesterolemic patients. To date, only two monoclonal antibodies targeting PCSK9 are available for treating hypercholesterolemia: evolocumab and alirocumab. They were tested in the OSLER trial (21) and in the ODYSSEY LONG TERM trial (22), respectively (**Table 1**). Both studies showed a ∼60% decrease of LDL particles in blood and a decrease in cardiovascular events including myocardial infarction, unstable angina or stroke (2.18% in placebo and 0.95% in evolocumab-treated patients in the OSLER trial and 5.1% in placebo and 4.6% in alirocumab-treated patients in the ODYSSEY LONG TERM study). However, the cardiovascular events reported during these studies were too low to demonstrate clinical relevance in this area. The FOURIER trial enrolled patients with previous atherosclerotic cardiovascular disease that were on statin therapy (23). Results showed a 59% reduction of LDL content in bloodstream and decreased cardiovascular events including cardiovascular mortality, myocardial infarction, stroke, hospitalization for unstable angina or coronary revascularization by more than 15% in evolocumab treated patients after 26 months follow-up. The ODYSSEY OUTCOMES study in patients with recent acute coronary syndrome at maximum tolerated dose of statins showed that alirocumab administration was associated with a reduced risk of recurrent ischemic cardiovascular events and also with a reduced mortality (24). Finally, the SPIRE 1 and SPIRE 2 trials were randomized trials that compared the efficacy of bococizumab, another anti-PCSK9 antibody, with placebo in patients that suffered previous cardiovascular events. These studies did not show benefits from bococizumab treatment despite showing significant improvements for patients with a high cardiovascular risk. There was reduced clinical efficacy because half of patients receiving bococizumab therapy developed antidrug antibodies probably because bococizumab is a murine humanized antibody containing approximately a 3% of murine sequence. Contrarily, alirocumab and evolocumab are antibodies with full human sequence. The negative results concluded in a premature stop of the trial by the sponsor (25).

Besides monoclonal antibodies, other approaches that target PCSK9 have been developed. Inclisiran (a small interference RNA) and statin administration in patients with atherosclerotic cardiovascular disease or heterozygous hypercholesterolemia patients reduced PCSK9 levels in blood and LDL-cholesterol levels in ORION-9 and ORION-10/ORION-11 phase 3 clinical trials (26, 27).

Regulation of cholesterol-rich LDL blood levels is not the only role that PCSK9 drives in atherosclerosis pathogenesis. There is a strong background suggesting alternative roles for PCSK9 in the development of atherosclerosis (28, 29). Indeed, a prospective cohort of 4.232 sixty-year-old men and women living in Stockholm County showed that independently of LDL plasma levels, PCSK9 levels correlate with elevated probability of future cardiovascular events (30). In another study that included 643 participants, high plasma PCSK9 levels correlated with enhanced atherosclerosis progression independently of LDL, as measured by carotid plaque formation and total plaque area (31). However, prospective studies have failed to demonstrate a relationship between PCSK9 expression levels and future risk of cardiovascular events despite revealing correlations between PCSK9 plasma levels and atherosclerotic markers including LDL-cholesterol, blood triglycerides or insulin (32, 33).

This review will discuss the role of PCSK9 in modulating the activity of different cell lineages involved in atherosclerosis progression including macrophages, vascular smooth muscle cells (VSMC), endothelial cells (EC), lymphocytes and platelets and its associated cardiovascular risk. We will comment on PCSK9 effector roles showing that they extend far beyond the regulation of LDL particles and reveal new insights by which PCSK9 inhibitors may lower the incidence of atherosclerosis progression.

PCSK9 MODULATES MACROPHAGE'S LIPID-UPTAKE RECEPTORS

Atherosclerosis is commonly described as a chronic inflammatory disease that starts with an excess of cholesterol accumulation in the vascular wall triggering inflammation (34). Macrophages are inflammatory cells that play a key role in lipid uptake and atherosclerosis progression. In 2012, it was shown that LDLR expressed in the surface of human macrophages were downregulated by PCSK9 produced by VSMC, reducing the ability of macrophages to internalize native LDL molecules and avoiding the formation of foam cells, indicating that PCSK9-stimulated macrophages reduce

TABLE 1 | Study characteristics and outcomes of clinical trials with monoclonal antibodies against PCSK9.

	Dosing	Patients/ Treatment ratio	Inclusion criteria	Results	Study limitations
OSLER TRIAL					
• OSLER-1: open-label, randomized and controlled study of patients from Phase II Evolocumab trials • OSLER-2: open-label, randomized and controlled study of patients from Phase III Evolocumab trials	420 mg/month or 140 mg/2 weeks	2:1 2,976 patients on Evolocumab : 1,489 patients on previous treatment (± statins)	• No adverse events in previous evolocumab studies. • Not having unstable medical condition. • Not expected to need adjustments of background lipid-regulating therapy.	• 61% reduction in LDL levels • 56% reduction in adverse CVE	• Open-label design • Low number of adverse CVE • Only patients who did not suffer CVE during previous Evolocumab therapy were accepted • High variability in patients' cardiovascular risk and use of statins
ODYSSEY LONG TERM					
A Phase III, randomized, double-blind, placebo-controlled, parallel-group and multinational study	150 mg/2 weeks	2: 1 1,553 patients on Alirocumab : 788 patients on placebo	• Heterozygous FH, coronary heart disease or equivalent risk • LDL-cholesterol levels above 70 mg/dL at screening • Patients under high-dose statin therapy or maximum-tolerated dose	• 62% reduction in LDL levels • 48% reduction adverse CVE	• Short follow-up period for a chronic disease evaluation (20 months). • Low number of CVE, limiting the robustness of the data.
FOURIER TRIAL					
Randomized, double-blinded, placebo-controlled, multicenter trial	140 mg/2 weeks or 420 mg/month	1: 1 13,784 patients on Evolocumab : 13,780 patients on placebo	• ≥40 and ≤ 85 years-old • Clinical evidence of atherosclerotic cardiovascular disease • LDL cholesterol ≥ 70 mg/dL, non-HDL cholesterol ≥ 100 mg/dL while on lipid lowering therapy	• 59% reduction in LDL cholesterol after 42 weeks • 15% reduction in CVE after 26 months	Median of 2,2 years
ODYSSEY OUTCOMES					
Randomized, double-blinded, placebo-controlled, multicenter trial	75 mg/2 weeks	1: 1 9,462 Patients on Alirocumab : 9,462 patients on placebo	• ≥40 years old • Hospitalization 1 ≤ and ≥ 12 months with acute coronary syndrome • LDL cholesterol ≥ 70 mg/dL, non-HDL cholesterol ≥ 100 mg/dL and apoB ≥ 80 mg/dL	• 54,7% reduction in LDL cholesterol after 48 months • 15% reduction of CVE and 15% reduction of death	Median of 2,8 years
SPIRE-1 and SPIRE-2					
• Spire-1 patients were eligible with at least 70 mg/dL of LDL cholesterol at screening • Spire-2 patients were eligible with at least 100 mg/dL of LDL cholesterol at screening	150 mg/2 weeks	1: 1 13,720 Patients on Bococizumab : 13,718 patients on placebo	• Men ≥ 50/Women ≥ 60, in case of FH Men ≥35/Women ≥ 45 • Previous CVE or a history of diabetes, chronic kidney disease or peripheral vascular disease with cardiovascular risk or familial hypercholesterolemia • Additional risk factors • On statin-therapy unless completely intolerance to statins is presented.	• 59% reduction in LDL cholesterol after 14 weeks • 12% reduction of CVE incidence	Median of 10 months (the study was not finished)

LDL, low density lipoprotein; HDL, high density lipoprotein; FH, familial hypercholesterolaemia; apoB, apolipoprotein B; CVE, cardiovascular event.

foam cells formation and hence, reduce atherosclerosis progression (35). However, native LDL molecules are not the major source of cholesterol accumulation in macrophages. Upon vascular extravasation, LDL molecules undergo several modifications including aggregation and oxidation. LDL aggregation and oxidation occur after extracellular matrix components such as glycosaminoglycans (36) or chondroitin sulfate proteoglycans (37) retain native LDL particles and facilitate their modification by several secreted enzymes including secretory phospholipase A2, sphingomyelinase, lipoxygenase or myeloperoxidase (38–40). Modified LDL particles generate aggregated (agLDL) and oxidized (oxLDL) LDLs, which are the major source of cholesterol ester accumulation in macrophages and VSMCs [**Figure 1**; (41–44)]. Macrophages do not internalize agLDL or oxLDL through LDLR but through a different group of receptors

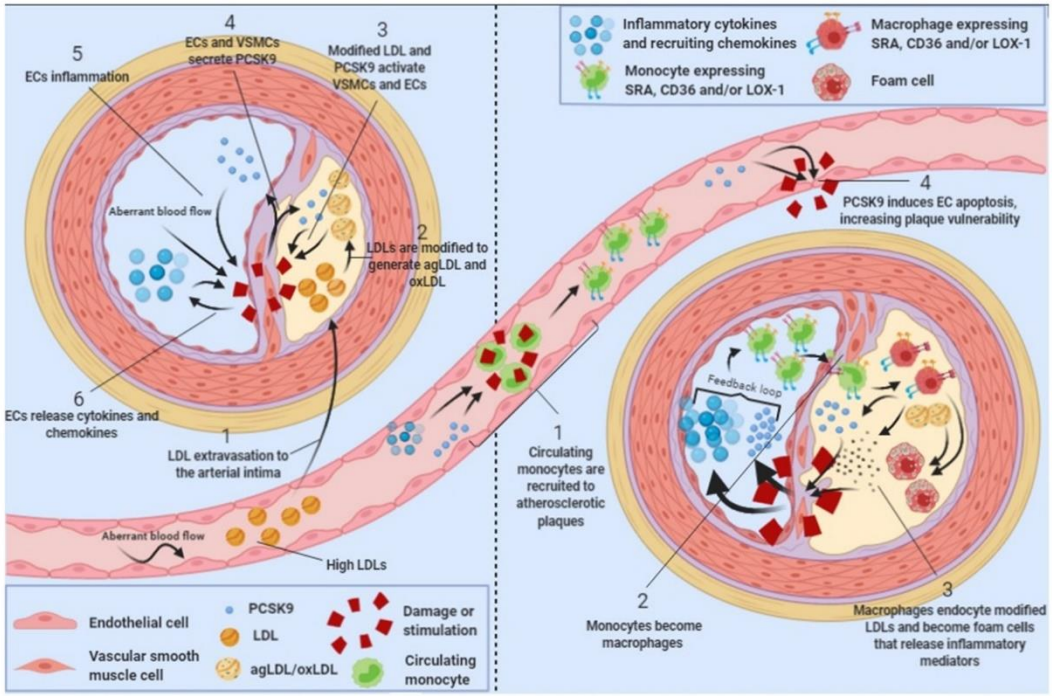

FIGURE 1 | PCSK9 in atherosclerosis progression. Schematic showing the role of PCSK9 in different stages of atherosclerosis progression.

called scavenger receptors (45) and LDLR related proteins [LRPs; (46–48)].

Scavenger receptors including scavenger receptor A (SRA), cluster of differentiation 36 (CD36) and lectin-like oxidized low-density lipoprotein receptor 1 (LOX-1) promote the endocytosis of oxLDL particles in monocytes and macrophages and their expression is highly increased under different inflammatory stimulus including lipopolysaccharide (LPS) or tumor necrosis factor-α [TNFα; **Figure 1**; (49, 50)]. Main features of scavenger receptors are summarized in **Table 2**. LPS are major components of the outer membrane of Gram-negative bacteria that are recognized by Toll-Like Receptor 4 (TLR4) expressed in macrophage's cell surface. Binding of LPS to TLR4 triggers an intracellular response that activates both MAPK and NFκB pathways triggering inflammation. PCSK9 expression levels are increased in mouse macrophages after LPS stimulation as a result of the activation of the NLRP3 (NOD-Like Receptor Protein 3) inflammasome. Indeed, NLRP3 and its downstream signals IL-1β, IL-18, and caspase 1 all participate in PCSK9 secretion as confirmed by specific gene deletion experiments (51).

PCSK9 expression in macrophages after TNFα stimulation relies on the generation of reactive oxygen species (ROS). ROS inhibitors diphenyleneiodonium (DPI) and apocynin reduce PCSK9 expression while ROS inducers pyocyanin and antimycin A increase PCSK9 release showing that PCSK9 is expressed during macrophage proinflammatory procedures (50). ROS production is dependent on NADPH oxidase. Upon TNFα-stimulation lack of different NADPH oxidase complex subunits reduces the amount of scavenger receptors in the surface of macrophages (50). Recombinant PCSK9 administration increases SRA, CD36, and LOX-1 both at gene and protein levels in cultured mouse macrophages. Concomitantly, oxLDL uptake is increased (**Figure 1**). This increased lipid uptake is abolished in macrophages that lack SRA, CD36, or LOX-1 suggesting that all three receptors are involved in oxLDL uptake and consequently, in the generation of foam cells in atherosclerosis (50). **Table 2** summarizes the involvement and regulation of scavenger receptors and LDLR in different processes associated with atherosclerosis.

Other cell surface receptors expressed in macrophages modulated by PCSK9 are LRP1, LRP5, and LRP8. These receptors belong to the LRP subfamily of the LDLR superfamily of receptors and conserve the characteristic EGF domain that allows PCSK9 binding (52). LRP1 surface levels, together with LDLR, are downregulated by human PCSK9 in atherosclerotic mouse macrophages inducing increased gene expression of

TABLE 2 | Scavenger Receptors and LDLR main features.

	LOX-1	SRA	CD36	LDLR
Cell expression	• VSMCs, endothelial cells, macrophages, platelets, fibroblasts	• Macrophages, VSMCs, endothelial cells	• Macrophages, monocytes, platelets, endothelial cells, erythrocytes	• Particularly elevated in hepatocytes • Ubiquitous expression
Upon PCSK9 stimulation	↑ expression	↑ expression	↑ expression	↓ expression
Deficiency	• Reduced oxLDL uptake in macrophages • Atheroprotective and anti-inflammatory	• Reduced oxLDL uptake in macrophages • Reduced inflammatory response • Macrophage apoptosis	• Reduced oxLDL uptake in macrophages • Atheroprotective	• Responsible for FH
Functions	• Pro-atherogenic • Pro-inflammatory • Pro-thrombotic • Induces PCSK9 expression in VSMCs • Endocytosis of oxLDL • Endothelial dysfunction • Foam cell formation • Macrophages, VSMC, endothelial cell apoptosis	• Pro-atherogenic • Pro-inflammatory • Endocytosis of oxLDL • In antigen presenting cells, mediates pathogen phagocytosis	• Pro-atherogenic • Pro-inflammatory • Pro-thrombotic • Endocytosis of oxLDL • Inhibits macrophage migration • Promotes platelet activation/aggregation	• Atheroprotective • Endocytosis of nLDL
Other regulations	Upregulated in VSMCs, macrophages and monocytes during oxidative stress and inflammation	Upregulated in VSMCs and endothelial cells during oxidative stress Upregulated in macrophages and monocytes during inflammation	Upregulated in macrophages by fat-rich diets, inflammation and oxidative stress	

nLDL, native low density lipoproteins; oxLDL, oxidized low density lipoproteins; VSMCs, vascular smooth muscle cells; FH, familial hypercholesterolemia.

the proinflammatory markers TNFα and IL-1β and decreased gene expression of the anti-inflammatory markers IL-10 and arginase-1 indicating enhanced macrophage polarization toward a pro-inflammatory phenotype (53). LRP8 (aka apoER2) a receptor known for recognizing ApoE protein is also downregulated upon recombinant PCSK9 binding in different cell lines including HEK293, 3T3 fibroblasts, CHO, NeuroA2 and HuH7 (54). We have recently described that LRP5 is required for lipid internalization in human macrophages as in the absence of PCSK9 and/or LRP5, macrophages show reduced cholesterol ester accumulation (55). Both proteins form a complex at the perinuclear area of human macrophages that immunoprecipitate together. Their interaction is stronger in lipid loaded macrophages (55). In addition, macrophages silenced for LRP5 show reduced release of PCSK9, indicating that LRP5 is involved in soluble PCSK9 release, probably by participating in the intracellular transport of PCSK9 to the plasma membrane (55). Furthermore, we also show that the complex LRP5-PCSK9 up-regulates TLR4/NFκB signaling to favor macrophage inflammation. Interestingly, LRP5 surface levels remain unaltered by secreted PCSK9 (55).

Finally, VLDLR, a receptor that also belongs to the LDLR superfamily and displays a similar structure to that of LDLR is also downregulated by PCSK9 binding. Indeed, treatment of HEK293 cells or 3T3 fibroblasts cells with human recombinant PCSK9 shows a downregulation of VLDLR expression levels (54). Both VLDLR and LRP8 are known to generate anti-inflammatory signaling in macrophages (56).

PCSK9 MODULATES VASCULAR INFLAMMATION

PCSK9 is mainly produced in liver, kidney and small intestine (4). However, it is also expressed in vascular cells including endothelial cells (ECs) and vascular smooth muscle cells [VSMCs; (35, 57, 58)]. Vascular cells are affected by hemodynamic factors like blood flow that, by inducing wall shear stress, play a critical role in atherosclerosis development and progression (59). Human ECs and VSMCs under low-blood flow have higher PCSK9 protein expression than cells under high blood flow, an effect conserved even after LPS stimulation. Indeed, aortas from *Wt* mice showed significantly higher PCSK9 expression in high shear stress regions, an effect further potentiated by LPS administration (60). Also, in rabbits fed at high-fat diet, low-flow aortic regions had higher PCSK9 expression while regions with high flow such the aortic arch showed lower vascular PCSK9 expression [**Figure 1**; (61)]. Therefore, there is a negative correlation between PCSK9 vascular expression levels and blood flow.

PCSK9 has been shown to promote vascular inflammation. Binding of PCSK9 to the inflammatory receptor TLR4 was first hypothesized by the structural homology of the C-terminal domain of PCSK9 and the TLR4 ligand resistin in *in silico* simulations (62). TLRs are cell receptors that recognize pathogens and regulate the expression of pro-inflammatory cytokines and also the early immune responses to infection (63). Among TLRs, TLR4 acts as a receptor for LPS and activates NF-κB to promote an inflammatory response (64). PCSK9

expression in ECs and VSMCs is dependent on the TLR4/NFκB signaling pathway as inhibition of different components of the activation cascade show that PCSK9 expression relies on the TLR4-MyD88-NFkB axis and is independent of the TLR4/TRIF signaling, postulating the MyD88 pathway as a possible target for future therapies to prevent excessive PCSK9 production in the vasculature (61). Hence, PCSK9 synthesis is regulated by the TLR4 receptor signaling pathway through MyD88 and NFκB activation, and soluble PCSK9 can act as an inflammatory mediator by TLR4 binding and recognition as demonstrated in *ApoE* knockout mice (65).

Vascular stability depends on cellular apoptosis. PCSK9 modulates the expression of the apoptosis inducer Bax and the apoptosis inhibitor Bcl-2. The balance between these two proteins is key to prevent or trigger apoptosis (66, 67). Lipid loaded endothelial cells show increased Bax protein levels and decreased Bcl-2 levels that lead to caspase 3 and caspase 9 activation inducing cell apoptosis (68). PCSK9 silencing by siRNA, inhibits apoptosis as silenced PCSK9 cannot phosphorylate p38 and JNK (both members of the MAPK signaling pathway) allowing the activation of the apoptosis inhibitor Bcl-2 (69–72). Interestingly, p38 and JNK are also responsible of Bax and Bad phosphorylation that activate programmed cell death (73, 74). Hence, PCSK9 may be promoting MAPK signaling cascade activation and endothelial cell apoptosis [**Figure 1**], a mechanism that has already been described in cancer cells (75).

PCSK9 PARTICIPATES IN PLAQUE FORMATION

Plaque formation is a complex process that includes lipoprotein retention, inflammatory cells recruitment, VSMC proliferation, matrix synthesis, apoptosis, and necrosis (76). Several lines of evidence sustain that PCSK9 promotes plaque formation in mice and human (29, 67, 77). Indeed, PCSK9 increases LDL uptake by macrophages scavenger receptors contributing to cell foam formation (50); it favors inflammation at the atherosclerotic vascular wall by inducing the expression of adhesion molecules, chemoattractants and inflammatory cytokines (78) and it induces ECs apoptosis reducing vessel stability (69). Furthermore, increased PCSK9 expression levels are associated to low shear stress (60, 61). Therefore, PCSK9 is an efficient target for the development therapies toward the prevention and treatment of atherosclerotic plaque formation.

Anti-PCSK9 therapy in mice reduced by half the plaque area in the aortic root, and the infiltration of pro-inflammatory macrophages in the atherosclerotic plaque was decreased (79). Serum levels of CXCL1, CXCL3, and CXCL10 (known chemoattractants for leukocytes), mainly produced by ECs and VSMCs, were reduced (79). Also, *Pcsk9* knockout mice show reduced expression of vascular cell adhesion molecule 1 (VCAM-1), a protein needed for immune cell adhesion to the vascular wall (57).

Anti-PCSK9 vaccination is an alternative to monoclonal antibody therapy. Vaccination involves the conjugation of a peptide (8–13 amino acids) that mimics the N-terminal domain of mature PCSK9 to a carrier protein that confers immunogenic properties to activate the immune system. Syntheses of host specific antibodies against PCSK9 generating long-term inhibition are obtained. Vaccination therapy aims to overcome monoclonal antibody therapy disadvantages including short *in vivo* half-lives, frequent dosage administration and high costs (80). In atherosclerosis mice models, inhibition of PCSK9 activity through vaccination decreased the expression of intercellular adhesion molecule 1 (ICAM-1) in the diseased aortic root and consequently there was a reduction in monocyte adhesion and migration to the endothelium that contributed to a reduction in atherosclerotic lesions (81). The anti-PCSK9 vaccine AT04A, which generates persistent humoral immune response against PCSK9 for 1 year in mice, reduced LDL content by more than 50% (81). It also reduced NLRP3 inflammasome expression in macrophages (81), a powerful inducer for PCSK9 expression and secretion in macrophages needed for the formation and progression of atherosclerotic plaques (51).

In humans, PCSK9 inhibitors therapy added to statin therapy is capable of increasing fibrous cap thickening in acute coronary syndrome patients, reducing plaque vulnerability (82). However, the LDL-cholesterol lowering capacities of both PCSK9 inhibitors and statin treatment cannot solely explain the increased fibrous cap thickness suggesting that an unknown pleiotropic effect such as an anti-inflammatory effect independent of lowering LDL-cholesterol may be involved (82). PCSK9 inhibitor treatment in an atherogenic mouse model increased the number of circulating endothelial progenitor cells and circulating angiogenic cells, markers of endothelial and vascular health associated with positive outcomes as reduced occurrence of cardiovascular events and death associated to cardiovascular causes (83).

ROLE OF PCSK9 IN INFLAMMATION IN THE ADAPTIVE IMMUNE SYSTEM

The role of PCSK9 during atherosclerosis progression in the adaptive immune system has been studied. Dendritic cells (DCs) and T lymphocytes are localized in the atherosclerotic plaque, usually at sites prone to rupture (84). DCs mainly work as antigen presenting cells to T lymphocytes. They phagocyte antigens and present them to T lymphocytes in a process that involves MHC and TCR complexes (in DCs and T lymphocytes, respectively). In atheroma plaques, DCs present oxLDL fragments to T-lymphocytes that are then activated (85). The importance of T cell activation in atherosclerosis was demonstrated because *ApoE* knockout and immunodeficient (severe combined immunodeficiency mice without functional B and T lymphocytes) mice had less atherosclerotic lesions than *ApoE* knockout mice alone. Furthermore, CD4 T lymphocytes from *ApoE* knockout mice transferred to immunodeficient *ApoE* knockout mice induce the generation of atherosclerotic lesions (86). PCSK9 is induced by oxLDL in DCs and enhances the expression of proteins involved in T cell activation including CD80, CD83, CD86, and HLA-DR and the production of

pro-inflammatory cytokines including TNFα, IL-1β, and IL-6. The expression of all these proteins was reduced when PCSK9 was silenced, and TGFβ and IL-10 expression levels were increased (87). T cells activated by oxLDL-stimulated DCs produced mainly IFNγ and IL-17, indicating a polarization toward an anti-inflammatory Th1/Th17 phenotype. These anti-inflammatory T regulatory cells inhibit foam cell formation and reverse the pro-inflammatory phenotype of macrophages reducing atherosclerosis progression (88). PCSK9 is a key molecule in Th17 response as atherosclerotic *Pcsk9/Ldlr/Apobec* (apolipoprotein B mRNA-editing catalytic polypeptide-1) triple knockout mice had significant lower Th17 production in comparison with atherosclerotic *Ldlr/Apobec* double knockout mice. This was associated with changes in the different cellular sources of Th17 (Th17 lymphocytes or $\gamma\delta TCR^+$ T cells). Indeed, mice lacking PCSK9 had a reduced number of Th17 lymphocytes as well as a reduced expression of RORγT, the transcription factor needed for Th17 lymphocyte differentiation (89).

A very recent work shows that PCSK9 downregulates the expression of MHC class I proteins in tumor cells by promoting its internalization and degradation in lysosomes (in a similar manner to that of PCSK9 with LDLR). Therefore, PCSK9 decreases the cytotoxic T lymphocyte response against the tumor (90). In an atherosclerotic context it seems plausible that modified LDLs could stimulate antigen presenting cells such as DCs or B cells to produce a variety of cytokines that would guide T lymphocytes differentiation toward a particular inflammatory subtype.

PCSK9'S ROLE IN FAMILIAL HYPERCHOLESTEROLEMIA

In 2003, after the discovery of PCSK9 gain-of-function mutations in FH patients the first monoclonal antibodies against PCSK9 were tested in preclinical and clinical studies (including ODYSSEY LONG TERM, ODYSSEY OUTCOMES, and FOURIER) demonstrating efficacy in reducing LDL cholesterol plasma levels in patients (91). In 2020 a recent sub analysis of the FOURIER and ODYSSEY OUTCOMES trials revealed that PCSK9 inhibition in patients with stable atherosclerosis and hyperlipidemia on statin therapy significantly reduces the risk of venous thromboembolism supporting a protective role for antiPCSK9 antibodies in human cardiovascular diseases (92). Monoclonal antibodies against PCSK9 are also capable of reversing the pro-inflammatory phenotype of atherogenic macrophages in patients with FH. PCSK9 inhibitors reduced CCR2, CX3CR1, and integrins CD11b and CD18 expression in circulating monocytes suggesting a lower infiltrating and chemoattractant capacity. PCSK9 antibody treatment reduced the production of TNFα by monocytes while the production of anti-inflammatory cytokine IL-10 was enhanced (93). In fact, circulating monocytes from FH patients were enriched with lipid droplets despite non-detectable LDLR expression but increased expression of CD36 and SRA [**Figure 1**; (93)]. Also, ABCA1 protein, a protein responsible for cholesterol efflux in macrophages, was inhibited upon PCSK9 expression (94). Taken together, these results suggest that circulating monocytes are pre-conditioned in FH patients due to PCSK9 activity, which enhances their infiltrating capacity, lipid accumulation and pro-inflammatory activity. Indeed, a prospective study with heterozygous FH patients under standard statin therapy revealed a positive correlation between circulating levels of PCSK9 and adverse cardiovascular events (95).

PCSK9 AND PLATELET THROMBOSIS

Several risk factors associated with cardiovascular disease, including hyperlipidaemia, induce endothelial dysfunction and lead to arterial or venous thrombosis (96). In arteries with ongoing atherosclerosis progression, atherosclerotic plaque rupture is the main cause for thrombosis (97).

Pcsk9 knockout mice show reduced carotid artery thrombosis induced by $FeCl_3$ (a technique to rapidly and accurately induce thrombi formation) in different sized arteries and veins (98). Upon $FeCl_3$ stimulation, 70% of *Pcsk9* knockout mice developed non-occlusive non-stable thrombi after 30 min while 57% of *Wt* mice showed total artery occlusion before 15 min after $FeCl_3$ administration suggesting a role for PCSK9 in platelet reactivity (98). Furthermore, platelets from *Pcsk9* knockout mice show a significant reduction in glycoprotein IIB/IIIA expression levels, P-selectin expression levels and in circulating platelet-leukocyte aggregates in comparison with *Wt* mice indicating lower platelet activation in *Pcsk9* knockout mice (98). Similarly, *Pcsk9* knockout mice also show reduced thrombi formation after inferior vena cava ligation in comparison to *Wt* mice (99). Thrombi generated by inferior vena cava ligation in *Pcsk9* knockout mice have less leukocyte attachment as leukocyte recruitment is dependent on P-selectin and CXCL1, which are downregulated in *Pcsk9* knockout mice (100). However, it is unknown whether this inflammatory cell recruitment is downregulated because of PCSK9's role in lipid uptake or because PCSK9 has lipid-independent functions on platelet's steady-state (**Figure 2** illustrates some of the mechanisms by which PCSK9 induces thrombosis).

NETosis is the process by which neutrophils release their nuclei content composed of DNA and antimicrobial proteins including neutrophil elastases and histones, creating networks of extracellular fibers that trap and facilitate the killing of pathogens (101). NETosis is linked to thrombosis because it causes platelet activation, aggregation and adhesion (102) and promotes the initiation of the coagulation cascade (100). In *Pcsk9* knockout mice NETosis is significantly reduced, despite that the total number of blood neutrophils and leukocytes are increased suggesting that PCSK9 can induce thrombosis by stimulating NETosis [**Figure 2**; (99)].

The PCSK9-REACT study is an observational, prospective study where patients with recent acute coronary syndromes underwent coronary intervention and received $P2Y_{12}$ inhibitors (103). $P2Y_{12}$ is a chemoreceptor for adenosine diphosphate (ADP) involved in platelet aggregation (104) and a target for thromboembolism treatments using antagonists as ticagrelor or

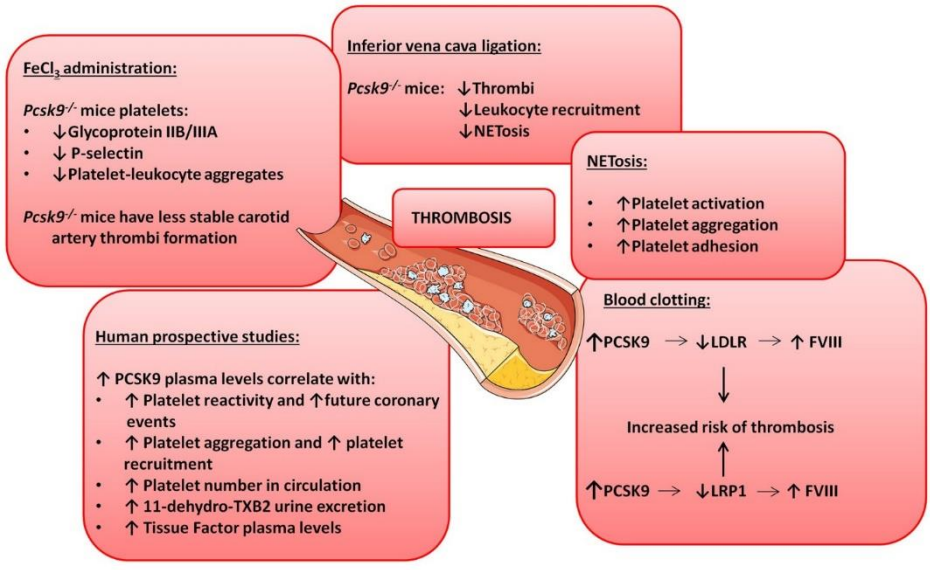

FIGURE 2 | PCSK9 aggravates thrombosis. Schematic showing the involvement of PCSK9 in different thrombotic processes.

prasugrel (105). The study revealed a strong correlation between PCSK9 blood levels and platelet reactivity (103). It also showed that elevated PCSK9 plasma levels are associated with future coronary events as 22% of patients with the highest PCSK9 plasma levels suffered coronary events while only 2% of the patients in the lower tertile experienced coronary events. In line with these results, human recombinant PCSK9 added to healthy human plasma was capable of significantly increasing platelet aggregation and reducing aggregation lag time when platelets were stimulated with epinephrine (98). The platelet enhancing capacity is because addition of PCSK9 increased the total number of platelets that express the activation marker glycoprotein IIB/IIIA by 36% [**Figure 2**; (98)].

A relationship between PCSK9 plasma levels and total number of circulating platelets has also been shown in patients with stable coronary artery disease (106). Similarly, atrial fibrillation patients show a strong correlation between PCSK9 plasma levels and platelet reactivity as elevated PCSK9 levels positively correlate with elevated risk for this cardiovascular event (107). These patients also have higher rate of platelet aggregation and recruitment coincidentally with higher expression levels of thromboxane B_2 (TxB_2, a platelet activation marker), higher release of P-selectin and enhanced ROS formation (108). Correlation between elevated PCSK9 plasma levels and elevated urine excretion of TxB_2 was also found (108). Taken together, these results show that not only platelet number but also platelet reactivity is enhanced when PCSK9 plasma levels are elevated (**Figure 2**).

Cholesterol incorporation into platelet membranes induces platelet reactivity while cholesterol depletion from membranes is associated with platelet stability (109). Thus, PCSK9 inhibition would decrease plasma LDL levels reducing platelet reactivity. As a matter of fact, statins treatment in hypercholesterolemic patients, is able to reduce platelet membrane cholesterol (110). It remains a matter of discussion whether PCSK9 exerts a direct effect on platelets or the effects depend on the dyslipidaemia generated by PCSK9 binding to LDLR. Dyslipidaemia induces the generation of oxLDL and agLDL, which in turn, facilitate platelet activation by binding scavenger receptors on platelet's surface including LOX-1 and CD36 (111–113). Once activated, platelets are capable of oxidizing LDLs, generating a positive feedback of platelet activation (114). PCSK9 inhibition also downregulates lipoprotein (a) [Lp(a)] serum levels in patients with inherited dyslipidemias (115). Since Lp(a) enhances platelet activation and thrombosis (116–119), PCSK9 may prevent thrombosis by lowering Lp(a) levels. A direct effect of PCSK9 on platelets independent of its effects on dyslipidaemia has been recently shown as PCSK9 inhibitors can enhance oxidative stress (as a result of the activation of the Nox2 and $cPLA_2$ signaling cascades) and block platelet activation in *Wt* human platelets (108).

PCSK9 inhibitors are being tested to modulate platelet activation in humans. Patients with primary hypercholesterolemia with previous statin treatment were treated for 12 months with alirocumab or evolocumab and after only 2 months treatment a significant decrease in the platelet activation marker CD62P was found (120). Soluble CD40, soluble P-selectin and platelet factor 4 plasma levels were

also reduced after 12 months of statin and PCSK9 inhibitor treatment. The study also shows that hypercholesterolemic patients with additional acetylsalicylic acid administration to statins and PCSK9 inhibitors have decreased platelet aggregation (120). A trend in the reduction of platelet aggregation in patients without acetylsalicylic acid administration was observed but there were no significant differences because of the low number of patients that followed this treatment (120).

PCSK9 is also involved in blood clotting. Clotting formation is a complex chemical process were circulating blood clotting factors will sequentially induce protein cleavages to generate thrombin and fibrin (121). A correlation between elevated blood clotting Factor VIII (FVIII) plasma levels and arterial thrombosis has been shown in both animal and human studies (122–124). FVIII synthesis and clearance (and therefore FVIII plasma levels) are regulated by the liver. Indeed, LDLR and LRP1 expressed in hepatocytes promote FVIII endocytosis and degradation (125–128). Although not demonstrated yet, a connection between PCSK9 and FVIII seems plausible. Indeed, downregulation of LDLR expression in hepatocytes cell surface regulated by PCSK9 induces an increase in FVIII plasma levels and therefore an increased risk of thrombosis and cardiovascular events (127). PCSK9 can also reduce LRP1 cell surface expression further increasing FVIII plasma levels (53, 129). Finally, in patients that produce anti-phospholipidic antibodies, polymorphisms in PCSK9 and LDLR genes are associated with thrombosis progression supporting a role in clotting formation for the PCSK9-LDLR axis [**Figure 2**; (130)].

CONCLUDING REMARKS

Since PCSK9 was first described as the inducer of some FH pathologies, a lot of interest has been placed in the achievement of an effective inhibitory treatment. PCSK9 inhibitors administered to patients revealed a key role of PCSK9 in atherosclerotic disease as its inhibition reduced plasma LDL-cholesterol levels with improved clinical cardiovascular outcomes demonstrating a multifactorial and pathophysiological role for PCSK9 in atherosclerosis progression. Interestingly, PCSK9 functions are far from only regulating LDL-cholesterol plasma levels by reducing hepatic LDLR expression. Indeed, recent findings demonstrate that PCSK9 is also actively modulating inflammation, plaque formation and thrombosis. Hence, the benefits observed from PCSK9 inhibitory therapies may not only be induced by its plasma lipid-lowering capacities but also by reducing the impact of several other mechanisms in which PCSK9 is involved that are actively promoting atherosclerosis. Unfortunately, the information on PCSK9 interactome is still limited and further investigations on the role of PCSK9's activity on different signaling pathways are still needed to generate a clear vision of PCSK9 full potential during atherosclerosis progression. Despite PCSK9 has been studied mostly in cardiovascular diseases, it also participates in general mechanisms shared by many other diseases, and hence it is conceivable that PCSK9 is involved in the initiation and progression of other pathologies with powerful inflammatory or thrombotic components.

AUTHOR CONTRIBUTIONS

AL: research performance, draft manuscript preparation, writing and review. MB-P: conceptualization, funding acquisition, draft manuscript preparation, writing, review, and editing. LB: conceptualization and funding acquisition. All authors contributed to the article and approved the submitted version.

FUNDING

This work was supported by the Spanish Ministry of Science and Innovation and FEDER funds (PID2019-107160RB-I00 to LB); the Instituto de Salud Carlos III (CIBERCV CB16/11/00411 to LB, TERCEL RD16/0011/018 to LB and FIS2020-01282 to MB-P); the Generalitat of Catalunya-Secretaria d'Universitats i Recerca del Departament d'Economia i Coneixement de la Generalitat (2017SGR1480 to LB); the Spanish Society of Cardiology (FEC 2019 to MB-P); and the Fundación Investigación Cardiovascular-Fundación Jesus Serra for their continuous support.

ACKNOWLEDGMENTS

We thank S. Huertas and M. A. Velasco for their continuous support to the group.

REFERENCES

1. Poirier S, Mayer G. The biology of PCSK9 from the endoplasmic reticulum to lysosomes: new and emerging therapeutics to control low-density lipoprotein cholesterol. *Drug Des Devel Ther.* (2013) 7:1135–48. doi: 10.2147/DDDT.S36984
2. Zhang DW, Lagace TA, Garuti R, Zhao Z, McDonald M, Horton JD, et al. Binding of proprotein convertase subtilisin/kexin type 9 to epidermal growth factor-like repeat A of low density lipoprotein receptor decreases receptor recycling and increases degradation. *J Biol Chem.* (2007) 282:18602–12. doi: 10.1074/jbc.M702027200
3. Benjannet S, Rhainds D, Essalmani R, Mayne J, Wickham L, Jin W, et al. NARC-1/PCSK9 and its natural mutants: zymogen cleavage and effects on the low density lipoprotein (LDL) receptor and LDL cholesterol. *J Biol Chem.* (2004) 279:48865–75. doi: 10.1074/jbc.M409699200
4. Seidah NG, Benjannet S, Wickham L, Marcinkiewicz J, Bélanger Jasmin S, Stifani S, et al. The secretory proprotein convertase neural apoptosis-regulated convertase 1 (NARC-1): liver regeneration and neuronal differentiation. *Proc Natl Acad Sci USA.* (2003) 100:928–33. doi: 10.1073/pnas.0335507100
5. Abifadel M, Varret M, Rabès JP, Allard D, Ouguerram K, Devillers M, et al. Mutations in PCSK9 cause autosomal dominant hypercholesterolemia. *Nat Genet.* (2003) 34:154–6. doi: 10.1038/ng1161
6. Soutar AK. Unexpected roles for PCSK9 in lipid metabolism. *Curr Opin Lipidol.* (2011) 22:192–6. doi: 10.1097/MOL.0b013e32834622b5
7. Seidah NG, Abifadel M, Prost S, Boileau C, Prat A. The proprotein convertases in hypercholesterolemia and cardiovascular

diseases: emphasis on proprotein convertase subtilisin/Kexin 9. *Pharmacol Rev*. (2017) 69:33–52. doi: 10.1124/pr.116.012989

8. Timms KM, Wagner S, Samuels ME, Forbey K, Goldfine H, Jammalapati S, et al. A mutation in PCSK9 causing autosomal-dominant hypercholesterolemia in a Utah pedigree. *Hum Genet*. (2004) 114:349–53. doi: 10.1007/s00439-003-1071-9
9. Fasano T, Sun XM, Patel DD, Soutar AK. Degradation of LDLR protein mediated by "gain of function" PCSK9 mutants in normal and ARH cells. *Atherosclerosis*. (2009) 203:166–71. doi: 10.1016/j.atherosclerosis.2008.10.027
10. Cariou B, Ouguerram K, Zaïr Y, Guerois R, Langhi C, Kourimate S, et al. PCSK9 dominant negative mutant results in increased LDL catabolic rate and familial hypobetalipoproteinemia. *Arterioscler Thromb Vasc Biol*. (2009) 29:2191–7. doi: 10.1161/ATVBAHA.109.194191
11. Benjannet S, Hamelin J, Chrétien M, Seidah NG. Loss- and gain-of-function PCSK9 variants: cleavage specificity, dominant negative effects, and low density lipoprotein receptor (LDLR) degradation. *J Biol Chem*. (2012) 287:33745–55. doi: 10.1074/jbc.M112.399725
12. Reiner Z. Resistance and intolerance to statins. *Nutr Metab Cardiovasc Dis*. (2014) 24:1057–66. doi: 10.1016/j.numecd.2014.05.009
13. Dubuc G, Chamberland A, Wassef H, Davignon J, Seidah NG, Bernier L, et al. Statins upregulate PCSK9, the gene encoding the proprotein convertase neural apoptosis-regulated convertase-1 implicated in familial hypercholesterolemia. *Arterioscler Thromb Vasc Biol*. (2004) 24:1454–9. doi: 10.1161/01.ATV.0000134621.14315.43
14. Costet P, Cariou B, Lambert G, Lalanne F, Lardeux B, Jarnoux AL, et al. Hepatic PCSK9 expression is regulated by nutritional status via insulin and sterol regulatory element-binding protein 1c. *J Biol Chem*. (2006) 281:6211–8. doi: 10.1074/jbc.M508582200
15. Miserez AR, Muller PY, Barella L, Barella S, Staehelin HB, Leitersdorf E, et al. Sterol-regulatory element-binding protein (SREBP)-2 contributes to polygenic hypercholesterolaemia. *Atherosclerosis*. (2002) 164:15–26. doi: 10.1016/S0021-9150(01)00762-6
16. Mayne J, Dewpura T, Raymond A, Cousins M, Chaplin A, Lahey KA, et al. Plasma PCSK9 levels are significantly modified by statins and fibrates in humans. *Lipids Health Dis*. (2008) 7:22. doi: 10.1186/1476-511X-7-22
17. Careskey HE, Davis RA, Alborn WE, Troutt JS, Cao G, Konrad RJ. Atorvastatin increases human serum levels of proprotein convertase subtilisin/kexin type 9. *J Lipid Res*. (2008) 49:394–8. doi: 10.1194/jlr.M700437-JLR200
18. Dong B, Wu M, Li H, Kraemer FB, Adeli K, Seidah NG, et al. Strong induction of PCSK9 gene expression through HNF1α and SREBP2: mechanism for the resistance to LDL-cholesterol lowering effect of statins in dyslipidemic hamsters. *J Lipid Res*. (2010) 51:1486–95. doi: 10.1194/jlr.M003566
19. Sui GG, Xiao HB, Lu XY, Sun ZL. Naringin activates AMPK resulting in altered expression of SREBPs, PCSK9, and LDLR to reduce body weight in obese C57BL/6J mice. *J Agric Food Chem*. (2018) 66:8983–90. doi: 10.1021/acs.jafc.8b02696
20. Li X, Hu X, Pan T, Dong L, Ding L, Wang Z, et al. Kanglexin, a new anthraquinone compound, attenuates lipid accumulation by activating the AMPK/SREBP-2/PCSK9/LDLR signalling pathway. *Biomed Pharmacother*. (2021) 133:110802. doi: 10.1016/j.biopha.2020.110802
21. Sabatine MS, Giugliano RP, Wiviott SD, Raal FJ, Blom DJ, Robinson J, et al. Efficacy and safety of evolocumab in reducing lipids and cardiovascular events. *N Engl J Med*. (2015) 372:1500–9. doi: 10.1056/NEJMoa1500858
22. Robinson JG, Farnier M, Krempf M, Bergeron J, Luc G, Averna M, et al. Efficacy and safety of alirocumab in reducing lipids and cardiovascular events. *N Engl J Med*. (2015) 372:1489–99. doi: 10.1056/NEJMoa1501031
23. Sabatine MS, Giugliano RP, Keech AC, Honarpour N, Wiviott SD, Murphy SA, et al. Evolocumab and clinical outcomes in patients with cardiovascular disease. *N Engl J Med*. (2017) 376:1713–22. doi: 10.1056/NEJMoa1615664
24. Schwartz GG, Steg PG, Szarek M, Bhatt DL, Bittner VA, Diaz R, et al. Alirocumab and cardiovascular outcomes after acute coronary syndrome. *N Engl J Med*. (2018) 379:2097–107. doi: 10.1056/NEJMoa1801174
25. Ridker PM, Revkin J, Amarenco P, Brunell R, Curto M, Civeira F, et al. Cardiovascular efficacy and safety of bococizumab in high-risk patients. *N Engl J Med*. (2017) 376:1527–39. doi: 10.1056/NEJMoa1701488
26. Raal FJ, Kallend D, Ray KK, Turner T, Koenig W, Wright RS, et al. Inclisiran for the treatment of heterozygous familial hypercholesterolemia. *N Engl J Med*. (2020) 382:1520–30. doi: 10.1056/NEJMoa1913805
27. Ray KK, Wright RS, Kallend D, Koenig W, Leiter LA, Raal FJ, et al. Two phase 3 trials of inclisiran in patients with elevated LDL cholesterol. *N Engl J Med*. (2020) 382:1507–19. doi: 10.1056/NEJMoa1912387
28. Cariou B, Ding Z, Mehta JL. PCSK9 and atherosclerosis: beyond LDL-cholesterol lowering. *Atherosclerosis*. (2016) 253:275–7. doi: 10.1016/j.atherosclerosis.2016.08.007
29. Shapiro MD, Fazio S. PCSK9 and atherosclerosis - lipids and beyond. *J Atheroscler Thromb*. (2017) 24:462–72. doi: 10.5551/jat.RV17003
30. Leander K, Mälarstig A, Van'T Hooft FM, Hyde C, Hellénius ML, Troutt JS, et al. Circulating proprotein convertase subtilisin/kexin type 9 (PCSK9) predicts future risk of cardiovascular events independently of established risk factors. *Circulation*. (2016) 133:1230–9. doi: 10.1161/CIRCULATIONAHA.115.018531
31. Xie W, Liu J, Wang W, Wang M, Qi Y, Zhao F, et al. Association between plasma PCSK9 levels and 10-year progression of carotid atherosclerosis beyond LDL-C: a cohort study. *Int J Cardiol*. (2016) 215:293–8. doi: 10.1016/j.ijcard.2016.04.103
32. Ridker PM, Rifai N, Bradwin G, Rose L. Plasma proprotein convertase subtilisin/kexin type 9 levels and the risk of first cardiovascular events. *Eur Heart J*. (2016) 37:554–60. doi: 10.1093/eurheartj/ehv568
33. Zhu YM, Anderson TJ, Sikdar K, Fung M, McQueen MJ, Lonn EM, et al. Association of proprotein convertase subtilisin/kexin type 9 (PCSK9) with cardiovascular risk in primary prevention. *Arterioscler Thromb Vasc Biol*. (2015) 35:2254–9. doi: 10.1161/ATVBAHA.115.306172
34. Ross R. The pathogenesis of atherosclerosis: a perspective for the 1990s. *Nature*. (1993) 362:801–9. doi: 10.1038/362801a0
35. Ferri N, Tibolla G, Pirillo A, Cipollone F, Mezzetti A, Pacia S, et al. Proprotein convertase subtilisin kexin type 9 (PCSK9) secreted by cultured smooth muscle cells reduces macrophages LDLR levels. *Atherosclerosis*. (2012) 220:381–6. doi: 10.1016/j.atherosclerosis.2011.11.026
36. Hurt-Camejo E, Camejo G, Rosengren B, López F, Ahlström C, Fager G, et al. Effect of arterial proteoglycans and glycosaminoglycans on low density lipoprotein oxidation and its uptake by human macrophages and arterial smooth muscle cells. *Arterioscler Thromb Vasc Biol*. (1992) 12:569–83. doi: 10.1161/01.ATV.12.5.569
37. Williams KJ. Arterial wall chondroitin sulfate proteoglycans: diverse molecules with distinct roles in lipoprotein retention and atherogenesis. *Curr Opin Lipidol*. (2001) 12:477–87. doi: 10.1097/00041433-200110000-00002
38. Deevska GM, Sunkara M, Morris AJ, Nikolova-Karakashian MN. Characterization of secretory sphingomyelinase activity, lipoprotein sphingolipid content and LDL aggregation in ldlr-/- mice fed on a high-fat diet. *Biosci Rep*. (2012) 32(Pt 5):479–90. doi: 10.1042/BSR20120036
39. Leitinger N, Watson AD, Hama SY, Ivandic B, Qiao JH, Huber J, et al. Role of group II secretory phospholipase A2 in atherosclerosis: 2. Potential involvement of biologically active oxidized phospholipids. *Arterioscler Thromb Vasc Biol*. (1999) 19:1291–8. doi: 10.1161/01.ATV.19.5.1291
40. Yoshida H, Kisugi R. Mechanisms of LDL oxidation. *Clin Chim Acta*. (2010) 411:1875–82. doi: 10.1016/j.cca.2010.08.038
41. Llorente-Cortés V, Otero-Viñas M, Camino-López S, Llampayas O, Badimon L. Aggregated low-density lipoprotein uptake induces membrane tissue factor procoagulant activity and microparticle release in human vascular smooth muscle cells. *Circulation*. (2004) 110:452–9. doi: 10.1161/01.CIR.0000136032.40666.3D
42. Costales P, Fuentes-Prior P, Castellano J, Revuelta-Lopez E, Corral-Rodríguez MÁ, Nasarre L, et al. K domain CR9 of low density lipoprotein (LDL) receptor-related protein 1 (LRP1) is critical for aggregated LDL-induced foam cell formation from human vascular smooth muscle cells. *J Biol Chem*. (2015) 290:14852–65. doi: 10.1074/jbc.M115.638361
43. Quinn MT, Parthasarathy S, Fong LG, Steinberg D. Oxidatively modified low density lipoproteins: a potential role in recruitment and retention of monocyte/macrophages during atherogenesis. *Proc Natl Acad Sci USA*. (1987) 84:2995–8. doi: 10.1073/pnas.84.9.2995

44. Parthasarathy S, Quinn MT, Steinberg D. Is oxidized low density lipoprotein involved in the recruitment and retention of monocyte/macrophages in the artery wall during the initiation of atherosclerosis? *Basic Life Sci.* (1988) 49:375–80. doi: 10.1007/978-1-4684-5568-7_58
45. Beppu M, Ohishi K, Kikugawa K. Modification of delipidated apoprotein B of low density lipoprotein by lipid oxidation products in relation to macrophage scavenger receptor binding. *Biol Pharm Bull.* (1994) 17:51–7. doi: 10.1248/bpb.17.51
46. Hu L, Boesten LSM, May P, Herz J, Bovenschen N, Huisman MV, et al. Macrophage low-density lipoprotein receptor-related protein deficiency enhances atherosclerosis in apoE/LDLR double knockout mice. *Arterioscler Thromb Vasc Biol.* (2006) 26:2710–5. doi: 10.1161/01.ATV.0000249641.96896.e6
47. Borrell-Pages M, Romero JC, Juan-Babot O, Badimon L. Wnt pathway activation, cell migration, and lipid uptake is regulated by low-density lipoprotein receptor-related protein 5 in human macrophages. *Eur Heart J.* (2011) 32:2841–50. doi: 10.1093/eurheartj/ehr062
48. Waltmann MD, Basford JE, Konaniah ES, Weintraub NL, Hui DY. Apolipoprotein E receptor-2 deficiency enhances macrophage susceptibility to lipid accumulation and cell death to augment atherosclerotic plaque progression and necrosis. *Biochim Biophys Acta Mol Basis Dis.* (2014) 1842:1395–405. doi: 10.1016/j.bbadis.2014.05.009
49. Hossain E, Ota A, Karnan S, Takahashi M, Mannan SB, Konishi H, et al. Lipopolysaccharide augments the uptake of oxidized LDL by up-regulating lectin-like oxidized LDL receptor-1 in macrophages. *Mol Cell Biochem.* (2015) 400:29–40. doi: 10.1007/s11010-014-2259-0
50. Ding Z, Liu S, Wang X, Theus S, Deng X, Fan Y, et al. PCSK9 regulates expression of scavenger receptors and ox-LDL uptake in macrophages. *Cardiovasc Res.* (2018) 114:1145–53. doi: 10.1093/cvr/cvy079
51. Ding Z, Wang X, Liu S, Zhou S, Kore RA, Mu S, et al. NLRP3 inflammasome via IL-1β regulates PCSK9 secretion. *Theranostics.* (2020) 10:7100–10. doi: 10.7150/thno.45939
52. Go GW, Mani A. Low-density lipoprotein receptor (LDLR) family orchestrates cholesterol homeostasis. *Yale J Biol Med.* (2012) 85:19–28.
53. Giunzioni I, Tavori H, Covarrubias R, Major AS, Ding L, Zhang Y, et al. Local effects of human PCSK9 on the atherosclerotic lesion. *J Pathol.* (2016) 238:52–62. doi: 10.1002/path.4630
54. Poirier S, Mayer G, Benjannet S, Bergeron E, Marcinkiewicz J, Nassoury N, et al. The proprotein convertase PCSK9 induces the degradation of low density lipoprotein receptor (LDLR) and its closest family members VLDLR and ApoER2. *J Biol Chem.* (2008) 283:2363–72. doi: 10.1074/jbc.M708098200
55. Badimon L, Luquero A, Crespo J, Peña E, Borrell-Pages M. PCSK9 and LRP5 in macrophage lipid internalization and inflammation. *Cardiovasc Res.* (2020) cvaa254. doi: 10.1093/cvr/cvaa254. [Epub ahead of print].
56. Baitsch D, Bock HH, Engel T, Telgmann R, Müller-Tidow C, Varga G, et al. Apolipoprotein e induces antiinflammatory phenotype in macrophages. *Arterioscler Thromb Vasc Biol.* (2011) 31:1160–8. doi: 10.1161/ATVBAHA.111.222745
57. Ding Z, Liu S, Wang X, Deng X, Fan Y, Shahanawaz J, et al. Cross-Talk between LOX-1 and PCSK9 in vascular tissues. *Cardiovasc Res.* (2015) 107:556–67. doi: 10.1093/cvr/cvv178
58. Ding Z, Liu S, Wang X, Mathur P, Dai Y, Theus S, et al. Cross-Talk between PCSK9 and damaged mtDNA in vascular smooth muscle cells: role in apoptosis. *Antioxidants Redox Signal.* (2016) 25:997–1008. doi: 10.1089/ars.2016.6631
59. Chatzizisis YS, Coskun AU, Jonas M, Edelman ER, Feldman CL, Stone PH. Role of endothelial shear stress in the natural history of coronary atherosclerosis and vascular remodeling. molecular, cellular, and vascular behavior. *J Am Coll Cardiol.* (2007) 49:2379–93. doi: 10.1016/j.jacc.2007.02.059
60. Ding Z, Liu S, Wang X, Deng X, Fan Y, Sun C, et al. Hemodynamic shear stress via ROS modulates PCSK9 expression in human vascular endothelial and smooth muscle cells and along the mouse aorta. *Antioxidants Redox Signal.* (2015) 22:760–71. doi: 10.1089/ars.2014.6054
61. Liu S, Deng X, Zhang P, Wang X, Fan Y, Zhou S, et al. Blood flow patterns regulate PCSK9 secretion via MyD88-mediated pro-inflammatory cytokines. *Cardiovasc Res.* (2019) 116:1721–32. doi: 10.1093/cvr/cvz262
62. Hampton EN, Knuth MW, Li J, Harris JL, Lesley SA, Spraggon G. The self-inhibited structure of full-length PCSK9 at 1.9 Å reveals structural homology with resistin within the C-terminal domain. *Proc Natl Acad Sci USA.* (2007) 104:14604–9. doi: 10.1073/pnas.0703402104
63. Takeda K, Akira S. Toll-like receptors in innate immunity. *Int Immunol.* (2005) 17:1–14. doi: 10.1093/intimm/dxh186
64. Guijarro-Muñoz I, Compte M, Álvarez-Cienfuegos A, Álvarez-Vallina L, Sanz L. Lipopolysaccharide activates toll-like receptor 4 (TLR4)-mediated NF-κB signaling pathway and proinflammatory response in human pericytes. *J Biol Chem.* (2014) 289:2457–68. doi: 10.1074/jbc.M113.521161
65. Tang ZH, Peng J, Ren Z, Yang J, Li TT, Li TH, et al. New role of PCSK9 in atherosclerotic inflammation promotion involving the TLR4/NF-κB pathway. *Atherosclerosis.* (2017) 262:113–22. doi: 10.1016/j.atherosclerosis.2017.04.023
66. Molostvov G, Morris A, Rose P, Basu S. Modulation of Bcl-2 family proteins in primary endothelial cells during apoptosis. *Pathophysiol Haemost Thromb.* (2002) 32:85–91. doi: 10.1159/000065081
67. Yurtseven E, Ural D, Baysal K, Tokgözoglu L. An update on the role of PCSK9 in atherosclerosis. *J Atheroscler Thromb.* (2020) 27:909–18. doi: 10.5551/jat.55400
68. Wu CY, Tang ZH, Jiang L, Li XF, Jiang ZS, Liu LS. PCSK9 siRNA inhibits HUVEC apoptosis induced by ox-LDL via Bcl/Bax-caspase9-caspase3 pathway. *Mol Cell Biochem.* (2012) 359:347–58. doi: 10.1007/s11010-011-1028-6
69. Li J, Liang X, Wang Y, Xu Z, Li G. Investigation of highly expressed PCSK9 in atherosclerotic plaques and ox-LDL-induced endothelial cell apoptosis. *Mol Med Rep.* (2017) 16:1817–25. doi: 10.3892/mmr.2017.6803
70. De Chiara G, Marcocci ME, Torcia M, Lucibello M, Rosini P, Bonini P, et al. Bcl-2 phosphorylation by p38 MAPK: identification of target sites and biologic consequences. *J Biol Chem.* (2006) 281:21353–61. doi: 10.1074/jbc.M511052200
71. Willis SN, Fletcher JI, Kaufmann T, Van Delft MF, Chen L, Czabotar PE, et al. Apoptosis initiated when BH3 ligands engage multiple Bcl-2 homologs, not Bax or Bak. *Science.* (2007) 315:856–9. doi: 10.1126/science.1133289
72. Dhanasekaran DN, Premkumar Reddy E. JNK-signaling: a multiplexing hub in programmed cell death. *Genes Cancer.* (2017) 8:682–94. doi: 10.18632/genesandcancer.155
73. Donovan N, Becker EBE, Konishi Y, Bonni A. JNK phosphorylation and activation of bad couples the stress-activated signaling pathway to the cell death machinery. *J Biol Chem.* (2002) 277:40944–9. doi: 10.1074/jbc.M206113200
74. Tsuruta F, Sunayama J, Mori Y, Hattori S, Shimizu S, Tsujimoto Y, et al. JNK promotes Bax translocation to mitochondria through phosphorylation of 14-3-3 proteins. *EMBO J.* (2004) 23:1889–99. doi: 10.1038/sj.emboj.7600194
75. Xu B, Li S, Fang Y, Zou Y, Song D, Zhang S, et al. proprotein convertase subtilisin/kexin type 9 promotes gastric cancer metastasis and suppresses apoptosis by facilitating MAPK signaling pathway through HSP70 up-regulation. *Front Oncol.* (2021) 10:609663. doi: 10.3389/fonc.2020.609663
76. Bentzon JF, Otsuka F, Virmani R, Falk E. Mechanisms of plaque formation and rupture. *Circ Res.* (2014) 114:1852–66. doi: 10.1161/CIRCRESAHA.114.302721
77. Ruscica M, Tokgözoglu L, Corsini A, Sirtori CR. PCSK9 inhibition and inflammation: a narrative review. *Atherosclerosis.* (2019) 288:146–55. doi: 10.1016/j.atherosclerosis.2019.07.015
78. Kühnast S, Van Der Hoorn JWA, Pieterman EJ, Van Den Hoek AM, Sasiela WJ, Gusarova V, et al. Alirocumab inhibits atherosclerosis, improves the plaque morphology, and enhances the effects of a statin. *J Lipid Res.* (2014) 55:2103–12. doi: 10.1194/jlr.M051326
79. Schuster S, Rubil S, Endres M, Princen HMG, Boeckel JN, Winter K, et al. Anti-PCSK9 antibodies inhibit pro-atherogenic mechanisms in APOE*3Leiden.CETP mice. *Sci Rep.* (2019) 9:11079. doi: 10.1038/s41598-019-47242-0
80. Galabova G, Brunner S, Winsauer G, Juno C, Wanko B, Mairhofer A, et al. Peptide-based anti-PCSK9 vaccines-an approach for long-term LDLc management. *PLoS ONE.* (2014) 9:e114469. doi: 10.1371/journal.pone.0114469

81. Landlinger C, Pouwer MG, Juno C, Van Der Hoorn JWA, Pieterman EJ, Jukema JW, et al. The AT04A vaccine against proprotein convertase subtilisin/kexin type 9 reduces total cholesterol, vascular inflammation, and atherosclerosis in APOE*3Leiden.CETP mice. *Eur Heart J.* (2017) 38:2499–507. doi: 10.1093/eurheartj/ehx260
82. Yano H, Horinaka S, Ishimitsu T. Effect of evolocumab therapy on coronary fibrous cap thickness assessed by optical coherence tomography in patients with acute coronary syndrome. *J Cardiol.* (2020) 75:289–95. doi: 10.1016/j.jjcc.2019.08.002
83. Werner N, Kosiol S, Schiegl T, Ahlers P, Walenta K, Link A, et al. Circulating endothelial progenitor cells and cardiovascular outcomes. *N Engl J Med.* (2005) 353:999–1007. doi: 10.1056/NEJMoa043814
84. Bobryshev YV, Watanabe T. Ultrastructural evidence for association of vascular dendritic cells with T-lymphocytes and with B-cells in human atherosclerosis. *J Submicrosc Cytol Pathol.* (1997) 29:209–21.
85. Frostegård J, Zhang Y, Sun J, Yan K, Liu A. Oxidized low-density lipoprotein (OxLDL)-treated dendritic cells promote activation of T cells in human atherosclerotic plaque and blood, which is repressed by statins: microRNA let-7c is integral to the effect. *J Am Heart Assoc.* (2016) 5:e003976. doi: 10.1161/JAHA.116.003976
86. Zhou X, Nicoletti A, Elhage R, Hansson GK. Transfer of $CD4^+$ T cells aggravates atherosclerosis in immunodeficient apolipoprotein E knockout mice. *Circulation.* (2000) 102:2919–22. doi: 10.1161/01.CIR.102.24.2919
87. Liu A, Frostegård J. PCSK9 plays a novel immunological role in oxidized LDL-induced dendritic cell maturation and activation of T cells from human blood and atherosclerotic plaque. *J Intern Med.* (2018) 284:193–210. doi: 10.1111/joim.12758
88. Foks AC, Lichtman AH, Kuiper J. Treating atherosclerosis with regulatory T cells. *Arterioscler Thromb Vasc Biol.* (2015) 35:280–7. doi: 10.1161/ATVBAHA.114.303568
89. Kim YU, Kee P, Danila D, Teng BB. A critical role of PCSK9 in mediating il-17-producing T cell responses in hyperlipidemia. *Immune Netw.* (2019) 19:e41. doi: 10.4110/in.2019.19.e41
90. Liu X, Bao X, Hu M, Chang H, Jiao M, Cheng J, et al. Inhibition of PCSK9 potentiates immune checkpoint therapy for cancer. *Nature.* (2020) 588:693–8. doi: 10.1038/s41586-020-2911-7
91. El Khoury P, Elbitar S, Ghaleb Y, Khalil YA, Varret M, Boileau C, et al. PCSK9 mutations in familial hypercholesterolemia: from a groundbreaking discovery to anti-PCSK9 therapies. *Curr Atheroscler Rep.* (2017) 19:49. doi: 10.1007/s11883-017-0684-8
92. Marston NA, Gurmu Y, Melloni GEM, Bonaca M, Gencer B, Sever PS, et al. The effect of PCSK9 inhibition on the risk of venous thromboembolism. *Circulation.* (2020) 141:1600–7. doi: 10.1161/CIRCULATIONAHA.120.046397
93. Bernelot Moens SJ, Neele AE, Kroon J, Van Der Valk FM, Van Den Bossche J, Hoeksema MA, et al. PCSK9 monoclonal antibodies reverse the pro-inflammatory profile of monocytes in familial hypercholesterolaemia. *Eur Heart J.* (2017) 38:1584–93. doi: 10.1093/eurheartj/ehx002
94. Adorni MP, Cipollari E, Favari E, Zanotti I, Zimetti F, Corsini A, et al. Inhibitory effect of PCSK9 on Abca1 protein expression and cholesterol efflux in macrophages. *Atherosclerosis.* (2017) 256:1–6. doi: 10.1016/j.atherosclerosis.2016.11.019
95. Cao YX, Jin JL, Sun D, Liu HH, Guo YL, Wu NQ, et al. Circulating PCSK9 and cardiovascular events in FH patients with standard lipid-lowering therapy. *J Transl Med.* (2019) 17:367. doi: 10.1186/s12967-019-2123-9
96. Gresele P, Momi S, Migliacci R. Endothelium, venous thromboembolism and ischaemic cardiovascular events. *Thromb Haemost.* (2010) 103:56–61. doi: 10.1160/TH09-08-0562
97. Santos-Gallego CG, Picatoste B, Badimón JJ. Pathophysiology of acute coronary syndrome. *Curr Atheroscler Rep.* (2014) 16:401. doi: 10.1007/s11883-014-0401-9
98. Camera M, Rossetti L, Barbieri SS, Zanotti I, Canciani B, Trabattoni D, et al. PCSK9 as a positive modulator of platelet activation. *J Am Coll Cardiol.* (2018) 71:952–4. doi: 10.1016/j.jacc.2017.11.069
99. Wang H, Wang Q, Wang J, Guo C, Kleiman K, Meng H, et al. Proprotein convertase subtilisin/kexin type 9 (PCSK9) deficiency is protective against venous thrombosis in mice. *Sci Rep.* (2017) 30:14360. doi: 10.1038/s41598-017-14307-x
100. von Brühl ML, Stark K, Steinhart A, Chandraratne S, Konrad I, Lorenz M, et al. Monocytes, neutrophils, and platelets cooperate to initiate and propagate venous thrombosis in mice *in vivo*. *J Exp Med.* (2012) 209:819–35. doi: 10.1084/jem.20112322
101. Brinkmann V, Reichard U, Goosmann C, Fauler B, Uhlemann Y, Weiss DS, et al. Neutrophil extracellular traps kill bacteria. *Science.* (2004) 303:1532–5. doi: 10.1126/science.1092385
102. Fuchs TA, Brill A, Duerschmied D, Schatzberg D, Monestier M, Myers DD, et al. Extracellular DNA traps promote thrombosis. *Proc Natl Acad Sci USA.* (2010) 107:15880–5. doi: 10.1073/pnas.1005743107
103. Navarese EP, Kolodziejczak M, Winter MP, Alimohammadi A, Lang IM, Buffon A, et al. Association of PCSK9 with platelet reactivity in patients with acute coronary syndrome treated with prasugrel or ticagrelor: the PCSK9-REACT study. *Int J Cardiol.* (2017) 227:644–9. doi: 10.1016/j.ijcard.2016.10.084
104. Dorsam RT, Kunapuli SP. Central role of the P2Y12 receptor in platelet activation. *J Clin Invest.* (2004) 113:340–5. doi: 10.1172/JCI20986
105. Hollopeter G, Jantzen HM, Vincent D, Li G, England L, Ramakrishnan V, et al. Identification of the platelet ADP receptor targeted by antithrombotic drugs. *Nature.* (2001) 409:202–7. doi: 10.1038/35051599
106. Li S, Zhu CG, Guo YL, Xu RX, Zhang Y, Sun J, et al. The relationship between the plasma PCSK9 levels and platelet indices in patients with stable coronary artery disease. *J Atheroscler Thromb.* (2015) 22:76–84. doi: 10.5551/jat.25841
107. Pastori D, Nocella C, Farcomeni A, Bartimoccia S, Santulli M, Vasaturo F, et al. Relationship of PCSK9 and urinary thromboxane excretion to cardiovascular events in patients with atrial fibrillation. *J Am Coll Cardiol.* (2017) 70:1455–62. doi: 10.1016/j.jacc.2017.07.743
108. Cammisotto V, Pastori D, Nocella C, Bartimoccia S, Castellani V, Marchese C, et al. PCSK9 regulates Nox2-mediated platelet activation via CD36 receptor in patients with atrial fibrillation. *Antioxidants.* (2020) 9:296. doi: 10.3390/antiox9040296
109. Shattil SJ, Anaya-Galindo R, Bennett J, Colman RW, Cooper RA. Platelet hypersensitivity induced by cholesterol incorporation. *J Clin Invest.* (1975) 55:636–43. doi: 10.1172/JCI107971
110. Panes O, González C, Hidalgo P, Valderas JP, Acevedo M, Contreras S, et al. Platelet tissue factor activity and membrane cholesterol are increased in hypercholesterolemia and normalized by rosuvastatin, but not by atorvastatin. *Atherosclerosis.* (2017) 257:164–71. doi: 10.1016/j.atherosclerosis.2016.12.019
111. Chen K, Febbraio M, Li W, Silverstein RL. A specific cd36-dependent signaling pathway is required for platelet activation by oxidized low-density lipoprotein. *Circ Res.* (2008) 102:1512–9. doi: 10.1161/CIRCRESAHA.108.172064
112. Hofmann A, Brunssen C, Morawietz H. Contribution of lectin-like oxidized low-density lipoprotein receptor-1 and LOX-1 modulating compounds to vascular diseases. *Vascul Pharmacol.* (2017). doi: 10.1016/j.vph.2017.10.002. [Epub ahead of print].
113. Shen MY, Chen FY, Hsu JF, Fu RH, Chang CM, Chang CT, et al. Plasma L5 levels are elevated in ischemic stroke patients and enhance platelet aggregation. *Blood.* (2016) 127:1336–45. doi: 10.1182/blood-2015-05-646117
114. Carnevale R, Bartimoccia S, Nocella C, Di Santo S, Loffredo L, Illuminati G, et al. LDL oxidation by platelets propagates platelet activation via an oxidative stress-mediated mechanism. *Atherosclerosis.* (2014) 237:108–16. doi: 10.1016/j.atherosclerosis.2014.08.041
115. Sahebkar A, Watts GF. New therapies targeting apoB metabolism for high-risk patients with inherited dyslipidaemias: what can the clinician expect? *Cardiovasc Drugs Ther.* (2013) 27:559–67. doi: 10.1007/s10557-013-6479-4
116. Rand ML, Sangrar W, Hancock MA, Taylor DM, Marcovina SM, Packham MA, et al. Apolipoprotein(a) enhances platelet responses to the thrombin receptor-activating peptide SFLLRN. *Arterioscler Thromb Vasc Biol.* (1998) 18:1393–9. doi: 10.1161/01.ATV.18.9.1393
117. Martínez C, Rivera J, Loyau S, Corral J, González-Conejero R, Lozano ML, et al. Binding of recombinant apolipoprotein(a) to human platelets and effect on platelet aggregation. *Thromb Haemost.* (2001) 85:686–93. doi: 10.1055/s-0037-1615654

118. Dentali F, Gessi V, Marcucci R, Gianni M, Grandi AM, Franchini M. Lipoprotein(a) as a risk factor for venous thromboembolism: a systematic review and meta-analysis of the literature. *Semin Thromb Hemost.* (2017) 43:614–20. doi: 10.1055/s-0036-1598002
119. Nguyen S, Ilano L, Oluoha N, Pakbaz Z. Lipoprotein(a) a risk factor for venous thrombosis and pulmonary embolism in patients younger than 50 years of age. *Blood.* (2018) 132(Suppl. 1):5055. doi: 10.1182/blood-2018-99-113975
120. Barale C, Bonomo K, Frascaroli C, Morotti A, Guerrasio A, Cavalot F, et al. Platelet function and activation markers in primary hypercholesterolemia treated with anti-PCSK9 monoclonal antibody: a 12-month follow-up. *Nutr Metab Cardiovasc Dis.* (2020) 30:282–91. doi: 10.1016/j.numecd.2019.09.012
121. Smith SA, Travers RJ, Morrissey JH. How it all starts: initiation of the clotting cascade. *Crit Rev Biochem Mol Biol.* (2015) 50:326–36. doi: 10.3109/10409238.2015.1050550
122. Bank I, Libourel EJ, Middeldorp S, Hamulyák K, Van Pampus ECM, Koopman MMW, et al. Elevated levels of FVIII:C within families are associated with an increased risk for venous and arterial thrombosis. *J Thromb Haemost.* (2005) 3:79–84. doi: 10.1111/j.1538-7836.2004.01033.x
123. Milgrom A, Lee K, Rothschild M, Makadia F, Duhon G, Min S, et al. Thrombophilia in 153 Patients With Premature Cardiovascular Disease ≤Age 45. *Clin Appl Thromb.* (2018) 24:295–302. doi: 10.1177/1076029617703481
124. Machlus KR, Lin FC, Wolberg AS. Procoagulant activity induced by vascular injury determines contribution of elevated factor VIII to thrombosis and thrombus stability in mice. *Blood.* (2011) 118:3960–8. doi: 10.1182/blood-2011-06-362814
125. Saenko EL, Yakhyaev AV, Mikhailenko I, Strickland DK, Sarafanov AG. Role of the low density lipoprotein-related protein receptor in mediation of factor VIII catabolism. *J Biol Chem.* (1999) 274:37685–92. doi: 10.1074/jbc.274.53.37685
126. Bovenschen N, Herz J, Grimbergen JM, Lenting PJ, Havekes LM, Mertens K, et al. Elevated plasma factor VIII in a mouse model of low-density lipoprotein receptor-related protein deficiency. *Blood.* (2003) 101:3933–9. doi: 10.1182/blood-2002-07-2081
127. Bovenschen N, Mertens K, Hu L, Havekes LM, Van Vlijmen BJM. LDL receptor cooperates with LDL receptor-related protein in regulating plasma levels of coagulation factor VIII *in vivo*. *Blood.* (2005) 106:906–12. doi: 10.1182/blood-2004-11-4230
128. Paciullo F, Gresele P. Effect of statins on measures of coagulation: potential role of low-density lipoprotein receptors. *Eur Heart J.* (2019) 40:392. doi: 10.1093/eurheartj/ehy680
129. Canuel M, Sun X, Asselin MC, Paramithiotis E, Prat A, Seidah NG. Proprotein convertase subtilisin/kexin type 9 (PCSK9) can mediate degradation of the low density lipoprotein receptor-related protein 1 (LRP-1). *PLoS ONE.* (2013) 8:e64145. doi: 10.1371/journal.pone.0064145
130. Ochoa E, Iriondo M, Manzano C, Fullaondo A, Villar I, Ruiz-Irastorza G, et al. LDLR and PCSK9 are associated with the presence of antiphospholipid antibodies and the development of thrombosis in aPLA carriers. *PLoS ONE.* (2016) 11:e0146990. doi: 10.1371/journal.pone.0146990

Conflict of Interest: The authors declare that the research was conducted in the absence of any commercial or financial relationships that could be construed as a potential conflict of interest.